# Systematic and taxonomic revision of Late Miocene Eurasian rhinocerotids, with a focus on *Chilotherium* Ringström, 1924

**Dissertation**

der Mathematisch-Naturwissenschaftlichen Fakultät

der Eberhard Karls Universität Tübingen

zur Erlangung des Grades eines

Doktors der Naturwissenschaften

(Dr. rer. nat.)

vorgelegt von

M.Sc. Panagiotis Kampouridis

aus Herford

Tübingen

2026

Gedruckt mit Genehmigung der Mathematisch-Naturwissenschaftlichen Fakultät der Eberhard Karls Universität Tübingen.

| | |
|---|---|
| Tag der mündlichen Qualifikation: | 11.06.2026 |
| Dekan: | Prof. Dr. Thilo Stehle |
| 1. Berichterstatterin: | Prof. Dr. Madelaine Böhme |
| 2. Berichterstatter: | Prof. Dr. Nikolai Spassov |
| 3. Berichterstatter: | PD Dr. Damien Becker |

## Table of Contents

**Acknowledgments**

First, I would like to thank my two supervisors, Prof. Dr. Madelaine Böhme and Prof. Dr. Nikolai Spassov for the supervision of this Dissertation. I am grateful to Prof. Böhme for giving me the opportunity to pursue this project about extinct rhinoceroses and supporting me during all this time. She made sure that I always had all necessary tools to conduct my research. She also gave me the chance to spend time in the field and to visit the collections that were necessary for realising this project. I want to thank Prof. Dr. Spassov for his kindness and for encouraging me to follow my research. I am grateful for him always being open to my ideas and supportive in publishing my findings, all while providing his extensive experience in the field. I would also like to thank PD Dr. Damien Becker, who generously shared his expertise on rhinoceroses and served as the third examiner for this Dissertation.

In addition to my supervisors, I am indebted to several people who played major roles, not only in realising the present Doctoral Dissertation, but also in my broader development as a researcher. First, I need to thank PD Dr. Andreas T. Matzke for his consistent support and for constantly being available for discussions about various aspects of palaeontological research. I am particularly grateful for his willingness to share his experience and for his genuine dedication to supporting the next generation of palaeontologists. Next, I would like to extend my gratitude to Prof. Dr. Socrates Roussiakis, my Bachelor's Thesis supervisor at the University of Athens in Greece. His expertise in large mammal anatomy and his commitment to scientific rigor were instrumental in my early development as a researcher. I am deeply indebted to Emer. Prof. Dr. George Theodorou, who had a pivotal role in my early development as a palaeontologist. He gave me and many other Geology students the opportunity to participate in excavations in Greece and Cyprus. His support was unwavering; he consistently went above and beyond for his students, continuing to offer guidance even as we pursued careers abroad. Very few individuals have impacted my professional journey as profoundly as he has.

I am grateful to my colleagues in the working group, both past and present, for creating a supportive environment. In alphabetical order, they are: Dr. Felix J. Augustin, Marie Biesinger, Dr. Christian Dietzel, Aaron Ebner, PD Dr. Haytham El Atfy, Dr. Gabriel de Souza Ferreira, Nina Frank, Dr. Josi Hartung, Vivien Hirsch, Dr. Nikolaos Kargopoulos, Dr. Uwe Kirscher, Maja Körber, Christina Kyriakouli, Dr.

Thomas Lechner, Florian Ludwig, Dr. Tobias Massonne, Paulina Moctezuma Duclaud, Miguel Díaz de León Muñóz, Michelle Poltze, Angie Ride, Tim Treiber, Kelly Ann Vega Pagán, and Darius Wedekind. I would further like to thank all the colleagues with whom I collaborated over the years. Their contributions and assistance at various stages of my research have been greatly appreciated.

To my friends and family: thank you for your unconditional support and endless encouragement throughout my years at the university. I owe a special debt of gratitude to my best friends—Vassilis Pappas, Iliana Kantzeli, and Anastasia Kounoupi. You were always there to provide a sanctuary outside of my research, consistently reminding me of the world beyond the university walls. I am incredibly lucky to have you in my life. Your enduring friendship allowed me to reach this milestone. I am deeply grateful to my parents, Zacharias Kampouridis and Assimo Mavrogianni, and my brothers, Miltiadis Kampouridis and Spiridon Kampouridis, for their enduring support of my path in Palaeontology and for providing the foundation that allowed me to flourish. I owe a special debt of gratitude to my grandfather, Miltiadis Kampouridis, who first sparked and nurtured my love for the natural world; without his early inspiration, I would not be where I am today.

Finally, my deepest gratitude goes to my fiancée, Sara Roci, for her unconditional love and unwavering support. You have been the North Star of my life throughout the past eleven years, enduring my long discussions on rhinoceros and chalicothere taxonomy with remarkable patience. Thank you for keeping me grounded, for ensuring I had a life beyond research, and for being the steady pillar that gave me strength. You have always been my greatest inspiration.

**List of Publications/Manuscripts of the Dissertation**

## a) Publications

1.) **Kampouridis, P.**, Svorligkou, G., Kargopoulos, N., & Augustin, F. J. 2022. Reassessment of '*Chilotherium wegneri*' (Mammalia, Rhinocerotidae) from the late Miocene of Samos (Greece) and the European record of *Chilotherium*. Historical Biology, 34, 412–420. https://doi.org/10.1080/08912963.2021.1920939

(Online publication date: 13.05.2021)

Author contributions: PK designed the study. PK studied the material. PK wrote the first draft of the manuscript. All authors reviewed and edited the manuscript.

2.) **Kampouridis, P.**, J. Hartung, G. S. Ferreira, and M. Böhme. 2022. Reappraisal of the Late Miocene elasmotheriine *Parelasmotherium schansiense* from Kutschwan (Shanxi Province, China) and its phylogenetic relationships. Journal of Vertebrate Paleontology 41(6):e2080556. https://doi.org/10.1080/02724634.2021.2080556

(Online publication date: 05.07.2022)

Author contributions: PK and JH designed the study. PK and JH studied the material. PK, JH, and GSF conducted the analyses. MB supervised the study. PK wrote the first draft of the manuscript. All authors reviewed and edited the manuscript.

3.) **Kampouridis, P.**, G. Svorligkou, N. Kargopoulos, N. Spassov, and M. Böhme. 2023. Revision of the Late Miocene hornless rhinocerotids from Samos Island (Greece) with the designation of neotypes and implications for the European chilotheres. Journal of Vertebrate Paleontology 43(1):e2254360. https://doi.org/10.1080/02724634.2023.2254360

(Online publication date: 02.11.2023)

Author contributions: PK, GS, and MB designed the study. All authors studied part of the material. MB and NS supervised the study. PK wrote the first draft of the manuscript. All authors reviewed and edited the manuscript.

4.) Svorligkou, G**., P. Kampouridis**, N. Kargopoulos, and L. Pandolfi. 2025. Craniodental anatomy of the hornless rhinocerotid *Chilotherium schlosseri* (Mammalia, Perissodactyla) from the Late Miocene of Samos Island, Greece. Journal of Mammalian Evolution 32:36. https://doi.org/10.1007/s10914-025-09777-0

(Online publication date: 17.10.2025)

Author contributions: PK and GS designed the study. All authors studied part of the material. PK and GS wrote the first draft of the manuscript. All authors reviewed and edited the manuscript.

5.) **Kampouridis, P.**, G. Svorligkou, N. Spassov, and M. Böhme. 2025. Postcranial anatomy of the Late Miocene Eurasian hornless rhinocerotid *Chilotherium*. PLOS ONE 20(12):e0336590. https://doi.org/10.1371/journal.pone.0336590

(Online publication date: 05.12.2025)

Author contributions: PK designed the study. PK studied the material. MB and NS supervised the study. PK wrote the first draft of the manuscript. All authors reviewed and edited the manuscript.

6.) **Kampouridis, P.**, L. Pandolfi, C. Kyriakouli, N. Spassov, and M. Böhme. Deciduous dentition and ontogenetic development of the skull and teeth of *Chilotherium*

(Mammalia, Perissodactyla, Rhinocerotidae) from the Late Miocene of Eurasia. Fossil Record 29(1):373–410. https://doi.org/10.3897/fr.29.192018

(Submission date: 04.06.2026)

Author contributions: PK designed the study. PK and LP studied the material. PK and CK conducted the analyses. MB and NS supervised the study. PK wrote the first draft of the manuscript. All authors reviewed and edited the manuscript.

**Additional publications produced during the doctoral studies**

Below a list of works is presented with all additional peer-reviewed publications that arose during the period of the doctoral studies but were not directly part of the Dissertation:

**1.)** Böhme, M., **P. Kampouridis**, G. N. Markov, L. Hristova, and N. Spassov. 2021. Large mammals (Proboscidea, Perissodactyla) from the late Miocene Burel Basin in West Bulgaria. Neues Jahrbuch Für Geologie Und Paläontologie - Abhandlungen 302(2):117–129. DOI: 10.1127/njgpa/2021/1022

**2.)** Hartung, J., F. J. Augustin, **P. Kampouridis**, and D. J. Chure. 2021. A unique notostracan trace fossil assemblage from the Upper Triassic Chinle Formation (northeastern Utah, USA) and its paleoecological and paleoenvironmental implications. Palaeogeography, Palaeoclimatology, Palaeoecology 583:110667. DOI: 10.1016/j.palaeo.2021.110667

**3.)** Kargopoulos, N., A. Valenciano, **P. Kampouridis**, T. Lechner, and M. Böhme. 2021. New early late Miocene species of *Vishnuonyx* (Carnivora, Lutrinae) from the hominid locality of Hammerschmiede, Bavaria, Germany. Journal of Vertebrate Paleontology 41(3):e1948858. DOI: 10.1080/02724634.2021.1948858

**4.)** Kargopoulos, N., **P. Kampouridis**, T. Lechner, and M. Böhme. 2021. A review of *Semigenetta* (Viverridae, Carnivora) from the Miocene of Eurasia based on material from the hominid locality of Hammerschmiede (Germany). Geobios 69:25–36. DOI: 10.1016/j.geobios.2021.07.001

**5.) Kampouridis, P.**, J. Hartung, and M. Böhme. 2022. Large mammals from the late Middle Miocene of Markt Rettenbach (Bavaria, Germany). Neues Jahrbuch für Geologie und Paläontologie - Abhandlungen 304(3):299–312. DOI: 10.1127/njgpa/2022/1072

**6.) Kampouridis, P.**, S. J. Roussiakis, I. X. Giaourtsakis, N. Kargopoulos, G. Svorligkou, and G. E. Theodorou. 2022. *Ancylotherium pentelicum* (Mammalia, Chalicotheriidae) from the late Miocene of Kerassia (Greece) and remarks on its intraspecific variability. Palaeobiodiversity and Palaeoenvironments 102:193–203. DOI: 10.1007/s12549-021-00497-w

**7.)** Augustin, F. J., **P. Kampouridis**, J. Hartung, R. Albersdörfer, and A. T. Matzke. 2022. The geologically oldest specimen of *Pterodactylus*: a new exquisitely preserved skeleton from the Upper Jurassic (Kimmeridgian) Plattenkalk deposits of Painten (Bavaria, Germany). Fossil Record 25:331–343. DOI: 10.3897/fr.25.90692

**8.)** Augustin, F. J., A. T. Matzke, M. W. Maisch, **P. Kampouridis**, and Z. Csiki-Sava. 2022. The first record of pterosaurs from the Lower Cretaceous Hutubei Formation (lower Tugulu Group) of the southern Junggar Basin (NW China) – A glimpse into an unusual ecosystem. Cretaceous Research 130:105066. DOI: 10.1016/j.cretres.2021.105066

**9.)** Kargopoulos, N., **P. Kampouridis**, T. Lechner, and M. Böhme. 2022. Hyaenidae (Carnivora) from the Late Miocene hominid locality of Hammerschmiede (Bavaria, Germany). Historical Biology 34(11):2249–2258. DOI: 10.1080/08912963.2021.2010193

**10.)** Kargopoulos, N., A. Valenciano, J. Abella, **P. Kampouridis**, T. Lechner, and M. Böhme. 2022. The exceptionally high diversity of small carnivorans from the Late Miocene hominid locality of Hammerschmiede (Bavaria, Germany). PLOS ONE 17(7):e0268968. DOI: 10.1371/journal.pone.0268968

**11.)** Roussiakis, S., N. Kargopoulos, **P. Kampouridis**, G. Svorligkou, and G. Theodorou. 2022. The fossil aardvark *Amphiorycteropus gaudryi* (Forsyth Major, 1888) from the late Miocene of Kerassia (Euboea, Greece). Historical Biology 34(3):493–506. DOI: 10.1080/08912963.2021.1931167

**12.) Kampouridis, P.**, J. Hartung, F. J. Augustin, H. El Atfy, and G. S. Ferreira. 2023. Dental eruption and adult dentition of the enigmatic ptolemaiid *Qarunavus meyeri* from the Oligocene of the Fayum Depression (Egypt) revealed by micro-computed tomography clarifies its phylogenetic position. Zoological Journal of the Linnean Society 199(4):1078–1091. DOI: 10.1093/zoolinnean/zlad065

**13.) Kampouridis, P.**, B. Ratoi, and L. Ursachi. 2023. New evidence for the unique coexistence of two subfamilies of clawed perissodactyls (Mammalia, Chalicotheriidae) in the Upper Miocene of Romania and the Eastern Mediterranean. Journal of Mammalian Evolution 30:641–656. DOI: 10.1007/s10914-023-09657-5

**14.)** Augustin, F. J., M. Rabi, F. Spindler, **P. Kampouridis**, J. Hartung, R. Albersdörfer, A. T. Matzke. 2023. A new specimen of *Solnhofia parsonsi* from the Upper Jurassic

(Kimmeridgian) Plattenkalk deposits of Painten (Bavaria, Germany) and comments on the relationship between limb taphonomy and habitat ecology in fossil turtles. PLoS ONE 18(7): e0287936. DOI: 10.1371/journal.pone.0287936

**15.)** Kargopoulos, N., **P. Kampouridis**, J. Hartung, and M. Böhme. 2023. Hyaenid remains from the Late Miocene of Kutschwan (Shanxi Province, China). PalZ 97:653–666. DOI: 10.1007/s12542-023-00658-6

**16.)** Kargopoulos, N., S. Roussiakis, **P. Kampouridis**, and G. D. Koufos. 2023. Interspecific competition in ictitheres (Carnivora: Hyaenidae) from the Late Miocene of Eurasia. Comptes Rendus Palevol 22(3):33-44. DOI: 10.5852/cr-palevol2023v22a3

**17.)** Konidaris, G. E., T. Lechner, **P. Kampouridis**, and M. Böhme. 2023. *Deinotherium levius* and *Tetralophodon longirostris* (Proboscidea, Mammalia) from the Late Miocene hominid locality Hammerschmiede (Bavaria, Germany), and their biostratigraphic significance for the terrestrial faunas of the European Miocene. Journal of Mammalian Evolution 30:923–961. DOI: 10.1007/s10914-023-09683-3

**18.) Kampouridis, P.**, J. Hartung, and F. J. Augustin. 2023. The Eocene–Oligocene vertebrate assemblages of the Fayum Depression, Egypt; pp. 373–405 in Z. Hamimi, H. Khozyem, T. Adatte, F. H. Nader, F. Oboh-Ikuenobe, M. K. Zobaa, and H. El Atfy (eds.), The Phanerozoic Geology and Natural Resources of Egypt. Springer Nature Switzerland AG. DOI: 10.1007/978-3-030-95637-0_14

**19.)** Augustin, F. J., J. Hartung, and **P. Kampouridis**. 2023. Dinosaur faunas of Egypt - the terrestrial Late Cretaceous vertebrate record; pp. 253–284 in Z. Hamimi, H. Khozyem, T. Adatte, F. H. Nader, F. Oboh-Ikuenobe, M. K. Zobaa, and H. El Atfy (eds.), The Phanerozoic Geology and Natural Resources of Egypt. Springer Nature Switzerland AG. DOI: 10.1007/978-3-030-95637-0_9

**20.) Kampouridis, P.**, J. Hartung, T, Lechner, N. Kargopoulos, and M. Böhme. 2024. Disparate occurrences of a chalicotheriine and a schizotheriine chalicothere (Mammalia, Chalicotheriidae) at the Late Miocene hominid locality Hammerschmiede (Germany). PalZ. DOI: 10.1007/s12542-024-00685-x

**21.) Kampouridis, P.**, M. Mirzaie Ataabadi, J. Hartung, and F. J. Augustin. 2024. The easternmost occurrence of the Late Miocene schizotheriine chalicothere *Ancylotherium pentelicum* at the classical locality of Maragheh (Iran). Journal of Mammalian Evolution. DOI: 10.1007/s10914-024-09730-7

**22.)** Kargopoulos, N., J. Abella, A. Daasch, T. Kaiser, **P. Kampouridis**, T. Lechner, M. Böhme. The primitive giant panda *Kretzoiarctos beatrix* (Ursidae, Carnivora) from the hominid locality of Hammerschmiede: dietary implications. Papers in Palaeontology. DOI: 10.1002/spp2.1588

**23.)** Kargopoulos, N., A. Valenciano, J. Abella, M. Morlo, G. E. Konidaris, **P. Kampouridis**, T. Lechner, and M. Böhme. The carnivoran guilds from the Late Miocene hominid locality of Hammerschmiede (Bavaria, Germany). Geobios. DOI: 10.1016/j.geobios.2024.02.003

**24.)** Kargopoulos, N., A. Valenciano, **P. Kampouridis**, S. Vasile, L. Ursachi, and B. Ratoi. The carnivoran record from the Neogene of eastern Romania. Rivista Italiana di Paleontologia e Stratigrafia. 130(2):331-371. DOI: 10.54103/2039-4942/22194

**25.) Kampouridis, P.**, C. Kyriakouli, and G. S. Ferreira. 2025. Unique pathological phalangeal fusion in the chalicothere subfamily Chalicotheriinae and the interphalangeal immobilization in chalicotheres. The Science of Nature. 112:59. DOI: 10.1007/s00114-025-02011-0

**26.)** Kargopoulos, N., A. Valenciano, Q. Jiangzuo, D. Liakopoulou, N. Gerakakis, **P. Kampouridis**, N. Paparizos, G Svorligkou, P. Filis, S. Sklavounou, S. Roussiakis. In press. A new genus of badger from Pikermi (Greece) and a review of the systematics and evolution of Miocene Melinae (Mammalia, Carnivora, Mustelidae). Journal of Systematic Palaeontology. 24(1): 2647483. DOI: 10.1080/14772019.2026.2647483

**27.)** Submitted: **Kampouridis, P.**, M. Mirzaie Ataabadi, M. Albrecht, and F. J. Augustin. First evidence of bioerosion on large mammal bones from the classical Upper Miocene locality of Maragheh in Iran provides insights into the palaeoenvironment. Lethaia (under review)

## List of conference contributions during the doctoral studies

**1.) Kampouridis, P.** and J. Hartung. 2021. Re-appraisal of the late Miocene elasmothere *Parelasmotherium schansiense* using high resolution X-ray computed tomography. 3rd Palaeontological Virtual Congress. (presentation)

**2.) Kampouridis, P.**, G. Svorligkou, C. Kyriakouli, N. Kargopoulos, S. Roussiakis and M. Böhme. 2022. Dental hypoplasias in the late Miocene hornless rhinocerotid *Chilotherium* (Mammalia, Rhinocerotidae) from Eurasia. 16th International Congress of the Geological Society of Greece. (poster)

**3.)** Svorligkou, G., **P. Kampouridis**, E. Alifieri and S. Roussiakis. 2022. The Late Miocene Rhinocerotids (Perissodactyla, Rhinocerotidae) from Samos Island - New Insights from the Historical T. Skoufos Collection. 16th International Congress of the Geological Society of Greece. (presentation)

**4.) Kampouridis, P.**, J. Hartung, F. J. Augustin, H. El Atfy and G. S. Ferreira. 2023. Dental eruption and adult dentition of the enigmatic ptolemaiid *Qarunavus meyeri* from the Oligocene Fayum Depression (Egypt) revealed by micro-computed tomography clarifies its phylogenetic position. 4th Palaeontological Virtual Congress. (presentation)

**5.)** Kargopoulos, N., J. Abella, A. Daasch, T. Kaiser, **P. Kampouridis**, T. Lechner and M. Böhme. 2023. *Kretzoiarctos beatrix* (Carnivora, Ursidae) from the Late Miocene of Hammerschmiede (Germany): dietary implications. 20th European Association of Vertebrate Palaeontologists Conference. (presentation)

**6.) Kampouridis, P.** 2024. The chilotheres from the Upper Miocene of Samos Island (Greece). Rencontres sur le Rhinoceros in Gannat (France) (presentation)

**7.)** Coombs, M. C., **P. Kampouridis**, and S. Cote. 2025. Chalicotheres (Perissodactyla) from La Grive, Southeast France: A transition from the Mid to Late Miocene. 5th Palaeontological Virtual Congress. (presentation)

**8.)** Svorligkou, G., and **P. Kampouridis**. 2025. Morphological characterization of *Chilotherium schlosseri* (Perissodactyla, Rhinocerotidae) from the Late Miocene of Samos Island, Greece). 5th Palaeontological Virtual Congress. (presentation)

**9.) Kampouridis, P.** 2025. Unique morphological adaptations in the hand of the Late Miocene chalicothere *Ancylotherium pentelicum*. 5th Palaeontological Virtual Congress. (presentation)

**10.) Kampouridis, P.**, G. Svorligkou, N. Kargopoulos, N. Spassov, and M. Böhme. 2025. The Late Miocene hornless rhinocerotids from Samos Island (Greece). 20th Annual Conference of the European Association of Vertebrate Palaeontologists. (presentation)

**11.) Kampouridis, P.**, G. Svorligkou, N. Kargopoulos, N. Spassov, and M. Böhme. 2025. The Late Miocene hornless rhinocerotids from Samos Island (Greece). RCMNS Workshop – Shaping the Neogene: Climate, Tectonics, Life. Exploring the ecological drivers of continental ecosystem change in time and space. (presentation)

**Abstract**

Rhinoceroses are amongst the most iconic animals alive today. However, today's only five existing species constitute only a small fraction of a remarkably diverse lineage that spanned the Cenozoic Era. The group's extensive fossil record reveals a rich evolutionary history, marked by significant taxonomic and ecomorphological variety. Rhinocerotidae reached their highest diversity during the Miocene, but in spite of their richness many details about their systematics are shrouded in mystery. Beyond the Rhinocerotinae that comprises all extant rhinoceroses, the family includes two extinct groups: the Aceratheriinae, also known as hornless rhinoceroses and the Elasmotheriinae, relatives of the Siberian unicorn. Despite over a century of palaeontological research the phylogeny, biogeography, and ecology of extinct rhinoceroses remain poorly resolved.

This Dissertation addresses many of the persisting issues in the systematics of extinct Rhinocerotidae. An important component of this research was to clarify the phylogenetic relationships of *Parelasmotherium*, a key taxon in the evolutionary history of derived elasmotheriines and revise the systematics of the group as a whole. This was accomplished through the reevaluation of the type species of the genus, *Parelasmotherium schansiense*, using micro-computed tomography to study previously unknown features in the dentition of the species. These novel data clarify the phylogenetic position of the genus and demonstrate that two taxa previously assigned to *Parelasmotherium* are not closely related to the type species, necessitating their taxonomic from this genus.

The primary focus of this Dissertation, however, was to elucidate the systematics of the chilotheres and resolve the taxonomy of the included species. This was achieved by revising historical material from several fossil sites across Eurasia that belonged to different species. This allowed the verification of some hypothesis about the systematic affinities of the group' representatives, such as the synonymisation of *Teleoceras ponticus*, *Aceratherium wegneri*, and *Aceratherium angustifrons* with *Chilotherium schlosseri* from the Upper Miocene of Samos (Greece). It further enabled the rejection of some other past hypotheses like the synonymisation of *Chilotherium kowalevskii* from the Upper Miocene of Grebeniki (Ukraine) with *C. schlosseri*, which in fact represent distinct species. The systematics of the group were further improved by redefining the Chilotheriina at the subtribe level and restricting it to

the three genera: *Chilotherium*, *Shansirhinus*, and *Eochilotherium*. The latter genus was re-established for the species *Eochilotherium samium*, which exhibits features distinguishing it from all *Chilotherium*, as well as *Shansirhinus*, species. For this purpose, neotypes were designated for the two valid chilothere species from Samos, *C. schlosseri* and *E. samium*. The conclusions were further refined by integrating previously neglected chilothere material, which includes elements of the appendicular skeleton and juvenile cranial, mandibular, and dental elements housed in collections across Europe. This provides new insight into the taxonomy and relationships of the chilothere species, suggesting a more complex biogeographical history for the group than previously hypothesised.

**Zusammenfassung**

Nashörner gehören zu den emblematischsten Tieren der heutigen Zeit. Die lediglich fünf noch existierenden Arten stellen jedoch nur einen kleinen Bruchteil einer höchst diversen und erfolgreichen Evolutionslinie dar, die sich über das gesamte Känozoikum erstreckte. Der umfangreiche Fossilbericht der Gruppe offenbart eine reiche Evolutionsgeschichte, die durch eine signifikante taxonomische und ökomorphologische Vielfalt gekennzeichnet ist. Die Familie der Rhinocerotidae erreichte während des Miozäns ihre höchste Diversität, doch trotz dieses Reichtums sind viele Details ihrer Systematik noch immer ungeklärt. Neben den Rhinocerotinae, welche alle rezenten Nashörner umfassen, beinhaltet die Familie zwei ausgestorbene Gruppen: die Aceratheriinae, auch bekannt als hornlose Nashörner, und die Elasmotheriinae, Verwandte des „Sibirischen Einhorns“. Trotz über eines Jahrhunderts paläontologischer Forschung bleiben die Phylogenie, Biogeographie und Ökologie ausgestorbener Nashörner in großem Maße unklar.

Diese Dissertation befasst sich mit vielen der hartnäckigen Probleme in der Systematik der ausgestorbenen Rhinocerotidae. Ein wesentlicher Bestandteil dieser Forschung war die Klärung der phylogenetischen Beziehungen von *Parelasmotherium*, einem Schlüsseltaxon in der Evolutionsgeschichte der abgeleiteten Elasmotheriinen, sowie die Revision der Systematik dieser Gruppe als Ganzes. Dies wurde durch eine Neubewertung der Typusart der Gattung, *Parelasmotherium schansiense*, erreicht, wobei Mikro-Computertomographie eingesetzt wurde, um bisher unbekannte Merkmale der Zähne dieser Art zu untersuchen. Diese neuen Daten klären die phylogenetische Position der Gattung und zeigen, dass zwei zuvor *Parelasmotherium* zugeordnete Taxa nicht eng mit der Typusart verwandt sind, was ihre taxonomische Ausgliederung aus dieser Gattung erforderlich macht.

Der Hauptfokus dieser Dissertation lag jedoch bei der Klärung der Systematik der Chilotherien und der Taxonomie der enthaltenen Arten. Dies gelang durch die Revision von historischem Material verschiedener Arten von mehreren Fundstellen aus ganz Eurasien. Dadurch konnten Hypothesen über die systematischen Verwandtschaftsverhältnisse der Vertreter dieser Gruppe überprüft werden, wie etwa die Synonymisierung von *Teleoceras ponticus*, *Aceratherium wegneri* und *Aceratherium angustifrons* mit *Chilotherium schlosseri* aus dem Obermiozän von

Samos (Griechenland). Des Weiteren ermöglichte dies die Ablehnung anderer früherer Hypothesen, wie der Synonymisierung von *Chilotherium kowalevskii* aus dem Obermiozän von Grebeniki (Ukraine) mit *C. schlosseri*, die in der Tat unterschiedliche Arten darstellen. Die Systematik der Gruppe wurde zudem durch die Neudefinition der Chilotheriina auf Subtribus-Ebene verbessert, die nun nur noch die drei Gattungen *Chilotherium*, *Shansirhinus* und *Eochilotherium* umfasst. Letztere Gattung wurde für die Art *Eochilotherium samium* wiedererrichtet, die Merkmale aufweist, die sie von allen *Chilotherium*- sowie *Shansirhinus*-Arten unterscheiden. Zudem Zweck wurden Neotypen für die zwei validen Chilotherien Arten aus Samos, *C. schlosseri* und *E. samium*, festgelegt. Die Schlussfolgerungen wurden durch den Einbezug von zuvor vernachlässigtem Chilotherien-Material weiter präzisiert, welches Elemente des Appendikularskellets sowie juvenile kraniale, mandibulare und dentale Elemente aus europäischen Sammlungen umfasst. Dies liefert neue Einblicke in die Taxonomie und die Verwandtschaftsverhältnisse der Chilotherien-Arten und deutet auf eine komplexere biogeographische Geschichte der Gruppe hin als bisher angenommen.

**Abbreviations**

AMNH, American Museum of Natural History, New York (USA);

AMPG, Athens Museum of Palaeontology and Geology of the National and Kapodistrian University of Athens (Greece);

BSPG, Bayerische Staatssammlung für Paläontologie und Geologie, Munich (Germany);

GMM, Geomuseum of the University of Münster (Germany);

GPIT, Geologisch-Paläontologisches Institut der Universität Tübingen (Germany);

GPIH, Geologisch-Paläontologisches Institut der Universität Hamburg (Germany);

HLMD, Hessisches Landesmuseum Darmstadt (Germany);

IPUW, Institut für Paläontologie, Universität Wien (Austria);

MGP-PD, Museo di Geologia e Paleontologia, Padua, Italy;

MLU, Martin-Luther-Universität Halle-Wittenberg (Germany);

MNHN, Muséum national d'Histoire naturelle, Paris (France);

NHMW, Naturhistorisches Museum in Wien (Austria);

NMB, Naturhistorisches Museum Basel (Switzerland);

NMNHU-P; Department of Palaeontology, National Museum of Natural History, National Academy of Sciences of Ukraine in Kyiv;

PMU, Museum of Evolution (Palaeontological Museum), Uppsala (Sweden);

SMF, Senckenberg Museum in Frankfurt (Germany);

SMNS, Staatliches Museum für Naturkunde Stuttgart (Germany);

SNSB, Staatliche Naturwissenschaftliche Sammlungen Bayerns (Germany); and

UCBL-FSL, Paleontological-Geological Collection of the University Claude Bernard Lyon 1 (France).

# 1. Introduction

Rhinoceroses are among the most emblematic animals today. The Rhinocerotidae represent a unique group within the order Perissodactyla, being closely related to extant horses and tapirs and the extinct perissodactyls like the clawed Chalicotheriidae. Today only five species of Rhinocerotidae exist and they all belong to the group of Rhinocerotinae or Rhinocerotini, depending on the authors (Heissig, 1973, e.g., 1981; Cerdeño, 1995; Antoine, 2002; Kampouridis et al., 2022a; Lu et al., 2023; Borrani et al., 2025; Fraser et al., 2025). They all exhibit one or two keratine horns attached to respective horn bosses on the skull, which is the most characteristic feature of the whole family (Osborn, 1900; Heissig, 1981). This feature makes them some of the most recognisable animals today. However, the family of Rhinocerotidae was much more diverse in the past with many taxa completely lacking the characteristic horn and many other taxa exhibiting only a very small horn or in some cases two horns paired side-by-side next to each other, like *Diceratherium* Marsh, 1875 and *Menoceras* Troxell, 1921 (Prothero, 2005), instead of in front of each other. The family includes, along with Rhinocerotinae, also the subfamilies Elasmotheriinae and Aceratheriinae. Elasmotheriinae is an extinct clade of large and horned rhinoceroses, with its last representative being *Elasmotherium sibiricum* Fischer, 1808, also known as the Siberian unicorn (Noskova, 2001; Antoine, 2002; Kosintsev et al., 2019). Representatives of this group were especially common during the Late Miocene in Asia (e.g., Fortelius and Heissig, 1989; Antoine, 2003; Deng, 2003; Kampouridis et al., 2022a), but were also frequent in Europe and Africa during the Miocene (e.g., Fortelius and Heissig, 1989; Noskova, 2001; Sanisidro et al., 2012; Geraads and Zouhri, 2021). Aceratheriinae, often referred to as the hornless rhinoceroses, represent a highly diverse and species rich subfamily of rhinoceroses, which were generally hornless, though many representatives in fact had a small horn boss (e.g., Sun et al., 2024). The relationships of taxa within Aceratheriinae, are often debated (for examples see Kampouridis et al., 2022a; Borrani et al., 2025; Fraser et al., 2025). Another issue is the often-debated inclusion of Aceratheriinae into the Rhinocerotinae (e.g., Antoine et al., 2010; Becker et al., 2013; Pandolfi, 2016; Fraser et al., 2025). Depending on that, the group is either considered a subfamily, having the same rank as elasmotheriines and rhinocerotines (e.g., Cerdeño, 1995; Lu et al., 2023; Borrani et al., 2025), or a tribe or even subtribe that is included in the rhinocerotines (Antoine et al., 2003a, 2010; Becker et al., 2013; Tissier et al., 2020). Though many studies regard elasmotheriines sister to

rhinocerotines and aceratheriines representing a distinct group (e.g., Cerdeño, 1995; Geraads and Zouhri, 2021; Lu et al., 2023; Borrani et al., 2025).

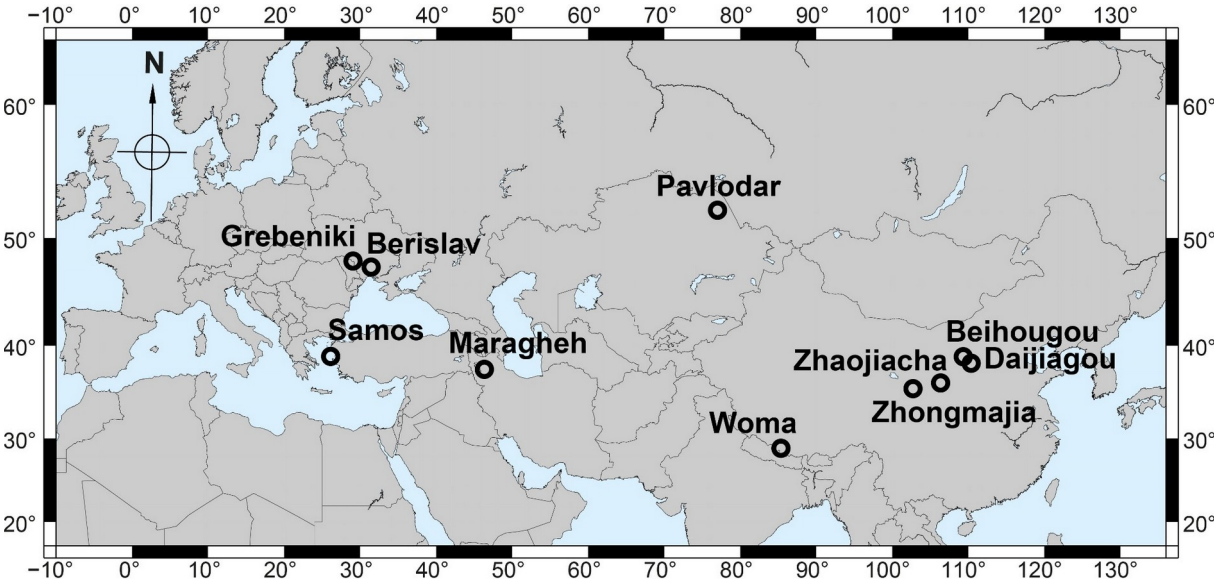


**Figure 1.** Geographical map with the type localities of chilotheres. Samos Island in Greece: *Chilotherium schlosseri* (Weber, 1905) and *Eochilotherium samium* (Weber, 1905); Grebeniki in Ukraine: *Chilotherium kowalevskii* (Pavlow, 1913); Berislav in Ukraine: *Chilotherium sarmaticum* Korotkevich, 1958; Maragheh in Iran: *Chilotherium persiae* (Pohlig, 1885); Pavlodar in Kazakhstan: *Chilotherium orlovi* Bayshashov, 1982; Woma (Deihagou) in Gyirong County, Xizang (Tibet) in China: *Chilotherium xizangense* Ji et al., 1980; Zhongmajia, Gansu Province in China: '*Chilotherium*' *primigenium* Deng, 2006; Zhaojiacha, Huachi County, Gansu Province in China: *Chilotherium licenti* Sun et al., 2018; Beihougou, Wulangou, Shaanxi Province in China: '*Chilotherium*' *wimani* Ringström, 1924; and Daijiagou, Baode, Shanxi Province in China: *Chilotherium anderssoni* Ringström, 1924. The map was generated using Generic Mapping Tools 6 (GMT6) (Wessel et al., 2019).

Rhinoceroses have a complex evolutionary history, especially when the superfamily Rhinocerotoidea is concerned, which includes several families of extinct rhinoceros relatives, beside the Rhinocerotidae. Depending on the authors this group includes the Amynodontidae, Eggysodontidae, Forstercooperiidae, Hyracodontidae, and the giant Paraceratheriidae (e.g., Heissig, 1989; Tissier et al., 2018; Bai et al., 2020; Lu et al., 2026). Some of the earliest certain representatives of the Rhinocerotoidea were found in the Arshanto Formation, Nei Mongol, China, though the exact relationships of these early taxa remain uncertain (Wang et al., 2016; Bai et al., 2020). The family Rhinocerotidae first appeared during the late Middle Eocene in North America and Asia with *Penetrigonias* Tanner and Martin, 1976 and *Teletaceras* Hanson, 1989, respectively (e.g., Antoine et al., 2003b). In Europe, the first

rhinoceroses appeared at the Eocene-Oligocene boundary during the Grande Coupure, arriving from Asia (Antoine and Becker, 2013; Böhme et al., 2013; Jame et al., 2019). From that time onwards rhinoceroses are constant faunal elements across Eurasia, North America and Africa, reaching their highest diversity during the Miocene (e.g., Heissig, 1989; Antoine et al., 2003b; Geraads, 2010; Hullot et al., 2024b, 2024a; Fraser et al., 2025).

During the Middle and Late Miocene, the rhinoceros' assemblages are especially diverse across Eurasia, including representatives that are closely related to the extant species, like *Ceratotherium neumayri* (Osborn, 1900), but also species belonging to the two extinct groups of aceratheriines and elasmotheriines. One of the best examples for such a sympatry is the classical Upper Miocene locality of Maragheh in Iran (Fig. 1), which includes four different rhinoceros' species: the dicerotine *Ceratotherium neumayri*, which is closely related to the extant African rhinoceroses, the large elasmotheriine *Iranotherium morgani* (Mecquenem, 1908a), which is a relative of *Elasmotherium sibiricum*, and the two hornless rhinoceroses *Chilotherium persiae* (Pohlig, 1885), which is the most common rhinoceros of the locality, and the much rarer *Persiatherium rodleri* Pandolfi, 2016. During the Late Miocene, rhinocerotines were already widespread and commonly found all over Eurasia, whereas elasmotheriines, persevered mainly in Asia, where they exhibit a high diversity. Aceratheriine diversity was declining in Europe, with the group vanishing from the continent at the very end of the Miocene. In Asia the aceratheriines remained very abundant and diverse throughout the Late Miocene, with their final extinction during the basal Pliocene (e.g., Deng et al., 2023; Antoine et al., 2025). During the Late Miocene, we also see the rise of the chilotheres, with *Chilotherium* being one of the most diverse and abundant rhinoceros genera (e.g., Tong, 2001; Antoine et al., 2025).

The presented Dissertation is structured as follows: First the goals of this work will be clarified (1.1.), then the research history of chilotheres and elasmotheriines will be presented in detail, concerning the taxonomy, ecology, and phylogeny of these rhinoceros' groups (1.2.–1.5.), and the relevant fossil sites for this Dissertation will be introduced (1.6.). Afterwards it will be explained what material was studied in the context of this Dissertation and what methods were used (2.). Following this, the results of the respective published works that are part of this Dissertation will be discussed (3.) and a comprehensive conclusion will be drawn with an outlook of the future

perspectives of this work (4.). After the references (5.), an appendix with the complete published works themselves is attached.

### 1.1. Aims and Objectives

Chilotheres are amongst the most common large mammals found in Upper Miocene deposits in Asia. Despite the large number of fossils of this rhinoceros' group, its' systematics remain obscured by the large number of taxa that have been attributed to the genus *Chilotherium*. These taxonomic issues have resulted in important collections of chilothere material remaining unstudied, which further added to the problems revolving around this rhinoceros group. Chilothere material of new localities is usually neglected altogether, hindering any kind of progress in understanding the group. Therefore, the overarching goal of this Dissertation is to provide a comprehensive revision of the taxonomic scheme of chilotheres, which is currently lacking and will facilitate more detailed studies on the taxonomy and systematics of this group.

The genus *Chilotherium* is possibly one of the most species-rich rhinoceros genera with more than 30 species having variably been attributed to the genus. Of these, a large number did, in fact, not represent chilotheres at all, and many others are now regarded synonyms of other chilothere species. Although several studies have discussed potential synonymities, there is no detailed account of these synonyms based on morphological features that would allow the differentiation of the valid species. This has led to the assumption that the genus is morphologically very conservative, which was even suggested in the original description of the genus. The different species often cannot be identified even based on complete skulls, primarily due to the lack of formal descriptions and depictions of the existing chilotheres. Another important factor is that most of the chilothere material is found either in eastern Asia or eastern Europe, with very little being known about potential occurrences between these two regions. Eastern Europe is an especially interesting region to study the systematics and evolution of chilotheres, because a large number of species were erected in a very restricted geographical area. Much has remained unknown about the validity and potential relationships of these species for a very long time, because the type material of four species (*Aceratherium schlosseri* Weber, 1905, *Aceratherium samium* Weber, 1905, *Aceratherium wegneri* Andree, 1921, and *Aceratherium angustifrons* Andree, 1921), all coming from the Upper Miocene locality of Samos, is considered lost. Adding to the difficulties, the whereabouts of the holotype of another species (*Teleoceras ponticus* Niezabitowski, 1912) were unknown for the longest time, and the type material of another species (*Aceratherium kowalevskii* Pavlow, 1913) was never defined.

Therefore, the first goal of this Dissertation is to provide a detailed account of the European fossil record of chilotheres. For this purpose, the only still existing part of the type material of *Aceratherium wegneri* Andree, 1921 (GMM 567) will be described and compared to establish it as a junior synonym of *Chilotherium schlosseri*. This specimen is the mandible (GMM 567) that was associated with the type skull of *Aceratherium wegneri* and was relocated in the collections of the GMM in 2019 (Markus Bertling pers. comm.). In addition to this specimen and the description of the research history of the chilotheres from Samos, also the information about the other European chilotheres will be revised. Based on new information *C. schlosseri* can be established as the senior synonym of *Aceratherium wegneri* and *Aceratherium angustifrons*. Further, it will be shown that *C. schlosseri* is a well-defined species, distinct from its' previously presumed junior synonym, *Chilotherium kowalevskii*. After reviewing the fossil record of chilotheres in Europe, the next goal is to establish the validity of the two historically oldest European species, *Aceratherium schlosseri* Weber, 1905 and *Aceratherium samium* Weber, 1905, by proposing specimens that will replace the lost type material. For this purpose, two complete skulls and their associated mandibles will be designated as the neotypes (GPIH 3015 and SMF M 3601) of the two species, respectively. The comparison of these specimens to the original descriptions and drawings of the type material and to each other confirms that they are well-separated species, which can be separated on a generic level. The next step of this Dissertation is to study historical material of different chilothere species from across Eurasia and propose diagnostic features for them. This will be achieved by describing and comparing postcranial elements, in addition to juvenile cranial and dental material of chilotheres, which are rarely mentioned in literature.

This comparative approach allows for the discovery of new diagnostic traits essential for species distinction, while providing the necessary framework to address broader ecological and phylogenetic questions in the future. The primary objective of this Dissertation is to combine these findings to clarify the taxonomic affinities of chilotheres, offering a comprehensive reappraisal of the group's diversity and systematics.

## 1.2. Taxonomic History

### 1.2.1. Chilotheres

The genus *Chilotherium* was erected by Ringström (1924) for a group of hornless rhinos that shared a set of characters, including most prominently a wide mandibular symphysis, with large lower incisors (i2s) that are separated by a wide diastema, depressed frontal region, widely separated parietal crests, and short limbs. Although Ringström (1924) did not provide a proper etymology for the genus name *Chilotherium*, it is formed from the Greek words “χείλος“ and “θηρίο“ and the literal translation of the genus name means “lip beast”, probably as a references to its wide mandibular symphysis, which could have resulted in the living animal looking like it has a large mouth.

As already mentioned, the genus was erected for a group of hornless rhinoceros species, most of which were already known, but had been included in the genera *Rhinoceros* Linnaeus, 1758, *Aceratherium* Kaup, 1832, or *Teleoceras* Hatcher, 1894 before (Ringström, 1924; Heissig, 1975; Deng, 2006; Kampouridis et al., 2022b; Svorligkou et al., 2025). The genus *Aceratherium* specifically acted as a wastebasket genus for most hornless rhinos in the 19$^{th}$ and beginning of the 20$^{th}$ century. Therefore, the research history of *Chilotherium* begins much earlier than the initial description of the genus itself (Ringström, 1924). The first ever described species that was later on included in the genus *Chilotherium* by Ringström (1924) is *Chilotherium persiae* (Fig. 2A). This species was originally erected as “*Rhinoceros persiae* Pohl.” without a formal morphological description. It remained rather enigmatic until Mecquenem (1908a, 1924) provided a relatively detailed description of the species from the type locality of Maragheh (Iran). In the meantime, several other chilothere species were described, like *Chilotherium habereri* (Schlosser, 1903), based on a series of mostly isolated teeth that were bought at pharmacies in China (Fig. 2E). The morphology of these teeth was initially considered to be very similar to that of *Teleoceras fossiger* (Cope, 1878) from North America (Schlosser, 1903), which was previously already suggested for *Chilotherium persiae* by Osborn (1900); thus starting a long-lasting debate about the potential relationship between *Chilotherium* and *Teleoceras* that to this day is not fully settled (e.g., Ringström, 1924; Bayshashov, 1982; Borrani et al., 2025). However, it is generally accepted that chilotheres are not closely related to teleoceratines and the shared similarities, such as the complicated tooth morphology, broad mandibular

symphysis, large tusk-like incisors, wide skull, and short limb bones are homoplasies (Heissig, 1973, 1989). Later, *Chilotherium schlosseri* (Weber, 1905) and *Eochilotherium samium* (Weber, 1905) were described based on well-preserved cranial and mandibular material from the Upper Miocene of Samos Island (Greece). It is mentioned that *C. schlosseri* seems to be quite similar to *C. persiae*, though no detailed comparison was possible due to the lack of any proper descriptions of the Maragheh fossils at that point (Weber, 1905). Afterwards, two chilotheres were described based on material from Ukraine: *Chilotherium ponticum* (Niezabitowski, 1912) from Odessa and *Chilotherium kowalevskii* (Pavlow, 1913) from Grebeniki (Ukraine). Both of these species were very quickly synonymised with *C. schlosseri* from Samos (Kiernik, 1913; Krokos, 1917). Both these species have been considered as junior synonyms of *C. schlosseri* by most authors (e.g., Krokos, 1917; Korotkevich, 1970; Bayshashov, 1993; Antoine and Sen, 2016; Kampouridis et al., 2022b; Țibuleac et al., 2023) and only few have considered *C. kowalevskii* as an distinct species over the last century (e.g., Heissig, 1975; Deng, 2006). The situation revolving around the taxonomic issues of *C. schlosseri* and its potential synonymity with other species got even more complicated after Andree (1921) erected two more chilotheres based on cranial material from Samos in Greece: *Chilotherium wegneri* (Andree, 1921) and *Chilotherium angustifrons* (Andree, 1921). These two species have variably been considered synonyms of either *C. schlosseri* or *C. kowalevskii*. Though recent studies have accepted them as junior synonyms of *C. schlosseri* (Giaourtsakis, 2022; Țibuleac et al., 2023).

Ringström (1924) offered a revision of all previously described chilotheres and erected several new taxa, along with the genus *Chilotherium* itself. The material he studied and based on which he described the new species came from Upper Miocene deposits of China, with the richest material coming from the Baode area (Ringström, 1924). He selected *Chilotherium anderssoni* Ringström, 1924 as the type species of the genus. This species is represented by about 40 skulls from its Upper Miocene type locality Daijiagou in the Shanxi Province, China. Based on this rich material Ringström (1924) provided detailed descriptions of the skull, mandible, and dentition of this species, even describing some postcranial aspects. Despite the detailed description that Ringström (1924) provided based on dozens of skulls, he decided to figure only four specimens of this species, including only a single adult skull (Fig. 2C). This heavily restricts our understanding of the species and its potential intraspecific variability,

which is shortly mentioned in the original description (Ringström, 1924). Nevertheless, the validity of this species has never been questioned since its initial description, although it has also not been revised since and it is rarely used in detailed comparisons.

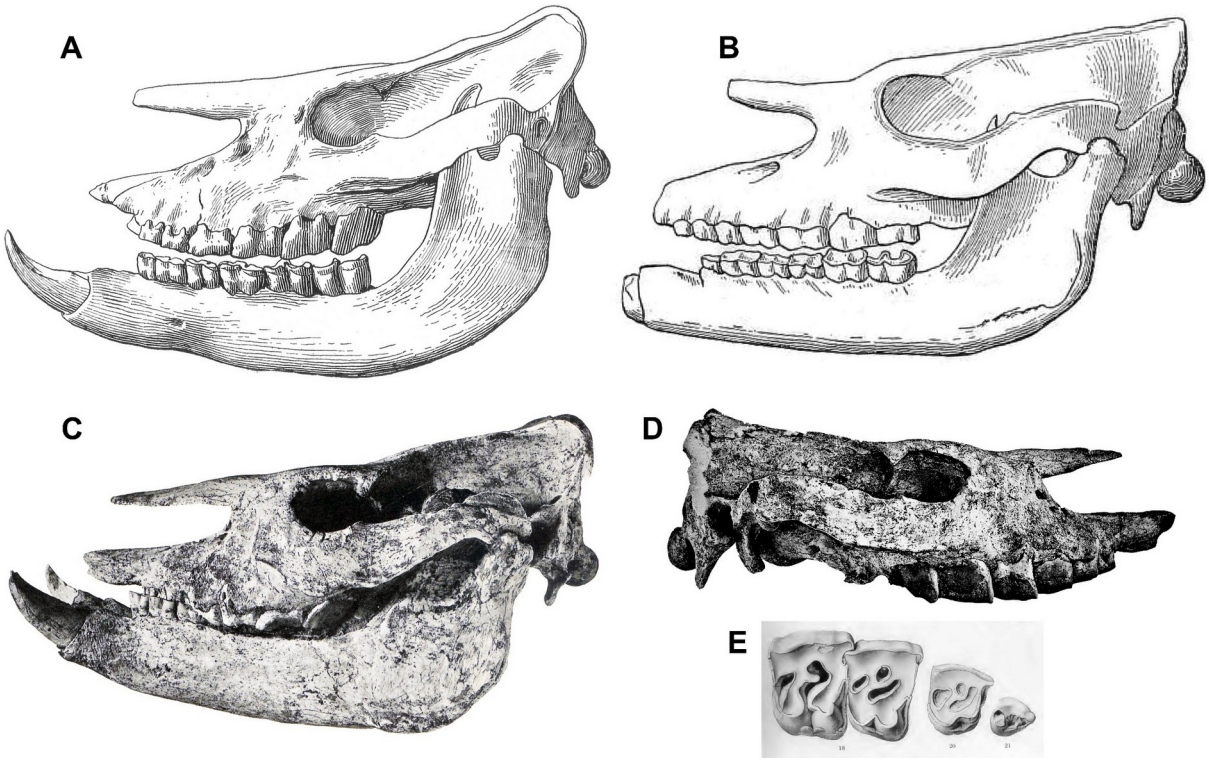


**Figure 2.** Skulls, mandibles, and teeth of chilotheres described at the beginning of the 20th century. A, Skull and mandible of *Chilotherium persiae* (Pohlig, 1885) from the Upper Miocene of Maragheh in Iran in left lateral view (taken from Mecquenem, 1908a, fig. 24); B, Skull and mandible of *Chilotherium schlosseri* (Weber, 1905) from the Upper Miocene of Samos Island in Greece in right lateral view, mirrored (taken from Mecquenem, 1908a, fig. 25); C, Skull and mandible of *Chilotherium anderssoni* Ringström, 1924 from the Upper Miocene of Daijiagou in China in left lateral view (Ringström, 1924, pl. 2, fig. 2); D, Skull of *Chilotherium habereri* (Schlosser, 1903) from the Upper Miocene of Yuejiali in China in right lateral view (taken from Ringström, 1924, pl. 4, fig. 2); and E, Upper teeth of *Chilotherium habereri* (Schlosser, 1903) from the Upper Miocene of China (taken from Schlosser, 1903, pl. 5, figs 18, 20-21).

Since then, several new species were described, most of which fit the general morphology of *Chilotherium*, such as *Chilotherium sarmaticum* Korotkevich, 1958, *Chilotherium xizangense* Ji et al., 1980, *Chilotherium orlovi* Bayshashov, 1982, *Chilotherium licenti* Sun et al., 2018. These species come mainly from Asia and only one species, *C. sarmaticum*, comes from the lower Upper Miocene of Berislav in Ukraine. A rather puzzling, hornless rhinoceros was described from the Vallesian locality Pentalophos 1 (Greece), based on a rich collection of cranial and mandibular

material, and was named *Aceratherium kiliasi* Geraads and Koufos, 1990. This may represent the most heavily discussed chilothere, as its' taxonomic affinities were the subject of intense debate following its initial description. It was quickly suggested that the material from Pentalophos 1 that was assigned to this species, in fact represented two distinct hornless rhinoceroses (e.g., Heissig, 1999; Fortelius et al., 2003; Giaourtsakis, 2003, 2022; Athanassiou et al., 2014): a small chilothere, which includes the holotype skull of *Aceratherium kiliasi* (PNT-135) and today is considered to represent *E. samium*, and the somewhat smaller non-chilothere *Acerorhinus* sp. (Athanassiou et al., 2014). Another interesting chilothere, '*Chilotherium*' *primigenium* Deng, 2006, was described relatively recently based on a complete skull and mandible of a senile individual from the earliest Upper Miocene of Zhongmajia in the Gansu Province, China (Deng, 2006). The holotype exhibits one of the most typical chilothere characters, which is the very wide mandibular symphysis with tusk-like incisors. Additionally, the species lacks upper incisors, has a rather small P2 and complicated enamel folds, though the teeth are heavily worn due to the ontogenetic age of the individual. However, the skull also exhibits several features untypical for the genus *Chilotherium*, such as the convex frontal region, which is concavely depressed in *Chilotherium*, the parietal crests that form a sagittal keel, whereas in *Chilotherium* they are widely separated, and the thick and long nasal bones, which are thinner and usually shorter in *Chilotherium*. Due to this peculiar combination of primitive and derived features it was suggested that '*C.*' *primigenium* represents the most primitive *Chilotherium* species (Deng, 2006). However, it is also possible that this species represents a different, though closely related genus and a reevaluation of the holotype is needed to address this question.

Overall, the work of Deng (2006) also provided an overview on the complicated taxonomic affinities of chilotheres, which was the first update since the work of Heissig (1975). However, both these studies only provided synonym lists that updated the status of the chilothere species (Heissig, 1975, tab. 6; Deng, 2006, tab. 4), without any detailed discussions about the diagnostic features of these species. As already mentioned before, Ringström (1924) had already provided an overview of the species that he included into *Chilotherium*. However, even this detailed study left many open questions about the exact features that distinguish each species, their taxonomy, what their intrageneric relationships are, and how *Chilotherium* fits into the rhinocerotid family tree. Later, Kretzoi (1942) discussed the evolutionary history of rhinoceroses

that lived during the Neogene and Quaternary and erected two genera that have been regarded as closely allied with *Chilotherium*: *Acerorhinus* Kretzoi, 1942 and *Shansirhinus* Kretzoi, 1942. The first one was erected to include *Acerorhinus zernowi* (Borissiak, 1914) from Sebastopol (Ukraine) and *Acerorhinus palaeosinensis* (Ringström, 1924) from China. Later also other species were assigned to this genus like *Acerorhinus neleus* Athanassiou et al., 2014 from the Upper Miocene of Kerassia in Greece (Athanassiou et al., 2014). The second genus, *Shansirhinus*, was coined for two peculiar species of hornless rhinoceroses that are characterised by very complicated enamel plications in the upper teeth. These two species are *Shansirhinus brancoi* (Schlosser, 1903), which is based on isolated teeth that were bought in pharmacies in China (Schlosser, 1903), and *Shansirhinus ringstromi* Kretzoi, 1942, which is based on a right maxilla, with all cheek teeth, that was initially referred to as *Rhinoceros* aff. *brancoi* (Ringström, 1927). The exact relationship of these two genera to *Chilotherium* is not clear, though *Shansirhinus* is usually recovered as a sister taxon to *Chilotherium* in most recent phylogenetic analyses (e.g., Pandolfi, 2016; Sun et al., 2018; Lu et al., 2023; Borrani et al., 2025).

Later, Heissig (1975) divided *Chilotherium* into different subgenera, in an attempt to revise it and to clarify the relationships of the species. He considered *Acerorhinus* as a subgenus of *Chilotherium* and coined a new subgenus, *Chilotherium* (*Subchilotherium*) Heissig, 1975, for the species *Subchilotherium intermedium* (Lydekker, 1884) from the Siwaliks (Heissig, 1975). He further regarded *Shansirhinus brancoi* as part of the subspecies "*Chilotherium* (*Chilotherium*)"; a scheme that he also used in some later studies (e.g., Heissig, 1973, 1989). However, today *Shansirhinus* is recognised as a closely related but distinct genus from *Chilotherium* (e.g., Deng, 2005a, 2006; Lu et al., 2015). The taxonomic arrangement concerning the separation of the genus into subgenera was not followed by later studies, as exemplified by Heissig (1989), who used *Chilotherium*, *Acerorhinus*, and *Subchilotherium* at the genus rank. Nevertheless, a few studies adopted this taxonomic scheme, like Tsiskarishvili (1987), who even erected a new species, *Chilotherium* (*Subchilotherium*) *eldaricum* Tsiskarishvili, 1987, based on an almost complete mandible. This specimen exhibits a narrow mandibular symphysis and can therefore definitely be excluded from the genus *Chilotherium* (Tsiskarishvili, 1987). It is likely that it should actually be assigned to the genus *Acerorhinus*, as also suggested before (e.g., Giaourtsakis, 2022). However, the holotype is an isolated mandible, which is usually not very diagnostic in aceratheriines,

and it is difficult to distinguish it from other aceratheriine species and it might be regard it as a nomen dubium. Geraads and Spassov (2009) also separated *Chilotherium* into subgenera but followed an alternative arrangement compared to that of Heissig (1975). They included most chilotheres in the subgenus *Chilotherium* (*Chilotherium*), and they coined a new subgenus, *Chilotherium* (*Eochilotherium*), for *E. samium* and the Pentalophos 1 chilothere, which they regarded as a distinct species (Geraads and Spassov, 2009). This subgenus was later elevated to the genus level to separate the Samian species *E. samium* from *Chilotherium* sensu stricto (Kampouridis et al., 2023).

Concerning *Subchilotherium intermedium* from the Siwaliks, its' relationship and potential inclusion into the genus *Chilotherium* has often been debated (e.g., Heissig, 1972, 1975; Deng, 2006, 2006; Khan et al., 2008, 2011). Recently, an inclusion of the species into the genus *Chilotherium* was re-attempted (Khan et al., 2011), despite the species lacking most of the autapomorphic features of the genus. For instance, the protocone constriction in the upper teeth of *Subchilotherium intermedium* is relatively weak, compared to the strong constriction in chilotheres, the hypocone is either not constricted at all or only very weakly constricted, the antecrochet is only present in the molars and only moderately developed, and the paracone fold is stronger than in *Chilotherium* spp. (Colbert, 1935, fig. 91; Khan et al., 2011, fig. 3A). Therefore, herein it is preferred to remove the species from *Chilotherium* and referred to it as *Subchilotherium intermedium*, outside Chilotheriina overall as also supported by several phylogenetic analyses that did not recover it within or close to *Chilotherium* (e.g., Pandolfi, 2016; Sun et al., 2018; Lu et al., 2023).

Over the last century, several other species were associated with the genus *Chilotherium*, either being assigned to the genus at some point, or being erected within the genus to begin with. This way dozens of different species have found themselves under the genus name *Chilotherium*. Notable misidentifications are *Chilotherium quintanelensis* Zbyszewsky, 1952 and *Chilotherium ibericum* Antunes, 1972 from Portugal, both of which in fact represent the elasmotheriine *Hispanotherium matritense* (Lartet in Prado, 1864) (Deng, 2006). Due to their complicated enamel folds, upper teeth of *Chilotherium* can sometimes be confused with those of small elasmotheriines. For instance, a single tooth from the Upper Miocene of Skoura in Morocco was originally identified as aff. *Chilotherium* sp. (Zouhri et al., 2012), but was later correctly attributed to an elasmotheriine (Geraads et al., 2019; Geraads and Zouhri, 2021). Another peculiar case of a potential identification of a chilothere in Africa, were three

upper teeth that were identified as *Chilotherium* sp., which was actually the first time it was suggested that *Chilotherium* might have been present in Africa (Hooijer, 1966). Later, these specimens, were included in *Chilotheridium pattersoni* Hooijer, 1971, a rhinoceros species that was based on a fragmented and deformed skull from the Upper Miocene of Loperot in Kenya (Hooijer, 1971). This species has been suggested to be a close relative of *Chilotherium*; however, the two taxa exhibit immense differences in the cranial anatomy (Geraads, 2010). In *Chilotheridium pattersoni* the frontal region is not at all depressed, the parietal crests are closely situated, and there are prominent horn bosses on the nasal bones, unlike any *Chilotherium* species (Hooijer, 1971). Additionally, the limb bones of *Chilotheridium pattersoni* are elongated, in contrast to the shortened appendicular skeleton of *Chilotherium* (compare Ringström, 1924; Hooijer, 1971). The affinities of this species remain doubtful, but an attribution to the elasmotheriines seems plausible, as was also suggested by Geraads and Zouhri (2021). Numerous other species were also at some point assigned to *Chilotherium*, significantly complicating its research history. To this day it is highly debated which species should or should not be included in the genus *Chilotherium*, how exactly the Chilotheriina should be defined and how the chilotheres fit into the family tree of rhinoceroses, with most recent phylogenetic analyses yielding contradicting results (e.g., Lu et al., 2023; Borrani et al., 2025; Fraser et al., 2025).

### 1.2.2. Elasmotheriines

The species *Parelasmotherium* schansiense Killgus, 1923 was erected by Killgus (1923) based on associated dental material from the Upper Miocene locality of Kutschwan (China). It is the fifth elasmotheriine rhinocerotid taxon that was ever named. The first elasmotheriine ever described is the Late Pleistocene *Elasmotherium sibiricum*, the second one is the Middle Miocene *Hispanotherium matritense*, and the third one is the Late Miocene *Iranotherium morgani* (Fig. 3A). Later, Ringström (1923) erected another elasmotheriine, *Sinotherium lagrelii* Ringström, 1923, based on an isolated M3 from the Upper Miocene of Daijiagou in Shanxi Province (China). Shortly after, Killgus (1923) published an extended abstract based on his Doctoral Dissertation (Killgus, 1922), in which he studied the Late Miocene fauna of Kutschwan in the Shanxi Province, China. He described three new large mammal species, including *Parelasmotherium schansiense*. One year later, Ringström (1924) published his

findings on the rhino material from the Sino-Swedish expedition (e.g., Andersson, 1923; Mateer and Lucas, 1985; Ebbestad, 2021). In this work, he presented additional material of *Sinotherium lagrelii*, including a subadult skull fragment (Fig. 3B) and made a detailed comparison to the known elasmotheriine rhinos. In this context he coined the genus *Iranotherium* for the Maragheh elasmotheriine (*Iranotherium morgani*) and discussed the shortly before described *Parelasmotherium schansiense*.

*Parelasmotherium schansiense* is only known based on the type material that is housed at the GPIT (Fig. 3C). It is represented by four teeth, a heavily worn D4, a little worn M1, an unworn M2, and an unerupted P4 still embedded in the maxilla, and some postcranial elements, a radius, an ulna, an astragalus, and an cuboid, which was not originally identified as belonging to *Parelasmotherium* (Killgus, 1922, 1923), but is in fact associated with the astragalus from Kutschwan. The radius and ulna cannot be relocated in the collections of the GPIT, but casts of these are housed at the AMNH (AMNH FM 32503).

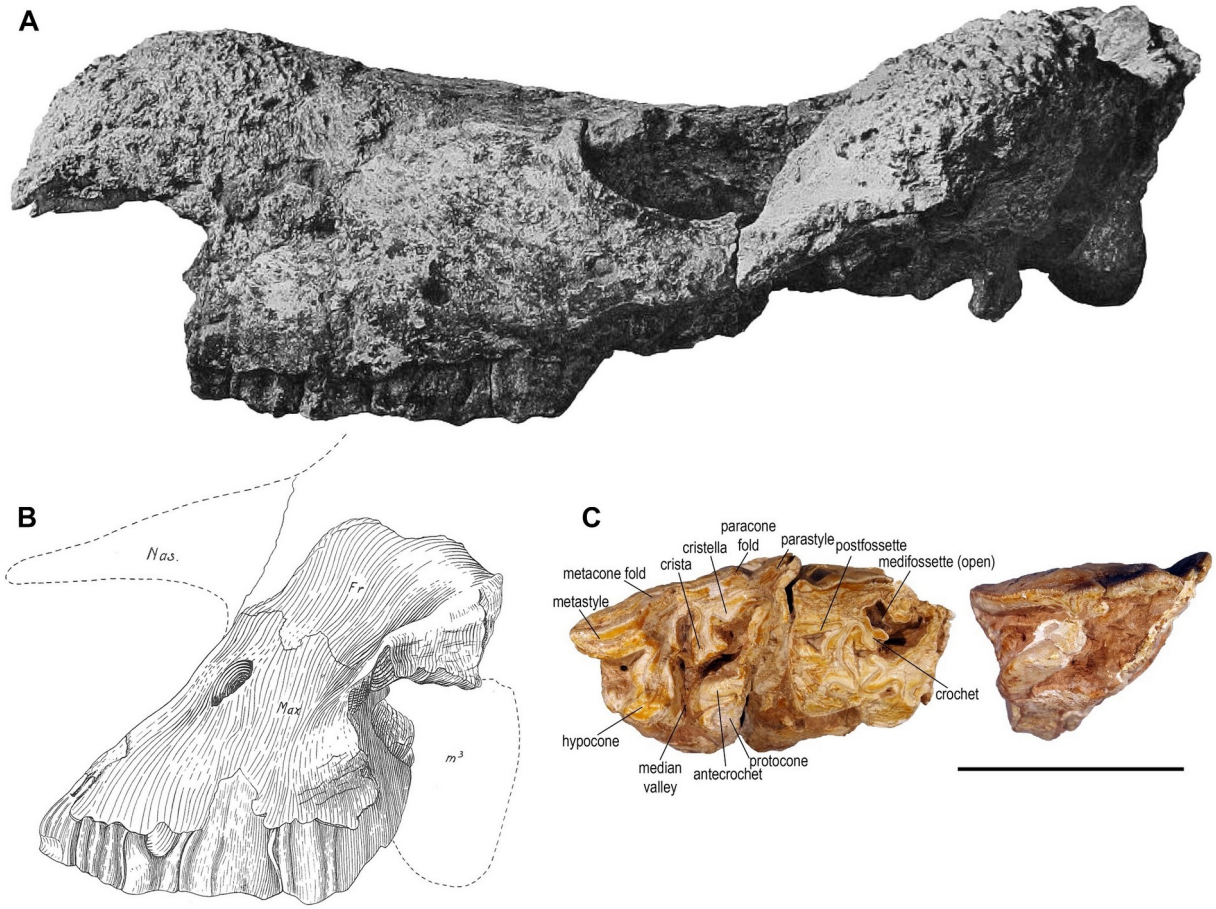


**Figure 3.** Skulls and teeth of Late Miocene elasmotheriines. A, Holotype skull of *Iranotherium morgani* (Mecquenem, 1908a) from the Upper Miocene of Maragheh in Iran (taken from Mecquenem, 1908a, pl. 8, fig. 1); B, Skull of *Sinotherium lagrelii* Ringström, 1923 from the Upper Miocene of Daijiagou in China (taken from Ringström, 1924, textfig. 76); and C, Holotype

teeth of *Parelasmotherium schansiense* Killgus, 1923 from the Upper Miocene of Kutschwan in China (modified after Kampouridis et al., 2022a, fig. 1). Scale bar equals 7.5 cm for C, and A–B are not to scale.

Due to the fragmentary nature of the type material the relationship of this species to other elasmotheriines has been difficult to resolve. Ringström (1924) considered *Parelasmotherium* a synonym of *Sinotherium* and discussed the possibility of *Parelasmotherium schansiense* representing a junior synonym of *Sinotherium lagrelii* altogether. Chow (1958) described three new elasmotheriine species from the Upper Miocene of China and considered *Parelasmotherium schansiense* a junior synonym of *Sinotherium lagrelii*. Qiu and Xie (1998) discussed the differences between *Sinotherium* and *Parelasmotherium* and concluded that they should be regarded as distinct genera, with *Parelasmotherium simplum* (Chow, 1958) belonging to the latter. While the synonymity of *Sinotherium lagrelii* and *Parelasmotherium schansiense* (Ringström, 1924) has not been suggested again, *Parelasmotherium schansiense* has had questionable affinities with several other Late Miocene elasmotheriines. As mentioned above, *Parelasmotherium simplum* was assigned to the same genus; however, this species is based on an isolated M3 (Chow, 1958), and two additional upper teeth were later added to the species (Qiu and Xie, 1998). Therefore, only the moderately worn M1s could be compared between the two species.

Later, *Ninxiatherium longirhinus* Chen, 1977 was erected based on a well-preserved skull from the Upper Miocene of Ningxia in China (Chen, 1977). This species was later suggested as a junior synonym of *Parelasmotherium schansiense* (Antoine, 2002, 2003), which lead to the scoring of *P. schansiense* based on the type skull of *Ninxiatherium longirhinus*, complicating the systematics of both species. Deng (2007) separated the two species, on the basis of a well-preserved skull that he assigned to *Parelasmotherium linxiaense* Deng, 2001a, a species that was previously known only from fragmentary dental remains (Deng, 2001a). Therefore, *Parelasmotherium* was suggested to include three species, the relationship of which was not clear (Deng, 2008). Elasmotheriine taxonomy and phylogeny is generally speaking fairly well resolved (e.g., Antoine, 2002; Deng, 2008; Geraads and Zouhri, 2021; Sun et al., 2023), with few cases as historically problematic as the affinities of *Parelasmotherium*.

### 1.3. Systematic Palaeontology of Chilotheriina

Due to the high taxonomic complexity of chilotheres a detailed overview of their systematics is provided below that includes herein considered valid chilothere taxa. This comprises in total 10 species of *Chilotherium*, counting also '*C.*' *wimani* and '*C.*' *primigenium*, which should actually be excluded from the genus, pending their revision (see below for details). Additionally, the two *Shansirhinus* species and the single *Eochilotherium* species are listed below as belong to Chilotheriina.

Class Mammalia Linnaeus, 1758

Order Perissodactyla Owen, 1848

Family Rhinocerotidae Gray, 1821

Subfamily Aceratheriinae Dollo, 1885 (sensu Lu et al., 2023)

Tribe Aceratheriini Dollo, 1885 (sensu Lu et al., 2023)

Subtribe Chilotheriina Qiu et al., 1987 (sensu Kampouridis et al., 2023)

Included genera

*Chilotherium* Ringström, 1924, *Shansirhinus* Kretzoi, 1942, and *Eochilotherium* Geraads and Spassov, 2009.

Diagnosis

Aceratheriine rhinocerotids that feature the following autapomorphic traits: separated parietal crests; upper molars featuring a marked protocone constriction and a moderate to strong antecrochet that tends to project lingually; a mandible that is characterised by a very wide mandibular symphysis with a flat to concave ventral surface; large, sexually dimorphic i2s that exhibit a trend to become more flattened and tusk-like, especially in males, and are separated from each other by a wide diastema and from the p2 by a long diastema with a marked crest. The group also exhibits an upper first deciduous premolar retained into adulthood, whereas the first lower deciduous premolar, when present, is shed and not replaced by a permanent one. Additionally, the group lacks any upper incisor and the upper cheek teeth have generally pronounced secondary enamel folds (i.e., crista, crochet, and antecrochet),

and the appendicular skeleton is notably shortened and relatively robust, especially the metapodials (after Kampouridis et al., 2023).

Remarks

The group Chilotheriini was originally established by Qiu et al. (1987) as a tribe, to encompass the genera *Acerorhinus* and *Chilotherium* and specifically excluding the genus *Aceratherium*. However, the relationship between these two genera is not clear, as shown in the contradicting results of some recent phylogenetic analyses (Pandolfi, 2016; Lu et al., 2023). Therefore, it has not been possible to prove that these two genera comprise a monophyletic clade. In fact, *Acerorhinus* shows many characters separating it from representatives of *Chilotherium*. *Aceratherium* shows characters that are more similar to *Chilotherium*, like the shortened limb bones (Hünermann, 1989), whereas in *Acerorhinus zernowi* from the Middle Miocene of Tung Gur the plesiomorphic state of more elongated limb bone is seen (Cerdeño, 1996). Another enigmatic hornless rhino, *Shansirhinus*, is much more similar to *Chilotherium* in many regards, such as the wide mandibular symphysis, the more complicated enamel folds, and the higher tooth crowns (Deng, 2005a). A closer relationship between these two genera has also been suggested in recent phylogenetic analyses (Pandolfi, 2016; Lu et al., 2023). It would therefore be best to remove *Acerorhinus* from this group and to restrict it to the genera *Chilotherium*, *Shansirhinus*, and *Eochilotherium*, with the latter one having been regarded a member of *Chilotherium* sensu stricto up until recently (Giaourtsakis, 2022; Kampouridis et al., 2022b, 2023).

The type genus of Chilotheriini was not designated by Qiu et al. (1987), who coined the group; however, based on ICZN Arts. 29.1 and 64, a suprageneric name must derive from its type genus, which would naturally make *Chilotherium* the type genus. Following, the recommendation of Kampouridis et al. (2023), the clade is herein used at a subtribe rank (as Chilotheriina) with *Chilotherium* as the type genus and also including the genera *Shansirhinus* and *Eochilotherium*.

Genus *Chilotherium* Ringström, 1924

Type species

*Chilotherium anderssoni* Ringström, 1924

Included species

*Chilotherium persiae* (Pohlig, 1885), *Chilotherium habereri* (Schlosser, 1903), *Chilotherium schlosseri* (Weber, 1905), *Chilotherium kowalevskii* (Pavlow, 1913), '*Chilotherium*' *wimani* Ringström, 1924, *Chilotherium sarmaticum* Korotkevich, 1958, *Chilotherium xizangense* Ji et al., 1980, *Chilotherium orlovi* Bayshashov, 1982, '*Chilotherium*' *primigenium* Deng, 2006, *Chilotherium licenti* Sun et al., 2018.

Diagnosis

Aceratheriine rhinocerotids that feature the following autapomorphic characters: flat and wide skull, flattened and depressed frontal region; well-developed postorbital processes; moderately to widely separated parietal crests; highly placed orbits; very wide mandibular symphysis that features a concave ventral side; very large, flattened, tusk-like second lower incisors, with a scalene triangle cross section and upturned, dorsomedially oriented wear facets; reduced premaxillary bones that lack upper incisors; and very strong secondary enamel folds, including a lingually flattened and strongly constricted protocone, almost pyramidal in occlusal view, in the molars. It is also characterised by a relatively short length of the premolars compared with the molars, mainly due to the reduced size of the P2 and p2; and notably shortened metapodials and relative robust appendicular skeleton (modified after Ringström, 1924; Geraads and Spassov, 2009; Giaourtsakis, 2022; Kampouridis et al., 2023).

Remarks

Recently, it was shown that '*C.*' *wimani* and '*C.*' *primigenium* lack some of the autapomorphic features of *Chilotherium* (Kampouridis et al., 2023). In fact, these two species seem to share some morphological features with *Eochilotherium samium* and while it is not possible to include these species into the genus *Eochilotherium* at the moment, it seems most likely that they do not belong to the genus *Chilotherium* and may even represent independent genera. However, until the issue about their generic attribution is resolved it is preferable to retain them in their original genus as '*C.*' *wimani* and '*C.*' *primigenium*.

*Chilotherium persiae* (Pohlig, 1885)

Type material

Pohlig (1885) originally erected this species based on a collection of four adult and one juvenile skull from Maragheh, but he did not mention where exactly these specimens are housed (Pohlig, 1884a, 1884b, 1885, 1886), therefore the type material was never formally defined. He mentioned that the material he collected himself in Maragheh, Iran was sent to Halle, Germany (Pohlig, 1886) and is now housed in the palaeontological collection of the MLU (Fig. 4B–C). However, Pohlig (1885, 1886) did not specify whether he collected the specimens he referred to "*Rhinoceros persiae*" himself or if he saw them in some other collection. In the collections of the MLU some fragmentary cranial elements of *C. persiae* were able to be relocated. However, Pohlig (1885) mentioned explicitly the fact that the collection of fossils in the area was continued by Theodor Strauss, as explained also by Rodler (1885), who joined the excavation in Maragheh, collecting for the NHMW. The fact that Pohlig was aware of these excavations and also specifically mentioned the material housed at the NHMW – Pohlig (1885) referred to the Maragheh material that Gaudry (1885) saw in Vienna – along with the fact that several skulls were deposited in the collection of the NHMW until 1885, make it likely that Pohlig had seen or was at least aware of this material. Until further information becomes available, however, the type material cannot be determined with certainty.

Type locality

Upper Miocene deposits of Maragheh (Iran); exact locality unknown

Diagnosis

Medium-sized *Chilotherium* species with a weakly to moderately depressed frontal region, straight and relatively thick nasal bones, parietal crests that are moderately separated from each other (minimal distance between parietal crests up to 54 mm, n=11) and a unique combination of dental characters: M3 with a somewhat quadrangular outline; long crochet; small crista sometimes present in the premolars that may close off the medifossette; very strong mesial and distal constriction of the protocone, which is lingually flattened, resulting in a very long antecrochet that may close off the median valley; a strong mesial constriction of the hypocone; crista rarely present in molars but when present may close off the medifossette; and a weak,

discontinuous lingual cingulum mainly present at the entrance of the median valley in the premolars (after Kampouridis et al., 2025).

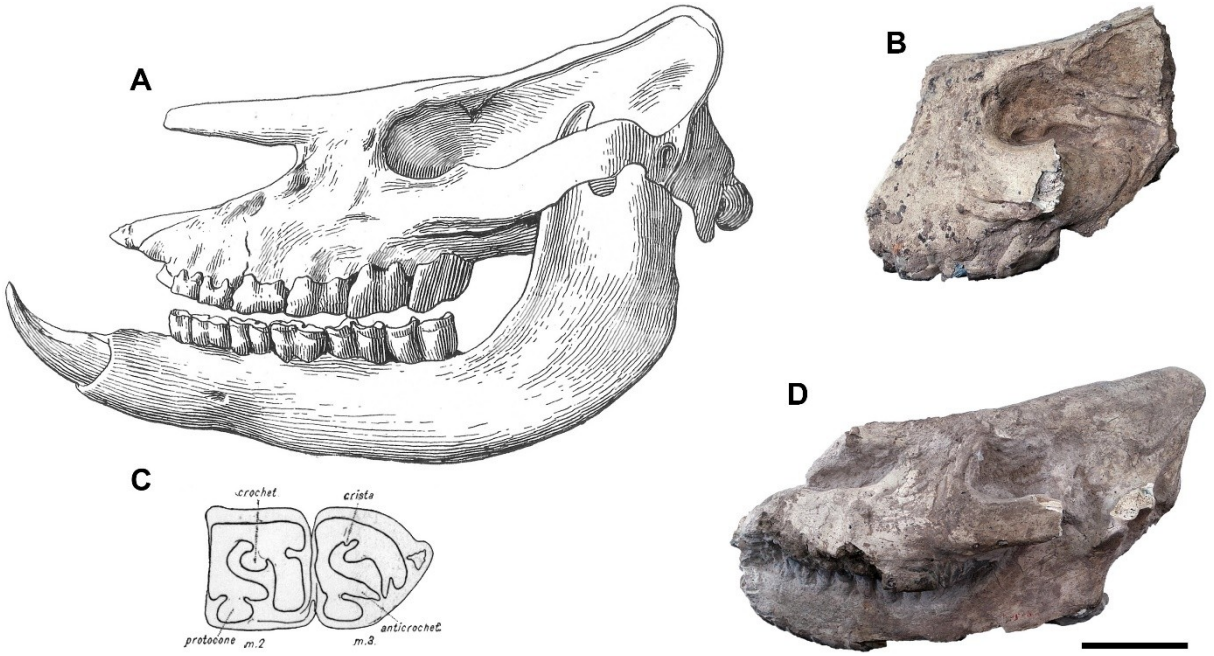


**Figure 4.** Skulls of *Chilotherium persiae* (Pohlig, 1885) from the Upper Miocene of Maragheh (Iran). A, Skull and mandible housed at the MNHN (taken from Mecquenem, 1908a, fig. 24); B, partial adult skull (MLU.GeoS.-Unnumbered); C, sketch of second and third upper molars (taken from Osborn, 1900, fig. 12a); D, almost complete juvenile skull with associated mandible (MLU.GeoS.8030). Scale bar equals 10 cm for B and D; A and C are not to scale.

*Chilotherium habereri* (Schlosser, 1903)

Lectotype

Schlosser (1903) assigned several teeth (Fig. 5B) to the new species he erected, without assigning any specific holotype. Therefore, all studied teeth (Schlosser, 1903, pl. 5, figs. 5-10, 12-21, pl. 7, figs. 1-3, 6, 8, 10-11) constitute the type material of *Chilotherium habereri*. The articulated P3 and P4 (SNSB-BSPG 1900 XII 622, Fig. 5A), illustrated by Schlosser (1903, pl. 5, fig. 18), were designated as the lectotype of the species under the provisions of ICZN Art. 74 by Kampouridis et al. (2025). These were also used as the basis for the identification of the species by Ringström (1924), who revised its morphological affinities.

Type locality

Upper Miocene red clay deposits of Shanxi (China); exact locality unknown

Diagnosis

Medium- to large-sized *Chilotherium* species with a moderately depressed frontal region, straight nasal bones, parietal bones that are moderately separated and a unique combination of dental characters: long crochet; usually closed off, round medifossette; crista absent in molars; very strong mesial and distal constriction of the protocone, which is lingually flattened, resulting in a long antecrochet that may close off the median valley at a very advanced wear stage; a strong mesial constriction of the hypocone of the molars; medifossette commonly closed in premolars; and a discontinuous lingual cingulum is mainly present in the premolars (after Kampouridis et al., 2025).

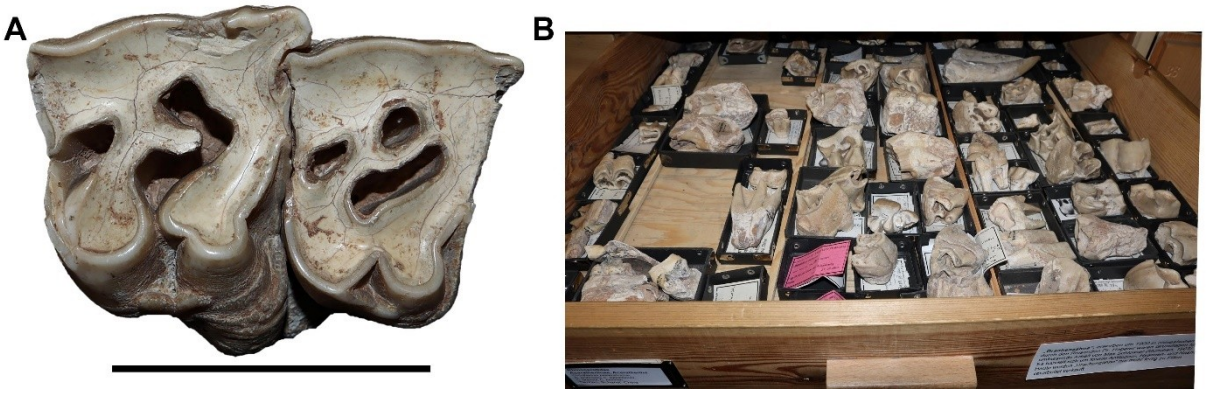


**Figure 5.** A, Lectotype of *Chilotherium habereri* (Schlosser, 1903) from the Upper Miocene of China; associated right P4 and P3, originally illustrated by Schlosser (1903, pl. 5, fig. 18). B, Drawer with the original chilothere material from China studied by Schlosser (1903) at the SNSB-BSPG. Scale bar equals 5 cm for A, and B is not to scale.

*Chilotherium schlosseri* (Weber, 1905)

Neotype

A well-preserved skull (GPIH 3015, Fig. 6A–D) with an associated mandible (GPIH 3015a, Fig. 6E), designated by Kampouridis et al. (2023).

Type locality

Upper Miocene deposits of Samos Island (Greece); exact locality unknown.

Junior synonyms

*Teleoceras ponticus* Niezabitowski, 1912, *Aceratherium wegneri* Andree, 1921, and *Aceratherium angustifrons* Andree, 1921 (see Fig. 7).

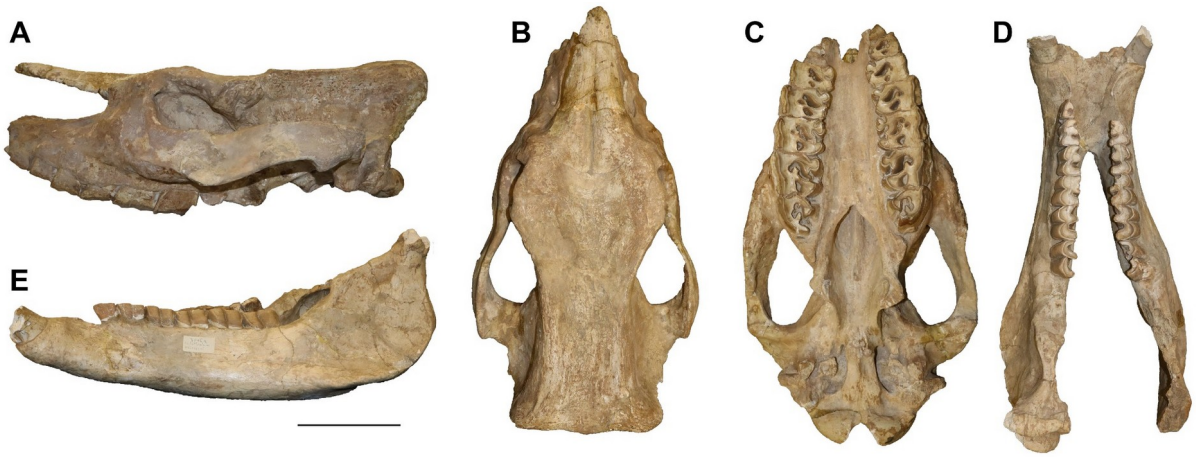


**Figure 6.** Neotype of *Chilotherium schlosseri* (Weber, 1905) from the Upper Miocene of Samos Island (Greece). Skull (A–C: GPIH 3015) and its' associated mandible (D–E: GPIH 3015a) in lateral (A, E), dorsal (B, D) and ventral (C) views. Scale bar equals 10 cm.

Diagnosis

A large *Chilotherium* species characterised by widely separated parietal crests (minimal distance between parietal crests always over 70 mm in adult individuals), notably depressed frontal and nasal bones, nasal bones that bear a central longitudinal groove on the dorsal side, and a unique combination of dental characters: very long crochet; very strong mesial and distal constriction of the protocone, which is lingually flattened, resulting in a very long antecrochet that usually closes off the median valley at an early wear stage in all teeth; a prominent mesial constriction of the hypocone; crista frequently present that closes the medifossette; and a discontinuous lingual cingulum that is occasionally moderately developed in the premolars; often a closed prefossette is present in the P2; in addition to sporadically present enamel plications in the upper teeth; very short trigonid in p2, with a highly reduced paralophid and a weak protoconid; and discontinuous lingual and buccal cingulids in the lower teeth (modified after Kampouridis et al., 2023).

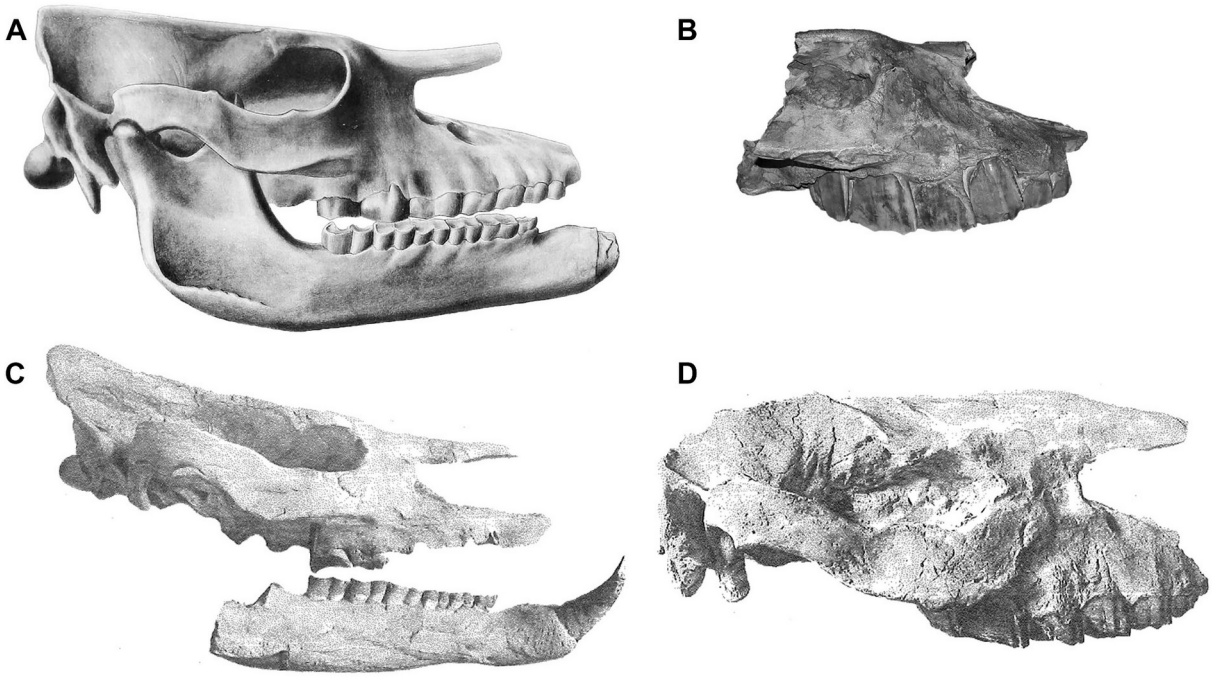


**Figure 7.** A, Original illustration of the now lost lectotype of *Chilotherium schlosseri* (Weber, 1905) from the Upper Miocene of Samos Island in Greece (Weber, 1905, pl. 8, fig. 1); and type material of the junior synonyms of *C. schlosseri*: B, holotype of *Teleoceras ponticus* Niezabitowski, 1912 from Upper Miocene of Odessa in Ukraine; C, original illustration of the, now lost, holotype of Aceratherium wegneri (Andree, 1921); and D, original illustration of the, now lost, lectotype of *Aceratherium angustifrons* (Andree, 1921). Both from the Upper Miocene of Samos Island of Greece (taken from Andree, 1921). Not to scale.

*Chilotherium kowalevskii* (Pavlow, 1913)

Type Material

The species was erected based on a large collection of cranial and postcranial elements (Fig. 8), without designating a specific holotype or syntype (Pavlow, 1913). Thereby, all referred material by Pavlow (1913) represents the syntype of *Chilotherium kowalevskii* (see Pavlow, 1913, pl. 4-5).

Type locality

Upper Miocene deposits of Grebeniki (Ukraine).

Diagnosis

Dorsal skull profile gently concave, zygomatic arch very robust, paroccipital process rather short; upper premolars large, with strong crochet, and long antecrochet

connecting the metaloph, thus closing the median valley almost up to the top of the crown; i1 shed late in life; limb bones stocky (after Geraads and Spassov, 2009).

Remarks

The species was erected by Marie Vasilievna Pavlova in an article that was part of an a volume published between the years 1907 and 1915 in memory of the renowned geologist Albert Gaudry, well known for its contributions to mammalian palaeontology (Pavlow, 1913). The authority of this species is often cited with the year 1914, which is probably due to the fact that there are two parts to this work, which were published separately, but as part of the same volume in honor of A. Gaudry. The first part, in which *C. kowalevskii* was erected was published in 1913, whereas the second part was published in 1914 (Pavlow, 1913, 1914). Therefore, the correct name for the species should be *Chilotherium kowalevskii* (Pavlow, 1913). However, there has not been any re-evaluation of these specimens since Krokos (1917).


**Figure 8.** Type material of *Chilotherium kowalevskii* (Pavlow, 1913) from the Upper Miocene of Grebeniki in Ukraine (from Pavlow, 1913, pl. 4). Not to scale.

*Chilotherium anderssoni* Ringström, 1924

Type Material

The species was erected based on a number of cranial and postcranial elements that were housed in the collections of the PMU, without designating a specific holotype or

syntype (Ringström, 1924). Thereby, all material referred by Ringström (1924) to *Chilotherium anderssoni* represents the syntype. This material is mainly housed in the collections of the PMU, however, part of it has been given to other collections such as the SMF.

Type locality

Upper Miocene deposits of Daijiagou in Shanxi (China), also referred to as “Lok. 30” in the Lagrelius Collection.

Remarks

This species was erected by Ringström (1924) and used as the basis for defining the genus *Chilotherium*. While different species have been assigned to the genus over time, the validity of *C. anderssoni* has never been questioned and it represents the type species of the genus. Therefore, any change to the diagnosis of the genus must conform with the morphology of *C. anderssoni*, including the flat and wide skull, wide mandibular symphysis, well-separated parietal crests, and complicated enamel folds, such as strongly developed crochet, strongly constricted protocone and long lingually bent antecrochet.


**Figure 9.** Skulls of *Chilotherium anderssoni* Ringström, 1924 from the Upper Miocene fossil site Daijiagou (or Lok. 30) in Shanxi (China). A, original illustration of a skull taken from Ringström (1924, tab. 2, fig. 2); and B, a skull with its’ associated mandible (SMF M 3599) from the same site, now housed at the SMF. Not to scale.

‘*Chilotherium*’ *wimani* Ringström, 1924

Type Material

The species was erected based on six adult skulls, three with their mandibles, and some additional material (Ringström, 1924). However, Ringström (1924) did not designate a specific holotype or syntype for the species. Deng (2001b) designated the skull illustrated in figure 1 of plate 7 of Ringström (1924) as the lectotype of ‘*C.*’ *wimani*; however, this skull was attributed to *C. planifrons*, a junior synonym of *C. anderssoni* (Heissig, 1975, tab. 6; Deng, 2006, tab. 4). Therefore, this skull cannot be regarded as the lectotype of ‘*C.*’ *wimani* and consequently, all material referred by Ringström (1924) to ‘*C.*’ *wimani* from the site Beihougou (or Lok. 51) represents its’ type material (see Ringström, 1924, p. 49).

Type locality

Upper Miocene deposits of Beihougou in Shaanxi (China), also referred to as “Lok. 51” in the Lagrelius Collection.

Diagnosis

Small chilothere. Almost bell-shaped occipital surface. Occipital crest with wide middle groove. Large orbits in comparatively low positions, strong supraorbital tubercles, weak postorbital processes on frontal and zygomatic bones, and irregular infraorbital foramina. Narrow and long rhombic cranial dorsal surface, strongly concave cranial dorsal profile, with highly elevated nuchal crest. Little separated parietal crests and steep outer walls of the braincase. Convex frontal bones and highly positioned nasal bones that are wide with a deep nasal notch. Relatively steep zygomatic arches. Robust postglenoid processes and thick posttympanic processes, which are fused together. Particularly wide mandibular symphysis with concave dorsal and ventral surface. Sexually dimorphic i2s, which are very large in males with an upturned medial flange. Mental foramina located under p3. Well-developed parastyle folds and paracone ribs, and weakly constricted protocones and hypocones on premolars but strong constriction on molars (modified after Deng, 2001b).

Remarks

This species was erected by Ringström (1924) to be included in the genus *Chilotherium*. He described its skull as being almost identical to that of the type species

*C. anderssoni*, with only minor differences. Based on additional cranial material of this species, described by Deng (2001b) it has become apparent that this species differs significantly from typical representatives of the genus *Chilotherium*, such as *C. anderssoni* and *C. schlosseri* (see Kampouridis et al., 2023). Therefore, the scheme of Kampouridis et al. (2023) is followed that proposed that '*C.*' *wimani* does not belong to the genus *Chilotherium*. However, until its generic attribution is clarified the species will be tentatively referred to as '*C.*' *wimani*.

*Chilotherium sarmaticum* Korotkevich, 1958

Holotype

An almost complete skull with its' associated mandible (NMNHU-P-28-355).

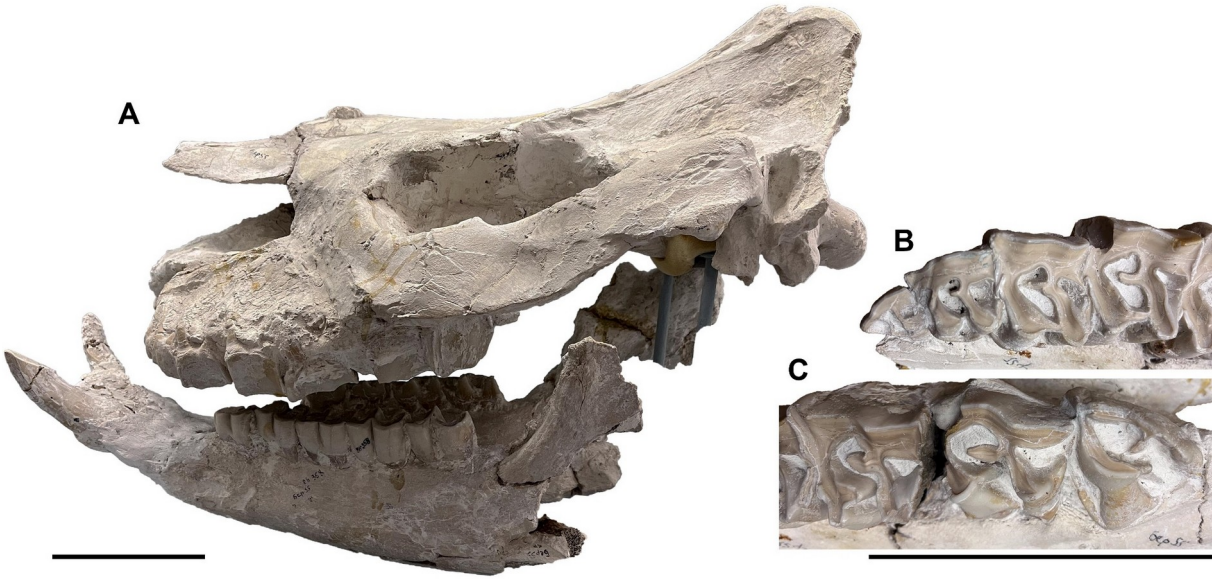


**Figure 10.** Holotype (NMNHU-P-28-355) of *Chilotherium sarmaticum* Korotkevitch, 1958 from the Upper Miocene of Berislav in Ukraine (courtesy of L. Gorobets). A, skull and associate mandible; B, right upper premolars (P1–P4); C, right upper molars. Scale bars equal 10 cm.

Type locality

Upper Miocene deposits of Berislav (Ukraine).

Diagnosis

Relatively small *Chilotherium* species. The parietal ridges diverge more widely than in most other species (smallest distance between them is 51–76.2 mm, n=4). The nasal bones are relatively short (the ratio of their length to the main length of the skull is 30.0-

31.5). The distal portions of the limbs (metapodials) are less massive, and the shortening of the limbs is more pronounced than in other species. The astragalus has predominantly two (rarely three) articular facets for articulation with the calcaneus (modified after Korotkevich, 1970).

*Chilotherium xizangense* Ji et al., 1980

Holotype

A fragmented skull with its' associated mandible (V5197-1, 2).

Type locality

Upper Miocene of the Lower Woma Formation in the Gyirong Basin in Tibet (China).

Diagnosis

A relatively small species of *Chilotherium*. Longitudinal groove in the middle of the nasal bones and abaxially convex; flat and concave frontal region; narrow mandibular symphysis; with high horizontal branch and straight lower margin; the D1 is wider than long; the protocone and hypocone connect in the premolars; the paralophid in the lower molars has a flat, nearly square outer wall; and the hypolophid has a rounded, crescent-shaped outer wall (modified after Ji et al., 1980).

Remarks

The species *C. xizangense* was described based on a fragmentary skull with its associated mandible and a few fragmentary dental remains, without any specimen being figured (Ji et al., 1980). Based on the provided diagnosis and description of the holotype, *C. xizangense* seems to feature typical characters of the genus *Chilotherium*, such as the wide mandibular symphysis and the depressed frontal bones (Ji et al., 1980). Therefore, an attribution to this genus seems justified.

*Chilotherium orlovi* Bayshashov, 1982

Holotype

A skull with its' associated mandible (Specimen No. 2802-03).

Type locality

Upper Miocene deposits of “Goose flight” at Pavlodar (Kazakhstan).

Diagnosis

Large *Chilotherium* species. Skull and lower jaw long. Flat skull, with only little elevated nuchal crest. Nasal bones short (ratio of their length to basic skull length 26.1%). Parietal crests widely separated (minimal distance 45–75 mm). Crochet and antecrochet strongly developed, parastyle and metastyle weakly expressed. The symphysis of the lower jaw is long, wide and curved upwards. The mandibular angle is weakly expressed (100-110°). The medial facet of the astragalus is oval and often elongated from below. The metapodials are relatively large and their distal epiphyses relatively narrow (modified after Bayshashov, 1982, 1993).

‘*Chilotherium*’ *primigenium* Deng, 2006

Holotype

A skull with its’ associated mandible (HMV 0102).

Type locality

Zhongmajia, 6 km southeast to the Hezheng County in Gansu Province, China. The specimen is collected from the gray green sandstone and conglomerates in the bottom of the Liushu Formation. The fossiliferous horizon is of early Late Miocene age, corresponding to early and middle MN9.

Diagnosis

Small chilothere. The species is characterised by a flat ventral surface of mandibular symphysis and parietal crests that are very slightly separated, even forming a sagittal crest (modified after Deng, 2006).

*Chilotherium licenti* Sun et al., 2018

Holotype

A skull with the articulated atlas (TNP-03978).

Type locality

Zhaojiacha, Huachi County, about 60 km northeast of Qingyang in Gansu Province, China. The fossiliferous horizon is of late Late Miocene age.

Diagnosis

Wide nasals become narrow gradually before the orbits; the zygomatic arch is fairly thin, particular in its posterior part; protocones and hypocones are strongly constricted, with straight lingual margins; crochet and crista are well developed and link together to form a medifossette on P2–M2, and antecrochet is also well developed; M1 has a projecting parastyle; lingual and buccal cingula are nearly absent; the buccal wall on the upper premolars and M1 is straight and smooth; the posterior valleys of the upper cheek teeth are almost closed (after Sun et al., 2018).

Genus *Shansirhinus* Kretzoi, 1942

Type Species

*Shansirhinus ringstromi* Kretzoi, 1942

Included Species

*Shansirhinus brancoi* (Schlosser, 1903)

Diagnosis

Aceratheriine rhinocerotids that feature very complicated enamel folds with a very strong protocone constriction and a prominent paracone fold. The premolars have a very strong crochet and crista that connect, creating additional fossettes.

Remarks

The genus *Shansirhinus* was erected by Kretzoi (1942) to distinguish two aceratheriine species, which are characterised by the presence of prominent enamel plications in the upper teeth, from the genera *Chilotherium* and *Acerorhinus*.


**Figure 11.** Dentition of *Shansirhinus* Kretzoi, 1942. A, holotype of *Shansirhinus ringstromi* Kretzoi, 1942 (from Ringström, 1927); B, skull of *Shansirhinus ringstromi* (PMU M 536, mirrored); C–F, syntype of *Shansirhinus brancoi* (Schlosser, 1903): C, 3D model of the D3 (SNSB-BSPG 1900 XII 678 [ex 25]); D, P2 (SNSB-BSPG 1900 XII 679 [ex 25]); E, P4 (MB.Ma. 28258); F**,** M1 (MB.Ma. 28259). Scale bar equals 5 cm for B–F and A is not to scale.

*Shansirhinus ringstromi* Kretzoi, 1942

Holotype

An upper tooth row (PMU M 536) by original designation by Kretzoi (1942, p. 311-312). Deng (2005a, p. 302) referred this specimen as the lectotype of the species. However, Kretzoi (1942, p. 311) refers specifically to “the palate-half described by Ringström as *Rh. aff. Brancoi* from Shanxi” („von Ringström als *Rh. aff. Brancoi* aus Shansi beschriebene Gaumenhälfte“ in the original German), which can only be referring to PMU M 536 (Ringström, 1927, pl. 1, fig. 3).

Type Locality

Upper Miocene to Lower Pliocene deposits of Huangshigou in Shanxi Province (China).

Diagnosis

The nasals are short and raised, with a rough horn boss on the tip. The mandibular symphysis is moderately expanded, with a concave labial surface. D1 is very small. The protocone is strongly constricted. The bridge and medifossette are well-developed on the premolars, with elaborate enamel plications and a continuous lingual cingulum present. The trigonid is angularly U-shaped (modified after Deng, 2005a)

Remarks

The holotype (PMU M 536) was originally described by Ringström (1927, pl. 1, fig. 3) as *Rhinoceros* aff. *brancoi*. This specimen was later used by Kretzoi (1942) to erect the species *Shansirhinus ringströmi* Kretzoi, 1942, named after Torsten Ringström, who described the specimen in the first place. Based on the rules of the ICZN (Art. 27) diacritic marks are not allowed in taxon names and need to be removed (ICZN Art. 32.5). In most studies, it was assumed that the correct spelling would be "*Shansirhinus ringstroemi*" (e.g., Athanassiou et al., 2014; Lu et al., 2015; Pandolfi, 2016). This is probably due to misinterpretation of ICZN Art. 32.5.2.1, which states that "…in a name published before 1985 and based upon a German word, the umlaut sign is deleted from a vowel and the letter "e" is to be inserted after that vowel…" However, the name Ringström is of Swedish origin, and not a German word, hence the diacritic used is not a German umlaut sign, but its Swedish equivalent. Therefore, the correct spelling of the species name should be *Shansirhinus ringstromi*, for other similar cases see Koerber (2009), as well as Snitting and Blom (2009).

*Shansirhinus brancoi* (Schlosser, 1903)

Type Material

Schlosser (1903) described this species based on four isolated teeth: a D3 (SNSB-BSPG 1900 XII 678 [ex 25]), a P2 (SNSB-BSPG 1900 XII 679 [ex 25]), a P4 (MB.Ma.28258), and M1 (MB.Ma.28259) (Schlosser, 1903, pl. 5, figs. 1-4).

Type Locality

The type material was bought as "dragon teeth" at a pharmacy in Tianjin, thus no locality information is available.

Diagnosis

*Shansirhinus* species that differs from *Shansirhinus ringstromi* in having more hypsodont teeth and more secondary enamel folds and plications (modified after Kretzoi, 1942).

Genus *Eochilotherium* Geraads and Spassov, 2009

Type and only species

*Aceratherium samium* Weber, 1905.

Diagnosis

Same as for the type and only species.

Remarks

*Eochilotherium* was coined by Geraads and Spassov (2009) as a subgenus, *Chilotherium* (*Eochilotherium*), with *Aceratherium kiliasi* as its type species and the authors also included *Aceratherium samium* in it. Based on the provisions of ICZN Art. 43.1 when taxon is established as a subgenus it is simultaneously established at the genus level as well; therefore, it was afterwards raised to the genus level by Kampouridis et al. (2023).

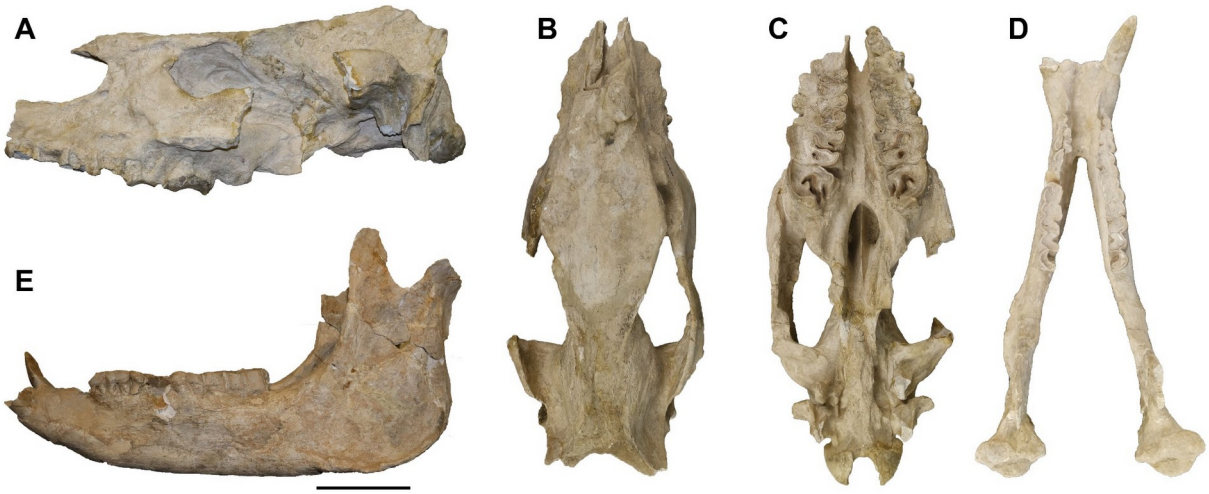


**Figure 12.** Neotype of *Eochilotherium samium* (Weber, 1905) from the Upper Miocene of Samos Island (Greece). Skull (A–C: SMF M 3601) and its' associated mandible (D–E) in lateral (A, E), dorsal (B, D) and ventral (C) views. Scale bar equals 10 cm.

*Eochilotherium samium* (Weber, 1905)

Neotype

A well-preserved skull with associated mandible of an old individual (SMF M 3601), designated by Kampouridis et al. (2023).

Type locality

Upper Miocene deposits on Samos Island in Greece; exact locality unknown.

Diagnosis

Aceratheriine rhinocerotid of medium size with a unique combination of craniodental features separating it from all other chilotheres: dolichocephalic skull; transversally concave dorsal surface of the parietal bones, while their frontal bones are convex in the anterior part, becoming flattened posteriorly; moderately separated parietal crests (~40 mm); weak to absent groove that would separate the nasal bones from each other; raised posterior part of the skull; wide mandibular symphysis with moderately enlarged and slightly flattened second lower incisors; the relative length of the premolars with respect to the molars is reduced, primarily due to the reduction of the size of the second upper and lower premolars; and complex enamel folds: moderate crochet and constriction of the protocone of the molars, with a strong antecrochet that bends lingually; neither the protocone nor the hypocone of the P2 are constricted; no crista in the molars; and discontinuous lingual cingula (after Kampouridis et al., 2023).

## 1.4. Phylogeny

### 1.4.1. Chilotheres

The phylogenetic position of Chilotheriina and the internal relationships of the included genera and species has been debated ever since the genus was first coined. Initially, the genus *Chilotherium* was included in the subfamily “Teleocerinae” (Ringström, 1924), which refers to the previously erected subfamily Teleoceratinae, which today is used variably at the subfamily, tribe, or subtribe level (Teleoceratinae, Teleoceratini, and Teleoceratina respectively) to include genera like the North American *Teleoceras* and the Eurasian *Brachypotherium* Roger, 1904 (e.g., Antoine et al., 2010; Sun et al., 2024; Borrani et al., 2025). Peculiarly, *Chilotherium* shares some features like the wide mandibular symphysis, a generally rather wide skull with widely separated parietal crests, along with complicated enamel folds in the upper teeth and short limbs with this group. For this reason, in the past many researchers assumed that *Chilotherium* also belonged to this group (Niezabitowski, 1912, 1913; Ringström, 1924; Korotkevich, 1958, 1970; Bayshashov, 1982, 1993), with a junior synonym of *Chilotherium schlosseri* even being erected as *Teleoceras ponticus* (Niezabitowski, 1912, 1913; Kiernik, 1913). Kretzoi (1942) proposed that his newly named genus *Shansirhinus*, with its two included species *Shansirhinus ringstromi* and *Shansirhinus brancoi*, should be closely affiliated with the genus *Chilotherium*, without establishing a new family-group taxon to unite them; thereby, foreshadowing the much later on described Chilotheriina. This taxon was originally erected as a tribe by Qiu et al. (1987) to include the two genera *Acerorhinus* and *Chilotherium*, removing *Chilotherium* from the teleoceratines. A close relationship between *Chilotherium* and *Acerorhinus* had previously been suggested by Heissig (1975), who studied the Late Miocene Anatolian rhinoceroses and placed *Acerorhinus* as a subgenus within *Chilotherium* and also included *Shansirhinus brancoi* within the genus *Chilotherium*. Qiu et al. (1987) did not explicitly mention the relationship of the two included genera to the genus *Shansirhinus*; however, they included the species *Acerorhinus cornutus* (Qiu and Yan, 1982) in this group, assuming its generic attribution to *Acerorhinus*. It was later shown that the skull for which the species *Chilotherium* (*Acerorhinus*) *cornutum* was erected, actually belongs to the genus *Shansirhinus* (Deng, 2006; Athanassiou et al., 2014); thereby, indirectly suggesting a close relationship between these taxa. Later, Heissig (1989) as well suggested that there is a “group around *Chilotherium* Ringström, 1924”, but he did not use the taxon Chilotheriina that had been created two years earlier. Nonetheless,

he considered the genera *Subchilotherium*, *Acerorhinus*, and *Chilotherium* to be most closely related (Heissig, 1989).

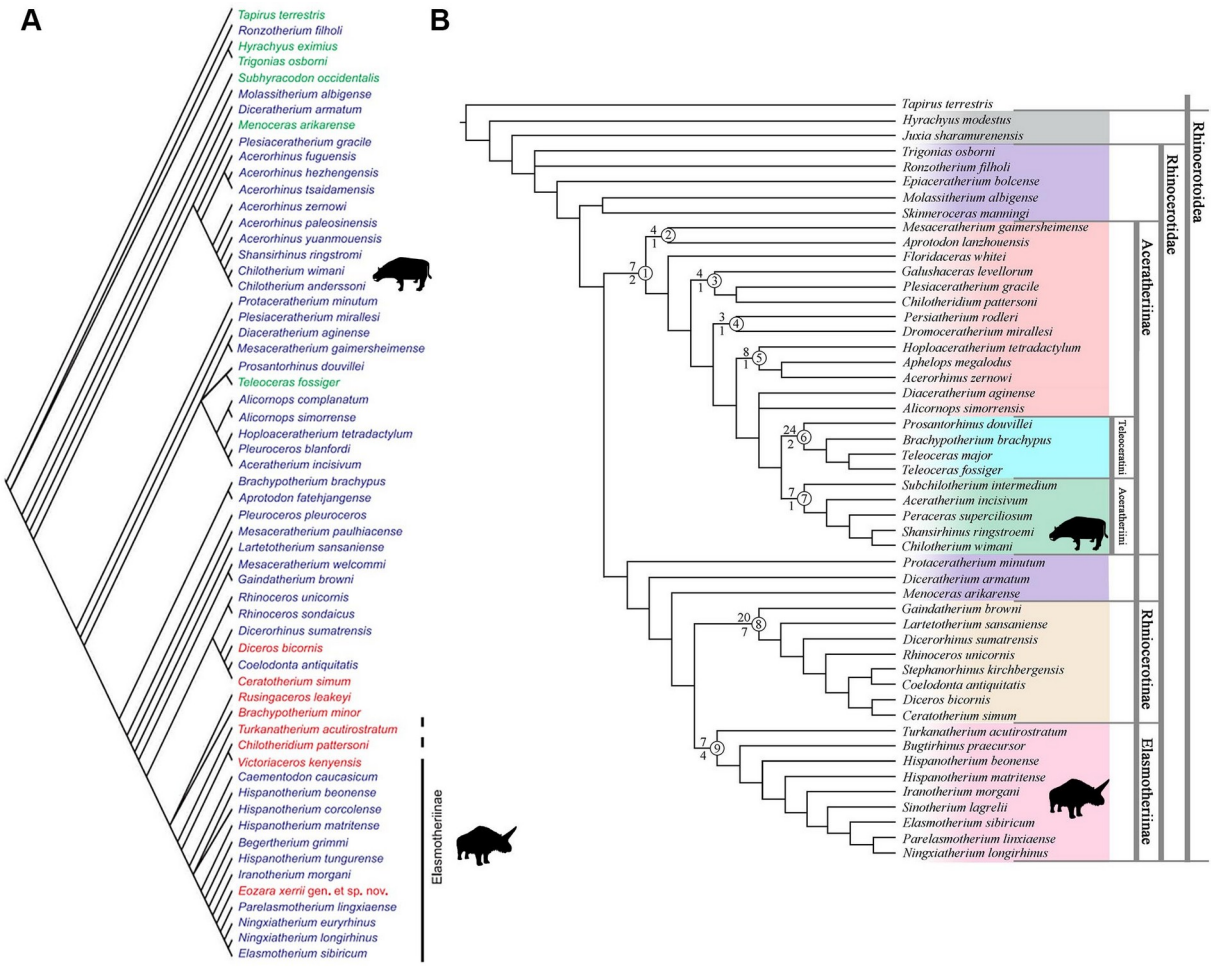


**Figure 13.** Phylogenetic analyses of Rhinocerotidae, including both chilotheres and elasmotheriines. A, phylogenetic analysis mainly focused on elasmotheriines (modified after Geraads and Zouhri, 2021, fig. 4); B, phylogenetic analysis mainly focused on chilotheres (modified after Lu et al., 2023, fig. 1). Silhouettes mark the position of chilotheres and elasmotheriines respectively. Silhouettes by Zimices via PhyloPic, licensed under CC BY-NC 3.0 (https://creativecommons.org/licenses/by-nc/3.0/).

Recently some phylogenetic analyses (e.g., Pandolfi, 2016; Sun et al., 2018; Lu et al., 2023; Borrani et al., 2025) that included members of the genera *Acerorhinus*, *Chilotherium*, and *Shansirhinus*, showed that *Chilotherium* and *Shansirhinus* are consistently recovered as sister taxa, whereas *Acerorhinus* is more distantly related to these genera. Based on this notion, Kampouridis et al. (2023) suggested that the Chilotheriina should be placed at the subtribe level and restricted to the genera *Chilotherium*, *Eochilotherium*, and *Shansirhinus*. However, the phylogenetic position of the group within Aceratheriinae is a highly debated topic and the proposed scheme

involving the chilotheres is very likely to be adjusted in the future, based on new findings. This is exemplified by two recent studies on rhinoceros phylogeny (Borrani et al., 2025; Fraser et al., 2025). In one of these (Fraser et al., 2025), *C. anderssoni*, the only included species of *Chilotherium* is placed at the base of the clade containing the extant Asian rhinoceroses (*Rhinoceros* and *Dicerorhinus* Gloger, 1941) and *Nesorhinus philippinensis* (Koenigswald, 1956), within crown Rhinocerotinae; whereas *Shansirhinus ringstromi* is recovered as a sister taxon to *Plesiaceratherium gracile* (Roman, 1924) and their clade is sister to *Molassitherium albigense* (Crusafont et al., 1955), a taxon that is variably recovered as a basal rhinocerotine or basal rhinocerotid, but consistently outside aceratheriines (Becker et al., 2013; Lu et al., 2023). The positions of both *C. anderssoni* and *S. ringstromi* are most curious, since they do not share many morphological features with the taxa with which they are placed in this phylogenetic analysis and their questionable placement is not further discussed by the authors of the study (Fraser et al., 2025). In the second study (Borrani et al., 2025), *Chilotherium kowalevskii*, *Chilotherium wimani*, *Chilotherium anderssoni*, and *Shansirhinus ringstromi*, are recovered in a clade along with *Chilotheridium pattersoni*. The latter species is a rhino with a highly debated phylogenetic position that has been suggested as a close relative of *Chilotherium* in the past, though this is most definitely not the case, due to its cranial morphology strongly deviating from that of *Chilotherium*. For instance, the frontal region is not at all depressed in *Chilotheridium pattersoni*, it has closely situated parietal crests, and prominent horn bosses on the nasal bones, unlike any *Chilotherium* species (Hooijer, 1971). Additionally, the appendicular skeleton does not exhibit the shortening that is observed in *Chilotherium* (compare Hooijer, 1971; Kampouridis et al., 2025). Therefore, the scheme proposed by Borrani et al. (2025) is most peculiar and is not supported by any morphological characters except for a general similarity in the tooth morphology, which is also similar to some elasmotheriines, to which *Chilotheridium* has also been attributed (Geraads and Zouhri, 2021). Nonetheless, Borrani et al. (2025) went as far as placing *Chilotheridium pattersoni* in the genus *Chilotherium*, which cannot be supported. *Chilotherium pattersoni* represents a clearly distinct genus from *Chilotherium* that is not closely related to it based on the morphology of the skull, mandible and appendicular skeleton. In the same phylogenetic analysis, the already discussed clade consisting of *Chilotherium*, *Chilotheridium*, and *Shansirhinus*, is placed within Teleoceratinae (Borrani et al., 2025). This is another old misconception, which is only supported by

three characters, which are actually not exclusive to this group and can be observed in several rhinoceros' taxa outside Teleoceratinae like the loss of the p1 and fusion of the metaconid to a constricted metalophid in the m3. These two studies, demonstrate the difficulty to resolve the phylogenetic position of Chilotheriina and the intrageneric relationships.

Herein, we accept the notion proposed by Kampouridis et al. (2023), based on morphological comparisons, that the Chilotheriina includes only three genera – *Chilotherium*, *Eochilotherium*, and *Shansirhinus*. They share a number of apomorphic features that are not observed in *Acerorhinus*. For instance, all three have a wide mandibular symphysis, fairly high-crowned teeth, along with complicated enamel folds in the upper teeth like a very prominent protocone constriction and a very long lingually oriented antecrochet, which are generally absent in the representatives of *Acerorhinus* (Cerdeño, 1996; Athanassiou et al., 2014).

### 1.4.2. Elasmotheriines

In contrast to the confusing systematic context of chilotheres, the phylogenetic relationships of elasmotheriines have had a much more stable and consistent research history. Nevertheless, the phylogenetic relationships of *Elasmotherium* were rather ambiguous in the past, for instance Osborn (1900) suggested a close relationship to *Aceratherium incisivum* Kaup, 1832 and other taxa that are now known to be hornless rhinoceroses. Later, Mecquenem (1908a) described a new rhinoceros species from the Upper Miocene of Maragheh in Iran, *Iranotherium morgani* (originally as *Rhinoceros morgani*). He compared this species mainly to *Elasmotherium* and *Coelodonta* Bronn, 1831, but he did not specifically suggest any closer relationship between the two species (Mecquenem, 1908a). Killgus (1922, 1923) attributed teeth from the Upper Miocene of Kutschwan in China to a new species, *Parelasmotherium schansiense*, which he considered an ancestor of *Elasmotherium sibiricum* in the beginning (Killgus, 1922), but later abandoned this hypothesis (Killgus, 1923). However, he (Killgus, 1923) suggested that *Elasmotherium* is not closely related to either *Aceratherium incisivum* nor to *Coelodonta antiquitatis* (Blumenbach, 1799). Almost at the same time, Ringström (1923) described a new species from similarly aged sediments from China, *Sinotherium lagrelii*, which he placed in the subfamily Elasmotheriinae; thus, being closely related to *Elasmotherium*. Shortly after, Ringström (1924) discussed the

relationship of *Elasmotherium* and *Sinotherium* in more detail, based on more complete material of the latter species, placing them within the same group, separated from all other rhinoceroses and suggesting that *Sinotherium* is a senior synonym of *Parelasmotherium*. He also coined the genus name *Iranotherium* for *Iranotherium morgani*, which is also included in the elasmotheriine group, but separated from *Elasmotherium* and *Sinotherium* (Ringström, 1924).

This general scheme of *Elasmotherium*, *Sinotherium*, *Parelasmotherium*, and *Iranotherium* representing the elasmotheriines, has remained more or less unchanged and other taxa have only been added to this group. In the last century, many new elasmotheriine taxa were identified, showing that this group was much more diverse than previously thought and covered the whole Old Word (e.g., Chow, 1958; Heissig, 1999; Deng, 2008; Geraads, 2010; Geraads et al., 2012; Sanisidro et al., 2012; Geraads and Zouhri, 2021; Sun et al., 2023). Their internal phylogenetic relationships are well resolved with only few specific taxa being problematic. For instance, *Chilotheridium pattersoni* was initially regarded as a close relative to *Chilotherium* (Hooijer, 1966, 1971) but most probably represents an elasmotheriine (Geraads and Zouhri, 2021), though additional studies need to confirm this. Another relatively problematic taxon is *Parelasmotherium schansiense*, as already mentioned shortly after its initial description it was synonymised with *Sinotherium* (Ringström, 1924). Later, it was recognised as a distinct species and two additional species were attributed to *Parelasmotherium* (e.g., Chow, 1958; Qiu and Xie, 1998; Deng, 2001a, 2007). It was also considered that another Late Miocene Chinese elasmotheriine, *Ninxiatherium longirhinus*, was a junior synonym of *Parelasmotherium schansiense*, which led to the use of a complete skull of the former species for scoring *Parelasmotheirum schansiense* (Antoine, 2002; Antoine et al., 2002). The inclusion of two further species in *Parelasmotherium* and the synonymisation of the type species with *N. longirhinus*, severely complicate the phylogenetic relationships of the genus, which left an important gap in our understanding of elasmotheriine evolution. This is further worsened by the fact that *Parelasmotherium schansiense*, the type species of the genus, has not been included in some recent phylogenetic analyses (e.g., Geraads and Zouhri, 2021; Lu et al., 2023; Borrani et al., 2025), because it is represented only by four associated teeth, one of which is a deciduous premolar, another being the unerupted P4 and another being completed unworn (Killgus, 1922, 1923).

## 1.5. Ecology

### 1.5.1. Chilotheres

The ecology of chilotheres has also been a matter of much debate. The discussion about their ecology has traditionally revolved around their prominent cranial and postcranial features that include the mandibular symphysis with large tusk-like incisors, toothless premaxillary bones, the relatively high-crowned teeth with complicated enamel folds, and the short limb bones. More specifically, early on it was suggested that the large tusk-like incisors were used for digging (Killgus, 1922), though already Ringström (1924) rejected this notion. He suggested that the large incisors were used in combination with a highly flexible upper lip to cut off grass. He supported this idea with the explanation that *Chilotherium* had rather strong attachment areas for the muscles associated with the upper lip, including relatively large toothless premaxillary bones. Additionally, he referred to the high-crowned teeth for the fact that these animals fed on highly abrasive vegetation, such as grass (Ringström, 1924). Similarly, Qiu and Yan (1982) studied the muscle attachments in the skull of *Chilotherium* and suggested that it must have had a hard upper lip that was used as a counterpart to the large incisors, while cutting low vegetation. Heissig (1989) suggested that the shortening of the limbs in *Chilotherium* was an adaptation to grazing low vegetation, though he admitted that it was questionable whether the genus represented true grazers. However, the notion of *Chilotherium* possibly being a grazer due to the high-crowned teeth was also supported by other researchers (e.g., Ringström, 1924; Heissig, 1999; Deng and Downs, 2002; Chen et al., 2010). Recent analysis of their teeth, including micro-, mesowear, and stable isotopes paint a more complicated picture about their ecology, showing that chilotheres were selective mixed feeders, adapted to open habitats (e.g., Biasatti et al., 2018; Deng et al., 2023; Hullot et al., 2023).

Another ecological aspect that has been discussed in the past and has already been mentioned herein, is the usage of the large incisors. It has been shown that these incisors are actually sexually dimorphic, with males have large tusk-like incisors and females having smaller ones (Chen et al., 2010 and literature therein). Therefore, it has been hypothesised that males used their large incisors in intraspecific combat, which is also supported by the fact that these animals were most probably living in herds and the adult male to female ratio is favoured towards females (Liang and Deng, 2005;

Chen et al., 2010). However, the incisors were most likely also used in combination with a flexible upper lip in foraging for food (e.g., Ringström, 1924; Qiu and Yan, 1982).

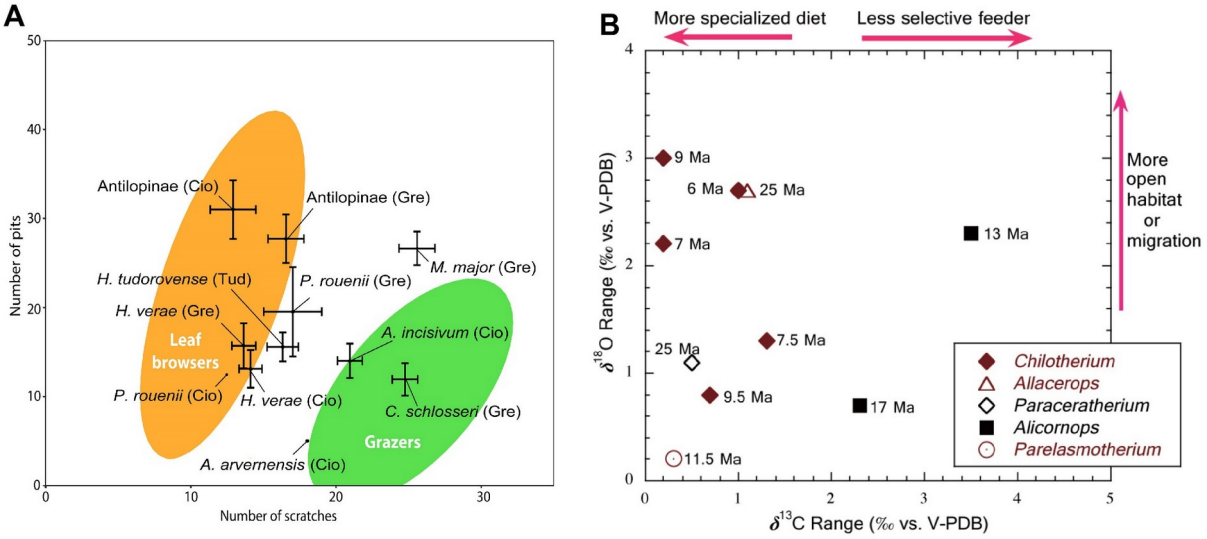


**Figure 14.** Palaeoecological data on herbivorous mammals including chilotheres. A, bivariate diagram with the results of a microwear analysis (average number of pits vs. scratches) of large herbivore mammals of three Upper Miocene localities of Moldova (Cio: Cioburciu 1 and Tud: Tudorovo) and Ukraine (Gre: Grebeniki) (from Rivals et al., 2024, fig. 7); and B, Bivariate plot of stable isotope values ($\delta^{18}O$ vs $\delta^{13}$ from rhinocerotoid tooth enamel across various Oligocene and Miocene localities in China (from Biasatti et al., 2018, fig. 4)

### 1.5.2. Elasmotheriines

Similarly to chilotheres, elasmotheriines have traditionally been considered to have had a very abrasive diet due to their complicated tooth morphology. Both groups display a trend towards more complicating enamel folds and plications, a trend typically observed in equids. This is especially evident in the type genus of the Elasmotheriinae, *Elasmotherium*, which has highly plicated enamel and extremely high-crowned teeth, that continue growing throughout the life of the animals. However, this is not the case in all elasmotheriines. In fact, only the most derived elasmotheriines like *Parelasmotherium*, *Sinotherium* and *Elasmotherium* have such high-crowned teeth that are heavily plicated (see Ringström, 1924; Kampouridis et al., 2022a; Sun et al., 2022). More basal elasmotheriines have a much simpler tooth morphology and less hypsodont teeth (see Deng, 2005b; Geraads et al., 2012; Sanisidro et al., 2012; Geraads and Zouhri, 2021), but even they are usually considered to represent animals that fed on a more abrasive diet and preferred more open habitats.

This agrees with the overall suggested palaeoenvironmental conditions in the regions they inhabited. For instance, it was suggested that during the Late Miocene within the Balkan-Iranian province the isolated presence of *Iranotherium morgani* in Maragheh in Iran, the easternmost locality of this region, implies a more arid environment (Giaourtsakis, 2022). The high diversity of elasmotheriines in China during the Late Miocene is also fits well into this narrative, because the environment in China is considered to have been more arid with more extensive open habitats compared to Europe (e.g., Li et al., 2014, 2020; Ciner et al., 2015; Liu et al., 2016; Deng et al., 2023).

### 1.6. Relevant localities with chilotheres

Chilotheres have a geographical distribution that spans the majority of Asia and extends westward into Eastern and Southeastern Europe. They are very common in many localities especially in Asia and even emerge as the most common large mammal in some isolated cases (e.g., Deng et al., 2023). Here, an overview of the most important and most relevant localities is provided where representatives of the group are found. The list is more exhaustive for the European localities, due to them being more limited. Due to the high number of Asian localities with the occurrence of chilotheres, it is preferred to only provide some of the most prominent cases that are relevant for this study.

#### 1.6.1. Studied localities

Samos

Age: Late Miocene, Turolian age (8-6.7 Mya; Kostopoulos et al., 2003; Koufos et al., 2009a)

Taxa: *Chilotherium schlosseri* (senior synonym of *Chilotherium wegneri* and *Chilotherium angustifrons*), *Eochilotherium samium, Ceratotherium neumayri, and Dihoplus pikermiensis*

The island of Samos (Fig. 1) has been known to yield Late Miocene vertebrate fossils since the mid-19$^{th}$ century (e.g., Koufos, 2009), with the first excavations taking place in the 1880s, led by C. I. Forsyth Major (e.g., Forsyth-Major, 1888). Since then, numerous palaeontologists and fossil hunters have visited the island to collect fossils (Koufos, 2009). This led to several impressive collections of Samos material in famous natural history museums throughout the world, including the AMNH, NHMW, and SMNS. Most recently, Prof. George Koufos from the Aristotle University of Thessaloniki, led new excavational campaigns on the island of Samos in Greece that brought to light a rich mammalian fauna (e.g., Kostopoulos et al., 2009; Koufos, 2009). Detailed studies of this material along with historically excavated fossils from Samos provided crucial information about the (bio-)stratigraphical context and the fauna itself (e.g., Kostopoulos et al., 2003, 2009; Koufos et al., 2009b, 2011). The Neogene deposits on Samos are separated into five formations. The Samos fossils come from numerous different fossiliferous sites, which are found in the Turolian (Upper Miocene) Mytilinii Formation (Kostopoulos et al., 2009). Most recent studies attributed these fossil sites to

four different, chronologically succeeding “mammal assemblages” (e.g., Koufos et al., 2009b, 2011).

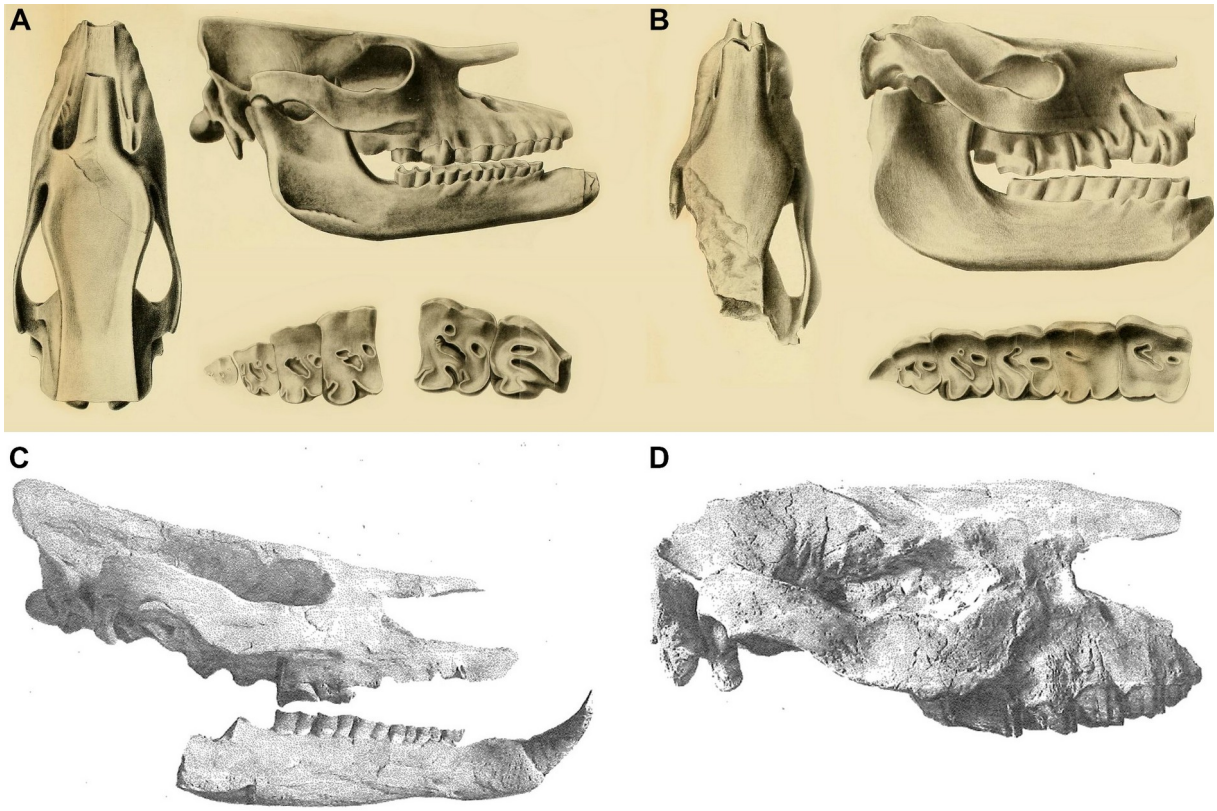


**Figure 15.** Original type material of all four species that were described from the Upper Miocene of Samos Island in Greece. A, *Aceratherium schlosseri* Weber, 1905 now *Chilotherium schlosseri* (modified after Weber, 1905, pl. 8-9); B, *Aceratherium samium* Weber, 1905 now *Eochilotherium samium* (modified after Weber, 1905, pl. 9-10); C, *Aceratherium wegneri* Andree, 1921, now synonym of *Chilotherium schlosseri* (modified after Andree, 1921, pl. 1, fig. 1); and D, *Aceratherium angustifrons* Andree, 1921, now synonym of *Chilotherium schlosseri* (modified after Andree, 1921, pl. 3, fig. 1). All illustrated specimens are considered lost today. Not to scale.

Chilotheres were probably present in all mammal assemblages, with *E. samium* probably being present in the older assemblages and *C. schlosseri* in the latter ones, possibly overlapping in the Intermediary Mammal Assemblage of Samos (Koufos et al., 2009b). However, it has to be noted that overall the rhino material from Samos has been assigned to several different taxa over years (for an overview see Giaourtsakis, 2022). Today, it is generally accepted that two large tandem-horned rhinos are present, *Ceratotherium neumayri* and *Dihoplus pikermiensis*, along with two smaller, hornless rhinocerotids, belonging to the Chilotheriina. The taxonomy of chilotheres (Fig. 15) has experienced many difficulties in the past, with the suggested presence of five species

(*Chilotherium schlosseri*, *Eochilotherium samium*, *Chilotherium wegneri*, *Chilotherium angustifrons*, and *Chilotherium kowalevskii*) by different authors (Weber, 1905; Krokos, 1917; Andree, 1921; Giaourtsakis, 2003, 2009, 2022; Athanassiou et al., 2014). Recently, it has been confirmed that *C. wegneri* and *C. angustifrons* represent junior synonyms of *C. schlosseri* and that *C. schlosseri* and *E. samium* are the two valid chilothere species present in Samos (Giaourtsakis, 2022; Kampouridis et al., 2022b, 2023; Svorligkou et al., 2025).

Daijiagou

Age: Late Miocene, Baodean age (5.7 Ma) (Kaakinen et al., 2013)

Taxa: *Chilotherium anderssoni* and *Sinotherium lagrelii*

The Upper Miocene red clay deposits in China are famous for their density of fossiliferous localities. In the late 1910s and early 1920s the Sino-Swedish expedition, led by Johan Gunnar Andersson, collected a large number of fossils from these fossil sites, as well as other mainly Miocene to Pleistocene localities. These fossils were transported to Uppsala where they are still housed and are known as the Lagrelius Collection in the PMU. Several palaeontologists from the University of Uppsala joined these expeditions in the early 20$^{th}$ century, collaborating with the Geological Survey of China. Axel Lagrelius, after whom the collection is named, was able to secure stable funding for the expeditions over the years (Mateer and Lucas, 1985). Close to 20000 specimens collected through this Sino-Swedish collaboration are now housed at the palaeontological collection of the PMU. This includes different types of fossils, including palaeobotanic, vertebrate, and invertebrate remains from different geological time periods. A large amount of chilothere specimens was also uncovered, including the type material of several species (Ringström, 1924). The most important fossil site for chilotheres is Daijiagou (also spelled Taijiagou and Taichiakou or called Lok. 30) that is found close to the Yellow River (Huang He) situated in the county of Baode in Shanxi Province, China (Fig. 1). The excavation of this locality, which is referred to as “Lok. 30” in several publications, and many other localities in China between 1921 and 1923 was undertaken by Otto Zdansky and later by other palaeontologists like Birger Bohlin, who also studied part of the excavated material (Zdansky, 1924, 1925a, 1925b, 1927a, 1927b; Bohlin, 1926, e.g., 1935). The Late Miocene faunal assemblages were

mainly made up of horses, bovids, and rhinoceroses (Ringström, 1923, 1924, 1927; Sefve, 1927; Bohlin, 1935).

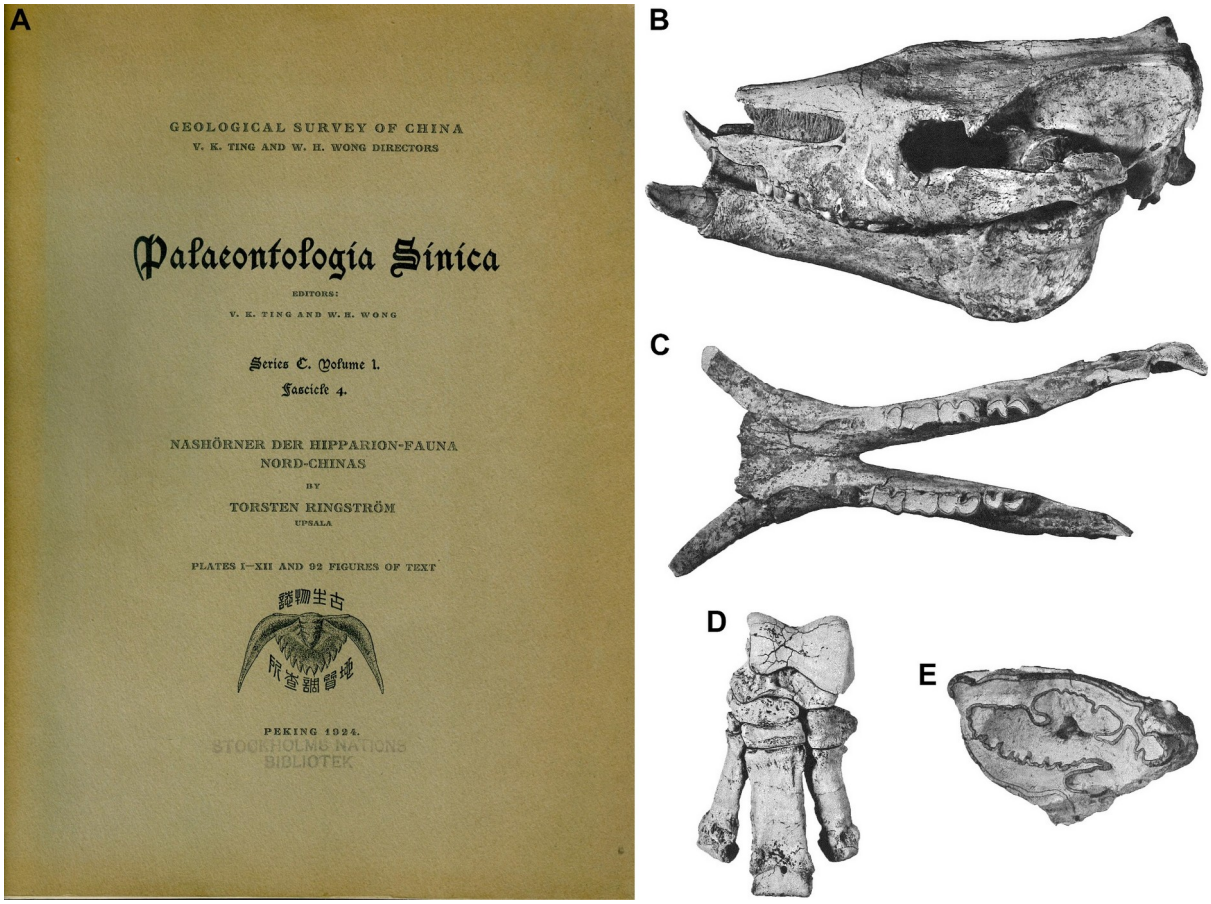


**Figure 16.** Publication of the rhinoceros material from the Upper Miocene red clays of China by Ringström (1924). A, Cover of the issue (modified after Ringström, 1924); B, Skull and mandible of *Chilotherium anderssoni* Ringström, 1924 from the Upper Miocene of Daijiagou in China (modified after Ringström, 1924, pl. 2, fig. 1); C, mandible of '*Chilotherium*' *wimani* Ringström, 1924 from the Upper Miocene of Beihougou in China (modified after Ringström, 1924, pl. 8, fig. 1); D, articulated partial tarsus of *C. anderssoni* from the Upper Miocene of Daijiagou in China (modified after Ringström, 1924, pl. 9, fig. 3); and E, holotype M3 of *Sinotherium lagrelii* Ringström, 1923 from the Upper Miocene of Daijiagou in China (modified after Ringström, 1924, pl. 12, fig. 2). Not to scale.

The rhinoceros material was described early on by Ringström (1924) and the chilothere and elasmotheriine material comes from six different fossil sites from the Upper Miocene Red Clays of China (Table 1). Based on this material Torsten Ringström (1924) erected the genus *Chilotherium* and its type species *C. anderssoni*. The locality of Daijiagou was only a small portion of the overall excavated material during the Sino-Swedish expedition but nonetheless, except for a large sample of *C. anderssoni* specimens also the elasmotheriine *Sinotherium lagrelii* was erected based

on a left M3, and additional material was described later on (Ringström, 1923, 1924). The stratigraphy of this classical Upper Miocene locality in the Baode county was recently re-evaluated and the age of many localities was able to be refined, dating Daijiagou to approximately 5.7 Ma (Kaakinen et al., 2013).

**Table 1.** List of J. G. Andersson's localities, which yielded rhinoceros fossils that were studied by Ringström (1924), with the locality numbers, names, and updated species that are found there. Type localities are marked by bold species names. Abbreviated genera: *A*., *Acerorhinus*; *C*., *Chilotherium*; and *D*., *Dihoplus*.

| Ringström loc. | Species | Loc. Name | County | Province |
|---|---|---|---|---|
| **11** | *D. ringstromi* | Zhengouwan | Xinan Xian | Henan |
| **12** | *A. palaeosinensis,* ***D. ringstromi*** | Shangyingou | Xinan Xian | Henan |
| **13** | *D. ringstromi* | Zhengouwan | Xinan Xian | Henan |
| **30** | ***C. anderssoni, Sinotherium lagrelii*** | Daijiagou | Baode | Shanxi |
| **31** | *C. habereri* | Liuwangou | Baode | Shanxi |
| **35** | *D. ringstromi* | Shangyingou | Xinan Xian | Henan |
| **43** | *C. habereri, D. ringstromi* | Jijiagou, Sangjialianggou | Baode | Shanxi |
| **44** | *C. habereri, C. anderssoni, A. palaeosinensis* | Yuejiali, Shenshuzui | Baode | Shanxi |
| **49** | ***A. palaeosinensis**, D. ringstromi* | Jijiagou, Yangmugou | Baode | Shanxi |
| **51** | ***‚C.' wimani*** | Wulangou, Beihougou | Fugu Xian | Shaanxi |
| **52** | *C. habereri, D. ringstromi* | Yuejiali, Linwangou | Baode | Shanxi |

Kutschwan

Age: Late Miocene, probably late Bahean to Baodean age

Taxa: *Chilotherium habereri* and *Parelasmotherium schansiense*

The locality of Kutschwan is another fossil site from the Upper Miocene red clays in China (Fig. 1). It was discovered before the Sino-Swedish expedition, by the German geographer Albert Tafel in Shanxi during his trip to China in 1905 (Killgus, 1923). No information about the exact location of the fossil site is known, but the material was collected from horizontal red clay deposits close to the Yellow River (Huang He) in Shanxi Province, China (Killgus, 1923). The material that was excavated by Albert Tafel, collecting a noteworthy sample of mammalian remains, composed of both cranial and postcranial elements. The whole collection was initially prepared at the

SMNS (Germany) before being deposited in the collections of the GPIT (Germany), where it is still housed today.

Hugo Killgus studied the whole collection for his Doctoral Dissertation (Killgus, 1922) and recognised a quite rich mammalian fauna, based on this limited material, including an ictithere hyaena (Kargopoulos et al., 2023), two rhino species, *Chilotherium habereri*, *Parelasmotherium schansiense*, a hipparionine horse, the giraffe *Schansitherium tafeli* Killgus, 1923, a large and up to three small bovids (Killgus, 1923). The hornless rhino *C. habereri* is the most abundant taxon in this collection, including several skulls (Fig. 17) and a small sample of postcranial material that was recently reevaluated. The cranial and dental morphology of the species were revised by Ringström (1924) after its' original description (Schlosser, 1903), but almost nothing was known about the postcranial anatomy of the species until recently.

**Figure 17.** Original photograph of cranial material from the Upper Miocene of Kutschwan in China taken by Albert Tafel and figured in his book (modified after Tafel, 1914, pl. 16). Scale bars equal 1 m.

Maragheh

Age: Late Miocene, Turolian age (9–7.4 Ma) (Mirzaie Ataabadi et al., 2013)

Taxa: *Chilotherium persiae*, *Ceratotherium neumayri*, *Iranotherium morgani*, *Persiatherium rodleri*

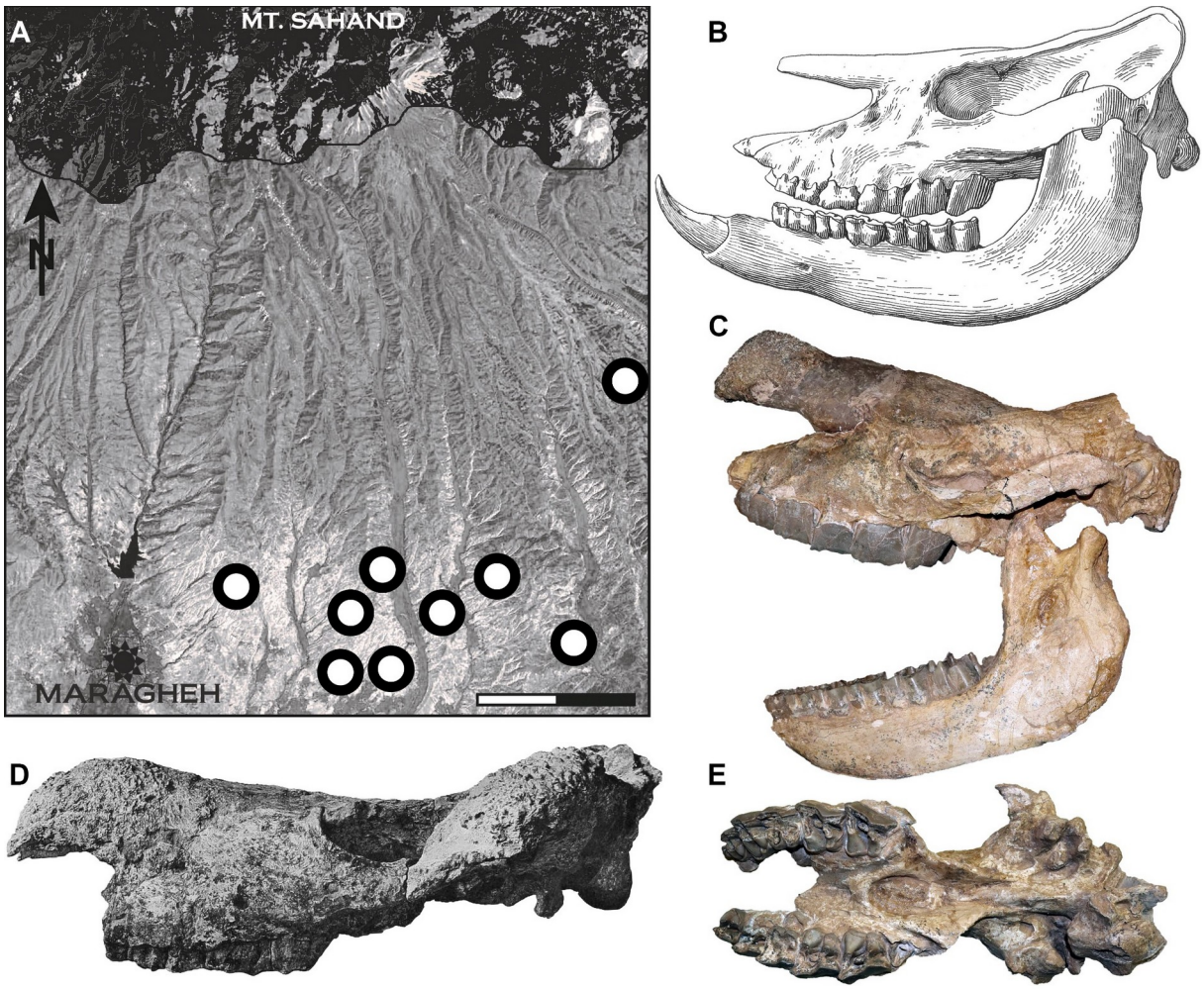


**Figure 18.** The Upper Miocene locality of Maragheh in Iran and its rhinoceros' assemblage. A, Topographical map of the fossil sites in the region (modified after Kampouridis et al., 2024, fig. 2); B, Skull and mandible of *Chilotherium persiae* (Pohlig, 1885) in left side view (modified after Mecquenem, 1908a, fig. 24); C, Holotype, skull and mandible of *Ceratotherium neumayri* (Osborn, 1900) in left side view ; D, Holotype skull of *Iranotherium morgani* (Mecquenem, 1908a) in left side view (modified after Mecquenem, 1908a, pl. 8, fig. 1); and E, Holotype skull of *Persiatherium rodleri* (Pandolfi, 2016) from the Upper Miocene of Maragheh in Iran in ventral view. Scale bar for A equals 10 km and B–E are not to scale.

Maragheh is a world-famous locality (Fig. 1) known for the detailed record of its' Late Miocene mammal fauna. The Upper Miocene deposits in the area make up the Maragheh Formation, which consists of continental volcanoclastic rocks that have yielded a large number of fossil sites (Fig. 18A). The Late Miocene fauna from this locality has been known since the 19$^{th}$ century (Rodler, 1885; Pohlig, 1886; Mecquenem, 1908b; Mirzaie Ataabadi et al., 2013, 2016). Several fossil sites were excavated over the last more than 100 years, with recent studies suggesting the

existence of three distinct fossiliferous levels to which also the historical fossil sites were associated (Campbell et al., 1980; Bernor, 1986). Material from Maragheh is scattered throughout many collections, such as the NHMW, MLU, MNHN, NHMUK, and SNSB-BSPG.

The rhino assemblage in Maragheh is quite rich (Fig. 18B–E) comprising four distinct species, the huge single-horned *Iranotherium morgani*, the large tandem-horned *Ceratotherium neumayri*, and two small hornless rhinoceroses, *Chilotherium persiae* and *Persiatherium rodleri* (e.g., Pohlig, 1885; Mecquenem, 1924; Pandolfi, 2016; Kampouridis et al., 2025). Most notably, Maragheh represents the type locality for all four of these rhinocerotid species, three of which have also been used as the type species to erect new genera. Pohlig (1885) erected *Rhinoceros persiae* for the chilothere from the Late Miocene of Maragheh. Therefore, this species is the first ever described species that is assignable to the genus *Chilotherium* and has, thus, priority over any other chilothere species name. In its original contributions, Pohlig (1884a, 1884b, 1885, 1886) did not describe any material. *Chilotherium persiae* is the most common and most characteristic representative of the family in the Maragheh fauna and several adult and juvenile cranial, mandibular, dental, and postcranial elements have been found. Several more recent studies have been able to refine the stratigraphic position of the Maragheh fossil sites and their ages (e.g., Kamei et al., 1977; Bernor et al., 1980; Swisher, 1996; Salminen et al., 2016; Sawada et al., 2016). This allowed restricting the chronological age of the fossiliferous strata to between 9 and 7.4 Ma. However, the majority of the collected vertebrate fossils come from the interval between 8.2 and 7.4 Ma (Mirzaie Ataabadi et al. 2016).

### 1.6.2. Chilothere localities from the Eastern Mediterranean

Bulgaria

In Europe, Bulgaria preserves the richest record of *Chilotherium*, with its occurrence having been reported from six localities to date. The presence of *Chilotherium* in the country was discussed in detail by Geraads and Spassov (2009), who revised the rhinoceros assemblages of Bulgaria in general. They provided a detailed account of all occurrences of the genus with revised taxonomic assignments, employing a subgeneric separation of *Chilotherium*. However, these assignments must be revised based on recent findings about the taxonomic affinities of the genus. Most of these

occurrences should be referred to *Chilotherium* sp. until a detailed re-examination is conducted.

Oranovo

Age: “early Upper Miocene age” from Spassov et al. (2006)

Taxa: *Chilotherium* cf. *sarmaticum* (here *Chilotherium* sp.)

A single i2 was described by Spassov et al. (2006) as *Chilotherium* cf. *sarmaticum*, which was later supported by Geraads and Spassov (2009). The authors mainly compared the specimen to incisors of *C. persiae*, *C. kowalevskii*, and *C. sarmaticum* (Spassov et al., 2006; Geraads and Spassov, 2009). The identification of such a specimen is not possible due to the taxonomic issues and the interspecific uniformity of the European *Chilotherium*. However, it has to be noted that the incisor is close in size to the incisors of female *C. schlosseri* specimens such as NMB-Sam25 and AMPG-SAM500 (Svorligkou et al., 2025), which have a width of about 30 mm at their bases, without being fully erupted. However, until more material becomes available, the specimen from Oranovo is best referred to as *Chilotherium* sp.

Kromidovo

Age: Late Miocene, Turolian (MN12?) (Spassov et al., 2006; Geraads and Spassov, 2009)

Taxa: *Chilotherium* (*Eochilotherium*) cf. *kiliasi* (here Chilotheriina indet.)

Geraads and Spassov (2009) described a partial skull that preserves only the ventral portion, including the teeth. They compared this specimen with the chilothere material from Pentalophos 1, due to similarities in the teeth, without going into detail about the specific morphological features. Based on their description of the specimen, it has a long crochet, which is visible in the illustration of the specimen (Geraads and Spassov, 2009, pl. 1A, B), this feature that does not exist in primitive chilotheres like *E. samium* from Pentalophos 1 and Samos. Additionally, the antecrochet is described as weak, which contrasts the strong antecrochet usually seen in chilotheres. The specimen from Kromidovo, however, is a rather young individual and while the antecrochet is not very prominent, a strong constriction is present in the protocone (both mesially and distally), which probably would lead to a strong antecrochet when worn enough. When compared to a *C. kowalevskii* skull of more or less similar age, based on the erupting

M3 (Pavlow, 1913, pl. 4, fig. 5), the development of the antecrochet does not seem to differ significantly. Geraads and Spassov (2009) also mentioned that the premolars have a lingual cingulum, and that the median valley remains open. Both these features are rather uncommon in *Chilotherium* spp. Even in primitive chilotheres such as *E. samium* the median valley in the premolars usually closes, except for the P2, which often remains open until very late, and the lingual cingulum is not continuous, unlike the Kromidovo specimen. The closing of the median valley, however, is a very variable feature and even in derived chilotheres such as *C. schlosseri* there are specimens where it remains open (Svorligkou et al., 2025). The lingual cingulum on the other hand is never continuous in derived chilotheres of Europe. The only cases of a continues lingual cingulum in the premolars are found in the primitive chilothere '*C.*' *wimani* from China (Ringström, 1924). It is very difficult to identify such a specimen based solely on the upper dentition. Even the generic attribution of the Kromidovo specimen is difficult to be established and it is best to refer this specimen to as Chilotheriina indet.

Yambol

Age: Late Miocene to Pliocene, Maeotian to Dacian age (Geraads and Spassov, 2009)

Taxa: *Chilotherium* cf. *kowalevskii*

Geraads and Spassov (2009) described some isolated remains of a chilothere from Yambol in Bulgaria. This also included mandibular fragments that were not illustrated and the identification to the species level of such material is in most cases impossible. However, they also described and illustrated some upper premolars (Geraads and Spassov, 2009, pl. 1C). These show some derived features like a very strong crochet and very strong protocone constriction resulting in a long antecrochet that connect the protocone and the hypocone at a very early wear stage. In fact, the teeth seem to be little worn and the proto- and hypocone seem to have established a wide connection (Geraads and Spassov, 2009, pl. 1C). The very early connection of the proto- and hypocone is characteristic for *C. kowalevskii* from Grebeniki (Ukraine) and differs from most other chilotheres. However, a crista and some plications, as well as a continuous cingulum are present in both specimens (P3 and P4). These are features that are not seen in the illustrated sample of *C. kowalevskii* from Grebeniki (Pavlow, 1913; Krokos, 1917) and beyond the few depicted tooth rows of *C. kowalevskii* not much is known about the potential intraspecific variability of the upper dentition of the species. A crista in the premolars that often closes the medifossette is rather common in *C. schlosseri*

and plications are also present in some specimens. However, the combination of all these features is not observed in any chilothere; nonetheless, it would be plausible for *C. kowalevskii* to exhibit a crista and/or plications in some premolar specimens, as plications are at least sometimes also observed in some other chilotheres such as *C. persiae* from Maragheh (Iran), which does not regularly exhibit them. Therefore, a preliminary attribution of these specimens to *C*. cf. *kowalevskii* seem plausible.

Ahmatovo

Age: Late Miocene, Turolian, probably post-Pikermian due to the presence of *Anancus* sp. (Geraads and Spassov, 2009)

Taxa: *Chilotherium* sp.

Geraads and Spassov (2009) described a single M3 from Ahmatovo in Bulgaria. They compared it to *C. sarmaticum*, *C. kowalevskii*, and *C. schlosseri*, arguing that this specimen could most probably be assigned to *C. schlosseri*. However, they preferred to assigning it to *Chilotherium* sp., due to the limited taxonomic value of an isolated molar.

Staniantsi

Age: Late Miocene, late Maeotian to Pontian age (Utescher et al., 2009)

Taxon: *Chilotherium* cf. *sarmaticum* (here *Chilotherium* sp.)

Geraads and Spassov (2009) described a single incisor tip from the coal deposits of Staniantsi in Bulgaria. They found that it is similar to the one from Oranovo that they assigned to *C.* cf. *sarmaticum* and tentatively assigned it to the same taxon. However, as already mentioned above, such a specimen is difficult to be identified and should be assigned to *Chilotherium* sp. Later, a more complete collection of chilothere material from Staniantsi was described showing many features separating it from most known chilothere species, with few characters possible suggesting a closer affinity to *C. schlosseri* from Samos, though even differing from that species (Kampouridis, 2020). Until a detailed description of this material is provided, along with in depth comparison, all the material from Staniantsi should be referred to as *Chilotherium* sp.

Gorna Sushitsa

Age: Late Miocene, Turolian age (Böhme et al., 2018)

Taxa: *Chilotherium* sp.

Spassov et al. (2019) mentioned several postcranial elements that they attributed to *Chilotherium* sp., but the specific identification of postcranial material is rather problematic. The material includes a MtIV with a length of approximately 98 mm, which is larger than the range provided for *C. sarmaticum* from Berislav in Ukraine (L=83.5–87 mm, n=4) and '*C.*' *wimani* from the Linxia Basin in China (L=83–90 mm, n=4), but falls within the range of *C. kowalevskii* from Grebeniki in Ukraine (L=91.8–100.5 mm, n=9), *C. orlovi* from Pavlodar in Kazakhstan (L=90–105 mm, n=4) and close to that of *C. schlosseri* from Samos in Greece (L=91.7–96 mm, n=2) (Weber, 1905; Krokos, 1917; Korotkevich, 1970; Bayshashov, 1993; Deng, 2002; Kampouridis et al., 2025). Unfortunately, the information on postcranial material of *Chilotherium* is still rather limited. Therefore, the identification will remain as *Chilotherium* sp. for the time being, though an assignment to either *C. schlosseri* or *C. kowalevskii* seems very likely, with *C. schlosseri* being the most plausible due to the similar age between Gorna Sushitsa and Samos. Several other postcranial elements, such as a calcaneus, three carpal bones and a fragment of a humerus, are mentioned but not described nor compared. However, postcranial elements of chilotheres can be identified as such due to them being relatively stout, as stated for the calcaneus (Spassov et al., 2019). Thus, these specimens at least confirm the presence of *Chilotherium* sp. in three different horizons of Gorna Sushitsa (GS3, GS4, GS8), dated to between 7.41 and 7.36 Ma (Böhme et al., 2018)

Greece

Pentalophos 1

Age: Late Miocene, Vallesian age (Geraads and Koufos, 1990; Koufos, 2006)

Taxa: *Eochilotherium samium* (considered the senior synonym of *Aceratherium kiliasi*), *Acerorhinus* sp., and *Ceratotherium neumayri*

Remarks: Geraads and Koufos (1990) described the species *Aceratherium kiliasi* from the early Late Miocene (Vallesian) of Pentalophos 1 (Greece). The holotype of the species is a moderately well-preserved skull of an old individual, which was later assigned to the genus *Chilotherium* (Heissig, 1996; Fortelius et al., 2003; Athanassiou et al., 2014). Geraads and Koufos (1990) also attributed to this species material that

actually belongs to the genus *Acerorhinus* (Heissig, 1996; Fortelius et al., 2003; Athanassiou et al., 2014). Heissig (1996, 1999) interpreted the Pentalophos chilothere as a primitive *Chilotherium*, which could be closely related to *E. samium* (which he included in *Chilotherium*) or potentially even conspecific. Giaourtsakis (2003) preferred to keep this species under its original name '*Aceratherium*' *kiliasi*, as a detailed re-evaluation of the material was needed. Fortelius et al. (2003) also pointed out the problems concerning this species, attributing it to a primitive *Chilotherium*, and noting its similarities to *E. samium*. Geraads and Spassov (2009) erected the new subgenus *Eochilotherium* with *C.* (*Eochilotherium*) *kiliasi* as its type species and also included *C. samium*. They studied numerous rhinocerotid remains from several Late Miocene localities of Bulgaria, attributing a skull from Kromidovo to *C.* (*Eochilotherium*) cf. *kiliasi*. Athanassiou et al. (2014) revised the record of the genus *Acerorhinus* from the Upper Miocene of the Eastern Mediterranean, erecting the new species *Acerorhinus neleus*. They attributed to this genus much of the material from Pentalophos 1, which was initially included in *Aceratherium kiliasi*. Athanassiou et al. (2014) also noted that the holotype skull of *Aceratherium kiliasi* represents a relatively primitive *Chilotherium*, but concerning the specific identification, they considered the loss of the type material of *E. samium* as a barrier that did not allow a definitive association and thus preferred to refer to it as *C.* cf. *samium* (Athanassiou et al., 2014, tab. 5). Finally, Giaourtsakis (2022) and Kampouridis et al. (2023) considered the Pentalophos chilothere to be synonymous to *E. samium*.

North Macedonia

Morievo area

Age: Late Miocene, Turolian age (Spassov et al., 2018)

Taxon: *Chilotherium* sp.

North Macedonia is known to have a number of rich vertebrate localities from the Late Miocene and most of them are found in the area of Veles for over a century (e.g., Laskarev, 1921; Schlosser, 1921; Garevski, 1974; Garevski and Markov, 2011; Spassov et al., 2018; Radović et al., 2025). These, mainly mammalian, assemblages have been compared with the "*Hipparion* fauna" of Pikermi (Greece), due to the similar taxa lists. Spassov et al. (2018) mentioned some dental elements that are assignable

to *Chilotherium* sp. They did not mention the exact position of the teeth, due to their fragmentary nature, but provide a short description, which is adequate to support the identification as *Chilotherium* sp. The fact that the specimens include also a long antecrochet may point to a derived chilothere. Any further identification is impossible, as the localities has only yielded isolated teeth. Thus, the Morievo area marks the westernmost occurrence of the genus *Chilotherium*.

Republic of Moldova

Lungu and Rzenik-Kowalska (2011) provided an overview of the Late Miocene localities of the Republic of Moldova with detailed taxa lists, in which several localities are referred to include *Chilotherium* representatives. More specifically, the existence of *C. schlosseri* was suggested in Chimishliya (as *C.* cf. *schlosseri*) and Gura-Galbene. *Chilotherium kowalevskii* was suggested to have been present in the localities of Răspopeni (or Respopen) and Pokshesht (as *C.* aff. *kowalevskii*). For Răspopeni it is specifically mentioned that *Chilotherium* is the most abundant large mammal with 20 skulls having been found. However, Lungu (2008) mentioned the existence of *Chilotherium schlosseri* in the fauna of Răspopeni, without any description of material, whereas Vangengeim and Tesakov (2013) assigned the Răspopeni chilothere to *Chilotherium kowalevskii* without a detailed discussion. The fact that for most localities there is no detailed description and comparison of the chilothere material with illustrations, prevents a specific identification. All these chilotheres are best referred to as either *Chilotherium* sp. of Chilotheriina indet. until detailed descriptions and comparisons are conducted. Additional potential occurrences of *Chilotherium* sp. were suggested from several other Upper Miocene localities like Pitushka, Varnitsa, Donich, and Peresechina (Lungu and Rzebik-Kowalska, 2011).

Romania

Reghiu

Age: Late Miocene, late Vallesian to early Turolian? age (Codrea et al., 2011)

Taxa: *Chilotherium* cf. *sarmaticum* or *Chilotherium schlosseri* (here *Chilotherium* sp.)

Rădulescu et al. (1995) described a rather complete skull of a chilothere from Reghiu in Romania (Fig. 19A). The skull was subsequently considered lost for several decades until recently. It was redescribed and assigned to *C. schlosseri*, due to the suggested synonymisation of *C. schlosseri* and *C. kowalevskii* (Țibuleac et al., 2023). The skull from Reghiu exhibits several features that would indicate a closer affinity to *C. kowalevskii* like the parietal crests that are 64.2 mm apart, the raised nuchal crest, and the premolars that features a closed off median valley even at a very early wear stage. In *C. schlosseri* the parietal crests are always at least 70 mm apart and the dorsal profile of the skull is completely flat without any upwards curve in the posterior part (Svorligkou et al., 2025). Therefore, a detailed re-examination of the skull is needed in light of the distinction between the species *C. schlosseri* and *C. kowalevskii*. Until then, the Reghiu specimen should be referred to as *Chilotherium* sp., though an assignment to *C. kowalevskii* seems plausible.


**Figure 19.** Romanian chilothere material. A, Skull of *Chilotherium* sp. from the Upper Miocene of Reghiu in Romania (modified after Țibuleac et al., 2023, fig. 3A); B, Right D2 of *Chilotherium* sp.; and C, Left M1 of *Chilotherium* sp. from the Upper Miocene of Pogana in Romania (courtesy of B. Ratoi). Not to scale.

Pogana

Age: Late Miocene, Turolian age (Codrea et al., 2011)

Taxa: *Chilotherium* sp.

Codrea et al. (2011) described two teeth of a small rhino from the Upper Miocene of Pogana, which they assigned to *Chilotherium* sp. This assignment seems most appropriate, because the M2 has a long crochet, a very strong protocone constriction,

both mesially and distally, which results in a very long antecrochet that bends lingually. Based on this material any further identification is impossible. Recently, new material, including dental (see Fig. 19B–C) and postcranial elements, from the Pogana has been unearthed but has not been described yet (R. Bogdan pers. comm.). The study of this material may shed some light on the taxonomy of the Pogana chilothere and help understanding the chilotheres of Romania in general.

Russia

Forstadt

Age: Late Miocene, middle Turolian age (Titov and Tesakov 2013)

Taxa: *Chilotherium* cf. *schlosseri* (here Chilotheriina indet.)

Titov and Tesakov (2013) mentioned the existence *Chilotherium* cf. *schlosseri* in the faunal list of the locality. They did not describe or even mention any specific material. Without the description of any specimen the identification cannot be verified. It would probably be best to tentatively attribute this occurrence to Chilotheriina indet. until further information becomes available.

Ukraine

Grebeniki

Age: Late Miocene, late Vallesian(?) age (Vangengeim and Tesakov, 2013)

Taxa: *Chilotherium kowalevskii*

Pavlow (1913) described *Aceratherium kowalevskii* based on rather rich material from the Upper Miocene of Grebeniki in Ukraine (Fig. 20A–B). A few years later, Krokos (1917) re-examined the material describing also the postcranial material in more detail and synonymised it with *C. schlosseri*. This notion was followed by many authors in until very recently (e.g., Krokos, 1917; Korotkevich, 1958, 1970; Bayshashov, 1993; Țibuleac et al., 2023), though Ringström (1924) supported the validity of *Chilotherium kowalevskii*. Heissig (1975) argued that this species is distinct from the other European chilotheres and that *C. angustifrons* represents a junior synonym of *C. kowalevskii*. Since then, the species has been variably treated either as valid (e.g., Geraads and

Spassov, 2009) or as a junior synonym of *C. schlosseri* (e.g., Antoine and Sen, 2016; Țibuleac et al., 2023). The discussion about the validity of this species has been rather complicated, while little attention has been given to a proper description of the features supporting or opposing its validity. Herein, *C. kowalevskii* is considered a valid species.

Odessa

Age: Late Miocene, late(?) Maeotian age (Kiernik, 1913)

Species: *Chilotherium schlosseri* (originally described as *Teleoceras ponticus*)

A partial skull (Fig. 20D) from the Upper Miocene deposits of Odessa in Ukraine was described by Niezabitowski (1912, 1913) as *Teleoceras ponticus*, but later attributed to *C. schlosseri* by Kiernik (1913), which was further supported by Krokos (1917). The synonymy of *C. ponticum* and *C. schlosseri* is rather well established and has not been challenged by anyone since Kiernik (1913). It is herein further supported by the fact that nasals are clearly depressed in a similar manner to *C. schlosseri*, a feature not observed in any other chilotheres.

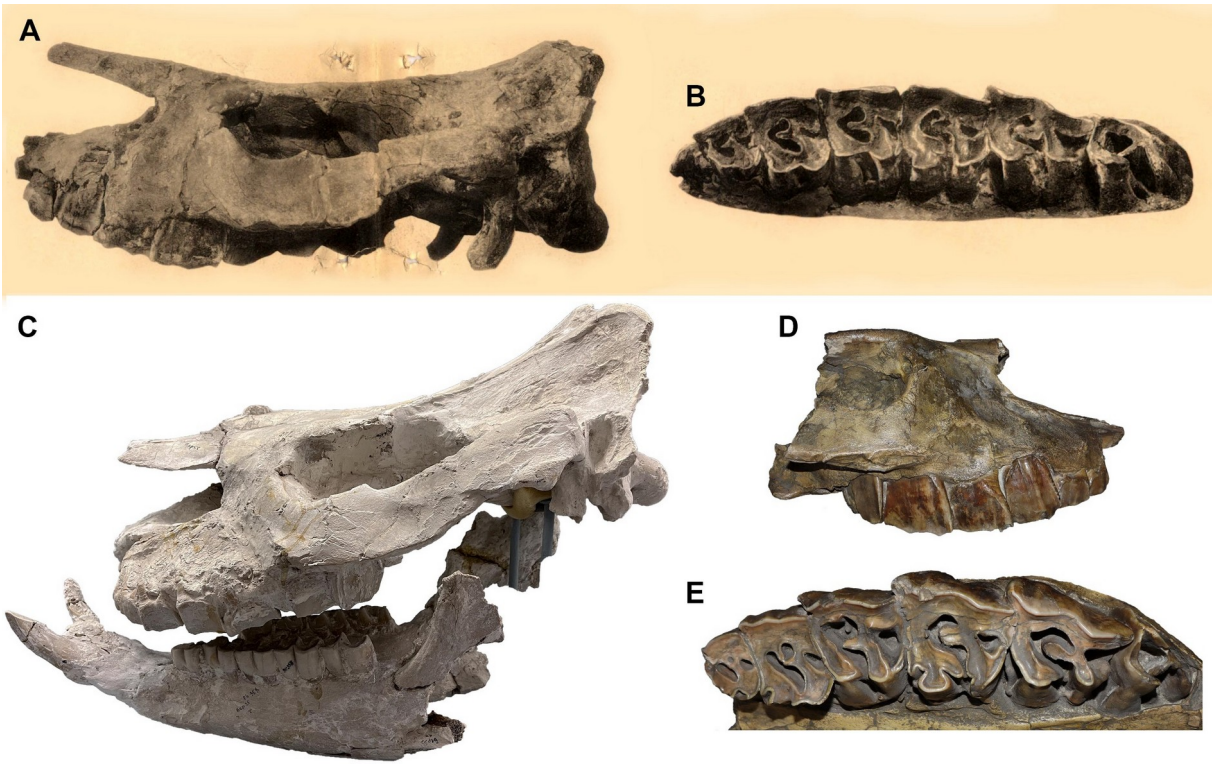


**Figure 20.** Skulls of the Ukrainian chilotheres. A–B, Skull (A) and upper dentition (B) of *Chilotherium kowalevskii* (Pavlow, 1913) from the Upper Miocene of Grebeniki (Ukraine); C, Holotype skull of *Chilotherium sarmaticum* Korotkevitch, 1958 from the Upper Miocene deposits of Berislav in Ukraine (courtesy of L. Gorobets); and D–E, Holotype skull and upper

dentition of *Teleoceras ponticus* Niezabitowski, 1912, now *Chilotherium schlosseri* (Weber, 1905), from the Upper Miocene of Odessa in Ukraine. Not to scale.

Berislav

Age: Late Miocene, Vallesian age (Vangengeim and Tesakov, 2013)

Taxa: *Chilotherium sarmaticum*

Korotkevitch (1958) erected *C. sarmaticum* based on a fairly complete skull with its mandible (Fig. 20C) from the Upper Miocene of Berislav in Ukraine. An ample collection of additional material of *C. sarmaticum* was also described in detail including cranial, dental, and postcranial elements from Berislav (Korotkevich, 1970). This material showed that *C. sarmaticum* is characterised by widely separated parietal crests and relatively small postcranial elements. Despite the rich available material of the species, it was neglected for many years and not used in comparative studies and even missing in the revisions of the genus (Heissig, 1975; Deng, 2006); therefore, the potential synonymy of this species has not been investigated. The widely separated parietal crests are a rare feature in chilotheres, otherwise only known in *C. schlosseri*. However, the relationship of *C. sarmaticum* to *C. schlosseri* is unknown, it only known that while relatively widely separated, the valued range of the minimal distance between the parietal crests is lower than *C. schlosseri* and should thus represent a distinct species.

### 1.6.3. Turkish chilothere localities

A plethora of Upper Miocene fossil localities exist in Türkiye that have yielded very rich fossil records of the mammalian communities during this time period. Many of these localities record also the presence of chilotheres. However, due to their taxonomic complexity the collected material belonging to this group has generally been neglected. Heissig (1975) studied a rich collection of Late Miocene rhinoceroses from several localities across Anatolia and provided a short overview of their taxonomy and biostratigraphy (Fig. 21). A major part represents the study of the chilothere material from these localities and the revision of their taxonomy, without any detailed discussion on the diagnostic characters, though.

In total, Heissig (1975) found that chilotheres were present at more than 15 localities. At these localities he suggested the presence of four different chilothere species, excluding *Subchilotherium intermedium* and *Acerorhinus zernowi*, which he included in the genus *Chilotherium*, though under different subgenera (Heissig, 1975). However, the fact that he did not provide any descriptions or illustrations of the material makes it impossible to verify the identifications and place them in the currently accepted taxonomic scheme for the chilotheres. Since then, some studies have provided information of chilotheres from other specific localities in Anatolia, such as Çorakyerler, where Geraads (2013) suggested the presence of either *Chilotherium* or *Acerorhinus*, based on ample cranial, mandibular and postcranial material. He discussed the previously suggested attribution of the material to *C. kowalevskii* and while finding significant similarities with its' teeth, the differences in the morphology of the skull and mandible led him to suggest that the material most probably belongs to a new species of *Acerorhinus*. The cranial morphology of *C. kowalevskii* seems to vary within the Grebeniki sample (Pavlow, 1913; Krokos, 1917). Therefore, an attribution to this species might still be plausible, but needs to be re-examined. Until then, the material is best referred to as *Chilotherium* sp.

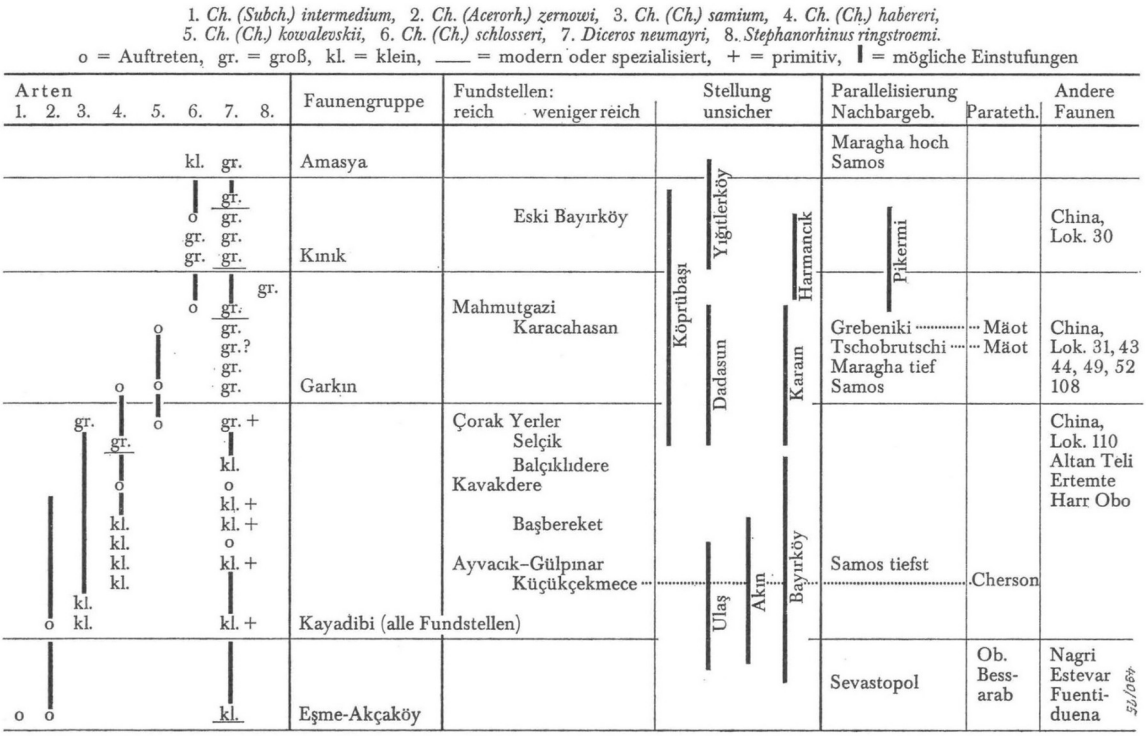


**Figure 21.** Table summarising the evolution of the rhinoceros assemblage in Anatolia compared with Europe and East Asia during the Late Miocene (taken from Heissig, 1975, tab. 7).

A rich collection of rhinoceros material from the Sinap region was studied and the presence of two different chilothere taxa was suggested, along with additional material from different fossil sites in the region that was not possible to be identified (Fortelius et al., 2003). An isolated m3 and a partial juvenile mandible from Loc. 49 were attributed to *C.* cf. *habereri*, a species that otherwise is only found in China (Schlosser, 1903; Killgus, 1923; Ringström, 1924). Lower teeth are generally not at all diagnostic within the chilotheres, and even complete mandibles can usually not be identified. This is also the case with these two specimens from Loc. 49. It is stated that the material is very hypsodont, and the mandible seems to somewhat widened anteriorly, though being broken a few centimetres in front of the d2. These features indicate an attribution to a chilothere, but further identification is possible. Several other specimens from the same fossil site (Loc. 49) were attributed to *Chilotherium kiliasi* (Fortelius et al., 2003), which herein is considered a junior synonym of *E. samium*. The relatively plesiomorphic dental morphology seen in the Loc. 49 material in combination with a mandible that bears a wide symphysis with large incisors makes an attribution of the material to *E. samium* plausible. However, a revision of this material is necessary to verify this hypothesis. The rest of the chilothere material from Sinap was not assigned to any species and instead much of the material was labelled as *Chilotherium* indet. (Fortelius et al., 2003), which was probably the best choice, because isolated and fragmented elements are almost impossible to be identified. The remaining material was referred to as "*Chilotherium* sp. (primitive)" (Fortelius et al., 2003). This identification is at least in some cases problematic, because some specimens are not diagnostic like some isolated dental and postcranial elements from Loc. 72 and 51. An interesting case is presented with an associated forelimb from Loc. 12. This specimen exhibits a fully functional fifth metacarpal (Fortelius et al., 2003, fig. 12.15A-B), whereas chilotheres have a highly reduced fifth metacarpal (Kampouridis et al., 2025). Instead, this specimen is morphologically relatively similar to *Aceratherium incisivum* from Höwenegg in Germany (Hünermann, 1989). However, until the material is revised it should be referred to as Aceratheriinae indet.

From the area of Kemiklitepe, several fossil sites have yielded a rich Late Miocene (Turolian age, MN11 and MN12) fauna (Sen et al., 1994). Amongst this material, Geraads (1994) reported several chilothere specimens, including both dental and postcranial elements. This material came primarily from the fossil site Kemiklitepe D (KTD) and was assigned to *C.* aff. *persiae*. The material was mainly compared to *C.*

*persiae* from Maragheh and the comparisons to other species like *C. anderssoni* and *C. schlosseri* were less significant (Geraads, 1994). Further, the material includes mainly isolated remains, and the most complete specimen is a partial mandible. A described third metacarpal is extremely small (L = 110 mm?) and is in fact smaller than any reported chilothere so far (compare to Krokos, 1917; Korotkevich, 1970; Deng, 2002; Kampouridis et al., 2025). However, the lack of a skull makes an identification almost impossible, and the material as a whole should be assigned to *Chilotherium* sp. An additional specimen comes from Kemiklitepe B (KTB) and was assigned to *Chilotherium* sp. (Geraads, 1994).

The Upper Miocene (Turolian age, MN12) locality of Akkaşdagi has also yielded a rich mammalian fauna that was studied in much detail (Kazanci et al., 2005). Antoine and Saraç (2005) described the rhinoceros material from the locality and reported a calcaneus that they assigned to *Chilotherium* sp., which seems plausible considering the morphology of the isolated postcranial element.

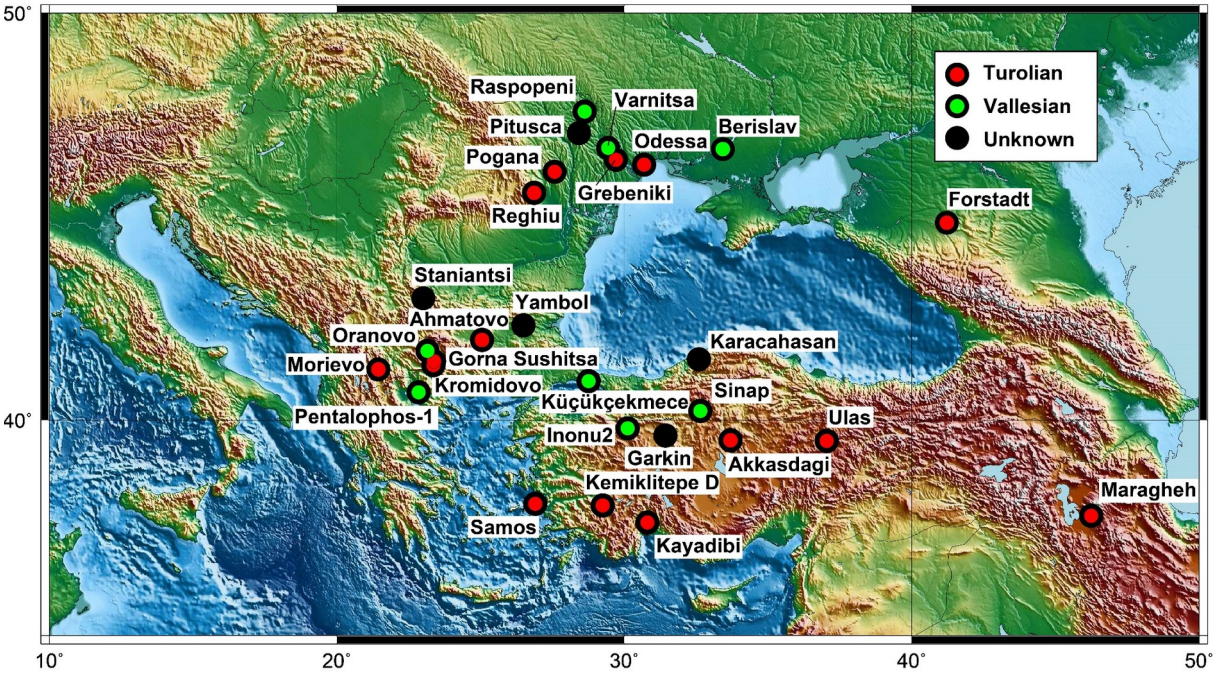


**Figure 22.** Topographical map of the Eastern Paratethys region showing the Upper Miocene localities that have yielded material assignable to a chilothere.

Most recently, Antoine and Sen (2016) studied the rhinoceros and chalicotheres from the Upper Miocene (late Vallesian age, MN 10) locality of Küçükçekmece and reported several isolated dental and postcranial elements of *C. schlosseri*. However, due to the taxonomic difficulties of the genus and the fact that the

material from Küçükçekmece is very limited it would be best to refer this material to *Chilotherium* sp.

# 2. Material and Methods

## 2.1. Material

For the purpose of this dissertation, I studied rhinoceros' material from different species and localities that were housed mainly in European collections. More specifically, the initial focus was to reevaluate the chilothere material of the historical excavations on Samos Island (Greece). This material is distributed in collections all over Europe and I studied this material in many of these institutions (i.e., AMPG, GMM, GPIH, GPIT, HLMD, IPUW, MGL, MNHN, NMB, NHMW, SMF, SMNS, SNSB-BSPG, UCBL-FSL). Many of these collections did not house any chilothere material and much of the material studied included fragmentary, either dental or postcranial, elements. Nonetheless, in the end I was able to study in total nine fairly complete chilothere skulls in person, and another two were studied based on photos provided by colleagues (AMNH – courtesy of N. Kargopoulos, and MGP-PD – courtesy of L. Pandolfi). This allowed the revision of the chilotheres of Samos, *C. schlosseri* and *E. samium*. In many of these institutions, which housed Samos material, also chilothere material from other localities were housed, such as Maragheh (Iran) at the IPUW, MNHN, and NHMW or material from different localities of China at the GPIT and SMF. This allowed me to also study the anatomy of *C. persiae* from Maragheh, *C. habereri* from Kutschwan and *C. anderssoni* from Daijiagou.

The initial goal was to revise the cranial and dental anatomy of the Samos chilotheres (Kampouridis et al., 2022b, 2023; Svorligkou et al., 2025). However, during the course of the project, it was adjusted to incorporate also other chilothere species and involve also the postcranial anatomy (Kampouridis et al., 2025) and juvenile cranial and dental morphology (Kampouridis et al. in prep.). Additionally, it was even expanded to include the revision of some other rhinocerotid taxa, such as the elasmotheriine *Parelasmotherium* (Kampouridis et al., 2022a). Material of several non-chilothere rhinoceroses housed in the same and additional collections were studied, including the hornless rhinos *Shansirhinus ringstromi*, *Aceratherium incisivum*, *Acerorhinus neleus*, *Persiatherium rodleri*, and *Hoploaceratherium tetradactylum* (Lartet, 1837), and the horned rhinos *Ceratotherium neumayri*, *Dihoplus pikermiensis*, *Dihoplus megarhinus* (de Christol, 1835), *Iranotherium morgani*, and *Parelasmotherium schansiense*.

## 2.2. Methods

### 2.2.1. Measurements and anatomical nomenclature

The measurements of cranial, dental, and postcranial elements were taken based on Guérin (1980) and Peter (2002). Despite the very detailed measurement protocol provided by Guérin (1980), some additional measurements were taken in some cases, especially in some postcranial elements (Kampouridis et al., 2025). It has to be mentioned that the literature before the 1980s did not follow a specific measurement protocol; therefore, the measurements in the older literature was not always taken in the same way. This is especially unfortunate, when studies such as Krokos (1917) and Korotkevitch (1970) are compared. These studies provide detailed measurements for basically all postcranial elements of *C. kowalevskii* from Grebeniki and *C. sarmaticum* from Berislav (both Ukraine). Even the exact translation of each measurement, which were provided in Russian, can already be rather tricky, and then the fact that many measurements have similar names but were actually measured in a slightly different way makes detailed comparisons sometimes impossible. This is especially problematic in more complicated bones such as carpals and tarsals.

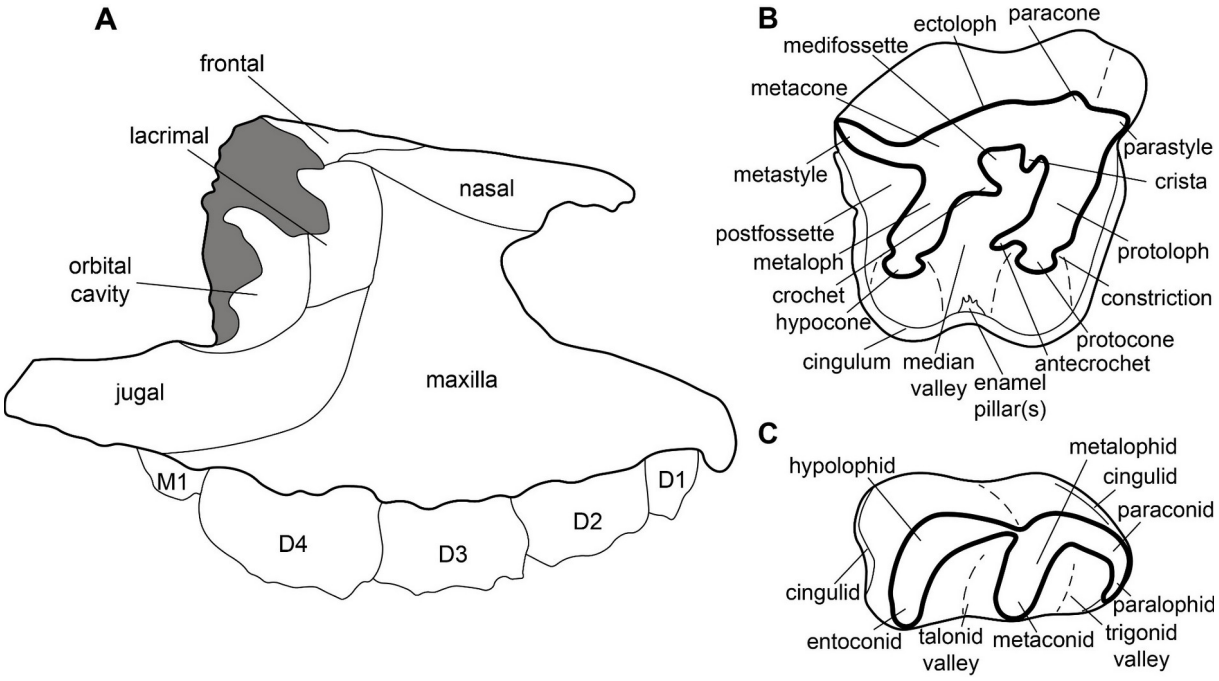


**Figure 23.** Anatomical nomenclature. A, Juvenile skull of *Chilotherium persiae* (Pohlig, 1885) from the Upper Miocene of Maragheh in Iran in lateral view; B, Upper molar; and C, lower molar in occlusal view showing the anatomical nomenclature used in this study. Not to scale.

The anatomical nomenclature of the described cranial, dental, and postcranial elements (Fig. 23) follows previous studies (e.g., Getty, 1975; Guérin, 1980; Antoine, 2002; Barone, 2010; Heissig, 2012; Mallet et al., 2019). More specifically, the cranial anatomy mainly follows Guérin (1980) and Antoine (2002), the dental anatomy follows Peter (2002), and postcranial anatomy follows mainly Guérin (1980) and Mallet et al. (2019).

### 2.2.2. Phylogenetic analysis

In order to assess the phylogenetic affinities of *Parelasmotherium schansiense* from the Upper Miocene of Kutschwan (China) a phylogenetic analysis was performed. I modified the character-taxon matrix of Sun et al. (2022), which modified the matrix of Deng (2008) by adding *Elasmotherium primigenium*, which is based on the matrix of Antoine (2002). I also added *Eoazara xerrii* Geraads and Zouhri, 2021 to the matrix, based on Geraads and Zouhri (2021) but removed the 32 new characters added by Lu (2013) to the matrix of Antoine (2002). '*Parelasmotherium*' *simplum* was scored based on published figures (Chow, 1958; Qiu and Xie, 1998) and *P. schansiense* was rescored based on the holotype (GPIT-PV-86051) studied herein. The final matrix includes 282 characters and 33 taxa; it is available in Kampouridis et al. (2022a, supplementary data 1) and at MorphoBank under http://morphobank.org/permalink/?P4228. The phylogenetic analysis was performed with TNT version 1.5 (Goloboff et al., 2008). All characters were unordered. The matrix was analysed using 'traditional search' (1000 replications), hold = 10, and random seed = 0, followed by tree bisection-reconnection. The analysis resulted in two most parsimonious trees with a length of 1101 steps. A strict consensus tree and decay values (Bremer support) were obtained using the implemented functions in TNT. Consistency (CI) and Retention indices (RI) were calculated for the whole tree (CI = 0.351 and RI = 0.543) using the script available in TNT.

### 2.2.3. Enamel Hypoplasia

Enamel hypoplasia is a defect in the development of the teeth, leading to the malformation of the enamel in part of a tooth and presents a unique marker for high levels of stress in an individual (e.g., Goodman and Rose, 1990; Guatelli-Steinberg,

2001; Hullot et al., 2021; Hullot and Antoine, 2022). Herein we studied enamel hypoplasia in deciduous teeth of four *Chilotherium* species. For this purpose, the hypoplasias in deciduous premolars, upper and lower second (d/D2), third (d/D3), and fourth (d/D4) premolars were investigated. In total, 149 teeth were studied. If hypoplasia appeared on the same tooth position on both sides, it was counted as a single occurrence. Teeth with damaged enamel or those that had not fully erupted were excluded from this study. Additionally, in some cases where some teeth from Kutschwan and Samos had not fully erupted, the respective specimens were CT-scanned, as proposed by Hullot and Antoine (2022), to investigate the occurrence of a potential hypoplasia (Fig. 24C–D).

### 2.2.4. µCT-scanning

To study the internal tooth and bone morphology in detail in different specimens, micro-computed tomography (µCT) scans were acquired with a Nikon XTH 320 µCT scanner operated by the 3D Imaging Lab at the Eberhard Karls University Tübingen and Senckenberg Centre for Human Evolution and Palaeoenvironment Germany (SHEP). An X-ray tube containing a multi metal reflection target with a maximum acceleration voltage of 225 kV was used in all scans. These scans are parts of two different projects within the frames of this Dissertation:

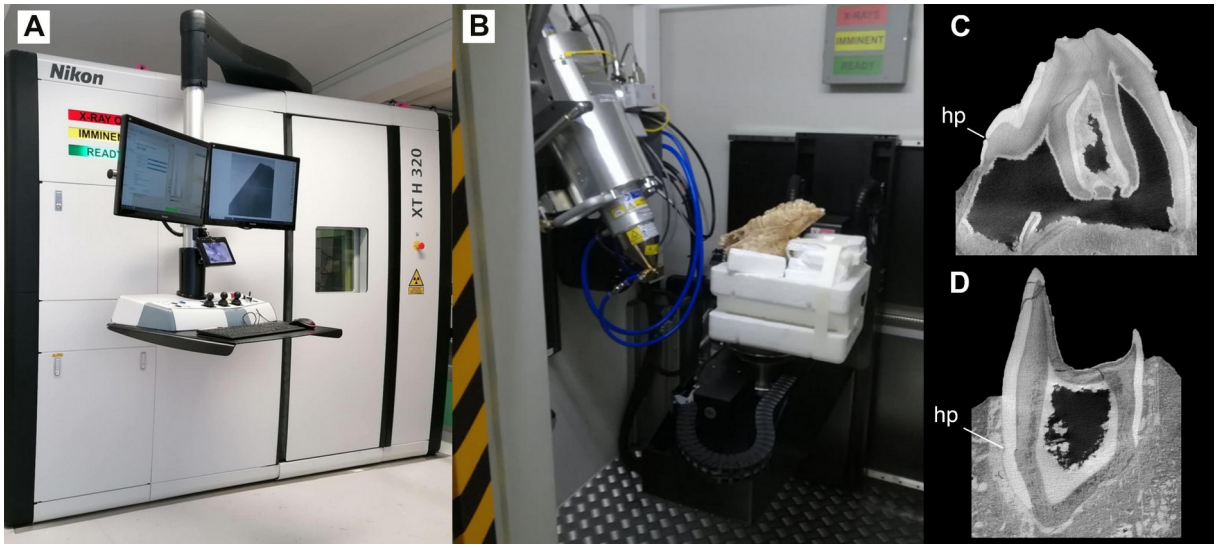


**Figure 24.** µCT-scanning of the specimens. A, Nikon XTH 320 µCT scanner at the University of Tübingen; B, Juvenile skull (GPIT/MA/04842) of *Chilotherium habereri* (Schlosser, 1903) from Kutschwan (China) being scanned in the aforementioned MCT-scanner; C, Virtual cross-section of the D4 of the same specimen (GPIT/MA/04842); and D, Virtual cross-section of the

d4 of a juvenile mandible (GPIT/MA/04849) of *Chilotherium habereri* (Schlosser, 1903) from Kutschwan (China). Abbreviation: hp, linear enamel hypoplasia. Not to scale.

*Parelasmotherium schansiense* tooth morphology

The holotype teeth of *P. schansiense* were µCT-scanned, more specifically the articulated D4, P4, and M1 were scanned at 220 kV and 140 µA with a voxel size of 0.05932821 mm, using a copper filter of 0.5 mm thickness. The isolated M2 of the same specimen was scanned at 220 kV and 190 µA with a voxel size of 0.05002721 mm, with the same copper filter. Images were processed using VG Studio Max. The results are virtual orthoslices of the actual teeth (Kampouridis et al., 2022a, fig. 2). The scans are available on MorphoSource (https://www.morphosource.org/) under the following IDs: Media ID—000415992 (D4, P4, and M1) and 000416854 (M2).

Hypoplasias in chilotheres

Several juvenile crania, mandibles, and isolated deciduous teeth of *C. habereri* from Kutschwan (China) and *C. schlosseri* from Samos (Greece) were also µCT-scanned for the purpose of studying the linear enamel hypoplasias that, in most case, were observed on the external surfaces of the teeth. The specimens were scanned at different kV and µA values with different metal filters depending on the specific element. Images were processed using VG Studio Max and the results are virtual orthoslices of the actual teeth. The scans will be made available on MorphoSource (https://www.morphosource.org/) upon publication under the Project ID 000840545.

### 2.2.5. Surface Scanner

To directly compare specimens housed in different institutions and to confirm the morphological traits of the studied specimens that may help to differentiate the chilothere species, I acquired surface scans for 66 chilothere specimens and a large number of additional rhinoceros' specimens. Three-dimensional surface data were acquired using an Artec Space Spider structured light scanner and initially processed in the software Artec Studio (versions 14 and 19). The scanner and the software were provided by the 3D Imaging Lab of the Senckenberg Centre for Human Evolution and Palaeoenvironment (SHEP) and the Eberhard Karls University of Tübingen, Germany and were used during several collection visits. The 3D models of the neotypes of

*Chilotherium schlosseri* (GPIH 3015) and *Eochilotherium samium* (SMF M 3601) are available on MorphoSource (https://www.morphosource.org/) under the Project ID 000521964.

# 3. Results and Discussion

This section presents summaries of the results on the systematics of the extinct hornless rhinoceros *Chilotherium* and other extinct rhinoceroses of the Late Miocene, divided into subsections based on the respective published article (9.1–9.5) or submitted manuscript (9.6). The publications are attached in the appendix below (Appendix 1–6).

## 3.1. Reassessment of '*Chilotherium wegneri*' (Mammalia, Rhinocerotidae) from the late Miocene of Samos (Greece) and the European record of *Chilotherium*

The first step during the course of this dissertation was to get an overview of the European fossil record of the genus *Chilotherium* and identify the specific problems that affect its taxonomy. Therefore, we provide in this publication a literature review of the fossil record of *Chilotherium* in Europe, in addition to reevaluating the holotype of the species *Chilotherium wegneri*. This species was erected by Andree (1921) based on a complete skull and its mandible (Fig. 25) from the Upper Miocene deposits of Samos in Greece over a century ago. The holotype is part of a fairly large collection of fossils from Samos that was excavated by T. Wegner during a 3-month campaign in 1909 (Andree, 1926). This material was then brought to Münster in Germany, where it remains part of the palaeontological collection of the GMM. The only parts of the collection that have been studied are the rhinoceroses, bovids and horses, which were published mainly during the first half of the 19$^{th}$ century (Andree, 1921, 1926; Wehrli, 1941). The collection has received very little attention in the last decades, despite it housing several holotypes. This also includes the holotypes of *Chilotherium wegneri* and *Chilotherium angustifrons*, which were originally established under the genus *Aceratherium* (Andree, 1921). It was Ringström (1924), who later on placed them in his new genus, *Chilotherium*, in which they have remained ever since, due to the clear shared morphological features, such as the wide mandibular symphysis with large tusk-like incisors in *C. wegneri*, along with the concave frontal region and the complicated enamel folds in both species. While cataloguing the types and published housed in the GMM, it was noted that the holotypes of both species have been lost, which is also the case for several other specimens from Samos housed in the GMM (Meiburg and Siegfried, 1970). However, the type mandible of *C. wegneri* (Fig. 26) was

found in 2019 by the curator of the collection, Dr. Markus Bertling, and his student, Denis Theda. Unfortunately, the skull is still missing, neither M. Bertling, nor Dr. Steffen Trümper, the current curator of the collection, were able to find it. During a visit to Münster in December of 2023, I was also able to confirm that the type skulls of both *C. wegneri* and *C. angustifrons* are not among the specimens in the Samos collection of the GMM. Several other important specimens from Samos that were housed in the GMM are also considered lost, including holotypes and complete skulls.

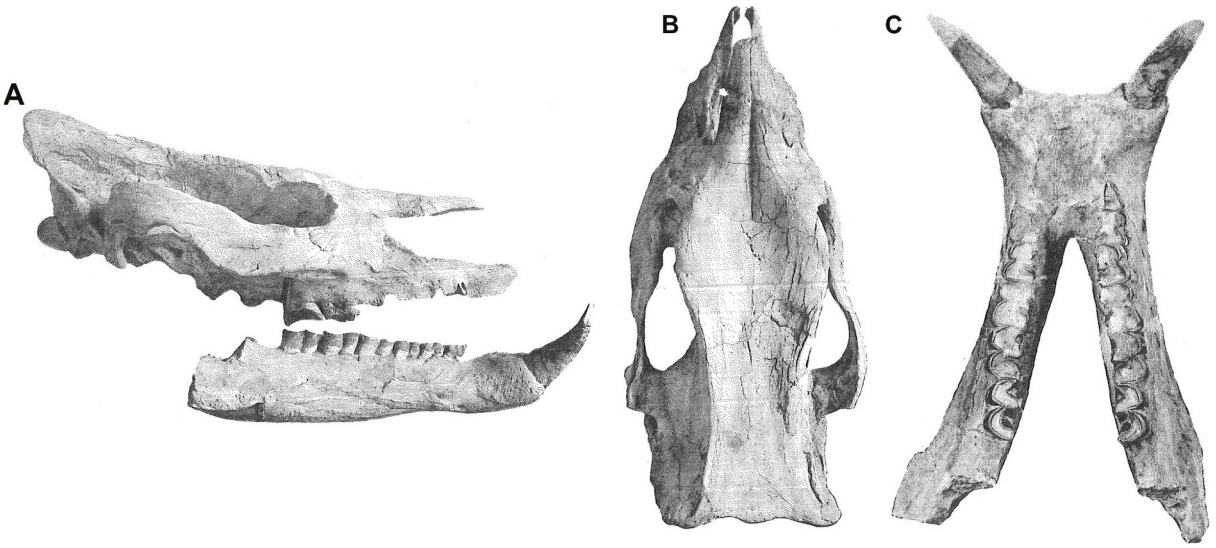


**Figure 25.** Holotype skull and mandible of *Aceratherium wegneri* Andree, 1921 in right side (A: both skull and mandible) and dorsal (B: skull and C: mandible) views (modified after Andree, 1921, tab. 1). Not to scale.

The discovery of the lost mandible of *C. wegneri* (GMM 567) along with the original illustrations and description, however, allowed us to revise this species, along with *C. angustifrons* and propose that both species are synonymous with another species from the Upper Miocene of Samos, *Chilotherium schlosseri*. More specifically, all three species feature the strongly depressed frontal region that also affects the position of the nasal bones. Additionally, the nasal bones feature a longitudinal groove in the middle and most importantly, at least in the type skulls of *C. wegneri* and *C. schlosseri*, it is visible that the parietal crests are very widely separated, more so than in any other chilothere species. This can now be regarded as a clear diagnostic feature for the species *C. schlosseri*, in which the parietal crests are always more than 70 mm apart in adult individuals. Unfortunately, in the holotype of *C. angustifrons* the right parietal region of the skull is completely lacking, and it is not possible to measure the distance between the parietal crests. However, *C. angustifrons* also shares a very complicated

dental morphology with *C. schlosseri*, like the very quick lingual closure of the median valley at a very early wear stage and the presence of a closed medifossette. Therefore, both *C. wegneri* and *C. angustifrons* represent junior synonyms of *C. schlosseri*.

The validity of the chilotheres erected by Andree (1921), *C. wegneri* and *C. angustifrons*, has been a matter of discussion with some researchers suggesting that the former is a junior synonym of *C. schlosseri* and the latter a junior synonym of *C. kowalevskii* (e.g., Heissig, 1975; Giaourtsakis, 2003; Deng, 2006), which is otherwise only known from Ukraine. This debate is just a small part of the confusion surrounding the European chilotheres, which include in total ten erected species.

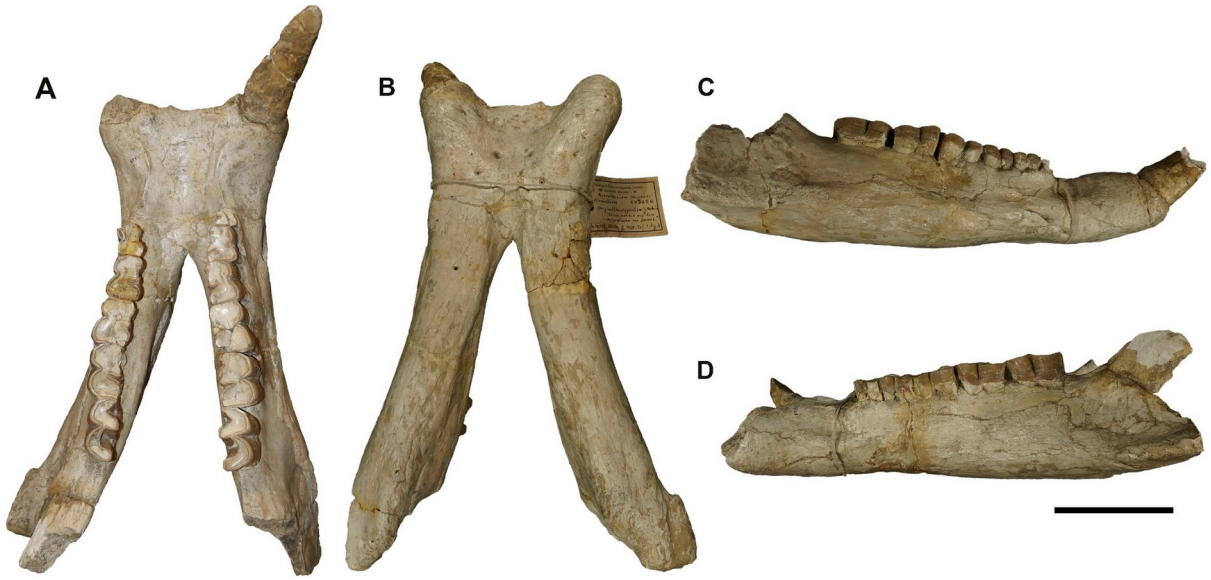


**Figure 26.** Type mandible of *Aceratherium wegneri* Andree, 1921 (GMM 567; now *Chilotherium schlosseri*) in dorsal (A), ventral (B), right lateral (C), and left lateral (D) view. Scale bar is 10 cm.

The first two species that come from Europe and were later attributed to *Chilotherium*, are *C. schlosseri* and *E. samium*, which were described by Weber (1905) based on skulls from the Upper Miocene of Samos Island (Greece). Both of these species have a complicated taxonomic history, with many suggested synonymities. Their type material was housed in the palaeontological collections of Munich and were destroyed during the Second World War (e.g., Giaourtsakis, 2003, 2022).

The next species that was erected based on material from Europe and was afterwards assigned to the genus *Chilotherium* is *Teleoceras ponticus*. This species was based on a partial skull from Upper Miocene sediments at Odessa (Ukraine). Shortly after its original description (Niezabitowski, 1912, 1913), the species was

synonymised with *C. schlosseri* from Samos (Kiernik, 1913). The status of this species has remained as such ever since (Heissig, 1975; Deng, 2006), without any further debate about a potential validity of the species.

Shortly after, *C. kowalevskii* was erected based on a rich collection of chilothere material from the Upper Miocene of Grebeniki in Ukraine (Pavlow, 1913). This material includes both cranial and postcranial elements, though the postcranial material was not describe din much detail when the species was first described (Pavlow, 1913). Later, Krokos (1917) revised the species, described the postcranial material and provided measurements, and synonymised it with *C. schlosseri* from Samos (Greece).

Over half a century later, *C. sarmaticum* was described based on a skull with an associated mandible from the Upper Miocene of Berislav in Ukraine (Korotkevich, 1958). Additionally, a rich collection of postcranial elements was described, and it was shown that *C. sarmaticum* differs in the proportions of some postcranial elements such as the metapodials from *C. kowalevskii* from Grebeniki (Korotkevich, 1970).

The last chilothere species that has been described so far is "*Aceratherium kiliasi*", which was erected based on a several cranial and mandibular elements (Geraads and Koufos, 1990). It was later suggested that part of the material actually belonged to a member of the genus *Acerorhinus* and that the holotype represents a chilothere (e.g., Fortelius et al., 2003; Athanassiou et al., 2014).

## 3.2. Reappraisal of the Late Miocene elasmotheriine *Parelasmotherium schansiense* from Kutschwan (Shanxi Province, China) and its phylogenetic relationships

During the course of this Dissertation I also studied the chilothere material from the Upper Miocene locality of Kutschwan (China), which was part of the doctoral dissertation of Hugo Killgus (Killgus, 1922). The fossils was collected by Albert Tafel during a journey to China (Tafel, 1914; Killgus, 1922, 1923). Unfortunately, there are no details about the exact location of the fossil other than that it is in Shanxi Province and close to the Yellow River. Nonetheless, the material is fairly rich and Killgus (1922, 1923) studied the complete fauna of this locality, erecting several new taxa, like the huge-sized elasmotheriine *Parelasmotherium schansiense*. This species remained rather elusive, and its taxonomic affinities are somewhat unclear due to the fragmentary nature of its holotype. The holotype of this species consists only of a partial right tooth row, that includes the erupted D4, M1 and unerupted P4 and M2 (Fig. 27). The dental morphology could only be studied in the D4 and M1 thus far. However, the D4 is at a quite advanced wear stage and the M1 hast just started being worn; additionally, the M2 is completely unworn and filled with sediment, with no enamel folds visible and the P4 remains within the maxillary bone below the D4. Therefore, the information from simple observation of the specimen is extremely limited and has not been able to clarify the systematics of the species. To solve these issues, we decided to acquire µCT-scans of the holotype and study the dental morphology through virtual horizontal cross-sections at different levels of the teeth (Fig. 28). This enabled detailed descriptions of the teeth, the assessment of the variation of the enamel folds throughout each tooth's height and comparisons to the other suggested *Parelasmotherium* species and to other elasmotheriines in general.

More specifically, *P. schansiense* differs from '*P.*' *simplum* in having a much longer crista, lacking a crochet, and featuring enamel plications. The species '*P.*' *linxiaense* is more similar to *P. schansiense*, but nonetheless differ in the latter exhibiting a pseudometaloph, a stronger metacone fold and more prominent enamel plications. The species *P. schansiense* also differs from all other elasmotheriines in the development of the enamel folds. These results support that the other two suggested *Parelasmotherium* species, '*P.*' *simplum* and '*P.*' *linxiaense*, should be removed from *Parelasmotherium* and possibly be placed in their own genus/genera. However, in the

absence of any other available genus names, we decided to refer to them as "*Parelasmotherium*".

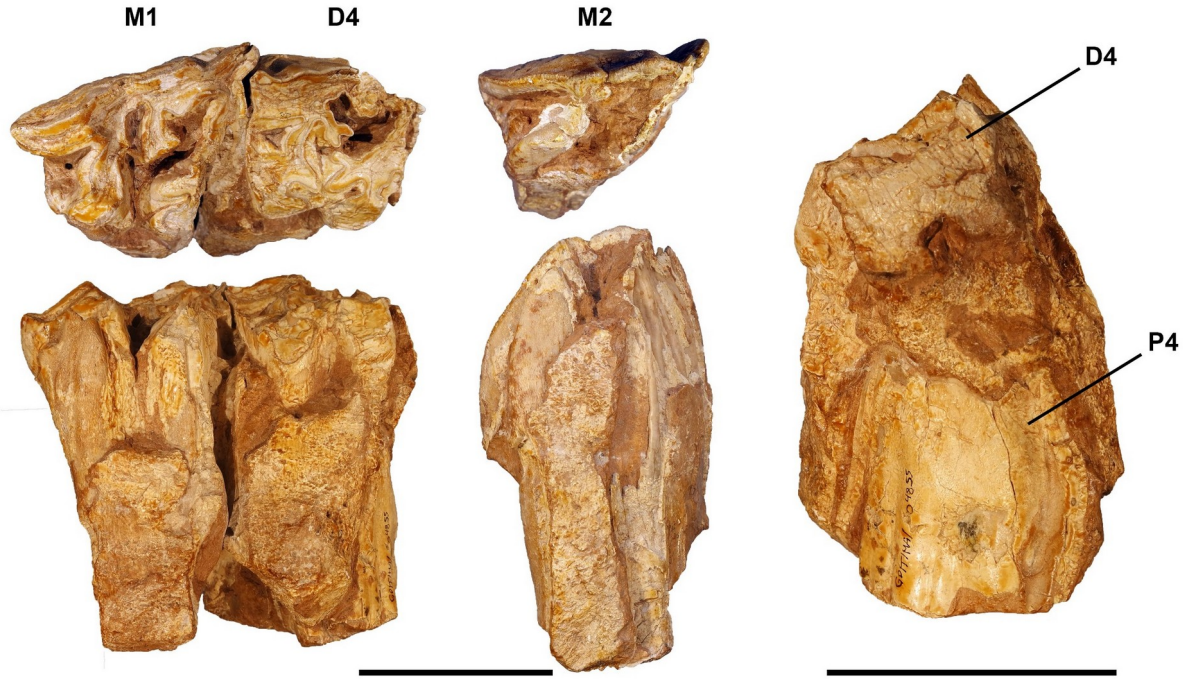


**Figure 27.** Holotype teeth of *Parelasmotherium schansiense* Killgus, 1923 from the Upper Miocene of Kutschwan (China). Scale bars equal 5 cm.

The new study of the material allowed us to also score many more characters for *P. schansiense* in the phylogenetic character-taxon matrix of Sun et al. (2022), which was modified from Deng (2008), which in turn represents a modified version of the classic rhinoceros matrix Antoine (2002). For the purpose of this study, we rescored *P. schansiense*, scored "*P.*" *simplum* based on the descriptions and figures in the literature (Chow, 1958; Qiu and Xie, 1998) and added the species *Eoazara xerrii*, based on the scorings of Geraads and Zouhri (2021). The results of the phylogenetic analysis support the hypothesis about the other two *Parelasmotherium* species representing other genera. More specifically, three suggested *Parelasmotherium* species are not recovered in a monophyletic clade. Instead, "*P.*" *simplum* and "*P.*" *linxiaense* are recovered in a more basal position and *Ninxiatherium longirhinus* is recovered as the sister to the clade including *P. schansiense*, *Sinotherium lagrelii* and *Elasmotherium* spp.

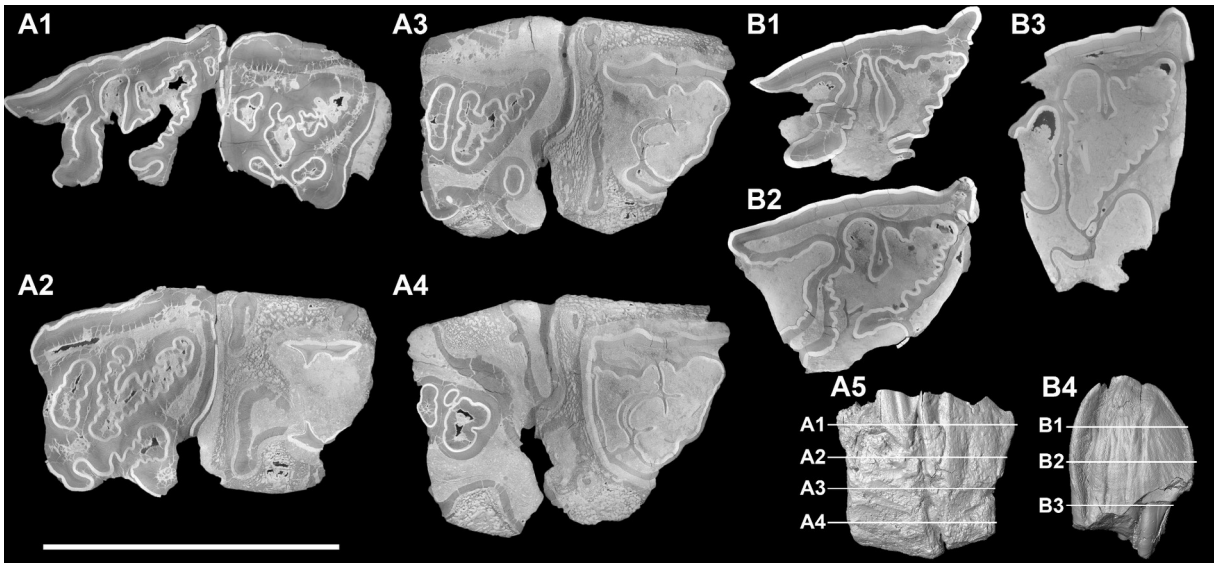


**Figure 28.** µCT-scan orthoslices of the holotype of *Parelasmotherium schansiense* Killgus, 1923 (GPIT-PV-86051) from the Upper Miocene of Kutschwan in China (modified after Kampouridis et al., 2022a, fig. 2). A, articulated right M1 and D4 (A1) or P4 (A2-4), in occlusal (A1–4) and buccal (A5) view; B, isolated right M2, in occlusal (B1-3) and buccal (B4) view. The virtual orthoslices are taken at different positions, as shown in A5 and B4, respectively. Scale bar equals 10 cm for A1–4 and B1-3 and 20 cm for A5 and B4.

### 3.3. Revision of the Late Miocene hornless rhinocerotids from Samos Island (Greece) with the designation of neotypes and implications for the European chilotheres

In this publication we were able to address the issues about the systematics of the Samian chilotheres, that had remained prevalent in the respective literature. This was achieved by designating neotypes for the two valid chilothere species from Samos, which are *Chilotherium schlosseri* (Weber, 1905) and *Eochilotherium samium* (Weber, 1905). The original type material of the two species comprised two well-preserved skulls that were housed at the collections of the BSPG (Weber, 1905). These skulls, along with the largest portion of the Samos material that was housed at the BSPG was destroyed during the Second World War (Giaourtsakis, 2022; Kampouridis et al., 2022b) when the Allied forces bombed Munich (Nothdurft and Smith, 2002). Thes loss of the type material significantly impacted the taxonomy of these two species, especially for *E. samium*, the validity of which has been rather controversial. There have been many assumptions about potential of the Samian species synonymities with other species such as *C. habereri*, *C. wegneri*, *C. angustifrons*, *C. kowalevskii*, and *Aceratherium kiliasi*. The synonymity of *C. schlosseri* and *C. kowalevskii* has been an often discussed topic (e.g., Krokos, 1917; Korotkevich, 1970; Antoine and Sen, 2016), even very recently (e.g., Țibuleac et al., 2023; Rivals et al., 2024). This demonstrates the need for resolving the taxonomy of the Samian chilotheres. For this purpose, I studied most of the still available chilothere skulls from Samos in person at the different institutions in which they are housed (AMPG, GPIH, HLMD, NMB, NHMW, and SMF) and studied the remaining two skulls through photographs that were kindly provided by colleagues (AMNH – courtesy of N. Kargopoulos, and MGP-PD – courtesy of L. Pandolfi). This allowed me to study the morphological variability and disparity seen in the available chilothere skulls from Samos; thereby enabling me to determine that there are two chilothere morphotypes in the Samos collection. The vast majority of chilothere skulls from Samos belong to *C. schlosseri* and only a single skull represents *E. samium*. To secure the stability of these two species for the future, enable detailed comparisons, and revise their diagnoses neotypes were designated. The best-preserved skull of *C. schlosseri* (GPIH 3015, Fig. 29A) and the only available skull of *E. samium* (SMF M 3601, Fig. 29B) were selected to represent the two species and were designated as neotypes based on the qualifying conditions set forth by the ICZN (Art. 75.3).

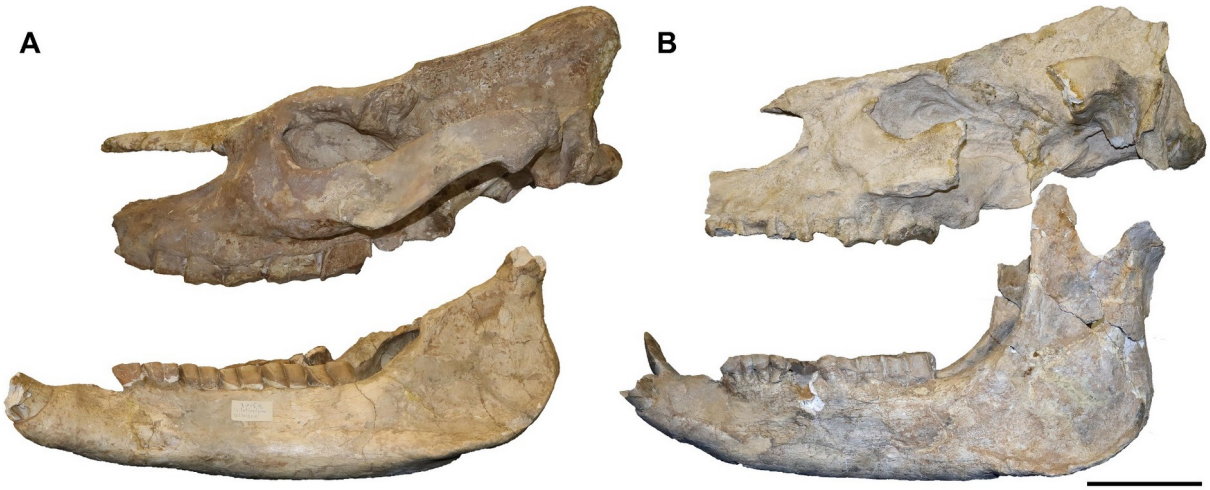


**Figure 29.** Neotypes of (A) *Chilotherium schlosseri* (Weber, 1905) and (B) *Eochilotherium samium* (Weber, 1905) from the Upper Miocene deposits of Samos Island (Greece). Scale bar is 10 cm.

Detailed comparisons of the two neotypes showed that the two Samian species significantly differ from each other in many cranial features (Fig. 30, Table 2). More specifically, *C. schlosseri* has a much wider and flatter skull, which is larger, whereas in *E. samium* the skull is much narrower and somewhat higher. Further, *C. schlosseri* has very widely separated parietal crests (>70 mm, n=12), whereas in the neotype of *E. samium*, while the relevant portion of the skull is a bit damaged, the parietal crest most likely were about 45 mm apart, similar to the measurement given for the lectotype. Other important features separating the two species are found in the occipital region, more specifically, the ridge that act as muscle attachments for the neck musculature have different shapes and positions in the two species: in *C. schlosseri*, the ridge are much broader, whereas in *E. samium* they are much more prominent and acute. Similarly, the occipital condyles are narrower and more angular in *E. samium*, whereas in *C. schlosseri* they are wider and more rounded. Other more minor features distinguishing between the two species include the somewhat thicker nasal bones, and the lack of a longitudinal groove in the middle of the nasal bones in *E. samium*, in addition to slightly narrower lower incisors, which are less flattened than in *C. schlosseri*. The comparison of the neotypes also showed that the upper molar morphology is quite similar between chilotheres; nonetheless, there were a few minor differences between the two Samian species that could be observed. More specifically, it seems that in *E. samium* the protocone is not as strongly constricted and that the

antecrochet is not as long. Thereby, the two Samian can clearly and easily be distinguished from one another.

**Table 2.** List of the most important morphological features differentiating *Chilotherium schlosseri* (Weber, 1905) and *Eochilotherium samium* (Weber, 1905) from the Upper Miocene deposits of Samos Island (Greece).

| | ***Chilotherium schlosseri*** | ***Eochilotherium samium*** |
|---|---|---|
| **1** | somewhat larger size | smaller size |
| **2** | relatively more brachycephalic | more dolichocephalic |
| **3** | wider skull | narrower skull |
| **4** | longitudinal groove on nasal bones | very weak or absent longitudinal groove on nasal bones |
| **5** | prominent depression in frontal bones | convex frontal bones |
| **6** | parietal crests widely separated | parietal crests moderately separated |
| **7** | zygomatic archs posteriorly widening | zygomatic archs constant width |
| **8** | dorsoventrally relatively compressed skull | dorsoventrally relatively higher skull |
| **9** | upper border of orbit at similar level to nasal bones | orbit positioned lower than nasal bones |
| **10** | wide occipital condyles | narrow and high occipital |
| **11** | dorsal incision in foramen magnum | dorsally rounded border of foramen magnum |
| **12** | deeper occipital fossa | shallow occipital fossa |
| **13** | lateral occipital crests broad and not marked | lateral occipital crests narrow and more pronounced |
| **14** | outer lateral crests subtle and rounded | outer lateral crests more prominent and longer |
| **15** | almost flat posterior part of the skull | raised posterior part of the skull |
| **16** | median valley closes early in premolars | median valley closes late or not at all |
| **17** | very strong constriction in premolars | weak or absent constriction in premolars |
| **18** | median valley closes at a moderate wear stage in molars | median valley closes late or not at all in molars |
| **19** | very strong constriction in molars | moderate constriction in molars |
| **20** | enamel plications present | enamel plications absent |

The magnitude of the observed differences surpasses the expected range for simple interspecific variation within the same genus. Also, *E. samium* lacks several key features of the genus *Chilotherium*, such as the depression of the frontal region and the wide skull that also flattened. Therefore, it is preferable to remove *E. samium* from *Chilotherium* sensu stricto. As was also previously suggested (Heissig, 1996; Giaourtsakis, 2022) and is further supported herein, *E. samium* represents the senior synonym of *Aceratherium kiliasi*, which was established based on material from the Upper Miocene of Pentalophos 1 (Greece). Later on, the subgenus *Chilotherium* (*Eochilotherium*) was established for the latter species. Herein, we use *Eochilotherium* at the genus level for the senior synonym of *Aceratherium kiliasi*, *Eochilotherium samium*.

These taxonomic revisions of the Samian species set the stage for a broader comparison among chilotheres. This comparison showed that *C. schlosseri* resemblance closer the classical *Chilotherium* representatives, being *C. anderssoni*,

*C. persiae*, *C. habereri*, *C. kowalevskii*, *C. sarmaticum*, and *C. orlovi*, and differ from the suggested “primitive” chilotheres, ‘*C*.’ *wimani* and ‘*C*.’ *primigenium*. In fact, the two “primitive” chilothere are much more similar to *E. samium*, as all three have slightly convex frontal region, fairly narrow and high skulls, and closely situated to only moderately separated parietal crests, contrasting the depressed frontal region, wide and flat skulls, and well-separated parietal crests in *Chilotherium* spp. Therefore, iit is suggested that ‘*C*.’ *wimani* and ‘*C*.’ *primigenium*, similar to *E. samium*, also do not represent *Chilotherium* sensu stricto and should be placed either in *Eochilotherium*, or in different genera. However, this matter needs to be resolved in a detailed revision of the two Chinese species and until then the two species will preliminarily be left in *Chilotherium* and referred to as ‘*Chilotherium*’ *wimani* and ‘*Chilotherium*’ *primigenium*.

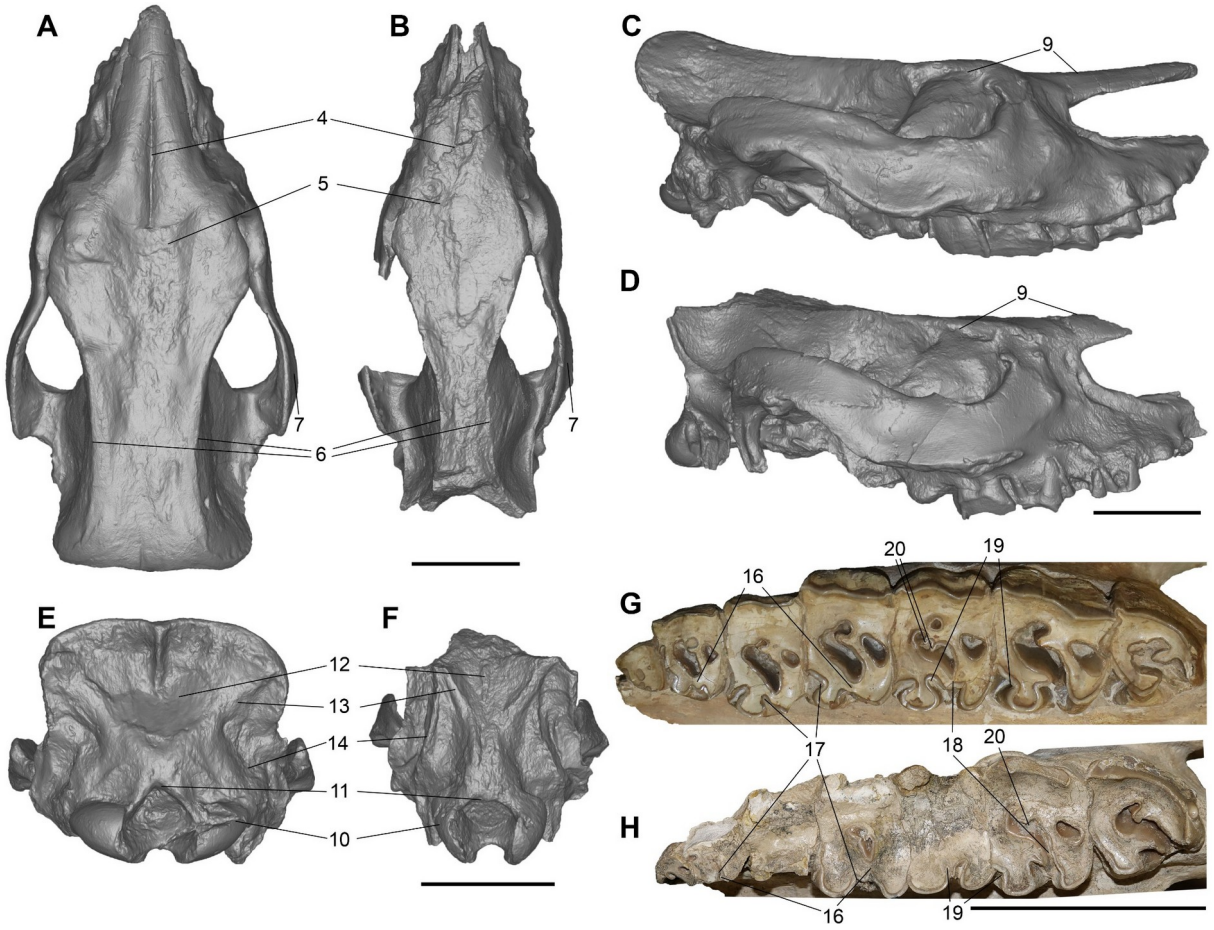


**Figure 30.** Comparison of the neotype skulls of *Chilotherium schlosseri* (Weber, 1905) (GPIH 3015) and *Eochilotherium samium* (Weber, 1905) (SMF M 3601) from the Upper Miocene of Samos Island (Greece). The numbers indicating the diagnostic features are given in Table 2. Scale bars equal 10 cm.

Lastly, based on these findings, the subtribe Chilotheriina, previously used at the tribe level, was comprehensively revised. This group has been used under variable schemes by

different authors. To make this group more useful for systematic works, the genus *Acerorhinus*, which differs from the other chilotheres and was erroneously included in the group, was removed. Based on features on the upper teeth and most importantly the wide mandibular symphysis, the genus *Eochilotherium*. Accordingly, a new diagnosis of Chilotheriina was established, to include the three genera *Chilotherium*, *Eochilotherium*, and *Shansirhinus*. This provides a coherent systematic scheme for this classical rhinoceros group that will be the foundation for subsequent comprehensive taxonomic and phylogenetic studies.

### 3.4. Craniodental anatomy of the hornless rhinocerotid *Chilotherium schlosseri* (Mammalia, Perissodactyla) from the Late Miocene of Samos Island, Greece

The next step was to understand the potential intraspecific variability chilothere may present, which has not been evaluated for any chilothere in the past. For this purpose we studied all available skulls of *C. schlosseri* from its type locality, Samos (Greece). This included a total of eight more or less complete skulls (Fig. 31) and four partial skulls. These specimens were housed in a number of different collections including AMNH, AMPG, GPIH, HLMD, MGP-PD NHMW, and NMB. The study of all these specimens and their comparison to the published skulls of *C. schlosseri* that have been lost (Weber, 1905; Andree, 1921) and cannot be directly studied anymore elucidated many morphological aspects about this species and further clarified its distinction from all other chilotheres, especially the sympatric *E. samium*.

The cranial features observed in the neotype (GPIH 3015) of *C. schlosseri* (Kampouridis et al., 2023) are consistent with the morphology of the other specimens, which suggests a pronounced intraspecific cranial uniformity. All studied skulls exhibit a strongly depressed frontal region that is more strongly concave than most other chilothere species and also affects the relative position of the nasal bones, which also seem to be depressed compared to the orbit. This feature is not seen in any other chilothere (e.g., Mecquenem, 1908a; Pavlow, 1913; Ringström, 1924; Korotkevich, 1958; Bayshashov, 1982; Deng, 2001b, 2006; Sun et al., 2018) and allows a very clear distinction of *C. schlosseri*. Additionally, the dorsal profile of the skull is almost completely straight with the skull being highly flattened, which is the case in all specimens. The nuchal crest is not at all raised, which is the case in chilotheres, including some *Chilotherium* species. Further, the nasal bones feature a deep longitudinal groove in all specimens and the nasal and the nasofrontal sutures remain unfused. Moreover, the parietal crests are always at least 70 mm apart in all adult specimens, which is a clear autapomorphic feature only seen in this species.

Only the teeth showed a relatively high degree of variability with the enamel folds varying depending on the specimen and the wear stage of the teeth. Although the enamel folds are generally very strong, they do seem to vary intraspecifically to some extent. However, even in the upper teeth there were several constant features observable in all teeth, some of which can be used for the identification of the species. For instance, both in the premolars and the molars, the crochet is quite strong and in

some specimens after moderate wear closes off the medifossette. Also, the premolars feature a discontinuous cingulum. But most importantly, *C. schlosseri* features more regularly enamel plications in the upper teeth, which are much more rarely observed in other *Chilotherium* species.

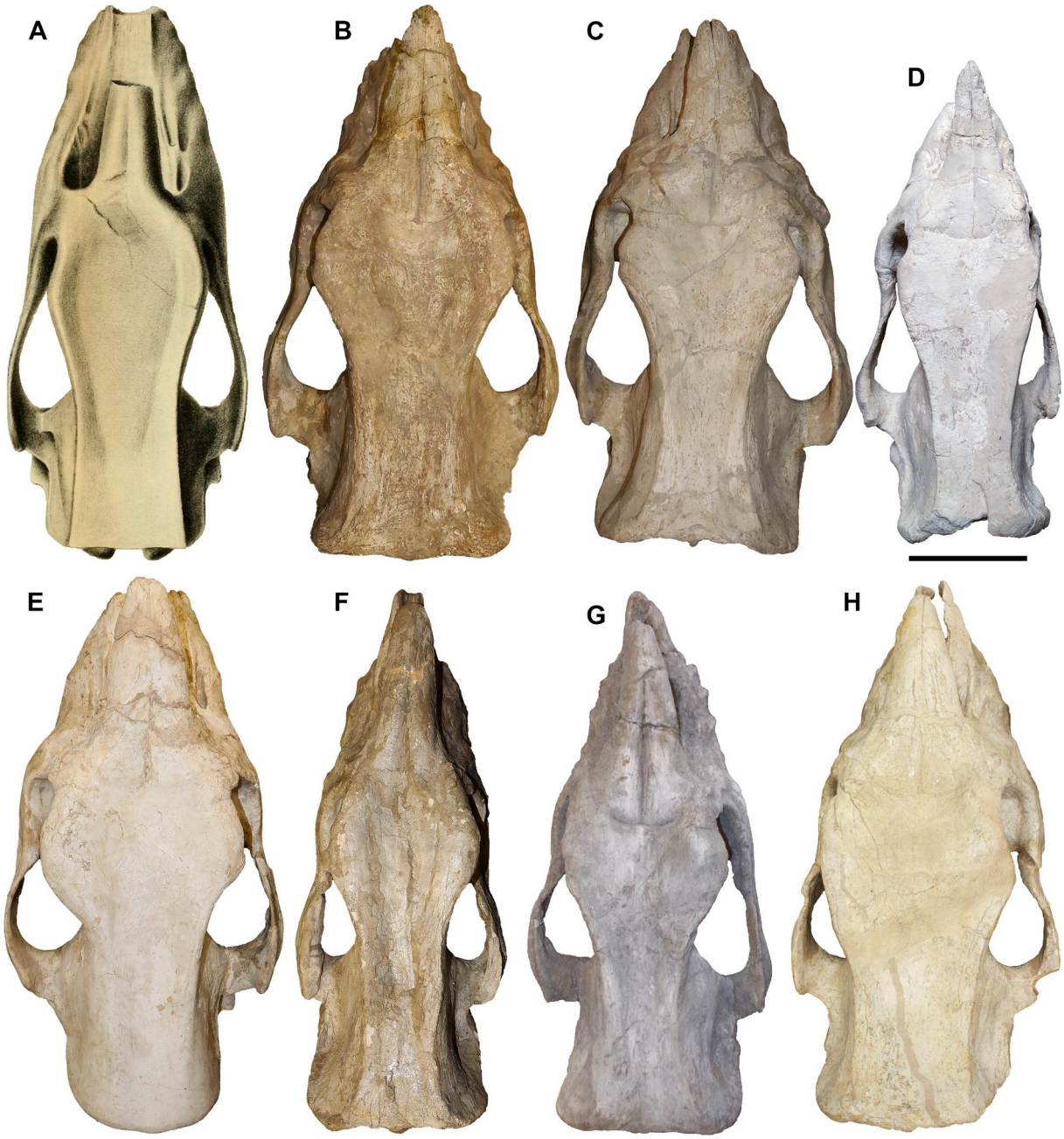


**Figure 31.** Comparison of the skulls of *Chilotherium schlosseri* (Weber, 1905) from the Upper Miocene of Samos Island (Greece). A, lectotype skull (modified after Weber, 1905, tab. 8, fig. 2); B, GPIH 3015 (neotype skull); C, NMB-Sam.25; D, NHMW-GEO-2009z0088/0001; E, HLMD-Sam192; F, NHMW-GEO-1911/0005/0128; G, MGP-PD 25302 (courtesy of L. Pandolfi); and H, AMNH 20794 (courtesy of N. Kargopoulos). Scale bar equals 10 cm for B–H, A is not to scale.

The comparison of all available cranial and mandibular specimens of *C. schlosseri* from its' type locality Samos shows that skull of the species is characterised by a high morphological uniformity. This further confirms assumptions about its morphology and taxonomic affinity of previous studies that were based on fewer specimens. Nonetheless, the teeth did exhibit a more pronounced degree of variation. This suggests that the skull morphology is a much better indicator for taxonomic studies than the dental morphology in chilotheres. These findings also provide important insight into the potential taxonomic affinities of the group in general.

## 3.5. Postcranial anatomy of the Late Miocene Eurasian hornless rhinocerotid *Chilotherium*

The postcranial material of chilotheres is neglected in most studies and if studied only basic descriptions with little comparison are provided. This adds to the issues about the taxonomy and phylogeny of these animals. Therefore, the purpose of this study was to describe new material of three *Chilotherium* species and compare with the specimens available in the literature and compile a revision of the postcranial anatomy of this group. One major issue that was addressed in the context of this study was that postcranial descriptions for three of the five chilothere species with documented postcrania were previously available only in Russian and another species only in German. More specifically, the initial description of *C. kowalevskii* was in French (Pavlow, 1913) that also included a short description of the postcranial material. A more analysis of the species, which also included more detailed descriptions of the postcranial material, was done a few years later and was in Russian (Krokos, 1917). For both *C. sarmaticum* and *C. orlovi* only Russian descriptions and comparison are available (Korotkevich, 1958, 1970; Bayshashov, 1982, 1993) and *C. anderssoni* was erected in German, including short descriptions of the postcranial material (Ringström, 1924), and no redescription exists.

The only species for which fairly detailed descriptions of the postcranium are available in English is '*C.*' *wimani*. Otherwise, descriptions of isolated postcranial elements have been provided by different researchers (e.g., Fortelius et al., 2003; Antoine and Sen, 2016; Spassov et al., 2019). However, there has not been any detailed study of the postcranial anatomy of chilotheres that was able to combine all existing information and metrical data for these species. This was, for the first time, attempted in this study and offered novel insight into the group's systematics.

Postcranial material of the following three chilothere species was studied: *C. persiae* from the Upper Miocene of Maragheh (Iran), *C. habereri* from the Upper Miocene of Kutschwan (China), and *C. schlosseri* from the Upper Miocene of Samos (Greece). In total, 210 postcranial elements of these species were studied in seven different collections (AMNH, AMPG, GMM, GPIT, MLU, MNHN, and NHMW). The vast majority of these specimens were isolated and not associated with any other skeletal elements. There were only few associated or articulated specimens, such as partial

tarsi of *C. persiae* from Maragheh in Iran (NHMW-GEO-2020/0014/0145) and *C. schlosseri* from Samos in Greece (AMPG-SAM516).

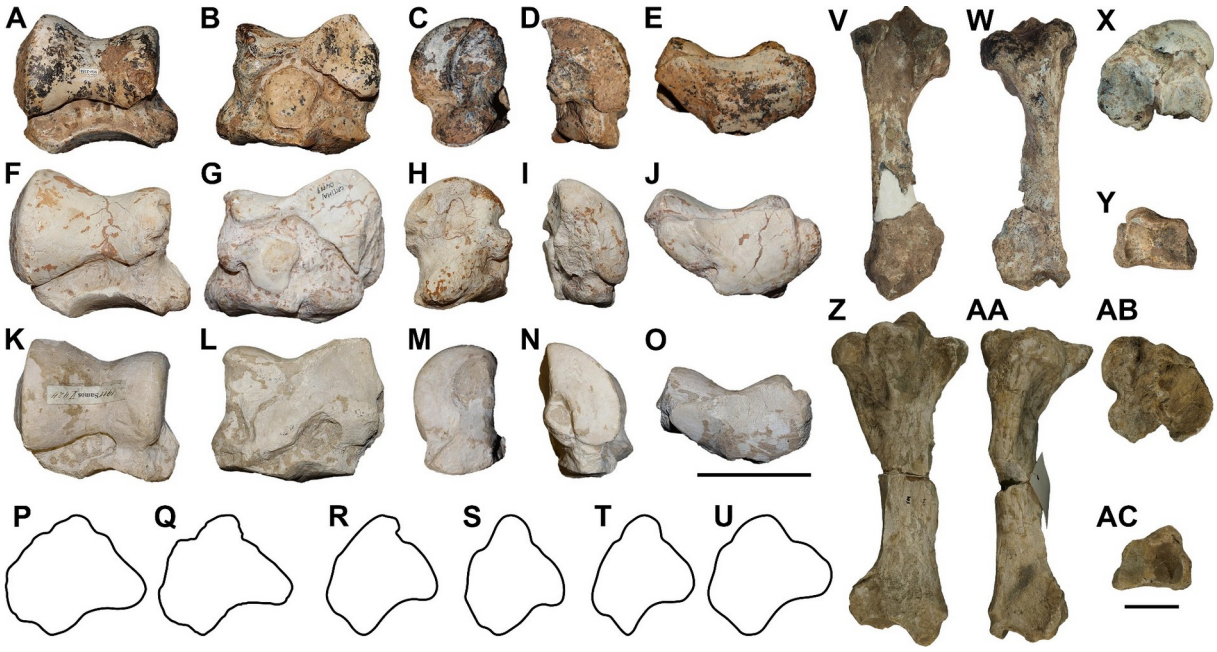


**Figure 32.** A selection of postcranial elements of different chilotheres from Eurasia. A–O, Astragali of *Chilotherium persiae* (Pohlig, 1885) from the Upper Miocene of Maragheh in Iran (A–E), *Chilotherium habereri* (Schlosser, 1903) from the Upper Miocene of Kutschwan in China (F–J), and *Chilotherium schlosseri* (Weber, 1905) from the Upper Miocene of Samos in Greece (K–O) in anterior (A, F, and K), posterior (B, G, and L), medial (C, H, and M), lateral (D, I, and N), and distal (E, J, and O) views; P–U, outline of patellae *C. habereri* (P), *C. persiae* (Q), *C. kowalevskii* (R), *C. sarmaticum* (S), '*C.*' *wimani* (T), and *Aceratherium incisivum* (U) in anterior view; and V–AC, tibiae of *C. persiae* (V–Y) and *C. schlosseri* (Z–AC) in anterior (V and Z), posterior (W and AA), proximal (X and AB), and distal (Y and AC) views. Scale bars equal 5 cm for A–O and V–AC, and P–U are not to scale.

The detailed study of this material showed that there are several morphological features that can offer clues to how to differentiate some chilothere species and inform their systematics. More specifically, it was shown that the astragalus exhibits several diagnostic traits, such as connections between the articular facets for the calcaneus (Fig. 33), which distinguish *C. schlosseri*, '*C.*' *wimani*, and *C. sarmaticum*. Only the former species exhibits a connection between the sustentacular and the ectal articular facet for the calcaneus (Fig. 33B). The species *C. schlosseri* is also the only species that features a connection between the medial lip of the articular trochlea for the tibia and the navicular facet (Fig. 32K). The morphology of the patella indicates that there are two morphotypes, one having more proximodistally elongated patellae, being exemplified by '*C.*' *wimani*, and the other exhibiting wider and more

rounded patellae, which are found in *C. persiae* and *C. habereri*. Unfortunately, for most other species no illustrations or measurements of the patella are available. However, the morphology of the proximal articulation of the tibia may offer some additional insight. In *C. persiae*, the lateral tuberosity of the proximal articulation of the tibia for the patellar ligaments, is mediolaterally oriented, being wider than high, corresponding well with the wider morphology of the patella; whereas in *C. schlosseri* the lateral tuberosity is higher than wide and anteroposteriorly oriented, possibly indicating a more proximodistally elongated patella.

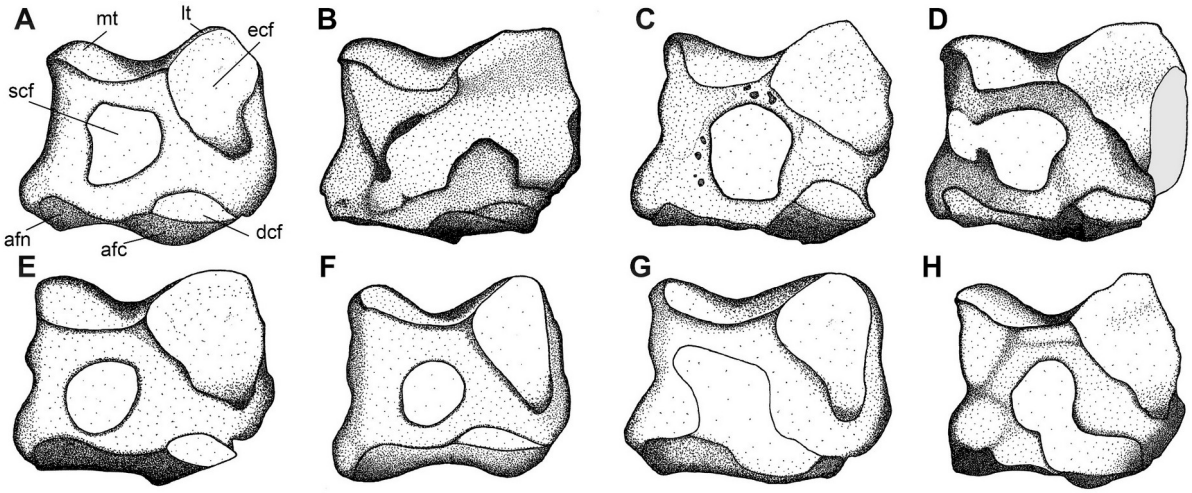


**Figure 33.** Schematic comparison of chilothere astragali in posterior view. A, *Aceratherium incisivum* Kaup, 1832, B, *Chilotherium schlosseri* (Weber, 1905), C, *Chilotherium persiae* (Pohlig, 1885), D, *Chilotherium habereri* (Schlosser, 1903), E, *Chilotherium orlovi* Bayshashov, 1982, F, *Chilotherium kowalevskii* (Pavlow, 1913), G, *Chilotherium sarmaticum* Korotkevitch, 1958, and H, '*Chilotherium*' *wimani* Ringström, 1924. Abbreviations: afc, articular facet for the cuboid; afn, articular facet for the navicular; dcf, distal calcaneal facet; ecf, ectal calcaneal facet; lt, lateral lip of the trochlea; mt, medial lip of the trochlea; and scf, sustentacular calcaneal facet. Not to scale.

There are also some more minor differences that can be observed in other postcranial elements but the value of which cannot be evaluated due to the limited number of specimens that can be compared. For instance, the axis features several differences in the studied specimens of *C. persiae* and *C. schlosseri*, as well as the shape of supraglenoid tubercle of the scapula that is more compressed in *C. habereri* than in *C. persiae* and *C. schlosseri*, and also more protruding in *C. schlosseri*. Also, the metapodials provide additional insight into the separation of the species, as revealed by their metrical comparison, based on which it is possible to divide the

chilotheres into two size groups and evaluate the degree of shortening of the metapodials.

Overall, this study was able to provide new clues for the interspecific distinction of the chilotheres. Combined with diagnostic features that were known from the skulls, mandibles and their dentition, this new information improves our understanding of the systematics of the group. The comparison of the collected metrical data of the postcranial material of the three studied species to the data from the literature further illuminated our understanding of chilothere evolution, which is characterised by a gradual increase in size in addition to a progressive shortening of the limbs.

### 3.6. Deciduous dentition and ontogenetic development of the skull and teeth of the Late Miocene hornless rhinocerotid *Chilotherium* of Eurasia

The taxonomy of chilotheres is almost exclusively based on adult cranial and dental material, with the infrequent addition of postcranial material. However, juvenile skulls, mandibles, and teeth have been almost completely neglected throughout their research history. There is almost no published data available on the deciduous dentition of chilotheres and their ontogenetic development. The goal of this study was to fill this gap by providing an overview of the available juvenile material of four chilothere species (Fig. 34) and compare this to the limited information in the literature.

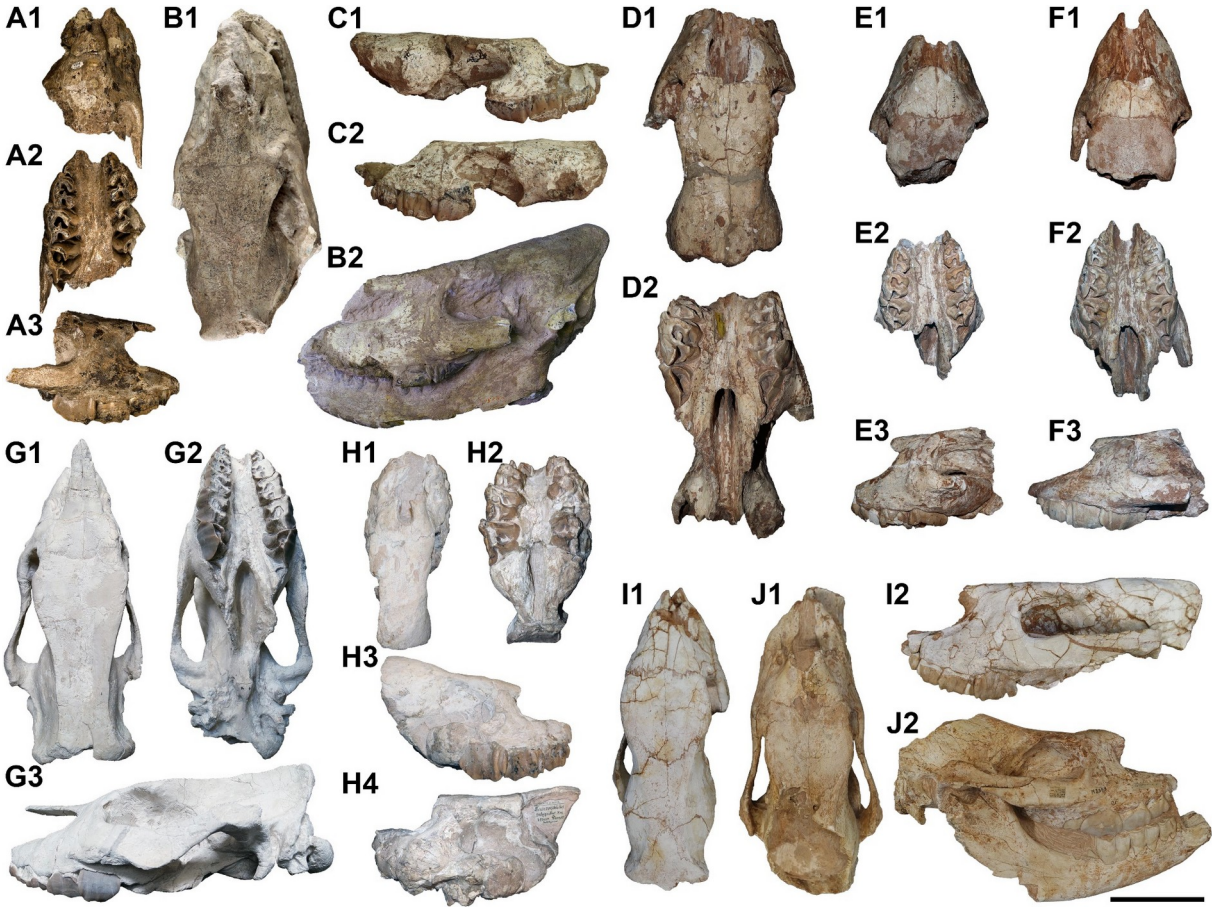


**Figure 34.** A selection of juvenile skull of different chilotheres from Eurasia. A–C, *Chilotherium persiae* (Pohlig, 1885) from the Upper Miocene of Maragheh in Iran; D–F, *Chilotherium habereri* (Schlosser, 1903) from the Upper Miocene of Kutschwan in China; G–H, *Chilotherium schlosseri* (Weber, 1905) from the Upper Miocene of Samos in Greece; and I–J, *Chilotherium anderssoni* Ringström, 1924 from the Upper Miocene of Daijiagou in China in different views. Scale bar equals 10 cm.

In total, 24 cranial, 21 mandibular, and 14 dental elements were studied belonging to the following four species: *C. persiae* from the Upper Miocene of

Maragheh (Iran), *C. habereri* from the Upper Miocene of Kutschwan (China), *C. schlosseri* from the Upper Miocene of Samos (Greece), and *C. anderssoni* from the Upper Miocene of Daijiagou (China). The material is housed in nine different collections across Europe (GPIT, GMM, MGL, MLU, MNHN, NHMW, NHMUK, SMF, and SMNS). The cranial material showed that although most features seem to ontogenetically develop in a similar manner, there is a difference in the development of the region between the orbital cavity and the nasal notch (nasorbital bar). More specifically, there seems to be a somewhat delayed development of the nasorbital bar in *C. schlosseri* compared to the other species.

Moreover, when the teeth of the crania were compared, it was observed that there is a slight difference in the eruption sequence of the upper deciduous premolars. In *C. persiae*, *C. habereri*, and *C. anderssoni* the D2 and D3 erupt almost simultaneously, followed by the D1 that erupts shortly before the D4. The dentition of *C. schlosseri* presents a slight deviation with the D4 erupting before the D1. The dentition itself also presents certain differences that allow the separation of some species. For instance, the size and morphology of the D1 seem to distinguish some species, with *C. habereri* exhibiting the smallest dimensions amongst the chilotheres. Moreover, *C. schlosseri* exhibits more pronounced enamel folds, including also frequently enamel plications, which are rarer in the other species. Additionally, in the D2 the presence of a prefossette is a consistent feature in *C. habereri* and *C. schlosseri*, whereas in *C. persiae* its presence varies. The comparison of the deciduous teeth also allowed to refine the differentiation of chilotheres from other rhinocerotids. More specifically, all chilotheres have strongly constricted protocones and hypocones in the D3 and D4 and most also exhibit a constriction in the D2 protocone and a weak constriction in the hypocone. Additionally, the parastyle of the D2 is very long and the shape of the ectoloph of the same tooth is convex.

Another important feature found in the teeth is the existence of hypoplasias (Fig. 35). Enamel hypoplasia is a deficiency in enamel thickness resulting from stress, when a certain threshold is met during the secretory phase of amelogenesis, with linear enamel hypoplasia being the most frequent form (Goodman and Rose, 1990). In the studied material several teeth were found to bear such a hypoplasia; while they were sporadically present in all deciduous teeth both in the maxilla and the mandible, the frequency in the d/D4 was rather surprising. In fact, a hypoplasia was present in every studied d/D4 that was adequately preserved (n=52).

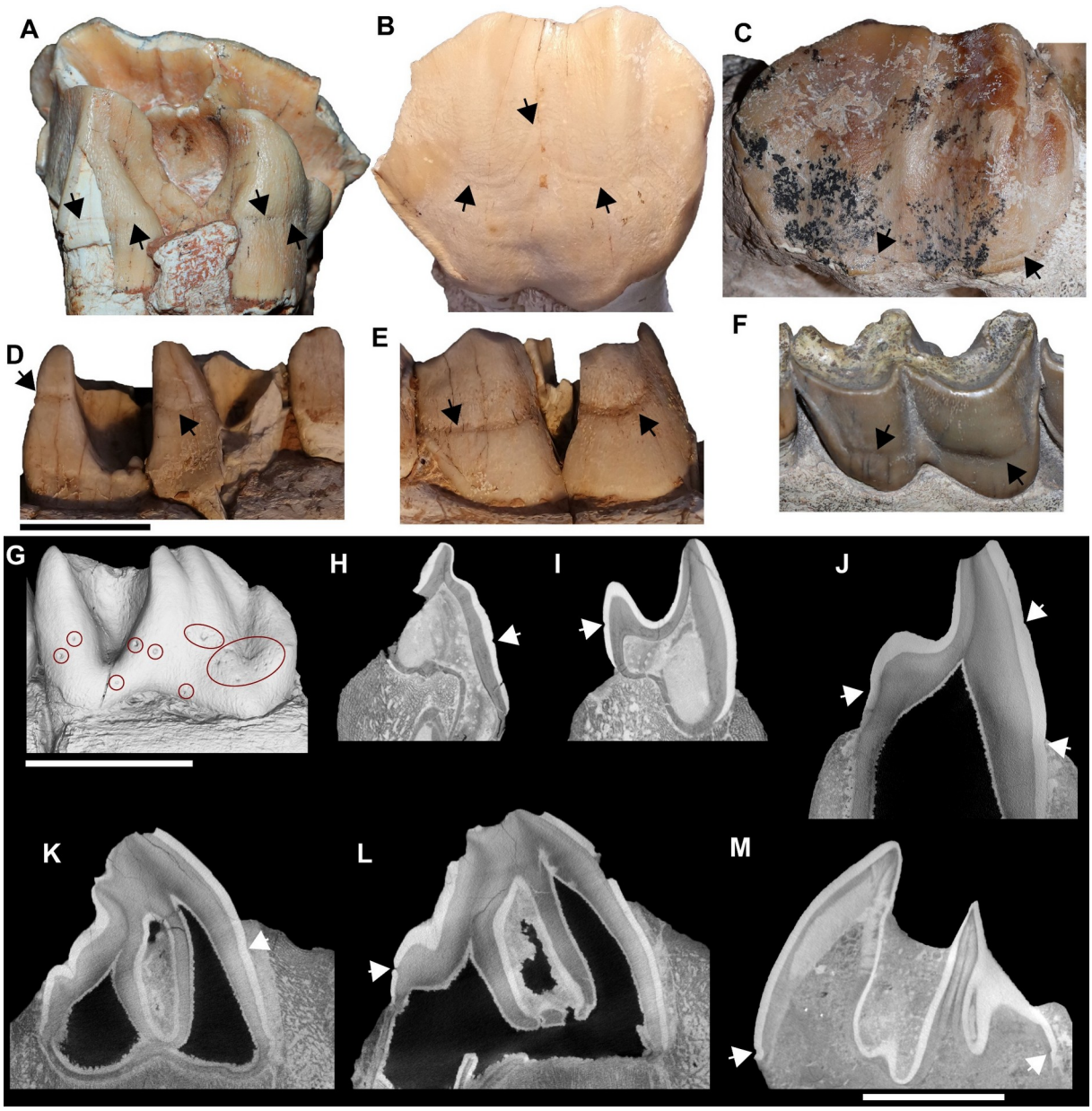


**Figure 35.** Hypoplasias in deciduous teeth of *Chilotherium* Ringström, 1924. A–F, photos of deciduous teeth *Chilotherium habereri* from the Upper Miocene of Kutschwan in China (A–B: same D4 and D–E: same d4) and *Chilotherium schlosseri* from the Upper Miocene of Samos in Greece (C: D4 and F: d4) in lingual (A and D) and buccal (B–C and E–F) views; and G–M, virtual cross-sections of deciduous teeth of C. habereri (G–I: same d2, J: d4, and K–L: same D4) and C. schlosseri (M: D4). Black and white arrows, as well as red circles indicate the hypoplasias. Scale bars equal 2 cm.

These new data differ from what had been reported before for other rhinoceroses (e.g., Mead, 1999; Hullot et al., 2021, 2023, 2024b), where a hypoplasia in the d/D4 may frequently be present, but never a constant feature in all specimens of a species. *Chilotherium* seems to be the only rhinoceros where such a pattern is observed. To interpret this difference the aetiology of the hypoplasias, which has been

extensively discussed in the past in primates (Skinner, 1986; Eckhardt and Protsch von Zieten, 1993; Hillson and Bond, 1997; Guatelli-Steinberg and Lukacs, 1998; Guatelli-Steinberg and Skinner, 2000; Guatelli-Steinberg, 2001; Chollet and Teaford, 2010; Skinner et al., 2014), has to be examined. The aetiology of hypoplasias is very complex and often controversial topic but the main factors are: 1. trauma, 2. genetic defects, and 3. physiological and systemic (nutritional) stress (Goodman and Rose, 1990). Due to the form, position, and prevalence of the presently observed hypoplasias the first twp potential causes can be rejected. Therefore, the hypoplasias in our chilothere sample result from systemic stress. The next step is to understand the fact that they are primarily found in the d/D4s.

Based on comparison with the extant African rhinoceros, *Ceratotherium simum* and *Diceros bicornis* (Goddard, 1970; Hillman-Smith et al., 1986), Mead (Mead, 1999) correlated the hypoplasias in the d/D4 of *Teleoceras* with the timing of birth of the individuals. Similar conclusions were also drawn by other studies for other mammalian groups (e.g., Goodman and Rose, 1990; Upex and Dobney, 2012; Davis and Mead, 2013). As a consequence, the fact that a hypoplasia is always present in every examined d/D4s of Chilotherium and always in the same position, without any deviation within the same species, implies that this hypoplasia is linked to an event that takes place in the life of every individual, without any exception. As also concluded for other groups, such a consistent event during the formation of the d/D4 can only be the birth of the animal.

However, there is an interesting disparity between the position of the hypoplasias in the different *Chilotherium* species. In *C. persiae*, *C. habereri*, and *C. anderssoni* the d/D4 hypoplasia is placed approximately in the middle of the tooth crown (Fig. 35B, E, J, K), In contrast to those species, in *C. schlosseri* the d/D4 hypoplasia is always found at the bottom of the tooth crown (Fig. 35C, F, M). Since the specific hypoplasia is connected to birth, the deviation in its' position might be related to some external environmental factor or interspecific differences that may affect the timing of birth to some degree. Nonetheless, confirming such differences in fossil taxa is very difficult. Its is, however, possible that this displacement of the hypoplasia in *C. schlosseri* can be used as a distinguishing feature for the species.

# 4. Conclusions and Outlook

Rhinoceroses were remarkably diverse in the past, with the existence of three distinct lineages comprising the extant Rhinocerotinae, and the two extinct Aceratheriinae and Elasmotheriinae. The research history of extinct representatives of the family is characterised by many debates and uncertainties about their taxonomy, phylogeny, and ecology. In this dissertation certain representatives of the aceratheriines and elasmotheriines were re-evaluated to shed light on persisting issues in these groups and shedding light on their systematics.

Among elasmotheriines, the genus *Parelasmotherium* has been a rather puzzling taxon, due to its synonymisation with other genera in the past and the fact that two additional species had been assumed members of the genus. To address this, µCT-scans of the holotype teeth of *P. schansiense*, the type species of the genus, were acquired. This revealed morphological features that were previously unknown due to the preservation and ontogenetic stage of the specimens. These findings clarified the phylogenetic position of the genus and showed that it should be limited to its type species, *P. schansiense*. This refined the phylogenetic relationship between elasmotheriines and also pointed out that the 'derived' species of elasmotheriines form a well-supported monophyletic clade.

Regarding, aceratheriines, chilotheres were amongst the most diverse rhinoceroses that have ever existed. They dominated the Late Miocene fauna in Eurasia. In some cases, such as the localities of Kutschwan and Daijiagou in China, their abundance rivaled that of hipparionine horses, which normally represent the most common faunal elements in these localities of the so-called "*Hipparion*"-fauna. Despite their abundance, the taxonomy, phylogenetic relationships, and ecology of chilotheres have remained poorly understood. This has led to a large amount of material remaining largely unstudied, which only further worsened our understanding about this rhinoceros group, with many researchers avoiding the chilothere material of a locality altogether.

This necessitated a comprehensive investigation of the taxonomy and evolutionary history of the chilotheres, which was the main goal of the present Dissertation. This work was able to elucidate important aspects of the taxonomy of these animals, by showing that in Europe alone at least four different species were present that belonged to two distinct genera: *Chilotherium*, including *C. schlosseri*, *C. kowalevskii* and, *C. sarmaticum*, and *Eochilotherium*, being represented only by *E.*

*samium*. It was shown that all four of these species are separated from each other as well as from the Asian chilotheres. Two of these species come from the same locality, Samos in Greece. However, it is unknown whether they co-occur in the same fossiliferous site, because all available material of these species comes from historical excavations, which often did not document the stratigraphical context. Four different chilothere species had been originally described based on material from Samos. During the course of this dissertation, it was shown that *C. schlosseri* and *E. samium* are the only valid species in the vertebrate assemblages of Samos with *E. samium* exhibiting features that are distinct from all typical *Chilotherium* representatives, thereby justifying its attribution to a different genus. It was also shown that two chilotheres that were considered the most primitive representatives of the genus *Chilotherium*, '*C*.' *wimani* and '*C*.' *primigenium*, present similarly plesiomorphic features as *E. samium*. They also lack apomorphic characters such as the flattened skull and depressed frontal region that are seen in *Chilotherium*, thereby suggesting that these two species also do not belong to the genus. This further demonstrates the complicated taxonomy of chilotheres and that this group is more diverse than previously thought (see Table 3).

These findings also enable a long-needed, comprehensive revision of the subtribe Chilotheriina. This group is herein raised to the subtribe rank and restricted to the three genera *Chilotherium*, *Eochilotherium*, and *Shansirhinus*, based on clear morphological features. The wide mandibular symphysis and the prominent enamel folds in the upper teeth represent synapomorphic features, linking these three genera together. The clarification of the diagnostic features and included genera of Chilotheriina facilitates future taxonomic work on other chilothere taxa and makes comparisons much easier.

The investigation of less studied skeletal remains such as the appendicular skeleton and cranial and dental elements of juvenile individuals showed that important differences can be found in such neglected material. The main finding is that the Chilotheriina are morphologically distinct from other rhinoceroses even in such often-overlooked material. They also exhibit important intraspecific morphological and metrical variability that often significantly overlaps between the species. Nonetheless, many postcranial elements exhibit specific features that can be considered diagnostic for some species, such as the morphology of the patella that differs between the Chinese chilotheres *C. habereri* and '*C*.' *wimani* or the arrangement of the articular

facets of astragalus that differentiates *C. schlosseri* from most other chilotheres. Similarly, the deciduous teeth present comparable results, showing that some morphological features such as the presence and development of some enamel folds can help in the identification of the species as well as the dimensions of the D1, which are characteristic for at least some species like *C. persiae*, *C. habereri*, and *S. ringstromi*. This provides new insights into the systematics of the Chilotheriina, validating some of the more enigmatic chilothere species and clarifying the relationships of some taxa.

**Table 3.** Summary of the taxonomic revision of Chilotheriina (modified after Heissig, 1975; Deng, 2006; Svorligkou et al., 2025).

| **Species** | **Authority** | **Revised species** | **Type locality** |
|---|---|---|---|
| *Rhinoceros persiae* | Pohlig, 1885 | *Chilotherium persiae* | Maragheh, Iran |
| *Rhinoceros habereri* | Schlosser, 1903 | *Chilotherium habereri* | Shanxi, China |
| *Aceratherium schlosseri* | Weber, 1905 | *Chilotherium schlosseri* | Samos, Greece |
| *Teleoceras ponticus* | Niezabitowski, 1912 | *Chilotherium schlosseri* | Odessa, Ukraine |
| *Aceratherium kowalevskii* | Pavlow, 1913 | *Chilotherium kowalevskii* | Grebeniki, Ukraine |
| *Aceratherium wegneri* | Andree, 1921 | *Chilotherium schlosseri* | Samos, Greece |
| *Aceratherium angustifrons* | Andree, 1921 | *Chilotherium schlosseri* | Samos, Greece |
| *Chilotherium anderssoni* | Ringström, 1924 | *Chilotherium anderssoni* | Daijiagou, Shanxi, China |
| *Chilotherium gracile* | Ringström, 1924 | *Chilotherium habereri* | Liuwangou, Shanxi, China |
| *Chilotherium planifrons* | Ringström, 1924 | *Chilotherium anderssoni* | Shenshuzui, Shanxi, China |
| *Chilotherium habereri* var. *laticeps* | Ringström, 1924 | *Chilotherium habereri* | Shanxi, China |
| *Chilotherium sarmaticum* | Korotkevitch, 1958 | *Chilotherium sarmaticum* | Berislav, Ukraine |
| *Chilotherium fenhoensis* | (Tung et al., 1975) | *Chilotherium anderssoni* | Anle, Shanxi, China |
| *Chilotherium xizangensis* | Ji et al., 1980 | *Chilotherium xijangense* | Woma, Xizang, China |
| *Chilotherium orlovi* | Bayshashov, 1982 | *Chilotherium orlovi* | Pavlodar, Kazakhstan |
| *Chilotherium licenti* | Sun et al., 2018 | *Chilotherium licenti* | Zhaojiacha, Gansu, China |
| *Chilotherium wimani* | Ringström, 1924 | "*Chilotherium*" *wimani* | Beihougou, Shaanxi, China |
| *Chilotherium primigenium* | Deng, 2006 | "*Chilotherium*" *primigenium* | Zhongmajia, Gansu, China |
| *Aceratherium samium* | Weber, 1905 | *Eochilotherium samium* | Samos, Greece |
| *Aceratherium kiliasi* | Geraads and Koufos, 1990 | *Eochilotherium samium* | Pentalophos 1, Greece |
| *Rhinoceros brancoi* | Schlosser, 1903 | *Shansirhinus brancoi* | Tianjin, China |
| *Shansirhinus ringströmi* | Kretzoi, 1942 | *Shansirhinus ringstromi* | Huangshigou, Shanxi, China |
| *Chilotherium yunnanensis* | (Tang et al., 1974) | *Shansirhinus ringstromi* | Shagou, Yunnan, China |
| *Chilotherium cornutum* | Qiu and Yan, 1982 | *Shansirhinus ringstromi* | Hanjiawa, Shanxi, China |

While important aspects of chilothere systematics were elucidated many questions remain about the taxonomic affinities of some species and their phylogenetic relationships. The next steps in chilothere research should be a revision of the “primitive” chilotheres ‘*C.*’ *wimani* and ‘*C.*’ *primigenium*, to resolve their generic attribution and subsequently to conduct a phylogenetic analysis in which all or at least most chilotheres are included to investigate their inter- and intrageneric relationships.

Another big issue in chilothere systematics is the chilothere material that has been described from Europe and Anatolia in the past, but under outdated taxonomic schemes. A revision should be conducted that will take into account the newest findings in chilothere taxonomy and compare with both the European and the Asian chilotheres. Such a study has the potential to answer many of the persisting questions about the phylogenetic relationships and biogeographical context of these animals. The biogeography of the Chilotheriina is a complicated topic that has never been addressed in detail but could be clarified through the revision of the previously described chilothere material combined with a detailed phylogenetic analysis of the group.

## 5. References


Andersson, J. G. 1923. Essays on the Cenozoic of northern China. Memoirs of the Geological Survey of China, Ser. A 3:1–152.

Andree, J. 1921. Rhinocerotiden aus dem Unterpliocän von Samos. Paläontologische Zeitschrift 3:189–212.

Andree, J. 1926. Neue Cavicornier aus dem Pliocän von Samos. Palaeontographica 67:135–175.

Antoine, P.-O. 2002. Phylogénie et évolution des Elasmotheriina (Mammalia, Rhinocerotidae). Mémoires du Muséum National d'Histoire Naturelle 188:1–359.

Antoine, P.-O. 2003. Middle Miocene elasmotheriine Rhinocerotidae from China and Mongolia: taxonomic revision and phylogenetic relationships. Zoologica Scripta 32:95–118.

Antoine, P.-O., and G. Saraç. 2005. Rhinocerotidae (Mammalia, Perissodactyla) from the late Miocene of Akkaşdağı, Turkey. Geodiversitas 27:601–632.

Antoine, P.-O., and D. Becker. 2013. A brief review of Agenian rhinocerotids in Western Europe. Swiss Journal of Geosciences 106:135–146.

Antoine, P.-O., and S. Sen. 2016. Rhinocerotidae and Chalicotheriidae (Perissodactyla, Tapiromorpha). Geodiversitas 38:245–259.

Antoine, P.-O., F. Alférez, and C. Iñigo. 2002. A new elasmotheriine (Mammalia, Rhinocerotidae) from the Early Miocene of Spain. Comptes Rendus Palevol 1:19–26.

Antoine, P.-O., F. Duranthon, and J.-L. Welcomme. 2003a. *Alicornops* (Mammalia, Rhinocerotidae) dans le Miocène supérieur des Collines Bugti (Balouchistan, Pakistan): implications phylogénétiques. Geodiversitas 25:575–603.

Antoine, P.-O., D. Becker, L. Pandolfi, and D. Geraads. 2025. Evolution and Fossil Record of Old World Rhinocerotidae; pp. 31–48 in M. Melletti, B. Talukdar, and D. Balfour (eds.), Rhinos of the World., . Fascinating Life Sciences Springer Nature Switzerland, Cham.

Antoine, P.-O., S. Ducrocq, L. Marivaux, Y. Chaimanee, J.-Y. Crochet, J.-J. Jaeger, and J.-L. Welcomme. 2003b. Early rhinocerotids (Mammalia: Perissodactyla) from South Asia and a review of the Holarctic Paleogene rhinocerotid record. Canadian Journal of Earth Sciences 40:365–374.

Antoine, P.-O., K. F. Downing, J.-Y. Crochet, F. Duranthon, L. J. Flynn, L. Marivaux, G. Métais, A. R. Rajpar, and G. Roohi. 2010. A revision of *Aceratherium blanfordi* Lydekker, 1884 (Mammalia: Rhinocerotidae) from the Early Miocene of Pakistan: postcranials as a key. Zoological Journal of the Linnean Society 160:139–194.

Antunes, M. T. 1972. Un nouveau Rhinocerotidé, <i>Chilotherium ibericus<i/> n. sp. Bolletim Do Museu e Laboratório Mineralógico e Geol´ggico Da Faculdade de Ciencias 13:25–33.

Athanassiou, A., S. J. Roussiakis, I. X. Giaourtsakis, G. E. Theodorou, and G. Iliopoulos. 2014. A new hornless rhinoceros of the genus *Acerorhinus* (Perissodactyla: Rhinocerotidae) from the Upper Miocene of Kerassiá (Euboea, Greece), with a revision of related forms. Palaeontographica Abteilung A 303:23–59.

Bai, B., J. Meng, C. Zhang, Y.-X. Gong, and Y.-Q. Wang. 2020. The origin of Rhinocerotoidea and phylogeny of Ceratomorpha (Mammalia, Perissodactyla). Communications Biology 3:509.

Barone, R. 2010. Anatomie Comparée Des Mammifères Domestiques. Tome 1: Ostéologie. Vigot Frères, Paris, pp.
Bayshashov, B. U. 1982. A new rhinoceros species of the genus *Chilotherium* from Pavlodar; pp. 72–83 in Mesozoic and Cenozoic vertebrate fauna and flora of North-Eastern and southern Kazakhstan. vol. 8. Academy of Sciences of Kazakhstan, Almaty.
Bayshashov, B. U. 1993. Neogene rhinoceroses of Kazakhstan. Academy of Sciences of Kazakhstan, Almaty, 152 pp.
Becker, D., P.-O. Antoine, and O. Maridet. 2013. A new genus of Rhinocerotidae (Mammalia, Perissodactyla) from the Oligocene of Europe. Journal of Systematic Palaeontology 11:947–972.
Bernor, R. L. 1986. Mammalian biostratigraphy, geochronology, and zoogeographic relationships of the Late Miocene Maragheh fauna, Iran. Journal of Vertebrate Paleontology 6:76–95.
Bernor, R. L., M. O. Woodburne, and J. A. Van Couvering. 1980. A contribution to the chronology of some Old World miocene faunas based on hipparionine horses. Geobios 13:705–739.
Biasatti, D., W. Yang, and D. Tao. 2018. Paleoecology of Cenozoic rhinos from northwest China: a stable isotope perspective. Vertebrata PalAsiatica 56:45–68.
Blumenbach, J. F. 1799. Handbuch Der Naturgeschichte. Dieterich, Göttingen, pp.
Bohlin, B. 1926. Die Famillie Giraffidae. Palaeontologia Sinica, Series C 4:1–178.
Bohlin, B. 1935. Cavicornier der *Hipparion*-Fauna Nord-Chinas. Palaeontologia Sinica, Series C 9:1–166.
Böhme, M., C. G. C. Van Baak, J. Prieto, M. Winklhofer, and N. Spassov. 2018. Late Miocene stratigraphy, palaeoclimate and evolution of the Sandanski Basin (Bulgaria) and the chronology of the Pikermian faunal changes. Global and Planetary Change 170:1–19.
Böhme, M., M. Aiglstorfer, P.-O. Antoine, E. Appel, P. Havlik, G. Métais, D. N. Tran, D. Uhl, and J. Prieto. 2013. Na Duong (northern Vietnam) – an exceptional window into Eocene ecosystems from Southeast Asia. Zitteliana A 53:120–167.
Borissiak, A. 1914. Mammifères fossiles de Sébastopol, I. Mémoires Du Comité Géologique, Nouvelle Série 87:105–154.
Borrani, A., P. Mackiewicz, O. Kovalchuk, Z. Barkaszi, C. Capalbo, A. Dubikovska, U. Ratajczak-Skrzatek, M. Sinitsa, K. Stefaniak, and P. P. A. Mazza. 2025. The evolutionary history of Rhinocerotidae: phylogenetic insights, climate influences and conservation implications. Cladistics 1–17.
Bronn, H. G. 1831. Italiens Tertiär-Gebilde Und Deren Organische Einschlüsse: Vier Abhandlungen. Groos, Heidelberg, 176 pp.
Campbell, B. G., M. H. Aminit, R. L. Bernor, W. Dickinsont, and R. Drake. 1980. Maragheh: a classical late Miocene vertebrate locality in northwestern Iran. Nature 287:837–841.
Cerdeño, E. 1995. Cladistic Analysis of the Family Rhinocerotidae (Perissodactyla). American Museum Novitates 3143:1–25.
Cerdeño, E. 1996. Rhinocerotidae from the Middle Miocene of the Tung-gur Formation, Inner Mongolia (China). American Museum Novitates 3184:1–43.
Chen, G. F. 1977. A new genus of Iranotheriinae of Ningxia. Vertebrata PalAsiatica 15:143–147.
Chen, S., T. Deng, S. Hou, Q. Shi, and L. Pang. 2010. Sexual Dimorphism in Perissodactyl Rhinocerotid *Chilotherium wimani* from the Late Miocene of the Linxia Basin (Gansu, China). Acta Palaeontologica Polonica 55:587–597.

Chollet, M. B., and M. F. Teaford. 2010. Ecological stress and linear enamel hypoplasia in *Cebus*. American Journal of Physical Anthropology 142:1–6.
Chow, M. 1958. New elasmotherine rhinoceros from Shansi. Vertebrata PalAsiatica 2:131–142.
de Christol, M. 1835. Recherches sur les caractères des grandes espèces de Rhinocèros fossiles. Annales Des Sciences Naturelles 2:44–112.
Ciner, B., Y. Wang, T. Deng, L. Flynn, S. Hou, and W. Wu. 2015. Stable carbon and oxygen isotopic evidence for Late Cenozoic environmental change in Northern China. Palaeogeography, Palaeoclimatology, Palaeoecology 440:750–762.
Codrea, V. A., L. Ursachi, D. Bejan, and C. Farcas. 2011. Early Late Miocene *Chilotherium* (Perissodactyla, Mammalia) from Pogana (Scythian Platform). North-Western Journal of Zoology 7:184–188.
Colbert, E. H. 1935. Siwalik mammals in the American Museum of Natural History. Transactions of the American Philosophical Society 26:1–401.
Cope, E. D. 1878. Descriptions of new extinct Vertebrata from the upper Tertiary and Dakota formations. Bulletin of the U.S. Geological and Geographical Survey of the Territories 4:379–396.
Crusafont, M., J. F. Villalta, and J. Truyols. 1955. El Burdigaliense continental de la Cuenca del Vallés-Penedés. Memorias y Comunicaciones Del Instituto Geológico de Barcelona 12:1–272.
Davis, H., and A. J. Mead. 2013. Enamel Hypoplasia as an Indicator of Nutritional Stress in Juvenile White-Tailed Deer. Georgia Journal of Science 71:95–101.
Deng, T. 2001a. New remains of *Parelasmotherium* from the late Miocene in Dongxiang Gansu China. Vertebrata PalAsiatica 39:306–311.
Deng, T. 2001b. New material of *Chilotherium wimani* (Perissodactyla, Rhinocerotidae) from the Late Miocene of Fugu, Shaanxi. Vertebrata PalAsiatica 39:129–138.
Deng, T. 2002. Limb bones of *Chilotherium wimani* (Perissodactyla, Rhinocerotidae) from the Late Miocene of the Linxia Basin in Gansu, China. Vertebrata PalAsiatica 40:305–316.
Deng, T. 2003. New material of *Hispanotherium matritense* (Rhinocerotidae, Perissodactyla) from Laogou of Hezheng County (Gansu, China), with special reference to the Chinese Middle Miocene elasmotheres. Geobios 36:141–150.
Deng, T. 2005a. New cranial material of *Shansirhinus* (Rhinocerotidae, Perissodactyla) from the Lower Pliocene of the Linxia Basin in Gansu, China. Geobios 38:301–313.
Deng, T. 2005b. New discovery of *Iranotherium morgani* (Perissodactyla, Rhinocerotidae) from the late Miocene of the Linxia Basin in Gansu, China, and its sexual dimorphism. Journal of Vertebrate Paleontology 25:442–450.
Deng, T. 2006. A primitive species of *Chilotherium* (Perissodactyla, Rhinocerotidae) from the Late Miocene of Linxia Basin (Gansu, China). Cainozoic Research 5:93–102.
Deng, T. 2007. Skull of *Parelasmotherium* (Perissodactyla, Rhinocerotidae) from the Upper Miocene in the Linxia Basin (Gansu, China). Journal of Vertebrate Paleontology 27:467–475.
Deng, T. 2008. A new elasmothere (Perissodactyla, Rhinocerotidae) from the late Miocene of the Linxia Basin in Gansu, China. Geobios 41:719–728.
Deng, T., and W. R. Downs. 2002. Evolution of Chinese Neogene Rhinocerotidae and Its Response to Climatic Variations. Acta Geologica Sinica 76:139–145.
Deng, T., X. Lu, D. Sun, and S. Li. 2023. Rhinocerotoid fossils of the Linxia Basin in northwestern China as late Cenozoic biostratigraphic markers. Palaeogeography, Palaeoclimatology, Palaeoecology 614:111427.

Dollo, L. 1885. Rhinocéros vivants et fossiles. Revue de Questions Scientifiques 17:293–299.
Ebbestad, J. O. R. 2021. Otto Zdansky: The Scientist Who Discovered Peking Man and Explored China's Fossil Past. Acta Universitatis Upsaliensis, Uppsala, 248 pp.
Eckhardt, R. B., and R. Protsch von Zieten. 1993. Enamel hypoplasias as indicators of developmental stress in pongids and hominids. Human Evolution 8:93–99.
Fischer, J. G. von W. 1808. La notice d'un animal fossile de Siberie inconnu aux naturalistes. Programme d'invitation a la seance publique de la Societe imperiale des naturalistes 23–28.
Forsyth-Major, C. I. 1888. Sur un gisement d'ossements fossiles dans l'île de Samos contemporains de l'âge de Pikermi. Comptes Rendus Hebdomadaires Des Séances de l'Académie Des Sciences 107:1178–1181.
Fortelius, M., and K. Heissig. 1989. The phylogenetic relationships of the Elasmotherini. Mitteilungen Der Bayerischen Staatssammlung Für Paläontologie Und Historische Geologie 29:227–233.
Fortelius, M., K. Heissig, G. Saraç, and S. Sen. 2003. Rhinocerotidae (Perissodactyla); pp. 282–307 in Geology and Paleontology of the Miocene Sinap Formation, Turkey. Columbia University Press, New York.
Fraser, D., N. Rybczynski, M. Gilbert, and M. R. Dawson. 2025. Mid-Cenozoic rhinocerotid dispersal via the North Atlantic. Nature Ecology & Evolution.
Garevski, R. 1974. Beitrag zur Kenntnis der Pikermifauna Mazedoniens. Fossilreste der Chalicotheriiden. Fragmenta Balcanica 9:201–209.
Garevski, R., and G. N. Markov. 2011. A *Deinotherium gigantissimum* (Mammalia, Proboscidea) palate with deciduous dentition from the area of Veles, Republic of Macedonia. Paläontologische Zeitschrift 85:33–36.
Gaudry, A. 1885. V.-Palaeontology in Germany and Austria. Geological Magazine 3:556–559.
Geraads, D. 1994. Les gisements de mammifères du Miocène supérieur de Kemiklitepe, Turquie: 4. Rhinocerotidae. Bulletin Du Muséum d'histoire Naturelle 16:81–95.
Geraads, D. 2010. Rhinocerotidae; pp. 675–689 in L. Werdelin (ed.), Cenozoic Mammals of Africa. University of California Press.
Geraads, D. 2013. Large Mammals from the Late Miocene of Çorakyerler,. Acta Zoologica Bulgarica 65:381–390.
Geraads, D., and G. Koufos. 1990. Upper Miocene Rhinocerotidae (Mammalia) from Pentalophos-1, Macedonia, Greece. Palaeontographica Abteilung A 210:151–168.
Geraads, D., and N. Spassov. 2009. Rhinocerotidae (Mammalia) from the Late Miocene of Bulgaria. Palaeontographica Abteilung A 287:99–122.
Geraads, D., and S. Zouhri. 2021. A new late Miocene elasmotheriine rhinoceros from Morocco. Acta Palaeontologica Polonica 66.
Geraads, D., M. McCrossin, and B. Benefit. 2012. A New Rhinoceros, *Victoriaceros kenyensis* gen. et sp. nov., and other Perissodactyla from the Middle Miocene of Maboko, Kenya. Journal of Mammalian Evolution 19:57–75.
Geraads, D., S. Zouhri, and G. N. Markov. 2019. The first *Tetralophodon* (Mammalia, Proboscidea) cranium from Africa. Journal of Vertebrate Paleontology 39:e1632321.
Getty, R. 1975. Sisson and Grossman's: The Anatomy of the Domestic Animals, Volume 1. W. B. Saunders, Philadephia, Pennsylvania, pp.
Giaourtsakis, I. X. 2003. Late Neogene Rhinocerotidae of Greece: distribution, diversity and stratigraphical range. Deinsea 10:235–253.

Giaourtsakis, I. X. 2009. The Late Miocene Mammal Faunas of the Mytilinii Basin, Samos Island, Greece: New Collection 9. Rhinocerotidae. Beiträge Zur Paläontologie 31:157–187.
Giaourtsakis, I. X. 2022. The Fossil Record of Rhinocerotids (Mammalia: Perissodactyla: Rhinocerotidae) in Greece; pp. 409–500 in E. Vlachos (ed.), Fossil Vertebrates of Greece Vol. 2. Springer International Publishing, Cham.
Gloger, C. 1941. Gemeinnütziges Hand-Und Hilfsbuch Der Naturgeschichte. Für Gebildete Leser Aller Stände, Besonders Für Die Reifere Jugend Und Ihre Lehrer. U. Schulz und Co., Wroclaw, 160 pp.
Goddard, J. 1970. Age criteria and vital statistics of a black rhinoceros population. East African Wildlife Journal 8:105–121.
Goloboff, P. A., J. S. Farris, and K. C. Nixon. 2008. TNT, a free program for phylogenetic analysis. Cladistics 34:407–437.
Goodman, A. H., and J. C. Rose. 1990. Assessment of systemic physiological perturbations from dental enamel hypoplasias and associated histological structures. American Journal of Physical Anthropology 33:59–110.
Gray, J. E. 1821. On the natural arrangemenet of vertebrose animals. London Medical Repository 15:297–310.
Guatelli-Steinberg, D. 2001. What can developmental defects of enamel reveal about physiological stress in nonhuman primates? Evolutionary Anthropology: Issues, News, and Reviews 10:138–151.
Guatelli-Steinberg, D., and J. R. Lukacs. 1998. Preferential expression of linear enamel hypoplasia on the sectorial premolars of rhesus monkeys (Macaca mulatta). American Journal of Physical Anthropology 107:179–186.
Guatelli-Steinberg, D., and M. Skinner. 2000. Prevalence and Etiology of Linear Enamel Hypoplasia in Monkeys and Apes from Asia and Africa. Folia Primatologica 71:115–132.
Guérin, C. 1980. Les Rhinocéros (Mammalia, Perissodactyla) du Miocène terminal au Pleistocène supérieur en Europe occidentale: comparaison avec les espèces actuelles. Documents des Laboratoires de Géologie de la Faculté des Sciences de Lyon 79:1–1185.
Hanson, C. B. 1989. *Teletaceras radinskyi*, a new primitive Rhinocerotid from the Late Eocene Clarno Formation of Oregon; pp. 379–398 in D. R. Prothero and R. M. Schoch (eds.), The evolution of perissodactyls. Oxford University Press, Oxford.
Hatcher, J. B. 1894. On a Small Collection of Vertebrate Fossils from the Loup Fork Beds of Northwestern Nebraska; with Note on the Geology of the Region. The American Naturalist 28:236–248.
Heissig, K. 1972. Paläontologische und geologische Untersuchungen im Tertiär von Pakistan 5. Rhinocerotidae (Mamm.) aus den unteren und mittleren Siwalik-Schichten. Bayerische Akademie der Wissenschaften Mathematisch-Naturwissenschaftliche Klasse Abhandlungen - Neue Folge 152:1–112.
Heissig, K. 1973. Die Unterfamilien und Tribus der rezenten und fossilen Rhinocerotidae (Mammalia). Säugetierkundliche Mitteilungen 21:25–30.
Heissig, K. 1975. Rhinocerotidae aus dem Jungtertiär Anatoliens. Geologisches Jahrbuch (B) 15:145–151.
Heissig, K. 1981. Probleme bei der cladistischen Analyse einer Gruppe mit wenigen eindeutigen Apomorphien: Rhinocerotidae. Paläontologische Zeitschrift 55:117–123.
Heissig, K. 1989. The Rhinocerotidae; pp. 399–417 in The Evolution of Perissodactyls. Oxford University Press, New York, NY.

Heissig, K. 1996. The stratigraphical range of fossil rhinoceroses in the Late Neogene of Europe and the Eastern Mediterranean; pp. 339–347 in The evolution of westermn Eurasian Neogene Mammal Faunas. Columbia University Press, New York.
Heissig, K. 1999. Family Rhinocerotidae; pp. 175–188 in The Miocene Land Mammals of Europe. Pfeil, München.
Heissig, K. 2012. Les Rhinocerotidae (Perissodactyla) de Sansan; pp. 317–485 in Mammifères de Sansan. Muséum national d'Histoire naturelle, Paris.
Hillman-Smith, A. K. K., R. N. Owen-Smith, J. L. Anderson, A. J. Hall-Martin, and J. P. Selaladi. 1986. Age estimation of the White rhinoceros (*Ceratotherium simum*). Journal of Zoology 210:355–379.
Hillson, S., and S. Bond. 1997. Relationship of enamel hypoplasia to the pattern of tooth crown growth: A discussion. American Journal of Physical Anthropology 104:89–103.
Hooijer, D. A. 1966. Fossil mammals of Africa No. 21 Miocene rhinoceroses of East Africa. Bulletin of the British Museum (Natural History) Geology 13:117–190.
Hooijer, D. A. 1971. A new rhinoceros from the Late Miocene of Loperot, Turkana district, Kenya. Bulletin of the Museum of Comparative Zoology 142:339–392.
Hullot, M., and P.-O. Antoine. 2022. Enamel hypoplasia on rhinocerotoid teeth: Does CT-scan imaging detect the defects better than the naked eye? Palaeovertebrata 45:e2.
Hullot, M., Y. Laurent, G. Merceron, and P.-O. Antoine. 2021. Paleoecology of the Rhinocerotidae (Mammalia, Perissodactyla) from Béon 1, Montréal-du-Gers (late early Miocene, SW France): Insights from dental microwear texture analysis, mesowear, and enamel hypoplasia. Palaeontologia Electronica 24:a27.
Hullot, M., C. Martin, C. Blondel, and G. E. Rössner. 2024a. Life in a Central European warm-temperate to subtropical open forest: Paleoecology of the rhinocerotids from Ulm-Westtangente (Aquitanian, Early Miocene, Germany). The Science of Nature 111:10.
Hullot, M., P.-O. Antoine, N. Spassov, G. D. Koufos, and G. Merceron. 2023. Late Miocene rhinocerotids from the Balkan-Iranian province: ecological insights from dental microwear textures and enamel hypoplasia. Historical Biology 35:1417–1434.
Hullot, M., C. Martin, C. Blondel, D. Becker, and G. E. Rössner. 2024b. Evolutionary palaeoecology of European rhinocerotids across the Oligocene–Miocene transition. Royal Society Open Science 11:240987.
Hünermann, K. A. 1989. Die Nashornreste (*Aceratherium incisivum*) aus dem Jungtertiär vom Höwenegg im Hegau. Andrias 6:5–116.
Jame, C., J. Tissier, O. Maridet, and D. Becker. 2019. Early Agenian rhinocerotids from Wischberg (Canton Bern, Switzerland) and clarification of the systematics of the genus *Diaceratherium*. PeerJ 7:e7517.
Ji, H. X., Q. Q. Xu, and W. B. Huang. 1980. The *Hipparion* fauna from Guizhong Basin, Xizang; pp. 18–32 in Palaeontology of Xizang, Book 1., . The Comprehensive Scientific Expedition to the Qinghai-Xizang Plateau of the Chinese Academy of Sciences Science Press, Beijing.
Kaakinen, A., B. H. Passey, Z.-Q. Zhang, L.-P. Liu, Z. Pesonen, and M. Fortelius. 2013. Stratigraphy and Paleoecology of the Classical Dragon Bone Localities of Baode County, Shanxi Province; pp. 203–217 in M. Fortelius, X. Wang, and L. Flynn (eds.), Fossil Mammals of Asia. Columbia University Press.

Kamei, T., J. Ikeda, H. Ishida, S. Ishida, I. Onishi, H. Partoazar, S. Sasajima, and S. Nishimura. 1977. A General Report of the Geological and Paleontological Survey in Maragheh Area, North-West Iran, 1973. Memoirs of the Faculty of Science, Kyoto University. Series of Geology and Mineralogy 43:131–164.

Kampouridis, P. 2020. Rhinocerotidae (Mammalia, Perissodactyla) from the Late Miocene of Staniantsi (Bulgaria). Master Thesis, Eberhard-Karls University of Tübingen, Tübingen, Germany, 68 pp.

Kampouridis, P., J. Hartung, G. S. Ferreira, and M. Böhme. 2022a. Reappraisal of the late Miocene elasmotheriine *Parelasmotherium schansiense* from Kutschwan (Shanxi Province, China) and its phylogenetic relationships. Journal of Vertebrate Paleontology 41:e2080556.

Kampouridis, P., G. Svorligkou, N. Kargopoulos, and F. J. Augustin. 2022b. Reassessment of ‘ *Chilotherium wegneri* ’ (Mammalia, Rhinocerotidae) from the late Miocene of Samos (Greece) and the European record of *Chilotherium*. Historical Biology 34:412–420.

Kampouridis, P., M. Mirzaie Ataabadi, J. Hartung, and F. J. Augustin. 2024. The easternmost occurrence of the Late Miocene schizotheriine chalicothere *Ancylotherium pentelicum* at the classical locality of Maragheh (Iran). Journal of Mammalian Evolution 31:36.

Kampouridis, P., G. Svorligkou, N. Spassov, and M. Böhme. 2025. Postcranial anatomy of the Late Miocene Eurasian hornless rhinocerotid *Chilotherium*. PLOS One 20:e0336590.

Kampouridis, P., G. Svorligkou, N. Kargopoulos, N. Spassov, and M. Böhme. 2023. Revision of the Late Miocene hornless rhinocerotids from Samos Island (Greece) with the designation of neotypes and implications for the European chilotheres. Journal of Vertebrate Paleontology.

Kargopoulos, N., P. Kampouridis, J. Hartung, and M. Böhme. 2023. Hyaenid remains from the Late Miocene of Kutschwan (Shanxi Province, China). PalZ.

Kaup, J. 1832. Über *Rhinoceros incisivus* Cuv., und eine neue Art, *Rhinoceros schleiermacheri*. Isis von Oken 898–904.

Kazanci, N., L. Karadenizli, G. Seyitog, S. Sen, M. C. Alçiçek, B. Varol, G. Saraç, and Y. Hakyemez. 2005. Stratigraphy and sedimentology of Neogene mammal bearing deposits in the Akkaşdagı area, Turkey. Geodiversitas 27:527–551.

Khan, A. M., E. Cerdeño, M. A. Khan, M. Akhtar, and M. Ali. 2011. *Chilotherium intermedium* (Rhinocerotidae: Mammalia) From the Siwaliks of Pakistan: Systematic Implications. Pakistan Journal of Zoology 43:651–663.

Khan, M. A., M. Iqbal, M. Akhtar, A. M. Khan, and A. A. Majeed. 2008. Some new fossil remains of *Chilotherium* sp. from the Dhok Pathan Formation of the Siwaliks. Journal of Animal and Plant Sciences 18:155–159.

Kiernik, E. 1913. Über einen Aceratheriumschädel aus der Umgebung von Odessa. Bulletin International de l’Académie Des Sciences de Cracovie 1913:808–864.

Killgus, H. 1922. Die Unterpliocaenen Chinesischen Säugetierreste der Tafelschen Sammlung zu Tübingen. Ph.D. Dissertation, Eberhard-Karls University of Tübingen, Tübingen, Germany, 87 pp.

Killgus, H. 1923. Unterpliozäne Säuger aus China. Paläontologische Zeitschrift 5:251–257.

Koenigswald, G. H. R. von. 1956. Fossil Mammals from the Philippines. National Research Council of the Philippines, Quezon City, 14 pp.

Koerber, S. 2009. From sponges to primates: emendation of 30 species nomina dedicated to the Swedish zoologist Einar Lönnberg. Zootaxa 2201.

Korotkevich, O. L. 1958. A new *Chilotherium* species from the Sarmatian deposits of the Ukraine. Dopovidi Akad. Nauk Ukrainskoi RSR 12:1372–1376.
Korotkevich, O. L. 1970. The mammals of the Berislav late Sarmatian *Hipparion*-fauna; pp. 24–121 in The Natural Environment and the fauna of the past, 5th ed. Naukova Dumka.
Kosintsev, P., K. J. Mitchell, T. Devièse, J. van der Plicht, M. Kuitems, E. Petrova, A. Tikhonov, T. Higham, D. Comeskey, C. Turney, A. Cooper, T. van Kolfschoten, A. J. Stuart, and A. M. Lister. 2019. Evolution and extinction of the giant rhinoceros *Elasmotherium sibiricum* sheds light on late Quaternary megafaunal extinctions. Nature Ecology & Evolution 3:31–38.
Kostopoulos, D. S., S. Sen, and G. D. Koufos. 2003. Magnetostratigraphy and revised chronology of the late Miocene mammal localities of Samos, Greece. International Journal of Earth Sciences 92:779–794.
Kostopoulos, D. S., G. D. Koufos, I. A. Sylvestrou, G. E. Syrides, and E. Tsombachidou. 2009. The Late Miocene Mammal Faunas of the Mytilinii Basin, Samos Island, Greece: New Collection: 2. Lithostratigraphy and Fossiliferous Sites. Beiträge Zur Paläontologie 31:13–26.
Koufos, G. D. 2006. Palaeoecology and chronology of the Vallesian (late Miocene) in the Eastern Mediterranean region. Palaeogeography, Palaeoclimatology, Palaeoecology 234:127–145.
Koufos, G. D. 2009. The Late Miocene Mammal Faunas of the Mytilinii Basin, Samos Island, Greece: New Collection: 1. History of the Samos Fossil Mammals. Beiträge Zur Paläontologie 31:1–12.
Koufos, G. D., D. S. Kostopoulos, and T. D. Vlachou. 2009a. The Late Miocene Mammal Faunas of the Mytilinii Basin, Samos Island, Greece: New Collection 16. Biochronology. 13.
Koufos, G. D., D. S. Kostopoulos, and T. D. Vlachou. 2009b. The Late Miocene Mammal Faunas of the Mytilinii Basin, Samos Island, Greece: New Collection 16. Biochronology. Beiträge Zur Paläontologie 31:397–408.
Koufos, G. D., D. S. Kostopoulos, T. D. Vlachou, and G. E. Konidaris. 2011. A synopsis of the late Miocene Mammal Fauna of Samos Island, Aegean Sea, Greece. Geobios 44:237–251.
Kretzoi, M. 1942. Bemerkungen zum System der Nachmiozänen Nashorn-Gattungen. Földtani Közlöny 72:4–12.
Krokos, W. I. 1917. *Aceratherium schlosseri* Web. du village de Grebeniki du gouvernement de Kherson. Memoires of the Agricultural Society of Southern Russia 82:1–96.
Lartet, E. 1837. Note sur les ossements fossiles des terrains tertiaries de Simorre et Sansan, dans le Departement de Gers et sur la decouverte recent d'une machoire de singe fossile. Comptes Rendus de l'Académie Des Sciences 4:85–93.
Laskarev, V. 1921. Sur la decourverte de la faune de Pikermi pres de Veles (Serbie meridionale). Bulletin of the Serbian Geographical Society 6:156–159.
Li, J., X. Fang, C. Song, B. Pan, Y. Ma, and M. Yan. 2014. Late Miocene–Quaternary rapid stepwise uplift of the NE Tibetan Plateau and its effects on climatic and environmental changes. Quaternary Research 81:400–423.
Li, Y., T. Deng, H. Hua, Y. Zhang, and J. Wang. 2020. Isotopic record of palaeodiet of a 7.4 Ma Hipparionine fauna from the central Loess Plateau, northern China: Palaeo-ecological and palaeo-climatic implications. Chemical Geology 532:119353.

Liang, Z., and T. Deng. 2005. Age structure and habitat of the rhinoceros *Chilotherium* during the Late Miocene in the Linxia Basin, Gansu, China. Vertebrata PalAsiatica 43:219–230.
Linnaeus, C. 1758. Systema Naturae. Laurentii Salvii, Stockholm, pp.
Liu, J., J. J. Li, C. H. Song, H. Yu, T. J. Peng, Z. C. Hui, and X. Y. Ye. 2016. Palynological evidence for late Miocene stepwise aridification on the northeastern Tibetan Plateau. Climate of the Past 12:1473–1484.
Lu, X. 2013. A juvenile skull of *Acerorhinus yuanmouensis* (Mammalia: Rhinocerotidae) from the Late Miocene hominoid fauna of the Yuanmou Basin (Yunnan, China). Geobios 46:539–548.
Lu, X., S. Chen, and W. He. 2015. New skulls of *Shansirhinus ringstroemi* from the upper Neogene of the Linxia Basin, and their paleoenvironmental context. Quaternary Research 35:539–549.
Lu, X., T. Deng, B. Sun, D. Sun, and S. Li. 2026. A new rhinocerotoid (Mammalia, Perissodactyla) from the early Oligocene of Ningdong, China, and its phylogenetic implications. Journal of Mammalian Evolution 32:47.
Lu, X.-K., T. Deng, and L. Pandolfi. 2023. Reconstructing the phylogeny of the hornless rhinoceros Aceratheriinae. Frontiers in Ecology and Evolution 11:1005126.
Lungu, A. 2008. Le developpement de la faune de *Hipparion* dans le Sarmatien sur le territoire de la Republique de Moldova. 6:181–186.
Lungu, A., and B. Rzebik-Kowalska. 2011. Faunal Assemblages, Stratigraphy and Taphonomy of the Late Miocene Localities in the Republic of Moldova. Institute of Systematics and Evolution of Animals, Krakow, Poland, 62 pp.
Lydekker, R. 1884. Additional Siwalik Perissodactyla and Proboscidea. Memoirs of the Geological Survey of India. Palaeontologia Indica 3:1–34.
Mallet, C., R. Cornette, G. Billet, and A. Houssaye. 2019. Interspecific variation in the limb long bones among modern rhinoceroses—extent and drivers. PeerJ 7:e7647.
Marsh, O. C. 1875. Notice of new Tertiary mammals, IV. American Journal of Science 3:239–250.
Mateer, N. J., and S. G. Lucas. 1985. Swedish vertebrate palaeontology in China: A history of the Lagrelius Collection. Bulletin of the Geological Institutions of the University of Uppsala, New Series 11:1–24.
Mead, A. J. 1999. Enamel hypoplasia in Miocene rhinoceroses (*Teleoceras*) from Nebraska: evidence of severe physiological stress. Journal of Vertebrate Paleontology 19:391–397.
Mecquenem, R. de. 1908a. Contribution à l'étude du gisement des vertébrés de Maragha et de ses environs. Annales d'histoire Naturelle 1:27–98.
Mecquenem, R. de. 1908b. Le lac D'ourmiah. Annales de Géographie 17:128–144.
Mecquenem, R. de. 1924. Contribution à l'étude des fossiles de Maragha. Annales de Paléontologie 13–14:135–160, 1–36.
Meiburg, P., and P. Siegfried. 1970. Katalog der Typen und Belegstücke zur Paläozoologie im Geologisch-Paläontologischen Institut der Westfälischen Wilhems-Universität Münster II. Teil: Vertebrata. Münstersche Forschungen Zur Geologie Und Paläontologie 15:1–84.
Mirzaie Ataabadi, M., R. L. Bernor, D. S. Kostopoulos, D. Wolf, Z. Orak, G. Zare, H. Nakaya, M. Watabe, and M. Fortelius. 2013. Recent Advances in Paleobiological Research of the Late Miocene Maragheh Fauna, Northwest Iran; pp. 546–565 in M. Fortelius, X. Wang, and L. Flynn (eds.), Fossil Mammals of Asia. Columbia University Press.

Mirzaie Ataabadi, M., A. Kaakinen, Y. Kunimatsu, H. Nakaya, Z. Orak, M. Paknia, T. Sakai, J. Salminen, Y. Sawada, S. Sen, G. Suwa, M. Watabe, G. Zaree, Z. Zhaoqun, and M. Fortelius. 2016. The late Miocene hominoid-bearing site in the Maragheh Formation, Northwest Iran. Palaeobiodiversity and Palaeoenvironments 96:349–371.

Niezabitowski, E. von L. 1912. *Teleoceras ponticus* n. sp. Vorläufige Notiz. Nowy Targ, pp.

Niezabitowski, E. von L. 1913. Über das Schädelfragment eines Rhinocerotiden (*Teleoceras ponticus* Niez.) von Odessa. Bulletin International de l'Academic des Sciences de Cracovie, Series B 223–235.

Noskova, N. G. 2001. Elasmotherians - evolution, distribution and ecology. The World of Elephants - International Congress 126–128.

Nothdurft, W., and J. B. Smith. 2002. The Lost Dinosaurs of Egypt. Random House, New York, 256 pp.

Osborn, H. F. 1900. Phylogeny of the rhinoceroses of Europe. Bulletin of the American Museum of Natural History 12:229–267.

Owen, R. 1848. Description of teeth and portions of jaws of two extinct anthracotherioid quadrupeds (*Hyopotamus vectianus* and *Hyop. bovinus*) discovered by the Marchioness of Hastings in the Eocene deposits on the N.W. coast of the Isle of Wight; with an attempt to develop Cuvier's idea of the classification of pachyderms by the number of their toes. Quarterly Journal of the Geological Society of London 4:103–141.

Pandolfi, L. 2016. *Persiatherium rodleri*, gen. et sp. nov. (Mammalia, Rhinocerotidae) from the upper Miocene of Maragheh (northwestern iran). Journal of Vertebrate Paleontology 36:e1040118.

Pavlow, M. 1913. Mammifères tertiaires de la Nouvelle Russie, 1. Partie: Artiodactyla, Perissodactyla (*Aceratherium kowalevskii* n.s.). Nouveaux Mémoires de La Société Impériale Des Naturalistes de Moscou 17:1–68.

Pavlow, M. 1914. Mammifères tertiaires de la Nouvelle Russie, 2. Partie: *Aceratherium incisivum*, *Hipparion*, Proboscidea, Carnivora. Nouveaux Mémoires de La Société Impériale Des Naturalistes de Moscou 17:1–78.

Peter, K. 2002. Odontologie der Nashornverwandten (Rhinocerotidae) aus dem Miozän (MN5) von Sandelzhausen (Bayern). Zitteliana 22:3–168.

Pohlig, H. 1884a. Ueber weitere Reiseergebnisse des Herrn Dr. Pohlig in Persien. Sitzungsberichte Der Naturforschenden Gesellschaft in Bonn 173–175.

Pohlig, H. 1884b. Geologische Untersuchungen in Persien. Verhandlungen Der Kaiserlich-Königlichen Geologischen Reichsanstalt 14:281–284.

Pohlig, H. 1885. Ueber eine Hipparionen-Fauna von Maragha in Nordpersien, über fossile Elephantenreste Kaukasiens und Persiens und über die Resultate einer Monographie der fossilen Elephanten Deutschalnds und Italiens. Zeitschrift Der Deutschen Geologischen Gesellschaft 37:1022–1027.

Pohlig, H. 1886. On the Pliocene of Maragha, Persia, and its resemblance to that of Pikermi in Greece. Quaterly Journal of the Geological Society of London 42:177–179.

Prado, de C. 1864. Descripción Física y Geológica de la Provincia de Madrid. Imprenta nacional, Madrid, Spain, 219 pp.

Prothero, D. R. 2005. The Evolution of North American Rhinoceroses. Cambridge University Press, Cambridge, UK, 218 pp.

Qiu, Z., and D. Yan. 1982. A horned *Chilotherium* skull from Yushe, Shansi. Vertebrata PalAsiatica 20:122–132.

Qiu, Z., and J. Xie. 1998. Notes on *Parelasmotherium* and *Hipparion* fossils from Wangji, Dongxiang, Gansu. Vertebrata PalAsiatica 36:13–23.
Qiu, Z. X., J. Y. Xie, and D. F. Yan. 1987. A new chilothere skull from Hezheng, Gansu, China, with special reference to the Chinese "*Diceratherium*". Scientia Sinica B 545–552.
Radović, P., M. M. Skinner, S. Alaburić, Z. Marković, J. Lindal, M. Roksandic, and S. Mayda. 2025. First record of a Late Miocene hominid from North Macedonia. Journal of Human Evolution 207:103734.
Ringström, T. 1923. *Sinotherium lagrelii*. Ringström. A new fossil rhinocerotid from Shansi, China. Bulletin of the Geological Survey of China 5:91–93.
Ringström, T. 1924. Nashörner der Hipparion-Fauna Nord-Chinas. Palaeontologia Sinica 1:1–156.
Ringström, T. 1927. Über quartäre und jungtertiäre Rhinocerotiden aus China und der Mongolei. Palaeontologia Sinica, Series C 4:1–21.
Rivals, F., R. I. Belyaev, V. B. Basova, and N. E. Prilepskaya. 2024. A tale from the Neogene savanna: Paleoecology of the hipparion fauna in the northern Black Sea region during the late Miocene. Palaeogeography, Palaeoclimatology, Palaeoecology 642:112133.
Rodler, A. 1885. Das Knochenlager und die Fauna von Maragha. Verhandlungen Der Kaiserlich-Königlichen Geologischen Reichsanstalt 14:333–337.
Roger, O. 1904. Wirbelthierreste aus dem Obermiocän der Bayerisch-Schwäbischen Hochebene. Bericht Des Naturwissenschaftlichen Vereins Für Schwäben Und Neuburg 36:1–52.
Roman, F. 1924. Contribution a l' étude de la faune de mammifères des Littorinenkalk (Oligocène supérieur) du Bassin de Mayence. Travaux Du Laboratoire de Géologie de La Faculté Des Sciences de Lyon 7:1–55.
Salminen, J., M. Paknia, A. Kaakinen, M. M. Ataabadi, G. Zare, Z. Orak, and M. Fortelius. 2016. Preliminary magnetostratigraphic results from the late Miocene Maragheh Formation, NW Iran. Palaeobiodiversity and Palaeoenvironments 96:433–443.
Sanisidro, O., M. T. Alberdi, and J. Morales. 2012. The first complete skull of *Hispanotherium matritense* (Prado, 1864) (Perissodactyla, Rhinocerotidae) from the middle Miocene of the Iberian Peninsula. Journal of Vertebrate Paleontology 32:446–455.
Sawada, Y., G. R. Zaree, T. Sakai, T. Itaya, K. Yagi, M. Imaizumi, M. Mirzaie Ataabadi, and M. Fortelius. 2016. K–Ar ages and petrology of the late Miocene pumices from the Maragheh Formation, northwest Iran. Palaeobiodiversity and Palaeoenvironments 96:399–431.
Schlosser, M. 1903. Die fossilen Säugethiere Chinas nebst einer Odontographie der recenten Antilopen. Abhandlungen Der Königlichen Bayerischen Akademie Der Wissenschaften 22:1–221.
Schlosser, M. 1921. Die Hipparionenfauna von Veles in Mazedonien. Abhandlungen der Bayerischen Akademie der Wissenschaften 24:1–55.
Sefve, I. 1927. Die Hipparionen Nord-Chinas. Palaeontologia SInica, Series C 4:1–91.
Sen, S., L. de Bonis, N. Dalfes, D. Geraads, and G. D. Koufos. 1994. Les gisements de mammifères du Miocène supérieur de Kemiklitepe, Turquie : 1. Stratigraphie et magnétostratigraphie. Bulletin Du Muséum National d'histoire Naturelle, Section C 16:5–17.
Skinner, M. F. 1986. Enamel hypoplasia in sympatric chimpanzee and gorilla. Human Evolution 1:289–312.

Skinner, M. F., A. T. Rodrigues, and C. Byra. 2014. Developing a pig model for crypt fenestration-induced localized hypoplastic enamel defects in humans: Localized Enamel Hypoplasia In Pigs. American Journal of Physical Anthropology 154:239–250.

Snitting, D., and H. Blom. 2009. Correcting taxon names containing diacritics—examples from Paleozoic vertebrates. Journal of Vertebrate Paleontology 29:269–270.

Spassov, N., T. Tzankov, and D. Geraads. 2006. Late Neogene stratigraphy, biochronology, faunal diversity and environments of South-West Bulgaria (Struma River Valley). Geodiversitas 28:477–498.

Spassov, N., D. Geraads, and G. Markov. 2019. The late Miocene mammal fauna from Gorna Sushitsa, southwestern Bulgaria, and the early/middle Turolian transition. Neues Jahrbuch Für Geologie Und Paläontologie - Abhandlungen 291:317–350.

Spassov, N., D. Geraads, L. Hristova, G. N. Markov, B. Garevska, and R. Garevski. 2018. The late Miocene mammal faunas of the Republic of Macedonia (FYROM). Palaeontographica Abteilung A 311:1–85.

Sun, D., T. Deng, and S. Wang. 2024. The first record of the genus *Prosantorhinus* (Perissodactyla: Rhinocerotidae) of East Asia. Zoological Journal of the Linnean Society 202:zlad183.

Sun, D., T. Deng, X. Lu, and S. Wang. 2023. A new elasmothere genus and species from the middle Miocene of Tongxin, Ningxia, China, and its phylogenetic relationship. Journal of Systematic Palaeontology 21:2236619.

Sun, D.-H., Y. Li, and T. Deng. 2018. A new species of *Chilotherium* (Perissodactyla, Rhinocerotidae) from the Late Miocene of Qingyang, Gansu, China. Vertebrata PalAsiatica 56:216–228.

Sun, D.-H., T. Deng, and Q. Jiangzuo. 2022. The most primitive *Elasmotherium* (Perissodactyla, Rhinocerotidae) from the Late Miocene of northern China. Historical Biology 1–11.

Svorligkou, G., P. Kampouridis, N. Kargopoulos, and L. Pandolfi. 2025. Craniodental anatomy of the hornless rhinocerotid *Chilotherium schlosseri* (Mammalia, Perissodactyla) from the Late Miocene of Samos Island, Greece. Journal of Mammalian Evolution 32:36.

Swisher, C. C. 1996. New 40Ar/39Ar dates and their contribution toward a revised chronology for the Late Miocene of Europe and west Asia; pp. 64–77 in R. L. Bernor, V. Fahlbusch, and H.-W. Mittmann (eds.), The evolution of western Eurasian Neogene mammal faunas. Columbia University Press, New York.

Tafel, A. 1914. Meine Tibetreise. Eine Studienfahrt Durch Das Nordwestliche China Und Durch Die Innere Mongolei in Das Östliche Tibet. Union Deutsche Verlagsgesellschaft, Stuttgart, 352 pp.

Tang, Y.-J., Y.-Z. You, H. Liu, and Y. Pan. 1974. New mammals from Banguo Basin of Yuanmou, Yunnan and their stratigraphical significance. Vertebrata PalAsiatica 12:60–67.

Tanner, L. G., and L. D. Martin. 1976. New rhinocerotids from the Oligocene of Nebraska. Life Science Miscellaneous Publications of the Royal Ontario Museum, Toronto 210–219.

Țibuleac, P., J. Tissier, A. Petculescu, and D. Becker. 2023. *Chilotherium schlosseri* (Weber, 1905) (Rhinocerotidae, M ammalia) from the late Miocene of the foreland of the Eastern Carpathians in Romania. Comptes Rendus Palevol 22:729–752.

Tissier, J., P.-O. Antoine, and D. Becker. 2020. New material of *Epiaceratherium* and a new species of *Mesaceratherium* clear up the phylogeny of early Rhinocerotidae (Perissodactyla). Royal Society Open Science 7:200633.
Tissier, J., D. Becker, V. Codrea, L. Costeur, C. Fărcaş, A. Solomon, M. Venczel, and O. Maridet. 2018. New data on Amynodontidae (Mammalia, Perissodactyla) from Eastern Europe: Phylogenetic and palaeobiogeographic implications around the Eocene-Oligocene transition. PLOS ONE 13:e0193774.
Tong, H.-W. 2001. Rhinocerotids in China - systematics and material analysis. Geobios 34:585–591.
Troxell, E. L. 1921. A study of *Diceratherium* and the diceratheres. American Journal of Science 5:197–208.
Tsiskarishvili, G. V. 1987. Late Tertiary Rhinoceroses (Rhinocerotidae) of the Caucasus. Izdatel'stvo Metsnierba, Tbilisi, Georgia, 141 pp.
Tung, Y., W. Huang, and Z. Qiu. 1975. Hipparion fauna in Anlo, Hohsien Shansi. Vertebrata PalAsiatica 13:34–47.
Upex, B., and K. Dobney. 2012. Dental enamel hypoplasia as indicators of seasonal environmental and physiological impacts in modern sheep populations: a model for interpreting the zooarchaeological record. Journal of Zoology 287:259–268.
Utescher, T., D. Ivanov, M. Harzhauser, V. Bozukov, A. R. Ashraf, C. Rolf, M. Urbat, and V. Mosbrugger. 2009. Cyclic climate and vegetation change in the late Miocene of Western Bulgaria. Palaeogeography, Palaeoclimatology, Palaeoecology 272:99–114.
Vangengeim, E., and A. Tesakov. 2013. Late Miocene mammal localities of Eastern Europe and Western Asia: toward biostratigraphic synthesis; pp. 521–537 in Fossil Mammals of Asia. Neogene Biostratigraphy and Chronology. Columbia University Press, New York.
Wang, H., B. Bai, J. Meng, and Y. Wang. 2016. Earliest known unequivocal rhinocerotoid sheds new light on the origin of Giant Rhinos and phylogeny of early rhinocerotoids. Scientific Reports 6:39607.
Weber, M. 1905. Über Tertiäre Rhinocerotiden von der Insel Samos. II. Bulletin de La Société Imperériale Des Naturalistes de Moscou 18:344–363.
Wehrli, H. 1941. Beitrag zur Kenntnis der „Hipparionen" von Samos. Paläontologische Zeitschrift 22:321–386.
Wessel, P., J. F. Luis, L. Uieda, R. Scharroo, F. Wobbe, W. H. F. Smith, and D. Tian. 2019. The Generic Mapping Tools Version 6. Geochemistry, Geophysics, Geosystems 20:5556–5564.
Zbyszewsky, G. 1952. Les mammifères miocènes de Quintanelas (Sabugo). Comuncòes Service Géologique Du Portugal 33:1–22.
Zdansky, O. 1924. Jungtertiäre Carnivoren Chinas. Palaeontologia Sinica, Series C 2:1–149.
Zdansky, O. 1925a. Quartäre Carnivoren aus Nord-Chiina. Palaeontologia Sinica, Series C 2:1–25.
Zdansky, O. 1925b. Fossile Hirsche Chinas. Palaeontologia Sinica, Series C 2:1–94.
Zdansky, O. 1927a. Weitere Bermerkungen über fossile Carnivoren aus China. Palaeontologia Sinica, Series C 4:1–30.
Zdansky, O. 1927b. Weitere Bermerkungen über fossile Cerviden aus China. Palaeontologia Sinica, Series C 5:1–21.
Zouhri, S., D. Geraads, S. El Boughabi, and A. El Harfi. 2012. Discovery of an Upper Miocene Vertebrate fauna near Tizi N'Tadderht, Skoura, Ouarzazate Basin (Central High Atlas, Morocco). Comptes Rendus Palevol 11:455–461.

# 6. Appendix

# Appendix 1

*Publication 1*

Reassessment of '*Chilotherium wegneri*' (Mammalia, Rhinocerotidae) from the late Miocene of Samos (Greece) and the European record of *Chilotherium*

**Panagiotis Kampouridis**[a], Georgia Svorligkou[b], Nikolaos Kargopoulos[a] and Felix J. Augustin[a]

[a]Department of Geoscience, Eberhard Karls University of Tübingen, Tübingen, Germany;

[b]Faculty of Geology and Geoenvironment, Department of Historical Geology and Palaeontology, National and Kapodistrian University of Athens, Athens, Greece

Published in

Historical Biology 22(3), 412–420

DOI: 10.1080/08912963.2021.1920939

Date of online publication: 13.05.2021

HISTORICAL BIOLOGY
2022, VOL. 34, NO. 3, 412–420
https://doi.org/10.1080/08912963.2021.1920939

Taylor & Francis
Taylor & Francis Group

ARTICLE



# Reassessment of '*Chilotherium wegneri*' (Mammalia, Rhinocerotidae) from the late Miocene of Samos (Greece) and the European record of *Chilotherium*

Panagiotis Kampouridis [a], Georgia Svorligkou [b], Nikolaos Kargopoulos [a] and Felix J. Augustin [a]

[a]Department of Geoscience, Eberhard Karls University of Tübingen, Tübingen, Germany; [b]Faculty of Geology and Geoenvironment, Department of Historical Geology and Palaeontology, National and Kapodistrian University of Athens, Athens, Greece

**ABSTRACT**

*Chilotherium* represents one of the most characteristic rhinocerotid genera during the late Miocene of Eurasia. In Europe, it is restricted to the eastern parts of the continent (Balkan Peninsula and Peri-Pontic region). In total, eight *Chilotherium* species have been described from European material, with Samos (Greece) representing the type locality of four of them. Herein, the type material of '*Chilotherium wegneri*' is revisited. The type cranium is considered lost for the past half-century, but the associated mandible is still housed in the collections of the Geomuseum Münster (Germany). The '*C. wegneri*' type mandible is redescribed and, taking into account the original illustration of the type cranium, compared to other chilotheres from Europe and Asia. Accordingly, the previously proposed synonymy of '*C. wegneri*' and *Chilotherium schlosseri*, which was also initially described from the late Miocene of Samos, is further supported. Lastly, an overview of the late Miocene record of *Chilotherium* in Europe is provided.

**ARTICLE HISTORY**
Received 12 March 2021
Accepted 19 April 2021

**KEYWORDS**
Taxonomy; rhinoceros; chilotheres; Neogene; Eastern Mediterranean; Greece

## Introduction

The late Miocene of the Eastern Mediterranean is characterised by a very rich and diverse mammalian faunal assemblage, which is known from numerous localities from Greece (e.g. Halmyropotamos, Axios Valley, Nikiti, Kerassia), Bulgaria (e.g. Hadjidimovo, Kalimantsi, Gorna Sushitsa, Staniantsi), North Macedonia (e.g. Karaslari, Prevalets) and Turkey (e.g. Akkaşdağı, Kemiklitepe, Mahmutgazi) (Bakalov and Nikolov 1962; Koufos 1987, 2006; de Bonis et al. 1992; Sen 1994; Theodorou et al. 2003; Antoine & Saraç 2005; Spassov et al. 2006, 2018, 2019; Kostopoulos 2009; Hristova 2012; Koufos et al. 2016; Geraads 2017; Böhme et al. 2018; Lechner and Böhme 2020; Kampouridis et al. 2020). The most renowned fossil localities of this region are certainly Pikermi (Gaudry 1862–1867; Theodorou et al. 2010; Böhme et al. 2017; Roussiakis et al. 2019) and Samos (Kostopoulos et al. 2003; Koufos 2009; Koufos et al. 2011) in Greece. The existence of vertebrate fossils on the island of Samos (Figure 1) has been known since the 19th century. The first systematic excavations took place in the 1880s and were led by C. I. Forsyth Major (Koufos 2009). In the following years Samos attracted the attention of many more researchers, such as the German palaeontologist E. Fraas (Koufos 2009), the Greek palaeontologist T. Skoufos (Svorligkou et al. 2019) and even the famed American fossil hunter B. Brown (Solounias 1981). The most recent systematic excavations on Samos were carried out by G. Koufos from the Laboratory of Geology and Palaeontology of the University of Thessaloniki (LGPUT, Greece) (Koufos 2009). The excavated material led to a detailed study of the faunal assemblage (e.g. Giaourtsakis 2009; Konidaris and Koufos 2009; Vlachou and Koufos 2009; Koufos et al. 2009a, 2009b, 2011) and the stratigraphical context, including a refined dating for the different fossiliferous horizons (Kostopoulos et al. 2003, 2009). The material of the recent LGPUT excavations is housed in the Natural History Museum of the Aegean (NHMA, Greece), while the material from the numerous older excavations is scattered in several collections throughout the world, some of the largest include the historical collections of the Bayerische Staatssammlung für Paläontologie und Geologie (BSPG, Germany), which unfortunately lost many specimens during the Second World War, the Naturhistorisches Museum in Wien (NHMW, Austria) and the American Museum of Natural History (AMNH, USA).

Another large collection of Samos fossils, which has received only little attention in the past (Andree 1921, 1926; Wehrli 1941), exists in the Geomuseum of the University of Münster (GMM, Germany). This material was uncovered by T. Wegner during 3 months of excavations in 1909 (Andree 1926). Andree (1926) also mentioned that 'the material comes from volcanic tuffs north of Mytilinii' (Andree 1926, p. 135). Wehrli (1941) noted that four different types of sediments can be identified associated with the Samos material in the GMM, which could be correlated to the sediment types mentioned by Schlosser (1904). However, he did not specify this any further and thus it is impossible to attribute the material of the GMM to any specific horizon(s) of Samos now and the exact age of the material cannot be assessed.

The Samos collection, housed in the GMM, comprises the type material of two hornless rhinos, described by Andree (1921), *Aceratherium wegneri* Andree (1921) and *Aceratherium angustifrons* Andree (1921). Later, they were referred to the genus *Chilotherium* by Ringström (1924). Heissig (1975) proposed that *Chilotherium wegneri* and *Chilotherium angustifrons* are junior synonyms of *Chilotherium schlosseri* (Weber 1905) and *Chilotherium kowalevskii* (Pavlow 1913), respectively. The type material of '*C. wegneri*' and *C. angustifrons* has been lost,

**CONTACT** Panagiotis Kampouridis pkampouridis94@gmail.com Department of Geoscience, Eberhard Karls University of Tübingen, Sigwartstr. 10, 72074, Tübingen, Germany



Published online 13 May 2021

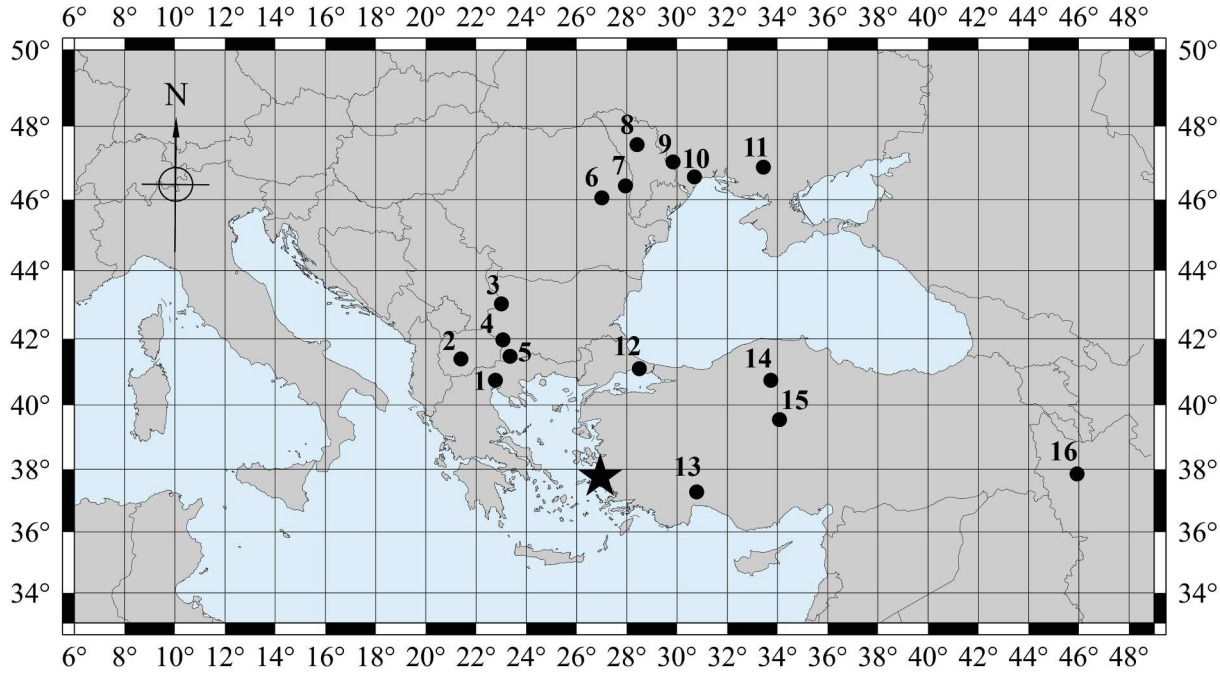


**Figure 1.** Distribution of *Chilotherium* spp. in the Balkan-Iranian province. Black star represents Samos (Greece) (Weber 1905; Andree 1921). 1, Pentalophos (Greece) (Geraads and Koufos 1990); 2, Morievo region (North Macedonia) (Spassov et al. 2018); 3, Staniantsi; 4, Oranovo; 5, Kromidovo (Bulgaria) (Geraads and Spassov 2009); 6, Reghiu (Codrea 1996); 7, Pogana (Romania) (Codrea 2011); 8, Raspopeni (Moldova) (Geraads et al. 2020); 9, Grebeniki (Pavlow 1913); 10, Odessa (unknown locality) (Niezabitowski 1913); 11, Berislav (Ukraine) (Korotkevich 1958); 12, Küçükçekmece (Antoine and Sen 2016); 13, Kayadibi (Geraads et al. 2020); 14, Sinap (several horizons) (Fortelius et al. 2003); 15, Akkaşdağı (Turkey) (Antoine and Saraç 2005); and 16, Maragha (Iran) (Pandolfi 2016).

with the type mandible of '*C. wegneri*' being the only exception (Meiburg and Siegfried 1970; Bertling pers. comm.), which is still housed in the GMM and, along with the associated skull described by Andree (1921), comprises the holotype of this species.

The aim of the present study is the redescription of the type mandible of '*C. wegneri*' and, based also on the original descriptions and illustrations of Andree (1921), the re-examination of the validity of this species. Additionally, a brief overview of all European *Chilotherium* species is provided (Table 1).

*Institutional Abbreviations*: AMNH, American Museum of Natural History, New York (USA); AMPG, Palaeontological and Geological Museum of the University of Athens (Greece); GMM, Geomuseum of the University of Münster (Germany); GPIT, Geologisch-Paläontologisches Institut der Universität Tübingen (Germany); LMU, Ludwig-Maximilians-University Munich (Germany); LGPUT, Laboratory for Geology and Palaeontology of the University of Thessaloniki (Greece); MNHN: Muséum national d'Histoire naturelle, Paris (France); NHMA, Natural History Museum of the Aegean, Samos (Greece); NHMW, Naturhistorisches Museum in Wien (Austria); NNPM, National Museum of Natural History, National Academy of Sciences of Ukraine, Kiev (Ukraine).

## Systematic palaeontology

Class Mammalia Linnaeus, 1758
Family Rhinocerotidae Gray, 1821

Tribe Chilotheriini Qiu et al., 1987

Genus *Chilotherium* Ringström, 1924

*Chilotherium schlosseri* (Weber, 1905)
*Synonym: Aceratherium wegneri* Andree 1921

*Material*: an almost complete mandible (GMM 567) (Figures 2–3)

*Locality*: Samos (unknown horizon; T. Wegner excavations in 1909)

*Remarks*: Andree (1921) erected the two hornless rhino species *Aceratherium wegneri* and *Aceratherium angustifrons* based on material from the late Miocene of Samos (Greece) housed in the GMM (Germany). He mentioned that the material of '*C. wegneri*' and *C. angustifrons* comes from the same sediment type and that the skull and the mandible, which represent the type material of '*C. wegneri*', were not found articulated, but right next to each

**Table 1.** Summary of the taxonomy of *Chilotherium* spp. from Europe.

| Species | Authority | Type Locality | Current Status |
|---|---|---|---|
| *Aceratherium schlosseri* | Weber 1905 | Samos (Greece) | *C. schlosseri* |
| *Aceratherium wegneri* | Andree 1921 | Samos (Greece) | *C. schlosseri* |
| *Aceratherium angustifrons* | Andree 1921 | Samos (Greece) | *C. schlosseri* |
| *Teleoceras ponticus* | Niezabitovski 1912 | Odessa (Ukraine) | *C. schlosseri*? |
| *Aceratherium samium* | Weber 1905 | Samos (Greece) | *C. samium* |
| *Aceratherium kowalevskii* | Pavlow 1913 | Grebeniki (Ukraine) | *C. kowalevskii* |
| *Chilotherium sarmaticum* | Korotkevich 1958 | Berislav (Ukraine) | *C. sarmaticum*? |
| *Aceratherium kiliasi* | Geraads and Koufos 1990 | Pentalophos (Greece) | *C. kiliasi* |

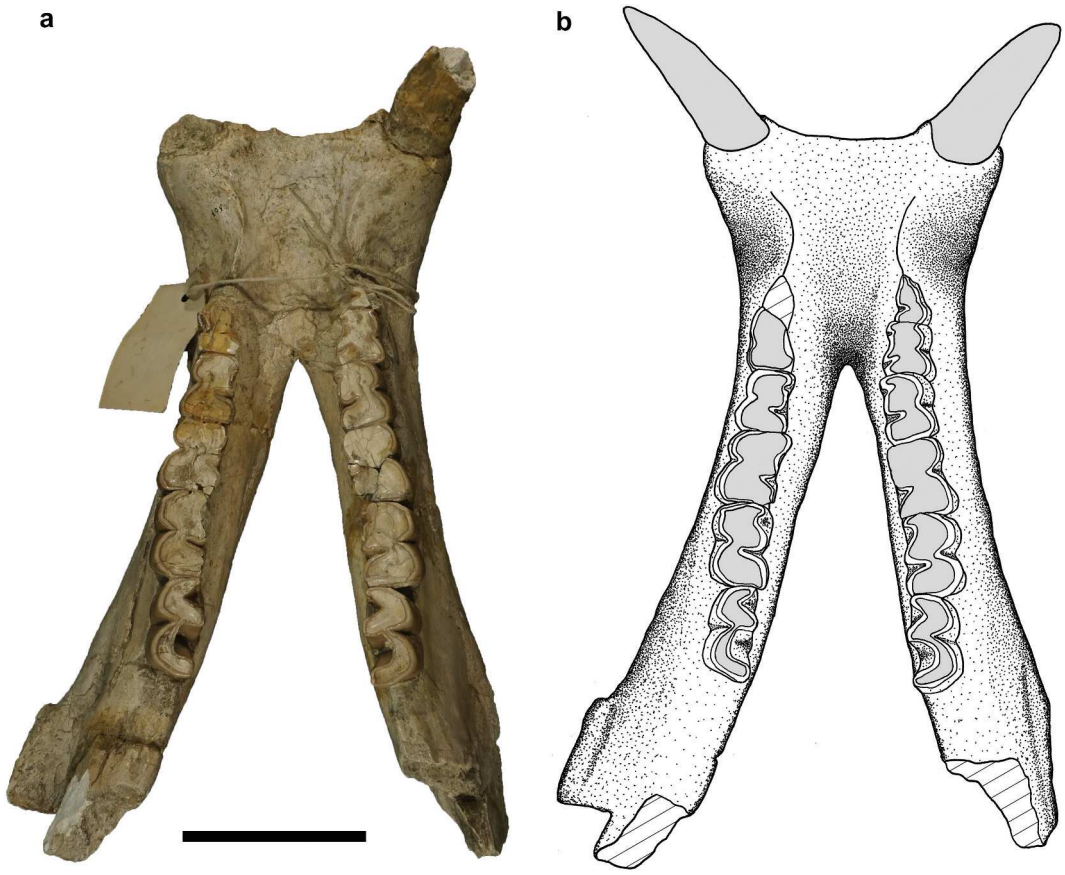


**Figure 2.** Type mandible of '*Chilotherium wegneri*' (GMM 567; herein assigned to *Chilotherium schlosseri*). (a), photograph; and (b), drawing in dorsal view, missing parts are reconstructed after Andree (1921, taf. I, Fig. 3). Scale bar is 10 cm.

other. However, their proximity and the similar wear stage should suffice to assign them to the same individual. The incisors, which were perfectly preserved during the time of their initial publication (Andree 1921), have been damaged since then and the left i2 is completely missing now (Figures 2, 3(b)). Therefore, the description of the incisors and the p2, which is also damaged, will take into account the description and illustrations provided by Andree (1921).

### *Description*

*Mandible*: Specimen GMM 567 (Figures 2–3) represents an almost complete mandible. The well-preserved symphysis is very wide and massive. In ventral view, it is transversally concave, and several foramina are visible on the ventral side of the symphysis: three on the left side and two on the right side (Figure 3(a)). In anterior view, between the incisors three other very large foramina are visible, one pair is situated on the right side and the third is larger and situated on the left side; the anterior end of the symphysis forms a thin edge (Figure 3(b)). In dorsal view, the symphysis terminates posteriorly at the distal end of the p3 (Figure 2). A long diastema exists between the p2 and the i2, which is marked by a well-developed dorsal ridge between these two teeth, on both sides. The dorsal surface of the symphysis, between these ridges is concave. The transversally narrowest part of the symphysis is at the middle of the p2. The ventral side of the symphysis is almost horizontal, showing a slight dorsal curve at its anterior end, right before the incisors. In lateral view, two mental foramina are present on each side, the anterior one is placed at the level of the anterior portion of the p2, somewhat more ventrally than the posterior one, which is situated below the border of p2-p3 (Figure 3(c–d)). A slight indentation on the ventral side of the mandibular body can be observed on both hemimandibles at the level of the p3, approximately at the beginning of the symphysis. The height of the mandibular body gradually increases posteriorly, as far as the level of the m3. Posteriorly, on both sides, the rami are broken off; however, enough of the left ramus is preserved to observe that the front edge of the ascending ramus is probably inclined slightly backwards. In lateral view, at the ventral portion of the mandible, posterior to the m3, both hemimandibles exhibit a well-developed anteroposteriorly oriented rugose attachment area for the M. masseter (Figure 3(c–d)).

*Lower dentition*: The dentition is relatively well preserved (Figure 2). The left incisor is completely broken off, leaving only the outline of the root visible within the alveolus (Figure 3(b)), whereas the right incisor is only missing its tip. The left toothrow is represented by the p3-m3, while the right toothrow also preserves part of the p2. The dentition is heavily worn, indicating an old age for the individual.

The i2s are large, tusk-like and dorsolaterally curved. The crown, when complete, was 103 mm long and 46 mm wide (Andree 1921, p. 212) and the two i2s are about 84 mm apart. The cross-section of the incisors is medially pointed and laterally rounded, as well as subelliptical at the base and subtriangular at the tip. Some remnants of enamel are exposed on the labial side of the preserved anterior edge of the right i2 (Figure 3(b)). The diastema separating the i2 from the p2 has a length of about 60 mm.

Some of the cheek teeth preserve remnants of their cement. The premolar/molar length ratio (sensu Athanassiou et al. 2014) is

67.5%. Most cheek teeth are heavily worn, and their morphology cannot be accurately assessed accordingly, only the m3 is moderately worn, allowing a more detailed description of its morphology. Anterior and posterior cingula are present in most teeth, in some cases reaching the lingual or buccal side of the tooth. Lingual and buccal cingula are very weakly developed, if present at all. All cheek teeth exhibit a well-developed ectolophid groove, except the p2 in which only a very shallow groove is visible. In the p2, the paralophid is very small, straight, and anteriorly pointing; the posterior valley remains open, albeit very small; there is no anterior valley; and the morphology of the protoconid cannot be assessed due to the wear stage.

All other cheek teeth exhibit a lingually projecting paralophid, although badly preserved in some, such as the damaged left m2 and both worn-down m1s. All cheek teeth preserve anterior and posterior valleys that remain open down to the cervix. Only in the p3, it seems possible that an even more advanced stage of wear would potentially close the posterior valley, thus forming a small 'fossettid'. In the p4 specifically, the anterior valley is extremely small and almost completely worn, without closing. In the same tooth, the posterior valley is deeper and narrow, reaching the centre of the tooth, despite its advanced wear stage. This can even be observed in the extremely worn m1. Similarly, in the m2, the anterior valley is almost completely worn, and the posterior one remains long and narrow.

The only exception is the less worn m3, which exhibits an anterolingually projecting paralophid, and a moderately deep anterior valley, in the trigonid. The metaconid is more developed than the paralophid and does not show any constriction. The trigonid is barely connected to the talonid, through a narrow (pre-)hypolophid. The hypolophid is similarly developed as the metaconid.

### *Comparison*

The mandible (GMM 567) bears two large, diverging incisors (Figures 2, 3(b)). This feature precludes the attribution of the mandible to any of the horned rhinos from the late Miocene of Europe, such as *Ceratotherium neumayri* (Osborn 1900) and *Dihoplus pikermiensis* (Toula 1906), which exhibit only small to moderate incisors if present at all, and never such tusk-like ones as seen in GMM 567 (Giaourtsakis et al. 2006; Giaourtsakis 2009; Pandolfi and Rook 2017). Furthermore, the premolar/molar length ratio (sensu Athanassiou et al. 2014) is relatively small (67.5%) and prevents its referral to the only other hornless rhino from the late Miocene of the Balkan Peninsula, *Acerorhinus neleus* Athanassiou et al. (2014) (compare Athanassiou et al. 2014, fig. 5).

Specimen GMM 567 exhibits the following features, characteristic for *Chilotherium*: a wide symphysis, with a strongly concave ventral surface; very strong i2s, separated from each other, and from the p2 by long diastemata (Ringström 1924; Deng 2001, 2006). Thus, the mandible (GMM 567) can be unambiguously attributed to the genus *Chilotherium*.

Within the genus *Chilotherium*, the identification of the species based solely on an isolated mandible is not possible. The morphology of both the mandibular body and the teeth is very uniform within the genus and shows only little variation which may be associated with intraspecific variability (Ringström 1924). In fact, Ringström (1924) does not provide any description of the lower teeth as a consequence. Furthermore, the anterior portion of the mandible is damaged in the, now lost, type material of *C. schlosseri* and no detailed description of the symphysis is available (Weber 1905, p. 346). Similarly, the type material of *C. samium* includes two mandibles, both of which lack the incisors. Only one of them, which Weber (1905, p. 356) considered belonging to a male individual, preserves the roots of the i2s and assumed that the teeth must have been large and tusk-like. The type material of *C. angustifrons*, which herein is considered a junior synonym of *C. schlosseri* (Table 1), does not include a mandible. Although no detailed comparison between the chilotheres from Samos is possible, some features such as the ramus that is slightly inclined backwards and the similarly developed attachment area for the M. masseter in the mandibles of both '*C. wegneri*' and *C. schlosseri* (Weber 1905, taf. VIII, fig. 1) indicate the great resemblance between the two species.

## Taxonomic status of '*C. wegneri*'

Andree (1921) initially described '*C. wegneri*' as a relatively large hornless rhino, most similar to *C. schlosseri*. This identification, however, has subsequently been questioned by several authors.

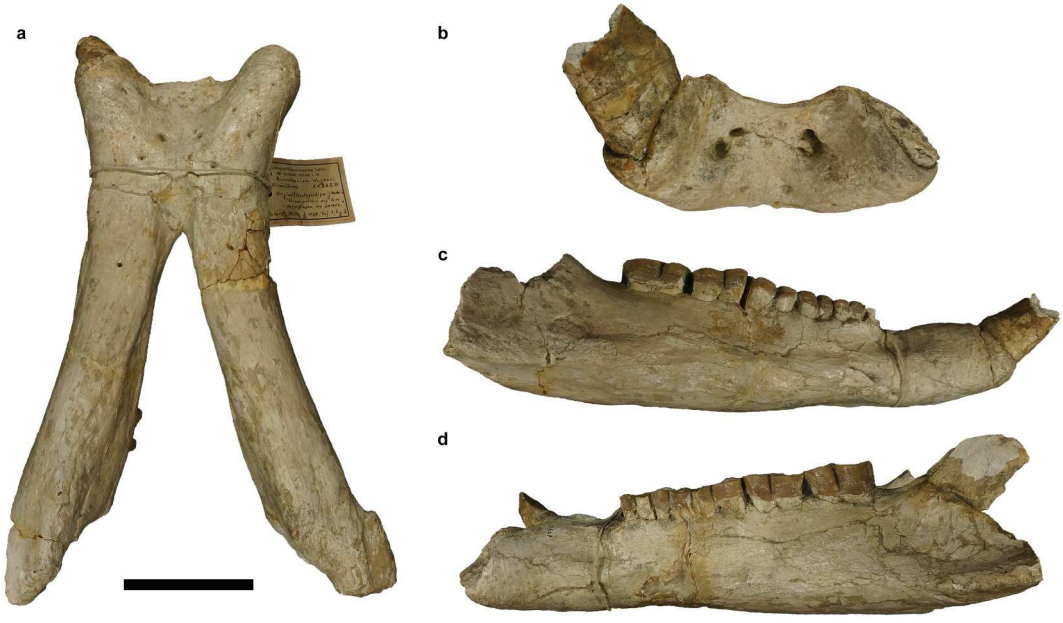


**Figure 3.** Type mandible of '*Chilotherium wegneri*' (GMM 567; herein assigned to *Chilotherium schlosseri*) in: (a), ventral; (b), anterior; (c), right lateral; and (d), left lateral view. Scale bar is 10 cm for (a), (c–d) and 7 cm for (b).

Killgus (1922, 1923) studied the late Miocene material of Kutschwan (China) housed in the GPIT, which includes a rich collection of *Chilotherium habereri* (Schlosser 1903) specimens. He provided a detailed description of the material and compared it to most of the known chilotheres. In his comprehensive comparison to '*C. wegneri*', Killgus (1922) noted many similarities between the two species and proposed their synonymy, a view also supported by Schlosser (1924). However, many of these suggested similarities are features that are relatively widespread within the genus *Chilotherium*, including the flat dorsal profile of the skull, the depression of the frontals and longitudinal groove between the two nasals (Ringström 1924).

One specific feature of both '*C. wegneri*' and *C. habereri*, noted by Killgus (1922), is the ventral profile of the mandible, which in both species seems to exhibit an indentation on the ventral side, below the premolars. However, this feature is also observed in some mandibles of the primitive *Chilotherium wimani* Ringström 1924 (Ringström 1924, p. 44) and in the more derived *Chilotherium persiae* (Pohlig 1886) (MNHN – MAR 3860) and *C. kowalevskii* (Pavlow 1913, pl. IV, fig. 11, 13 and 14). Another feature, discussed by Killgus (1922), is the minimal distance between the parietal crests. However, as can be seen in Table 2, in '*C. wegneri*' and *C. schlosseri* the minimal distance between the parietal crests is significantly higher than in the other *Chilotherium* species and, in fact, illustrates the resemblance of '*C. wegneri*' to *C. schlosseri*.

Ringström (1924) included '*C. wegneri*' in his new genus, *Chilotherium*. He noted that the premaxillae of '*C. wegneri*' are most similar to *Chilotherium anderssoni* Ringström 1924 because they are straight without a medial process, in contrast to *C. habereri* and *C. persiae* in which a cone-like process is present on the medial side of the premaxillae. However, a closer look into the illustrations provided by Andree (1921, taf. I, fig. 2) reveals that indeed a cone-like structure is present on the medial side of the premaxillae. Furthermore, Ringström (1924) discussed three morphological similarities to his new species *Chilotherium planifrons* Ringström 1924), most likely a junior synonym of *C. anderssoni* (Deng 2006). The first one concerns the form of the occipital. However, its morphology can vary as already indicated by the differences between '*C. planifrons*' and *C. anderssoni* (Ringström 1924, fig. 34–35). Furthermore, the type cranium of '*C. wegneri*' is somewhat deformed. The second feature, discussed by Ringström (1924) concerns the similar morphology of their paroccipital processes. However, in *C. kowalevskii* from Grebeniki (Pavlow 1913) the paroccipital processes seem to be very similar to '*C. wegneri*'. In addition, a skull (NHMW-1911/0005/0128) from Samos, housed in the NHMW, which can be assigned to *C. schlosseri*, exhibits a short paroccipital process, which, in posterior view, does not cover the postglenoid process, just like in '*C. wegneri*'. Similarly, in some *C. habereri* skulls from Kutschwan (China), housed in the GPIT, the paroccipital process is relatively short, compared to the one illustrated by Ringström (1924, fig. 22). Thus, the morphology and relative size of the paroccipital process cannot be used to associate '*C. wegneri*' with '*C. planifrons*' and might in fact indicate its affinity to the European species. The last feature used by Ringström (1924) to stress the similarity between '*C. wegneri*' and '*C. planifrons*' is the flat dorsal profile of the skull. This represents a common feature in derived species of *Chilotherium*. Additionally, the degree of flatness or concavity of the dorsal profile of the skull may vary within the same population as seen in Pavlow (1913, pl. IV, fig. 6–7).

As already pointed out by Heissig (1975), Deng (2006) and Giaourtsakis (2009), '*C. wegneri*' probably represents a junior synonym of *C. schlosseri*. However, none of them provided any arguments in favour of this hypothesis. Herein, we follow the abovementioned authors regarding the synonymy of '*C. wegneri*' and *C. schlosseri* because both are morphologically nearly indistinguishable, exhibiting the following features in the skull: a well-formed ('muldenförmige') depression in the frontals; weakly, anteriorly ascending nasals, which are separated from each other by a median, longitudinal groove; a flat dorsal profile in the skull; an orbita that ends anteriorly above the anterior portion of the M3; and widely separated parietal crests (see Table 2). Regarding the dental morphology, the two preserved teeth (right M2 and M3) in the type cranium of '*C. wegneri*' are almost identical to the respective teeth in *C. schlosseri* featuring: in both M2 and M3, a closed medifossette, an extremely strong protocone constriction and a very strong antecrochet; in the M2, a closed postfossette, a small, closed medifossette, a closed median valley, a strongly constricted hypocone and no visible paracone rib; and in the M3, an unconstricted hypocone, an open median valley and a weak paracone fold. In general, *C. schlosseri* (including '*C. wegneri*') seems to be distinct from all other chilotheres by featuring a minimal distance separating the parietal crests of at least 70 mm (see Table 2), a feature already mentioned by Ringström (1924, p. 85), which might, in fact, represent an autapomorphy of the species.

**Table 2.** Minimal distance (in mm) between the parietal crests in *Chilotherium* spp. Data sources: 1, Andree (1921); 2, own data; 3, Krokos (1917); 4, Killgus (1922); 5, Ringström (1924); 6, Deng (2006).

| Taxon | min | max | n |
|---|---|---|---|
| '*C. wegneri*'[1] | 87 | - | 1 |
| *C. schlosseri*[1,2] | 70 | 90 | 4 |
| *C. samium*[1] | ~40 | - | 1 |
| *C. kowalevskii*[3] | 40 | 66 | 10 |
| *C. persiae*[2] | 32 | 50 | 4 |
| *C. habereri*[4,5] | 42 | 60 | 9 |
| *C. anderssoni*[5] | 50 | 63 | 5 |
| *C. wimani*[6] | 28 | 64 | 10 |
| *C. primigenius*[6] | 18 | - | 1 |

## The European record of *Chilotherium*

The genus *Chilotherium* has a very limited stratigraphical and geographical distribution as it has only been reported from the late Miocene of Eurasia. *Chilotherium* was established by Ringström (1924), based on material from the late Miocene of China, for short-limbed, hornless rhinos, which are characterised by a depression in the frontals and a wide mandibular symphysis with enlarged tusks. In the late Miocene of Asia, especially in the '*Hipparion* Red Clay' localities (Flynn et al. 2011) of China, this group is extremely common, and, in some cases, it even appears as the dominant vertebrate taxon (Killgus 1922, 1923; Ringström 1924). The earliest representative of the genus is *Chilotherium primigenius* Deng 2006 from the early Late Miocene (early to middle MN9) of the Linxia Basin (China) (Deng 2006). Deng (2006) suggested that this species might have evolved into *C. wimani*, which in turn may be ancestral to several other species of the genus, such as *C. habereri* (Deng 2006). Heissig (1975) proposed the migration of the Chinese *C. habereri* into Anatolia during the Turolian, which then might have given rise to the European chilotheres.

Despite its rarity in Europe, at least eight chilotheres have been described from the Eastern and Southeastern parts of the continent. A short overview of the fossil record of the European *Chilotherium* representatives is given below, ordered by the date of their initial description:

### *Chilotherium schlosseri*

Weber (1905) described the first European chilotheres while studying the rhinocerotid remains from the late Miocene of Samos housed in the BSPG – the slightly larger, more derived *C. schlosseri* and the smaller, primitive *C. samium*, (Weber 1904, 1905). Andree (1921) described a badly damaged skull of *C. schlosseri* from the Samos material of the GMM, which is considered lost (Meiburg and Siegfried 1970; Bertling pers. comm.). Later, Killgus (1922) confirmed the validity of *C. schlosseri*, pointing out numerous differences separating it from the Chinese *C. habereri*, as also supported by Schlosser (1924). Ringström (1924) discussed similarities between *C. schlosseri* and the Chinese *C. anderssoni*, such as the morphology of the paroccipital process, while also pointing out important differences which separate the two species. Many authors (Kiernik 1913; Krokos 1917; Korotkevich 1970; Heissig 1975; Giaourtsakis 2003, 2009; Deng 2006; Antoine & Sen 2016) considered most of the later described European chilothere species to be potential junior synonyms of *C. schlosseri*. Furthermore, the potential presence of *C. schlosseri* has been recognised in some other late Miocene fossil sites in the Eastern Mediterranean (Heissig 1975, 1996; Vangengeim and Tesakov 2013; Antoine and Sen 2016). Unfortunately, the type material of this species was lost during the Second World War (Giaourtsakis 2003, 2009).

### *Chilotherium samium*

The second species described by Weber (1905), *C. samium*, represents a primitive chilothere. This species is based on two skulls and mandibles of very old individuals and Weber (1905) originally suggested a close affinity to *Aceratherium incisivum*, instead of *C. schlosseri*. Ringström (1924) included *C. samium* into *Chilotherium*, based on the high placement of the orbits, the straight nasals and the separated parietal crests, also pointing out the similarities to the other chilotheres instead of *Aceratherium incisivum*. Heissig (1975) also supported the attribution of *C. samium* to *Chilotherium* and described it as a primitive representative of the genus (or subgenus), distinct from *Acerorhinus* spp. and *Subchilotherium intermedium*. Geraads and Koufos (1990) followed the original assignment of *C. samium* to the genus *Aceratherium*, based on the description of Weber (1905). They also proposed a close relationship of *C. samium* and their new species *Aceratherium kiliasi* Geraads and Koufos 1990). Heissig (1996) mentioned *C. samium* as 'the most primitive form dentally', with its first occurrence in Anatolia potentially from the MN10. Fortelius et al. (2003) described *C. samium* as being at a comparable evolutionary stage as *C. wimani*, but because of the problematic taxonomy of *C. samium*, they proposed to restrict this name to its type material. Geraads and Spassov (2009) included this species in their new subgenus as *C.* (*Eochilotherium*) *samium* and pointed out important differences from the more derived *C. wimani*. The problems concerning *C. samium*, including the loss of the type material, have been discussed by several authors in the past (e.g. Geraads and Koufos 1990; Fortelius et al. 2003; Giaourtsakis 2003, 2009; Athanassiou et al. 2014).

### *Chilotherium ponticum*

Niezabitowski (1912) erected the species *Teleoceras ponticus* Niezabitowski 1912), probably from the late Miocene (Turolian) of Odessa. One year later he published a description of the type cranium, with a comparison to *C. schlosseri* and some teleoceratines, suggesting that despite its close affinity to the former, it should be included in the genus *Teleoceras* (Niezabitowski 1913). Kiernik (1913) published a detailed description and comparison of the type cranium of *C. ponticum*, in which he rejects the results of Niezabitowski (1912, 1913), synonymising *C. ponticum* from Odessa and *C. schlosseri* from Samos. Killgus (1922, 1923) argued that the type cranium of *C. ponticum* in fact belongs to *C. habereri*, based on the similarities of the tooth morphology. Ringström (1924) assigned it to the genus *Chilotherium*, based on the depression in the frontals and the very strong antecrochet and kept the name *C. ponticum* for the fragmentary skull from Odessa. More recently, Heissig (1975) and Deng (2006) referred *C. ponticum* to *C. schlosseri*, as previously proposed by Kiernik (1913).

### *Chilotherium kowalevskii*

Pavlow (1913) studied the rich fauna from the late Miocene of Grebeniki, including a large collection of rhino material, based on which she described the species *C. kowalevskii*. Krokos (1917) revised the Grebeniki material and attributed it to *C. schlosseri*. Ringström (1924, p. 93) mentioned it as 'a typical *Chilotherium* species' and pointed out that it resembles *C. habereri*, without synonymising them. Heissig (1975) attributed material from the late Miocene of Anatolia to *C. kowalevskii*, which he regarded as a valid *Chilotherium* species, noting its potential relationship to the younger '*Chilotherium*' *brancoi*. However, the latter in fact belongs to the distinct chilothere genus *Shansirhinus* (Kretzoi 1942; Deng 2005). Heissig (1996, 1999) supported the validity of *C. kowalevskii* and noted that it has sometimes been mentioned from Anatolia, but its presence there is rather doubtful. Geraads (2013) regarded the hornless rhino from Çorakyerler (Turkey), which had previously been identified as *C. kowalevskii* (Heissig 1975), as a potential new species, belonging to the genus *Acerorhinus*. In addition, Fortelius et al. (2003) assigned part of the hornless rhino material from the late Miocene (MN11-12) of Kavakdere (Turkey) to *C. kowalevskii*. Geraads and Spassov (2009) provided a short diagnosis for *C. kowalevskii* and referred material from the late Miocene of Yambol (Bulgaria) to *C.* cf. *kowalevskii*. Deng (2006) included *C. kowalevskii* in his revision of *Chilotherium* spp. and regarded it as a valid species. Vangengeim and Tesakov (2013, tab. 23.3) reported *C. kowalevskii* also from the late Miocene (MN10) of Raspopeni (Moldova). Antoine and Sen (2016) assigned the small hornless rhino material from the late Miocene of Küçükçekmece, which had previously been referred to *Aceratherium* cf. *kowalevskii* (Nicolas 1978), to *C. schlosseri*. Furthermore, they considered *C. kowalevskii* to be a junior synonym of *C. schlosseri*, based on their strong craniodental similarities and their overlapping spatio-temporal distribution. This hypothesis is further supported, although not explicitly stated, by the phylogenetic analysis of Pandolfi (2016), which considers the two species either as sister taxa or as synonyms (Antoine and Sen 2016). Herein, *C. kowalevskii* is kept as a separate species (Table 1) until its taxonomic issues are resolved.

### *Chilotherium angustifrons*

Andree (1921) described two new hornless rhino species, '*C. wegneri*' and *C. angustifrons*, based on cranial material from the late Miocene of Samos, housed in the GMM. The first has been discussed above and represents a junior synonym of *C. schlosseri* (Table 1). The second was described as a relatively small hornless rhino, which may be more closely related to *C. samium* and *Aceratherium incisivum* (Andree 1921). Killgus (1922, 1923) compared his *C. habereri* material from Kutschwan (China) to

*C. angustifrons* and concluded that they should be attributed to the same species. Accordingly, Ringström (1924) ascribed *C. angustifrons* to *Chilotherium*, with its teeth morphology being a typical example of a chilothere and differing significantly from *Aceratherium incisivum*. He also noted the similarities of *C. angustifrons* to *Chilotherium gracile* Ringström 1924, a junior synonym of *C. habereri* (Deng 2006), without synonymising them. Heissig (1975) suggested that *C. angustifrons* represents a synonym of *C. kowalevskii* from Grebeniki. Whereas Giaourtsakis (2009) mentioned that *C. angustifrons* represents a junior synonym of either *C. kowalevskii* or *C. schlosseri*. The taxonomic status of *C. angustifrons* is quite problematic due to the fact that the type skull is heavily damaged, lacking a significant portion of its right side (Andree 1921, taf. III, figs. 1–2), and is currently considered lost (Meiburg and Siegfried 1970). The deep groove separating the nasals, the depression of the frontals, the marked protocone constriction and the strong antecrochet in the M1 confirm its attribution to the genus *Chilotherium* and preclude its attribution to *C. samium*. Due to the absence of any morphological traits that would distinguish it from *C. schlosseri, C. angustifrons* is herein considered a junior synonym of the latter (Table 1) as previously indicated by Giaourtsakis (2009).

### *Chilotherium sarmaticum*

Korotkevich (1958) described the new species *Chilotherium sarmaticum* Korotkevich 1958) from the late Miocene of Berislav (Ukraine). This species is mainly discussed in Russian literature (Geraads and Spassov 2009) and is often neglected in most recent reviews of chilotheres (Heissig 1975, 1996, 1999; Fortelius et al. 2003; Deng 2006). A complete skull from Reghiu (Romania; MN10-11), which Codrea (1996) referred to as *Chilotherium* sp., was later associated with *C. sarmaticum* (Ştiucă 2003). However, Codrea (2011) noted that the skull from Reghiu (Romania) is regarded as 'lost or at least, mislaid'. Spassov et al. (2006) referred a single i2 from the late Miocene of Oranovo (Bulgaria) to *C.* cf. *sarmaticum*. Geraads and Spassov (2009) reviewed the Bulgarian fossil record of Neogene rhinos, ascribing additional material to this species. They provide a simplified diagnosis for *C. sarmaticum*, based on the ones given by Korotkevich (1958, 1970). However, neither the Romanian nor the Bulgarian material was definitively assigned to this species (referred to as *C.* cf. *sarmaticum*). Geraads and Spassov (2009) suggested that, despite the absence of *C. sarmaticum* in recent literature, it should be regarded as a valid species.

### *Chilotherium kiliasi*

Geraads and Koufos (1990) described the species *Aceratherium kiliasi* from the early late Miocene (Vallesian) of Pentalophos 1 (Greece). The holotype of the species is a moderately well-preserved skull of an old individual, which was later assigned to the genus *Chilotherium* (Heissig 1996; Fortelius et al. 2003; Athanassiou et al. 2014). Geraads and Koufos (1990) also attributed to this species material, which actually belongs to the genus *Acerorhinus* (Heissig 1996; Fortelius et al. 2003; Athanassiou et al. 2014). Heissig (1996, 1999) interpreted *C. kiliasi* as a primitive *Chilotherium*, which could be closely related to *C. samium* or potentially even conspecific. Giaourtsakis (2003) preferred to keep this species under its original name '*Aceratherium*' *kiliasi*, as a detailed re-evaluation of the material was needed. Fortelius et al. (2003) also pointed out the problems concerning this species, attributing it to a primitive *Chilotherium*, and noting its similarities to *C. samium*. They also referred to this species a number of specimens from the late Miocene of Loc. 49 of the Sinap Formation (Turkey). Geraads and Spassov (2009) erected the new subgenus *Eochilotherium* with *C.* (*Eochilotherium*) *kiliasi* as its type species and also included *C. samium*. They studied numerous rhinocerotid remains from several late Miocene localities of Bulgaria, attributing a skull from the late Miocene of Kromidovo to *C.* (*Eochilotherium*) cf. *kiliasi*. Athanassiou et al. (2014) revised the record of the genus *Acerorhinus* from the late Miocene of the Eastern Mediterranean, erecting the new species *Acerorhinus neleus*. They attributed to this species much of the material from Pentalophos 1, which was initially included in *Aceratherium kiliasi*. Athanassiou et al. (2014) also noted that the type cranium of *C. kiliasi* represents a relatively primitive *Chilotherium*, but concerning the specific identification, the loss of the type material of *C. samium* does not allow a definitive association and thus preferred to refer to it as *C.* cf. *samium* (Athanassiou et al. 2014, tab. 5). Herein, it is considered as a valid species, pending further investigations (Table 1).

### *Chilotherium habereri*

Lastly, the species *Aceratherium habereri* was initially described by Schlosser (1903) based on material from the late Miocene of China, but was later recorded in some European localities, many of these reports are however questionable and its presence outside Asia is doubtful. Killgus (1922, 1923) assigned a rich collection of cranial and postcranial elements from the late Miocene of Kutschwan (China), housed in the GPIT, to *Aceratherium habereri*. Later, Ringström (1924) incorporated it in *Chilotherium*, attributing new material from other late Miocene localities of China to *C. habereri*. In addition, the occurrence of the Chinese chilothere *C. habereri* has been suggested even in Europe, but the taxonomic status of this material is not clear (Antoine and Saraç 2005). As already discussed, Killgus (1922, 1923) proposed the synonymy of some European species with *C. habereri*, implying the presence of *C. habereri* in the late Miocene of Samos (Greece), but this hypothesis cannot be sustained. Heissig (1975) mentioned its presence in Anatolia, but without any detailed description (Heissig 1996). Saraç (1994) also identified the species based on material from the late Miocene of Turkey. Fortelius et al. (2003) attributed some material from the late Miocene fossil site Loc. 49 of the Sinap Formation (Turkey) to *C.* cf. *habereri* and noted that some material previously assigned to *C. habereri* belongs to an 'indeterminate *Chilotherium*'. Antoine & Saraç (2005) briefly discussed the issues concerning the taxonomy of this material and preferred to refer their specimen from the late Miocene of Akkaşdağı preliminarily to *Chilotherium* sp. until the issues concerning the presence of *C. habereri* in Turkey are resolved.

## Conclusion

The re-examination of the type material of '*C. wegneri*', from the late Miocene of Samos (Greece), led to its attribution to the derived *C. schlosseri*, also known from Samos material. The type crania of the two chilothere species share many similarities in the cranial anatomy and an identical dental morphology in the preserved teeth, but most importantly they exhibit widely separated (>70 mm)

parietal crests, in contrast to most other *Chilotherium* species. Furthermore, we provide an overview of the fossil record of *Chilotherium* in Europe. In total, eight species have been described, many of which evidently represent synonyms. Despite the fact that *Chilotherium* spp. was very common in the late Miocene of Asia (especially China), it is a rare faunal component in Europe, with its distribution being limited to the Balkan Peninsula and the Peri-Pontic region.

## Acknowledgments

We would like to thank M. Bertling and D. Theda (GMM) for providing photographs of the "*C. wegneri*" mandible housed in the GMM and information on the material. We thank I. Giaourtsakis (LMU) for fruitful discussions. We would like to thank A. Athanassiou (Ephorate for Palaeoanthropology and Speleology of Greece) for providing important literature. We would also like to thank M. Böhme (GPIT), S. Roussiakis (AMPG), G. Theodorou (AMPG), U. Göhlich (NHMW) and L. Gorobets (NNPM) for photographs and access to comparative material under their care. We would like to thank the Editor-in-Chief G. Dyke for his very fast and reliable handling of the manuscript. Lastly, we thank D. Geraads (MNHN) and an anonymous reviewer for their constructive comments, which improved the manuscript.

## Disclosure statement

No potential conflict of interest was reported by the author(s).

## ORCID

Panagiotis Kampouridis http://orcid.org/0000-0002-1812-4664
Georgia Svorligkou http://orcid.org/0000-0002-1472-0282
Nikolaos Kargopoulos http://orcid.org/0000-0002-6471-151X
Felix J. Augustin http://orcid.org/0000-0002-7787-5601

## References

Andree J. 1921. Rhinocerotiden aus dem Unterpliocän von Samos. Paläontol Zeitschrift. 3:189–212. doi:10.1007/BF03190415.
Andree J. 1926. Neue Cavicornier aus dem Pliocän von Samos. Palaeontographica. 67(6):135–175.
Antoine P-O, Saraç G. 2005. Rhinocerotidae (Mammalia, Perissodactyla) from the late Miocene of Akkaşdağı, Turkey. Geodiversitas. 27 (4):601–632.
Antoine P-O, Sen S. 2016. Rhinocerotidae and Chalicotheriidae (Perissodactyla, Tapiromorpha). Geodiversitas. 38(2):245–259. doi:10.5252/g2016n2a6.
Athanassiou A, Roussiakis SJ, Giaourtsakis IX, Theodorou GE, Iliopoulos G. 2014. A new hornless rhinoceros of the genus *Acerorhinus* (Perissodactyla: Rhinocerotidae) from the Upper Miocene of Kerassiá (Euboea, Greece), with a revision of related forms. Palaeontograp Abteilung A. 303(1–3):23–59. doi:10.1127/pala/303/2014/23.
Bakalov P, Nikolov IV. 1962. Les fossiles de Bulgarie: mammifères tertiaires. Sofia: Académie des Sciences de Bulgarie.
Böhme M, Spassov N, Ebner M, Geraads D, Hristova L, Kirscher U, Kötter S, Linnemann U, Prieto J, Roussiakis S, et al. 2017. Messinian age and savannah environment of the possible hominin *Graecopithecus* from Europe. PLoS ONE. 12(5):e0177347. doi:10.1371/journal.pone.0177347.
Böhme M, Van Baak CGC, Prieto J, Winklhofer M, Spassov N. 2018. Late Miocene stratigraphy, palaeoclimate and evolution of the Sandanski Basin (Bulgaria) and the chronology of the Pikermian faunal changes. Glob Planet Change. 170:1–19. doi:10.1016/j.gloplacha.2018.07.019.
de Bonis L, Bouvrain G, Geraads D, Koufos G. 1992. Diversity and paleoecology of Greek late Miocene mammalian faunas. Palaeogeogr Palaeoclimatol Palaeoecol. 91(1–2):99–121. doi:10.1016/0031-0182(92)90035-4.
Codrea V. 1996. Miocene rhinoceroses from Romania: an overview. Acta Zool Cravov. 39(1):83–88.
Codrea VA. 2011. Early Late Miocene *Chilotherium* (Perissodactyla, Mammalia) from Pogana (Scythian Platform). North-western J Zool. 7(2):184–188.
Deng T. 2001. New material of *Chilotherium wimani* (Perissodactyla, Rhinocerotidae) from the Late Miocene of Fugu, Shaanxi. Vertebr PalAsiatica. 39(2):129–138.
Deng T. 2005. New cranial material of *Shansirhinus* (Rhinocerotidae, Perissodactyla) from the Lower Pliocene of the Linxia Basin in Gansu, China. Geobios. 38(3):301–313. doi:10.1016/j.geobios.2003.12.003.
Deng T. 2006. A primitive species of *Chilotherium* (Perissodactyla, Rhinocerotidae) from the Late Miocene of Linxia Basin (Gansu, China). Cainozoic Res. 5(1–2):93–102.
Flynn LJ, Deng T, Wang Y, Xie G-P, Hou S-K, Pang L-B, Wang T-M, Mu Y-Q. 2011. Observations on the *Hipparion* red clays of the Loess Plateau. Vertebr PalAsiatica. 49(3):275–284.
Fortelius M, Heissig K, Saraç G, Sen S. 2003. Rhinocerotidae (Perissodactyla). In: Mikael F, John K, Sevket S, and Raymond LB, editors. Geology and paleontology of the Miocene sinap formation, Turkey. New York: Columbia University Press; p. 282–307.
Gaudry A. 1862–1867. Animaux fossiles et géologie de l'Attique. Paris: F. Savy.
Geraads D. 2013. Large mammals from the Late Miocene of Çorakyerler, Çankiri, Turkey. Acta Zool Bulgar. 65(3):381–390.
Geraads D. 2017. Late Miocene large mammals from Mahmutgazi, Denizli province, Western Turkey. Neues Jahrbuch für Geologie und Paläontologie - Abhandlungen. 284(3):241–257. doi:10.1127/njgpa/2017/0661.
Geraads D, Cerdeño E, Fernandez DG, Pandolfi L, Billia E, Athanassiou A, Albayrak E, Codrea V, Obada T, Deng T, et al. 2020. A database of Old World Neogene and quaternary rhino-bearing localities. [accessed 2021 Apr 04] http://www.rhinoresourcecenter.com/about/fossil-rhino-database.php
Geraads D, Koufos G. 1990. Upper Miocene Rhinocerotidae (Mammalia) from Pentalophos-1, Macedonia, Greece. Palaeontograp Abteilung A. 210:151–168.
Geraads D, Spassov N. 2009. Rhinocerotidae (Mammalia) from the Late Miocene of Bulgaria. Palaeontograp Abteilung A. 287(4–6):99–122. doi:10.1127/pala/287/2009/99.
Giaourtsakis I. 2003. Late Neogene Rhinocerotidae of Greece: distribution, diversity and stratigraphical range. Deinsea. 10:235–253.
Giaourtsakis I. 2009. The Late Miocene Mammal Faunas of the Mytilinii Basin, Samos Island, Greece: new collection 9. Rhinocerotidae. Beiträge Zur Paläontol. 31:157–187.
Giaourtsakis I, Theodorou G, Roussiakis S, Athanassiou A, Iliopoulos G. 2006. Late Miocene horned rhinoceroses (Rhinocerotinae, Mammalia) from Kerassia (Euboea, Greece). Neues Jahrbuch für Geologie und Paläontologie - Abhandlungen. 239(3):367–398. doi:10.1127/njgpa/239/2006/367.
Gray JE. 1821. On the natural arrangemenet of vertebrose animals. London Med Reposit. 15:297–310.
Heissig K. 1975. Rhinocerotidae aus dem Jungtertiär Anatoliens. Geol Jahrbuch (B). 15:145–151.
Heissig K. 1996. The stratigraphical range of fossil rhinoceroses in the Late Neogene of Europe and the Eastern Mediterranean. In: Raymond LB, Volker F, Hans-Walter M editor(s). The evolution of western Eurasian Neogene Mammal Faunas. New York: Columbia University Press; p. 339–347.
Heissig K. 1999. Family Rhinocerotidae. In: Gertrud R, Kurt H, editor. The Miocene Land Mammals of Europe. München: Pfeil Verlag; p. 175–188.
Hristova L. 2012. On the age of the Late Miocene localities of the Kalimantsi fossiliferous area based on *Cremohipparion* (Perissodactyla, Equidae) skull morphology polymorphism. His Natur Bulga. 20:143–150.
Kampouridis P, Michailidis D, Kargopoulos N, Roussiakis S, Theodorou G. 2020. First description of an ostrich from the late Miocene of Kerassia (Euboea, Greece): remarks on its cervical anatomy. Hist Biol. 1–8. doi:10.1080/08912963.2020.1779252.
Kiernik E. 1913. Über einen Aceratheriumschädel aus der Umgebung von Odessa. Bull Inter De l'Académie Des Sciences De Cracovie. 1913:808–864.
Killgus H 1922. Die Unterpliocaenen Chinesischen Säugetierreste der Tafelschen Sammlung zu Tübingen [Ph.D. Dissertation]. Tübingen (Germany): Eberhard-Karls University of Tübingen.
Killgus H. 1923. Unterpliozäne Säuger aus China. Paläontol Zeitschrift. 5 (3):251–257.
Konidaris GE, Koufos GD. 2009. The Late Miocene Mammal Faunas of the Mytilinii Basin, Samos Island, Greece: new collection: 8. Proboscidea. Beiträge Zur Paläontol. 31:139–155.
Korotkevich OL. 1958. A new *Chilotherium* species from the Sarmatian deposits of the Ukraine. Dopovidi Akad Nauk Ukrainskoi RSR. 12:1372–1376.
Korotkevich OL. 1970. The mammals of the Berislav late Sarmatian *Hipparion*-fauna. In: I.G. Pidoplichko (editor). The natural environment and the fauna of the past. Kiev: Naukova Dumka; p. 24–121.
Kostopoulos DS. 2009. The pikermian event: temporal and spatial resolution of the Turolian large mammal fauna in SE Europe. Palaeogeogr Palaeoclimatol Palaeoecol. 274(1–2):82–95. doi:10.1016/j.palaeo.2008.12.020.
Kostopoulos DS, Koufos GD, Sylvestrou IA, Syrides GE, Tsombachidou E. 2009. The Late Miocene Mammal Faunas of the Mytilinii Basin, Samos Island, Greece: new collection: 2. Lithostratigraphy and fossiliferous sites. Beiträge Zur Paläontol. 31:13–26.
Kostopoulos DS, Sen S, Koufos GD. 2003. Magnetostratigraphy and revised chronology of the late Miocene mammal localities of Samos, Greece. Inter J Earth Sci. 92(5):779–794. doi:10.1007/s00531-003-0353-8.

Koufos GD. 1987. Study of the Turolian Hipparions of the lower Axios Valley (Macedonia, Greece). Geobios. 20(3):293–312. doi:10.1016/S0016-6995(87)80045-1.
Koufos GD. 2006. The Neogene mammal localities of Greece: faunas, chronology and biostratigraphy. Hellenic J Geosci. 41:183–214.
Koufos GD. 2009. The Late Miocene Mammal Faunas of the Mytilinii Basin, Samos Island, Greece: new collection: 1. History of the Samos fossil mammals. Beiträge Zur Paläontol. 31:1–12.
Koufos GD, Kostopoulos DS, Merceron G. 2009a. The Late Miocene Mammal Faunas of the Mytilinii Basin, Samos Island, Greece: new Collection 17. Palaeoecology – palaeobiogeography. Beiträge Zur Paläontol. 31:409–430.
Koufos GD, Kostopoulos DS, Vlachou TD. 2009b. The Late Miocene Mammal Faunas of the Mytilinii Basin, Samos Island, Greece: new collection 16. Biochronology. Beiträge zur Paläontol. 31:397–408.
Koufos GD, Kostopoulos DS, Vlachou TD, Konidaris GE. 2011. A synopsis of the late Miocene Mammal Fauna of Samos Island, Aegean Sea, Greece. Geobios. 44(2–3):237–251. doi:10.1016/j.geobios.2010.08.004.
Koufos GD, Kostopoulos DS, Vlachou TD, Konidaris GE. 2016. Synthesis. Geobios. 49(1–2):147–154. doi:10.1016/j.geobios.2016.01.005.
Kretzoi M. 1942. Bemerkungen zum System der nachmiozänen Nashorn-Gattungen. Földtani Közlöny. 72:309–318.
Krokos WI. 1917. *Aceratherium schlosseri* Web. du village de Grebeniki du gouvernement de Kherson. Memoires Agri Soc South Russia. 82(2):1–96.
Lechner TS, Böhme M. 2020. *Castor*-like postcranial adaptation in an uppermost Miocene beaver from the Staniantsi Basin (NW Bulgaria). Fossil Imprint. 76(1):128–164. doi:10.37520/fi.2020.009.
Linnaeus C. 1758. Systema naturæ per regna tria naturæ, secundum classes, ordines, genera, species, cum characteribus, differentiis, synonymis, locis. Holmiae (Laurentii Salvii): Editio decima, reformata.
Meiburg P, Siegfried P. 1970. Katalog der Typen und Belegstücke zur Paläozoologie im Geologisch-Paläontologischen Institut der Westfälischen Wilhems-Universität Münster II. Teil: vertebrata. Münstersche Forschungen zur Geologie und Paläontologie. 15(1):1–84.
Nicolas J. 1978. Un nouveau gisement de vertébrés dans le Chersonien: kutchuk-Tchekmedje Ouest (Thrace turque). Comptes rendus de l'Académie de Sci. 287(D):455–458.
Niezabitowski EL. 1912. *Teleoceras ponticus* n. sp. Nowy Targ: Vorläufige Notiz.
Niezabitowski EL. 1913. Über das Schädelfragment eines Rhinocerotiden (*Teleoceras ponticus* Niez.) von Odessa. Bull Inter De l'Academie Des Sciences De Cracovie, Series B. 1913:223–235.
Osborn HF. 1900. Phylogeny of the rhinoceroses of Europe. Bull Am Mus Natural History. 12:229–267.
Pandolfi L. 2016. *Persiatherium rodleri*, gen. et sp. nov. (Mammalia, Rhinocerotidae) from the upper Miocene of Maragheh (northwestern Iran). J Vertebr Paleontol. 36(1):e1040118. doi:10.1080/02724634.2015.1040118.
Pandolfi L, Rook L. 2017. Rhinocerotidae (Mammalia, Perissodactyla) from the latest Turolian localities (MN 13; Late Miocene) of central and northern Italy. Bollettino della Società Paleontologica Italiana. 1:45–56.
Pavlow M. 1913. Mammifères tertiaires de la Nouvelle Russie, 1. Partie: artiodactyla, Perissodactyla (*Aceratherium kowalevskii* n.s.). Nouveaux Mémoires de la Société Impériale des Naturalistes de Moscou. 17:1–68.
Pohlig H. 1886. On the Pliocene of Maragha, Persia, and its resemblance to that of Pikermi in Greece. Quater J Geol Soc London. 42:177–179. doi:10.1144/GSL.JGS.1886.042.01-04.20.
Qiu ZX, Xie JY, Yan DF. 1987. A new chilothere skull from Hezheng, Gansu, China, with special reference to the Chinese "*Diceratherium*". Sci Sin B. 5:45–552.
Ringström T. 1924. Nashörner der Hipparion-Fauna Nord-Chinas. Palaeontologia Sinica. 1(4):1–156.
Roussiakis S, Filis P, Sklavounou S, Giaourtsakis I, Kargopoulos N, Theodorou G. 2019. Pikermi: a classical European fossil mammal geotope in the spotlight. Europ Geol. 48:28–32.
Saraç G 1994. The biostratigraphy and palaeontology of the rhinocerotidae (Mammalia - Perissodactyla) of the continental Neogene sediments in the Ankara Region [Ph.D. Dissertation]. Ankara (Turkey): Ankara University.
Schlosser M. 1903. Die fossilen Säugethiere Chinas nebst einer Odontographie der recenten Antilopen. Abhandlungen der Koniglichen Bayerischen Akademie der Wissenschaften. 22:1–221.
Schlosser M. 1904. Die fossilen Cavicornier von Samos. Beiträge zur Paläontologie und Geologie Österreich-Ungarns. 17:21–118.
Schlosser M. 1924. Tertiary Vertebrates from Mongolia. Palaeontol Series C. 1:1–133.
Sen S. 1994. Les gisements de mammifères du Miocène supérieur de Kemiklitepe, Turquie: 5. Rongeurs, Tubulidentés et Chalicothères. Bulletin du Muséum d'histoire naturelle sér C. 16(1):94–111.
Solounias N. 1981. The Turolian fauna from the island of Samos, Greece. Contribut Vertebr Evol. 6:1–232.
Spassov N, Geraads D, Hristova L, Markov GN, Garevska B, Garevski R. 2018. The late Miocene mammal faunas of the Republic of Macedonia (FYROM). Palaeontograp Abteilung A. 311(1–6):1–85. doi:10.1127/pala/2018/0073.
Spassov N, Geraads D, Markov G. 2019. The late Miocene mammal fauna from Gorna Sushitsa, southwestern Bulgaria, and the early/middle Turolian transition. Neues Jahrbuch für Geologie und Paläontologie - Abhandlungen. 291(3):317–350. doi:10.1127/njgpa/2019/0804.
Spassov N, Tzankov T, Geraads D. 2006. Late Neogene stratigraphy, biochronology, faunal diversity and environments of South-West Bulgaria (Struma River Valley). Geodiversitas. 28(3):477–498.
Ştiucă E. 2003. Note préliminaire sur les mammifères du Miocène de Reghiu (Dept. Vrancea, Roumanie). In: Alexandru P, Emanoil Ş, editors. Advances in Vertebrate Paleontology "Hen to Panta.". Bucuresti (Romania): Institute of Speleogy "Emil Racovita"; p. 113–116.
Svorligkou G, Giaourtsakis I, Roussiakis S. 2019. New material of the hornless rhinocerotid *Chilotherium* (Mammalia, Perissodactyla) from the Turolian fauna of Samos island, Greece. Bull Geol Soc Greece Special Public. 7:64–65.
Theodorou G, Athanassiou A, Roussiakis S, Iliopoulos G. 2003. Preliminary remarks on the Late Miocene herbivores of Kerassiá (Northern Euboea, Greece). Deinsea. 10:519–530.
Theodorou GE, Roussiakis SJ, Athanassiou A, Filippidi A. 2010. Mammalian remains from a new site near the classical locality of Pikermi (Attica, Greece). Sci Anna School Geol Aristotle Univ Thess. 99:109–119.
Toula F. 1906. Das Gebiss und Reste der Nasenbeine von *Rhinoceros* (*Ceratorhinus* Osborn) *hundsheimensis*. Abhandlungen der k k Geologischen Reichsanstalt Wien. 20(2):1–38.
Vangengeim E, Tesakov A. 2013. Late Miocene mammal localities of Eastern Europe and Western Asua: toward biostratigraphic synthesis. In: Xiaoming W, Lawrence JF, Mikael F, editors. Fossil Mammals of Asia Neogene biostratigraphy and chronology. New York: Columbia University Press; p. 521–537.
Vlachou TD, Koufos GD. 2009. The Late Miocene Mammal Faunas of the Mytilinii Basin, Samos Island, Greece: new Collection 11. Equidae Beiträge zur Paläontol. 31:207–281.
Weber M. 1904. Ueber Tertiäre Rhinocerotiden von der Insel Samos. Bull De La Société Impériale Des Naturalistes De Moscou. 17(4):477–501.
Weber M. 1905. Über Tertiäre Rhinocerotiden von der Insel Samos. II. Bull de la Société Imperériale des Naturalistes de Moscou. 18(4):344–363.
Wehrli H. 1941. Beitrag zur Kenntnis der „Hipparionen" von Samos. Paläontol Zeitschrift. 22(3–4):321–386. doi:10.1007/BF03042699.

# Appendix 2

*Publication 2*

Reappraisal of the late Miocene elasmotheriine *Parelasmotherium schansiense* from Kutschwan (Shanxi Province, China) and its phylogenetic relationships.

**Panagiotis Kampouridis**[a], Josephina Hartung[a], Gabriel de Souza Ferreira[a,b], and M. Böhme[a,b]

[a]Department of Geoscience, Eberhard Karls University of Tübingen, Tübingen, Germany;

[b]Senckenberg Centre for Human Evolution and Palaeoenvironment, Tübingen, Germany

Published in

Journal of Vertebrate Paleontology 41(6), e2080556

DOI: 10.1080/02724634.2021.2080556

Date of online publication: 05.07.2022

Journal of Vertebrate Paleontology e2080556 (7 pages)

DOI: 10.1080/02724634.2021.2080556



ARTICLE

# REAPPRAISAL OF THE LATE MIOCENE ELASMOTHERIINE *PARELASMOTHERIUM SCHANSIENSE* FROM KUTSCHWAN (SHANXI PROVINCE, CHINA) AND ITS PHYLOGENETIC RELATIONSHIPS

PANAGIOTIS KAMPOURIDIS, [1,*] JOSEPHINA HARTUNG, [1] GABRIEL S. FERREIRA, [1,2] and MADELAINE BÖHME[1,2]
[1]Eberhard Karls University of Tübingen, Tübingen 72076, Germany, pkampouridis94@gmail.com;
[2]Senckenberg Centre for Human Evolution and Palaeoenvironment, Tübingen 72076, Germany

ABSTRACT—Elasmotheres, such as the huge Siberian unicorn (*Elasmotherium sibiricum*), are amongst the most iconic large mammals ever to roam Eurasia. Several different elasmotheriine taxa are also known from the upper Miocene of Asia, including the large genus *Parelasmotherium*. Herein we present the re-examination of the holotype of its type species *Parelasmotherium schansiense*, using high resolution X-ray computed tomography. The μCT analysis reveals thus far unknown morphological features of the M1 and the unerupted P4 and M2, thereby adding to our knowledge about this species. This allows comparisons with other species that have been referred to *Parelasmotherium*, '*Parelasmotherium*' *simplum* and '*Parelasmotherium*' *linxiaense*, which, according to the results of the phylogenetic analysis, should not be included in the same genus as *P. schansiense*. Furthermore, based on comparisons to other Miocene elasmotheriines the diagnosis of *Parelasmotherium schansiense* was amended and its phylogenetic position was assessed. *Parelasmotherium schansiense* is placed in a monophyletic group of 'derived elasmotheriines,' which also includes the genera *Elasmotherium*, *Sinotherium*, and *Ninxiatherium*.

SUPPLEMENTAL DATA—Supplemental materials are available for this article for free at www.tandfonline.com/UJVP.

Citation for this article: Kampouridis, P., J. Hartung, G. S. Ferreira, and M. Böhme. 2022. Reappraisal of the late Miocene elasmotheriine *Parelasmotherium schansiense* from Kutschwan (Shanxi Province, China) and its phylogenetic relationships. Journal of Vertebrate Paleontology. DOI: 10.1080/02724634.2021.2080556

## INTRODUCTION

Elasmotheres are amongst the most characteristic rhinocerotids found in the fossil record. This group of rhinos existed throughout the Old World (e.g., Antoine, 2002; Geraads et al., 2012; Deng et al., 2013), but prevailed in Asia, where it survived until the latest Pleistocene (Kosintsev et al., 2019; Liu et al., 2021). The affinities and relationships of its representatives remained enigmatic for a long time, but during the last decades numerous new finds have elucidated the evolutionary history of this unique group (Antoine, 2002; Schvyreva, 2015; Kosintsev et al., 2019). However, the taxonomy and phylogeny of its pre-Quaternary representatives are not fully resolved (e.g., Fortelius and Heissig, 1989; Geraads et al., 2012; Deng et al., 2013). The aim of this study is to re-describe the holotype of the huge *Parelasmotherium schansiense* Killgus, 1923 (Fig. 1), a late Miocene representative of elasmotheriines. High resolution X-ray computed tomography was used to reveal previously unknown information about the internal tooth morphology of its holotype; thus, allowing for detailed comparisons to the other elasmotheriines, elucidating their phylogenetic relationships, especially within the genus *Parelasmotherium*.

## LOCALITY

*Parelasmotherium schansiense* was originally described by Killgus (1923), based on material from the upper Miocene locality of Kutschwan, Shanxi Province, China. The material was excavated by Albert Tafel from sediments on the Chinese Loess Plateau along the Yellow River in 1905 (Tafel, 1914; Killgus, 1922, 1923), over a decade before the first excavation of Johan Gunnar Andersson in Shanxi (Andersson, 1923). The material was later given to the Eberhard Karls University of Tübingen (Germany), where it was studied by Hugo Killgus for his Ph.D. dissertation (Killgus, 1922). Unfortunately, the exact geographical location of Kutschwan remains unknown. The fossils of Kutschwan represent a typical large mammal assemblage of the upper Miocene of China. They include the hornless rhino *Chilotherium habereri*, *Hipparion* sensu lato, the large giraffid *Schansitherium tafeli*, two bovids, and an ictithere hyaenid, along with the huge rhino *P. schansiense* (Killgus, 1922, 1923). Adhering particles of red fine silt on the fossils reveal that the embedding sediment represents the classical 'Chinese Red Clay.'

## MATERIAL AND METHODS

The holotype of *P. schansiense* consists of four upper teeth (GPIT-PV-86051; Fig. 1) housed in the Geological and Paleontological Institute at the University of Tübingen, Germany (GPIT). To study the internal tooth morphology in detail, micro-computed tomography (μCT) scans were acquired with a Nikon XTH 320 μCT scanner operated by the Centre for Visualisation, Digitisation and Replication at the Eberhard Karls University Tübingen and Senckenberg Centre for Human Evolution and Palaeoenvironment Germany (SHEP). An X-ray tube containing a multi metal reflection target with a maximum acceleration voltage of 225 kV was used. The articulated D4, P4, and M1 were

*Corresponding author
Color versions of one or more of the figures in the article can be found online at www.tandfonline.com/ujvp.

Published online 05 Jul 2022

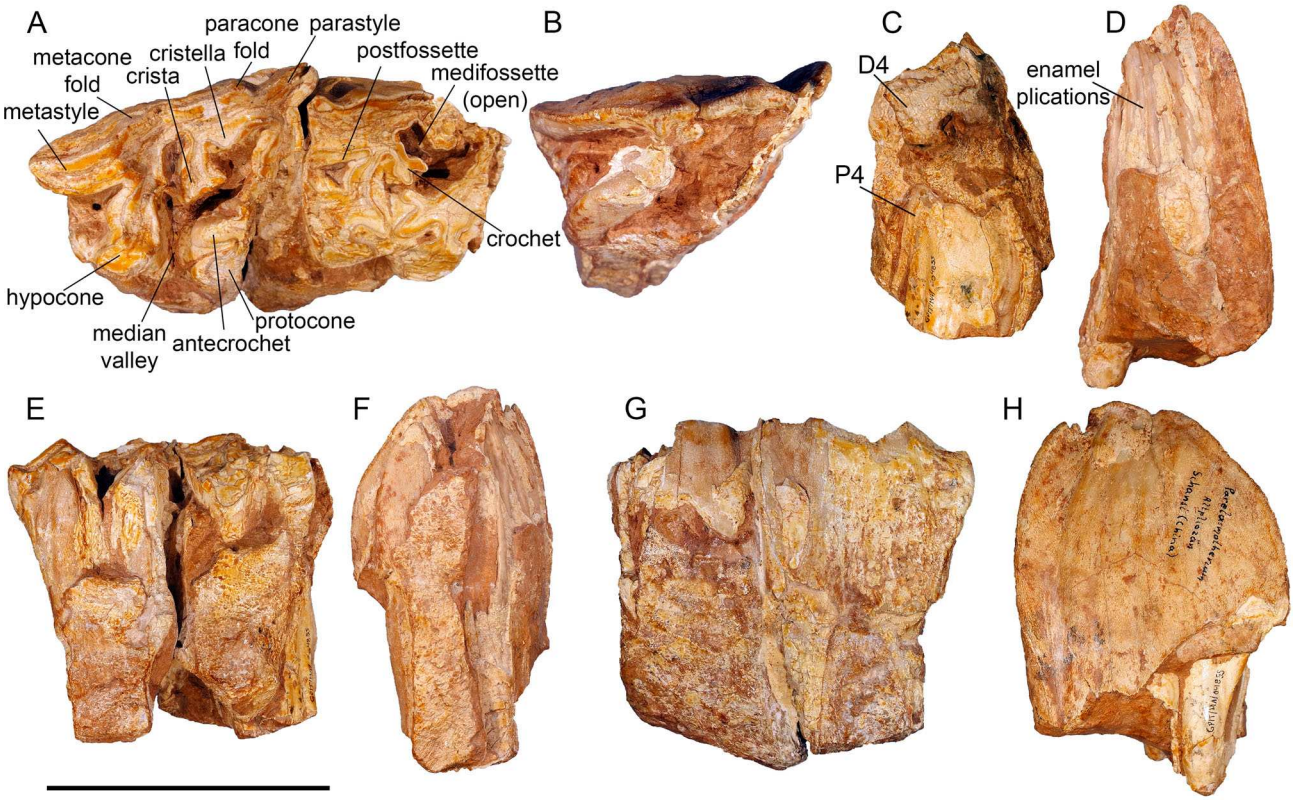


FIGURE 1. Photographs of the holotype of *Parelasmotherium schansiense* (GPIT-PV-86051) from the upper Miocene of Kutschwan (Shanxi Province, China). **A**, **C**, **E**, **G**, articulated right D4 and M1; and **B**, **D**, **F**, **H**, right M2 in occlusal (**A** and **B**), anterior (**C** and **D**), lingual (**E** and **F**), and buccal (**G** and **H**) view, respectively. Note that in posterior view (**C**), both the D4 and P4 are exposed. Scale bar equals 7.5 cm for **A-B** and 10 cm for **C-H**.

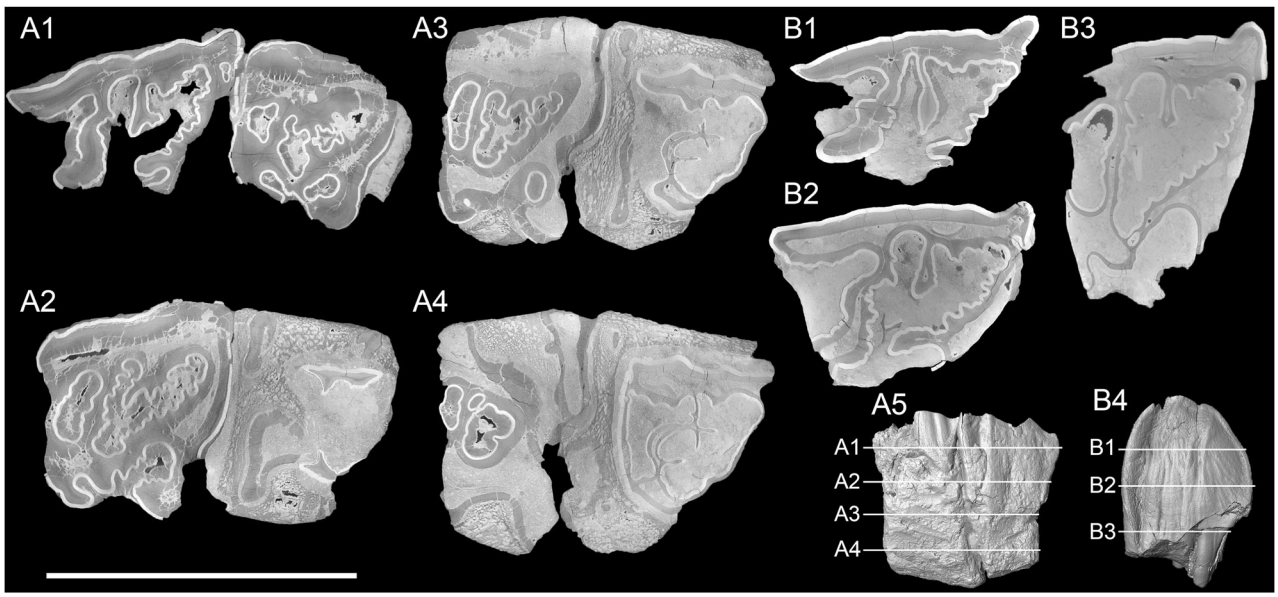


FIGURE 2. µCT-scan orthoslices of the holotype of *Parelasmotherium schansiense* (GPIT-PV-86051) from the upper Miocene of Kutschwan (Shanxi Province, China). **A**, articulated right M1 and D4 (**A1**) or P4 (**A2-4**), in occlusal (**A1–4**) and buccal (**A5**) view; **B**, isolated right M2, in occlusal (**B1-3**) and buccal (**B4**) view. The virtual orthoslices are taken at different positions, as shown in **A5** and **B4**, respectively. Scale bar equals 10 cm for **A1–4** and **B1-3** and 20 cm for **A5** and **B4**.

scanned at 220 kV and 140 μA with a voxel size of 0.05932821 mm, using a copper filter of 0.5 mm thickness. The isolated M2 was scanned at 220 kV and 190 μA with a voxel size of 0.05002721 mm, with the same copper filter. Images were processed using VG Studio Max. The results are virtual orthoslices of the actual teeth (Fig. 2). The scans are available on MorphoSource under the following IDs:

**Media ID**—000415992 (D4, P4, and M1) and 000416854 (M2).

The dental terminology used in this study is shown in Fig. 1A, D and follows Guérin (1980) and Antoine (2002). Measurements of the teeth are given in Table 1.

## SYSTEMATIC PALEONTOLOGY

Class MAMMALIA Linnaeus, 1758
Family RHINOCEROTIDAE Gray, 1821
Tribe ELASMOTHERIINI Dollo, 1885
*PARELASMOTHERIUM* Killgus, 1923

**Diagnosis**—Same as for the type species.

**Type Species**—*Parelasmotherium schansiense* Killgus, 1923.

**Remarks**—Three further species have been previously attributed to *Parelasmotherium*: *Sinotherium simplum* Chow, 1958, *Parelasmotherium linxiaense* Deng, 2001, and *Ninxiatherium longirhinus* Chen, 1977 (Qiu and Xie, 1998; Deng, 2001; Antoine, 2002). The first two are herein regarded as not belonging to this genus and will provisionally be referred to as '*Parelasmotherium*.' The third species was considered a junior synonym of *P. schansiense*, but was later re-established as a valid taxon, belonging to *Ninxiatherium*, along with *Ninxiatherium euryrhinus* Deng, 2008, which is also supported in this study.

### *PARELASMOTHERIUM SCHANSIENSE* Killgus, 1923 (Figs. 1–2)

**Holotype**—Partial right upper toothrow, with worn D4 and M1, and unerupted P4 and M2 (GPIT-PV-86051).

**Type Locality**—Kutschwan, Shanxi Province, China (Baodean; late Miocene).

**Amended Diagnosis**—Large elasmotheriine with a unique combination of dental features separating it from all other elasmotheriines: large crochets on D4 and P4; well-established protocone and hypocone connection at any wear stage, unconstricted hypocone, presence of a 'pseudometaloph,' and prominent metacone and paracone folds on P4; strongly constricted hypocone and highly plicated enamel in the hypsodont M1 and M2.

#### Description

**D4**—This tooth represents the only deciduous tooth preserved. The anterior half of the ectoloph is broken off and the lingual part of the D4 is heavily damaged (Fig. 1A, G). The tooth is moderately worn, and its preserved maximal height is 41 mm. The protocone is very strongly constricted, anteriorly and posteriorly, resulting in a large antecrochet. A large plication is present at the buccal side of the antecrochet. The hypocone is strongly constricted anteriorly, forming a large enamel fold that connects to the antecrochet (Fig. 2A1) with advanced wear, closing the median valley. A small crista is present. A large crochet exists, which splits into two small enamel folds. The lingual one fuses with the enamel plication of the antecrochet, when slightly more worn (Fig. 2A1). The postfossette is closed. On the ectoloph, two folds at the level of the metacone are present and the beginning of a paracone fold can be traced. The tooth is partially filled with cement and some remnants cover part of the ectoloph.

**P4**—It is not yet erupted. In fact, it is not even fully formed yet, remaining beneath the D4 that is still in use (Fig. 1C). The μCT analysis reveals the previously unknown morphology of the thus far formed P4 (Fig. 2A2–3). The anterior enamel wall of this tooth is completely lacking, due to damage; thus, its morphology cannot be assessed. The P4 exhibits a protocone and hypocone, which are fused right from the beginning. A large double crochet is present that connects to the long but thin crista very early in occlusion. A cristella and a postcrista are present as short enamel bumps. The postfossette closes posteriorly at a very early wear stage, but remains anteriorly connected to the medifossette at all levels of the thus far formed tooth. The hypocone does not connect to the metacone at any level of the formed P4, while the crochet and the crista form a 'pseudometaloph' (sensu Antoine, 2002). Buccally, well-developed metacone and paracone folds are present. The enamel within the tooth exhibits some small enamel bumps, much less distributed than the enamel plications in the two molars.

**M1**—The M1 is the best-preserved tooth, only lacking the lingual half of the anterior wall and part of the protocone (Fig. 1A, E). It is moderately worn. The protocone bears a very strong posterior constriction, forming a large, lingually-oriented antecrochet. The anterior part of the protocone is damaged, but a small curve in the enamel at the middle of the tooth (Fig. 2A2) confirms the occurrence of an anterior protocone constriction. The hypocone bends posteriorly and bears a strong anterior constriction and a very small posterior constriction on its lingual tip. The protocone and the hypocone fuse when moderately worn. A large crista is present, with a strong anteriorly oriented plication. Though, when heavily worn the crista would become less distinct (see Fig. 2A3). Anterior to the crista, a distinct, but weak cristella is present, which connects to the anterior plication of the crista when slightly more worn. A very small crochet is visible that does not connect with the crista. A weak anterior cingulum is present. A posterior cingulum exists, leading to the closure of the postfossette. The ectoloph is relatively flat, albeit exhibiting a prominent paracone fold and a strong parastyle. The M1 has strong internal enamel plications, which are already visible on the posterior enamel wall of the protoloph of the only little worn M1 (Fig. 1A), but become much more widespread and prominent with further wear (Fig. 2A1–3). The M1 exhibits extensive cement covering internally and externally, on all sides of the tooth. The surface of the outer enamel layer is quite wavy and rough.

**M2**—It is the only tooth that is completely isolated and not enclosed in the maxillary bone (Fig. 1B–F). The tooth is completely unworn, but the protocone and the anterior enamel wall are broken off. Only the μCT analysis reveals the morphology of the M2 (Fig. 2B). It exhibits a strongly posteriorly-constricted protocone that forms a large antecrochet. The presence of an anterior constriction cannot be assessed. The hypocone is strongly constricted anteriorly, forming a large enamel fold that fuses with the antecrochet when moderately worn, closing the median valley. The crista is well developed at an early wear stage (Fig. 2B1), but becomes smaller when heavily worn (Fig. 2B3), a

TABLE 1. Dental measurements of the holotype of *Parelasmotherium schansiense* Killgus, 1923 (GPIT-PV-86051) in mm. The measurements were taken with a digital caliper with an error of 0.01 mm and then rounded. Height: the preserved height is given, the D4 and M1 are already significantly worn and M2 is probably not fully formed yet; HI (Hypsodonty Index = Height/Length) is a minimal value, because the height of the teeth is not complete.

| Tooth | Height | Length | Width | HI |
|---|---|---|---|---|
| D4 | 41 | ~55 | 57 | - |
| M1 | 115 | 80 | ~70 | 1.44 |
| M2 | 145 | 85 | ~70 | 1.71 |

feature that is also visible in *Sinotherium lagrelii* Ringström, 1924 (Ringström, 1924:textfigs. 87–88). A small cristella is present throughout the tooth's height. A small crochet is present. An anterior cingulum is present as shown by a small remnant right below the parastyle. A posterior cingulum is present, leading to the closure of the postfossette, when moderately worn. The ectoloph is slightly wavy with a strong parastyle. The enamel within the tooth is very wrinkled, with strong plications being present mostly on the posterior enamel wall of the protoloph (Fig. 2B). The plications would be visible at a very early wear stage, as demonstrated by the high-placed (about 1 cm below the occlusal surface) enamel plications that are visible through the broken protoloph (see Fig. 1D). The M2 exhibits remnants of cement within the median valley, the postfossette, and on the ectoloph. The surface of the outer enamel layer is quite wavy and rough.

### Comparison to Other Species of *Parelasmotherium*

The genus *Parelasmotherium* was erected by Killgus (1923) for *P. schansiense*, based on the material studied here (Figs. 1–2). It was originally based on its large dimensions, high hypsodonty, extensive cement covering and low enamel thickness of the teeth (Killgus, 1922, 1923). Later, three species were included in this genus: *N. longirhinus*, '*P.*' *simplum*, and '*P.*' *linxiaense* (Qiu and Xie, 1998; Deng, 2001; Antoine, 2002). The first taxon was later re-established and is herein treated as a valid taxon. The other two were based on isolated teeth (Chow, 1958; Qiu and Xie, 1998; Deng, 2001), but from the latter a complete skull was later reported (Deng, 2007). The morphology of *P. schansiense* is evidently more complex than the other two species. In '*P.*' *simplum*, the crista is rather small, and a small crochet may be present in the molars, while the enamel shows no signs of plications in the molars (Chow, 1958; Qiu and Xie, 1998). These features remain relatively constant throughout the height of the teeth, as demonstrated by the cross section of the M2 figured by Qiu and Xie (1998:pl. 1, figs. 4-5), thus differing from the molars of *P. schansiense* that bear a huge crista, no crochet and are highly plicated.

The differences of *P. schansiense* to '*P.*' *linxiaense* are somewhat more subtle. The P4 morphology resembles that of *P. schansiense* in having a fused protocone and hypocone, an unconstricted hypocone, as well as a long crochet and crista that connect when worn enough (Deng, 2007:fig. 3). However, the hypocone does not fuse with the metacone and the metacone fold is much stronger in *P. schansiense*, in contrast to '*P.*' *linxiaense*. Although, the missing connection between the hypocone and the metacone might represent a somewhat variable feature, as seen in the 'pseudometaloph' (sensu Antoine, 2002) variably occurring in the P3s of *Sinotherium* (Ringström, 1924:figs. 77-80). More importantly, in the molars of '*P.*' *linxiaense* enamel plications are very weak or absent, as seen both in its holotype (IVPP V 12650; Deng, 2001:pl. 1, figs. 1-3), as well as in the skull discovered later at the same locality (HMV 1411; Deng, 2007:fig. 3). In contrast, in *P. schansiense* plications are very prominent and would be visible on both the M1 and M2 after some slight to moderate wear (Fig. 2A1, B1), and are already beginning to show in the little worn M1 (Fig. 1A). Thus, both '*P.*' *simplum* and '*P.*' *linxiaense* differ from *P. schansiense*, as well as from one another.

### Comparison to Other Elasmotheriines from the upper Miocene of China

***Iranotherium***—*Iranotherium morgani* (Mecquenem, 1908), is best known from its type locality Maragheh, from the upper Miocene of Iran (Mecquenem, 1908; Pandolfi, 2016), but two complete skulls have also been recovered from upper Miocene deposits of the Linxia Basin in China (Deng, 2005). The cheek teeth of *I. morgani* are covered and filled with cement (NHMW 2014/0425/001, pers. obs.; Deng, 2005; Pandolfi, 2016), a common feature in elasmotheriines (Geraads et al., 2016; Geraads and Zouhri, 2021). However, *I. morgani* differs from 'derived elasmotheriines' like as *P. schansiense* in having small or absent cristae, no or extremely weak enamel plications, and the hypocone of the M1 and M2 not posteriorly bent as seen in *I. morgani* from Maragheh (NHMW 2014/0425/001, pers. obs. by P.K.) and from the Linxia Basin (see Deng, 2005:fig. 6).

***Ninxiatherium***—*Ninxiatherium longirhinus*, is based on a complete skull from Ningxia (China). Antoine et al. (2002) synonymized *P. schansiense* and *N. longirhinus*, considering their differences as possible intraspecific variation, whereas Deng (2007) separated the two genera. This was based on some cranial and dental characters, following the discovery of a complete skull of '*P.*' *linxiaense* that was later further supported by Deng (2008). The present study of the *P. schansiense* holotype confirms the existence of significant differences between *Ninxiatherium* and *Parelasmotherium*. In *N. longirhinus* the P4 bears only very small crista and crochet, and the ectoloph seems very flat (Chen, 1977:fig. 1), in contrast to the long crista and crochet of *P. schansiense*, as revealed by the μCT-scan of the specimen from Kutschwan (Fig. 2A2–4). Moreover, in contrast to *P. schansiense*, the molars of *N. longirhinus* bear widely connected protocone and hypocone, a very small crista, and exhibit no distinct parastyle (Chen, 1977:fig. 1).

Deng (2008) erected the new species *N. euryrhinus*, which differs from *N. longirhinus* in having a larger size, wider nasals, and a shallower nasal notch. The P4 of *N. euryrhinus* bears very short crista and crochet compared to *P. schansiense* (Fig. 2A3–4). The molars of *N. euryrhinus* exhibit a small crista, and the cristella, when present, is very small, in contrast to *P. schansiense*.

Both *N. longirhinus* and *N. euryrhinus* exhibit a hypocone, which is not as posteriorly bent as in *P. schansiense*, '*P.*' *simplum*, '*P.*' *linxiaense*, and *S. lagrelii*. Moreover, *Ninxiatherium* bears very weak or no enamel plications, and its teeth are not as hypsodont. Although it is not known to what degree these features may have varied, due to the existence of only a single skull of *N. longirhinus* and *N. euryrhinus*, respectively, the differences between these two species and *P. schansiense* and *S. lagrelii* are significant enough to confirm their validity as distinct taxa. In fact, these features are somewhat more similar to '*P.*' *simplum* and '*P.*' *linxiaense*, which also bear only weak secondary enamel folds and lack the highly plicated enamel of *P. schansiense*.

***Sinotherium***—Ringström (1923) erected *S. lagrelii* based on a left M3 from the upper Miocene of the Shanxi Province in China. Shortly after, Ringström (1924) synonymized the genera *Parelasmotherium* and *Sinotherium*, based on their similar morphology, noting though the difference in their dimensions. The present study shows that the two elasmotheriine genera exhibit some important morphological differences. For instance, in *S. lagrelii* the D4 features a very strong crista and no crochet, while the protocone and hypocone are widely connected at about 3 cm height from the base (Ringström, 1924:fig. 4, table 12). On the contrary, in *P. schansiense* the crista is very small, and the crochet is largely developed and splits into two, while the protocone and hypocone remain separated until a later wear stage and only barely connect before the tooth is completely worn. Concerning the P4, *S. lagrelii* has a strong crista, no crochet, unfused protocone and hypocone, a strongly constricted protocone, and some enamel plications in the median valley (Ringström, 1924:fig. 1, table 12). Whereas *P. schansiense* exhibits long and narrow crista and crochet, completely fused protocone and hypocone that do not exhibit any constriction, while not exhibiting enamel plication as seen in *S. lagrelii*, as shown by the μCT analysis (Fig. 2A3–4). The molars in both *S. lagrelii* and *P. schansiense*

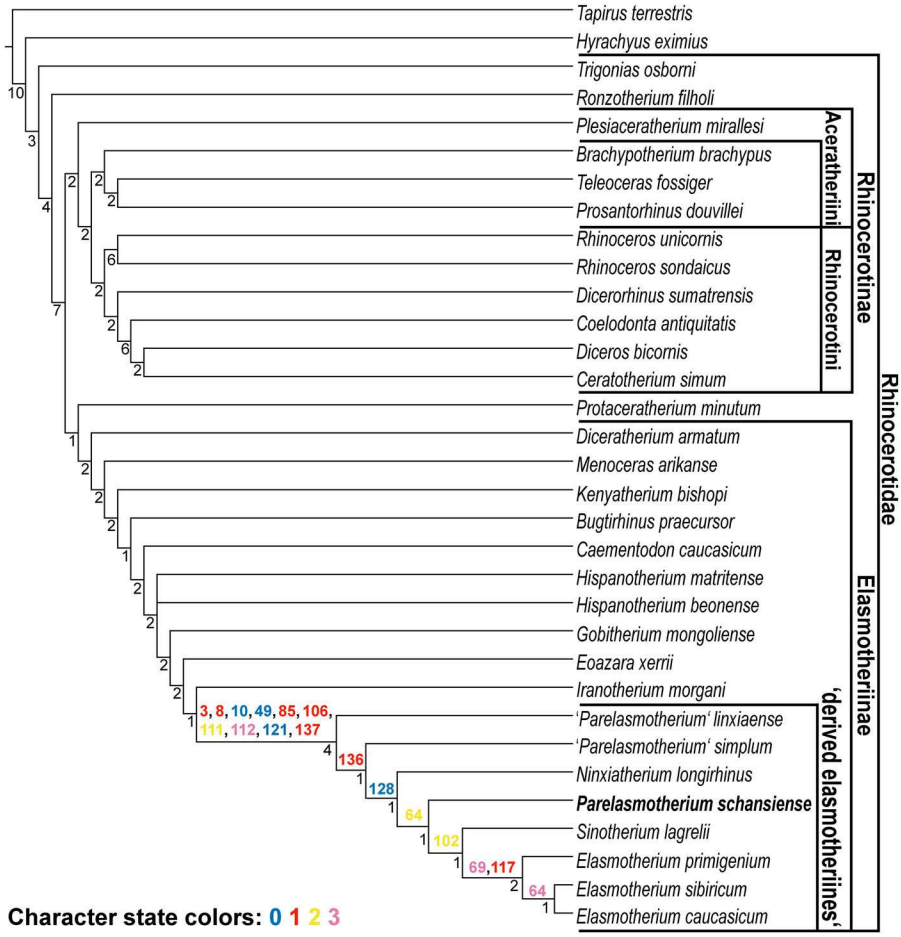


FIGURE 3. Strict consensus of the two most parsimonious trees resulting from the phylogenetic analysis. Bremer support values are reported below each branch. Synapomorphies are reported for the 'derived elasmotheriines' above the branches.

show similarly well-developed enamel plications when moderately worn (Ringström, 1924:textfigs. 87-88). However, *S. lagrelii* is much more hypsodont.

## PHYLOGENETIC ANALYSIS

In order to assess the phylogenetic affinities of *Parelasmotherium* a phylogenetic analysis was performed. We modified the character-taxon matrix of Sun et al. (2021), which modified the matrix of Deng (2008) by adding *Elasmotherium primigenium*, which is based on the matrix of Antoine (2002). We also added *Eoazara xerrii* to the matrix, based on Geraads and Zouhri (2021) but removed the 32 new characters added by Lu (2013) to the matrix of Antoine (2002). '*P.*' *simplum* was scored based on published figures (Chow, 1958; Qiu and Xie, 1998) and *P. schansiense* was rescored based on the holotype (GPIT-PV-86051) studied herein. The current matrix includes 282 characters and 33 taxa (Supplementary Data 1; it is also available at MorphoBank under http://morphobank.org/permalink/?P4228). The phylogenetic analysis was performed with TNT version 1.5 (Goloboff et al., 2008). All characters were unordered. The matrix was analyzed using 'traditional search' (1000 replications), hold = 10, and random seed = 0, followed by tree bisection-reconnection. The analysis resulted in two most parsimonious trees (Figs. S1–2) with a length of 1101 steps. A strict consensus tree and decay values (Bremer support; Supplementary Data 2) were obtained using the implemented functions in TNT. Consistency (CI) and Retention indices (RI) were calculated for the whole tree (CI = 0.351 and RI = 0.543) using the script available in TNT.

## DISCUSSION

*Parelasmotherium schansiense* has been known for almost a century (Killgus, 1923) but its exact taxonomic and phylogenetic affinities and its relationship to the other elasmotheriines of Eurasia have been debated and remain ambiguous (e.g., Deng, 2001, 2007, 2008; Antoine, 2002). The comparison to the other elasmotheriines from the upper Miocene of China showed that *P. schansiense* is a valid taxon that can be distinguished from all other species. It also showed that '*P.*' *simplum* and '*P.*' *linxiaense* exhibit important morphological differences to *P. schansiense*, such as the lack of any prominent enamel plications, implying a more derived evolutionary stage for the latter species, as suggested by the phylogenetic analysis (Fig. 3). The former two species also seem to differ from each other, as shown by the very small crista in '*P.*' *simplum*, in contrast to the largely developed crista in '*P.*' *linxiaense* and other 'derived elasmotheriines,' as suggested by the phylogenetic analysis (Fig. 3), which separates them and places both species in a more basal position than *Ninxiatherium*. Therefore, implying that *Parelasmotherium*, as it stands now, is paraphyletic and that both '*P.*' *simplum* and '*P.*' *linxiaense* should not be included in the same genus as *P. schansiense*. Thus, it might be more appropriate to refer to these two species as '*Parelasmotherium*' until these issues have been resolved.

Unfortunately, because no skulls of '*P.*' *simplum* and *P. schansiense* have been reported so far (Killgus, 1923; Chow, 1958; Qiu and Xie, 1998), important morphological features such as the morphology, number, and position of the horn boss (es) are unknown, thus making the phylogenetic position of these species more uncertain. Furthermore, the species assigned to *Parelasmotherium* and *Ninxiatherium* are represented by very few or even a single specimen. Therefore, their intraspecific variability cannot be assessed, thus complicating their comparison even further. Until additional material of these taxa becomes available, a careful and detailed description and comparison of the already known material is the only way to enhance our understanding of their relationships. Concerning *P. schansiense*, the very hypsodont teeth bearing a large crista, and rich enamel plications in the molars suggest a position among the 'derived elasmotheriines', as a sister to the clade including *Sinotherium* and *Elasmotherium*. This position is also supported by our phylogenetic analysis (Fig. 3), which might also point to an early Baodean age (Qiu et al., 2013) for Kutschwan. Furthermore, the analysis showed that the clade (marked in Fig. 3) sometimes referred to as 'derived elasmotheriines' (Deng, 2008; Deng et al., 2013) is a well-supported group (Bremer support = 4), defined by 10 synapomorphies (characters 3, 8, 10, 49, 85, 106, 111, 112, 121, 137).

## CONCLUSION

Herein the holotype of the huge elasmotheriine rhinocerotid *Parelasmotherium schansiense* from the upper Miocene of Kutschwan (Shanxi, China) was re-evaluated to answer questions about its taxonomy and phylogenetic relationships. CT-scans of the specimen revealed the previously unknown morphology of the unerupted P4 and unworn M2. Comparisons with the other late Miocene elasmotheriines from China and a phylogenetic analysis showed that the genus *Parelasmotherium* is paraphyletic and therefore '*Parelasmotherium*' *simplum* and '*Parelasmotherium*' *linxiaense* should not be included in the same genus as *P. schansiense*. Furthermore, the phylogenetic analysis placed *P. schansiense* within the 'derived elasmotheriines' as a sister to the clade which includes *Sinotherium* and *Elasmotherium*.

## ACKNOWLEDGMENTS

We acknowledge the support of the Centre of Visualisation, Digitisation and Replication at the Eberhard Karls Universität in Tübingen for instrument use, scientific and technical assistance and A. Tröscher (SHEP) for µCT-scanning the specimens. We thank I. Werneburg (SHEP) for the curation of the material housed in the GPIT. We would like to thank U. Göhlich (NHMW) for providing access to the collections of Maragheh. This research received support from the SYNTHESYS+ project http://www.synthesys.info/ which is financed by European Community Research Infrastructure Action under the H2020 Integrating Activities Programme, Project number 823827 (AT-TAF-TA3-9). We would like to thank the Handling Editor F. Bibi, the Technical Editor J. Harris, as well as P.-O. Antoine, and an anonymous reviewer for their helpful comments that greatly improved this work.

## ORCID

Panagiotis Kampouridis http://orcid.org/0000-0002-1812-4664
Josephina Hartung http://orcid.org/0000-0002-2084-0328
Gabriel S. Ferreira http://orcid.org/0000-0003-1554-8346

## LITERATURE

Andersson, J. G. 1923. Essays on the Cenozoic of northern China. Memoirs of the Geological Survey of China, Ser. A 3:1–152.
Antoine, P.-O. 2002. Phylogénie et évolution des Elasmotheriina (Mammalia, Rhinocerotidae). Mémoires du Muséum National d'Histoire Naturelle 188:1–359.
Antoine, P.-O., F. Alférez, and C. Iñigo. 2002. A new elasmotheriine (Mammalia, Rhinocerotidae) from the Early Miocene of Spain. Comptes Rendus Palevol 1:19–26.
Chen, G. F. 1977. A new genus of Iranotheriinae of Ningxia. Vertebrata PalAsiatica 15:143–147.
Chow, M. 1958. New elasmotherine rhinoceros from Shansi. Vertebrata PalAsiatica 2:131–142.
Deng, T. 2001. New remains of *Parelasmotherium* from the late Miocene in Dongxiang Gansu China. Vertebrata PalAsiatica 39:306–311.
Deng, T. 2005. New discovery of *Iranotherium morgani* (Perissodactyla, Rhinocerotidae) from the late Miocene of the Linxia Basin in Gansu, China, and its sexual dimorphism. Journal of Vertebrate Paleontology 25:442–450.
Deng, T. 2007. Skull of *Parelasmotherium* (Perissodactyla, Rhinocerotidae) from the upper miocene in the Linxia Basin (Gansu, China). Journal of Vertebrate Paleontology 27:467–475.
Deng, T. 2008. A new elasmothere (Perissodactyla, Rhinocerotidae) from the late Miocene of the Linxia Basin in Gansu, China. Geobios 41:719–728.
Deng, T., S. Wang, and S. Hou. 2013. A bizarre tandem-horned elasmothere rhino from the Late Miocene of northwestern China and origin of the true elasmothere. Chinese Science Bulletin 58:1811–1817.
Dollo, L. 1885. Rhinocéros vivants et fossiles. Revue de Questions Scientifiques 17:293–299.
Fortelius, M., and K. Heissig. 1989. The phylogenetic relationships of the Elasmotherini. Mitteilungen Der Bayerischen Staatssammlung Für Paläontologie Und Historische Geologie 29:227–233.
Geraads, D., and S. Zouhri. 2021. A new late Miocene elasmotheriine rhinoceros from Morocco. Acta Palaeontologica Polonica 66.
Geraads, D., M. McCrossin, and B. Benefit. 2012. A new rhinoceros, *Victoriaceros kenyensis* gen. et sp. nov., and other Perissodactyla from the Middle Miocene of Maboko, Kenya. Journal of Mammalian Evolution 19:57–75.
Geraads, D., T. Lehmann, D. J. Peppe, and K. P. McNulty. 2016. New Rhinocerotidae from the Kisingiri localities (lower Miocene of western Kenya). Journal of Vertebrate Paleontology 36:e1103247.
Goloboff, P. A., J. S. Farris, and K. C. Nixon. 2008. TNT, a free program for phylogenetic analysis. Cladistics 34:407–437.
Gray, J. E. 1821. On the natural arrangemenet of vertebrose animals. London Medical Repository 15:297–310.
Guérin, C. 1980. Les rhinocéros (Mammalia, Perissodactyla) du Miocène terminal au Pleistocène supérieur en Europe occidentale: comparaison avec les espèces actuelles. Département des sciences de la terre, Université Claude-Bernard Lyon 1, Villeurbanne, 3 pp.
Killgus, H. 1922. Die Unterpliocaenen Chinesischen Säugetierreste der Tafelschen Sammlung zu Tübingen. Ph.D. Dissertation, Eberhard-Karls University of Tübingen, Tübingen, Germany, 87 pp.
Killgus, H. 1923. Unterpliozäne Säuger aus China. Paläontologische Zeitschrift 5:251–257.
Kosintsev, P., K. J. Mitchell, T. Devièse, J. van der Plicht, M. Kuitems, E. Petrova, A. Tikhonov, T. Higham, D. Comeskey, C. Turney, A. Cooper, T. van Kolfschoten, A. J. Stuart, and A. M. Lister. 2019. Evolution and extinction of the giant rhinoceros *Elasmotherium sibiricum* sheds light on late Quaternary megafaunal extinctions. Nature Ecology & Evolution 3:31–38.
Linnaeus, C. 1758. Systema Naturae. Laurentii Salvii, Stockholm, pp.
Liu, S., M. V. Westbury, N. Dussex, K. J. Mitchell, M.-H. S. Sinding, P. D. Heintzman, D. A. Duchêne, J. D. Kapp, J. von Seth, H. Heiniger, F. Sánchez-Barreiro, A. Margaryan, R. André-Olsen, B. De Cahsan, G. Meng, C. Yang, L. Chen, T. van der Valk, Y. Moodley, K. Rookmaaker, M. W. Bruford, O. Ryder, C. Steiner, L. G. R. Bruins-van Sonsbeek, S. Vartanyan, C. Guo, A. Cooper, P. Kosintsev, I. Kirillova, A. M. Lister, T. Marques-Bonet, S. Gopalakrishnan, R. R. Dunn, E. D. Lorenzen, B. Shapiro, G. Zhang, P.-O. Antoine, L. Dalén, and M. T. P. Gilbert. 2021. Ancient and modern genomes unravel the evolutionary history of the rhinoceros family. Cell S0092867421008916.
Lu, X. 2013. A juvenile skull of *Acerorhinus yuanmouensis* (Mammalia: Rhinocerotidae) from the Late Miocene hominoid fauna of the Yuanmou Basin (Yunnan, China). Geobios 46:539–548.
Mecquenem, R. de. 1908. Le lac D'ourmiah. Annales de Géographie 17:128–144.

Pandolfi, L. 2016. *Persiatherium rodleri*, gen. et sp. nov. (Mammalia, Rhinocerotidae) from the upper Miocene of Maragheh (northwestern iran). Journal of Vertebrate Paleontology 36:e1040118.

Qiu, Z., and J. Xie. 1998. Notes on *Parelasmotherium* and *Hipparion* fossils from Wangji, Dongxiang, Gansu. Vertebrata PalAsiatica 36:13–23.

Qiu, Z. X., Z. D. Qiu, T. Deng, C. K. Li, Z. Q. Zhang, B. Y. Wang, and X. Wang. 2013. Neogene land mammal stages/ages of China; pp. 29–90 in X. Wang, L. J. Flynn, and M. Fortelius (eds.), Fossil Mammals of Asia. Columbia University Press, New York.

Ringström, T. 1923. *Sinotherium lagrelii*. Ringström. A new fossil rhinocerotid from Shansi, China. Bulletin of the Geological Survey of China 5:91–93.

Ringström, T. 1924. Nashörner der Hipparion-Fauna Nord-Chinas. Palaeontologia Sinica 1:1–156.

Schvyreva, A. K. 2015. On the importance of the representatives of the genus *Elasmotherium* (Rhinocerotidae, Mammalia) in the biochronology of the Pleistocene of Eastern Europe. Quaternary International 379:128–134.

Sun, D.-H., T. Deng, and Q. Jiangzuo. 2021. The most primitive *Elasmotherium* (Perissodactyla, Rhinocerotidae) from the Late Miocene of northern China. Historical Biology 1–11.

Tafel, A. 1914. Meine Tibetreise. Eine Studienfahrt Durch Das Nordwestliche China Und Durch Die Innere Mongolei in Das Östliche Tibet. Union Deutsche Verlagsgesellschaft, Stuttgart, 352 pp.

Submitted January 28, 2022; revisions received April 28, 2022;
accepted May 10, 2022.
Handling Editor: F. Bibi.

# Appendix 3

*Publication 3*

Revision of the Late Miocene hornless rhinocerotids from Samos Island (Greece) with the designation of neotypes and implications for the European chilotheres.

**Panagiotis Kampouridis**[a,b], Georgia Svorligkou[c], Nikolaos Kargopoulos[d,e], Nikolai Spassov[f], and Madelaine Böhme[a,b]

[a]Department of Geoscience, Eberhard Karls University of Tübingen, Tübingen, Germany;

[b]Senckenberg Centre for Human Evolution and Palaeoenvironment, Tübingen, Germany;

[c]Faculty of Geology and Geoenvironment, Department of Historical Geology and Palaeontology, National and Kapodistrian University of Athens, Athens, Greece;

[d]Department of Biological Sciences, University of Cape Town, Cape Town, South Africa;

[e]Giraffe Conservation Foundations, Eros, Windhoek, Namibia; and

[f]National Museum of Natural History at the Bulgarian Academy of Sciences, Sofia, Bulgaria

Published in

Journal of Vertebrate Paleontology 43(1), e2254360

DOI: 10.1080/02724634.2023.2254360

Date of online publication: 02.11.2023

Journal of Vertebrate Paleontology e2254360 (24 pages)
Published with license by the Society of Vertebrate Paleontology
DOI: 10.1080/02724634.2023.2254360



ARTICLE

# REVISION OF THE LATE MIOCENE HORNLESS RHINOCEROTIDS FROM SAMOS ISLAND (GREECE) WITH THE DESIGNATION OF NEOTYPES AND IMPLICATIONS FOR THE EUROPEAN CHILOTHERES

PANAGIOTIS KAMPOURIDIS, *[,1,2] GEORGIA SVORLIGKOU, [3] NIKOLAOS KARGOPOULOS, [4,5] NIKOLAI SPASSOV, [6] and MADELAINE BÖHME [1,2]
[1]Terrestrial Palaeoclimatology section, Department of Geosciences, Eberhard Karls University of Tübingen, Tübingen, Germany, pkampouridis94@gmail.com;
[2]Palaeontology section, Senckenberg Centre for Human Evolution and Palaeoenvironment, Tübingen, Germany;
[3]Faculty of Geology and Geoenvironment, Department of Historical Geology and Palaeontology, National and Kapodistrian University of Athens, Athens, Greece;
[4]Department of Biological Sciences, University of Cape Town, Cape Town, South Africa;
[5]Giraffe Conservation Foundations, Eros, Windhoek, Namibia;
[6]National Museum of Natural History at the Bulgarian Academy of Sciences, Sofia, Bulgaria

ABSTRACT—Extant rhinoceroses are represented only by five species and are characterized by the presence of a nasal horn. In the past, they were much more diverse, with one of the best-known groups being the aceratheriines, i.e., hornless rhinoceroses. Chilotheres are a group of hornless rhinos that inhabited Eurasia during the Late Miocene. Their westernmost geographic range reached Eastern Europe, where overall eight species have been erected. Four of these were described based on material from the Upper Miocene of Samos Island (Greece), two of which are not considered valid anymore. Unfortunately, the type skulls of all four species are lost and there are several issues concerning their taxonomy. Therefore, we herein designate two skulls housed in historical collections from Samos as neotypes for the first two species, *Chilotherium schlosseri* (Weber, 1905) and *Eochilotherium samium* (Weber, 1905), and provide detailed comparisons for the separation of the species from each other and from any other chilotheres. Our results prove that the two species are valid and justify their separation on a generic level. *Chilotherium schlosseri* seems to be more closely affiliated with the other European *Chilotherium* species, whereas *E. samium* is more similar to the Chinese '*Chilotherium*' *wimani* and '*Chilotherium*' *primigenium*, based on their more plesiomorphic characters.

SUPPLEMENTARY FILES—Supplementary files are available for this article for free at www.tandfonline.com/UJVP. 3D surface models of the neotypes of *Chilotherium schlosseri* (GPIH 3015) and *Eochilotherium samium* (SMF M 3601) are available on MorphoSource (https://www.morphosource.org/) under the Project ID 000521964

Citation for this article: Kampouridis, P., Svorligkou, G., Kargopoulos, N., Spassov, N., & Böhme, M. (2023) Revision of the Late Miocene hornless rhinocerotids from Samos Island (Greece) with the designation of neotypes and implications for the European chilotheres. *Journal of Vertebrate Paleontology*. https://doi.org/10.1080/02724634.2023.2254360

Submitted: May 14, 2023
Revisions Received: July 10, 2023
Accepted: August 21, 2023

## INTRODUCTION

Rhinoceroses are among the last remnants of megafauna, comprising only five species today. In the past they were much more common, representing some of the most typical faunal elements in vertebrate assemblages during the Neogene and Quaternary in the Old World (Heissig, 1996, 1999). During this time diverse rhinoceros assemblages existed, with taxa that belonged to different groups, including the group of todays horned rhinos, the extinct elasmotheriines and the hornless rhinos (e.g., Kampouridis et al., 2022a; Pandolfi, 2016). The Late Miocene of Eurasia is an especially interesting time period for fossil rhinos, with several species being able to coexist in the same locality (Antoine, in press; Antoine & Saraç, 2005; Deng, 2006b; Fortelius et al., 2003; Heissig, 1999; Pandolfi, 2016). The Balkan–Iranian province (Bonis et al., 1992; Kampouridis et al., 2023; Spassov et al., 2019) is one of the best-studied regions with world-renowned Upper Miocene fossil localities such as Pikermi (Gaudry, 1862; Roussiakis et al., 2019; Wagner, 1848) and Samos (Kostopoulos et al., 2003; Koufos et al., 2011; Osborn, 1899; Solounias et al., 2010) in Greece, Hadjidimovo (Hristova et al., 2003; Spassov, 2002; Spassov & Geraads, 2004) in Bulgaria, Karaslari (Garevski, 1974; Schlosser, 1921; Spassov et al., 2018) in North Macedonia, and Maragheh (Ataabadi et al., 2013; Bernor, 1986; Hullot et al., 2022; Mecquenem,

*Corresponding author.

Color versions of one or more of the figures in the article can be found online at www.tandfonline.com/ujvp.

TABLE 1. Updated list of the European chilotheres species (modified after Kampouridis et al., 2022b).

| Species | Authority | Type Locality | Current Status |
|---|---|---|---|
| *Aceratherium schlosseri* | Weber, 1905 | Samos (Greece) | *C. schlosseri* |
| *Aceratherium samium* | Weber, 1905 | Samos (Greece) | *Eochilotherium samium* |
| *Aceratherium wegneri* | Andree, 1921 | Samos (Greece) | *C. schlosseri* |
| *Aceratherium angustifrons* | Andree, 1921 | Samos (Greece) | *C. schlosseri* |
| *Teleoceras ponticus* | Niezabitovski, 1912 | Odessa (Ukraine) | *C. schlosseri* |
| *Aceratherium kowalevskii* | Pavlow, 1913 | Grebeniki (Ukraine) | *C. kowalevskii* |
| *Chilotherium sarmaticum* | Korotkevich, 1958 | Berislav (Ukraine) | *C. sarmaticum* |
| *Aceratherium kiliasi* | Geraads & Koufos, 1990 | Pentalophos-1 (Greece) | *E. samium* |

1908; Pohlig, 1886) in Iran. Despite the abundance of material that has been excavated for over a century, many issues continue to exist regarding the rhinos. Samos has been known to yield vertebrate fossils for over a century (Forsyth-Major, 1888; Koufos, 2009; Solounias & Ring, 2007) and is of particular interest when fossil rhinos are concerned. Over the years, the existence of six species has been proposed (Andree, 1921; Weber, 1904, 1905). Most prominently, four chilothere species (originally referred to the genus *Aceratherium* Kaup, 1832) have been erected based on material from Samos (Andree, 1921; Weber, 1905). Weber (1905) erected *Aceratherium schlosseri* Weber, 1905, and *Aceratherium samium* Weber, 1905, based on a rich fossil collection, which, however, show a very worn-down dentition and Andree (1921) erected *Aceratherium wegneri* Andree, 1921, and *Aceratherium angustifrons* Andree, 1921, based on further complete cranial material. All of these were later (Heissig, 1975; Ringström, 1924) considered to belong to *Chilotherium* Ringström, 1924. Unfortunately, the type material of all four species has been lost and only the associated type mandible of *Chilotherium wegneri* is preserved in the collection of GPMM (Kampouridis et al., 2022b). This adds to the confusion that concerns this group with different synonymies having been proposed (e.g., Deng, 2006a; Giaourtsakis, 2003; Heissig, 1975; Kampouridis et al., 2022b).

The taxonomic and phylogenetic issues regarding the chilotheres became much more complicated, due to the description of four additional species assignable to the genus *Chilotherium* in Eastern Europe alone (Table 1; Geraads & Koufos, 1990; Korotkevich, 1958; Niezabitowski, 1912; Pavlow, 1913) and many more in East Asia (e.g., Deng, 2006a; Qiu et al., 1987; Ringström, 1924; Sun et al., 2018). The first European chilotheres are the herein revised species *C. schlosseri* and *E. samium* from Upper Miocene deposits of Samos in Greece (Weber, 1905), ranging from late early Turolian (MN 11) to the earliest late Turolian (MN 13), based on recent biochronological and magnetostratigraphic data (Kostopoulos et al., 2003; Koufos et al., 2009, 2011). Later, Niezabitowski (1912, 1913) described a fragmentary skull from Odessa in Ukraine, for which he established the species *Teleoceras ponticus* Niezabitowski, 1912. This species was later extensively reviewed and synonymized with *C. schlosseri* by Kiernik (1913), who suggested a Maeotian age, based on the sediment matrix and associated invertebrate remains. Pavlow (1913) described a large amount of rhino material from the Upper Miocene deposits of Grebeniki in Ukraine, which is considered to be of early Maeotian age (Vangengeim & Tesakov, 2013). This material was attributed to the new species *Aceratherium kowalevskii* Pavlow, 1913, which was subsequently placed in the genus *Chilotherium* (Ringström, 1924). Almost half a century later, another species, *Chilotherium sarmaticum* Korotkevich, 1958, was erected based on ample material from Berislav, a late Sarmatian locality in Ukraine (Vangengeim & Tesakov, 2013). More recently, the species *Aceratherium kiliasi* Geraads & Koufos, 1990, was described based on material from the Vallesian locality Pentalophos-1 in Greece (Geraads & Koufos, 1990). However, the material was a mixed sample of fossils that belong to *Acerorhinus neleus* Athanassiou et al., 2014, and a chilothere (Fortelius et al., 2003) that is herein synonymized with *E. samium*.

Overall, the European representatives of chilotheres include a variety of hornless rhino species that cover a stratigraphic range from the Vallesian to the late Turolian. Their inclusion in the genus *Chilotherium* was mainly based on the separated parietal crests, the wide mandibular symphysis with the large, flattened tusk-like lower incisors, the complicated upper tooth morphology, and their short and robust appendicular skeleton. Some of these features also occur in *E. samium*, which, however, also exhibits more plesiomorphic features that would sustain a generic separation.

The aim of the present study is to investigate the preserved aceratheriine fossils from the Upper Miocene of Samos housed in different collections throughout Europe and address the taxonomic issues revolving around this material and the other chilotheres from Eastern Europe, by assigning neotypes to the two valid aceratheriines from Samos. This revision allows us to re-establish the classical two species *Chilotherium schlosseri* and *Eochilotherium samium* and place them in separate genera, thus shedding light on some of the issues concerning the chilotheres.

**Institutional Abbreviations**—**AMPG**, Athens Museum of Palaeontology and Geology of the National and Kapodistrian University of Athens, Athens, Greece; **BSPG**, Bayerische Staatssammlung für Paläontologie und Geologie, Munich, Germany; **GMM**, Geomuseum of the University of Münster, Münster, Germany; **GPIH**, Geologisch-Paläontologisches Institut der Universität Hamburg, Hamburg, Germany; **GPIT**, Geologisch-Paläontologisches Institut der Universität Tübingen, Tübingen, Germany; **HLMD**, Hessisches Landesmuseum Darmstadt, Darmstadt, Germany; **MNHN**, Muséum national d'Histoire naturelle, Paris, France; **NHMW**, Naturhistorisches Museum, Vienna, Austria; **NMB**, Naturhistorisches Museum Basel, Basel, Switzerland.

## GEOLOGICAL SETTING

The island of Samos is situated in the easternmost part of the Aegean Sea in Greece, close to Asia Minor (Fig. 1) and is one of the richest Upper Miocene localities in the Eastern Mediterranean. All material studied herein comes from these fossiliferous Upper Miocene deposits (Drevermann, 1930; Gürich, 1911; Lehmann, 1984). Recent studies elucidated the stratigraphic context of these deposits (Kostopoulos et al., 2003, 2009; Koufos et al., 2009; Solounias & Mayor, 2004). The Neogene sediments of Samos Island are deposited on metamorphic and non-metamorphic rocks of Middle Triassic to Late Jurassic age, associated with the alpine orogenesis. The fossil vertebrate sites are all located in the Mytilinii Basin, in the eastern part of the island. The Neogene stratigraphy of Mytilinii Basin has been studied by many geologists in the past, mostly for the sake of the vertebrate fossils found there (see Kostopoulos et al., 2009). We follow the most recent study of Kostopoulos et al. (2009), who divided the Neogene sediments into five formations, the Basal Formation, the Mayradzei Formation, the Hora Formation, the Mytilinii

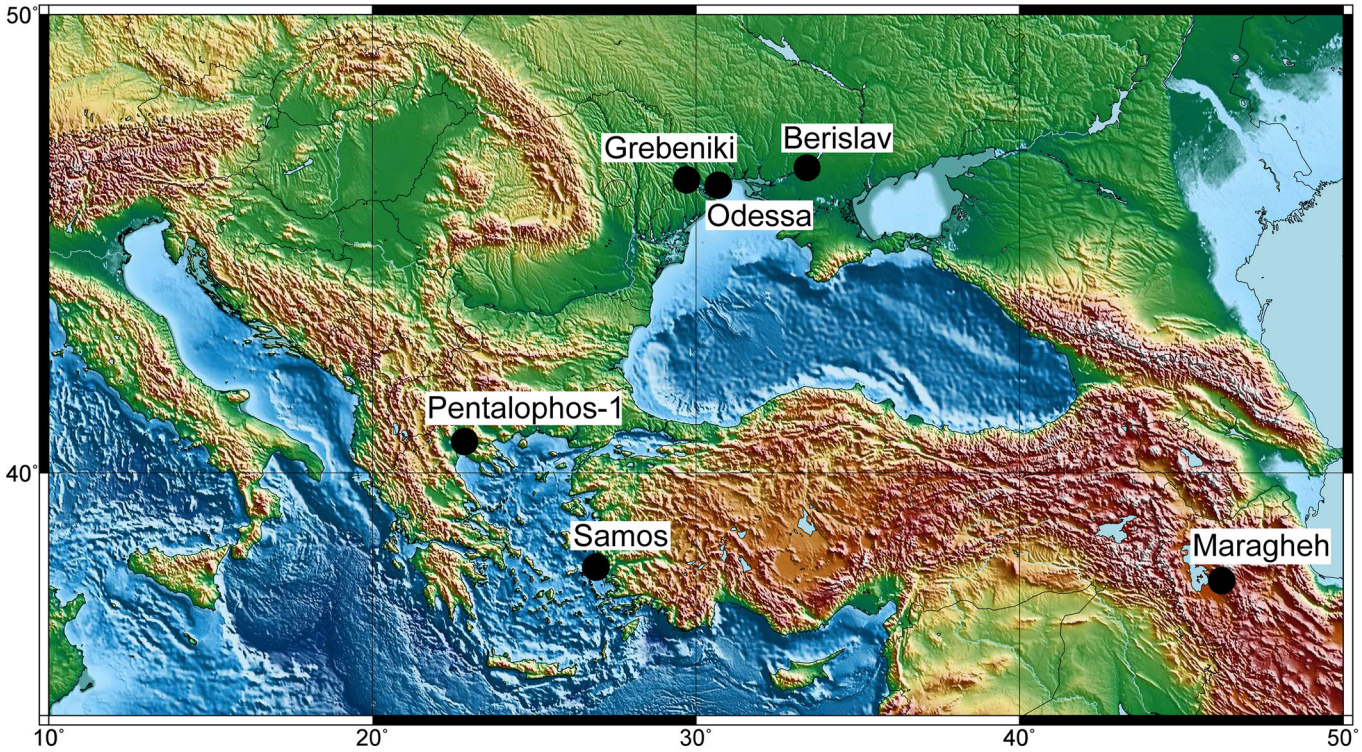


FIGURE 1. Geographic map indicating the type localities of the Chilotheriina species found in the Eastern Mediterranean: Samos (*Aceratherium schlosseri* Weber, 1905, *Aceratherium samium* Weber, 1905, *Aceratherium wegneri* Andree, 1921, and *Aceratherium angustifrons* Andree, 1921) and Pentalophos-1 (*Aceratherium kiliasi* Geraads and Koufos 1990) in Greece; Odessa (*Teleoceras ponticus* Niezabitowski, 1912), Grebeniki (*Aceratherium kowalevskii* Pavlow, 1913), and Berislav (*Chilotherium sarmaticum* Korotkevitch, 1958) in Ukraine; and Maragheh (*Rhinoceros persiae* Pohlig, 1886) in Iran. The map was made with GMT6 (Wessel et al. 2019).

Formation, and the Kokkarion Formation. The Mytilinii Formation, which comprises all fossiliferous layers, mainly constitutes debris-flows in complex with ephemeral lake and overflow deposits.

The Mytilinii Formation has been divided into four members. At the bottom are the Old Mill Beds, overlain by the Gravel Beds, both of which consist of green to brown silty sands in alternation with sandy tuffs and conglomerates. These are overlain by the White Beds member, which consists mainly of white marls and marly-sandy limestones. These lower members include only very few fossiliferous localities. The Main Bone Beds member consists primarily of brownish to reddish silty sands, but includes also white tuffites, yellow to brownish conglomerates and tuffaceous sandstones. At the top of the Mytilinii Formation characteristic marker tuffs are found that comprise red tuffaceous sandy silts with intercalations of massive tuffs.

The Main Bone Beds member includes the vast majority of all vertebrate fossil sites discovered on the island of Samos and the material studied herein probably comes from these deposits. Most collectors did not specify the exact location or stratigraphic context of the excavated material. Thus, stratigraphic correlations between the different collections of fossil material from Samos, including the material studied herein, is not possible (see also Kostopoulos et al., 2009). The only knowledge on the stratigraphic context of the two chilothere species is that provided by Weber (1905), who was not in the field himself and only stated that they come from different horizons, based on the different sediment adhering to the type material. During the most recent excavations on Samos (Koufos, 2009), no chilothere material was found (Giaourtsakis, 2009). Koufos et al. (2009) tried to assess the potential position of the two species in the stratigraphic column of Samos, based on the associated fauna for *C. schlosseri*, that is well-known from the historical collections of Samos and according to the suggested stratigraphic distribution by previous authors that was based on its possible existence in other localities for *E. samium* (Heissig, 1975, 1996). It is likely that the two species do not co-occur in the same strata and that *E. samium* is found in the stratigraphically older layers, whereas *C. schlosseri* is present in the younger fossiliferous horizons of Samos. However, the lack of stratigraphic information for the specimens prevents their association with any of the fossiliferous horizons; and thus, inhibits certain stratigraphic correlations.

## MATERIAL AND METHODS

For the purpose of the present work, material from several collections was studied including the NHMW (Austria), MNHN (France), GMM, GPIH, GPIT, HLMD, SMF, and SMNS (Germany), AMPG (Greece), and NMB (Switzerland). The goal was to find the most appropriate specimens to be designated as neotypes to compensate for the loss of the holotypes of *Aceratherium schlosseri* Weber, 1905, and *Aceratherium samium* Weber, 1905. The names *Aceratherium schlosseri* and *Aceratherium samium* will be used only to refer to the type material of the two species that was described by Weber (1905). The names *Chilotherium schlosseri* and *Eochilotherium samium* will be used to refer to the species in general and when only the neotypes are concerned the specimen numbers (GPIH 3015 and SMF M 3601) will be stated, to avoid confusion.

**Qualifying Conditions for the Designation of the Neotypes**

The International Code on Zoological Nomenclature (ICZN) lists seven qualifying conditions (ICZN Art. 75.3) that ought to be met for a neotype designation to be valid (Ride et al., 1999). Based on these, the situation of both *C. schlosseri* and *E. samium* justifies the designation of neotypes.

The two Samian chilothere species *C. schlosseri* and *E. samium* have a problematic taxonomic history. At the moment, it is extremely difficult to assign any new material to either of these species, because the comparison can only be based on old illustrations. This is especially the case for *E. samium*, for which virtually no additional material from its type locality has ever been described after its erection. Also, no certain attribution has been made from other localities (see also Fortelius et al., 2003). Thus, the first qualifying condition (ICZN Art. 75.3.1) is met. The skull GPIH 3015 and its associate mandible are definitely assignable to *C. schlosseri* based on the morphological similarities, which include the very wide parietal crests and the complex tooth morphology, with a very strong crochet, antecrochet, protocone constriction, and the existence of a crista in some teeth that closes off the medifossette. The taxonomic attribution of GPIH 3015 to *C. schlosseri* was also encouraged by previous authors (Giaourtsakis, 2022; Lehmann, 1984). Specimen SMF M 3601, on the other hand, lacks the depression in the frontals, its parietal crests are much closer together, and the secondary folds in the maxillary teeth are not as prominent. These features allow the identification of SMF M 3601 as *E. samium*. This attribution was also supported by Geraads and Spassov (2009), thus covering the second qualifying condition (ICZN Art. 75.3.2). The specimens herein designated as the neotypes of *Aceratherium schlosseri* Weber, 1905 (GPIH 3015) and *Aceratherium samium* Weber, 1905 (SMF M 3601) will be described and illustrated (Figs. 2–13, S1–2) in detail and 3D surface models of both specimens are provided (ICZN Art. 75.3.3). The type material of both *Aceratherium schlosseri* and *Aceratherium samium*, including all material described by Weber (1905), was formerly housed in the BSPG, but cannot be relocated and it is believed that it was destroyed in the Second World War (Giaourtsakis, 2003, 2022; Kampouridis et al., 2022b), during the bombing of Munich by the Allied Royal Air Force on April 24, 1944 (Nothdurft & Smith, 2002), thus meeting the condition of ICZN Art. 75.3.4. As mentioned above, the skulls GPIH 3015 and SMF M 3601, which are selected as neotypes exhibit the same key features as the lectotypes of *Aceratherium schlosseri* and *Aceratherium samium*, respectively. These include the notably depressed frontal bones, widely separated (over 70 mm) parietal crests, and the complex dental morphology for *C. schlosseri*, and the convex frontal bones, the more closely situated parietal crests (approx. 40 mm), and the somewhat less developed secondary folds in the upper teeth in *E. samium* (ICZN Art. 75.3.5). The material described by Weber (1905), as well as the material studied herein and selected as the neotypes, all come from the Upper Miocene deposits of the Mytilinii Basin on Samos Island (Greece). During the excavations on Samos in the course of the 19th and beginning of the 20th century only little attention was paid to documenting the exact location and stratigraphic context of the findings (Koufos, 2009). Therefore, almost nothing is known about it for these specimens, except for the fact that they come from the same basin, where the Turolian fossiliferous deposits on Samos Island are found (Kostopoulos et al., 2003), thus being the best option to meeting the conditions of ICZN Art. 75.3.6. Specimen GPIH 3015 has been part of the geological-paleontological collections of the University of Hamburg, an official university in Germany, since at least 1911 (Gürich, 1911; Lehmann, 1984). These collections are currently administered by the Leibniz Institute for the Analysis of Biodiversity. Similarly, specimen SMF M 3601 has been part of the collection of the Senckenberg Research Institute in Frankfurt, a scientific institution in Germany, since 1910 (R. Brocke, pers. comm.). In both cases, the material is housed in proper collections and will be accessible for further study in perpetuity (ICZN Art. 75.3.7); thereby, meeting all qualifying conditions set forth by ICZN Art. 75.3.

## SYSTEMATIC PALEONTOLOGY

Class MAMMALIA Linnaeus, 1758
Order PERISSODACTYLA Owen, 1848
Family RHINOCEROTIDAE Gray, 1821
Subfamily ACERATHERIINAE Dollo, 1885 (sensu Lu, Deng, & Pandolfi, 2023)
Tribe ACERATHERIINI Dollo, 1885 (sensu Lu, Deng, & Pandolfi, 2023)
Subtribe CHILOTHERIINA Qiu, Xie, and Yan, 1987

**Included Genera**—*Chilotherium* Ringström, 1924, *Shansirhinus* Kretzoi, 1942, and *Eochilotherium* Geraads and Spassov, 2009.

**Amended Diagnosis**—Aceratheriine rhinocerotids that feature the following autapomorphic traits: separated parietal crests; upper molars featuring a marked protocone constriction and a moderate to strong antecrochet with a trend to turn lingually; a mandible that is characterized by a very wide mandibular symphysis that features a concave ventral side; large, sexually dimorphic i2s with a trend to become flattened and tusk-like that are separated from each other by a wide diastema and from the p2 by a long diastema with a marked crest. The group also exhibits an upper first deciduous premolar retained into adulthood, whereas the first lower deciduous premolar, when present, is shed and not replaced by a permanent one. Additionally, the upper cheek teeth have generally pronounced secondary enamel folds, and the appendicular skeleton is notably shortened and relatively robust, especially the metapodials.

**Remarks**—The clade Chilotheriini (sensu Qiu et al., 1987) was erected as a tribe to encompass the genera *Chilotherium* and *Shansirhinus*. However, the rank of this group is not clear. Different phylogenetic analyses have placed the clade of the hornless rhinos variably as a subfamily, Aceratheriinae (e.g., Cerdeño, 1995; Fortelius & Heissig, 1989; Heissig, 1999; Lu et al., 2023), or as a tribe, Aceratheriini (e.g., Antoine, 2002; Pandolfi, 2016). This leads to an ambiguous rank for the clade that includes the chilotheres, which in the latest phylogenetic analysis concerning hornless rhinos was placed as a subclade (*Chilotherium* + *Shansirhinus*) within the tribe Aceratheriini that includes both *Chilotherium* and *Aceratherium* (Lu et al., 2023). Therefore, we tentatively place Chilotheriina as a subtribe that includes the three genera *Chilotherium*, *Shansirhinus*, and *Eochilotherium*.

### Genus *CHILOTHERIUM* Ringström, 1924

**Type Species**—*Chilotherium anderssoni* Ringström, 1924.

**Type Locality**—Lok. 30 Shanxi, China (Ringström, 1924).

**Included Species**— *Chilotherium persiae* (Pohlig, 1886), *Chilotherium habereri* (Schlosser, 1903), *Chilotherium schlosseri* (Weber, 1905), *Chilotherium kowalevskii* (Pavlow, 1913), '*Chilotherium*' *wimani* Ringström, 1924, *Chilotherium sarmaticum* Korotkevich, 1958, *Chilotherium orlovi* Bayshashov, 1982, '*Chilotherium*' *primigenium* Deng, 2006a, *Chilotherium licenti* Sun et al., 2018.

**Amended Diagnosis**—Aceratheriine rhinocerotids that feature the following autapomorphic characters: flattened and depressed frontal region; well-developed postorbital processes; moderately to widely separated parietal crests; highly placed orbits; very wide mandibular symphysis; very large, flattened, tusk-like second lower incisors, with a scalene

triangle cross section and upturned, dorsomedially oriented wear facets; reduced premaxillary bones that lack upper incisors; and very strong secondary enamel folds, including a lingually flattened and strongly constricted protocone in the molars. It is also characterized by a relatively short length of the premolars compared with the molars, mainly due to the reduced size of the P2 and p2; and notably shortened metapodials and relative robust appendicular skeleton (Geraads & Spassov, 2009; Giaourtsakis, 2022; modified after Ringström, 1924).

**Differential Diagnosis**—Differs from *Eochilotherium* in having a less dolichocephalic skull; concave frontals; flat dorsal profile of the skull; more complicated enamel folds in the upper teeth, including constricted protocones in P2 and P3, more strongly constricted molars, and more prominent antecrochets; and much larger lower incisors that are more flattened. Differs from *Shansirhinus* in having concave frontals; a wider mandibular symphysis; more reduced second upper premolar; less pronounced lingual cingula; much weaker paracone folds; and less enamel plications.

## *CHILOTHERIUM SCHLOSSERI* (Weber, 1905) (Figs. 2–5)

**Neotype**—A well-preserved skull (GPIH 3015) with an associated mandible (GPIH 3015a), by present designation under the provisions of ICZN Art. 75.

**Type Locality**—Upper Miocene deposits (Turolian age, Mytilinii Formation) of Samos Island; exact locality unknown.

**Junior Synonyms**—*Teleoceras ponticus* Niezabitowski, 1912, *Aceratherium wegneri* Andree, 1921, and *Aceratherium angustifrons* Andree, 1921.

**Amended Diagnosis**—A large *Chilotherium* species characterized by widely separated parietal crests (minimal width always over 70 mm in adult individuals), notably depressed frontal and nasal bones and a unique combination of dental characters: very long crochet; very strong mesial and distal constriction of the protocone, which is lingually flattened, resulting in a very long antecrochet that usually closes off the median valley at an early wear stage in all teeth; a prominent mesial constriction of the hypocone; crista frequently present that closes the medifossette; and a discontinuous lingual cingulum that is occasionally moderately developed in the premolars; often a closed prefossette is present in the P2; in addition to sporadically present enamel plications in the upper teeth; and discontinuous lingual and buccal cingulids in the lower teeth.

**Remarks**—The lectotype (designated by Giaourtsakis, 2022) is a relatively well-preserved adult cranium with its associated mandible described and figured as *Aceratherium schlosseri* by Weber (1905:table 8, figs. 1–4; table 9, fig. 1). It was housed in the BSPG, but it is believed to have been destroyed during the Second World War (Giaourtsakis, 2009, 2022). Due to the loss of the type material, a neotype must be designated to solve the taxonomic issues and to secure the stability of this species. We herein choose the specimen GPIH 3015 as the neotype of *C. schlosseri*. It is housed in the collections of the GPIH in Germany and comes from the same locality as the lectotype of *Aceratherium schlosseri* (Weber, 1905:table 8, figs. 1–4; table 9, fig. 1), the Upper Miocene deposits of Samos Island (Greece). It was described as *Chilotherium schlosseri* and illustrated by Lehmann (1984:pl. 3, figs. 2–3). In fact, it shows all morphological features characteristic for this species, as also supported by Giaourtsakis (2022). Therefore, all qualifying conditions for the designation of a neotype (see ICZN Art. 75.3) are met.

*Chilotherium schlosseri* is much more common in the material collected from Samos than *E. samium*. Several almost complete skulls of *C. schlosseri* are available in different collections (e.g., NHMW, HLMD). Herein, we select GPIH 3015 as the neotype as it is virtually complete, preserves its associated mandible and its teeth are at a wear stage that allows the detailed study of the dental morphology.

The lower incisors of the neotypic mandible (GPIH 3015a) are very damaged and only their bases are preserved. Nonetheless, it can be seen that they were very large (i2 width = ~45 mm). Based on the very wide i2s, it can be assumed that the skull (GPIH 3015) with its mandible (GPIH 3015a) belonged to a male individual.

### Description

**Skull**—The skull is almost complete, lacking only the premaxillary bones, part of the left zygomatic arch, which has been modeled with plaster, parts of the postglenoid and posttympanic processes, and the left D1 and P2 (Figs. 2–4). Additionally, some areas on the dorsal side of the skull seem to have been modeled, covered with plaster but do not affect any important morphological traits. The specimen has not been affected by any other kind of distortion or deformation.

In lateral view (Fig. 3), the dorsal profile of the skull seems flat, with a very slight elevation of the nuchal crest in the posterior portion of the skull. The nasal bones extend slightly past the D1, anteriorly. The nasal notch is almost U-shaped and terminates at the level above the middle of the M1. On the maxillary bone, three infraorbital foramina are present within the nasal notch. There is no apparent facial crest. The orbit is located very high in the skull, with its anterior margin being above the mesial portion of the M2. A small lacrimal tubercle is visible, but the number of lacrimal foramina cannot be assessed, due to the presence of sediment in that area. The postorbital process on the frontal bones is very strong and marks the widest portion of the skull roof, as well as the beginning of the parietal crests. Another, weaker postorbital process is also present on the zygomatic arch, slightly more anteriorly than the one on the frontal bones. The zygomatic arches exhibit a very slight depression behind the postorbital process. The postglenoid process is broken on both sides. But it is visible that they are very close to the posttympanic processes without contacting them. The paroccipital process is also broken.

In dorsal view (Fig. 2A), the nasal bones are rather narrow. Their tip is slightly rugose, and they are separated from each other by the internasal suture that forms a noticeable longitudinal groove. The suture between the nasals and the frontal remains visible despite the adult age of the individual. The suture is a curved line approximately at the level of the orbital margin. The frontal bones are strongly depressed. The whole skull roof is transversely concave from the nasal bones until the parietal crests. The parietal crests are widely separated, with a minimal distance of 89 mm between them and end in a well-developed nuchal crest.

In ventral view (Fig. 2B), the anterior end of the choana is slightly pointed and reaches the medial part of the M3. The tips of the pterygoid processes are damaged but seem simple and laterally extending. The intercondylar notch is U-shaped and the condyles are widely separated.

In posterior view, the upper portion of the skull forming the nuchal crest is broken, but the general shape seems to be somewhat trapezoidal. The nuchal tubercle is only weakly developed, from which moderately developed lateral occipital crests start and might have reached the nuchal crest. Laterally to them, weak outer lateral crests exist.

**Upper Dentition**—The upper dentition is almost completely preserved, only lacking the right D1 and P2 (Figs. 2B, 4). Most teeth are at a moderate wear stage. All of them preserve a layer of cement buccally and lingually. The D1 is retained into adulthood but is heavily worn. The hypocone is larger than the protocone. A large fossette, probably represents the closed

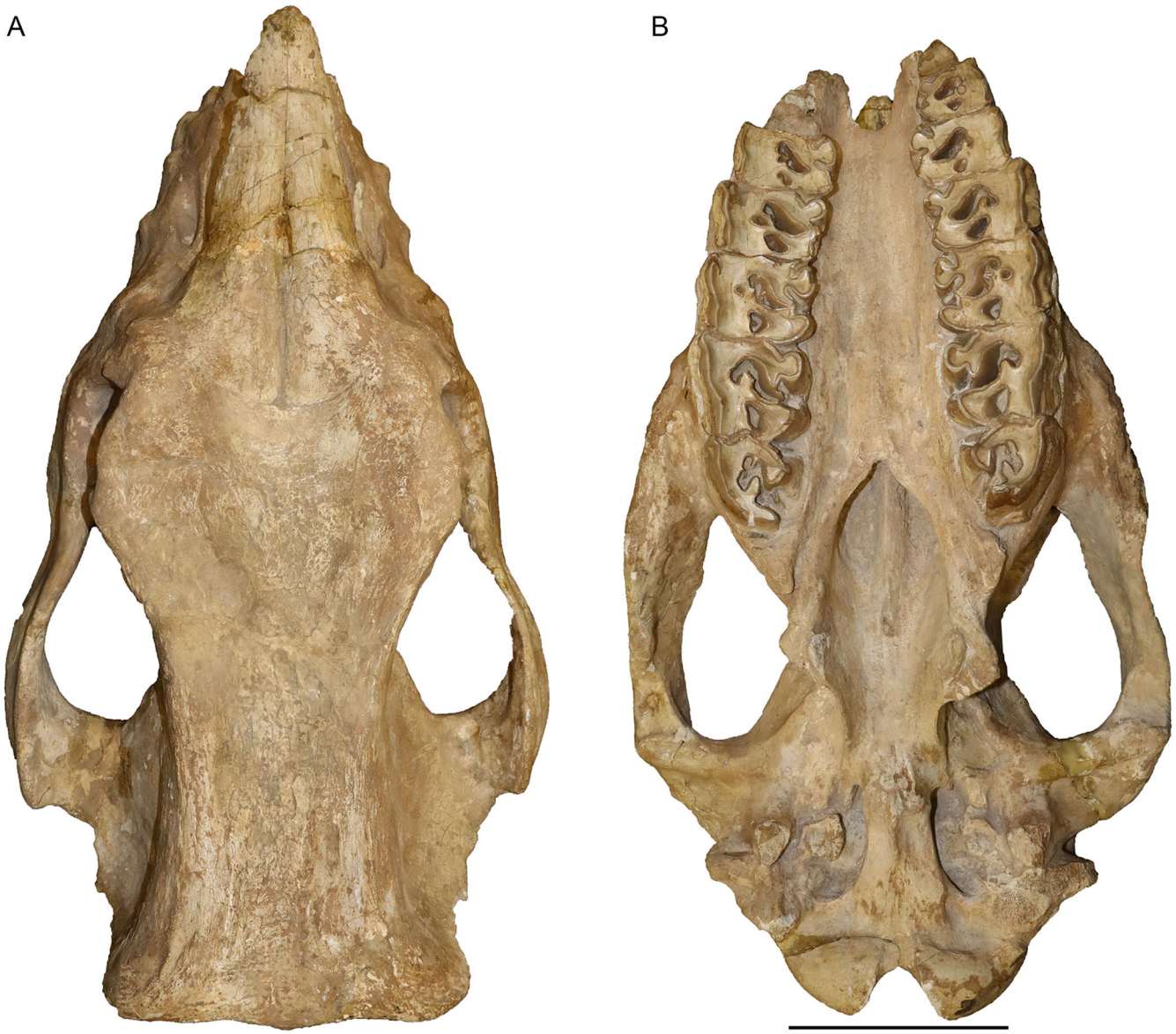


FIGURE 2. Neotype skull of *Chilotherium schlosseri* (Weber, 1905) (GPIH 3015) from the Upper Miocene of Samos Island (Greece) in dorsal (**A**) and ventral view (**B**). Scale bar equals 10 cm.

median valley, whereas a much smaller fossette should correspond to the postfossette. The P2 is well-worn revealing its morphology in much detail. The protocone is slightly smaller than the hypocone. The protocone is constricted mesially and distally, forming an antecrochet that is connected to the hypocone closing off the median valley. The hypocone is only mesially constricted. A crochet is present, along with a very small crista, with which it may fuse during a more advanced wear stage to form a closed medifossette. The prefossette remains open at this wear stage, but would close when slightly more worn, while the postfossette is already closed. Lingually, an almost continuous cingulum is present, whereas buccally the ectoloph is covered by cement. Nonetheless, a discontinuous buccal cingulum seems to be present. In the P3, the protocone and the hypocone are similarly well-developed. The protocone is strongly constricted mesially and distally, forming a long antecrochet that connects with the hypocone, closing off the median valley. The hypocone does not exhibit a constriction; this is very likely due to the fusion with the antecrochet and the advanced wear stage. A crochet is present, and the crista is very small, almost closing off the medifossette; in the right P3 the small crista is followed by an enamel plication. No prefossette is visible, but the postfossette is closed. A discontinuous lingual and buccal cingulum is present. The P4 features a strongly constricted protocone, with a prominent antecrochet, which fuses with the hypocone, resulting in a closed median valley. A crochet is present; in the right P4 it is much longer and closes off the medifossette. In the left P4, a weak enamel bulge is present that corresponds to the crista. A large postfossette is present. A discontinuous lingual cingulum is present on the right P4, whereas on the left this cannot be observed. On the ectoloph, both P4s exhibit a discontinuous cingulum.

The M1 is well-worn and exposes a very strongly constricted protocone, both mesially and distally, that forms a long, lingually projecting antecrochet. The protocone is lingually flattened and has an almost sub-triangular shape. The hypocone is mesially


FIGURE 3. Neotype skull of *Chilotherium schlosseri* (Weber, 1905) (GPIH 3015) from the Upper Miocene of Samos Island in left lateral (**A**) and right lateral view (**B**). Scale bar equals 10 cm.

strongly constricted and connects to the antecrochet, closing off the median valley. A closed medifossette and postfossette are present. Both lingually and buccally, discontinuous cingula are present, which form enamel pillars in the entrance of the median valley. Enamel plications are visible within the median valley and the postfossette in both M1s. Lastly, the M1 exhibits a hypoplasia visible only at the base of the lingual side, because the ectoloph is covered by cement. The M2 is less worn than the previous teeth. It exhibits a lingually flattened and strongly constricted protocone that results in a strong antecrochet, which turns lingually. The hypocone is only mesially constricted; at a more advanced wear stage the hypocone and the antecrochet would fuse and cut off the median valley. The crochet is strong but does not close the medifossette at this wear stage. The postfossette is just about to close. Both M2s feature discontinuous cingula lingually. Moreover, in lingual view, close to the base of the tooth crown a hypoplasia is visible. The M3 is the least worn tooth in this specimen. The protocone is lingually flattened and bears strong mesial and distal constrictions, which form a long lingually projecting antecrochet. A strong crochet is present, along with a crista and an additional enamel plication. Distally the cingulum is represented by a high enamel bar. Finally, a hypoplasia is present in the M3, only visible on the lingual side, due to the presence of cement coverage buccally on the ectoloph.

**Mandible**—The mandible is very well preserved, including almost the complete dentition and only lacking the left articular process and the coronoid process on both sides (Fig. 5). The symphysis is very wide with a diastema of 82.3 mm between the incisors. On the ventral side the symphysis is markedly concave and bears two large foramina that are also visible in anterior view. A small foramen is visible posterior to the large one on the left hemimandible. Other foramina are not visible due to the presence of plaster that covers part of the ventral surface. The anterior end of the symphysis forms a thin edge between the two incisors. In dorsal view, the symphysis ends at the posterior end of the p3s and is 127 mm long. Between the i2 and the p2 there is a long diastema of 60 mm, which is marked by a well-developed dorsal ridge between these two teeth. The dorsal surface of the symphysis, between these ridges is concave. In lateral view, on the left side one large and one small mental foramen are visible below the p2 and p3. On the left side the foramina are covered by plaster. The height of the mandibular body remains similar throughout its length, with a slight increase posteriorly. The vertical rami are only partially preserved, with the coronoid processes missing in both hemimandibles. The condylar process for the articulation


FIGURE 4. Neotype upper dentition of *Chilotherium schlosseri* (Weber, 1905) (GPIH 3015) from the Upper Miocene of Samos Island. Left (**A**) and right (**B**) upper toothrow. Scale bar equals 5 cm.

to the skull is 78.5 mm wide. The condylar process becomes medially thinner. Lastly, the mandibular angle bears a strong masseteric tuberosity.

**Lower Dentition**—The lower dentition only lacks the right p2 and the incisors are broken off (Fig. S1). Despite the damage to the incisors, it is visible that they would have been very large, and their wear facet is placed dorsally and turned abaxially, with enamel only on the ventral side. The cross section of the roots of the incisors is almond shaped with a width of 45 mm. Some of the cheek teeth preserve remnants of their cement. The premolar/molar length ratio (sensu Athanassiou et al., 2014) is 72%. All of the cheek teeth bear discontinuous lingual cingulids, the premolars also feature discontinuous buccal cingulids. The p2 has a thin mesially projecting paralophid and features a shallow anterior valley and a weak anterior groove on the ectolophid. Rather strong mesial and distal cingulids are also present, which slightly extend towards the buccal side of the side. Otherwise, the lower cheek teeth have a rather simple morphology that is relatively uniform. They have a paralophid that is slightly shorter than the metaconid. The metaconid and entoconid are relatively thick. The anterior valley is not as deep as the posterior one and the ectolophid groove is deep until a very advanced wear stage.

## Genus *EOCHILOTHERIUM* Geraads & Spassov, 2009

**Type and Only Species**—*Aceratherium samium* Weber, 1905.

**Diagnosis**— Same as for the type and only species.

**Remarks**—*Eochilotherium* was coined by Geraads and Spassov (2009) as a subgenus, *Chilotherium* (*Eochilotherium*), with *Aceratherium kiliasi* as its type species and the authors also included *Aceratherium samium* in it. Herein, we elevate *Eochilotherium* to the genus level, this does not affect *Aceratherium kiliasi* as its type species according to the provisions of the ICZN Art. 61.2.2. However, *Aceratherium kiliasi* is a junior synonym of *E. samium*, as stated also in previous studies (Athanassiou et al., 2014:table 3; Giaourtsakis, 2022). The type species of *Eochilotherium* is now fixed (under ICZN Article 70.3) as *Aceratherium samium* Weber, 1905, due to the misidentification of *Aceratherium kiliasi* Geraads and Koufos, 1990.

### *EOCHILOTHERIUM SAMIUM* (Weber, 1905) (Figs. 6–9)

**Neotype**—A well-preserved skull with associated mandible of an old individual (SMF M 3601), by present designation under the provisions of ICZN Art. 75.

**Type Locality**—Upper Miocene deposits (Turolian, Mytilinii Formation) on Samos Island; exact locality unknown.

**Junior Synonym**—*Aceratherium kiliasi* Geraads and Koufos, 1990.

**Amended Diagnosis**—Aceratheriine rhinocerotid of medium size with a unique combination of craniodental features separating it from all other chilotheres: dolichocephalic skull; transversally concave dorsal surface of the parietal bones, while their frontal bones are convex in the anterior part, becoming flattened posteriorly; moderately separated parietal crests (~40 mm); weak to absent groove that would separate the nasal bones from each other; raised posterior part of the skull; wide mandibular symphysis with moderately enlarged and slightly flattened second lower incisors; the relative length of the premolars with respect to the molars is reduced, primarily due to the reduction of the size of the second upper and lower premolars; and

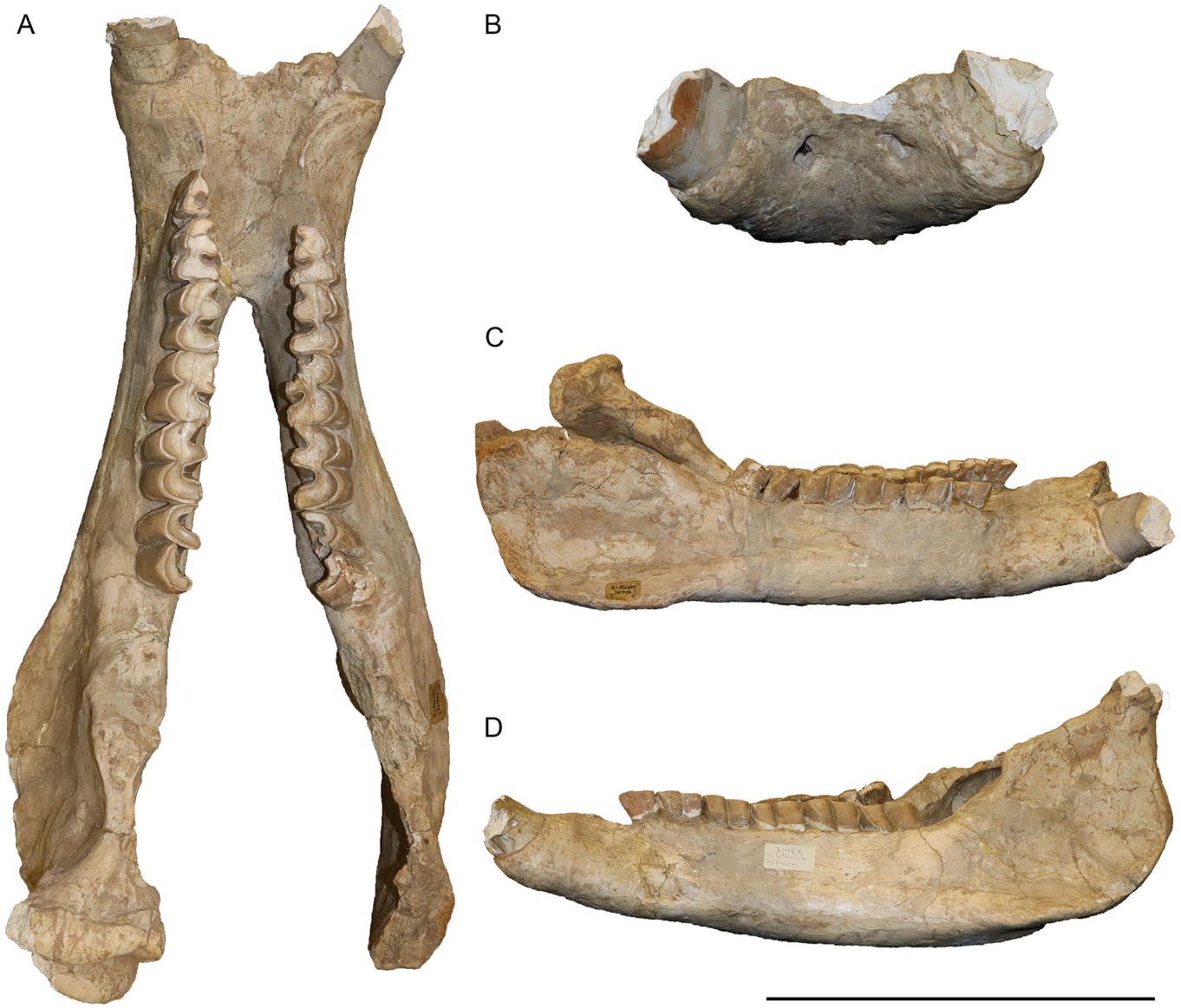


FIGURE 5. Neotype mandible of *Chilotherium schlosseri* (Weber, 1905) (GPIH 3015) from the Upper Miocene of Samos Island in dorsal (**A**), anterior (**B**), right lateral (**C**), and left lateral view (**D**). Scale bar equals 20 cm in **A**, 15 cm in **B**, and 30 cm in **C** and **D**.

complex enamel folds: moderate crochet and constriction of the protocone of the molars, with a strong antecrochet that bends lingually; neither the protocone nor the hypocone of the P2 are constricted; no crista in the molars; and discontinuous lingual cingula.

**Differential Diagnosis**—Differs from *Chilotherium* spp. in having flat to convex frontal bones and lacking the frontal depression characterizing the genus *Chilotherium*; the parietal crests are usually not as widely separated from each other as in *Chilotherium* spp.; the posterior portion of the skull is notably elevated, compared with the only weakly elevated or flat posterior part in *Chilotherium* spp.; in the P2 and P3 the protocone is not constricted; the hypocone is either not constricted or only weakly constricted; the lower incisor is narrower and less flattened in *E. samium* compared with *Chilotherium* spp. Differs from *Shansirhinus* spp. in lacking the complicated enamel folds that include the strongly constricted protocone and hypocone in all teeth and the presence of enamel plications in *Shansirhinus* spp. Furthermore, *Shansirhinus* spp. exhibits a prominent paracone fold, which is much weaker in *E. samium*.

**Remarks**—The lectotype (designated by Geraads & Koufos, 1990:p. 163) is a partially preserved adult cranium with associated mandible described and figured as *Aceratherium samium* by Weber (1905:table 9, fig. 5; table 10, fig. 1, 2). It was housed in the BSPG, but it is believed to have been destroyed during the Second World War (Giaourtsakis, 2009, 2022). We herein embrace the notion of Geraads and Spassov (2009), who considered specimen SMF M 3601 as the only specimen that can be assigned to *E. samium*, and designate this skull (SMF M 3601) as the neotype of *Aceratherium samium*. Specimen SMF M 3601 is housed in the collections of SMF in Germany and comes from the same locality as the lectotype of *Aceratherium samium* (Weber, 1905:table 9, fig. 5; table 10, fig. 1, 2), Upper Miocene deposits of Samos Island (Greece). This specimen was initially illustrated by Drevermann (1930:fig. 6) as *C. schlosseri*, without any detailed description or comparison. Geraads and

Spassov (2009) mentioned that this is the only specimen that can be assigned to *E. samium*. It has to be noted that Giaourtsakis (2022) seemingly disagreed with the identification of SMF M 3601 as *C. schlosseri* by Drevermann (1930:fig. 6), but preferred to keep SMF M 3601 as *Chilotherium* sp., without mentioning a potential assignment to *E. samium* that was already suggested by Geraads and Spassov (2009). Herein, we follow Geraads and Spassov (2009), because specimen SMF M 3601 shows the key features in the morphology of the skull and teeth of *E. samium*, as discussed below. Therefore, all qualifying conditions for the designation of a neotype (see ICZN Art. 75.3) are met.

*Eochilotherium samium* is a rare species in the Upper Miocene deposits of Samos (Greece). In total, only three skulls of this species have been mentioned: the lectotype and a second skull described by Weber (1905:table 9, fig. 5; table 10, figs. 1, 2), and specimen SMF M 3601. The first two were lost during the Second World War. Therefore, SMF M 3601 is the only reasonable choice for the neotype of this species.

In the neotype mandible (SMF M 3601) only the right lower incisor is preserved. It is almost triangular in shape and is relatively small (i2 width = 30 mm). Based on the small triangular i2, it can be assumed that the skull (SMF M 3601) with its mandible belonged to a female individual.

## Description

**Skull**—The skull SMF M 3601 is almost complete, missing only the right premolars, except the P4, the premaxillary bones, parts of the nasal bones and of the left zygomatic arch, the tips of the paroccipital processes, and the posterior part of its skull roof is damaged (Figs. 6–8). Beside this damage to the skull, the specimen has not undergone any kind of deformation and is symmetrically preserved. Due to missing premaxillary bones, we cannot directly assess the potential existence of upper incisors; however, the i2 in the mandible is only moderately worn, despite the advanced age of the individual, which might suggest that there was no upper incisor that would have worn it down. Also, the wear facet in the preserved i2 covers the whole tooth and is most similar to *Chilotherium*, which lacks upper incisors. Therefore, it is very likely that *E. samium* also lacked upper incisors.

In lateral view (Fig. 7), the dorsal profile of the skull seems flat; however, this is in part due to the damaged posterior part of the skull roof. Otherwise, the dorsal profile of the skull is slightly concave. The anterior part of the nasal bones is missing; therefore, its exact shape and orientation are not known. The nasal notch has an almost trapezoidal shape and terminates at the level above the anterior part of the M1. On the maxillary, laterally to the nasal notch two rather prominent infraorbital foramina are present. A facial crest is partially present on both sides. The orbit is located high in the skull, with its anterior margin being above the distal portion of the M2. A lacrimal tubercle is visible, but the number of lacrimal foramina cannot be assessed. The postorbital process on the frontal is present, but damaged. Another process is also present on the zygomatic arch, roughly at the same level as the one on the frontal. The preserved right zygomatic arch exhibits a strong depression behind the postorbital process. The postglenoid and posttympanic processes are close to each other but remain at least 5 mm apart and do not contact each other. They are both similarly long and extent slightly below the lower limit of the occipital condyle. The paroccipital process is much more ventrally extending than the posttympanic one.

In dorsal view (Fig. 6A), the preserved portion of the nasal bones is rather narrow. The internal nasal suture is not visible and there does not seem to have been a very prominent longitudinal groove present, though on their ventral side a weak longitudinal bulge is present. The frontals do not show the typical depression seen in most *Chilotherium* species but are in fact slightly convex. The posterior part of the frontals becomes flat but not concave at any point. The parietals are concave due to the elevation of the parietal crests. These end in the nuchal crest, which is not preserved in SMF M 3601, and despite being damaged the minimal distance between the parietal crests can be estimated to about 40 mm.

In ventral view (Fig. 6B), the anterior end of the choana is slightly pointed and reaches the mesial part of the M3. On the palatine bone two foramina are present at the level of the M2 on the right side. The other side is slightly compressed, and the foramina cannot be seen. The tips of the pterygoid processes are broken but seem simple. The intercondylar notch is U-shaped, and the condyles are widely separated.

In posterior view, the upper portion of the skull forming the nuchal crest is broken, but the general shape seems to be somewhat trapezoidal. The nuchal tubercle is only weakly developed, from which marked lateral occipital crests start and might have reached the nuchal crest. Laterally to them, prominent outer lateral crests exist.

**Upper Dentition**—The upper dentition is almost completely preserved, only lacking the right D1, P2, and P3. However, the teeth are very worn due to the old age of the individual. Most teeth preserve a thin cement layer on their enamel. The D1 is retained into adulthood and despite the old age of the individual is only moderately worn. It exhibits a lingually projecting parastyle, a very small protocone in contrast to the more prominent hypocone, a closed postfossette and a lingual cingulum. The P2 is almost completely worn and not much of its enamel is preserved, but a closed prefossette is visible and a weak cingulum seems to be present. It can be observed that neither the protocone nor the hypocone exhibit a constriction and that the median valley remains open until the tooth is completely worn off. The P3 does not retain any enamel and its morphology cannot be evaluated. The P4 is similarly well preserved on both sides, the only difference being that the right one preserves the enamel that represents the closed prefossette, whereas on the left side this is already worn off. On both sides, the constriction of the protocone is visible and a portion of the antecrochet which connected with the hypocone and resulted in a closed median valley. Moreover, a prominent enamel pillar is situated at the entrance of the median valley.

The M1 is also extremely worn and only the right one preserves some remains of enamel that confirm the presence of a closed postfossette. Also, both the protocone and the hypocone are constricted and a lingually projecting antecrochet is present, closing off the median valley. The M2 is less worn than the previous teeth, but is nonetheless very worn, with less than 1 cm high enamel remaining on its ectoloph. The closed postfossette is well-visible, the protocone is constricted both mesially and distally, with the presence of a lingually projecting antecrochet, while the hypocone is only mesially constricted. Despite the advanced wear stage and the prominent antecrochet, the median valley remains open in both M2s. The M3 is the least worn tooth in this specimen. It bears mesial and distal constrictions only in the protocone, which form a lingually projecting antecrochet. Additionally, a small crochet is present and distally a cingulum is present.

**Mandible**—The mandible is very well preserved, including almost the complete dentition (Fig. 9). The symphysis is very wide with a diastema of 58 mm between the incisors. On the ventral side the symphysis is slightly concave and bears two foramina that are also visible in anterior view. Other foramina are not visible due to the presence of sediment and plaster that cover part of the ventral surface. The anterior end of the symphysis forms a thin edge between the two incisors. In dorsal view, the symphysis ends posteriorly at the middle of the p3s and is 119 mm long. Between the i2 and the p2 there is a long diastema of 65 mm, which is marked by a well-developed dorsal ridge between these two teeth. The dorsal surface of the


FIGURE 6. Neotype skull of *Eochilotherium samium* (Weber, 1905) (SMF M 3601) from the Upper Miocene of Samos Island in dorsal (**A**) and ventral view (**B**). Scale bar equals 10 cm.

symphysis, between these ridges is concave. In lateral view, only one mental foramen is visible on right horizontal ramus below the p3. On the left side this foramen is covered by some plaster. The height of the mandibular body remains almost the same throughout its length. The vertical rami are almost completely preserved, only the right one lacking the tip of the coronoid process. They almost form a 90° angle to the horizontal rami. The preserved left coronoid process is 63 mm high and the condylar process for the articulation to the skull is 68 mm wide. The condylar process becomes medially much thinner. Lastly, the mandibular angle bears a strong masseteric tuberosity.

**Lower Dentition**—The lower dentition only lacks the left i2, p4, and parts of the p2. It is better preserved than the upper dentition and is slightly less worn. The right i2 is only moderately worn despite the high age of the individual. Its crown has a


FIGURE 7. Neotype skull of *Eochilotherium samium* (Weber, 1905) (SMF M 3601) from the Upper Miocene of Samos Island in left lateral (**A**) and right lateral view (**B**). Scale bar equals 10 cm.

triangular shape with a length of about 52 mm and a width of 30 mm. The labial side of the tooth preserves the complete enamel, whereas on the lingual side only a small surface of enamel is preserved, which nonetheless shows that the tooth was completely covered by enamel, both labially and lingually. The cross section of the root is oval.

Some of the cheek teeth preserve remnants of their cement. The premolar/molar length ratio (sensu Athanassiou et al., 2014) is 66.9%. Most cheek teeth are heavily worn, and their morphology cannot be accurately assessed, only the m3 is moderately worn, allowing a more detailed description of its morphology. The p2 has a mesially projecting paralophid and features a shallow anterior valley and a weak anterior groove on the ectolophid. None of the cheek teeth bear lingual or buccal cingulids. In most teeth neither mesial nor distal cingulids can be observed, due to the advanced wear stage, but in the m3 a distal cingulid is well visible and a slight extension of the mesial cingulid towards the lingual side can be traced.

## COMPARISON

Both species described above, *C. schlosseri* and *E. samium*, come from the Upper Miocene of Samos, though the stratigraphic context is unknown, and they probably were not found in the same fossiliferous horizons (Weber, 1905). The taxonomy of the latter one has been very controversial, to the extent where it has been suggested that usage of the species name *E. samium* should be restricted only to its type material (Fortelius et al., 2003). Therefore, the first part of the comparison is dedicated to the comparison of the herein designated neotypes of the two Samian species to the lectotypes. This proves the attribution of GPIH 3015 to *C. schlosseri* and SMF M 3601 to *E. samium*. Next, the two Samian species, *C. schlosseri* and *E. samium*, will be compared with each other, pointing out the morphological features distinguishing the two taxa. This confirms the existence of two distinct chilothere species in the Upper Miocene deposits on Samos Island, as shown by the prominent morphological


FIGURE 8. Neotype upper dentition of *Eochilotherium samium* (Weber, 1905) (SMF M 3601) from the Upper Miocene of Samos Island. Left (**A**) and right upper toothrows (**B**). Scale bar equals 5 cm.

differences, though no evidence exists that the two species occurred in the same stratigraphic layer. Afterwards, each of them will be carefully compared with other relevant chilothere species across Eurasia, to verify them as valid species and investigate their potential relationships.

### Comparison to the Lectotypes of *Aceratherium schlosseri* Weber, 1905 and *Aceratherium samium* Weber, 1905

The comparison of the two specimens selected as neotypes for *C. schlosseri* (GPIH 3015) and *E. samium* (SMF M 3601) to the descriptions and illustrations provided by Weber (1905) for the original type material of *Aceratherium schlosseri* and *Aceratherium samium* is crucial for their proper establishment as neotypes. The lectotype of *Aceratherium schlosseri* (Weber, 1905:pl. 8, figs. 1–3) is an almost complete skull with an associated mandible, the teeth of which were in an advanced wear stage (Giaourtsakis, 2022). Weber (1905) mentioned another rather complete skull with its mandible and several maxillary and mandibular elements with teeth that he assigned to this species. The lectotype of *Aceratherium samium* (Weber, 1905:pl. 10, figs. 1, 2) is a skull with its mandible, which is posteriorly damaged (Athanassiou et al., 2014; Geraads & Koufos, 1990). Weber (1905) assigned another partially preserved skull that lacked almost all teeth with its mandible and a maxillary element of a juvenile individual to this species. All this material is now considered lost.

There are several characters that allow the association of the neotypes to their respective species. In general, the skulls of *Aceratherium samium* and SMF M 3601 are more dolichocephalic and smaller than the ones of *Aceratherium schlosseri* and GPIH 3015 (Figs. 10, 11). Weber (1905) mentioned that the most prominent feature in the two skulls of *Aceratherium schlosseri* is the depression in the frontal bones. For *Aceratherium samium*, Giaourtsakis (2022) mistakenly translated the description of Weber (1905) of the frontal region as "slightly depressed," whereas Weber (1905:p. 354) wrote "etwas gewölbte Stirnregion," which should be translated as "slightly convex frontal region," thus meaning the opposite. A frontal depression is clearly present in GPIH 3015 as in *Aceratherium schlosseri*, whereas in SMF M 3601 the frontal region is convex as in *Aceratherium samium* (Fig. 10). Weber (1905) also mentioned that in *Aceratherium schlosseri* the nasal bones are separated by an anteroposterior longitudinal groove, which is well visible on its lectotype (Weber, 1905:pl. 8, fig. 2). He also mentioned that a longitudinal bulge is present on the ventral side of the nasal bones. Both the groove on the dorsal side and the bulge on the ventral side of the nasal bones are present in GPIH 3015, with the groove stretching posteriorly until the nasofrontal suture (Fig. 10A). In *Aceratherium samium*, this groove is only weakly visible, more similar to SMF M 3601, where the groove is not visible due to some damage in that region. If it was present, when SMF M 3601 was complete, it must have been rather weak and definitely did not extent as posteriorly as in *C. schlosseri* (Fig. 10B). Moreover, Weber (1905) mentioned that the nasal bones of *Aceratherium schlosseri* slightly slope upwards, as is the case in GPIH 3015, in contrast to *Aceratherium samium* where they are completely straight, which also seems to be the case in SMF M 3601 (Fig. 11). He also mentioned that the

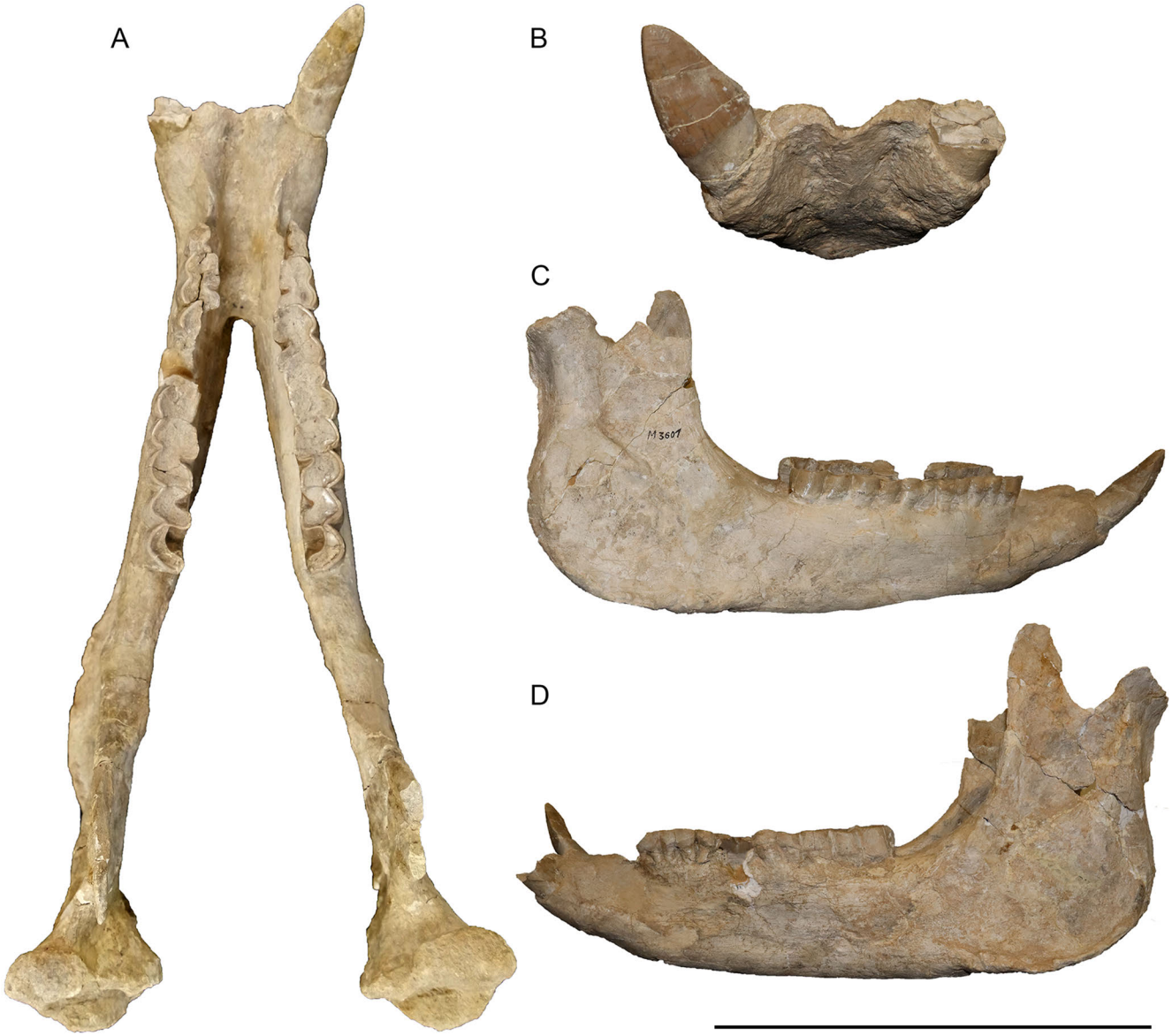


FIGURE 9. Neotype mandible of *Eochilotherium samium* (Weber, 1905) (SMF M 3601) from the Upper Miocene of Samos Island in dorsal **A**, anterior, **B**, right lateral, **C**, and left lateral view, **D**. Scale bar equals 20 cm in **A**, 15 cm in **B**, and 30 cm in **C** and **D**.

orbit is placed very highly in the skull of *Aceratherium schlosseri*, as in GPIH 3015, whereas in the figure of the skull of *Aceratherium samium* it is visible that is not the case (Weber, 1905:table 10, fig. 1). In SMF M 3601 the orbit also seems to be placed somewhat lower. Another feature that Weber (1905) pointed out in *Aceratherium schlosseri* is the big minimal distance between the parietal crests, which is 90 mm in the lectotype. This was also discussed by Kampouridis et al. (2022b) who considered a minimal distance between the parietal crests of over 70 mm as a diagnostic feature of *C. schlosseri* that is not seen in other chilotheres (Table 2). In GPIH 3015 this distance is 89 mm, thus very close to the lectotype of *Aceratherium schlosseri*. In the lectotype of *Aceratherium samium* this portion is heavily damaged, but the right parietal crest is adequately preserved to assess that the minimal distance would be close to 40 mm, as also pointed out by Andree (1921). In SMF M 3601, this portion is also damaged, but the minimal distance between the parietal crests can be estimated to about 40 mm (Fig. 10B), thereby being the same as in *Aceratherium samium*. In general, the parietal region in the lectotype of *Aceratherium schlosseri* and in GPIH 3015 is much wider than in SMF M 3601 (Fig. 10). Additionally, in *Aceratherium schlosseri* the skull roof is very flat and posteriorly slopes up only very slightly as in GPIH 3015 (Fig. 11A). In *Aceratherium samium* and SMF M 3601 the posterior part of the skull roof is damaged but based on the preserved parts it can be assumed that in both skulls it would slope up more abruptly. The zygomatic arches in *Aceratherium schlosseri* are posteriorly widening, as in GPIH 3015, whereas in *Aceratherium samium* and SMF M 3601 they are positioned closer to the skull and do not become wider posteriorly (Fig. 10).

Moreover, in posterior view there are several features distinguishing GPIH 3015 and SMF M 3601 (compare in Fig. 12).

TABLE 2. Comparison of the minimal distance between the parietal crests (in mm) of Chilotheriina (modified after Kampouridis et al., 2022b).

| Taxon | Min | Max | n | Literature |
|---|---|---|---|---|
| *Chilotherium schlosseri* (Weber, 1905) | 70 | 90 | 7 | Andree, 1921, own data |
| *Eochilotherium samium* (Weber, 1905) | ~40 | | 2 | Andree, 1921; own data |
| *Chilotherium persiae* (Pohlig, 1886) | 36.5 | 53.7 | 11 | own data |
| *Chilotherium habereri* (Schlosser, 1903) | 42 | 60 | 9 | Killgus, 1922, Ringström, 1924 |
| *Chilotherium kowalevskii* (Pavlow, 1913) | 40.1 | 66 | 10 | Krokos, 1917 |
| *Chilotherium anderssoni* Ringström, 1924 | 50 | 63 | 5 | Ringström, 1924 |
| '*Chilotherium*' *wimani* Ringström, 1924 | 28 | 64 | 10 | Deng, 2006b |
| *Chilotherium sarmaticum* Korotkevich, 1958 | 51 | 76.2 | 4 | Korotkevich, 1970 |
| *Chilotherium orlovi* Bayshashov, 1982 | 45 | 75 | 3 | Bayshashov, 1982 |
| '*Chilotherium*' *primigenium* Deng, 2006b | 18 | - | 1 | Deng, 2006b |

The illustration of the lectotype of *Aceratherium schlosseri* in posterior view (Weber, 1905:pl. 8, fig. 3), however, is very simplistic and many of these features are not visible and the posterior portion of the lectotype of *Aceratherium samium* was severely damaged and was never illustrated by Weber (1905). The only features comparable between *Aceratherium schlosseri* and GPIH 3015 are the generally wide skull in posterior view with very wide occipital condyles, which are much higher and longer in SMF M 3601 (Fig. 12) and the fact that the lateral occipital crests are relatively weak and widely spaced in comparison to the more prominent and closer situated occipital crests in SMF M 3601.

Weber (1905) described the mandibles of both species in the same manner without pointing out any differentiating features that might be diagnostic. Giaourtsakis (2022:438) mentioned that the mandible of the lectotype of *Aceratherium samium* does not feature a masseteric tuberosity, which is mentioned for the mandible of the male individual described by Weber (1905:356). This could be explained through some damage to that region that is not clearly depicted in the figure or by a potential simplification of the morphology in the drawing of the lectotype of *Aceratherium samium*; a strong masseteric tuberosity is definitely present in the mandible of SMF M 3601, which belongs to a female individual just like the lectotype of *Aceratherium samium*. In the mandibles of *Aceratherium schlosseri* and GPIH 3015 this tuberosity is clearly visible. In SMF M 3601 the symphysis is rather narrow when compared with *Aceratherium schlosseri* and GPIH 3015. The preserved lower incisor of SMF M 3601 has also a more triangular shape than GPIH 3015. The shape and size of this tooth is heavily affected by sexual dimorphism in chilotheres (Chen et al., 2010), but the narrow triangular shape and rather small size in SMF M 3601 is a more plesiomorphic feature, not seen in material that is assignable to *C. schlosseri*.

Considering differentiating features in the upper cheek teeth of these two species is more difficult, especially for *E. samium*, because both the lectotype of *Aceratherium samium* and SMF M 3601 belonged to ontogenetically very old individuals and their dentition is very worn, more so in SMF M 3601. Nonetheless, there are some features that can be used to attribute specimens GPIH 3015 and SMF M 3601 to *C. schlosseri* and *E. samium* (see Fig. 13). As also pointed out by previous studies (e.g., Geraads & Koufos, 1990; Giaourtsakis, 2022) the enamel folds in *E. samium* are not as complex as in *C. schlosseri*. This is easily visible when the toothrows of the two lectotypes are compared (Weber, 1905:table 9, fig. 1, 5). The lectotype of *Aceratherium schlosseri* features an extremely strong protocone constriction, with a very strong antecrochet that closes off the median valley, which is not the case in the lectotype of *Aceratherium samium*. In GPIH 3015 the protocone is also much more strongly constricted than in SMF M 3601 and the resulting antecrochet would close off the median valley in all teeth, whereas in SMF M 3601 it remains open in the P2 and M2 despite the advanced wear stage. Another important feature seen in both the lectotype of *Aceratherium schlosseri* and GPIH 3015 is the strong crochet that results in a closed medifossette in most teeth, whereas in the lectotype of *Aceratherium samium* and SMF M 3601 the crochet is not as prominent, and most teeth do not feature a closed medifossette. Thereby, GPIH 3015 can safely be attributed to *C. schlosseri* and SMF M 3601 respectively to *E. samium*.

### Comparison Between *Chilotherium schlosseri* and *Eochilotherium samium*

The two Samian species exhibit many important features that distinguish them from each other that not only allow their specific separation but would also justify their placement in different genera. The general shape of the two skulls is very different, with the skull of *C. schlosseri* being generally larger, but relatively shorter and wider (Fig. 10). The skull of *E. samium* is much more dolichocephalic and narrower, as seen in the narrow palate and the narrow parietal region. The most striking evidence that they represent distinct taxa is the marked depression in the frontal bones that also lowers the position of the nasals in *C. schlosseri*, whereas in *E. samium* the frontal bones are slightly convex anteriorly and become flat posteriorly. On the nasals, in *C. schlosseri* a deep longitudinal groove is found that reaches the nasofrontal suture, whereas in *E. samium* this groove is either absent or does not extend as far posteriorly. The parietal crests are much wider apart in *C. schlosseri* (always >70 mm in adult individuals, n=7) than in *E. samium* (~40 mm) and the zygomatic arches become wider in the posterior part in *C. schlosseri*, whereas in *E. samium* they are generally closer to the skull and do not show an important degree of widening. In lateral view, despite the damage to the posterior portion of the lectotype and the neotype skulls of *E. samium*, the posterior skull portion would have been much more raised than in *C. schlosseri*, where the skull is almost flat (Fig. 11). It is also visible that in *C. schlosseri* the dorsal border of the orbit is positioned higher than the nasals, whereas in *E. samium* it is situated at a lower position. In posterior view, several striking differences are visible, despite some damage to the neotypes of both species (Fig. 12). The skull of *C. schlosseri* is generally much wider than *E. samium*. This is also the case for the occipital condyles, which are very wide and rounded in *C. schlosseri*, whereas in *E. samium* they are in relation much higher, transversally narrower, but anteroposteriorly longer and more angular. The lateral occipital crests are also broader and more rounded in *C. schlosseri*, compared with *E. samium*, where they are closer to each other and are more pronounced. The occipital fossa is also deeper in *C. schlosseri*. The outer lateral crests are much more prominent and longer in *E. samium*, connecting to the lateral crests, in contrast to *C. schlosseri*, where they are more subtle and rounded. In *C. schlosseri*, the foramen magnum features an incision at its dorsal border, which does not exist in *E. samium*.

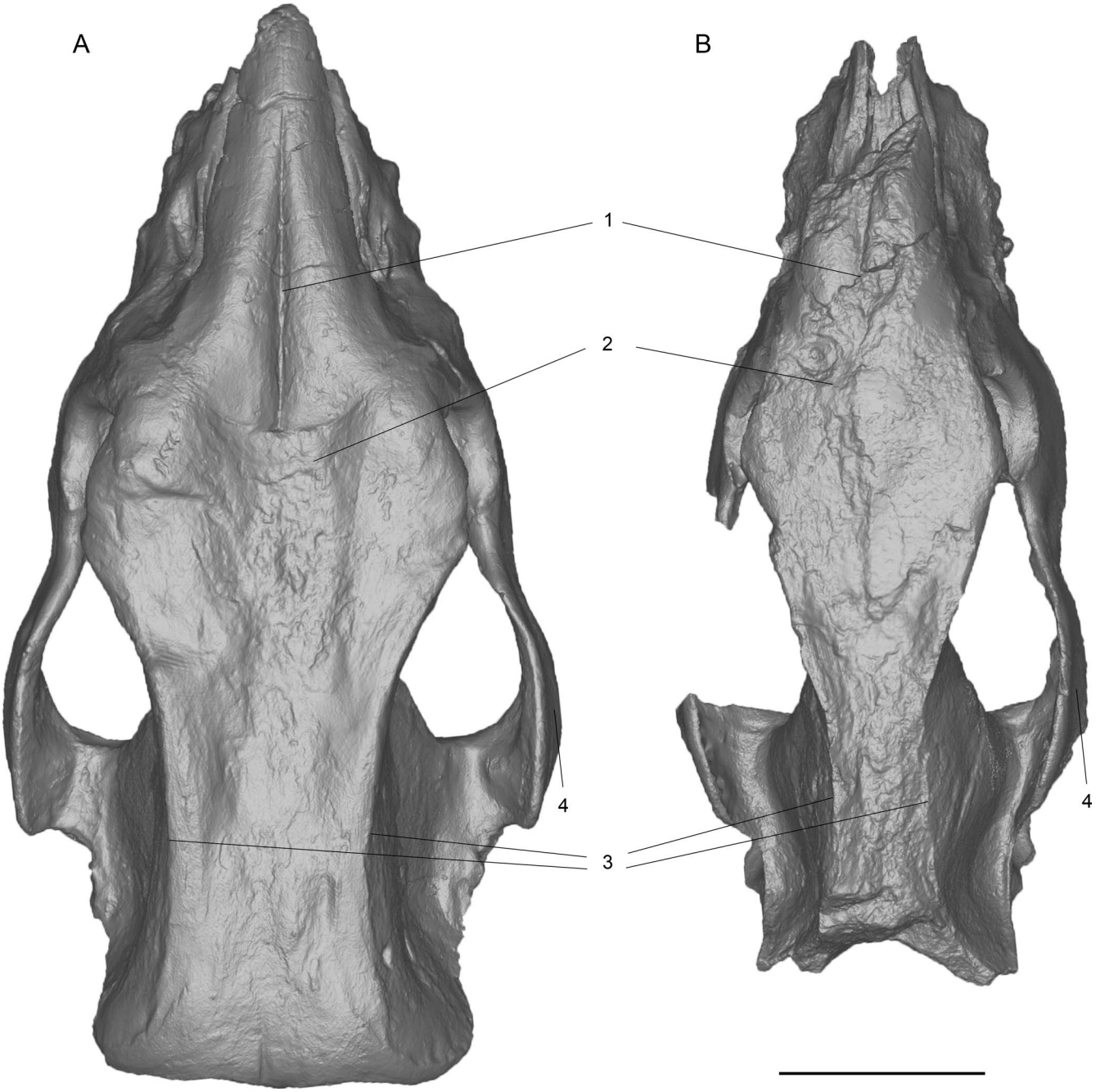


FIGURE 10. Comparison of 3D surface models of the neotype skulls of *Chilotherium schlosseri* (Weber, 1905) (GPIH 3015) (**A**) and *Eochilotherium samium* (Weber, 1905) (SMF M 3601) (**B**) from the Upper Miocene of Samos Island (Greece) in dorsal view. **Abbreviations—1**, longitudinal groove on nasal bones: present in *C. schlosseri* (**A**) and weak or absent in *E. samium* (**B**); **2**, shape of frontal bones: strongly depressed in *C. schlosseri* (**A**) and slightly convex in *E. samium* (**B**); **3**, distance between parietal crests: very widely separated (>70mm) in *C. schlosseri* (**A**) and moderately separated in *E. samium* (**B**); and **4**, shape of zygomatic archs: posteriorly widening in *C. schlosseri* (**A**) and constant width in E. *samium* (**B**). Scale bar equals 10 cm.

The upper teeth of both the neotype and the lectotype of *E. samium* are very worn, due to the high ages of the individuals; nonetheless, some differentiating characters for the two chilothere species are still visible (Fig. 13). The P2 in *E. samium* has an unconstricted protocone and in the P4 the protocone is only moderately constricted, in contrast to the strongly constricted protocone in all three permanent premolars in *C. schlosseri*. Additionally, in the P2 the protocone and the hypocone remain separated and in the P4 they barely touch in *E. samium*, despite their advanced wear stage. In *C. schlosseri*, the protocone and the hypocone are connected in all premolars. Similarly, in the M2 of *E. samium* the median valley remains open and would only close when the tooth is almost completely worn down, whereas in the M1 of *C. schlosseri* they are already connected, and in the M2 they would connect at an earlier wear stage than in *E. samium*. Both the M2 and the M3 of *E. samium* feature small crochets that do not close off the medifossette, whereas in the M1 of *C. schlosseri* the medifossette is

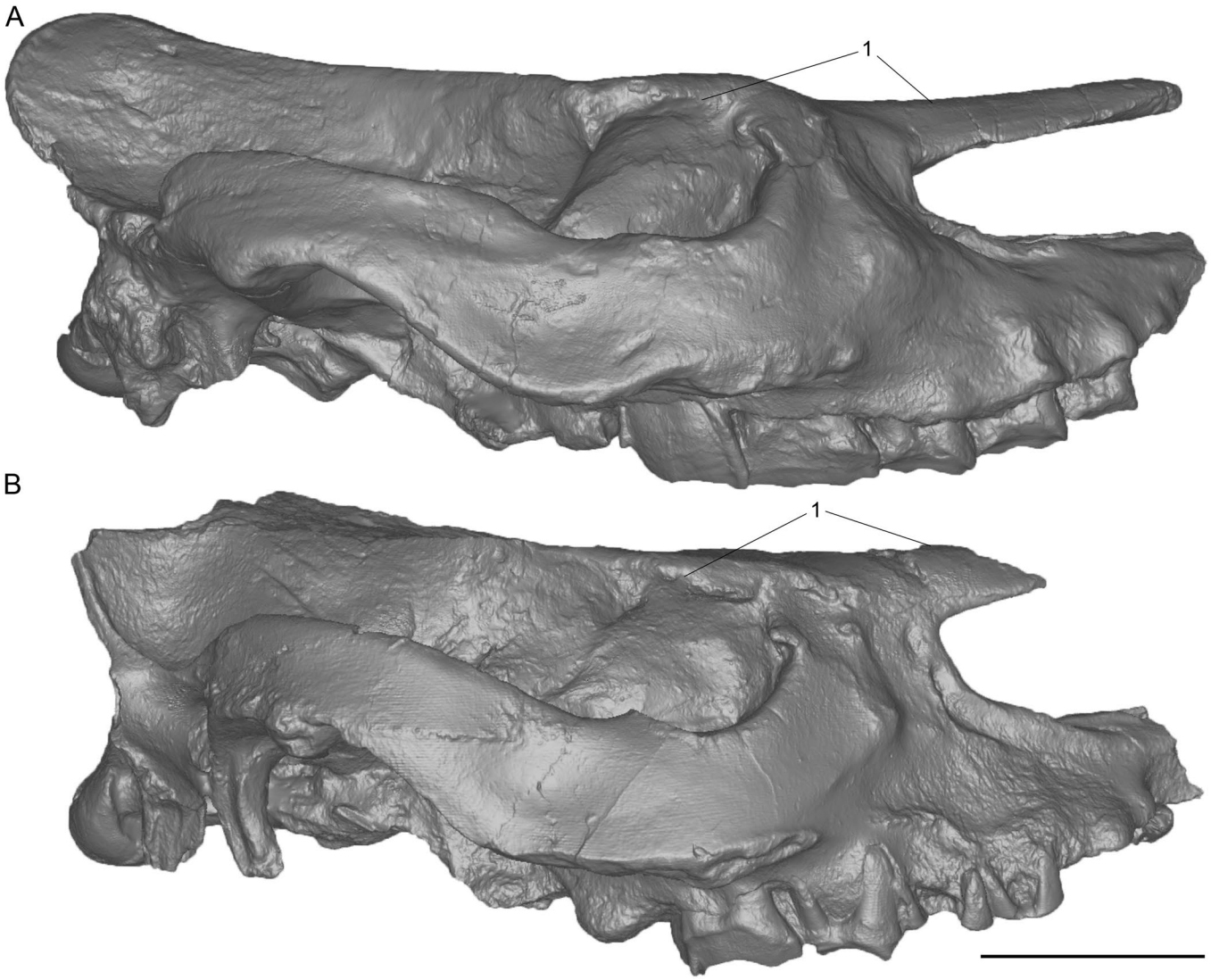


FIGURE 11. Comparison of 3D surface models of neotype skulls of *Chilotherium schlosseri* (Weber, 1905) (GPIH 3015) (**A**) and *Eochilotherium samium* (Weber, 1905) (SMF M 3601) (**B**) from the Upper Miocene of Samos Island (Greece) in right lateral view. **Abbreviations—1**, relative position of nasal bones to dorsal wall of the orbit: at the same level in *C. schlosseri* (**A**) and lower position of orbit in *E. samium* (**B**). Scale bar equals 10 cm.

closed off, in the M2 the crochet is relatively small due to the early wear stage and in M3 the crochet is already large and would close off the medifossette at a slightly more advanced wear stage. In general, the molars of *C. schlosseri* feature much stronger constricted protocones than in *E. samium*. Interestingly, in both species the protocone constriction leads to strong antecrochets that are lingually oriented, a feature common among chilotheres, but somewhat more pronounced in *C. schlosseri*. Lastly, *C. schlosseri* differs from *E. samium* in sporadically exhibiting enamel plications, which seems to be absent in *E. samium*.

The mandibles of the two species also seem to offer some clues for their separation. However, they must be taken with much caution, as the lectotype and the neotype of *E. samium* seem to have belonged to female individuals, whereas the neotype of *C. schlosseri* belonged to a male individual. This is mainly based on the wider symphysis in *C. schlosseri* with larger incisors. The width of the incisors at their base is 45 mm in *C. schlosseri* and 30 mm in *E. samium*. The most prominent differences are found in the anterior part of the mandible. The symphysis is very wide in both species, reaching posteriorly the p3 in both species and is similarly long, with a diastema between the i2 and the p2 of 60 mm in *C. schlosseri* and 65 mm in *E. samium*. Despite the similar length, the symphysis is much wider in *C. schlosseri*, with the incisors being 82.3 mm apart, whereas in *E. samium* they are only 58 mm apart. This makes the symphyseal area of *E. samium* look much more elongated than *C. schlosseri*.

All these characters prove that *C. schlosseri* and *E. samium* show significant differences to each other. This not only confirms that they represent distinct species but also justifies a separation at the generic level with *C. schlosseri* being a member of the genus of *Chilotherium* that was erected by Ringström (1924) and *E. samium* belonging to *Eochilotherium* that was initially erected by Geraads and Spassov (2009) as a subgenus of *Chilotherium* and is herein raised to the genus level. Moreover, a clear separation of the two taxa is possible based on consistent morphological features that do not seem to vary importantly in the more ample material of *C. schlosseri* crania from Samos (Greece). The diagnostic traits of the two species do not overlap at all, making a subjective synonymy practically impossible.

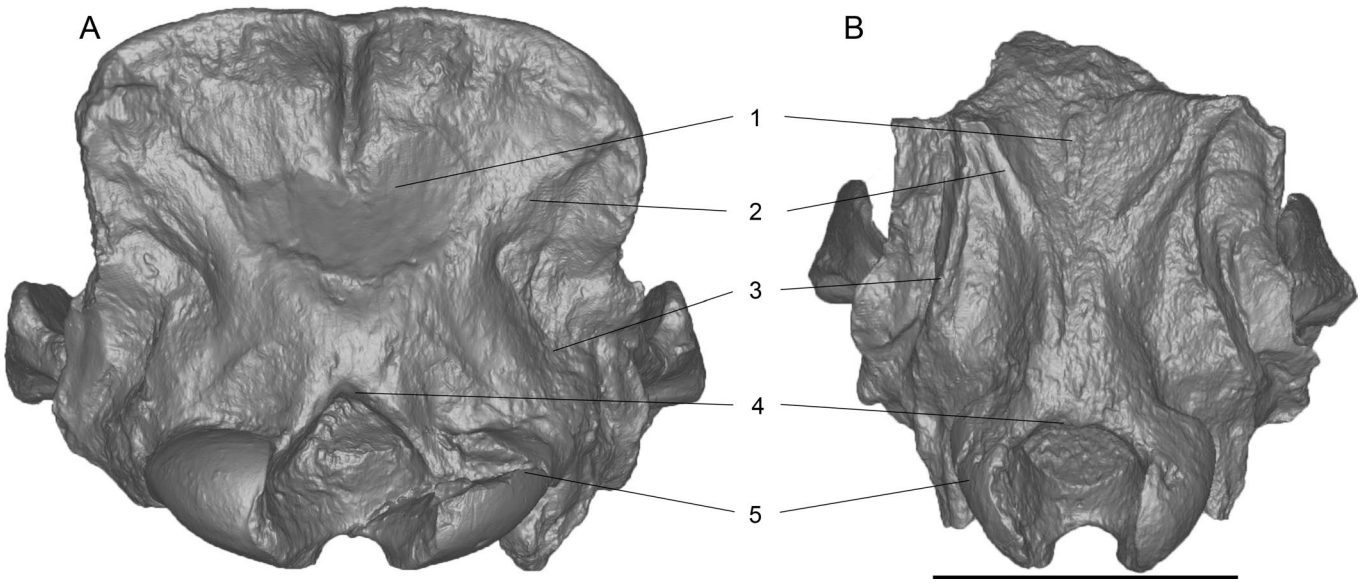


FIGURE 12. Comparison of of 3D surface models of neotype skulls of *Chilotherium schlosseri* (Weber, 1905) (GPIH 3015) (**A**) and *Eochilotherium samium* (Weber, 1905) (SMF M 3601) (**B**) from the Upper Miocene of Samos Island (Greece) in posterior view. **Abbreviations—1**, occipital fossa: deep in *C. schlosseri* (**A**) and shallow in *E. samium* (**B**); 2, lateral occipital crests: broad and not marked in *C. schlosseri* (**A**) and narrow but more pronounced in *E. samium* (**B**); 3, outer lateral occipital crests: subtle and rounded in *C. schlosseri* (**A**) and more prominent and longer in *E. samium* (**B**); 4, dorsal shape of the foramen magnum: dorsal incision in *C. schlosseri* (**A**) and rounded dorsal border in *E. samium* (**B**); and 5, shape of occipital condyles: wide in *C. schlosseri* (**A**) and narrow and high in *E. samium* (**B**). Scale bar equals 10 cm.

### Comparison of *Chilotherium schlosseri* to Other Species of *Chilotherium*

The species *C. schlosseri* belongs in the Chilotheriina based on the wide mandibular symphysis, the hypsodont teeth and their complex enamel folds, including the strong constrictions of the protocone and hypocone and the very long antecrochet that bends lingually. However, it differs from the genera *Eochilotherium*, as mentioned above, and *Shansirhinus* (Kretzoi, 1942). Deng (2005) described an almost complete adult skull of the species *Shansirhinus ringstroemi* (Kretzoi, 1942). It does not exhibit the prominent depression in the frontal bones seen in *C. schlosseri*, and has thicker nasal bones, closer situated parietal crests (~40 mm), a narrower mandibular symphysis, with smaller and more triangular lower incisors (Deng, 2005). However, both species exhibit similarly developed secondary enamel folds, such as a crochet that often closes the medifossette, strong protocone constrictions, the connection between protocone and hypocone in the premolars, and the variable presence of enamel plications in the upper teeth. Though, *S. ringstroemi* exhibits a much more prominent paracone fold and the hypocone is additionally distally constricted, as seen in the M1 (Deng, 2005:fig. 6), in contrast to *C. schlosseri*. Based on features in its cranial morphology like the very widely separated parietal crests, the prominent frontal depression, the flat dorsal profile of the skull, along with its rather complex tooth morphology *C. schlosseri* can be attributed to the genus *Chilotherium*. The comparison of *C. schlosseri* will involve the following members of *Chilotherium* sensu stricto *Chilotherium persiae* from Maragheh in Iran (Pandolfi, 2016; Pohlig, 1886), *Chilotherium habereri* from various localities in China (Killgus, 1922, 1923; Ringström, 1924; Schlosser, 1903), *Chilotherium kowalevskii* from Grebeniki in Ukraine (Korotkevich, 1970; Pavlow, 1913), *Chilotherium anderssoni* from Loc. 30 in China (Ringström, 1924), *Chilotherium sarmaticum* from Berislav in Ukraine (Korotkevich, 1958, 1970), and *Chilotherium orlovi* from Palvodar in Kazakhstan (Bayshashov, 1982, 1993). These species have a very similar cranial and dental morphology. They share all typical features known for the genus *Chilotherium*, such as the depression in the frontal bones, the separated parietal crests, the highly placed orbit, the hypsodont teeth with very complicated enamel folds and the wide mandibular symphysis with large tusk-like incisors that are dorsolaterally upturned, with large wear facets and have an obtuse triangular shape in cross section (Geraads & Spassov, 2009; Ringström, 1924). Additionally, another feature that seems to be similar in these species is the shape of the zygomatic arches, which are relatively robust and tend to become wider posteriorly. In *C. schlosseri*, some of these features are, however, more developed than in the other species of *Chilotherium*. For instance, the frontal depression in *C. schlosseri* is very strong and also involves the nasal bones, which as a result are placed more ventrally in comparison to the orbit (Fig. 3A). Thereby, even in lateral view the 'nasofrontal' depression is easily distinguishable, due to the placement of the nasal bones (Fig. 11A; Weber, 1905:pl. 8, fig. 1), a feature that is more rarely observed in other *Chilotherium* species. Another important trait is that *C. schlosseri* exhibits parietal crests that are always separated from each other by at least 70 mm (n = 7). This represents an autapomorphic feature of this species, not seen in any other *Chilotherium*. The only other *Chilotherium* species where the minimal distance between the parietal crests may reach over 70 mm, but not consistently, seem to be *C. sarmaticum* and *C. orlovi*, varying from 51–76 mm (n = 4; Korotkevich, 1970) and from 45–75 mm (n = 3; Bayshashov, 1982), respectively (Table 2). These two species have been given only little attention since their first description and are not considered in most recent studies about *Chilotherium*. In almost all other species the parietal crests are always less than 70 mm apart (Table 1; Kampouridis et al., 2022b:table 2).

The comparison of the upper teeth of *Chilotherium* spp. is somewhat more complicated, because an important degree of intraspecific variability exists and has to be taken into

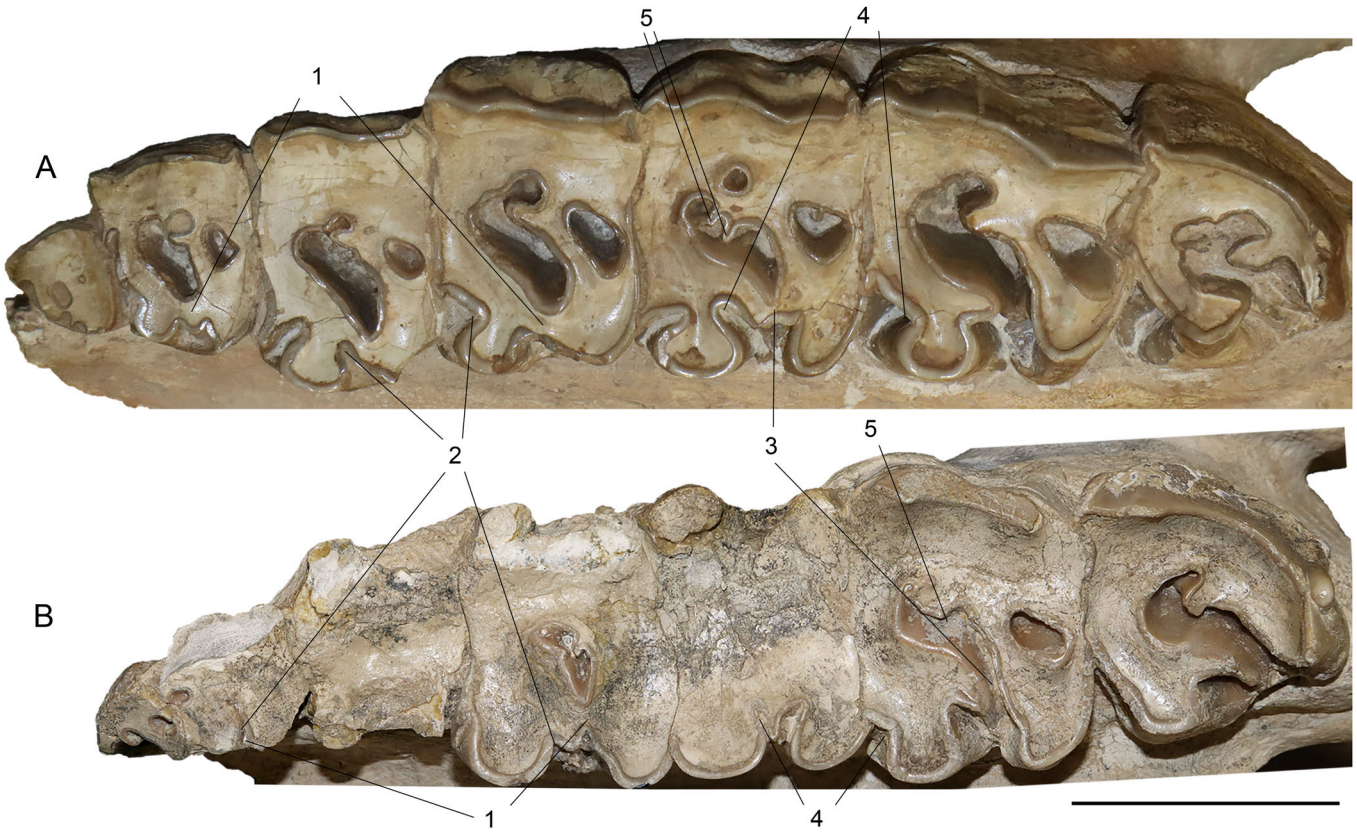


FIGURE 13. Comparison of the left upper tooth row of the neotypes of *Chilotherium schlosseri* (Weber, 1905) (GPIH 3015) (**A**) and *Eochilotherium samium* (Weber, 1905) (SMF M 3601) (**B**) from the Upper Miocene of Samos Island (Greece) in occlusal view. **Abbreviations—1**, closure of the median valley in the premolars: at an early wear stage in *C. schlosseri* (**A**) and at a late wear stage or not at all in *E. samium* (**B**); **2**, protocone constriction in the premolars: very strong in *C. schlosseri* (**A**) and weak or absent in *E. samium* (**B**); **3**, closure of the median valley in the molars: at a moderate wear stage in *C. schlosseri* (**A**) and at a late wear stage in *E. samium* (**B**); **4**, proto- and hypocone constriction in molars: very strong in *C. schlosseri* (**A**) and moderate in *E. samium* (**B**); and **5**, enamel plications: present *C. schlosseri* (**A**) and absent in *E. samium* (**B**). Scale bar equals 5 cm.

account. The dentition of *C. schlosseri* (Fig. 4) exhibits relatively hypsodont teeth, with very complicated secondary enamel folds. Most prominently, the crochet is usually very strong and the protocone is always very strongly constricted, leading to a prominent antecrochet that usually closes off the median valley. Specifically in the molars, the protocone constriction is very strong and it has a flat lingual side. This leads the protocone to have a subtriangular shape. These features are usually also observed in *C. persiae*, *C. habereri*, *C. kowalevskii*, *C. anderssoni*, *C. sarmaticum*, and *C. orlovi*. A lingual cingulum, which seems to be almost continuous, is always present in the premolars of *C. schlosseri* but may also be present in these species. In *C. schlosseri*, a crista can also be present both in the premolars and the molars. This enamel fold is usually lacking in most *Chilotherium* species, like in *C. habereri* and *C. anderssoni*, where it is only occasionally present, and *C. kowalevskii*, where it seems to be lacking completely. In *C. schlosseri*, the crochet very frequently leads to the closure of the medifossette, in which the crista is often involved, whereas in most other species, this is not as common. Although, in the holotype of *C. orlovi* figured by Bayshashov (1993), a closed medifossette exists in most premolars and in the M1. Another dental feature that seems to separate *C. schlosseri* from most other *Chilotherium* species is the fact that it frequently exhibits small enamel plications in the upper cheek teeth, as seen in the right M1 in GPIH 3015 (Fig. 4). These plications are not constantly present, and their appearance may vary intra-specifically and depending on the wear stage of the teeth. Nonetheless, the upper teeth of the well-sampled species *C. persiae* almost never exhibit such plications. Similarly, in the figured toothrows assigned to *C. kowalevskii* by Pavlow (1913), to *C. anderssoni* by Ringström (1924), and to *C. sarmaticum* by Korotkevitch (1970), also no plications are visible in the permanent dentition and the authors also do not mention any such features.

The mandible bears maybe the most prominent feature of the group: the wide mandibular symphysis with widely separated large incisors (Ringström, 1924). The width of the symphysis and the size and shape of the incisors is characterized by notable sexual dimorphism, with males having wider symphyses and large tusks, whereas females have somewhat narrower symphyses and notably smaller incisors (e.g., Chen et al., 2010; Weber, 1905). The neotype of *C. schlosseri* does not preserve the complete crown of the lower incisors, only the bases of the teeth, where they are very wide (about 45 mm). The mandibular symphysis is, however, almost perfectly preserved and is very massive, reaches posterior the p3s and the incisors are widely separated from each other. These features clearly separate *C. schlosseri* from any non-chilothere rhino; however, within the genus *Chilotherium* these features are rather common and

relatively uniform, not allowing a specific identification of a mandible (e.g., Kampouridis et al., 2022b). Nonetheless, the features of the skull and upper dentition allow the distinction of *C. schlosseri* from all other chilothere species.

### Comparison of *Eochilotherium samium* to *Aceratherium kiliasi*

The problematic taxonomic status of *Aceratherium kiliasi* has been discussed by several authors (Athanassiou et al., 2014; Fortelius et al., 2003; Geraads & Spassov, 2009; Giaourtsakis, 2003; Heissig, 1996, 1999; Kampouridis et al., 2022b). It was originally erected by Geraads and Koufos (1990) for aceratheriine material from the Vallesian locality Pentalophos-1 in Northern Greece. Later, it was pointed out that the material belongs to two distinct aceratheriine taxa (Fortelius et al., 2003). The holotype and some other specimens belong to a chilothere (herein *E. samium*), whereas the rest of the material belongs to *Acerorhinus neleus* (Athanassiou et al., 2014). A potential close relationship between *Aceratherium kiliasi* and *E. samium* was already hinted by Heissig (1996) and Giaourtsakis (2022) suggested that *Aceratherium kiliasi* actually represents a junior synonym of *E. samium*.

We herein agree with the synonymy of these two species, because the holotype of *Aceratherium kiliasi* (PNT 135) exhibits the key features that characterize *E. samium*. More specifically *Aceratherium kiliasi* has flattened frontal bones, lacking the depression seen in *Chilotherium*. It also lacks the longitudinal groove in the middle of the nasal bones, just like *E. samium*. Regarding the upper dentition, the holotypic skull of *Aceratherium kiliasi* has a quite worn dentition, yet less worn than the dentitions of the lectotype and neotype of *E. samium*. The premolars feature either weakly constricted or unconstructed proto- and hypocones, similar to the P2 of *E. samium*. In the P2, despite the advanced wear stage, the protocone and the hypocone remain separated, as in *E. samium*. Similarly, the M1 is almost completely worn, and yet the protocone and the hypocone are barely connected, without being fully fused. This is very similar to the M2 in the neotype of *E. samium*. The protocone constriction in the molars in *Aceratherium kiliasi* also seems to be weaker than in *Chilotherium* and similar to *E. samium*. Both in the M2 and M3 the crochet is similarly developed to the lectotype and neotype of *E. samium*. Thus, the two species represent synonyms, with the earlier described *E. samium* (Weber, 1905), having priority over *Aceratherium kiliasi* that was described much later (Geraads & Koufos, 1990) according to the Principle of Priority (ICZN Art. 23.3).

### Comparison of *Eochilotherium samium* to 'Primitive' *Chilotherium* Species

The species *E. samium* belongs in the Chilotheriina based on the wide mandibular symphysis, the hypsodont teeth, and their relative complex enamel folds. However, it differs from the genera *Chilotherium*, as mentioned above, and *Shansirhinus.* Despite the fact that *Eochilotherium* and *Shansirhinus* exhibit several similarities such as the lack of the prominent depression in the frontal bones seen in *Chilotherium*, the moderately separated parietal crests (~40 mm in both species), a comparably narrower mandibular symphysis, with smaller and more triangular lower incisors (Deng, 2005), the two taxa exhibit several characters that distinguish them. *Shansirhinus ringstroemi* exhibits more prominent secondary enamel folds, such as a crochet that often closes the medifossette, stronger protocone and hypocone constrictions, a stronger paracone fold, a connection between protocone and hypocone in the premolar, and the existence of enamel plications in the upper teeth. Therefore, *E. samium* is placed in a different genus. The comparison of *E. samium* will only include the more 'primitive' chilotheres '*C.*' *wimani* and '*C.*' *primigenium*. These species lack the autapomorphic traits seen in the typical *Chilotherium* species. All three species lack the depression in the frontal bones that is visible in *Chilotherium*, as seen in *C. schlosseri* (Fig. 2) and *C. anderssoni* (Ringström, 1924:table 2, figs. 1, 2). On the contrary, in *E. samium*, '*C.*' *wimani* and '*C.*' *primigenium*, the frontal bones are convex and become flat posteriorly. In *E. samium* and '*C.*' *wimani* the parietal bones are transversally concave as in typical *Chilotherium* species, whereas in '*C.*' *primigenium* they are only very slightly separated, forming a sagittal crest, a feature not seen in any other chilothere species. All three species exhibit convex frontal bones that posteriorly become more flattened and in *E. samium* and '*C.*' *wimani* the surface between the parietal crests is transversally concave, in contrast to the convex sagittal crest seen in '*C.*' *primigenium*, though Deng (2006a) mentioned that '*C.*' *wimani* may also form a sagittal crest. Also, the parietal region, in which the brain would be situated is transversally generally narrower in these three species than in typical *Chilotherium*. The skulls of *E. samium* and '*C.*' *wimani* are also rather dolichocephalic, whereas '*C.*' *primigenium* seems to have a comparably more brachycephalic skull. Although, in *E. samium*, the occipital region seems to not have been as highly elevated as in '*C.*' *wimani* and '*C.*' *primigenium*.

Regarding the mandible, both '*C.*' *primigenium* and '*C.*' *wimani* exhibit a very wide mandibular symphysis with very large tusk-like incisors. In *E. samium* the mandibular symphysis is somewhat narrower, and the incisors are much smaller, most likely due to the mandible of SMF M 3601 belonging to a female individual. The existence of prominent sexual dimorphism is known in chilotheres and especially well-documented in '*C.*' *wimani* (Chen et al., 2010). Otherwise, both the mandible and the lower dentition do not seem to show any differentiating features. Though, in '*C.*' *primigenium* both the upper and lower dentition is extremely worn and only badly preserved. In the upper teeth, however, it is visible that all three species exhibit weakly constricted or unconstricted premolars, as seen in the completely unconstructed protocone and hypocone in the P2 that is preserved in all three species (Fig. 8; Deng, 2001, 2006a), thereby showing that *E. samium* must be closer affiliated with "*C.*" *wimani* and possibly "*C.*" *primigenium* than with the species of the genera *Chilotherium* and *Shansirhinus.*

## DISCUSSION

### Taxonomy

The Eastern European hornless rhinos have remained rather elusive, despite their existence in several localities during the Late Miocene (e.g., Athanassiou et al., 2014; Geraads & Spassov, 2009; Korotkevich, 1970). This is mainly due to the high number of described species that have been primarily associated with the genus *Chilotherium* and the fact that most of the type material of these new species has been unavailable for further study (Kampouridis et al., 2022b). This is also the case for the type skulls of the four species of hornless rhinos that have been erected based on material from the Upper Miocene deposits of Samos Island in Greece (Giaourtsakis, 2022; Kampouridis et al., 2022b). The four species *C. schlosseri*, *E. samium*, *C. wegneri*, and *C. angustifrons* were initially placed in the genus *Aceratherium* (Andree, 1921; Weber, 1905) and later incorporated into the genus *Chilotherium* (Heissig, 1975; Ringström, 1924). The type material of all four species is considered lost, with the exception of the type mandible of *C. wegneri*, which was relocated in the collections of the GMM (Kampouridis et al., 2022b). After careful comparisons, based on the illustrations of the type material, the two species *C. wegneri* and *C. angustifrons* can undoubtedly be considered

junior synonyms of *C. schlosseri*, supporting the notion of previous studies (Giaourtsakis, 2022; Kampouridis et al., 2022b). Thereby only *C. schlosseri* and *E. samium* remain, which in fact are the first chilothere species that were described from Europe. This makes the affirmation of their validity even more important. For this purpose, we decided to establish neotypes to replace the destroyed lectotypes of both species that Weber (1905) described. The skulls that were selected as neotypes (GPIH 3015 for *C. schlosseri* and SMF M 3601 for *E. samium*) show all essential characters that are known from the lectotypes of *Aceratherium schlosseri* and *Aceratherium samium*, as described and illustrated by Weber (1905).

The two taxa also exhibit important differences from each other, primarily in their skull morphology (Figs. 10–12), confirming that they represent distinct species. These differences include: a generally much wider skull in *C. schlosseri* compared with the dolichocephalic skull of *E. samium* (Fig. 10); the presence of a prominent depression in the frontal bones in *C. schlosseri* (Fig. 10A) that leads to a lower position of the nasal bones (Fig. 11A), whereas in *E. samium* the frontal bones are convex in the anterior part and posteriorly become flat (Figs. 10B, 11B); slightly upwards turning nasal bones with a deep longitudinal groove in the middle in *C. schlosseri*, in contrast to the straight nasal bones without a prominent groove in *E. samium* (Fig. 11); widely separated parietal crests (>70 mm) in *C. schlosseri*, whereas in *E. samium* they are more closely situated (~40 mm) (Table 2; Fig. 10); and the posteriorly widening zygomatic arches in *C. schlosseri* compared with the straight zygomatic arches with a constant width seen in *E. samium* (Fig. 10).

The upper dentition of the neotype of *C. schlosseri* (GPIH 3015) is very well preserved and only moderately worn (Fig. 4), thereby revealing the dental morphology of all teeth. This specimen shows that *C. schlosseri* has a very complex tooth morphology that involves many secondary enamel folds like a very strong crochet, which along with the potential crista close off the medifossette, an early closure of the postfossete, strongly constricted protocones in all teeth that create a prominent antecrochet that closes off the median valley. These are all features that are also visible in the lectotype of *Aceratherium schlosseri* (Weber, 1905:table 9, fig. 1), including also the presence of some enamel plications, which seem to be variably present in the teeth of this species, in contrast to most other *Chilotherium* species, where usually no plications are present. This makes *C. schlosseri* a highly derived member of the chilotheres. Unfortunately, the teeth in the neotype of *E. samium* (SMF M 3601) are almost completely worn down and badly preserved, so only little can be said about its dental morphology. It seems that the secondary folds are well developed in comparison to other genera of rhinoceroses, but not as prominent as in *C. schlosseri* (Fig. 13) and other members of the genus *Chilotherium*, as seen by the crochet in the left M2, which despite its advanced wear stage is only moderately long and does not close off the medifossette and the antecrochet in the same tooth does not cut off the median valley. In both P4s of SMF M 3601 the antecrochet barely connects to the hypocone and closes the median valley. The dentition of the lectotype of *Aceratherium samium* seems to offer similar insights, as in the P2, P4, M1, and M2 no medifossette exists and the median valley in the P4 remains open. These are generally more plesiomorphic features among chilotheres and separate *E. samium* from all species of *Chilotherium*, justifying an attribution to a distinct genus, which is herein applied to bring clarity into the confusion concerning the chilotheres.

### Relationships with Other Chilothere Species

The complex secondary enamel folds, the features of the skull and the wide mandibular symphysis with large incisors of *C. schlosseri* show that it is a typical representative of the genus *Chilotherium*. Moreover, it seems to be closely aligned to the Vallesian species *C. sarmaticum* from Berislav (Ukraine) and the Turolian *C. orlovi* from Pavlodar (Kazakhstan), based on the distance between the parietal crests. Additionally, the dentition of *C. schlosseri* seems to be very similar to *C. kowalevskii* from the Turolian of Grebeniki (Ukraine), with complicated enamel folds such as the strong protocone constriction that results in a very strong antecrochet and the infrequently present cingulum in the upper premolars. A close relationship between *C. schlosseri* and *C. kowalevskii* is also suggested by the similar dimensions of their metapodials that differ from those of *C. sarmaticum* (Korotkevich, 1970; Krokos, 1917; Weber, 1905). Thus, it seems likely that these species share a close relationship and are more distantly related to the other chilotheres known from Europe and Asia.

*Eochilotherium samium* seems to share a more distant relationship to the other European species and is probably closer aligned to the "primitive" chilotheres found in China: '*C.*' *wimani* and '*C.*' *primigenium*. They share some of the defining features that are also present in the typical members of *Chilotherium*, such as the wide mandibular symphysis with large tusk-like incisors and a small P2/p2 (Deng, 2001, 2006a). Additionally, *E. samium* and '*C.*' *wimani* also exhibit a transversally concave parietal region. However, they also exhibit plesiomorphic features such as slightly convex frontal bones that flatten posteriorly, straight nasal bones, without a prominent longitudinal groove, and a raised occipital region of the skull. In addition, *E. samium* features also a somewhat simpler tooth morphology than '*C.*' *wimani* (Deng, 2006a). Thus, *E. samium* lacks many of the apomorphic characters seen in *Chilotherium*, justifying its placement in a different genus. A potential inclusion of '*C.*' *wimani* in *Eochilotherium* is more ambiguous, and the species is herein provisionally kept in its original genus, pending further studies clarifying its generic attribution. '*Chilotherium*' *primigenium*, on the other hand, exhibits an unusual combination of characters. It features a very wide mandibular symphysis with large tusk-like incisors and a small p2, which suggests a close relationship to the genus *Chilotherium*. However, '*C.*' *primigenium* includes also more plesiomorphic traits than *Eochilotherium* such as the closely situated parietal crests that form a sagittal crest instead of more widely separated crests with a concave interior, while also exhibiting convex frontal bones that lack the characteristic frontal depression of the genus *Chilotherium*. '*Chilotherium*' *primigenium* additionally exhibits rather thick nasal bones that are long, and completely straight, without any longitudinal groove separating the nasal bones from each other. Moreover, in lateral view the posterior part of the skull is extremely elevated and in caudal view the skull is bell-shaped. These features separate '*C.*' *primigenium* from the typical representatives of *Chilotherium*, but also from the 'primitive' *E. samium* and '*C.*' *wimani* and suggest that it should probably be placed in a different genus. However, further study is needed to clarify its exact taxonomic status and phylogenetic affinities. For the time being, we therefore decided to temporarily keep it in its original genus, while pointing out the issues and suggesting that a generic separation might be preferable.

The comparison of the three genera included in the Chilotheriina, *Chilotherium*, *Eochilotherium*, and *Shansirhinus*, demonstrates their shared similarities, such as the wide mandibular symphysis, the tusk-like lower incisors, the moderately to widely separated parietal crests, the hypsodont teeth, and the very complex enamel folds in the upper teeth. However, it also illustrates the important differences, such as the morphology of the frontal bones, which are notably depressed in *Chilotherium*, but are flat to convex in *Eochilotherium* and *Shansirhinus*, the posterior portion of the skull that is transversally rather wide

in *Chilotherium*, whereas in the other two genera it is narrower, the size and form of the lower incisors, which are large, flat, asymmetrical and tusk-like in *Chilotherium* and somewhat smaller, more symmetrical and less flattened in *Eochilotherium* and *Shansirhinus*. Additionally, the tooth morphology is variably developed in these genera, with *Shansirhinus* having the most complicated secondary folds in the Chilotheriina. This supports that they represent distinct genera and shows that '*C.*' *wimani* and '*C.*' *primigenium* do not exactly fit the description of either genus and might actually represent different genera.

## CONCLUSIONS

The European chilotheres have a very complicated taxonomic history, with the erection of over eight species. Herein, we attempt to solve some of the issues involving this group by designating neotypes for the first two described chilothere species from Europe, *Chilotherium schlosseri* and *Eochilotherium samium*, both from the Upper Miocene deposits of Samos Island (Greece). The revision showed that they represent two distinct taxa, with *E. samium* being placed in a distinct genus, based on some cranial features such as the missing depression in the frontal bones and its less complex dental morphology, such as the less pronounced protocone constriction. *Chilotherium schlosseri* represents one of the most derived species of the genus, based on its very widely separated parietal crests and its very complex tooth morphology, which frequently includes enamel plications. This species is closely allied with other Eastern European *Chilotherium* species, *Chilotherium kowalevskii*, *Chilotherium sarmaticum* from Ukraine and the Asian species *Chilotherium orlovi* from Kazakhstan. *Eochilotherium samium* on the other hand, seems to be more similar to the Chinese '*Chilotherium*' *wimani* and '*Chilotherium*' *primigenium*.

## ACKNOWLEDGMENTS

We would like to thank S. Roussiakis, G. Theodorou (AMPG), O. Sandrock, M. Blume, M. Kollbacher (HLMD), M. Bertling, D. Theda (GMM), U. Kotthoff (GPIH), I. Werneburg (GPIT), C. Argot (MNHN), U. Göhlich, F. Zachos, A. Bibl (NHMW), L. Costeur, F. Dammeyer (NMB), R. Brocke, G. Riedel, L. Kraus (SMF), and E. Amson (SMNS), for allowing us to study material under their care. We thank P.-O. Antoine (University of Montpellier, France), A. Athanassiou (Ephorate of Palaeoanthropology-Speleology at the Hellenic Ministry for Culture, Greece), B. U. Bayshashov (Institute of Zoology in Akademgorodok, Kazakhstan), I. Giaourtsakis (Ludwig-Maximilians-University of Munich, Germany) and K. Heissig (Staatliche Naturwissenschaftlichen Sammlungen Bayerns, Germany) for fruitful discussions and for providing literature about fossil rhinoceroses. We thank the Editor A. Friscia (University of California, U.S.A.), an anonymous reviewer and P.-O. Antoine (University of Montpellier, France) for their helpful comments that improved this study. This research received support from the SYNTHESYS + project (http://www.synthesys.info/) which is financed by European Community Research Infrastructure Action under the H2020 Integrating Activities Programme, Project number 823827 (AT-TAF-TA3-9 and AT-TAF-TA4-29 and FR-TAF-TA4-71).

## AUTHOR CONTRIBUTIONS

Conceptualization: P.K., G.S., M.B.; Investigation: P.K., G.S., N.K., N.S., M.B.; Project Administration: N.S., M.B.; Validation: P.K., N.S., M.B.; Writing original draft: P.K.; Review and approval: P.K., G.S., N.K., N.S., M.B.

## SUPPLEMENTARY FILES

Supplementary Data 1: figures of lower teeth and table with the most important features of the Samian chilotheres.

## ORCID

Panagiotis Kampouridis http://orcid.org/0000-0002-1812-4664
Georgia Svorligkou http://orcid.org/0000-0002-1472-0282
Nikolaos Kargopoulos http://orcid.org/0000-0002-6471-151X
Nikolai Spassov http://orcid.org/0000-0002-2891-7457
Madelaine Böhme http://orcid.org/0000-0003-2100-6164

## LITERATURE CITED

Andree, J. (1921). Rhinocerotiden aus dem Unterpliocän von Samos. *Paläontologische Zeitschrift*, *3*, 189–212.

Antoine, P.-O. (2002). Phylogénie et évolution des Elasmotheriina (Mammalia, Rhinocerotidae). *Mémoires du Muséum National d'Histoire Naturelle*, *188*, 1–359.

Antoine, P.-O. (In Press). Rhinocerotids from the Siwalik faunal sequence. In C. Badgley, D. Pilbeam, & M. Morgan (Hrsg.), *At the Foot of the Himalayas: Paleontology and Ecosystem Dynamics of the Siwalik Record of Pakistan*. Johns Hopkins University Press.

Antoine, P.-O., & Saraç, G. (2005). Rhinocerotidae (Mammalia, Perissodactyla) from the late Miocene of Akkaşdaği, Turkey. *Geodiversitas*, *27*(4), 601–632.

Ataabadi, M. M., Bernor, R. L., Kostopoulos, D. S., Wolf, D., Orak, Z., Zare, G., Nakaya, H., Watabe, M., & Fortelius, M. (2013). Recent Advances in Paleobiological Research of the Late Miocene Maragheh Fauna, Northwest Iran. In M. Fortelius, X. Wang, & L. Flynn (Hrsg.), *Fossil Mammals of Asia* (S. 546–565). Columbia University Press. https://doi.org/10.7312/columbia/9780231150125.003.0025

Athanassiou, A., Roussiakis, S. J., Giaourtsakis, I. X., Theodorou, G. E., & Iliopoulos, G. (2014). A new hornless rhinoceros of the genus *Acerorhinus* (Perissodactyla: Rhinocerotidae) from the Upper Miocene of Kerassiá (Euboea, Greece), with a revision of related forms. *Palaeontographica Abteilung A*, *303*(1–3), 23–59. https://doi.org/10.1127/pala/303/2014/23

Bayshashov, B. U. (1982). A new rhinoceros species of the genus *Chilotherium* from Pavlodar. In *Mesozoic and Cenozoic vertebrate fauna and flora of North-Eastern and southern Kazakhstan* (Bd. 8, S. 72–83). Academy of Sciences of Kazakhstan.

Bayshashov, B. U. (1993). *Neogene rhinoceroses of Kazakhstan*. Academy of Sciences of Kazakhstan.

Bernor, R. L. (1986). Mammalian biostratigraphy, geochronology, and zoogeographic relationships of the Late Miocene Maragheh fauna, Iran. *Journal of Vertebrate Paleontology*, *6*(1), 76–95. https://doi.org/10.1080/02724634.1986.10011600

Bonis, L. de, de Brunet, M., Heintz, E., & Sen, S. (1992). La province Greco-irano-afghane et la répartition des faunes mammaliennes au Miocène supérieur. *Paleontologia i Evolucio*, *24–25*, 103–112.

Cerdeño, E. (1995). Cladistic Analysis of the Family Rhinocerotidae (Perissodactyla). *American Museum Novitates*, 3143, 28.

Chen, S., Deng, T., Hou, S., Shi, Q., & Pang, L. (2010). Sexual Dimorphism in Perissodactyl Rhinocerotid *Chilotherium wimani* from the Late Miocene of the Linxia Basin (Gansu, China). *Acta Palaeontologica Polonica*, *55*(4), 587–597. https://doi.org/10.4202/app.2009.0001

Deng, T. (2001). New material of *Chilotherium wimani* (Perissodactyla, Rhinoceritdae) from the Late Miocene of Fugu, Shaanxi. *Vertebrata Palasiatica*, *39*(2), 129–138.

Deng, T. (2005). New cranial material of *Shansirhinus* (Rhinocerotidae, Perissodactyla) from the Lower Pliocene of the Linxia Basin in Gansu, China. *Geobios*, *38*(3), 301–313. https://doi.org/10.1016/j.geobios.2003.12.003

Deng, T. (2006a). A primitive species of *Chilotherium* (Perissodactyla, Rhinocerotidae) from the Late Miocene of Linxia Basin (Gansu, China). *Cainozoic Research*, *5*(1–2), 93–102.

Deng, T. (2006b). Neogene Rhinoceroses of the Linxia Basin (Gansu, China). *Courier Des Forschungsinstituts Senckenberg*, *256*, 43–56.

Dollo, L. (1885). Rhinocéros vivants et fossiles. *Revue de Questions Scientifiques*, *17*, 293–299.

Drevermann, F. (1930). Aus der Zeit des dreizehigen Pferdes. *Natur und Museum*, *60*(1), 2–13.

Forsyth-Major, C. I. (1888). Sur un gisement d'ossements fossiles dans l'île de Samos contemporains de l'âge de Pikermi. *Comptes Rendus Hebdomadaires des Séances de l'Académie des Sciences*, *107*, 1178–1181.

Fortelius, M., & Heissig, K. (1989). The phylogenetic relationships of the Elasmotherini. *Mitteilungen der Bayerischen Staatssammlung für Paläontologie und historische Geologie*, *29*, 227–233.

Fortelius, M., Heissig, K., Saraç, G., & Sen, S. (2003). Rhinocerotidae (Perissodactyla). In *Geology and Paleontology of the Miocene Sinap Formation, Turkey* (S. 282–307). Columbia University Press.

Garevski, R. (1974). Beitrag zur Kenntnis der Pikermifauna Mazedoniens. Fossilreste der Chalicotheriiden. *Fragmenta Balcanica*, *9*, 201–209.

Gaudry, A. (1862). *Animaux fossiles et géologie de l'Attique*. F. Savy.

Geraads, D., & Koufos, G. (1990). Upper Miocene Rhinocerotidae (Mammalia) from Pentalophos-1, Macedonia, Greece. *Palaeontographica Abteilung A*, *210*, 151–168.

Geraads, D., & Spassov, N. (2009). Rhinocerotidae (Mammalia) from the Late Miocene of Bulgaria. *Palaeontographica Abteilung A*, *287*(4–6), 99–122. https://doi.org/10.1127/pala/287/2009/99

Giaourtsakis, I. X. (2003). Late Neogene Rhinocerotidae of Greece: Distribution, diversity and stratigraphical range. *Deinsea*, *10*, 235–253.

Giaourtsakis, I. X. (2009). The Late Miocene Mammal Faunas of the Mytilinii Basin, Samos Island, Greece: New Collection 9. Rhinocerotidae. *Beiträge Zur Paläontologie*, *31*, 157–187.

Giaourtsakis, I. X. (2022). The Fossil Record of Rhinocerotids (Mammalia: Perissodactyla: Rhinocerotidae) in Greece. In E. Vlachos (Hrsg.), *Fossil Vertebrates of Greece Vol. 2* (S. 409–500). Springer International Publishing. https://doi.org/10.1007/978-3-030-68442-6_14

Gray, J. E. (1821). On the natural arrangemenet of vertebrose animals. *London Medical Repository*, *15*, 297–310.

Gürich, G. (1911). Fossile Säugetierreste aus Samos. *Verhandlungen des Naturwissenschaftlichen Vereins in Hamburg*, *3*(19), 79.

Heissig, K. (1975). Rhinocerotidae aus dem Jungtertiär Anatoliens. *Geologisches Jahrbuch (B)*, *15*, 145–151.

Heissig, K. (1996). The stratigraphical range of fossil rhinoceroses in the Late Neogene of Europe and the Eastern Mediterranean. In *The evolution of westermn Eurasian Neogene Mammal Faunas* (S. 339–347). Columbia University Press.

Heissig, K. (1999). Family Rhinocerotidae. In *The Miocene land mammals* (S. 175–188). Pfeil.

Hristova, L., Kovachev, D., & Spassov, N. (2003). *Hipparion brachypus* Hensel, 1862 from Hadjidimovo, souwestern Bulgaria (late Miocene). *Comptes rendus de l'Académie bulgare des Sciences*, *56*(2), 77–84.

Hullot, M., Antoine, P.-O., Spassov, N., Koufos, G. D., & Merceron, G. (2022). Late Miocene rhinocerotids from the Balkan-Iranian province: Ecological insights from dental microwear textures and enamel hypoplasia. *Historical Biology*, 1–18. https://doi.org/10.1080/08912963.2022.2095910

Kampouridis, P., Hartung, J., Ferreira, G. S., & Böhme, M. (2022a). Reappraisal of the late Miocene elasmotheriine *Parelasmotherium schansiense* from Kutschwan (Shanxi Province, China) and its phylogenetic relationships. *Journal of Vertebrate Paleontology*, *41*(6), e2080556. https://doi.org/10.1080/02724634.2021.2080556

Kampouridis, P., Ratoi, B., & Ursachi, L. (2023). New evidence for the unique coexistence of two subfamilies of clawed perissodactyls (Mammalia, Chalicotheriidae) in the Upper Miocene of Romania and the Eastern Mediterranean. *Journal of Mammalian Evolution*. https://doi.org/10.1007/s10914-023-09657-5

Kampouridis, P., Svorligkou, G., Kargopoulos, N., & Augustin, F. J. (2022b). Reassessment of '*Chilotherium wegneri*' (Mammalia, Rhinocerotidae) from the late Miocene of Samos (Greece) and the European record of *Chilotherium*. *Historical Biology*, *34*(3), 412–420. https://doi.org/10.1080/08912963.2021.1920939

Kaup, J. (1832). Über *Rhinoceros incisivus* Cuv., und eine neue Art, *Rhinoceros schleiermacheri*. *Isis von Oken*, *(8)*, 898–904.

Kiernik, E. (1913). Über einen Aceratheriumschädel aus der Umgebung von Odessa. *Bulletin international de l'Académie des sciences de Cracovie*, 1913, 808–864.

Killgus, H. (1922). *Die Unterpliocaenen Chinesischen Säugetierreste der Tafelschen Sammlung zu Tübingen* [Ph.D. Dissertation]. Eberhard-Karls University of Tübingen.

Killgus, H. (1923). Unterpliozäne Säuger aus China. *Paläontologische Zeitschrift*, *5*(3), 251–257. https://doi.org/10.1007/BF03160368

Korotkevich, O. L. (1958). A new *Chilotherium* species from the Sarmatian deposits of the Ukraine. *Dopovidi Akad. Nauk Ukrainskoi RSR*, *12*, 1372–1376.

Korotkevich, O. L. (1970). The mammals of the Berislav late Sarmatian *Hipparion*-fauna. In *The Natural Environment and the fauna of the past* (5. Aufl., S. 24–121). Naukova Dumka.

Kostopoulos, D. S., Koufos, G. D., Sylvestrou, I. A., Syrides, G. E., & Tsombachidou, E. (2009). The Late Miocene Mammal Faunas of the Mytilinii Basin, Samos Island, Greece: New Collection: 2. Lithostratigraphy and Fossiliferous Sites. *Beiträge Zur Paläontologie*, *31*, 13–26.

Kostopoulos, D. S., Sen, S., & Koufos, G. D. (2003). Magnetostratigraphy and revised chronology of the late Miocene mammal localities of Samos, Greece. *International Journal of Earth Sciences*, *92*(5), 779–794. https://doi.org/10.1007/s00531-003-0353-8

Koufos, G. D. (2009). The Late Miocene Mammal Faunas of the Mytilinii Basin, Samos Island, Greece: New Collection: 1. History of the Samos Fossil Mammals. *Beiträge Zur Paläontologie*, *31*, 1–12.

Koufos, G. D., Kostopoulos, D. S., & Vlachou, T. D. (2009). The Late Miocene Mammal Faunas of the Mytilinii Basin, Samos Island, Greece: New Collection 16. Biochronology. *Beiträge Zur Paläontologie*, *31*, 397–408.

Koufos, G. D., Kostopoulos, D. S., Vlachou, T. D., & Konidaris, G. E. (2011). A synopsis of the late Miocene Mammal Fauna of Samos Island, Aegean Sea, Greece. *Geobios*, *44*(2–3), 237–251. https://doi.org/10.1016/j.geobios.2010.08.004

Kretzoi, M. (1942). Bemerkungen zum System der Nachmiozänen Nashorn-Gattungen. *Földtani Közlöny*, *72*(1), 4–12.

Krokos, W. I. (1917). *Aceratherium schlosseri* Web. Du village de Grebeniki du gouvernement de Kherson. *Memoires of the Agricultural Society of Southern Russia*, *82*(2), 1–96.

Lehmann, U. (1984). Notiz für Säugerreste von der Insel Samos in der Sammlung des Geologisch-Paläontologischen Instituts und Museums Hamburg. *Mitteilungen des Geologisch-Paläontologischen Instituts der Universität Hamburg*, *57*, 147–156.

Linnaeus, C. (1758). *Systema Naturae*. Laurentii Salvii.

Lu, X.-K., Deng, T., & Pandolfi, L. (2023). Reconstructing the phylogeny of the hornless rhinoceros Aceratheriinae. *Frontiers in Ecology and Evolution*, *11*, 1005126. https://doi.org/10.3389/fevo.2023.1005126

Mecquenem, R. de. (1908). Contribution a l'étude du gisement des vertébrés de Maragha et de ses environs. *Annales d'histoire Naturelle*, *1*, 27–98.

Niezabitowski, E. von L. (1912). *Teleoceras ponticus* n. Sp. Vorläufige Notiz (S. 2). Nowy Targ.

Niezabitowski, E. von L. (1913). Über das Schädelfragment eines Rhinocerotiden (*Teleoceras ponticus* Niez.) von Odessa. *Bulletin International de l'Academic des Sciences de Cracovie, Series B*, 223–235.

Nothdurft, W., & Smith, J. B. (2002). *The lost dinosaurs of Egypt*. Random House.

Osborn, H. F. (1899). On *Pliohyrax kruppi* Osborn, a fossil hyracoid from Samos, Lower Pliocene in the Stuttgart collection. A new type and first known Tertiary hyracoid. *Proceedings of the 4th International Congress of Zoology*, 172–173.

Owen, R. (1848). Description of teeth and portions of jaws of two extinct anthracotherioid quadrupeds (*Hyopotamus vectianus* and *Hyop. Bovinus*) discovered by the Marchioness of Hastings in the Eocene deposits on the N.W. coast of the Isle of Wight; with an attempt to develop Cuvier's idea of the classification of pachyderms by the number of their toes. *Quarterly Journal of the Geological Society of London*, *4*, 103–141.

Pandolfi, L. (2016). *Persiatherium rodleri*, gen. Et sp. Nov. (Mammalia, Rhinocerotidae) from the upper Miocene of Maragheh (northwestern iran). *Journal of Vertebrate Paleontology*, *36*(1), e1040118. https://doi.org/10.1080/02724634.2015.1040118

Pavlow, M. (1913). Mammifères tertiaires de la Nouvelle Russie, 1. Partie: Artiodactyla, Perissodactyla (*Aceratherium kowalevskii* n.s.). *Nouveaux Mémoires de la Société Impériale des Naturalistes de Moscou*, *17*, 1–68.

Pohlig, H. (1886). On the Pliocene of Maragha, Persia, and its resemblance to that of Pikermi in Greece. *Quaterly Journal of the Geological Society of London*, *42*, 177–179.

Qiu, Z. X., Xie, J. Y., & Yan, D. F. (1987). A new chilothere skull from Hezheng, Gansu, China, with special reference to the Chinese "*Diceratherium*". *Scientia Sinica B*, *5*, 545–552.

Ride, W. D. L., Cogger, H. G., Dupris, C., Kraus, B., Minelli, A., Thompson, F. C., & Tubbs, P. K. (1999). *International Code of Zoological Nomenclature*. International Trust for the Zoological Nomenclature and the British Museum.

Ringström, T. (1924). Nashörner der Hipparion-Fauna Nord-Chinas. *Palaeontologia Sinica*, *1*(4), 1–156.

Roussiakis, S., Filis, P., Sklavounou, S., Giaourtsakis, I. X., Kargopoulos, N., & Theodorou, G. (2019). Pikermi: A classical European fossil mammal geotope in the spotlight. *European Geologist*, *48*, 28–32.

Schlosser, M. (1903). Die fossilen Säugethiere Chinas nebst einer Odontographie der recenten Antilopen. *Abhandlungen der Koniglichen Bayerischen Akademie der Wissenschaften*, *22*, 1–221.

Schlosser, M. (1921). Die Hipparionenfauna von Veles in Mazedonien. *Abhandlungen der Bayerischen Akademie der Wissenschaften*, *24*(4), 1–55.

Solounias, N., & Mayor, A. (2004). Ancient references to the fossils from the land of Pythagoras. *Earth Sciences History*, *23*(2), 283–296.

Solounias, N., & Ring, U. (2007). Samos Island, Part II: Ancient history of the Samos fossils and the record of earthquakes. *Journal of the Virtual Explorer*, *28*(3), 1–18. https://doi.org/10.3809/jvirtex.2007.00179

Solounias, N., Rivals, F., & Semprebon, G. M. (2010). Dietary interpretation and paleoecology of herbivores from Pikermi and Samos (late Miocene of Greece). *Paleobiology*, *36*(1), 113–136. https://doi.org/10.1666/0094-8373-36.1.113

Spassov, N. (2002). The Turolian Megafauna of West Bulgaria and the character of the Late Miocene ''Pikermian biome". *Bollettino della Società Paleontologica Italiana*, *41*(1), 69–81.

Spassov, N., & Geraads, D. (2004). *Tragoportax* Pilgrim, 1937 and *Miotragocerus* Stromer, 1928 (Mammalia, Bovidae) from the Turolian of Hadjidimovo, Bulgaria, and a revision of the late Miocene Mediterranean Boselaphini. *Geodiversitas*, *26*(2), 339–370.

Spassov, N., Geraads, D., Hristova, L., Markov, G. N., Garevska, B., & Garevski, R. (2018). The late Miocene mammal faunas of the Republic of Macedonia (FYROM). *Palaeontographica Abteilung A*, *311*(1–6), 1–85. https://doi.org/10.1127/pala/2018/0073

Spassov, N., Geraads, D., & Markov, G. (2019). The late Miocene mammal fauna from Gorna Sushitsa, southwestern Bulgaria, and the early/middle Turolian transition. *Neues Jahrbuch Für Geologie Und Paläontologie - Abhandlungen*, *291*(3), 317–350. https://doi.org/10.1127/njgpa/2019/0804

Sun, D.-H., Li, Y., & Deng, T. (2018). A new species of *Chilotherium* (Perissodactyla, Rhinocerotidae) from the Late Miocene of Qingyang, Gansu, China. *National Science Review*, *56*(3), 216–228. https://doi.org/10.19615/j.cnki.1000-3118.180109

Vangengeim, E., & Tesakov, A. (2013). Late Miocene mammal localities of Eastern Europe and Western Asua: Toward bistratigraphic synthesis. In *Fossil Mammals of Asia. Neogene Bistratigraphy and Chronology* (S. 521–537). Columbia University Press.

Wagner, A. (1848). Urweltliche Säugetier-Überreste aus Griechenland. *Abhandlungen der Bayerischen Akademie der Wissenschaften*, *5*, 335–378.

Weber, M. (1904). Ueber Tertiäre Rhinocerotiden von der Insel Samos. *Bulletin de la Société Impériale des Naturalistes de Moscou*, *17*(4), 477–501.

Weber, M. (1905). Über Tertiäre Rhinocerotiden von der Insel Samos. II. *Bulletin de la Société Imperériale des Naturalistes de Moscou*, *18*(4), 344–363.

Wessel, P., Luis, J. F., Uieda, L., Scharroo, R., Wobbe, F., Smith, W. H. F., & Tian, D. (2019). The Generic Mapping Tools version 6. *Geochemistry, Geophysics, Geosystems*, *20*, 5556–5564. https://doi.org/10.1029/2019GC008515

Handling Editor: Anthony Friscia.

# Appendix 4

*Publication 4*

Craniodental anatomy of the hornless rhinocerotid *Chilotherium schlosseri* (Mammalia, Perissodactyla) from the Late Miocene of Samos Island, Greece

Georgia Svorligkou[a], **Panagiotis Kampouridis**[b,c], Nikolaos Kargopoulos[d], and Luca Pandolfi[e]

[a]Faculty of Geology and Geoenvironment, Department of Historical Geology and Palaeontology, National and Kapodistrian University of Athens, Athens, Greece; and

[b]Department of Geoscience, Eberhard Karls University of Tübingen, Tübingen, Germany;

[c]Senckenberg Centre for Human Evolution and Palaeoenvironment, Tübingen, Germany;

[d]Departamento de Ciencias de la Tierra, Instituto Universitario de Investigación en Ciencias Ambientales de Aragón (IUCA), Universidad de Zaragoza, Zaragoza, Spain;

[e]Dipartimento di Scienze della Terra, Università di Pisa, Pisa, Italy

Published in

Journal of Mammalian Evolution 32, 36

DOI: 10.1007/s10914-025-09777-0

Date of online publication: 17.10.2025

Journal of Mammalian Evolution (2025) 32:36
https://doi.org/10.1007/s10914-025-09777-0

RESEARCH

# Craniodental anatomy of the hornless rhinocerotid *Chilotherium schlosseri* (Mammalia, Perissodactyla) from the Late Miocene of Samos Island, Greece

**Georgia Svorligkou**[1] · **Panagiotis Kampouridis**[2,3] · **Nikolaos Kargopoulos**[4] · **Luca Pandolfi**[5]

Accepted: 29 July 2025


## Abstract

The fossiliferous sites of Samos Island are of major importance amidst the numerous Turolian localities of Greece, partly because it is the type locality of two hornless rhinocerotids, *Chilotherium schlosseri* and *Eochilotherium samium* . For more than a century, the island has been excavated by Greek and international teams, leading to a dispersal of fossils in a plethora of museums around the World. In the present work, the entirety of the craniodental material of *Chilotherium schlosseri* available in different European and American collections is examined for the first time. Additionally, we compared the material to various *Chilotherium* species from the Late Miocene of Eurasia. A number of diagnostic characters are herein established for *C. schlosseri*: the markedly depressed frontal and nasal region, the widely separated parietal crests, the complicated enamel folds and the presence of enamel plications on the permanent upper dentition. In terms of morphology, the species that is phenotypically closest to *C. schlosseri* appears to be *C. orlovi* from the Late Miocene of Kazakhstan. Both species seem to be more distantly related to the other Samian chilothere, *E. samium*.

**Keywords** Biostratigraphy · Chilotheres · Eurasia · Taxonomy · Palaeoenvironment

## Introduction

### Nomenclatural and systematic review of the genus *Chilotherium*

Rhinoceroses are amongst the most iconic mammals that exist today. They are represented by five species that live in Africa and Asia, most of which are considered endangered. However, contrary to their limited taxonomic and phylogenetic diversity nowadays, rhinoceroses were much more diverse in the past, including multiple clades (Antoine et al. 2025). The most diverse clade was represented by the aceratheriines. They were very abundant during the Miocene in Eurasia, but they also spread to North America and Africa. The most frequent and characteristic genus of this group in Eurasia is probably *Chilotherium* Ringström, 1924. *Chilotherium* was extremely common during the Late Miocene, with its geographical distribution reaching from China all the way to Eastern Europe and, in many localities, it was among the most common large mammals (Deng et al. 2023). Representatives of this genus were characterised by the absence of horn-bosses (suggesting the absence of

✉ Georgia Svorligkou
geosvorligk@geol.uoa.gr

✉ Panagiotis Kampouridis
pkampouridis94@gmail.com

[1] Department of Historical Geology and Palaeontology, National Kapodistrian University of Athens, Athens, Greece

[2] Department of Geosciences, Eberhard Karls University of Tübingen, Tübingen, Germany

[3] Senckenberg Centre for Human Evolution and Palaeoenvironment, Tübingen, Germany

[4] Departamento de Ciencias de la Tierra, Instituto Universitario de Investigación en Ciencias Ambientales de Aragón (IUCA), Universidad de Zaragoza, Zaragoza, Spain

[5] Dipartimento di Scienze della Terra, Università di Pisa, Pisa, Italy

Published online: 17 October 2025

keratin horns), depressed skull, wide mandibular symphysis, well-developed lower incisors, and shortened limbs (e.g., Ringström 1924).

The genus *Chilotherium* was erected by Ringström (1924), based on abundant material from Upper Miocene strata in China that was collected in the beginning of the 20th century. Ringström erected the genus *Chilotherium* upon *Chilotherium anderssoni* Ringström, 1924, which he assigned as the type species for the genus; furthermore, he erected several new species for this genus: *Chilotherium planifrons* Ringström, 1924, and *C. wimani* Ringström, 1924. Ringström (1924) additionally referred 10 previously described species from Eurasia to this new genus. Some of these species are now considered junior synonyms (Table 1), while many of them have not be re-evaluated since then and their status remains somewhat unclear (e.g., Kampouridis et al. 2022; 2023). The situation is especially dire concerning the European chilotheres. Eight distinct chilothere species have been erected within the very restricted geographical region of southeastern Europe (Kampouridis et al. 2023, table 1): *Aceratherium schlosseri* Weber, 1905, *Aceratherium samium* Weber, 1905, *Teleoceras ponticus* Niezabitowski, 1912, *Aceratherium kowalevskii* Pavlow, 1913, *Aceratherium wegneri* Andrée, 1921, *Aceratherium angustifrons* Andrée, 1921, *Chilotherium sarmaticum* Korotkevich, 1958, *Aceratherium kiliasi* Geraads and Koufos, 1990. The generic attributions and relationships among these forms is discussed in detail below (Tables 2 and 3).

Many authors have suggested the synonymy of some of these species in the past (e.g., Kiernik 1913; Korotkevitch 1970; Heissig 1975; Antoine and Sen 2016; Țibuleac et al. 2023). Nonetheless, the status of most of them remains unclear. One reason for this ambiguity is the fact that the type specimens of *C. schlosseri* and *E. samium*, stored in Munich, were destroyed during WWII bombings (Geraads and Spassov 2009; Kampouridis et al. 2022; Giaourtsakis 2022 and references therein). From the types of *C. wegneri* and *C. angustifrons*, originally housed in Münster, only a mandible of *C. wegneri* has been relocated and described (Kampouridis et al. 2022). Closely related to *Chilotherium* is the genus *Shansirhinus* Kretzoi, 1942, that shares the complicated enamel folds, including a medifossette often closed by the crochet, markedly constricted protocone, connection between protocone and hypocone in the premolars, and enamel plications in the upper teeth (Kampouridis et al. 2023). This similarity increases the complexity of the genus's taxonomy and the diversity of the chilotheres group overall. Kampouridis et al. (2023) suggested that some species that were considered as belonging to *Chilotherium* lack certain apomorphies seen in all other *Chilotherium* species, such as the depression of the frontal region, and should probably be placed in different genera. Kampouridis et al. (2023) revised the species from Samos by fixing neotypes for the two valid species and separated them on the generic level, based on their differing skull morphology: *Chilotherium schlosseri* (Weber, 1905) and *Eochilotherium samium* (Weber, 1905). Additionally, they suggested that two species from Upper Miocene deposits of China, regarded as primitive members of the genus, "*Chilotherium*" *wimani* Ringström, 1924, and

**Table 1** Summary of the taxonomy of the Chilotheriina (modified after Heissig 1975; Deng 2006b; Kampouridis et al. 2022, 2023)

| Species | Authority | Revised species | Type locality |
|---|---|---|---|
| *Aceratherium schlosseri* | Weber, 1905 | *Chilotherium schlosseri* | Samos, Greece |
| *Teleoceras ponticus* | Niezabitovski, 1912 | *Chilotherium schlosseri* | Odessa, Ukraine |
| *Aceratherium angustifrons* | Andree, 1921 | *Chilotherium schlosseri* | Samos, Greece |
| *Aceratherium wegneri* | Andree, 1921 | *Chilotherium schlosseri* | Samos, Greece |
| *Aceratherium kowalevskii* | Pavlow, 1913 | *Chilotherium kowalevskii* | Grebeniki, Ukraine |
| *Chilotherium sarmaticum* | Korotkevich, 1958 | *Chilotherium sarmaticum* | Berislav, Ukraine |
| *Chilotherium orlovi* | Bayshashov, 1993 | *Chilotherium orlovi* | Pavlodar, Kazakhstan |
| *Rhinoceros persiae* | Pohlig, 1886 | *Chilotherium persiae* | Maragheh, Iran |
| *Chilotherium anderssoni* | Ringström, 1924 | *Chilotherium anderssoni* | Anlecun, China |
| *Chilotherium planifrons* | Ringström, 1924 | *Chilotherium anderssoni* | Anlecun, China |
| *Chilotherium fenhoensis* | Tung et al., 1975 | *Chilotherium anderssoni* | Anlecun, China |
| *Chilotherium habereri* | Schlosser, 1903 | *Chilotherium habereri* | Lantian, China |
| *Chilotherium gracile* | Ringström, 1924 | *Chilotherium habereri* | Lantian, China |
| *Chilotherium wimani* | Ringström, 1924 | *"Chilotherium" wimani* | Wangdaifuliang, China |
| *Chilotherium xijangensis* | Ji et al., 1980 | *Chilotherium xijangensis* | Xijang, China |
| *Chilotherium primigenium* | Deng, 2006a | *"Chilotherium" primigenium* | Zhongmajia, China |
| *Chilotherium licenti* | Sun et al., 2018 | *Chilotherium licenti* | Gansu, China |
| *Aceratherium samium* | Weber, 1905 | *Eochilotherium samium* | Samos, Greece |
| *Aceratherium kiliasi* | Geraads and Koufos, 1990 | *Eochilotherium samium* | Pentalophos, Greece |
| *Rhinoceros brancoi* | Schlosser, 1903 | *Shansirhinus brancoi* | Shanxi, China |
| *Shansirhinus ringstromi* | Kretzoi, 1942 | *Shansirhinus ringstromi* | Shanxi, China |
| *Chilotherium yunnanensis* | Tang et al., 1974 | *Shansirhinus brancoi* | Yunan, China |
| *Chilotherium cornutum* | Qiu and Yan, 1982 | *Shansirhinus ringstromi* | Shanxi, China |

**Table 2** The main differences observed on the craniodental material of *Chilotherium schlosseri* (Weber, 1905) and *Eochilotherium samium* (Weber, 1905) from the Late Miocene of Samos Island in Greece (modified after Kampouridis et al. 2023: table S1)

| Feature | *Chilotherium schlosseri* | *Eochilotherium samium* |
|---|---|---|
| Size | Somewhat larger | Smaller |
| Skull shape | More brachycephalic, wider, dorsoventrally compressed, not raised posteriorly | More dolichocephalic, narrower, dorsoventrally higher, raised posteriorly |
| Nasal bones | Longitudinal groove present | Longitudinal groove very weak or absent |
| Frontal bones | Prominent depression in frontal bones | Convex frontal bones |
| Parietal crests | Widely separated | Moderately separated |
| Zygomatic arches | Posteriorly widening | Constant width |
| Orbit position | Upper border at similar level to nasal bones | Lower than nasal bones |
| Occipital condyles | Wide | Narrow and high |
| Foramen magnum | Dorsal incision | Dorsally rounded border |
| Occipital fossa | Deeper | Shallow |
| Lateral occipital crests | Broad and not marked | Narrow and more pronounced |
| Outer lateral crests | Subtle and rounded | More prominent and longer |
| Median valley | Closing at early wear stage in premolars | Closing late or not at all |
| Protocone constriction | Very strong in premolars, molars | Weak or absent in premolars, strong in molars |
| Enamel plications on upper dentition | Sometimes present | Absent |

"*Chilotherium*" *primigenium* Deng, 2006a, also seem to be more similar to *E. samium* than to other *Chilotherium* species and should be excluded from this genus, either belonging to *Eochilotherium* Geraads and Spassov, 2009, or to a different genus. The study of Kampouridis et al. (2023) conducted such a revision of the Samian chilotheres by offering detailed descriptions and comparisons of the neotypes of the two chilothere species from Samos, along with diagnoses that clearly separate them from each other and from any other rhino species. However, it focused only on the two neotype skulls and their associated mandibles. There are several other skulls, mandibles and more fragmentary elements that would elucidate the relationship between these two hornless rhino species and assess their intraspecific variability.

Accordingly, the goal of the present work is to describe and compare all available skulls that can be assigned to *Chilotherium schlosseri* from the Upper Miocene horizons of Samos Island that are scattered throughout different institutions and provide a detailed overview of morphological variation of this species. Both skulls and mandibles are examined and compared to relevant chilothere species, evaluating the variability of *C. schlosseri*. This way, we aim to confirm the number of hornless rhinos co-occurring in Samos during the Late Miocene, as well as their interspecific abundance.

**Table 3** Distance between the parietal crests of all available *Chilotherium schlosseri* ( Weber, 1905 ) skulls from the Late Miocene of Samos Island (Greece) and the Chilotheriina species discussed in text

| Specimen or taxon | Distance (mm) | *N* | Source |
|---|---|---|---|
| Lectotype of *Chilotherium schlosseri* | 90 | - | Weber (1905) |
| Holotype of *Chilotherium angustifrons* | 70 | - | Andree (1921) |
| Holotype of *Chilotherium wegneri* | 87 | - | Andree (1921) |
| GPIH 3015 (neotype of *Chilotherium schlosseri*) | 89 | - | Present study |
| NHMW-GEO-1911/0005/0128 | 71 | - | Present study |
| HLMD-Sam192 | 72 | - | Present study |
| NMB-Sam.25 | 75 | - | Present study |
| AMNH-20794 | 100 | - | Present study |
| MGP-PD 25302 | 71.3 | - | Present study |
| AMPG-SAM513 | 75.5 | - | Present study |
| AMPG-SAM508 | 80 | - | Present study |
| AMPG-SAM510 | 72 | - | Present study |
| *Chilotherium schlosseri* (Weber, 1905) | 71–100 | 12 | Andree (1921); own data |
| *Eochilotherium samium* (Weber, 1905) | ~40 | 2 | Andree (1921); Kampouridis et al. (2023) |
| *Chilotherium persiae* (Pohlig, 1886) | 36.5–53.7 | 11 | Kampouridis et al. (2023) |
| *Chilotherium habereri* (Schlosser, 1903) | 42–60 | 9 | Killgus (1922); Ringström (1924) |
| *Chilotherium kowalevskii* (Pavlow, 1913) | 40.1–66 | 10 | Krokos (1917) |
| *Chilotherium anderssoni* Ringström, 1924 | 50–63 | 5 | Ringström (1924) |
| *"Chilotherium" wimani* Ringström, 1924 | 15.3–66.7 | 57 | Chen et al. (2010) |
| *Chilotherium sarmaticum* Korotkevich, 1958 | 51-76.2 | 4 | Korotkevich (1970) |
| *Chilotherium orlovi* Bayshashov, 1982 | 45–75 | 3 | Bayshashov (1982) |
| *"Chilotherium" primigenium* Deng, 2006b | 18 | 1 | Deng (2006b) |

## History of the Samos excavations

The palaeontological wealth of the Island of Samos has sparked the interest of researchers from Europe from the

early 1850 s until the first decade of the 21 st century. The first systematic excavations on the island were conducted in 1885–1887 and 1889 by C. Forsyth Major, in the sites Adrianos ravine, Potamies ravine, and Stefana. German scientists T. Stutzel and A. Hentschel also contributed to the excavations on the island between 1897 and 1902 (Schlosser 1903; Andrée 1926). In 1901, the renowned German paleontologist E. Fraas carried out new excavations on the island (Koufos 2009). Later on, the famed American "fossil hunter" B. Brown excavated a notable number of specimens (Brown 1927). Additionally, during the same time, several lesser-known excavation campaigns, often not organized by palaeontologists, took place (e.g., Gürich 1911; Andrée 1921; Drevermann 1930). The material of these excavations was transferred to different institutions around the world, where it is housed today.

As far as Greek researchers are concerned, the Samian doctor A. Stefanidis from Mytilinii village was among the pioneers of excavating and collecting fossils. In 1879, Stefanidis delivered a number of his collected specimens to Professor I. Mitzopoulos (University of Athens), though he never received any response from the professor. The whereabouts of this collection are currently unknown. Eventually, Stefanidis, who kept collecting fossils, gave his collection to C. Forsyth Major the second time the British expatriate came to Samos, in 1887; this collection, along with the rest of the material Forsyth-Major collected in Samos, is now housed in the museums of Geneva, Basel and Lausanne (Koufos 2009).

The curator of the Athens Museum of Palaeontology and Geology and later University of Athens Professor, T. Skoufos, was the first Greek academic to lead an organized excavation in the sites Adrianos, Katikoumena, Bartzikos and Bailntaki in 1903 (Koufos 2009). Postdating Skoufos, Aristotle University of Thessaloniki Professor I. Melentis conducted two new excavations at the fossiliferous site Mytilinii-1 A (MTLA) of Adrianos ravine, in 1963 and 1985 (Melentis 1968; Koufos 2009). In 1976, N. Solounias led new excavations on the island under the auspices of University of Colorado (Black et al. 1980; Solounias and Ring 2007). Solounias was the first to also excavate for small mammals, which were found in locality S3 (Solounias and Ring 2007). The latest systematic excavations in Samos were led by Aristotle University of Thessaloniki Professors G. Koufos and D. Kostopoulos between 1990 and 2006, shedding light on an immense number of specimens and resolving important issues on the stratigraphy and palaeoecology of the island's fossiliferous localities (Koufos 2009).

## Geological and stratigraphical context

The illustrious fossiliferous strata of Samos are part of the Mytilinii Formation, situated in the northwestern part of Mytilinii Basin, one of the three Neogene depressions present on the island (Mountrakis et al. 2003). The latter is characterized by a complicated stratigraphy, which has been an issue of study since the 19th century (Kostopoulos et al. 2009 and references therein). According to the most recent work of Kostopoulos et al. (2009), the vast majority of the fossils are found in the Main Bone Beds Member of the Mytilinii Formation, which consists mainly of brownish to reddish silty sands, along with yellow to brownish conglomerates, tuffaceous sandstones and white tuffites. The formation is overlain by tuffaceous red sandy silts with insertions of massive tuffs (Kostopoulos et al. 2009).

One major problem concerning the study of the Samos fauna is the striking lack of adequate stratigraphic data. The various excavations were led by different scientists, each one using their own methods for documenting their findings. Consequently, the same locality can be found in the literature under different names. Additionally, many specimens originate from unknown fossiliferous horizons. Thus, stratigraphic correlations between the different collections of fossil material from Samos, including the material studied herein, are not possible (Kostopoulos et al. 2009).

**Institutional abbreviations: AMNH**, American Museum of Natural History, USA; **AMPG**, Athens Museum of Palaeontology and Geology of the National and Kapodistrian University of Athens, Greece; **GMM**, Geomuseum der Universität Münster, Germany; **GPIH**, Geologisch-Paläontologisches Institut der Universität Hamburg, Germany; **GPIT**, Geologisch-Palaeontologisches Institut Tübingen, Germany; **HLMD**, Hessisches Landesmuseum Darmstadt, Germany; **MGP-PD**, Museo di Geologia e Paleontologia, Padua, Italy; **MNHN**, Muséum national d' Histoire naturelle, Paris, France; **NHMW**, Naturhistorisches Museum Wien, Austria; and **NMB**, Naturhistorisches Museum Basel, Switzerland.

## Systematic palaeontology

Mammalia Linnaeus, 1758
Perissodactyla Owen, 1848
Rhinocerotidae Gray, 1821
Aceratheriinae Dollo, 1885 (sensu Lu et al. 2023)
Aceratheriini Dollo, 1885 (sensu Lu et al. 2023)
Chilotheriina Qiu et al., 1987 (sensu Kampouridis et al. 2023)

**Included genera**: *Chilotherium* Ringström, 1924; *Shansirhinus* Kretzoi, 1942; and *Eochilotherium* Geraads and Spassov, 2009.

**Remarks**: The name Chilotheriini was originally proposed by Qiu et al. (1987) for a tribe that would encompass the genera *Acerorhinus* and *Chilotherium*, and to specifically exclude the more plesiomorphic genus *Aceratherium*. However, it has not yet been possible to prove that this comprises a monophyletic group. In fact, *Acerorhinus* shows many plesiomorphic characters separating it from representatives of the genus *Chilotherium*. It is therefore considered best to remove *Acerorhinus* from this group. Following the recommendation of Kampouridis et al. (2023), we herein use the name Chilotheriina at a subtribe rank that includes the genera *Chilotherium*, *Shansirhinus*, and *Eochilotherium*.

Genus *Chilotherium* Ringström, 1924

**Type species**: *Chilotherium anderssoni* Ringström, 1924

**Other included species**: *Chilotherium persiae* (Pohlig, 1886); *Chilotherium habereri* (Schlosser, 1903); *Chilotherium schlosseri* (Weber, 1905); *Chilotherium kowalevskii* (Pavlow, 1913); *Chilotherium sarmaticum* Korotkevich, 1958; *Chilotherium orlovi* Bayshashov, 1982; *Chilotherium licenti* Sun et al. 2018, and possibly *"Chilotherium" wimani* Ringström, 1924 and *"Chilotherium" primigenium* Deng 2006b.

**Diagnosis**: Aceratheriine rhinocerotids that bear the following features: flat and wide skull; flattened and depressed frontal region; absence of horn-bosses, suggesting the absence of keratin horns; well-developed postorbital processes; moderately to widely separated parietal crests; highly placed orbits; very wide mandibular symphysis that features a concave ventral side; very large, flattened, tusk-like second lower incisors, with a scalene triangle cross section and upturned, dorsomedially oriented wear facets; reduced premaxillary bones that lack upper incisors; and very strong secondary enamel folds, including a lingually flattened and strongly constricted protocone in the upper molars. The genus is also characterised by a relatively short length of the premolars compared with the molars, mainly due to the reduced size of the P2 and p2; and notably shortened metapodials and relative robust appendicular skeleton (modified after Ringström 1924; Geraads and Spassov 2009; Giaourtsakis 2022; Kampouridis et al. 2023).

**Remarks**: The validity of the different *Chilotherium* species and their potential synonymies have been debated for many years (see Kiernik 1913; Krokos 1917; Ringström 1924; Deng 2001; Kampouridis et al. 2022). We herein follow Geraads and Koufos (1990) and Kampouridis et al. (2023) and exclude *E. samium* from the genus *Chilotherium* and consider the species *"C." wimani* and *"C." primigenium* most likely not belonging to *Chilotherium*. Additionally, we consider *C. schlosseri* from Samos, *C. kowalevskii* from Grebeniki and *C. sarmaticum* from Berislav as distinct species, pending a comprehensive revision of the type material of these species. Many studies have argued in favour of *C. schlosseri* representing the senior synonym of *C. kowalevskii* (e.g., Krokos 1917; Korotkevich 1970; Antoine and Sen 2016; Țibuleac et al. 2023). Nevertheless, in *C. schlosseri* the parietal crests are much more widely separated, with the measured values not exhibiting any overlap. Moreover, the upper premolars of *C. kowalevskii* lack the complex enamel plications and the closed medifossette present in *C. schlosseri*. Korotkevich (1970) showed that *C. sarmaticum* from Berislav can be differentiated from *C. kowalevskii* from Grebeniki based on the postcranial material.

*Chilotherium schlosseri* (Weber, 1905)

**Neotype**: a well-preserved skull (GPIH 3015) with an associated mandible (GPIH 3015a), designated by Kampouridis et al. (2023).

**Type locality**: Upper Miocene deposits of Samos Island; precise locality unknown.

**Junior synonyms**: *Teleoceras ponticus* Niezabitowski, 1912; *Aceratherium wegneri* Andrée, 1921; *Aceratherium angustifrons* Andrée, 1921.

**Diagnosis**: A large *Chilotherium* species characterised by widely separated parietal crests (minimal distance between parietal crests always over 70 mm in adult individuals), frontal region notably depressed in the middle, constriction of the protocone very strong;constriction of the protocone very strong;nasal bones that bear a central longitudinal groove on the dorsal side, and a unique combination of dental characters: crochet very long; mesial and distal constriction of the protocone very strong; protoloph lingually flattened; antecrochet very long; median valley usually closed off the at an early wear stage in all teeth; mesial constriction of the hypocone prominent; crista frequently present on the premolars; medifossette normally closed; lingual cingulum discontinuous and occasionally moderately developed in the upper premolars; prefossette often closed on P2; enamel plications sporadically present in the upper teeth; lingual and buccal cingulids discontinuous in the lower teeth (after Kampouridis et al. 2023).

**Referred material**: AMNH 20794, complete skull with associated mandible; AMPG-SAM513, complete skull missing nasal and premaxillary bones; AMPG-SAM503, partial skull; AMPG-SAM506, partial skull; AMPG-SAM508, partial skull; AMPG-SAM509, partial skull; AMPG-SAM510, partial skull; GPIH 3015, complete skull with associated mandible; HLMD-Sam192, complete skull, with reconstructed posterior portion of dorsal surface; MGP-PD 25302, complete skull; NHMW-GEO-1911/0005/0128, complete skull; NHMW-GEO-2009z0088/0001, complete skull with deciduous teeth, missing premaxillary bones; NMB-Sam.25, complete skull with associated mandible; AMNH 22815, mandible; AMPG-SAM500, mandible; NHMW-GEO-1911/0005/0032, mandible; NHMW-GEO-1911/0005/0033; mandible (Fig. 1).

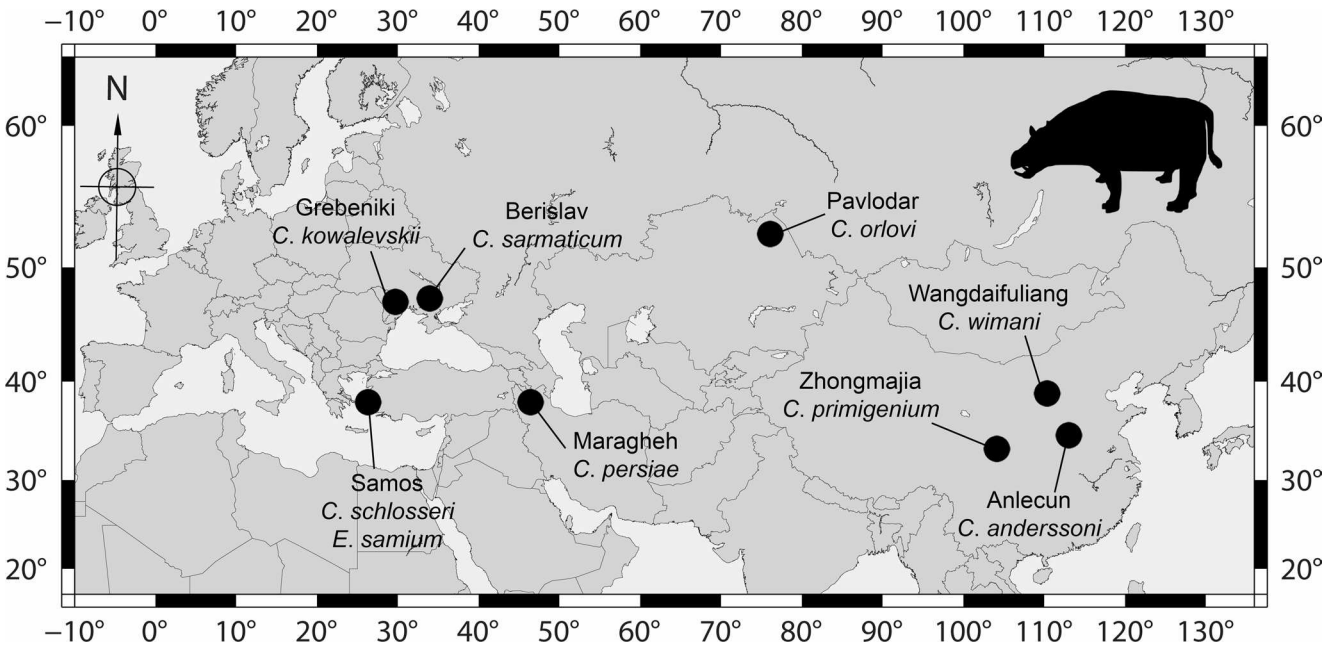


**Fig. 1** Map of the type localities of the species of *Chilotherium* and *Eochilotherium* discussed in the text. The map was created using Generic Mapping Tool (GMT) 6

Source of the silhouette of *C. anderssoni*: phylopic.org (by Zimices; CC BY-SA 3.0)

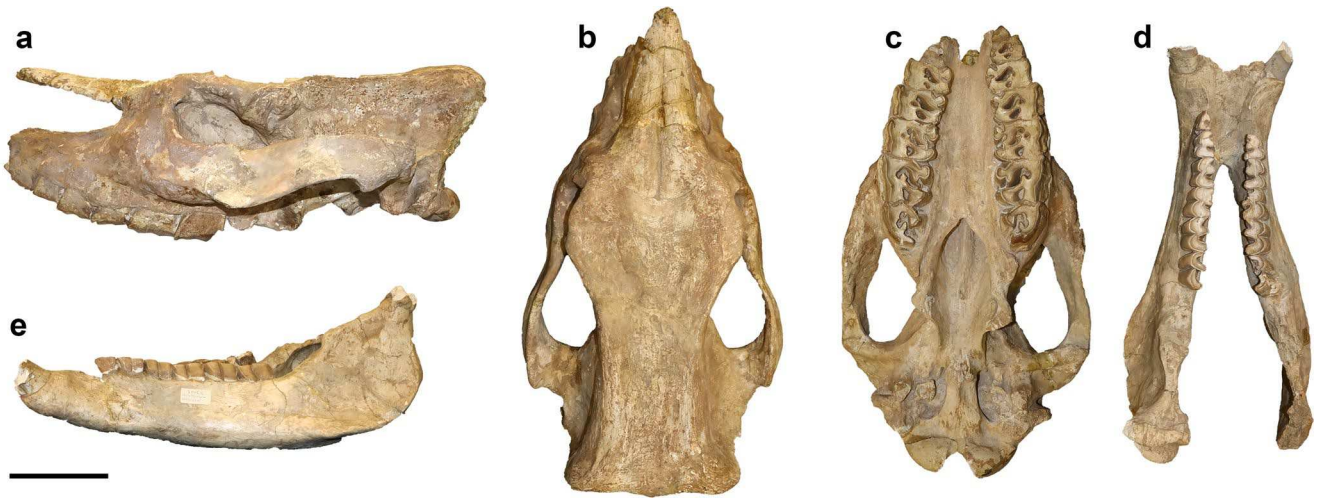


**Fig. 2** Neotype of the hornless rhinoceros *Chilotherium schlosseri* (Weber, 1905) (GPIH 3015) from the Upper Miocene of Samos Island, Greece. **a-c.** skull in lateral (**a**), dorsal (**b**) and ventral (**c**) views; **d-e.** mandible in dorsal (**d**) and lateral (**e**) view. Scale bar equals 10 cm

**Remarks**: Numerous *C. schlosseri* skulls and mandibles from Samos Island are housed in various European and American collections. Most are in an adequate preservation stage, though missing certain parts. Consequently, the descriptions will be based on observations from the whole of the available material. *Chilotherium schlosseri* is the first described species of the genus from Europe (Weber 1905). It was described based on material from Samos and was recently revised (Kampouridis et al. 2023). The neotype shares all diagnostic traits with the referred material (Fig. 2). More specifically, the neotype has a deep depression in its frontal bones, which also leads to more ventrally placed nasal bones, in lateral view. This is also visible in several studied specimens, like GPIH 3015, NMB-Sam.25, and MGP-PD 25302 (Fig. 3). *Chilotherium schlosseri* exhibits the most widely separated parietal crests (always over 70 mm in adult specimens) among the representatives of the genus. This is also also the case in all studied specimens, where the parietal crests are observed. Furthermore, the upper dentition of our studied material is identical with the *C. schlosseri* material available in the literature (Weber 1905; Andrée 1921; Giaourtsakis 2022; Kampouridis et

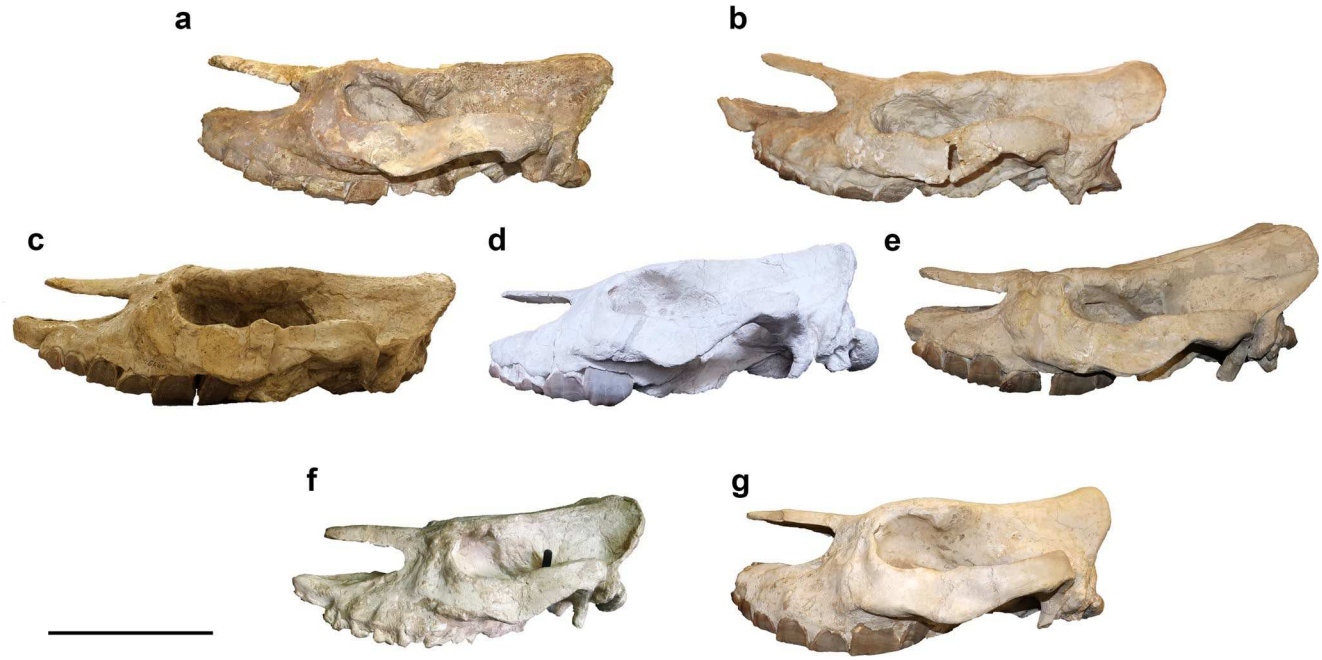


**Fig. 3** Skulls of the hornless rhinocerotid *Chilotherium schlosseri* (Weber, 1905) from the Upper Miocene of Samos Island, Greece, in lateral view **a.** GPIH 3015; **b.** MGP-PD 25302; **c.** AMNH 20794; **d.** NHMW-GEO-2009z0088/0001; **e.** NMB-Sam.25; **f.** NHMW-GEO-1911/0005/0128; **g.** HLMD-Sam192. Scale bar equals 10 cm

al. 2023), featuring extremely strong protocone constrictions and marked hypocone constriction, especially in the molars. The antecrochet is long, bending mesiolingually bending and closing off the median valley at an early wear stage in the premolars and at a moderate to advanced wear stage in the molars. A strong crochet is present in all teeth, a crista is frequently present and the medifossette usually closes at a moderate to advanced wear stage on P4 and M1. A characteristic trait for *C. schlosseri* is the variable presence of enamel plication in the upper dentition, which are also observable in many of the studied specimens. Thereby, the attribution of the studied material from Samos to this species is justified.

## Morphological description

### Skull

There are several almost complete and well-preserved skulls in the historical Samos collections, such as AMPG-SAM513, NHMW-GEO-1911/0005/0128 and NHMW-GEO-2009z0088/0001, HLMD-Sam192, and NMB-Sam.25. However, certain specimens are slightly deformed, such as the taphonomically transversally compressed skull NHMW-GEO-1911/0005/0128. Other are partially reconstructed with plaster, like NMB-Sam.25, in which the anterior part of the skull was broken off and then put back together incorrectly using plaster, leading to a distortion of the skull, and HLMD-Sam192, in which case most of the dorsal surface of the skull is covered in plaster, not allowing the detailed description of this region (Fig. 4).

The skull form ranges from slightly dolichocephalic (width/length ratio of ~42 in the transversally somewhat taphonomically compressed skull NHMW-GEO-1911/0005/0128 and ~43 in the juvenile skull NHMW-GEO-2009z0088/0001) to brachycephalic (width/length ratio of ~53 in HLMD-Sam192 and ~55 in NMB-Sam.25). It is worth noting that the oldest and youngest skulls amidst the referred material (NHMW-GEO-1911/0005/0128 and NHMW-GEO-2009z0088/0001 respectively) bear an almost identical skull width/length ratio, indicating that ontogeny has no impact on this feature. The skull is relatively short dorsoventrally. Although there are no horn bosses, the anterior tip of the nasal bones is somewhat rugose, a character most visible in the specimens GPIH 3015, NHMW-GEO-2009z0088/0001 and NMB-Sam.25 (Fig. 4). The frontal region is depressed in the middle, appearing transversally concave, affecting the position of the nasal bones. The latter remain separated, with a visible internasal suture until in most adult specimens, including the oldest available specimen NHMW-GEO-1911/0005/0128, in which even the M3 is heavily worn (Fig. 5). The region from the nasals to the parietal bones is notably depressed, with the parietal crests being very prominent, and widely separated (70–100 mm). The transversal development of the zygomatic arches seems to vary a little, but in all skulls, they tend to widen

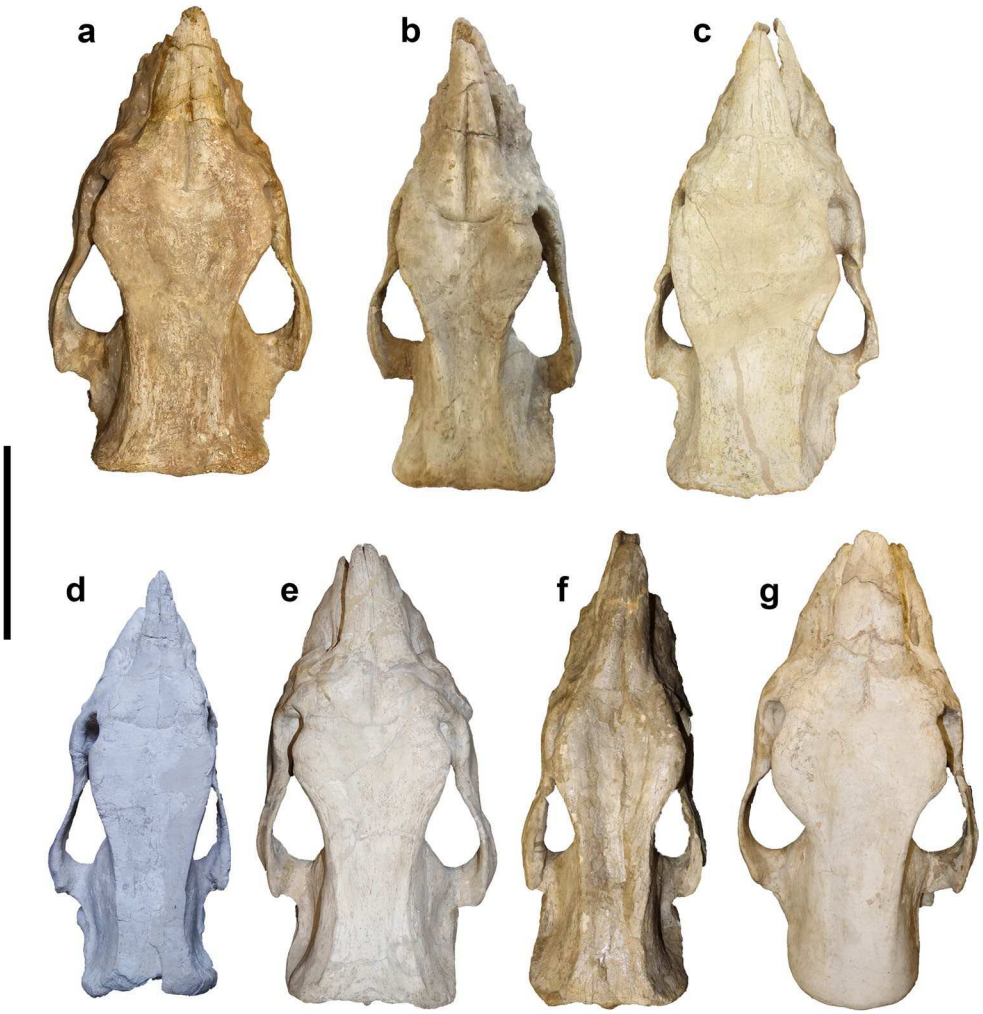


**Fig. 4** Skulls of the hornless rhinocerotid *Chilotherium schlosseri* (Weber, 1905) from the Upper Miocene of Samos Island, Greece, in dorsal view. **a.** GPIH 3015; **b.** MGP-PD 25302; **c.** AMNH 20794; **d.** NHMW-GEO-2009z0088/0001; **e.** NMB-Sam.25; **f.** NHMW-GEO-1911/0005/0128; **g.** HLMD-Sam192. Scale bar equals 10 cm

posteriorly. In lateral view, the nasal notch is deep, the exact position of its posterior border varying between the skulls from the level above the anterior part of the M2 to the level of the contact between the P4 and the M1. This feature also appears to be independent of the ontogeny of the specimens, as it is similarly positioned in both juvenile NHMW-GEO-2009z0088/0001 (a specimen of young ontogenetic age with deciduous dentition) and old NHMW-GEO-1911/0005/0128 (a specimen of old ontogenetic age, with deeply worn teeth).

Correlatively, the anterior margin of the orbit varies between the level of the middle of the M3 and the level of the middle of the M2. The distance between the orbit and the nasal notch is relatively short. The post-glenoid process extends further ventrally than the post-tympanic process, and the two remain well-separated. In posterior view, the occipital region is wide. Its dorsal part is fan-shaped. The occipital condyles are strong, very wide, and saddle shaped. In ventral view, the posterior border of the incisive foramen is located between P2 and P3 and the mesial border of the choanae is located anterior to M3 or mid of M3 in old individuals (M3 in wear), while in younger individuals, the incisive foramen is at the level of P2 and the mesial border of the choanae is located between M1 and M2. The shape of the postglenoidal apophysis varies from subtrapezoidal to elliptical, the hypoglossal foramen is located anteriorly on the condylar fossa and the sagittal crest is barely visible in all the specimens, with the exception of NHMW-GEO-2009z0088/0001, which belongs to a young individual with deciduous dentition).

### Upper dentition

Traces of cement are preserved in some of the specimens. The premolars have a quadrangular outline. Depending on the degree of the wearing of the enamel, the protocone and hypocone are either connected by a wide bridge or separated. The P2s bear an adamantine style and a lingual cingulum. They preserve a postfossette. A small, pointed crista is also present. The crochet is weak. The crista and crochet

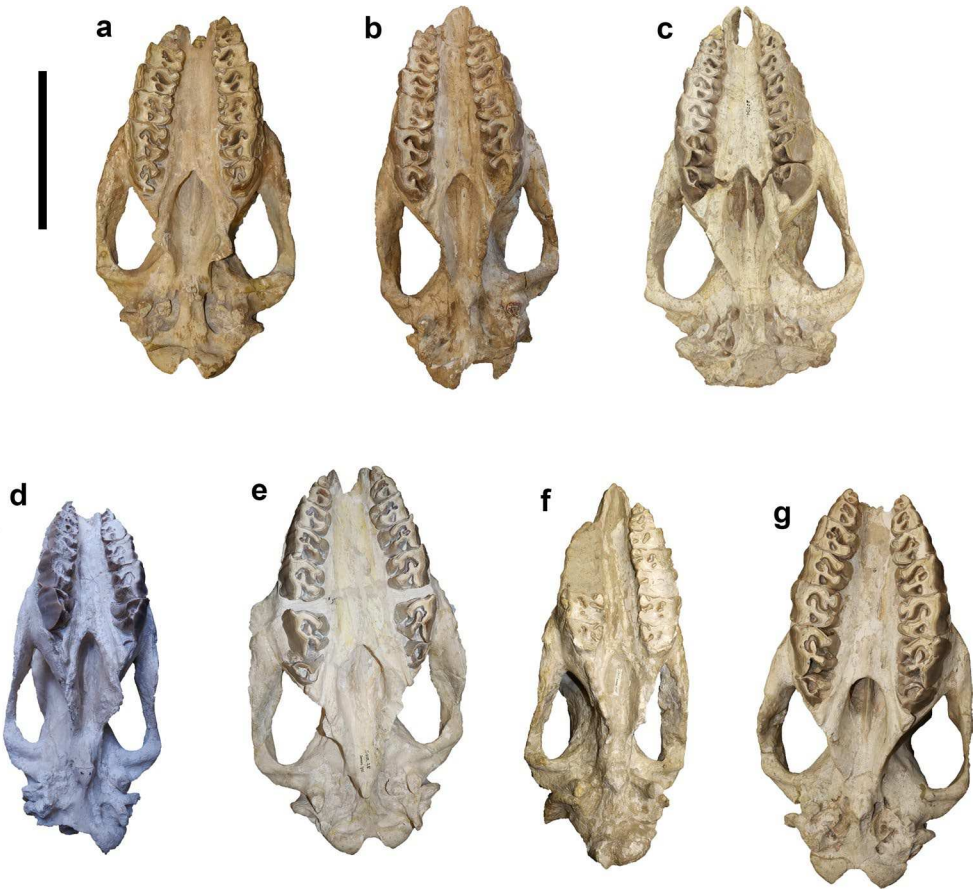


**Fig. 5** Skulls of the hornless rhinocerotid *Chilotherium schlosseri* (Weber, 1905) from the Upper Miocene of Samos Island, Greece, in ventral view. **a.** GPIH 3015; **b.** MGP-PD 25302; **c.** AMNH 20794; **d.** NHMW-GEO-2009z0088/0001; **e.** NMB-Sam.25; **f.** NHMW-GEO-1911/0005/0128; **g.** HLMD-Sam192. Scale bar equals 10 cm

are not joined. The antecrochet is smooth and rounded. The median valley is open. The parastyle extends mesially. The mesial part of the ectoloph is curved.

The P3s preserve cement traces both labially and, to a lesser degree, lingually. The protocone has a curved lingual margin. The hypocone constriction is weaker than that of the protocone. The antecrochet is smooth and rounded. The crista, when present, is very weak. The crochet is markedly curved. The postfossette is wide. The paracone and metacone folds are weak. A lingual cingulum is present. The parastyle is short, the metastyle is slightly longer and sharper. The median valley is narrow.

On the P4s, the protocone and hypocone, both well constricted, are roughly of the same size. The lingual margin of the protocone is almost straight. The antecrochet is thin. The paracone fold is weak. The crochet is well developed and markedly curved. On the contrary, the crista is miniscule. The postfossette is large and roughly triangular. The posterior wall is strong. The median valley is open lingually. The parastyle is stronger than the metastyle.

The M1s bear a very marked protocone constriction. The hypocone is also constricted, though to a lesser degree. The antecrochet is very strong and curved lingually. There is no crista. The crochet is strong and curved labially. The postfossette is triangular. The paracone fold is very weak, almost absent. A weak, discontinuous lingual cingulum is present.

The M2s bears a very sharp, mesially extended parastyle. The metastyle is long. The protocone is notably more constricted than the hypocone and has a roughly straight lingual margin. The crochet is very large and markedly curved labially, almost tear shaped. There is no crista. The antecrochet is present, though weak and rounded. There is no posterior wall. The posterior valley has a triangular outline. A lingual cingulum is also present.

The M3 preserves faint cement traces labially. It has a sharp parastyle. The ectoloph and metaloph are fused together, thus explaining the triangular outline of the tooth. The paracone fold is very weak. The crochet, though thin, is long and curved. A weak lingual cingulum is present. The posterior valley is wide.

As far as the deciduous upper dentition is concerned, some of the characters previously discussed are also present, as observed in the specimen NHMW-GEO-2009z0088/0001 (Fig. 6). The specimen bears a constricted protocone and hypocone as well as lingual cingula on the preserved teeth.

The DP3 bears a marked protocone constriction. A medifossette is present, as well as a lingual cingulum. The

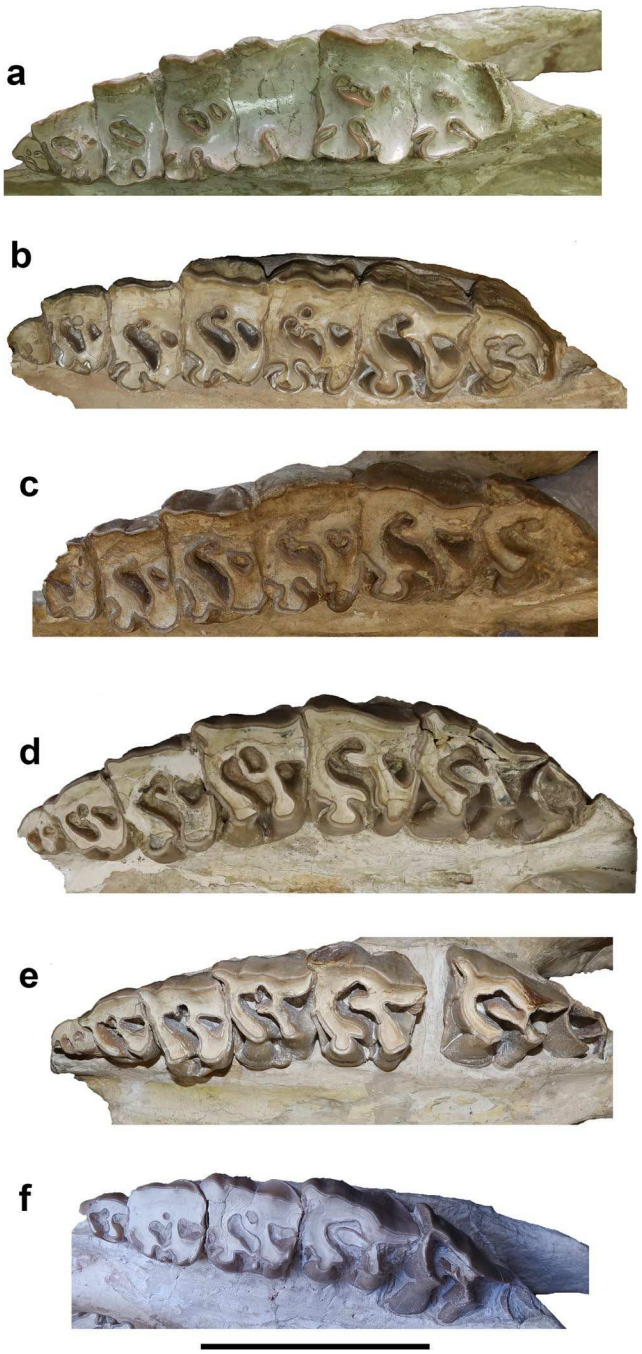


**Fig. 6** Ontogenetic series of upper dentition of the hornless rhinocerotid *Chilotherium schlosseri* (Weber, 1905) from the Upper Miocene of Samos Island, Greece, in occlusal view, from oldest (**a**) to youngest (**f**) - featuring a complete deciduous dentition - specimen. **a.** NHMW-GEO-1911/0005/0128; **b.** GPIH 3015; **c.** MGP-PD 25302; **d.** HLMD-Sam192; **e.** NMB-Sam.25; **f.** NHMW-GEO-2009z0088/0001. Scale bar equals 10 cm

antecrochet is elongated and lingually curved. The median valley is closed.

The DP4 bears a strong, elongated crochet and a short, pointed antecrochet. The postfossette, though in a mediocre preservation stage, is deep. The median valley remains open. A lingual cingulum is present.

### Mandible

The most notable characteristic of the mandible is the very wide symphysis, terminating posteriorly at the level of p3. The ascending ramus is preserved only on specimens AMNH 20794 and NMB-Sam.25 (Fig. 7). On AMNH 20794, which belongs to a male individual based on the large, dagger-like incisors (Chen et al. 2010), the ramus is markedly concave in lateral view. On the other hand, the ascending ramus of NMB-Sam.25, which based on the much shorter incisors belongs to a female individual, has a more concave shape in lateral view. The mandibular body is not very robust. Its base is nearly straight beneath the level of m3 to p2, gradually bending towards the symphysis. The angle between the body and the symphysis is somewhat more obtuse in NMB-Sam.25 compared to AMNH 20794. In lateral view, the foramen mentalis opens in front of p3. In the rostral part of the symphysis, a light sagittal linear groove is formed. In dorsal view, the referred material demonstrates a long diastema with a marked crista along the interalveolar margin.

### Lower dentition

Traces of cement are preserved in some of the specimens. The morphology of the lower dentition is simple and relatively uniform within the genus *Chilotherium*, bearing metalophids relatively longer than the paralophids, weakly constricted metaconids, relatively sharp trigonids and a deep ectolophid groove. The lower incisors are tusk-like, more or less straight in dorsal view and distinctly curved in lateral view, wide close to the basis, getting progressively narrower. They grow divergently. When partly preserved, the roots of the i1s are small and somewhat meniscus shaped (Fig. 8). The size of the lower incisors is indicative of strong sexual dimorphism in chilotheres, as they are larger in alleged male individuals compared to females (Chen et al. 2010).

## Comparison with non-chilothere aceratheriines

During the Turolian, three hornless rhinocerotid genera are present in Greece: derived *Chilotherium* and more "primitive" *Eochilotherium* and *Acerorhinus*. The type species of the latter genus is *Acerorhinus zernowi* (Borissiak, 1914). This species is well known from a rich collection of fossils from the Middle Miocene of Tung Gur in Mongolia (Cerdeño 1996). *Chilotherium schlosseri* presents significant differences with this species as well. *Acerorhinus zernowi* has narrowly separated parietal crests (Cerdeño 1996: fig. 2c), and a deeply concave dorsal skull profile, due to the


**Fig. 7** Mandibles of the hornless rhinocerotid *Chilotherium schlosseri* (Weber, 1905) from the Upper Miocene of Samos Island, Greece, in lateral view. **a.** AMNH 20794; **b.** NMB-Sam.25; **c.** AMNH 22815. Scale bar equals 10 cm


**Fig. 8** Mandibles of the hornless rhinocerotid *Chilotherium schlosseri* (Weber, 1905) from the Upper Miocene of Samos Island, Greece, in dorsal view. **a.** AMNH 20794; **b.** AMNH 22815; **c.** GPIH 3015; **d.** GMM SIII/1; **e.** NHMW-GEO-1911/0005/0032; **f.** NHMW-GEO-1911/0005/0033; **g.** AMPG-SAM500; **h.** GMM SIII/2. Scale bar equals 10 cm

prominent elevation of the occipital region (Cerdeño 1996: fig. 3a) compared to the well separated parietal crests and the flat dorsal skull profile of the studied skulls from Samos. The mandible of *A. zernowi* has a much narrower symphysis (Cerdeño 1996: fig. 3a) compared to the studied material. Furthermore, the upper dentition of *A. zernowi* lacks the strongly constricted protocone and the long, lingually bent antecrochet on the molars (Cerdeño 1996: fig. 4a) observed on the studied specimens.

The genus is represented in Greece by *Acerorhinus neleus* Athanassiou et al., 2014, first reported from the Turolian locality of Kerassia, Evia Island, but also present in the locality of Pikermi in Attica (Theodorou et al. 2003; Athanassiou et al. 2014; Kampouridis et al. 2019). There are several differences between the material under study and *A. neleus*: the dorsal profile of the Samos material is flat, with a notable depression in the frontal bones, whereas in *A. neleus* the skull is transversally convex and the dorsal profile is slightly concave (Athanassiou et al. 2014: pl. 1, fig. 3a–b); the parietal crests are less widely separated in *A. neleus* than in the Samos specimens (Athanassiou et al. 2014: table 1); the distance between the nasal incision and the rostral margin of the orbital fossa is longer in *A. neleus* (77 mm left and 88 mm right in *A. neleus*; Athanassiou et al. 2014: table 1), compared to 63.5–72.8 mm in the studied Samos material. The occipital region of *A. neleus* appeared to be bell-shaped and is dorsoventrally higher, compared with the wider and trapezium-like occipital region of the studied specimens (Athanassiou et al. 2014: pl. 1, fig. 3c). The mandibles from Samos bear one of the most notable apomorphies of the genus *Chilotherium*: the markedly wide symphysis (Ringström 1924), whereas in *A. neleus* the mandibular symphysis is much narrower. The diastema between i2 and p2 is longer and more curved in the Samos specimen than in *A. neleus*, and in lateral view, the anterior, incisors-bearing, part of the symphysis is straighter in the Samos specimens than in *A. neleus* (Athanassiou et al. 2014, pl. 2, fig. 2a–c).The upper teeth of the Samos specimens are generally more hypsodont compared to *A. neleus*, with a stronger protocone constriction, more pronounced and longer antecrochets and complicated enamel plications compared to *A. neleus* (Athanassiou et al. 2014: pl. 1, fig. 4a–b; pl. 2, fig. 1b). Finally, the Samos specimens bear shorter premolars mesio-distally, compared to *A. neleus* (Athanassiou et al. 2014). Thereby, the Samos material can easily be separated from that of *Acerorhinus*.

*Persiatherium rodleri* is an acerathere rhinocerotid from the early Upper Miocene of Maragheh, Iran, co-occurring with *C. persiae* (Pandolfi 2016) and coeval to the Samos fossil assemblage. As one badly preserved skull, preserving only a part of the basicranium and preserving M1-M2, D4, P3-P1 on the left hemimaxilla and M1-M2, D4, P3-P2 on the right hemimaxilla (Pandolfi 2016: fig. 2a), is the sole specimen available, the only possible comparison was with the available permanent dentition. Both the premolars and the molars of *P. rodleri* lack the marked protocone and hypocone constriction and the elongated, strong antecrochet that characterizes the referred material from Samos; additionally, the premolars of *P. rodleri* bear a notably strong, continuous lingual cingulum that is not present in the Samos material (Pandolfi 2016: fig. 2a, b).

## Comparison with *Eochilotherium samium*

Two valid species of hornless rhinocerotids are reported in the Upper Miocene deposits from Samos Island: *E. samium* and *C. schlosseri* (Kampouridis et al. 2023). *Eochilotherium samium* has had a strongly debated taxonomy (Fortelius et al. 2003; Geraads and Spassov 2009; Athanassiou et al. 2014; Kampouridis et al. 2023). *Chilotherium schlosseri* can be distinguished from *E. samium* based on the following morphological variations: the frontal region of *E. samium* is convex in the anterior part and flattens posteriorly, whereas *C. schlosseri* has a markedly concave frontal region. Furthermore, the parietal crests of *C. schlosseri* are more widely separated (at least 70 mm apart in all adult specimens) than in *E. samium*, in which they are roughly 40 mm apart (Kampouridis et al. 2023).

The upper dentition of *C. schlosseri* is characterized by a very strong protocone constriction, which results in a marked antecrochet closing off the median valley. On the other hand, in *E. samium* this constriction is weaker, with the median valley remaining open until very advanced wear stage. *Chilotherium schlosseri* also features a strong crochet and, consequently, a closed medifossette at an early to moderate wear stage, whereas in *E. samium* the crochet is weaker and the medifossette remains open until an advanced wear stage.

In terms of the mandible, the foramen mentalis of the studied material is located in front of p3, and the symphysis terminates posteriorly before p3. On the other hand, in the *E. samium* neotype the only visible foramen mentalis is located below p3, and the symphysis terminates posteriorly at the middle of the p3 (Kampouridis et al. 2023). Thereby, the attribution of the Samos specimens to *E. samium* can be excluded.

## Comparison with Chinese *Chilotherium* species

*Chilotherium schlosseri* from Samos was compared to the three chilotheres of the classical Chinese Linxia Basin: *"C." primigenium*, *"C." wimani*, and *C. anderssoni*. Small

aceratheriine *"C." primigenium* is the most primitive species of *Chilotherium* yet described, constituting the ancestral morphotype of the genus (Deng 2005). *"Chilotherium" wimani* also represents a primitive form of the genus. Both species were first described in the early Late Miocene of China (Deng 2001, 2005). *"Chilotherium" primigenium* presents numerous differences with most *Chilotherium* species, to the point that its belonging to the genus was recently questioned, as well as that of *"C." wimani* (Kampouridis et al. 2023). Some of those differences excluding *"C." primigenium* from other chilotheres are the very poorly separated parietal crests, which form a sagittal crest rearwards, the convex frontal bones with a posterior flattening, the narrowing of the parietal region, the short distance between the bases of i2 and p2, the dentition lacking the complex enamel folding of most chilotheres, the narrow nasal notch and the somewhat flat ventral surface of the symphysis, and the weak post-tympanic process.

Medium-sized *"C." wimani* is the dominant species in Linxia Basin (Deng 2006a). The main characters of this middle-sized aceratheriine are the transversal expansion of the mandibular symphysis and the upturned medial flange of the huge i2s (Chen et al. 2010). Compared to the cranial specimens under study, the parietal crests are only slightly separated, the zygomatic arch is narrow, and the orbita is in low position (Deng 2001, 2006a). Moreover, the upper dentition of *"C." wimani* features less strong crochets and small antecrochets (Deng 2001), the connection between the protocone and hypocone is quite narrow and no protocone constriction is visible (Ringström 1924; Deng 2001), markedly different from *C. schlosseri*. The mandible, as is a common trait of the genus, has a markedly wide symphysis. However, the mandibular symphysis terminates at the level of the middle of p3, where the foramen mentalis opens, while in *C. schlosseri* the same border is situated in front of the same tooth and the foramen mentalis opens in front of p3.

*Chilotherium anderssoni* comes from the Late Miocene of Loc. 30, Daijiagou, China; compared to the previous more primitive forms, it bears some of the more advanced features of the *Chilotherium* genus, such as the widely separated parietal crests, the long distance between i2 and p2, the thick posttympanic process, the wide nasal notch, and the concave ventral surface of the mandibular symphysis (Deng 2006a). However, the parietal crests of *C. anderssoni* are more narrowly separated and its upper dentition, complex as it is, is lacking the enamel plications that can be observed in *C. schlosseri*. Moreover, *C. Schlosseri* preserves a crista and a lingual cingulum on the upper molars, which are missing from *C. anderssoni* (Ringström 1924).

## Comparison with other Eurasian *Chilotherium* species

The specimens under study were also compared with a number of *Chilotherium* genera from the Late Miocene of Eurasia: *C. persiae*, *C. kowalevskii*, *C. sarmaticum* and *C. orlovi*.

*Chilotherium persiae* has been described from Maragheh, Iran, along with the tandem-horned *Diceros neumayri* Osborn, 1900, the huge elasmothere *Iranotherium morgani* (Mecquenem, 1908), and the acerathere *Persiatherium rodleri* (Pandolfi, 2016) (Pohlig 1886; Mecquenem 1908; Pandolfi 2016; Giaourtsakis 2022). Compared to *C. schlosseri*, *C. persiae* has less depressed frontals and a wider region before the orbit, the nasal incision is more rounded and smoother and the zygomatics are almost straight backwards. The dentition of *C. persiae* is also complex, similar to that of *C. schlosseri*. However, *C. persiae* is the only chilothere to bear a somewhat quadrangularly outlined M3 (Ringström 1924). Compared to *C. schlosseri*, the premolars of *C. persiae* bear a stronger and longer crochet, a more pointed crista and more pronounced paracone fold, while on the molars of the same species the antecrochet is less elongated. The mandibular symphysis is shorter in *C. persiae*, terminating at the mesial half of p2, instead of p3 as in *C. schlosseri*. The anterior part of the mandible is more markedly curved in *C. persiae*. This trait is easier to observe in juvenile mandibles compared to adult ones, indicating a potential correlation with the individual's ontogenetic stage, as this curve of the mandible probably facilitates the development of the tusks.

*Chilotherium kowalevskii* was originally described from the Upper Miocene of Grebeniki, Ukraine (Pavlow 1913). There are not many differences between *C. kowalevskii* and *C. schlosseri*. However, in *C. kowalevskii*, the frontal depression is less pronounced and the parietal parietal crests are less widely separated thank in *C. schlosseri*. Moreover, in lateral view, the zygomatics get posteriorly narrower more smoothly than in *C. schlosseri.* Unlike *C. schlosseri*, *Chilotherium kowalevskii* does not bear a closed medifossette on the upper premolars, the protocone and hypocone constriction is weaker, there is no crista present and the premolars do not have complex enamel plications. Additional differential characters can be detected looking at the morphology of the otic region, with the posttympanic process more narrow and straighter in *C. schlosseri* than in *C. kowalevskii*, and at the shape of the zygomatic arch, anteriorly higher in *C. kowalevskii*, in lateral view (Pavlow 1913).

*Chilotherium sarmaticum* comes from the Late Miocene locality of Berislav, Ukraine (Korotkevich 1958), and has also been reported from Romania and Bulgaria (Geraads & Spassov 2009; Kampouridis et al. 2022; Țibuleac et al.

2023). The main difference with *C. schlosseri* is, similarly to *C. kowalevskii*, the lack of enamel plications on the upper permanent dentition. Furthermore, in *C. sarmaticum* the distance between the parietal crests (51–76.2 mm; $N=4$) (Korotkevitch 1970) is generally shorter than *C. schlosseri* and overlaps only little, not reaching the extreme range of up to 100 mm seen in *C. schlosseri*. While in *C. sarmaticum* this distance can be greater than in *C. kowalevskii*, where it is between 40.1 and 66 mm (Krokos 1917), in *C. schlosseri* the mean value for this measurement is about 78 mm, thereby greater than the greatest value provided for *C. sarmaticum*.

*Chilotherium orlovi* has been reported from the Upper Miocene deposits of Pavlodar, Kazakhstan (Bayshashov 1982, 1993). In similar manner to *C. sarmaticum*, it has not been thoroughly studied after its first description and is rarely included in morphological and phylogenetical revisions of the genus. It is a fairly large chilothere, which shares many similarities with *C. schlosseri*. The dorsal profile of the skull is relatively flat in *C. orlovi*, similar to *C. schlosseri* and unlike some other species like *"C." primigenium*, *"C." wimani*, *C. kowalevskii* and *C. persiae*. The parietal crests can be up to 75 mm apart from each other, making it, along with *C. sarmaticum*, the only species that reaches the value range seen in *C. schlosseri*. As far as the upper dentition is concerned, the molars exhibit a marked protocone constriction and a very large antecrochet that may close off the median valley. The teeth also exhibit a strong crochet and in some molars a crista is visible. The medifossete is closed in the P2 and P3 and a prominent postfossette is visible. Additionally, there also seem to be few enamel plications visible in some teeth, which is fairly rare even within chilotheres (Bayshashov 1982, 1993). In conclusion, despite a few similarities present on the craniodental material of the two species, the most important feature in the comparison between *C. orlovi* and *C. schlosseri* is that the maximum distance between the parietal crests in *C. orlovi* (75 mm) remains smaller than the mean value of 78 mm at *C. schlosseri* (Bayshashov 1993).

## Discussion

### Diagnostic features of *C. schlosseri*

Under the scope of the present paper, we described all the skulls and mandibles of *C. schlosseri* available in numerous collections around Europe and the USA. We managed to conclude that *C. schlosseri* has certain craniodental features that allow for a comprehensive diagnosis of the species: depressed frontal bones; low position of the nasal bones with respect to the skull roof; presence of longitudinal groove on the nasal bones; widely separated parietal crests (>70 mm in adult specimens of various ontogenetic stages); complicated enamel folds and prevalent enamel plications on the upper dentition. As examined in the different specimens, the main aspects of the morphological characters where some intraspecific variability can be observed are the following: the skull-form, ranging from somewhat dolichocephalic to brachycephalic; the transversal development of the zygomatic arches; the exact position of the posterior border of the nasal notch, varying from the level above the anterior part of the M2 to the level of the contact between the P4 and the M1, and, respectively, the exact position of the anterior margin of the orbit, varying between the level above the middle of the M3 and the level above the middle of the M2; the shape of the postglenoidal apophysis ranging from subtrapezoidal to elliptical; the crochet and the crista usually lead to the closure of the medifossette. Furthermore, the most important morphological diagnostic character of the species, the width of the parietal crests, presents some morphometric variability: it is 64 mm in the youngest specimen examined in this work (NHMW-GEO-2009z0088/0001, juvenile individual that was not fully grown, with deciduous dentition), 89 mm and 100 mm in two similarly old adult individuals (neotype GPIH 3015 and AMNH 20794), 70 mm and 87 mm in two oldest individuals (NHMW-GEO-1911/0005/0128 and holotype of the species). Demonstrating that in all adult individuals the minimal distance between the parietal crests is always over 70 mm.

### Interspecific variability of craniodental features within *Chilotherium*

As previously discussed in the comparison chapters, many of these features are characterized by a marked variability among the different *Chilotherium* species. Chinese *C. anderssoni* features a prominent depression of the frontal region that does not affect the nasal bones. It also has widely separated parietal crests, yet to a lesser degree than *C. schlosseri*, while lacking the latter species' enamel plications on the upper dentition (Deng 2006a). *Chilotherium persiae* presents certain minor differences in the upper dentition along with flattened frontal bones, a wider preorbital region, a rounded nasal incision, straight zygomatics and a shorter mandibular symphysis, terminating at the mesial half of p2, instead of p3 as in the studied specimens. *Chilotherium kowalevskii* seems to lack a distinct frontal depression in contrast to *C. schlosseri*, as well as featuring narrower parietal crests and missing both a crista and any additional enamel plications on the upper dentition. The absence of enamel plication is also a main difference between *C. schlosseri* and *C. sarmaticum*, which also shares widely separated parietal crests, although this feature is much more prominent in *C.*

*schlosseri*. In general *C. schlosseri*, *C. sarmaticum*, and *C. orlovi* seem to be the only chilotheres where the parietal crests can have a minimal distance over 70 mm from each other, indicating, together with other characters such as the presence of a closed medifossette in the M1 and the premolars of *C. orlovi* (Bayshashov 1982) either a potential close relationship between these three species, or similar paleoecological adaptations. The more plesiomorphic species *E. samium*, *"C." primigenium* and *"C." wimani* feature an overall higher skull, thick nasal bones, convex frontal bones, narrowly separated parietal crests, and somewhat less complicated upper dentitions. *"C." primigenium* also has a narrow nasal notch, a shorter diastema between the i2 and p2, a ventrally flattened symphysis and a weak post-tympanic process. *"Chilotherium" wimani* bears a narrow zygomatic arch, a lowly positioned orbit and no protocone of the orbit.

## Biogeographical context and potential phylogenetic relations

Some chilotheres share specific morphological features, thus demonstrating a peculiar distribution of characters that may be affected by their biogeographical history. The widely separated parietal crests, a character that *C. schlosseri* shares with *C. sarmaticum* from Ukraine and *C. orlovi* from Kazakhstan, may indicate either a closer relationship between *C. schlosseri* and these two species than with other chilotheres, or similar palaeodietary habits, since the distance between the parietal crests is a character related to herbivory, as the parietal crests themselves represent attachment areas for the temporalis muscle, one of the main muscles associated with mastication. On the other hand, *C. persiae* from Iran and *C. kowalevskii* from Ukraine seem to be more distantly related to *C. schlosseri*, since they both lack the widely separated parietal crests, the strongly depressed frontal and nasal region, the flat dorsal profile of the skull, and usually the absence of a closed medifossette in the upper premolars. Additionally, in both *C. persiae* and *C. kowalevskii* the sutures between the nasal bones and between the nasal and the frontal bones seem to completely close in adult individuals *(C. persiae*: MNHN.F.MAR.3072 and *C. kowalevskii*: Pavlow 1914: pl. 5, fig. 31). Therefore, the morphological similarities observed between *C. schlosseri*, *C. sarmaticum*, and *C. orlovi* could either represent a close phylogenetic relationship or possibly similar palaeodietary habits. Based on the current data, it is not clear how they are related.

According to Kampouridis et al. (2023), C. *schlosseri*, *C. sarmaticum*, *C. kowalevskii*, *C. persiae*, *C. orlovi*, and *C. anderssoni* belong to *Chilotherium* sensu stricto, showcasing all apomorphies of the genus, such as complex upper dentition, wide mandibular symphysis and well separated parietal crests. Within *Chilotherium* sensu stricto, certain morphological features seem to separate the genus into distinct morpho-groups. If they are considered to be of phylogenetic value, it would mean *C. schlosseri*, *C. sarmaticum*, and *C. orlovi* are more closely related to each other than to *C. kowalevskii* and *C. persiae*. Additionally, *E. samium* is only distantly related to all of these species, as it does not exhibit any of the apomorphies of *Chilotherium*. This would mean that there must have been at least three different dispersal events from Eastern Asia, where the most primitive chilotheres originated (Deng 2006b), to the West, that led to the establishment of the European and western Asian chilotheres. The exact timing of these dispersal events cannot currently be assessed. The chilotheres vanished by the end of the Miocene from Europe, marking the end for the once abundant and diverse aceratheriines, or hornless rhinos, that inhabited the subcontinent for several millions of years.

**Acknowledgements** We would like to express our gratitude to S. Roussiakis, G. Theodorou, E. Koskeridou (AMPG), J. Meng (AMNH), O. Sandrock, M. Blume, M. Kollbacher (HLMD), U. Kothoff (GPIH), M. Böhme, I. Werneburg (GPIT), L. Gorobets (Kyiv), C. Argot (MNHN), U. Göhlich, F. Zachos, A. Bibl (NHMW), L. Costeur, F. Dammeyer (NMB), and R. Brocke, G. Riedel, L. Kraus (SMF) for allowing us to study material under their care. We would also like to thank the reviewers P.-O. Antoine and D. Geraads for their thorough and valuable remarks on our manuscript and Associate Editor P. Coster for her fast and reliable handling of the manuscript.

**Author contributions** All authors contributed to the study conception and design. GS and PK wrote the main manuscript text. All authors reviewed the manuscript.

**Funding** Open access funding provided by HEAL-Link Greece. GS was financially supported by the Hellenic Foundation for Research and Innovation (4th Call for H.F.R.I. Scholarships for PHD Candidates). PK received support from the SYNTHESYS+project http://www.synthesys.info/ which is financed by European Community Research Infrastructure Action under the H2020 Integrating Activities Programme, Project number 823827 (AT-TAF-TA3-9 and AT-TAF-TA4-29 and FR-TAF-TA4-71). NK was financially supported by the Spanish Ministry of Science, Innovation, and Universities ("Juan de la Cierva Formación", ref. JDC2023-051158-I), the American Museum of Natural History (Collection Study Grant Program), and the Deutscher Akademischer Austauschdienst (Research Grants – One-Year Grants for Doctoral Candidates 2021/22, ref. 57552339).

**Data availability** No datasets were generated or analysed during the current study.

## Declarations

**Competing interests** The authors declare no competing interests.

## References

Andrée J (1921) Rhinocerotiden aus dem Unterpliocän von Samos. Paläontol Z 20:189–212

Andrée J (1926) Neue Cavicornier aus dem Pliocän von Samos. Palaeontogr 65:135–175

Antoine PO, Sen S (2016) Rhinocerotidae and Chalicotheriidae (Perissodactyla, Tapiromorpha). Geodiversitas 38(2):245–259

Antoine PO, Becker D, Pandolfi L, Geraads D (2025) Evolution and Fossil Record of Old World Rhinocerotidae. In: Melletti M, Talukdar B, Balfour D (eds) Rhinos of the World. Fascinating Life Sciences. Cham: Springer Nature Switzerland, pp 31–48. https://doi.org/10.1007/978-3-031-67169-2_2

Athanassiou A, Roussiakis SJ, Giaourtsakis IX, Theodorou GE, Iliopoulos G (2014) A new hornless rhinoceros of the genus *Aceratherium* (Perissodactyla: Rhinocerotidae) from the Upper Miocene of Kerassiá (Euboea, Greece), with a revision of related forms. Palaeontogr Abt A 303(1–3):23–59

Bayshashov BU (1982) A new rhinoceros species of the genus *Chilotherium* from Pavlodar. In: Mesozoic and Cenozoic Vertebrate Fauna and Flora of North-eastern and Southern Kazakhstan. Academy of Sciences of Kazakhstan, Almaty, Kazakhstan, pp 72–83

Bayshashov BU (1993) Neogene Rhinoceroses of Kazakhstan. Almaty Gleimei, Kazakhstan

Black CC, Krishtalka L, Solounias N (1980) Mammalian fossils of Samos and Pikermi. Part 1. The Turolian rodents and insectivores of Samos. Ann Carnegie Mus 49:359–378

Borissiak A (1914) Mammifères fossiles de Sébastopol. Mem Com Geol 87:105–154

Brown B (1927) Samos-Romantic Island of the Aegean. Nat Hist 27:19–32

Cerdeño E (1996) Rhinocerotidae from the Middle Miocene of the Tung-gur Formation, Inner Mongolia (China). Am Mus Novit 3184:1–43

Chen S, Deng T, Hou S, Shi Q, Pang L (2010) Sexual dimorphism in perissodactyl rhinocerotid *Chilotherium wimani* from the late Miocene of the Linxia Basin (Gansu, China). Acta Palaeontol Pol 55(4):587–597

Deng T (2001) New material of *Chilotherium wimani* (Perissodactyla, Rhinocerotidae) from the Late Miocene of Fugu, Shaanxi. Vertebr Palasiat 39(2):129–138

Deng T (2005) New cranial material of *Shansirhinus* (Rhinocerotidae, Perissodactyla) from the Lower Pliocene of the Linxia Basin in Gansu, China. Geobios 38(3):301–313. https://doi.org/10.1016/j.geobios.2003.12.003

Deng T (2006a) Neogene rhinoceroses of the Linxia Basin (Gansu, China). Cour Forsch Senk 256:43–56

Deng T (2006b) A primitive species of *Chilotherium* (Perissodactyla, Rhinocerotidae) from the Late Miocene of Linxia Basin (Gansu, China). Cainoz Res 5(1–2):93–102

Deng T, Lu X, Sun D, Li S (2023) Rhinocerotoid fossils of the Linxia Basin in northwestern China as late Cenozoic biostratigraphic markers. Palaeogeogr Palaeoclimatol Palaeoecol 614:111427

Dollo L (1885) Rhinocéros vivants et fossiles. Rev Quest Sci 17:293–299

Drevermann F (1930) Zeit des dreizehigen Pferdes. Nat Mus 60(1):2–13

Fortelius M, Heissig K, Saraç G, Sen S (2003) Rhinocerotidae (Perissodactyla). In: Fortelius M, Kappelman J, Sen S, Bernor RL (eds) Geology and Paleontology of the Miocene Sinap Formation, Turkey. Columbia University Press, New York, pp 282–307

Geraads D, Koufos GD (1990) Upper Miocene Rhinocerotidae (Mammalia) from Pentalophos-1, Macedonia, Greece. Palaeontogr Abt A 210(4):151

Geraads D, Spassov N (2009) Rhinocerotidae (Mammalia) from the Late Miocene of Bulgaria. Palaeontogr Abt A 287(46):99–122. https://doi.org/10.1127/pala/287/2009/99

Giaourtsakis IX (2022) The fossil record of rhinocerotids (Mammalia: Perissodactyla: Rhinocerotidae) in Greece. In: Vlachos E (ed) Fossil Vertebrates of Greece Vol. 2: Laurasiatherians, Artiodactyles, Perissodactyles, Carnivorans, and Island Endemics. Springer International Publishing, Cham, Switzerland, pp 409–500

Gray JE (1821) On the natural arrangemenet of vertebrose animals. Lond Med Repos 15:297–310

Gürich, G. (1911). Fossile Säugetierreste aus Samos. Verh Naturwiss Ver Hamburg 3(19):79

Heissig K (1975) Rhinocerotidae aus dem Jungtertiär Anatoliens. Geol Jahrb (B) 15:145–151

Ji HX, Xu QQ, Huang WB (1980) The Hipparion fauna from Guizhong Basin, Xizang. In: Qinghai–Tibetan Plateau Comprehensive Scientific Investigation Team of Chinese Academy of Sciences (ed) Palaeontology of Xizang, Book 1 , The Comprehensive Scientific Expedition to the Qinghai-Xizang Plateau of the Chinese Academy of Sciences. Science Press, Beijing, China, pp 18–32

Kampouridis P, Roussiakis S, Kargopoulos N, Giaourtsakis I, Dimakopoulos G, Iliopoulos G, Svorligkou G, Theodorou G (2019) Faunal diversity at the Turolian locality of Kerassia (northern Euboea, Greece). Bull Geol Soc Greece Spec Publ 7(122):52–53

Kampouridis P, Svorligkou G, Kargopoulos N, Augustin F J (2022) Reassessment of '*Chilotherium wegneri*' (Mammalia, Rhinocerotidae) from the late Miocene of Samos (Greece) and the European record of *Chilotherium*. Hist Biol 34(3):412–420 https://doi.org/10.1080/08912963.2021.1920939

Kampouridis P, Svorligkou G, Kargopoulos N, Spassov N, Böhme M (2023) Revision of the Late Miocene hornless rhinocerotids from Samos Island (Greece) with the designation of neotypes and implications for the European chilotheres. J Vertebr Paleontol 43(1):e2254360

Kiernik E (1913) Über einen Aceratheriumschädel aus der Umgebung von Odessa. Bull Int Acad Sci Crac 1913:808–864

Killgus H (1922) Die Unterpliocaenen Chinesischen Säugetierreste der Tafelschen Sammlung zu Tübingen. Dissertation, Eberhard-Karls University of Tübingen

Korotkevich O L (1958) A new *Chilotherium* species from the Sarmatian deposits of the Ukraine. Dopov Akad Nauk Ukr RSR 12:1372–1376

Korotkevich O L (1970) The mammals of the Berislav late Sarmatian Hipparion-fauna. Nat Environ Fauna Past 5: 24–121

Kostopoulos DS, Koufos GD, Sylvestrou IA, Syrides GE, Tsombachidou E (2009) The Late Miocene mammal faunas of the Mytilinii Basin, Samos Island, Greece: New collection. 2. Lithostratigraphy and fossiliferous sites. Beitr Pal 31:13–26

Koufos GD (2009) The Late Miocene mammal faunas of the Mytilinii Basin, Samos Island, Greece: New collection. 1. History of the Samos fossil mammals. Beitr Pal 31:1–12

Kretzoi M (1942) Bemerkungen zum System der Nachmiozänen Nashorn-Gattungen. Földt Közlöny 72(1):4–12

Krokos WI (1917) *Aceratherium schlosseri* Web. du village de Grebeniki du gouvernement de Kherson. Mem Agricl Soc S Rus 82(2):1–96

Linnaeus C (1758). Systema Naturae. Laurentii Salvii, Stockholm

Lu XK, Deng T, Pandolfi L (2023) Reconstructing the phylogeny of the hornless rhinoceros Aceratheriinae. Front Ecol Evol 11:1005126. https://doi.org/10.3389/fevo.2023.1005126

Mecquenem R de (1908) Contribution à l'étude du gisement des vertébrés de Maragha et de ses environs. Ann Hist Nat 1:27–98

Melentis, JK (1968) Palaeontological excavations at Samos Island (preliminary report). Proc Acad Athens 43:344–349

Mountrakis D, Kilias A, Vavliakis E, Psilovikos A, Thomaidou E (2003) Neotectonic map of Samos Island (Aegean Sea, Greece): Implication of geographical information systems in the geological mapping. In: de Vivo B, Salminen R (eds) Proceedings of the 4th European Congress on Regional Geoscientific Cartography and Information Systems , Bologna , vol 1, pp 11–13

Niezabitowski E von L (1912) *Teleoceras ponticus* n. sp. Vorläuf Notiz. Nowy Targ, Poland

Owen R (1848). Description of teeth and portions of jaws of two extinct anthracotherioid quadrupeds (*Hyopotamus vectianus* and *Hyop*. *bovinus*) discovered by the Marchioness of Hastings in the Eocene deposits on the N.W. coast of the Isle of Wight; with an attempt to develop Cuvier's idea of the classification of pachyderms by the number of their toes. Quart J Geol Soc Lond 4:103–141

Pandolfi L (2016) *Persiatherium rodleri*, gen. et sp. nov. (Mammalia, Rhinocerotidae) from the upper Miocene of Maragheh (northwestern Iran). J Vertebr Paleontol 36(1):e1040118

Pavlow M (1913) Mammifères tertiaires de la Nouvelle Russie, 1. Partie: Artiodactyla, Perissodactyla (*Aceratherium kowalevskii* n.s.). Nouv Mem Soc Imp Nat Mosc 17:1–68.

Pavlow M (1914) Mammifères tertiaires de la Nouvelle Russie. 2 partie. *Aceratherium incisivum*, *Hipparon*, Proboscidaea, Carnivora. Nouv Mem Soc Imp Nat Mosc 17(4): 1–78.

Pohlig H (1886) On the Pliocene of Maragha, Persia, and its resemblance to that of Pikermi in Greece; on fossil elephant remains of Caucasia and Persia; and on the results of a monograph of the fossil elephants of Germany and Italy. Quart J Geol Soc 42(1–4):177–182.

Qiu ZX, Yan DF (1982) A horned *Chilotherium* skull from Yushe, Shansi. Vertebr Palasiat 20(2):122–132

Schlosser M (1903) Die fossilen Cavicornia von Samos. Beitr Pal Österr-Ung 17:21–118

Qiu Z X, Xie J Y, Yan D F (1987) A new chilothere skull from Hezheng, Gansu, China, with special reference to the Chinese "*Diceratherium*". Sci Sinica B 5:545–552

Ringström T (1924) Nashörner der Hipparion-Fauna Nord-Chinas. Palaeont Sin 1(4):1–156

Solounias N, Ring U (2007) Ancient history of the Samos fossils and the record of earthquakes. In: Lister G, Forster M, Ring U (eds): Inside the Aegean Metamorphic Core Complexes. J Virtual Explor 27:6. https://doi.org/10.3809/jvirtex.2007.00179

Sun DH, Yu L, Deng T (2018) A new species of *Chilotherium* (Perissodactyla, Rhinocerotidae) from the late Miocene of Qingyang, Gansu, China. Vertebr Palasiat 56(3):216

Tang YJ, You YZ, Liu HY, Pan YR (1974) New materials of Pliocene mammals from Banguo Basin of Yuanmou, Yunnan and their stratigraphical significance. Vertebr Palasiast 12(1):60–67

Țibuleac P, Tissier J, Petculescu A, Becker D, Weber (2023) *Chilotherium schlosseri* (Weber, 1905) (Rhinocerotidae, Mammalia) from the late Miocene of the foreland of the Eastern Carpathians in Romania. C R Palevol 22:729–752

Theodorou G, Athanassiou A, Roussiakis S, Iliopoulos G (2003) Preliminary remarks on the late Miocene herbivores of Kerassia (Northern Euboea, Greece). Deinsea 10(1):519–530.

Tung YS, Huang WP, Qiu ZD (1975) *Hipparion* fauna in Anlo, Hohsien, Shansi. Vertebr Palasiat 13(1):34–47

Weber M (1905) Über Tertiäre Rhinocerotiden von der Insel Samos. II. Bull Soc Imp Nat Mosc 18(4):344–363

# Appendix 5

*Publication 5*

Postcranial anatomy of the Late Miocene Eurasian hornless rhinocerotid *Chilotherium*

**Panagiotis Kampouridis**[a,b], Georgia Svorligkou[c], Nikolai Spassov[f], and Madelaine Böhme[a,b]

[a]Department of Geoscience, Eberhard Karls University of Tübingen, Tübingen, Germany;

[b]Senckenberg Centre for Human Evolution and Palaeoenvironment, Tübingen, Germany;

[c]Faculty of Geology and Geoenvironment, Department of Historical Geology and Palaeontology, National and Kapodistrian University of Athens, Athens, Greece; and

[f]National Museum of Natural History at the Bulgarian Academy of Sciences, Sofia, Bulgaria

Published in

PLoS One 20(12), e0336590

DOI: 10.1371/journal.pone.0336590

Date of online publication: 05.12.2025

PLOS One

RESEARCH ARTICLE

# Postcranial anatomy of the Late Miocene Eurasian hornless rhinocerotid *Chilotherium*

**Panagiotis Kampouridis**[1,2]*, **Georgia Svorligkou**[3], **Nikolai Spassov**[4], **Madelaine Böhme**[1,2]

**1** Terrestrial Palaeoclimatology section, Department of Geosciences, Eberhard Karls University of Tübingen, Tübingen, Germany, **2** Palaeontology Section, Senckenberg Centre for Human Evolution and Palaeoenvironment, Tübingen, Germany, **3** Faculty of Geology and Geoenvironment, Department of Historical Geology and Palaeontology, National and Kapodistrian University of Athens, Athens, Greece, **4** National Museum of Natural History at the Bulgarian Academy of Sciences, Sofia, Bulgaria

* pkampouridis94@gmail.com



OPEN ACCESS

**Citation:** Kampouridis P, Svorligkou G, Spassov N, Böhme M (2025) Postcranial anatomy of the Late Miocene Eurasian hornless rhinocerotid *Chilotherium*. PLoS One 20(12): e0336590. https://doi.org/10.1371/journal.pone.0336590

**Editor:** Luca Pandolfi, Universita degli Studi della Basilicata, ITALY

**Received:** July 24, 2025

**Accepted:** October 28, 2025

**Published:** December 5, 2025



**Data availability statement:** All relevant data are within the manuscript and its Supporting Information files.

**Funding:** This research received support from the SYNTHESYS+ project http://www.synthesys.info/ which is financed by European Community Research Infrastructure Action under the H2020 Integrating Activities

## Abstract

The hornless rhinocerotid genus *Chilotherium* is one of the most common rhinoceroses found in Eurasia during the Late Miocene, even being the most abundant large mammal in some localities. Despite its high frequency, much is still unknown about the anatomy and taxonomy of some representatives of the group, because most studies focus solely on cranial and dental remains. For this reason, we describe the postcranial material of the three well-known chilothere species *Chilotherium persiae* from the Upper Miocene of Maragheh (Iran), *Chilotherium habereri* from the Upper Miocene of Kutschwan (China), and *Chilotherium schlosseri* from the Upper Miocene of Samos (Greece). A comparison to postcranial material of other chilotheres from the literature reveals some characters that can assist the identification of some species, such as the morphology and dimensions of the patella and the metapodials, the morphology of the proximal articulation of tibia, and the arrangement of the articular facets for the calcaneum on the astragalus. The comparison supports previous hypotheses about the relationships of some chilotheres that were only based on cranial features, including the plesiomorphic nature of '*Chilotherium*' *wimani* from the Upper Miocene of China and the close relationship of *C. persiae* and *C. habereri*.

## Introduction

Rhinoceroses are amongst the most iconic large mammals to roam the earth today. Even though only five extant species exist, in the past this group was much more diverse [1–6]. During the Miocene a plethora of rhinoceros species existed and, although the extant representatives are characterised by the presence of horns on their heads, a highly diverse rhinocerotid group were the aceratheriines, also known as the hornless rhinos. One of the most characteristic and species-rich genera of this group was *Chilotherium* Ringström, 1924 [7] that lived in Asia and Eastern Europe

Programme, Project number 823827 (AT-TAF-TA3-9 and AT-TAF-TA4-29 and FR-TAF-TA4-71 granted to PK). The funders had no role in study design, data collection and analysis, decision to publish, or preparation of the manuscript.

**Competing interests:** The authors have declared that no competing interests exist.

during the Late Miocene [1,8,9]. This genus is characterised by a very wide mandibular symphysis with two large, tusk-like incisors, flat to concave frontal bones, very complex enamel folds in the upper teeth, and the appendicular skeleton is notably shortened and relatively robust, especially the metapodials [7,10].

Ringström (1924) [7] initially attributed over ten species to this newly erected genus, while also erecting several new species, based on material from the Upper Miocene of China. He discussed that the representatives of *Chilotherium* were extremely similar and that they could only be separated based on the morphology of the upper teeth. However, it has been shown that the morphology of the skull over all is more informative for the taxonomic attribution than the tooth morphology [e.g., 10,11]. Some studies actually suggested that also the postcranial anatomy of some species can be used for their distinction [11,12]. However, only few studies have reported postcranial material for members of this group [e.g., 7,13–15] and even less studies described and analysed this material in detail [11,16]. This creates a large gap in our understanding of the body plan of this rhino group and the potential interspecific variability. However, it was suggested early on that the appendicular skeleton of the genus *Chilotherium* is very derived [7], which was also confirmed by later studies, suggesting that the limb bones of chilotheres differ from those of other aceratheriines [3,16]. Korotkevitch [11], Krokos [17], and Deng [16] studied large samples of some chilothere species, suggesting that some elements, such as the metapodials, are also important for taxonomic purposes within the group. These findings have not been verified or re-evaluated by any later study, making some assumptions somewhat ambiguous.

The aim of this study is to evaluate the postcranial material of *Chilotherium* spp. available in different institutions to provide some insight into the taxonomy and interrelationships of this group. For this purpose, we studied collections of three historical fossil localities, Maragheh (Iran), Kutschwan (China), and Samos (Greece), that are known to include *Chilotherium* in their fauna (Fig 1). The studied specimens were compared with available material in the literature from Europe and Asia (Fig 1), thereby covering almost the complete geographical distribution of this taxon and offering new insight into the anatomy and taxonomy of these animals.

## Abbreviations

### Anatomical abbreviations

APD, anteroposterior diameter; APDbec, anteroposterior diameter measured at the level of the posterior astragalar facet; APDcaput, anteroposterior diameter of the humerus head; APDdia, anteroposterior diameter of the diaphysis; APDdist, distal anteroposterior diameter; APDdist art, anteroposterior diameter of the distal articular surface; APDinf, medial anteroposterior diameter; APDolecr, anteroposterior diameter of the olecranon; APDprox, proximal anteroposterior diameter; APDprox art, anteroposterior diameter of the proximal articular surface; APDsommet, anteroposterior diameter of the tuber calcis; DL, distance between the lips of the trochlea; TD, transversal diameter; TDcaput, transversal diameter of the humerus head; TDdia, transversal diameter of the diaphysis; TDdist artic, transversal diameter of the distal

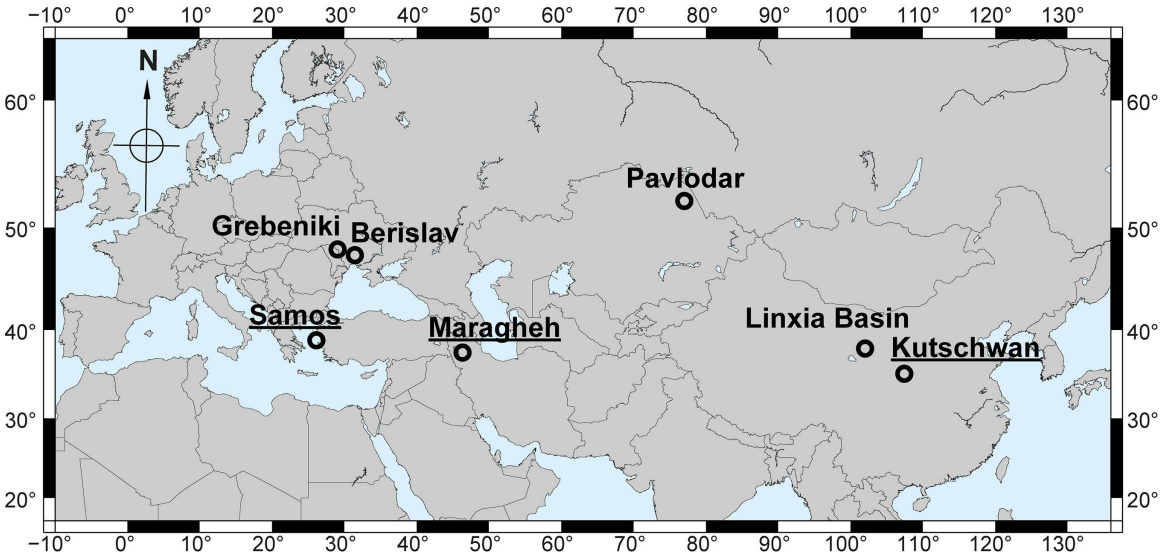


**Fig 1. Geographical map with the fossil localities of the compared chilotheres.** The localities where the herein studied material comes from (Samos in Greece, Maragheh in Iran, and Kutschwan in China) are underlined. The map was generated using Generic Mapping Tools 6 (GMT6) [18].

https://doi.org/10.1371/journal.pone.0336590.g001

articular surface; TDdist max, maximal distal transversal diameter; TD maxi dist, maximal distal transversal diameter; TDmini post, minimal transversall diameter; TDolecranon, transversal diameter of the olecranon; TDprox art, transversal diameter of the proximal articular surface; TDprox max, maximal proximal transversal diameter; TDsommet, transversal diameter of the tuber calcis; TDsust, maximal transversal diameter at the sustentacular tali; H, height; Hant, anterior height; Hface ant, height of anterior facet; H lateral condyle, height of the lateral distal condyle; H medial condyle, height of the medial distal condyle; Hpost, posterior height measured between the tubers calcis and the posterior astragalar facet; Htuberosity, height of the lateral tuberosity; L, length; Lmax, maximal length; L absolute, maximal length; L anatom, length in anatomical position; Lart sup, length of the anterior articular surface; Lart inf, length of the central articular surface; Lcaput, length measured from the humerus head; l, width; lart, width of articular surface; and lart sup, width of anterior articular surface.

### Institutional abbreviations

AMNH, American Museum of Natural History, New York (USA); AMPG, Athens Museum of Palaeontology and Geology of the National and Kapodistrian University of Athens (Greece); BSPG, Bayerische Staatssammlung für Paläontologie und Geologie, Munich (Germany); GMM, Geomuseum of the University of Münster (Germany); GPIT, Geologisch-Paläontologisches Institut der Universität Tübingen (Germany); GPIH, Geologisch-Paläontologisches Institut der Universität Hamburg (Germany); HLMD, Hessisches Landesmuseum Darmstadt (Germany); IPUW, Institut für Paläontologie, Universität Wien (Austria); MLU, Martin-Luther Universität Halle-Wittenberg (Germany); MNHN, Muséum national d'Histoire naturelle, Paris (France); NHMW, Naturhistorisches Museum in Wien (Austria); NMB, Naturhistorisches Museum Basel (Switzerland); and SMNS, Staatliches Museum für Naturkunde Stuttgart (Germany); and SNSB, Staatliche Naturwissenschaftliche Sammlungen Bayerns (Germany).

## Materials and methods

For the purpose of this study, material of three distinct chilotheres was studied: *Chilotherium persiae* (Pohlig, 1885) [19] from the Upper Miocene deposits of Maragheh in Iran [13,20–23], *Chilotherium habereri* (Schlosser, 1903) [24] from the

Upper Miocene deposits of Kutschwan in China [25,26], and *Chilotherium schlosseri* (Weber, 1905) [14] from the Upper Miocene deposits of Samos in Greece [8,27–29] (Fig 1). The material studied herein is housed in different palaeontological collections (GMM, GPIT, IPUW, MNHN, NHMW, and MLU).

Additionally, the studied material is compared to published data from the species '*Chilotherium*' *wimani* Ringström, 1924 [7] from the Upper Miocene of China [16], *Chilotherium kowalevskii* (Pavlow, 1913) [15], *Chilotherium sarmaticum* Korotkevitch, 1958, both from the Upper Miocene of Ukraine [11,15,17], and *Chilotherium orlovi* Bayshashov, 1982 [30] from the Upper Miocene of Pavlodar in Kazakhstan [12,30].

Measurements were taken according to Guérin (1980) [31] with some additions. Detailed measurements of all bones from the literature and those measured herein are provided in S1 Tables 1–23 and throughout the main text in the Tables. The anatomical terms used in this study are based on the literature [31–35]. It has to be noted that in the older literature [7,11,12,14,17] no standardised measuring protocol like that of Guérin (1980) [31] has been used. Therefore, it is difficult to make certain and detailed comparisons with some of the species. This is especially true for complex bones like carpals and tarsals, where it is even more difficult to compare measurements if they did not follow the exact same method of measuring.

### Taxonomic notes

The taxonomy of chilotheres has been a rather complicated matter for a long time [8,10,17,36–38]. The genus was erected over 100 years ago [7] and over a dozen species have been assigned to it over the years, with many attributions not being valid anymore (see [7,37–39]). Especially the European representatives have been the centre of great confusion, with the erection of overall 10 species, two of which come from Portugal and in fact belong to the elasmotheriine rhinoceros *Hispanotherium* [37,38]. All other European chilotheres come from Eastern and Southeastern Europe and are validly assigned to the chilotheres. The taxonomy of these other eight species, while representing chilotheres, has been a complicated matter to this day. From the Upper Miocene of Samos alone, four species have been erected, two of which, *Chilotherium wegneri* (Andree, 1921) [40] and *Chilotherium angustifrons* (Andree, 1921) [40], have subsequently been synonymised to *C. schlosseri* [8]. *Chilotherium schlosseri* and the fourth species, *Eochilotherium samium* (Weber, 1905), were recently revised and separated on a generic level, with both species belonging to the subtribe Chilotheriina (sensu [10]). The other chilothere species from Greece is *Aceratherium kiliasi* Geraads and Koufos, 1990 [41], which was erected based on craniomandibular material from the Upper Miocene of Pentalophos in northern Greece. The material from Pentalophos belongs in part to the non-chilothere aceratheriine *Acerorhinus neleus* Athanassiou et al., 2014 [42]. The holotype and some other specimens, do belong to a chilothere, but represent the species *E. samium*, making *Aceratherium kiliasi* a junior synonym of this species [10,42]. The other European chilotheres were all erected based on material from Ukraine. A partial skull from Upper Miocene deposits near Odessa represents the holotype of *Teleoceras ponticus* Lubicz-Niezabitowski, 1912 [43,44]. Shortly after its' erection it was suggested to represent a junior synonym of *C. schlosseri* [36] and is still considered as such [8]. The other two species are *Chilotherium kowalevskii* (Pavlow, 1913) [15] from the Upper Miocene of Grebeniki and *Chilotherium sarmaticum* Korotkevitch, 1958 [45] from the Upper Miocene of Berislav (Ukraine). The first of these two has repeatedly been suggested to be a junior synonym of *C. schlosseri* [11,17,46,47]; however, recent re-evaluations of the Samian chilotheres showed that the two species differ both in their cranial and dental morphology [8,10]. The species *C. schlosseri* features widely separated parietal crests, with a minimal distance of at least 70 mm (n = 7), whereas the material of *C. kowalevskii* from Grebeniki exhibits a value range of 40–66 mm (n = 10) for this measurement, thus clearly differing from *C. schlosseri*. *Chilotherium sarmaticum*, on the other hand, has received little attention after its initial description and was usually neglected in most comparative studies [8,48]. However, it was shown that *C. sarmaticum* differs from both *C. kowalevskii* from Grebeniki and *C. schlosseri* from Samos [10,11]. Therefore, both *C. kowalevskii* and *C. sarmaticum* are herein considered valid species. Regarding the *Chilotherium* species from China, there are several species that were attributed to the genus by Ringström (1924) [7], including some newly erected species

and subspecies. Some of these cannot be considered as valid species, while other do not belong to the genus *Chilotherium*. Several studies have tried to bring order into this matter [e.g., 37,38]. Heissig (1975) [38] attempted to distinguish different lineages within the genus *Chilotherium* by proposing subgenera. Only few researchers adopted this scheme [e.g., 48] and it is not used anymore. More recent work on the rhinocerotids from China has shed new light on the issue, separating distinct genera, and for instance erecting new chilothere species, like '*Chilotherium*' *primigenium* Deng, 2006 [37] and *Chilotherium licenti* Sun et al., 2018 [49]. Additionally, it was recently discussed that the two more 'primitive' species '*C.*' *primigenium* [37] and '*C.*' *wimani* [7] may in fact not belong to the genus *Chilotherium*. It was discussed that they lack the characteristic depression of the frontal region and exhibit some other more plesiomorphic characters that may associate these two species closer with *E. samium* instead [10]. A detailed re-evaluation of the type material is needed to clarify the generic status of these species. However, for the time being both species will be referred to as '*C.' primigenium* and '*C.' wimani*.

### Fossil sites

**Maragheh.** The locality of Maragheh is situated in northwestern Iran (Fig 1). The Late Miocene fauna is well known since the late 19th century [19,50,51]. Several fossil sites in the area have been excavated over the last century [13,23,50,52,53], recent studies suggested the existence of three distinct fossiliferous horizons and were able to correlate the old fossil sites with these three horizons [21,22]. Material from Maragheh is scattered throughout many collections, such as the MLU, MNHN, and NHMW. The rhino assemblage in Maragheh is quite rich and includes the huge elasmotheriine *Iranotherium morgani* (Mecquenem, 1908) [50] the large tandem-horned '*Ceratotherium*' *neumayri* (Osborn, 1900) [54], and two smaller aceratheriines, *Chilotherium persiae* and *Persiatherium rodleri* Pandolfi, 2016 [20]. The last species, was only recently described and is mainly known from its holotype – a subadult skull [20]. Maragheh is the type locality of all four of these rhinocerotid species and the first two are also well known from other localities in Eurasia, showing the importance of the locality for rhinocerotid systematics. *Chilotherium persiae* is by far the most common representative of the family in the Maragheh fauna and a rich collection of postcranial material is available for this species. Mecquenem (1924) [13] was the first to provide a more detailed description of *C. persiae* and while shortly describing also some postcranial elements he mainly focussed on the cranial and dental material. The studied material comes from different fossil sites situated in the area north of Maragheh, including 'Ketschawa' or Karajabad, Kara Kend, and Kopran, which represent the middle and lower fossiliferous beds of Maragheh [55,56].

As mentioned above, four rhinocerotid species existed in Maragheh and during the course of this project postcranial elements not only of *C. persiae* but also of the other species were found. The horned rhinoceroses '*Ceratotherium' neumayri* and *Iranotherium morgani* are much larger and their postcranial bones are easily distinguishable from *Chilotherium*. The other hornless species, *Persiatherium rodleri*, is basically only known from a single skull, apart from it only some isolated dental and fragmentary postcranial elements from the Upper Miocene of Küçükçekmece (Turkey) have been attributed to *Persiatherium* sp. [46]. However, they are not particularly helpful in distinguishing the species. Based on the phylogenetic analysis of Lu et al. (2023) [57], *Persiatherium rodleri* is placed in Aceratheriinae, but distinct from Chilotheriina, which is the clade made up by *Chilotherium* and *Shansirhinus* in Lu et al. (2023) [57], although not referred to as such by the authors. This further supports the notion that *Persiatherium rodleri* should not exhibit the shortened limbs that are known in *Chilotherium*. All herein reported specimens, fit both metrically and morphological the known postcranial elements of *Chilotherium*.

**Kutschwan.** The locality of Kutschwan in China is of Late Miocene age and was discovered by the German geographer and physician Albert Tafel in Shanxi during his trip to China in 1905 [25]. No information about the exact location of the fossil site is known, but the material was collected from horizontal red clay deposits close to the Yellow River (Huang He) in Shanxi (China, Fig 1) [25]. The material was excavated by A. Tafel, comprising of many cranial and postcranial elements. The whole collection was initially prepared at the SMNS (Germany) before being deposited in the

collections of the GPIT (Germany) and is still housed there today. Hugo Killgus studied the whole collection for his Ph.D. Dissertation [26] and recognised a quite rich mammalian fauna, based on this limited material, including an ictithere hyaena [58], two rhinocerotids, *Chilotherium habereri*, *Parelasmotherium schansiense* Killgus, 1923 [25], a hipparionine horse, the giraffe *Schansitherium tafeli* Killgus, 1923 [25], one large and up to three small bovids [25]. More recently, Kampouridis et al. (2022) [59] reassessed the taxonomy and phylogeny of *Parelasmotherium schansiense* by studying its holotype.

The chilothere *C. habereri* is the most abundant taxon in this collection, including several skulls and a small sample of postcranial material, which cannot be associated with the huge elasmotheriine. The cranial and dental morphology of the species were revised by Ringström (1924) [7] after the original description [24], but not much is known about the postcranial anatomy of the species. The herein reported postcranial elements can only be assigned to the single aceratheriine present in Kutschwan, *C. habereri*.

**Samos.** The island of Samos (Fig 1) has been known to yield Late Miocene vertebrate fossils since the 19th century [60]. Since then, numerous palaeontologists and fossil hunters have travelled to the island to collect fossils [60]. This led to several impressive collections of Samos material in famous natural history museums throughout the world, including among others the AMNH, NHMW, and SMNS. Most recently, the Aristotle University of Thessaloniki, led by Prof. George Koufos, excavated on Samos Island, bringing to light a rich collection of mammalian remains [60,61]. The material was studied in detail, providing crucial information about the (bio-)stratigraphical context and the fauna itself [e.g., 28,29,61,62]. The rhinocerotid material from Samos has been assigned to several different taxa over the years [8,10,27]. Today, it is generally accepted that two large tandem-horned rhinocerotines are present, '*Ceratotherium*' *neumayri* and *Dihoplus pikermiensis* (Toula, 1906) [63], along with two small aceratheriines, *Chilotherium schlosseri* and *Eochilotherium samium* [10,14,27,28,64]. The taxonomy of the Samian chilotheres has experienced many difficulties in the past, with the suggested presence of five different species depending on the authors – *C. schlosseri*, *E. samium*, *C. wegneri*, *C. angustifrons*, and *C. kowalevskii* [e.g., 8,14,17,27,40,42]. Most recently, Kampouridis et al. (2023) [8,10] suggested that the only valid chilothere species in Samos are *C. schlosseri* and *E. samium*, with *C. wegneri* and *C. angustifrons* representing junior synonyms of *C. schlosseri*. The species *E. samium* is much rarer than *C. schlosseri* and is currently only known from a single skull (SMF M 3601) with its associated mandible from the locality of Samos.

No postcranial material is assignable to *E. samium*, whereas *C. schlosseri* is represented by a large amount of material including, an impressive number of skulls [14,40,65–67] but also postcranial elements, which differ significantly from the much larger '*Ceratotherium*' *neumayri* and *Dihoplus pikermiensis*. This postcranial material is morphologically and metrically much closer to that of typical chilotheres, such as *C. kowalevskii*, *C. anderssoni* Ringström, 1924 [7], and *C. orlovi*, than to the more plesiomorphic '*C.*' *wimani* (see also below); therefore, an assignment to *E. samium* is excluded.

## Systematic Palaeontology

Class Mammalia Linnaeus, 1758 [68]
Order Perissodactyla Owen, 1848 [69]
Family Rhinocerotidae Gray, 1821 [70]
Subfamily Aceratheriinae Dollo, 1885 [71] (sensu Lu et al. (2023) [57])
Tribe Aceratheriini Dollo, 1885 [71] (sensu Lu et al. (2023) [57])
Subtribe Chilotheriina Qiu et al., 1987 [72] (sensu Kampouridis et al. (2023) [10])

## Included genera

*Chilotherium* Ringström, 1924 [7], *Shansirhinus* Kretzoi, 1942 [73], and *Eochilotherium* Geraads and Spassov, 2009 [48].

### Diagnosis

Aceratheriine rhinocerotids that feature the following autapomorphic traits: separated parietal crests; upper molars featuring a marked protocone constriction and a moderate to strong antecrochet that tends to project lingually; a mandible that is characterised by a very wide mandibular symphysis with a flat to concave ventral surface; large, sexually dimorphic i2s that exhibit a trend to become more flattened and tusk-like, especially in males, and are separated from each other by a wide diastema and from the p2 by a long diastema with a marked crest. The group also exhibits an upper first deciduous premolar retained into adulthood, whereas the first lower deciduous premolar, when present, is shed and not replaced by a permanent one. Additionally, the group lacks any upper incisor and the upper cheek teeth have generally pronounced secondary enamel folds (i.e., crista, crochet, and antecrochet), and the appendicular skeleton is notably shortened and relatively robust, especially the autopodium (modified after [10]).

### Remarks

The clade Chilotheriini was originally established by Qiu et al. (1987) [72] as a tribe, to encompass the genera *Acerorhinus* and *Chilotherium*, specifically excluding the genus *Aceratherium*. However, the relationship between these two genera is not clear, as shown in the contradicting results of some recent phylogenetic analyses [20,57]. Therefore, it has not been possible to prove that these two genera form a monophyletic clade. In fact, *Acerorhinus* shows many plesiomorphic characters and none of the apomorphic features characterising representatives of *Chilotherium*, therefore a close relationship cannot be supported. *Aceratherium* shows characters that are more similar to *Chilotherium*, like the somewhat shortened limb bones [74], whereas in *Acerorhinus zernowi* the plesiomorphic state of more elongated limb bone is seen [75]. Another more enigmatic hornless rhinocerotid, *Shansirhinus*, is much more similar to *Chilotherium* in many regards, such as the wide mandibular symphysis, the more complicated enamel folds, and the higher tooth crowns [76]. Their probably closer relationship has also been suggested in recent phylogenetic analyses [20,57]. It would therefore be best to remove *Acerorhinus* from Chilotheriina and to restrict this group to the genera *Chilotherium*, *Shansirhinus*, and *Eochilotherium*, with the latter one having been regarded as belonging to *Chilotherium* sensu stricto up until recently [8,10,27].

The type genus of Chilotheriini was not designated as such by Qiu et al. (1987) [72]; however, based on ICZN Arts. 29.1 and 64, a suprageneric name must derive from its type genus, which would naturally make *Chilotherium* the type genus. Following, the recommendation of Kampouridis et al. (2023) [10], we herein use the clade at a subtribe rank (as Chilotheriina) with *Chilotherium* as the type genus and also including the genera *Shansirhinus* and *Eochilotherium*.

Genus *Chilotherium* Ringström, 1924 [7]

### Type species

*Chilotherium anderssoni* Ringström, 1924 [7].

### Included species

*Chilotherium persiae* (Pohlig, 1885) [19], *Chilotherium habereri* (Schlosser, 1903) [24], *Chilotherium schlosseri* (Weber, 1905) [14], *Chilotherium kowalevskii* (Pavlow, 1913) [15], '*Chilotherium*' *wimani* Ringström, 1924 [7], *Chilotherium sarmaticum* Korotkevich, 1958 [45], *Chilotherium orlovi* Bayshashov, 1982 [30], '*Chilotherium*' *primigenium* Deng, 2006 [37], and *Chilotherium licenti* Sun et al., 2018 [49].

### Diagnosis

Aceratheriine rhinocerotids that feature the following autapomorphic characters: flat and wide skull, flattened and depressed frontal region; well-developed postorbital processes; moderately to widely separated parietal crests; highly

placed orbits; very wide mandibular symphysis that features a concave ventral side; very large, flattened, tusk-like second lower incisors, with a scalene triangle cross section and upturned, dorsomedially oriented wear facets; reduced premaxillary bones that lack upper incisors; and very strong secondary enamel folds, including a lingually flattened and strongly constricted protocone in the molars. It is also characterised by a relatively short length of the premolars compared with the molars, mainly due to the reduced size of the P2 and p2; and notably shortened metapodials and relative robust appendicular skeleton (modified after [7,10,27,39,48]).

### Remarks

Recently, it was shown that '*C.*' *wimani* and '*C.*' *primigenium* exhibit more plesiomorphic features than the other *Chilotherium* species [10]. In fact, these two species seem to share some morphological features with *Eochilotherium samium*, such as the flat to convex frontal region, the thickness of the nasal bones, and the highly elevated nuchal crest It seems most plausible that they do not belong to the genus *Chilotherium*; however, it is preferred not to include these species into the genus *Eochilotherium* at the moment. Nonetheless, until the issue about their generic attribution is resolved it is preferable to keep them in their original genus as '*C.*' *wimani* and '*C.*' *primigenium* [10,39].

*Chilotherium persiae* (Pohlig, 1885) [19]

### Type material

Pohlig (1885) [19] erected the species without fixing a holotype, providing any specimen numbers, photographs, or any information about the collection which housed the material he studied. He mentioned that the material he collected himself in Maragheh (Iran) was sent to Halle (Germany) [51]. This material is now housed in the palaeontological collection of the MLU. Pohlig (1885, 1886) [19,51] specifically mentioned that there were four adult and one juvenile skull that he assigned to this species. He did not specify whether these were collected by himself or if he saw them in some other collection. In the collections of the MLU only one adult and two juvenile skulls of *C. persiae* were able to be relocated. However, Pohlig (1886) [51] mentioned explicitly the fact that the collection of fossils in the area was continued by Theodor Strauss, as explained also by Rodler (1885) [77], who joined the excavation in Maragheh, collecting for the NHMW. The fact that Pohlig was well aware of these excavations and also specifically mentioned the material housed at the NHMW [51,78], along with the fact that several skulls were deposited in the collection of the NHMW until 1885, make it likely that Pohlig had seen at least some of these skulls and counted them into the, in total, five skulls he mentioned [51]. Until further information becomes available, however, the type material cannot be determined with certainty.

### Type locality

Upper Miocene deposits of Maragheh (Iran); exact locality unknown.

### Diagnosis

Medium-sized *Chilotherium* species with a weakly to moderately depressed frontal region, straight and relatively thick nasal bones, parietal crests that are moderately separated from each other (minimal distance between parietal crests up to 54 mm, n = 11) and a unique combination of dental characters: M3 with a somewhat quadrangular outline; long crochet; small crista sometimes present in the premolars that may close off the medifossette; very strong mesial and distal constriction of the protocone, which is lingually flattened, resulting in a very long antecrochet that may close off the median valley; a strong mesial constriction of the hypocone; crista rarely present in molars but when present may close off the medifossette; and a weak, discontinuous lingual cingulum mainly present at the entrance of the median valley in the premolars.

### Referred material

An axis (MNHN.F.MAR3939), five scapulae (MNHN.F.MAR1431, MNHN.F.MAR1433, MNHN.F.MAR2899, MNHN.F.MAR3898, and MNHN.F.MAR3900), 11 humeri (MNHN.F.MAR3901, MNHN.F.MAR3903, MNHN.F.MAR3904, MNHN.F.MAR3905, NHMW-GEO-2020/0014/0115, NHMW-GEO-2020/0014/0122, NHMW-GEO-2020/0014/0123, NHMW-GEO-2020/0014/0124, NHMW-GEO-2020/0014/0125, NHMW-GEO-2020/0014/0148, and NHMW-GEO-2020/0014/0147), 17 radii (MNHN.F.MAR1434, MNHN.F.MAR3906, MNHN.F.MAR3908, MNHN.F.MAR3909, MNHN.F.MAR3911, MNHN.F.MAR3912, MNHN.F.MAR3913, MNHN.F.MAR3963, NHMW-GEO-2020/0014/0107, NHMW-GEO-2020/0014/0108, NHMW-GEO-2020/0014/0109, NHMW-GEO-2020/0014/0110, NHMW-GEO-2020/0014/0111, NHMW-GEO-2020/0014/0126, NHMW-GEO-2020/0014/0127, NHMW-GEO-2020/0014/0128, NHMW-GEO-2020/0014/0149), a scaphoid (MNHN.F.MAR1412), two semilunars (MNHN.F.MAR1401 and MNHN.F.MAR1411), two pyramidals (MNHN.F.MAR1405, MNHN.F.MAR1413), a trapezoid (MNHN.F.MAR1409), six unciforms (MNHN.F.MAR1400, MNHN.F.MAR1403, MNHN.F.MAR1406, MNHN.F.MAR1408, NHMW-GEO-2020/0014/0140, and NHMW-GEO-2020/0014/0155), four second metacarpals (MNHN.F.MAR1375, MNHN.F.MAR1388, NHMW-GEO-2020/0014/0106, and NHMW-GEO-2020/0014/0142), five third metacarpals (MNHN.F.MAR1377, MNHN.F.MAR1379, MNHN.F.MAR1383, MNHN.F.MAR1429, and MLU.GeoS.6242), six fourth metacarpals (MNHN.F.MAR1376, MNHN.F.MAR1387, MNHN.F.MAR1390, MNHN.F.MAR1386, MLU.GeoS.6241, and NHMW-GEO-2020/0014/0143), seven femora (MNHN.F.MAR1416, MNHN.F.MAR1432, MNHN.F.MAR3920, MNHN.F.MAR3921, NHMW-GEO-1911/0005/0273, NHMW-GEO-2020/0014/0114, and NHMW-GEO-2020/0014/0152), 11 patellae (MNHN.F.MAR1463, MNHN.F.MAR3922, MNHN.F.MAR3923, MNHN.F.MAR3924, MNHN.F.MAR3925, MNHN.F.MAR3926, MNHN.F.MAR3927, MNHN.F.MAR3928, MLU.GeoS.6245, NHMW-GEO-2020/0014/0118, and NHMW-GEO-2020/0014/0130), 10 tibiae (MNHN.F.MAR1435, MNHN.F.MAR3931, MNHN.F.MAR3932, MNHN.F.MAR3933, MNHN.F.MAR3990a, MNHN.F.MAR4131, MNHN.F.MAR4132, NHMW-GEO-2020/0014/0112, NHMW-GEO-2020/0014/0113, and NHMW-GEO-2020/0014/0117), 14 astragali (IPUW-MFN21652, MNHN.F.MAR1360, MNHN.F.MAR1366, MNHN.F.MAR1367, MNHN.F.MAR1368, MNHN.F.MAR1369, MNHN.F.MAR1370, MNHN.F.MAR1371, MNHN.F.MAR1372, MNHN.F.MAR1373, MNHN.F.MAR1419, NHMW-GEO-2020/0014/0102, NHMW-GEO-2020/0014/0129, and NHMW-GEO-2020/0014/0137), 19 calcanei (MNHN.F.MAR1421, MNHN.F.MAR1422, MNHN.F.MAR1423, MNHN.F.MAR1424, MNHN.F.MAR1425, MLU.GeoS.6243, MLU.GeoS.6244, NHMW-GEO-2020/0014/0103, NHMW-GEO-2020/0014/0104, NHMW-GEO-2020/0014/0105, NHMW-GEO-2020/0014/0131, NHMW-GEO-2020/0014/0132, NHMW-GEO-2020/0014/0133, NHMW-GEO-2020/0014/0134, NHMW-GEO-2020/0014/0138, NHMW-GEO-2020/0014/0139, NHMW-GEO-2020/0014/0145, NHMW-GEO-2020/0014/0146, and NHMW-GEO-2020/0014/0151,), six naviculars (MNHN.F.MAR1407, MNHN.F.MAR1415, MNHN.F.MAR1427a, NHMW-GEO-2020/0014/0136, NHMW-GEO-2020/0014/0145, and NHMW-GEO-2020/0014/0156), three cuboids (MNHN.F.MAR1414, MNHN.F.MAR1427b, and NHMW-GEO-2020/0014/0145), three ectocuneiforms (MNHN.F.MAR1399, MNHN.F.MAR1427c, and NHMW-GEO-2020/0014/0145), three second metatarsals (MNHN.F.MAR1378, MNHN.F.MAR1381, and MNHN.F.MAR1385), three third metatarsals (MNHN.F.MAR1382, NHMW-GEO-2020/0014/0150, and NHMW-GEO-2020/0014/0154), and four fourth metatarsals (MNHN.F.MAR1452, NHMW-GEO-2020/0014/0121, NHMW-GEO-2020/0014/0144, and NHMW-GEO-2020/0014/0154).

### Remarks

*Chilotherium persiae*, originally erected as *Rhinoceros persiae*, represents the first described rhinoceros species that was later included in the genus *Chilotherium* [7,51]. Maragheh, the type locality of the species, has brought to light a very diverse mammalian fauna based on a large amount of fossil bones [21,22,53,79]. Along with many skulls, the species *C. persiae* is represented also by a large number of postcranial elements housed in different institutions, including the MLU,

MNHN, and NHMW. These fossils were excavated at different fossil sites in the area around Maragheh that correspond to different stratigraphical layers [23,e.g., 51,77]. More specifically the studied postcranial material comes from the sites Karajabad, Kara Kend, and Kopran that represent the middle and lower fossiliferous beds in Maragheh [21,55,56].

*Chilotherium habereri* (Schlosser, 1903) [24]

### Lectotype

Schlosser (1903) [24] assigned several teeth to the new species that he erected, *Rhinoceros habereri*, without assigning a holotype. Therefore, all studied teeth (Schlosser, 1903: plate 5, figs 5–10, 12–21; plate 7, figs 1–3, 6, 8, 10, 11) [24] constitute the syntype of *Chilotherium habereri*. The associated P3 and P4 (SNSB- BSPG 1900 XII 622), illustrated by Schlosser (1903, plate 5, fig 18) [24], are herein designated as the lectotype of the species under the provisions of ICZN Art. 74. These were also used as the basis for the identification of the species by Ringström (1924) [7], who revised its morphological affinities.

### Diagnosis

Medium- to large-sized *Chilotherium* species with a moderately depressed frontal region, straight nasal bones, parietal bones that are moderately separated and a unique combination of dental characters: long crochet; usually closed off, round medifossette; crista absent in molars; very strong mesial and distal constriction of the protocone, which is lingually flattened, resulting in a long antecrochet that may close off the median valley at a very advanced wear stage; a strong mesial constriction of the hypocone of the molars; medifossette commonly closed in premolars; and a discontinuous lingual cingulum is mainly present in the premolars.

### Type locality

Upper Miocene red clay deposits in Shanxi (China); exact locality unknown.

### Referred material

A scapula (GPIT/MA/04974), four humeri (GPIT/MA/04831, GPIT/MA/04832, GPIT/MA/04833, and GPIT/MA/04834), three radii (GPIT/MA/04778, GPIT/MA/04786, and GPIT/MA/04791), a scaphoid (GPIT/MA/04784), two second metacarpals (GPIT/MA/04782 and GPIT/MA/04783), two third metacarpals (GPIT/MA/04756 and GPIT/MA/04782), a fourth metacarpal (GPIT/MA/04776) a fifth metacarpal (GPIT/MA/04756), a femur (GPIT/MA/04835), a patella (GPIT/MA/04781), a tibia (GPIT/MA/04836), three astragali (GPIT/MA/04763, GPIT/MA/04779, and GPIT/MA/04792), three calcanei (GPIT/MA/04792, GPIT/MA/04859, and GPIT/MA/04860), a navicular (GPIT/MA/04782), and a third metatarsal (GPIT/MA/04796).

### Remarks

*Chilotherium habereri* is the first chilothere species described from China [24]. It was originally erected as *Rhinoceros habereri* [24] and later assigned to the genus *Chilotherium* [7]. However, the type material comprises only isolated teeth and dental characters are evidently not reliable for species identifications in the genus *Chilotherium* (see for example [47]). Ringström (1924) [7] tried to address this issue by using a skull from a different, but probably closely situated, locality with identical teeth to the type material as a basis to redefine the species. However, the morphological features seen in these teeth that were used to define the species are subject to intraspecific variation within the genus *Chilotherium*, therefore assigning a skull to the same species based solely on the morphology of the premolars may prove difficult. This complicates the matter and shows that a detailed revision of the type material, along with the material studied by Ringström (1924) [7], is needed. For the purpose of the current study, we tentatively refer the chilothere material from

Kutschwan housed in the GPIT to *C. habereri*, as also proposed in the initial description of the material [25,26] and later supported by Ringström (1924) [7].

Chilotherium schlosseri [Weber, 1905] [14]

### Neotype

A well-preserved skull (GPIH 3015) with an associated mandible (GPIH 3015a), designated by Kampouridis et al. (2023) [10].

### Diagnosis

A large *Chilotherium* species characterised by widely separated parietal crests (minimal distance between parietal crests always over 70 mm in adult individuals), notably depressed frontal and nasal bones, nasal bones that bear a central longitudinal groove on the dorsal side, and a unique combination of dental characters: very long crochet; very strong mesial and distal constriction of the protocone, which is lingually flattened, resulting in a very long antecrochet that usually closes off the median valley at an early wear stage in all teeth; a prominent mesial constriction of the hypocone; crista frequently present that closes the medifossette; and a discontinuous lingual cingulum that is occasionally moderately developed in the premolars; often a closed prefossette is present in the P2; in addition to sporadically present enamel plications in the upper teeth; and discontinuous lingual and buccal cingulids in the lower teeth (after [10]).

### Type locality

Upper Miocene deposits of Samos Island (Greece); exact locality unknown.

### Referred material

An axis (GMM FO-14), two scapulae (GMM 563 and NHMW-GEO-1911/0005/0245), seven humeri (GMM 495, GMM 496, GMM 599, GMM 601, GMM 602, GMM FO-18, and GMM FO-24), two radii (GMM 561 and GMM 564), two scaphoids (NHMW-GEO-1911/0005/0152 and NHMW-GEO-2009z0089/0001), four femora (GMM FO-10, GMM FO-11, GMM FO-12, and NHMW-GEO-1911/0005/0273), 10 tibiae (AMNH 22818, GMM 497, GMM 594, GMM 595, GMM 596, GMM FO-13, GMM FO-19, GMM FO-27, NHMW-GEO-1911/0005/0497, and NHMW-GEO-1911/0005/0498), six astragali (AMNH Unnumbered, AMPG-SAM516, AMPG-SAM517, AMPG-SAM518, GMM 571, and NHMW-GEO-1911/0005/0424), three calcanei (AMNH-20794, AMNH-95122, and AMNH Unnumbered), a navicular (AMPG-SAM516), a cuboid (AMPG-SAM516), a second metatarsal (GMM 572), four third metatarsals (AMNH-22818, AMPG-SAM520, GMM 572, and NHMW-GEO-1911/0005/0220), and two fourth metatarsals (AMPG-SAM520 and GMM 572)

### Description and comparison

**Axis.** The studied material includes only one axis belonging to *C. persiae* from Maragheh (MNHN.F.MAR3939) and one to *C. schlosseri* from Samos (GMM FO-14) (Fig 2). Both are missing the neural arch and preserve only the centrum of the vertebra. The two bones are very similar to each other, with the axis of *C. schlosseri* being slightly larger. The dens of the axis is quite narrow and elongated in comparison to the contemporary '*Ceratotherium*' *neumayri*, in which the dens is much shorter, wider, and bears a prominent articular facet for the atlas on its ventral side (as seen in GMM FO-21, pers. obs.). In both *Chilotherium* species, the anterior articular facet of the axis is not as clearly defined, though this might be caused by some damage to the bone. The two vertebrae exhibit some slight differences like the ventral crest is wider and looks more massive in *C. schlosseri*, whereas in *C. persiae* it seems narrower and constricted in the middle. Concerning the posterior articular facet for third cervical vertebra, in *C. schlosseri* it has a high-oval shape with a

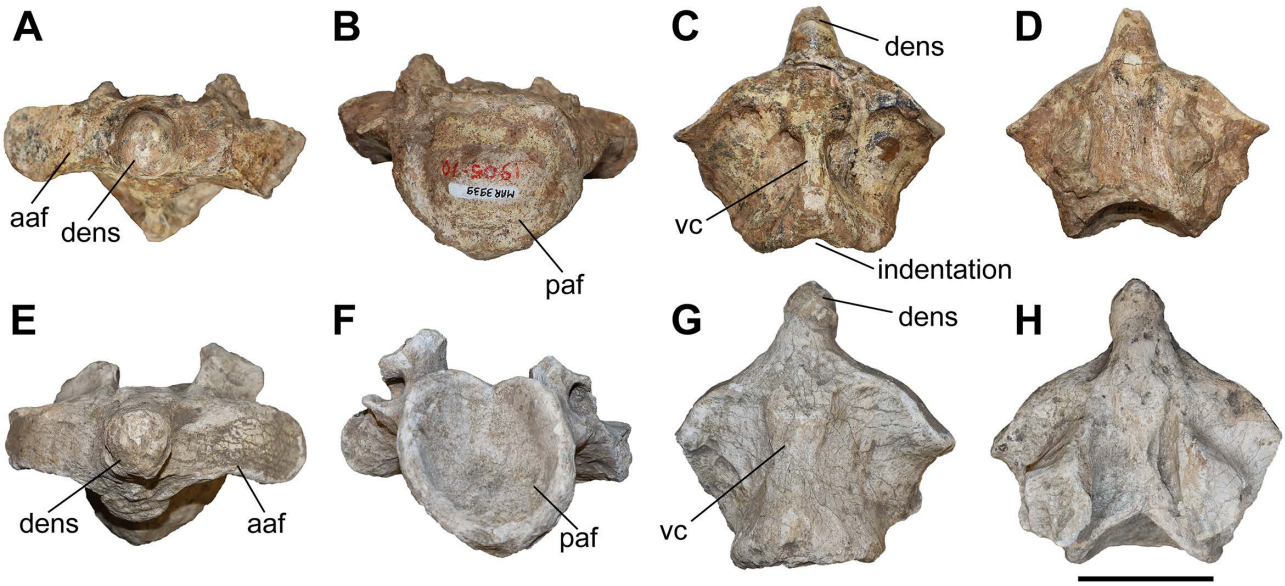


**Fig 2. The axis of chilotheres.** A–D, *Chilotherium persiae* (Pohlig, 1885) [19] (MNHN.F.MAR3939) from Maragheh (Iran) and E–H, *Chilotherium schlosseri* (Weber, 1905) [14] (GMM FO-14) from Samos (Greece) in anterior (A, E), posterior (B, F), ventral (C, G), and dorsal (D, H) views. Abbreviations: aaf, anterior articular facet; paf, posterior articular facet; and vc, ventral crest. Scale bar equals 5 cm.

https://doi.org/10.1371/journal.pone.0336590.g002

slight, dorsal indentation, whereas in *C. persiae* it is more rounded, and the dorsal surface is flat. Additionally, in ventral view there is an indentation on the posterior side in *C. persiae* (Fig 2C), whereas *C. schlosseri* lacks such an indentation (Fig 2G). Lastly, the area where the lateral walls of the neural canal of the axis connect to the vertebral body seems to extend more posteriorly in *C. schlosseri* than in *C. persiae*. A single axis was described for *C. kowalevskii* from Grebeniki [15]. Unfortunately, the description and illustration provided for this axis [15] are not sufficient for a comparison to our specimens. Additionally, due to the small sample size it is not possible to assess the intraspecific variability. Nonetheless, it is very likely that at least some of the observed differences are of taxonomic value.

**Scapula.** The studied material includes five partial scapulae of *C. persiae* from Maragheh, one of *C. habereri* from Kutschwan, and two of *C. schlosseri* from Samos (Fig 3). Unfortunately, none of them are complete, but in all specimens the proximal portion is adequately preserved to compare them, and in some specimens parts of the scapular spine is preserved. The spine is well developed and straight. In the more complete specimens, it is visible that the infraspinous fossa is only slightly larger than the supraspinous fossa. A spinous tuberosity is present, but not very prominent. In all specimens the articular facet for the humerus is oval and anteroposteriorly elongated (as indicated by Guerin (1980) [31]). The articular facet does not seem to differ among the scapulae of *C. persiae*, *C. habereri*, *C. schlosseri*, and *C. wimani* [16] neither in size, nor in shape. The supraglenoid tubercle and the coracoid process form a continuous tuberosity, the shape of which varies to some extent in the studied specimens. It is more rounded in *C. persiae* and *C. schlosseri* (Fig 3C, I) and rather flattened in *C. habereri* (Fig 3F). Furthermore, is seems to be more protruding in *C. schlosseri*; however, the small sample size may obscure the variability of these features. The specimens of *C. persiae* do in fact exhibit some variety in their morphology.

### Humerus

The studied material includes 12 humeri of *C. persiae* from Maragheh, four of *C. habereri* from Kutschwan, and seven of *C. schlosseri* from Samos (Fig 4, Table 1, S1 Table 1). Most specimens are only partially preserved. Their morphology is rather similar in all available specimens. The diaphysis is relatively straight. In the proximal part, the great and lesser tubercles

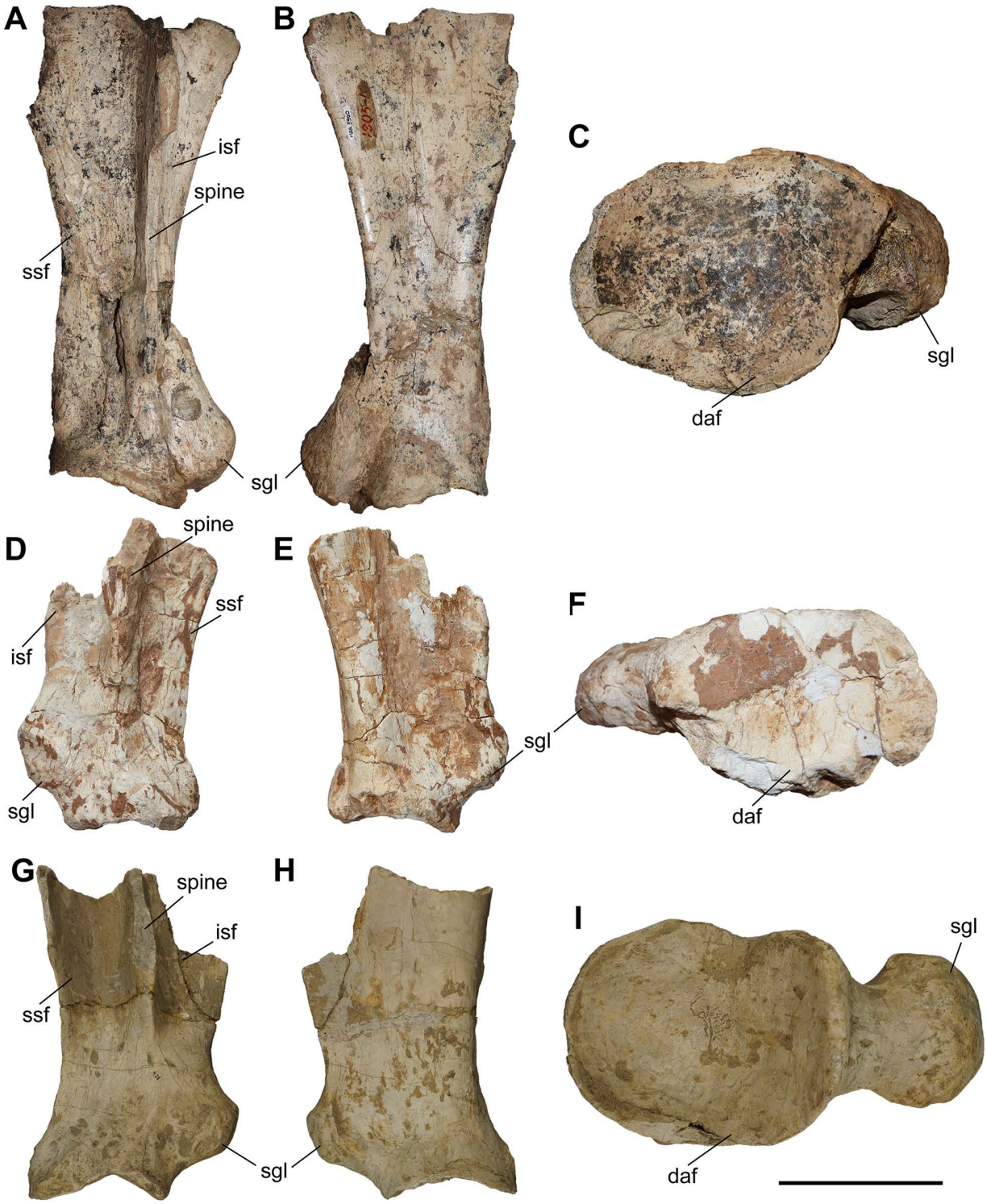


**Fig 3. The scapula of chilotheres.** A–C, *Chilotherium persiae* (Pohlig, 1885) [19] (MNHN.F.MAR3900, right) from Maragheh (Iran), D–F, *Chilotherium habereri* (Schlosser, 1903) [24] (GPIT/MA/04794, left) from Kutschwan (China), and G–I, *Chilotherium schlosseri* (Weber, 1905) [14] (GMM 428, right) from Samos (Greece) in anterior (A, D, and G), posterior (B, E, and H), and distal (C, F, and I) views. Abbreviations: daf, distal articular facet; isf, infraspinous fossa; sgl, supraglenoid tubercle; ssf, supraspinous fossa. Scale bar equals 10 cm for A, B, D, E, G, and H and 5 cm for C, F, and I.

https://doi.org/10.1371/journal.pone.0336590.g003

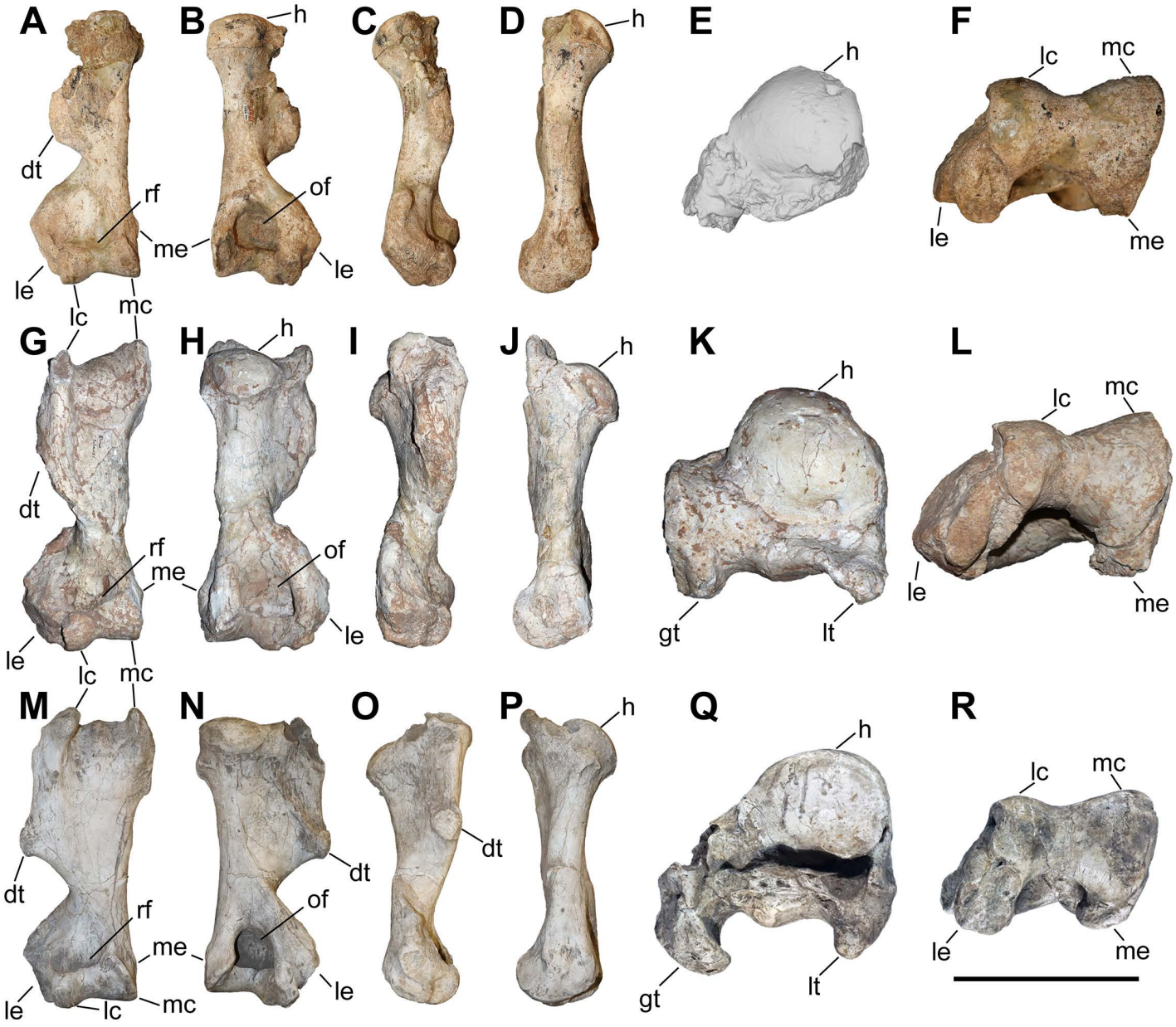


**Fig 4. The humerus of chilotheres.** A–F, *Chilotherium persiae* (Pohlig, 1885) [19] (MNHN.F.MAR3904, right) from Maragheh (Iran), G–L, *Chilotherium habereri* (Schlosser, 1903) [24] (GPIT/MA/04831, right) from Kutschwan (China), and M–R, *Chilotherium schlosseri* (Weber, 1905) [14] (GMM 601, right) from Samos (Greece) in anterior (A, G, and M), posterior (B, H, and N), medial (C, I, and O), lateral (D, J, and P), proximal (E: 3D model, K, and Q), and distal (F, L, and R) views. Abbreviations: dt, deltoid tuberosity; gt, greater trochanter; h, head of the humerus; lc, lateral condyle; le, lateral epicondyle; lt, lesser trochanter; mc, medial condyle; me, medial epidondyle; rf, radial fossa; and of, olecranon fossa. Scale bar equals 20 cm for A–D, G–J, and M–P, and 10 cm for E, F, K, L, Q, and R.

https://doi.org/10.1371/journal.pone.0336590.g004

are of similar size and their processes extend proximally to a similar degree, though the anterior part of the greater tubercle is broken in most specimens. The intermediate tubercle is somewhat less pronounced, without any distinct process. The two intertubercular grooves are smooth and relatively shallow. Anteriorly, the crest of the greater tubercle is prominent and extends distally to the deltoid tuberosity. The deltoid tuberosity is placed at the middle of the diaphysis. Its' morphology and

**Table 1. Measurements (in mm) of the humeri of the studied chilotheres.**

| | | L | Lca-put | TDprox max | TDprox art | APD-prox | TDdia | APD-dia | TDdist max | TDdist artic | APD-dist | TDca-put | APD-caput |
|---|---|---|---|---|---|---|---|---|---|---|---|---|---|
| ***C. persiae*** | min | | 305.5 | | | | 46.5 | 55.3 | 120 | 82.8 | 78.7 | 77.3 | 73.4 |
| | max | | 351.4 | | | | 63.9 | 63.4 | 139.5 | 93.4 | 94.4 | 78.1 | 75 |
| | mean | | 327.2 | | | 98.1 | 55.9 | 58.4 | 131.7 | 87.8 | 84.4 | 77.7 | 74.2 |
| | n | | 4 | | | 1 | 11 | 8 | 10 | 9 | 6 | 2 | 2 |
| ***C. habereri*** | min | 356 | 329 | 160 | 131.1 | 125.1 | 60 | 54.3 | 131.6 | 87.4 | 91.9 | 81.5 | 74 |
| | max | 365 | 334 | 161.3 | 138 | 127.2 | 63.4 | 62.3 | 150.1 | 98.4 | 97.4 | 94.6 | 90.1 |
| | mean | 360.5 | 331.5 | 160.7 | 134.6 | 126.2 | 61.8 | 57.8 | 142.7 | 93.9 | 95.5 | 88.4 | 84.4 |
| | n | 2 | 2 | 3 | 2 | 3 | 4 | 4 | 3 | 3 | 3 | 3 | 3 |
| ***C. schlosseri*** | min | 334 | 311 | 136 | 112.1 | 102 | 62.1 | 56.8 | 128.2 | 88.4 | 86 | 73 | 72.5 |
| | max | 353 | 320 | 152.2 | 134 | 139.5 | 76.2 | 78.6 | 146.8 | 98.3 | 91 | 84.1 | 83.8 |
| | mean | 343.5 | 314.3 | 145.5 | 126.6 | 124.7 | 69.1 | 63.0 | 138.0 | 93.9 | 89.5 | 79.9 | 78.4 |
| | n | 2 | 3 | 3 | 4 | 5 | 7 | 6 | 5 | 5 | 5 | 3 | 3 |

https://doi.org/10.1371/journal.pone.0336590.t001

only be assessed in GMM 601 of *C. schlosseri* and GPIT/MA/04832 of *C. habereri*, where it is similarly well developed and posteriorly projecting. In all available specimens, on the posterior side also the tricipital line is well visible, represented by a ridge starting at the middle of the proximal part, approximately at the beginning of the greater tubercle and merged into the deltoid tuberosity, also marking the limit of the muscle attachment area there. In the distal part, the medial epicondyle is relatively weak, especially when compared to the prominent lateral one, with its crest reaching almost the middle of the shaft. The radial fossa is almost triangular and well-developed, placed above the trochlea of the humerus. The medial condyle of the trochlea is larger than the lateral one and they are not separated by a trochlear scar. The olecranon fossa is fairly rounded and deep in all specimens, but it seems to be somewhat narrower transversally in *C. schlosseri* (Fig 4N) than in *C. habereri* (Fig 4H). In the latter species, the opening of the olecranon fossa is much wider, and the fossa has overall a transversally slightly elongated oval shape, as seen in the four available specimens.

Unfortunately, for *C. persiae* it was only possible to measure the length from the caput humeri and not the full length of any specimen. For both *C. schlosseri* and *C. habereri* two complete humeri were studied respectively, allowing most dimensions to be measured (S1 Table 1).

The measurements provided for a well-preserved humerus of the type species *C. anderssoni* from its type locality Lok. 30 [7] shows that the humerus of *Chilotherium* is only little shortened compared to The comparison of the measurements of the herein studied chilotheres (Table 1, S1 Table 1), a well-preserved humerus of the type species *C. anderssoni* from its type locality Lok. 30 (China) [7], and several other chilothere humeri from the literature [11,12,16,17] to other rhinocerotids, like the aceratheriines *Aceratherium incisivum* Kaup, 1832 [80] from Höwenegg (Germany) [74] and *Acerorhinus zernowi* from Tung-gur (China) [75] shows that humerus of *Chilotherium* is only little shortened compared. Among chilotheres, '*C.*' *wimani* from the Linxia Basin [16] and *E. samium* [14] seem to exhibit the smallest humeri, with the maximal length of the former being 335 mm and the single specimen of the latter being 312 mm. The species with the largest dimensions for the humerus seem to be *C. orlovi* from Pavlodar, with a length value range between 357 and 378 mm (n = 5) [12]. The dimensions of the humeri of *C. schlosseri*, *C. persiae*, *C. habereri*, *C. kowalevskii* from Grebeniki [15], and a potential chilothere from Loc. 51 of the Sinap Formation (Turkey) [81], are intermediate, with overlapping ranges.

### Radius

The studied material includes 17 radii *C. persiae* from Maragheh, three of *C. habereri* from Kutschwan, and two of *C. schlosseri* from Samos (Fig 5, Table 2, S1 Table 2). Most specimens are not complete and overall, poorly preserved. The

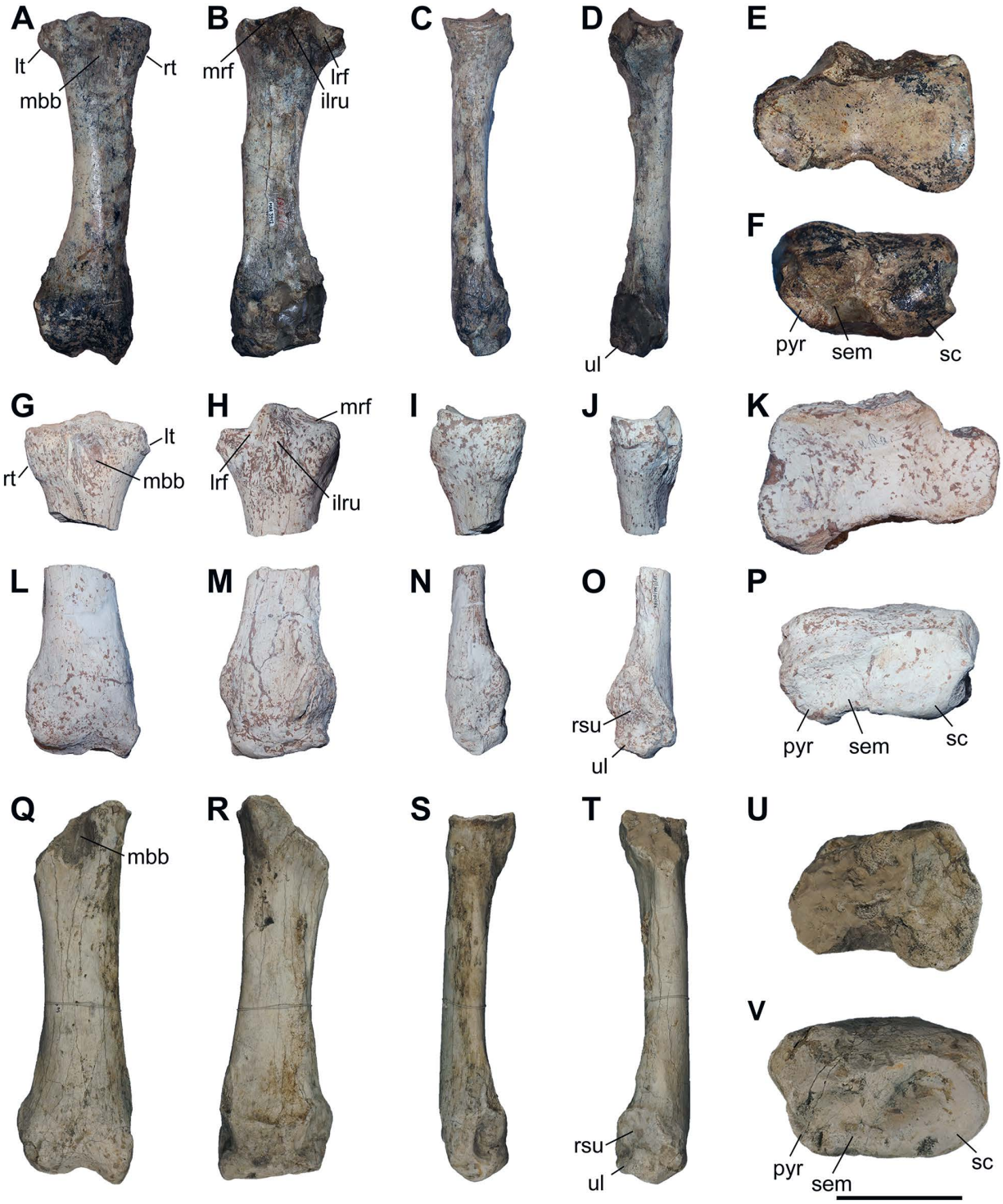


**Fig 5. The radius of chilotheres.** A–F, *Chilotherium persiae* (Pohlig, 1885) [19] (MNHN.F.MAR3912, right) from Maragheh (Iran), G–P, *Chilotherium habereri* (Schlosser, 1903) [24] (G–K: GPIT/MA/04878, left and L–P: GPIT/MA/04786, right) from Kutschwan (China), and Q–V, *Chilotherium schlosseri* (Weber, 1905) [14] (GMM 564, right) from Samos (Greece) in anterior (A, G, L, and Q), posterior (B, H, M, and R), medial (C, I, N, and S), lateral (D, J, O, and T), proximal (E, K, and U), and distal (F, P, and V) views. Abbreviations: ilru, attachment surface for the interosseous ligament between the radius and ulna; lrf, lateral radial facet; lt, lateral tuberosity; mbb, insertion for the musculus biceps brachii; mbb, medial radial facet; rt, radial tuberosity; pyr, articular facet for the pyramidal; rsu; rugose surface for the attachment of the ulna; sc, articular facet for the scaphoid; sem, articular facet for the semilunar; and ul, articular facet for the ulna. Scale bar equals 10 cm for A–D, G–J, L–O, and Q–T, and 5 cm for E, F, K, P, U, and V.

https://doi.org/10.1371/journal.pone.0336590.g005

**Table 2. Measurements of radii (in mm) of studied chilotheres.**

| | | L | TDproxmax | TDprox art | APDprox | TDdia | APDdia | TDdist max | TDdist artic | APDdist max | APDdist art |
|---|---|---|---|---|---|---|---|---|---|---|---|
| ***C. persiae*** | min | 270.5 | 76.5 | 73.1 | 53.9 | 44.5 | 26.5 | 72.3 | 60.9 | 47.8 | 33.4 |
| | max | 295.2 | 90.6 | 89.4 | 63 | 55.5 | 35.3 | 90.5 | 77.3 | 55.9 | 39.8 |
| | mean | 280.1 | 85.2 | 82.8 | 56.5 | 49.5 | 31.9 | 81.2 | 71.0 | 52.0 | 37.1 |
| | n | 5 | 13 | 8 | 15 | 15 | 15 | 7 | 7 | 7 | 7 |
| ***C. habereri*** | min | | 93.1 | 86.9 | 57.7 | 54 | 28.6 | 89.2 | 80.2 | 55 | 37.6 |
| | max | | 93.1 | 86.9 | 57.7 | 58 | 33.8 | 95.1 | 86.8 | 60 | 40.6 |
| | mean | | 93.1 | 86.9 | 57.7 | 56.0 | 31.2 | 92.2 | 83.5 | 57.5 | 39.1 |
| | n | | 1 | 1 | 1 | 2 | 2 | 2 | 2 | 2 | 2 |
| ***C. schlosseri*** | min | | | | | | 32.7 | 87.5 | 77.5 | 53.7 | 41 |
| | max | | | | | | 33.3 | 92.9 | 77.8 | 54.1 | 43.4 |
| | mean | 290.0 | | | 55.0 | 55.7 | 33.0 | 90.2 | 77.7 | 53.9 | 42.2 |
| | n | 1 | | | 1 | 1 | 2 | 2 | 2 | 2 | 2 |

https://doi.org/10.1371/journal.pone.0336590.t002

proximal articular facet for the humerus is transversally elongated, subtrapezoidal in shape with the medial side being much wider anteroposteriorly than the lateral side. In the middle of the proximal facet, there is an indentation on the anterior side and a protrusion on the posterior side. In anterior view, below the proximal articular facet the insertion for the musculus biceps brachii is represented byan excavation in the middle of the bone, with a rugose surface. This insertion is much deeper in the only specimen of *C. habereri* where it could be assessed (Fig 5G) than in *C. persiae*, *C. schlosseri* (Fig 5A, Q), and *C. wimani* from the Linxia Basin [16]. However, in *C. persiae* it seems to cover a wider area. In GMM 564, the only specimen of *C. schlosseri* in which the proximal part of the radius is preserved, it is not complete, and the morphology of this feature cannot be studied in detail. Medially placed, next to the insertion for the m. biceps brachii, the radial tuberosity is visible. This is also much more prominent in *C. habereri* (Fig 5G), where it covers almost one third of the bone's width in anterior view. In *C. persiae* (Fig 5A), the radial tuberosity is much smaller, and the surface is less rugose. In *C. schlosseri*, this feature cannot be observed. On the other side of the bone the lateral tuberosity is less prominent but extends towards the posterior side of the bone. On the posterior side, extending distally from the articular facet for the humerus, two articular facets for the ulna are visible. The medial one is a thin, transversally elongated stripe, whereas the lateral one is much larger and has an irregular shape and is larger in *C. persiae* than in *C. habereri* (Fig 5B, H). Around these two facets, a wide rugose area covers the whole proximal part of the posterior side of the bone, which represents an attachment area for the interosseous ligaments between the radius and the ulna. Further below a proximal interosseous space of about 2–3 cm is found in all specimens. From there on, the rugose crest for the attachment of the interosseous ligaments, runs down towards the distal part of the bone. A few centimeters above the distal epiphysis of the bone, a distal interosseous space of about 1 cm is placed. Right below this a large rugose area for the attachment of the ulna exists on the lateral side of the bone. At the distal end of this area, a small articular facet for the ulna is found, which seems somewhat larger in *C. persiae* and *C. schlosseri* (Fig 5D, T) than in *C. habereri* (Fig 5O). A discontinuous, rugose, and mediolaterally oriented crest is placed a few centimeters above the distal articulation. Its development varies between the specimens studied, even within the same species. For instance, for *C. persiae* in MNHN.F.MAR3908 it is rather weak, whereas in MNHN.F.MAR3906 it is much more distinct. In both specimens of *C. schlosseri* (GMM 561 and GMM 564) it is not very prominent. Concerning the two specimens of *C. habereri*, the crest is rather weak in GPIT/MA/04791 and almost absent in GPIT/MA/04786. Medially and laterally to this crest, two tuberosities are placed, which also exhibit a significant degree of variability. In *C. persiae* and *C. schlosseri* they have the shape of relative small tuberosities (Fig 5B–D, R–T), which may be somewhat proximodistally elongated in the case of MNHN.F.MAR3806 of *C. persiae*. In both specimens of *C. habereri* (Fig 5M–O), they actually form strong, proximodistally oriented crests of a few centimeters in length. The distal articular facets have a rather similar

arrangement and form among the species. Medially, the articular facet for the scaphoid is large and anteroposteriorly convex. Laterally to the scaphoid facet the articular facet for the semilunar is smaller, subtrapezoidal to rounded in shape, and concave. Next to it the articular facet for the pyramidal is represented by a slightly obliquely placed, small stripe, which is not visible in all specimens. For instance, in MNHN.F.MAR3806 it is very faintly visible, whereas in MNHN.F.MAR3808 there is no trace of it, which may mean that it just is confluent with the facet for the semilunar.

Concerning the dimensions of the radius, *C. sarmaticum* from Berislav exhibit the lowest values for the length of (247–280 mm) [11,16]. They are followed by those of '*C.*' *wimani* from the Linxia Basin and *C. kowalevskii* from Grebeniki with value ranges for the length of 266–278 mm and 262–286 mm, respectively [11,17]. The radii of *C. orlovi* from Pavlodar exhibit the largest dimensions, with a value range of 292–320 mm for the length [12]. The only species in which the radii seem to reach or almost reach the lowest values of *C. orlovi*, are *C. schlosseri*, *C. persiae* (Table 2), and a potential chilothere from Loc. 12 of the Sinap Formation [81]. The single radius of *C. anderssoni* from Lok. 30, seems to show intermediate dimensions, with a length of 280 mm [7]. For *C. habereri* no complete radius is known, but the measurable dimensions indicate that the radii were quite large, and almost comparable to *C. orlovi*.

### Scaphoid

The studied material includes one scaphoid of *C. persiae* from Maragheh, one of *C. habereri* from Kutschwan, and two from *C. schlosseri* from Samos (Fig 6, S1 Table 4). The specimens are fairly similar, though the Maragheh specimen is partially damaged. In proximal view, the articular facet for the radius is large with a subtrapezoidal outline and is in medial view sigmoidal. A prominent posteriolateral tuberosity is present, the morphology of which somewhat varies, medially to this a long thin stripe represents the proximal articular facet for the semilunar. In distal view, three articular facets for the trapezium, the trapezoid and the magnum are present. The medial facet for the trapezium is the smallest and its shape

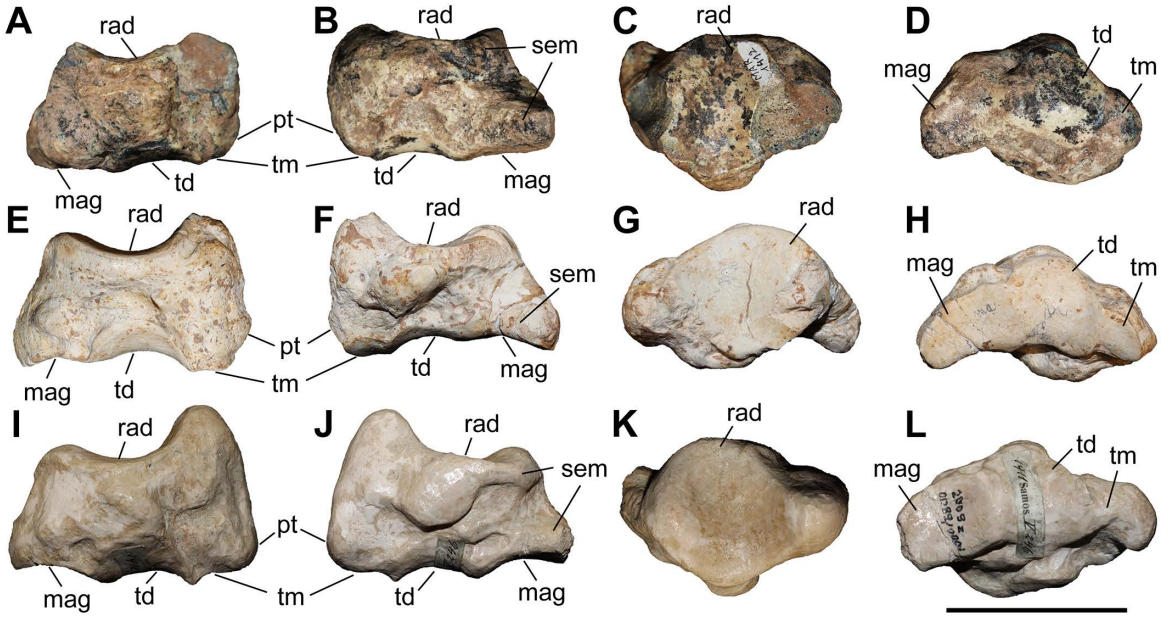


**Fig 6. The scaphoid of chilotheres.** A–D, *Chilotherium persiae* (Pohlig, 1885) [19] (MNHN.F.MAR1412, left) from Maragheh (Iran), E–H, *Chilotherium habereri* (Schlosser, 1903) [24] (GPIT/MA/04784, left) from Kutschwan (China), and I–L, *Chilotherium schlosseri* (Weber, 1905) [14] (NHMW-GEO-2009z0089/0001, left) from Samos (Greece) in anterior (A, E, and I), posterior (B, F, and J), proximal (C, G, and K), and distal (D, H, and L) views. Abbreviations: mag, articular facet for the magnum; pt, posterior tubersotiy; rad, articular facet for the radius; sem, articular facet for the semilunar; td, articular facet for the trapezoid; and tm, articular facet for the trapezium. Scale bar equals 5 cm.

https://doi.org/10.1371/journal.pone.0336590.g006

varies from triangular to semi-oval; this facet seems to be somewhat longer in *C. habereri* than in the other two species. The central facet for the trapezoid is the largest and has a subtrapezoidal shape with a convex medial border. The lateral articular facet for the magnum is subtriangular and connected to the laterodistal articular facet for the semilunar. The specimens are proximodistally short and lateromedially elongated, similar to '*C.*' *wimani* from the Linxia Basin [16], *C. sarmaticum* from Berislav [11], and *C. orlovi* from Pavlodar [12]. Although, the measurements provided for the scaphoid of *C. orlovi* represent the largest values for any chilothere yet [12].

### Semilunar

A single partial semilunar (MNHN.F.MAR.1411) of *C. persiae* from Maragheh has been examined. Only the anterior portion of the bone is preserved. The proximal articular facet for the radius is saddle-shaped, with a posteriorly extending stripe and the anterior border of the facet being convex. In medial view, it bears two suboval articular facets for the scaphoid. In lateral view, two articular facets for the pyramidal are visible, the proximal facet is subtrapezoidal, whereas the distal one is a small longitudinal stripe. In distal view, only two articular facets are visible in the preserved part, the medioproximal one is the one for the scaphoid and the lateral facet articulates to the unciform and the preserves portion is subcircular. The articular facet for the magnum, which would have been placed next to these facets, is not preserved. The measurable dimensions of the Maragheh specimen are almost identical to the measurements provided for the semilunar of '*C.*' *wimani* from the Linxia Basin [16]. Interestingly, they are significantly higher than the values provided for the dimensions of the semilunar of *C. sarmaticum* from Berislav and *C. orlovi* from Pavlodar [11,12]. It is possible that the measurements of the latter two species do not correspond to the same sections measured in *C. persiae* and '*C.*' *wimani*, which follow those proposed by Guérin (1980) [31].

### Pyramidal

Two pyramidals (MNHN.F.MAR.1405 and MNHN.F.MAR.1413) of *C. persiae* from Maragheh have been examined (Fig 7A–E). They are higher than wide. The proximal facet, for the ulna, is antero-posteriorly concave and transversely slightly convex and indistinguishable from the probably much smaller facet for the radius. In medial view, two articular facets for the semilunar are visible, they are separated by a wide groove and have a semi-oval outline. In lateral view, in the distal half of the bone a well-developed tubercle exists that extends towards the posterior side of the bone. In posterior view, the articular facet for the pisiform has an obtuse subtriangular shape and contacts the articular facet for the ulna. The distal articular facet, for the unciform, is concave and has a suboval outline. The dimensions of the two pyramidals of *C. persiae* and those of '*C.*' *wimani* from the Linxia Basin seem to overlap almost perfectly, despite the very limited sample size [16]. The single measurement for the pyramidal of *C. anderssoni* from Lok. 30 is also quite close to the height values provided for the other two species [7]. The values for the pyramidal of *C. orlovi* from Pavlodar are comparably higher [12]. The values provided for *C. sarmaticum* from Berislav [11] seem somewhat peculiar, as the given transversal diameter value is higher than the height of the bone, which is not the case in the other chilotheres and unusual for rhinoceroses in general. It would be more plausible to assume that distances measured by Korotkevitch (1970) [11], are not the same as those given by Guérin (1980) [31], which was followed in the current study.

### Trapezoid

Only one trapezoid (MNHN.F.MAR.1409) of *C. persiae* from Maragheh was studied (Fig 7F–J). In proximal view, the articular facet for the scaphoid has a subtrapezoidal outline. In medial view, it bears a small, elongated articular stripe for the trapezium. In lateral view, it bears a larger almost rectangular facet for the magnum. In distal view, the articular facet for the McII is oval. Deng (2002) [16] mentioned that the trapezoid of '*C.*' *wimani* from the Linxia Basin in China bears two articular facets for the magnum on its lateral side, in contrast to the single articular facet present in the Maragheh specimen. The measurements also show that the Maragheh trapezoid is transversally wider (see S1 Table 7). The dimensions

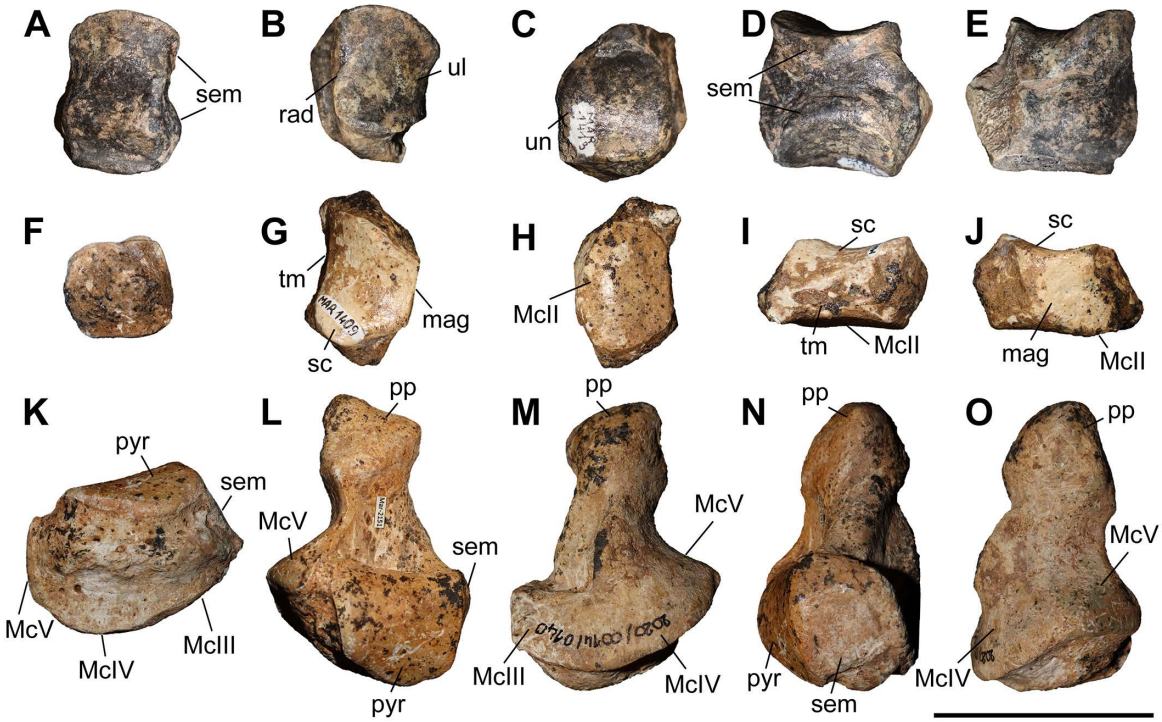


**Fig 7. Carpals of *Chilotherium persiae* (Pohlig, 1885) [19] from Maragheh (Iran).** A–E, pyramidal (MNHN.F.MAR1413, left), F–J, trapezoid (MNHN.F.MAR1409, right), and K–O, unciform (NHMW-GEO-2020/0014/0140, left) in anterior (A, F, and K), proximal (B, G, and L), distal (C, H, and M), medial (D, I, and N), and lateral (E, J, and O) views. Abbreviations: mag, articular facet for the magnum; McII, articular facet for the McII; McIII, articular facet for the McIII; McIV, articular facet for the McIV; McV, articular facet for the McV; pp, posterior process; pyr, articular facet for the pyramidal; rad, articular facet for the radius; sc, articular facet for the scaphoid; sem, articular facet for the semilunar; tm, articular facet for the trapezium; ul, articular facet for the ulna;and un, articular facet for the unciform. Scale bar equals 5 cm.

https://doi.org/10.1371/journal.pone.0336590.g007

of the trapezoid of '*C.*' *wimani* seem to be much closer to those of *C. sarmaticum* from Berislav [11]. The trapezoid of *C. anderssoni* from Lok. 30 seems to have dimensions that are more similar to *C. persiae* [7]. The trapezoid of the *C. orlovi* from Pavlodar, on the other hand, has generally greater dimensions, with only the transversal width being smaller [12]. It has to be noted that in complex bones like carpals, it is very difficult to compare measured dimensions if they did not follow the exact same method of measuring.

### Unciform

Six unciforms from Maragheh can be attributed to *C. persiae* (Fig 7K–O). In three of them the characteristic posterior process is broken off. In proximomedial view, the saddle-shaped facet for the pyramidal and the trapezoidal-shaped facet for the semilunar meet at an almost right angle. In distal view, the articular facets for the magnum, McIII, and McIV, are represented by a continuing wide stripe, without any well-defined separation. The articular facet for the magnum has posteriorly bent medial edge. The articular facet for the McIII has an irregular outline. The facet for the McIV is subtriangular to subtrapezoidal and forms a small, but notable, hump. In lateral view, the same articular stripe continues and forms the articular facet for the rudimentary McV. At the border between the articular facets for the McIV and McV a very subtle depression is present. In posterior view, a large curved posterior process is visible. The unciforms of *C. persiae* are much larger than those of '*C.*' *wimani* from the Linxia Basin [16], especially the length of the bone in the latter species is significantly smaller. The dimensions reported for the unciform of *C. anderssoni* from Lok. 30 [7] and *C. sarmaticum* from

Berislav [11] are only slightly smaller than those of *C. persiae*. The dimensions of the unciforms of *C. orlovi* from Pavlodar on the other hand are greater than in any other chilothere thus far [12].

### Second metacarpal

Four McII of *C. persiae* from Maragheh and two of *C. habereri* from Kutschwan were studied (Fig 8, Table 3). Only in a single specimen (NHMW-GEO-2020/0014/0142) the complete length of the bone is preserved and measurable, in the other specimens the distal portion is broken off. In proximal view the articular facet for the trapezoid is suboval to subtrapezoidal, transversally concave and anteroposteriorly convex. Laterally, it shares a wide connection to the obliquely placed longitudinal articular stripe for the magnum. The magnum facet contacts the articular facet(s) of the McIII in both species. In the two specimens of *C. persiae* where the proximal part is sufficiently preserved, the articular facet for the McIII is a continuous, wide stripe and is in proximal view concave (Fig 8C), whereas in the single specimen of *C. habereri* we see two small, distinct articular facets for the McIII (Fig 8I). No articular facet for the trapezium is visible on the proximomedial side of the bone. On the anterior side of the McII a prominent tuberosity covers the proximal part of the bone that

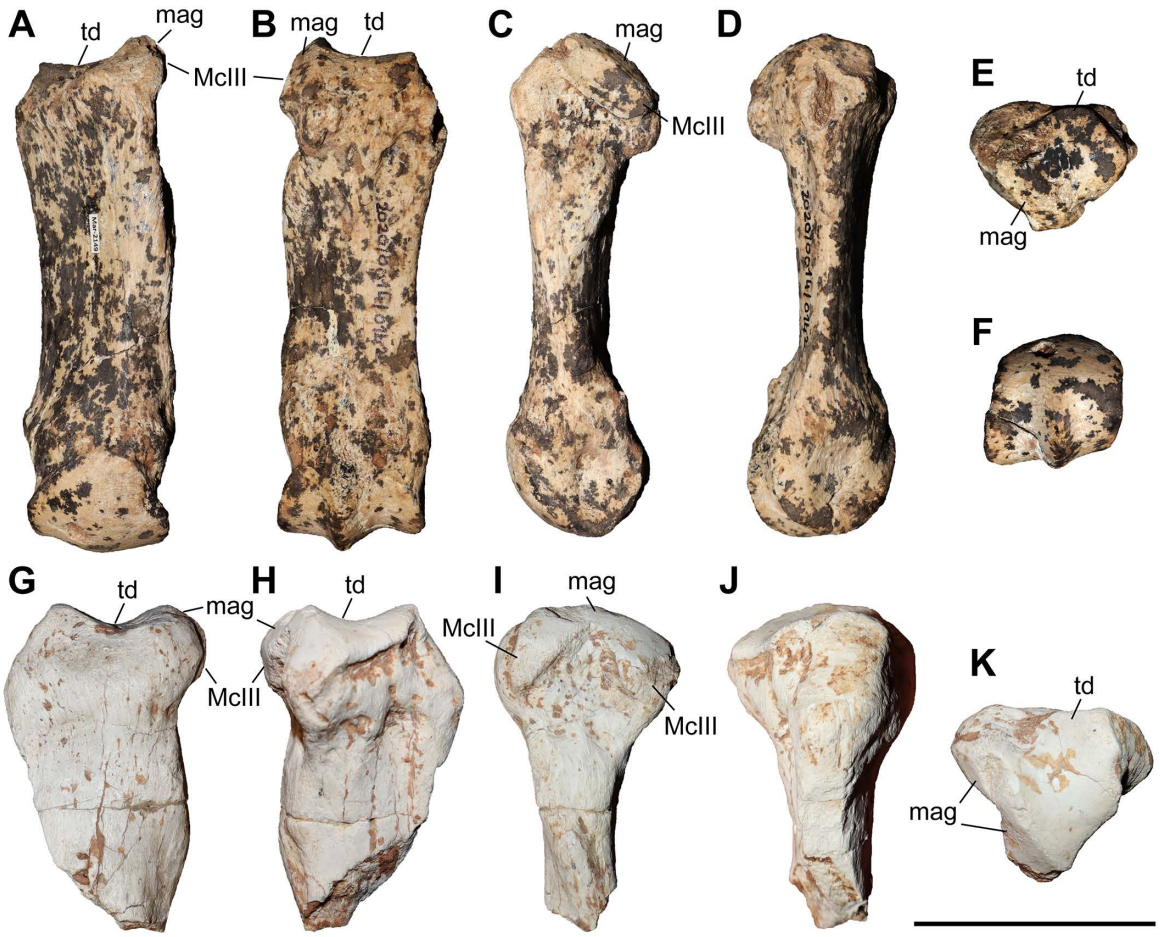


**Fig 8. The second metacarpal of chilotheres.** A–F, *Chilotherium persiae* (Pohlig, 1885) [19] (NHMW-GEO-2020/0014/0142, left) from Maragheh (Iran), and G–K, *Chilotherium habereri* (Schlosser, 1903) [24] (GPIT/MA/04783, left) from Kutschwan (China), in anterior (A, G), posterior (B, H), lateral (C, I), medial (D, J), proximal (E, K), and distal (F) views. Abbreviations: mag, articular facet for the magnum, McIII, articular facet for the McIII; and td, articular facet for the trapezoid. Scale bar equals 5 cm.

https://doi.org/10.1371/journal.pone.0336590.g008

**Table 3. Measurements (in mm) of second metacarpals of the studied chilotheres.**

| | | L | TDprox max | TDprox art | APDprox | TDdia | APDdia | TDdist max | TDdist artic | APDdist |
|---|---|---|---|---|---|---|---|---|---|---|
| *C. persiae* | min | | 37.1 | 31.1 | 36.3 | 30.4 | 15.4 | 34.6 | | |
| | max | | 42.5 | 39.6 | 41 | 33.1 | 15.7 | 37 | | |
| | mean | 108.5 | 39.1 | 33.4 | 38.3 | 31.8 | 15.6 | 35.8 | 31.1 | 31.9 |
| | n | 1 | 4 | 4 | 4 | 2 | 2 | 2 | 1 | 1 |
| *C. habereri* | GPIT/MA/04783 | | 46.4 | 37 | 40 | | | | | |
| | GPIT/MA/04782 | | | | | | | 40.3 | 37.5 | 33.3 |

https://doi.org/10.1371/journal.pone.0336590.t003

represents a muscle attachment area for the extension of the metapodials. The tuberosity forms a slight discontinuous groove between the articular facet for the trapezoid and the tuberosity. On the posterior side, the articular facets for the trapezoid and magnum end on a slight protuberance, from which a small but notable crest extends distally to a variable degree. The shaft of the bone is straight, and the distal articular head is somewhat asymmetrical. The median distal keel develops in the posterior half of the trochlea. Deng (2002) [16] described a similar arrangement and overall morphology for the proximal articular facets of the McII mentioning also that the facets for the magnum and the McIII create a marked crest, by meeting at an angle. The length of the sole complete McII from Maragheh (Table 3, S1 Table 9) is slightly lower than the values given for *C. kowalevskii* from Grebeniki and *C. orlovi* from Pavlodar but is comparable to the length measured in *C. anderssoni* from Lok. 30, '*C.*' *wimani* from the Linxia Basin, *C. sarmaticum* from Berislav, and a potential 'primitive' *Chilotherium* from Loc. 12 of the Sinap Formation [7,11,12,16,81]. The maximal transversal diameter of the proximal epiphysis is best comparable to those of '*C.*' *wimani*, *C. kowalevskii*, *C. orlovi*, and the potential 'primitive' *Chilotherium* from Sinap, while the proximal anteroposterior diameter is closer to *C. sarmaticum* and *C. orlovi*.

### Third metacarpal

Five McIII of *C. persiae* from Maragheh and two of *C. habereri* from Kutschwan were studied (Fig 9, Table 4). In only two of those (MNHN.F.MAR.1379 and MNHN.F.MAR.1383) the complete length of the bone is measurable. The proximal articular facet for the magnum has an almost subtriangular to subtrapezoidal outline, with a sigmoidal anterior border. It is transversally concave and anteroposteriorly convex and meets the small, oval articular facet for the McIII at an almost right angle, on the medial side. Laterally in the anterior part, the facet for the magnum meets the trapezoidal articular facet for the unciform at an almost right angle. This facet, in turn contacts the semi-oval anterior articular facet for the McIV. This facet is separated by a wide and deep groove from the elliptical posterior articular facet for the McIV, which meets the posterior part of the articular facet for the magnum at an acute angle.

All specimens have a rather straight shaft, with a slight concave lateral aspect in anterior view. In the proximal part of the anterior side, just below the proximal articular facet, a strong rugose surface for the insertion of the carpal extensor muscle exists. The distal articular head is fairly symmetrical, with a strongly convex proximal border on the anterior side and a prominent central keel on the posterior sides. The keel reaches approximately the middle of the head. Additionally, above this keel, on the posterior side, a small but prominent rugose crest extends proximally and vanishes before the middle of the bone. The overall morphology of the Maragheh specimens fits the descriptions provided for the McIII of other chilotheres like *C. anderssoni* from Lok. 30, '*C.*' *wimani* from the Linxia Basin, *C. sarmaticum* from Berislav, *C. kowalevskii* from Grebeniki, and *C. orlovi* from Pavlodar [7,11,12,16]. Metrically, the main aspect that could be used to differentiate them seems to be the length of the bones (S1 Table 10). More specifically, the length of the Maragheh specimens (132.9 and 140.7 mm, Table 4) is comparable to the reported values for *C. kowalevskii* (128.9–142.7 mm, n = 10), *C. orlovi* (128–153 mm, n = 15) and the potential 'primitive' *Chilotherium* from Loc. 12 of the Sinap Formation (135 mm, n = 1), which are greater than the reported values for '*C.*' *wimani* (120–123 mm, n = 2), *C. anderssoni* (127 mm, n = 1), and *C. sarmaticum* (113–129 mm, n = 6), having almost no overlap between them [7,11,12,16,81].

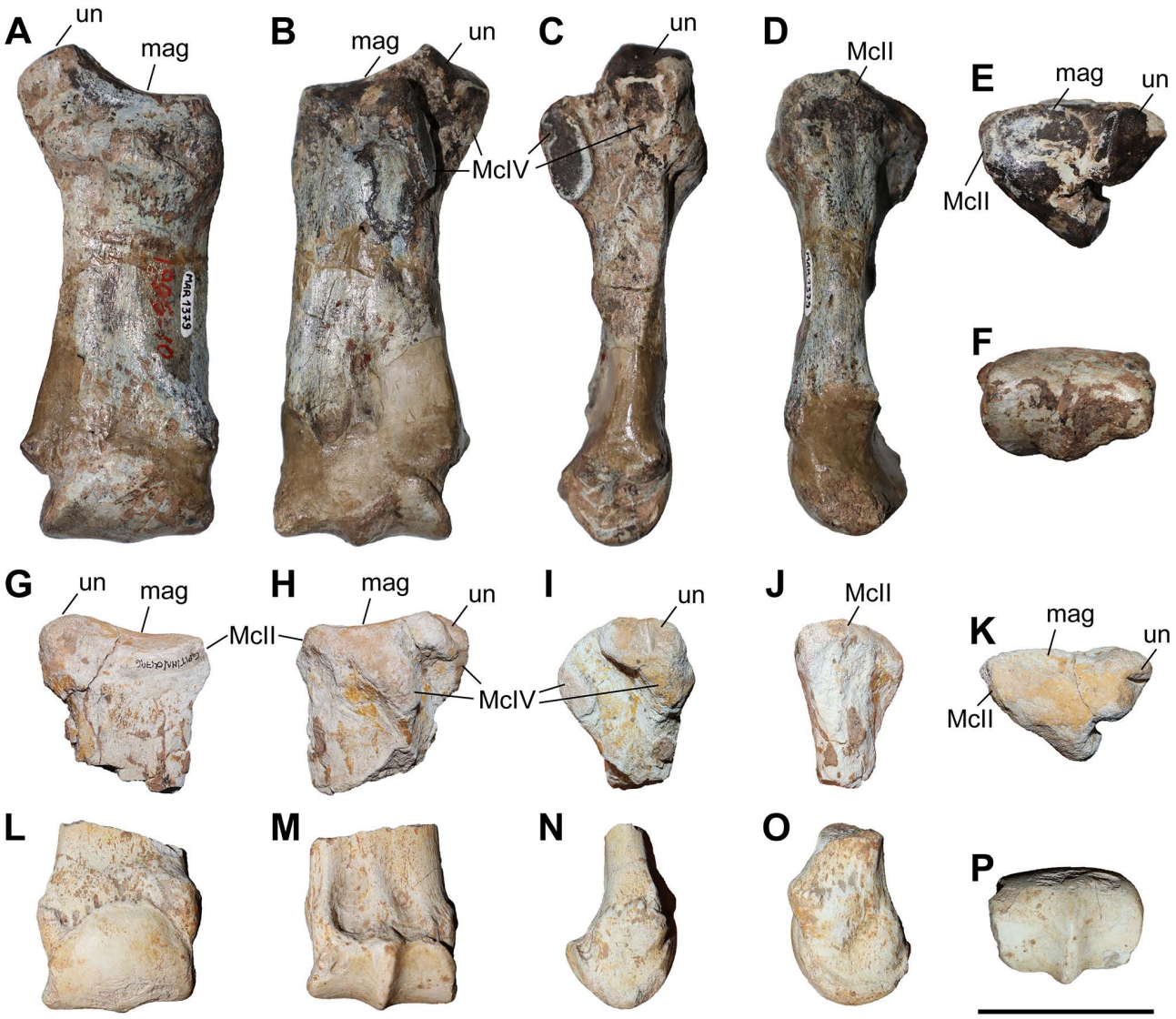


**Fig 9. Third metacarpal of chilotheres.** A–F, *Chilotherium persiae* (Pohlig, 1885) [19] (MNHN.F.MAR1379, right) from Maragheh (Iran), and G–P, *Chilotherium habereri* (Schlosser, 1903) [24] (G–K: GPIT/MA/04796 and L–P: GPIT/MA/04782, both right) from Kutschwan (China) in anterior (A, G, L), posterior (B, H, M), lateral (C, I, N), medial (D, J, O), proximal (E, K), and distal (F, P) views. Abbreviations: mag, articular facet for the magnum; McII, articular facet for the McII; McIV, articular facet for the McIV; and un, articular facet for the unciform. Scale bar equals 5 cm.

https://doi.org/10.1371/journal.pone.0336590.g009

**Table 4. Measurements (in mm) of third metacarpals of the *Chilotherium persiae* (Pohlig, 1885) [19].**

| | | L | TDprox max | APDprox | TDdia | APDdia | TDdist max | TDdist artic | APDdist |
|---|---|---|---|---|---|---|---|---|---|
| *C. persiae* | min | 132.9 | 45.9 | 39 | 24.4 | 17.1 | 46 | 46.5 | 35.6 |
| | max | 140.7 | 55.7 | 48.6 | 43.8 | 23.4 | 52.2 | 48.7 | 36.2 |
| | mean | 136.8 | 52.7 | 44.7 | 38.2 | 19.0 | 49.6 | 47.6 | 35.9 |
| | n | 2 | 4 | 4 | 4 | 5 | 3 | 3 | 2 |

https://doi.org/10.1371/journal.pone.0336590.t004

### APDAPD

**Fourth metacarpal.** Six McIV of *C. persiae* from Maragheh and one of *C. habereri* from Kutschwan were studied (Fig 10, Table 5), all of which are more or less complete. In proximal view, the shape of the articular facet for the unciform varies from subtriangular to subtrapezoidal. Posteriorly it bends distally, creating additional articulation area for the unciform. In medial view, the two articular facets for the McIII are separated by a groove. The anterior articular facet for the McIII shares a wide contact to the articular facet for the unciform and form a ridge. Its' shape varies from an elongated stripe to subtriangular. The posterior facet for the McIII either contacts the facet for the unciform only slightly or not at all. Its' shape varies from almost circular to almost rectangular. On the lateral side, the articular facet for the rudimentary McV is a relatively thin and poorly-defined articular stripe that connects to the posterior extension of the unciform facet.

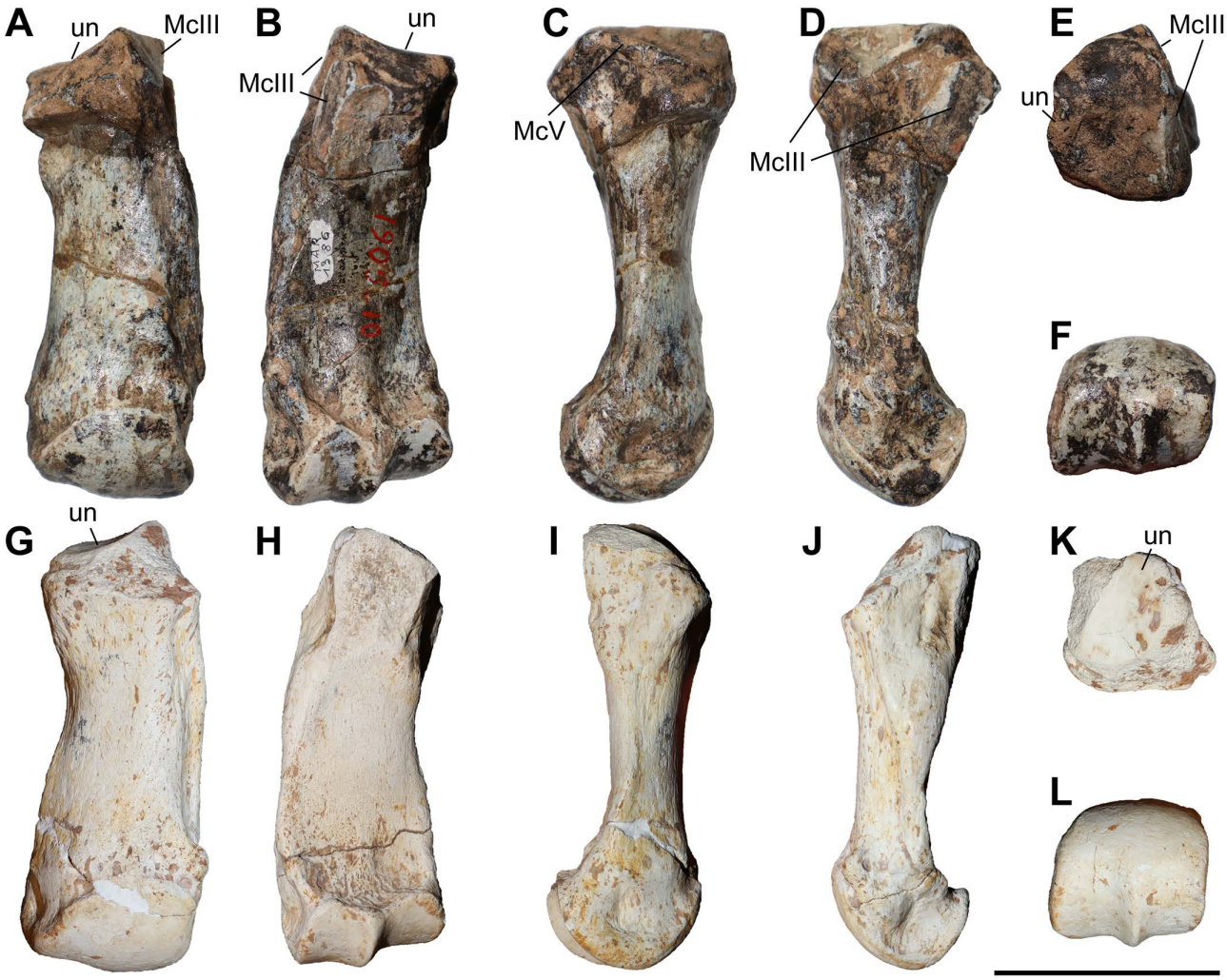


**Fig 10. The fourth metacarpal of chilotheres.** A–F, *Chilotherium persiae* (Pohlig, 1885) [19] (MNHN.F.MAR1386, right) from Maragheh (Iran), and G–L, *Chilotherium habereri* (Schlosser, 1903) [24] (GPIT/MA/04776, right) from Kutschwan (China), in anterior (A, G), posterior (B, H), lateral (C, I), medial (D, J), proximal (E, K), and distal (F, L) views. Abbreviations: McIII, articular facet for the McIII; McV, articular facet for the McV; and un, articular facet for the unciform. Scale bar equals 5 cm.

https://doi.org/10.1371/journal.pone.0336590.g010

**Table 5. Measurements (in mm) of fourth metacarpals of the studied chilotheres.**

| | | L | TDprox max | TDprox art | APDprox | TDdia | APDdia | TDdist max | TDdist artic | APDdist |
|---|---|---|---|---|---|---|---|---|---|---|
| *C. persiae* | min | 88.2 | 27.8 | 29.6 | 34.2 | 25.9 | 15.7 | 33.3 | 27.5 | 27.4 |
| | max | 106.1 | 35.8 | 29.6 | 43.1 | 34.2 | 20 | 39.6 | 36.4 | 34.6 |
| | mean | 101.1 | 30.9 | 29.6 | 40.1 | 30.6 | 17.9 | 37.1 | 32.3 | 31.7 |
| | n | 6 | 6 | 1 | 5 | 6 | 6 | 5 | 6 | 6 |
| *C. habereri* | GPIT/MA/04776 | 100 | >34 | | | 29.9 | 16.5 | 36.2 | 34.1 | 33.3 |

https://doi.org/10.1371/journal.pone.0336590.t005

Below the articular facets for the third metacarpal a long, almost triangular rugosity for the attachment of the interosseous ligament is placed. The shaft is slightly laterally curved, and the distal articular head is somewhat asymmetrical.

The McIV of the different chilotheres have a similar morphology overall. Though there are some potential differences found in the literature. For instance, while Korotkevich (1970) [11] and Bayshashov (1993) [12] described the existence of a small articular facet for the McV in *C. sarmaticum* from Berislav and *C. orlovi* from Pavlodar respectively, Deng (2002) [16] mentioned that in '*C.*' *wimani* from the Linxia Basin there is no articular facet for the McV. However, no lateral view of any McIV is provided to confirm this and it is possible that the McV facet in '*C.*' *wimani* remained unnoticed due to its very small size..

The metrical comparison of the McIV (S1 Table 11) indicates that there is a distinction between some species based on the values of the total length of this bone. More specifically, *C. persiae* (100.6–105.6 mm, n = 5) fits best among the greater values seen in *C. kowalevskii* (93.2–108.2 mm, n = 10), and is somewhat smaller than *C. orlovi* (107–115 mm, n = 8) [11,12]. Whereas '*C.*' *wimani* (91.5–93 mm, n = 4), *C. sarmaticum* (90.5–95 mm, n = 6), *Chilotherium* indet. from Kavakdere in Turkey (89.4–92.5 mm, n = 2) have smaller values [11,16,81]. The single McIVs of *C. anderssoni* (98 mm) and of the potential 'primitive' *Chilotherium* from Sinap (97 mm) have an intermediate length [7,81]. Additionally, some material from Loc. 26 in the Sinap region referred to as '*Acerorhinus* sp. nov.', includes a McIV with a length of 95.5 mm [81], which could also be associated with the smaller group, and probably belongs to a chilothere and not to *Acerorhinus*, as previously suggested [42]. Its' gracility index (TDdia/L = 30.3%) falls well into the value range of the chilotheres (27.5–34.8%, n = 14) and the overall morphology of this bone also fits the morphology seen in *Chilotherium*. A McIV (MNHN.F.TRQ329) from Küçükçekmece (Turkey) that was assigned to *C. schlosseri* is, with a length of 112 mm, longer than most *Chilotherium* species, being in the range of *C. orlovi* but very slender (TDprox = 29 mm and TDdia = 25 mm). Its' gracility index (TDdia/L = 22.3%) is lower than in any available chilothere (27.5–34.8%, n = 14) and even lower than in the non-chilothere *Aceratherium incisivum* from Höwenegg (24.3–27.4%, n = 4) but falls well into the range of *Acerorhinus zernowi* from Tung Gur (19.8–23.9%, n = 3), which has a significantly more elongated appendicular skeleton than any chilothere.

### Fifth metacarpal

A single McV (GPIT/MA/04756) of *C. habereri* from Kutschwan was studied (Fig 11). It is small, with a total length of 27.4 mm, and has a cone-like shape with a rounded tip. It has two articular facets: one large and quadrangular one for the unciform and a much smaller striper for the McIV. The two articular facets connect at a slightly acute angle and do not have any well-defined border. No other McV was found in the studied collections, and its morphology remains unknown for *C. persiae* and *C. schlosseri*. Ringström (1924) [7] described a simple, rudimentary McV for the type species *C. anderssoni* from Lok. 30. Deng (2002) [16] mentioned no McV of '*C.*' *wimani* from the Linxia Basin and noted that in the studied McIV sample there is no articular facet for the McIV. Unfortunately, no lateral view of any McIV is provided, to confirm the complete lack of this facet. Korotkevich (1970) [11] and Bayshashov (1993) [12] explicitly mentioned the presence of a small articular facet for the McV in the McIV of *C. sarmaticum* from Berislav and *C. orlovi* from Pavlodar, respectively. Interestingly, the potential 'primitive' *Chilotherium* from Loc. 12 of the Sinap Formation exhibits a well-developed, and not

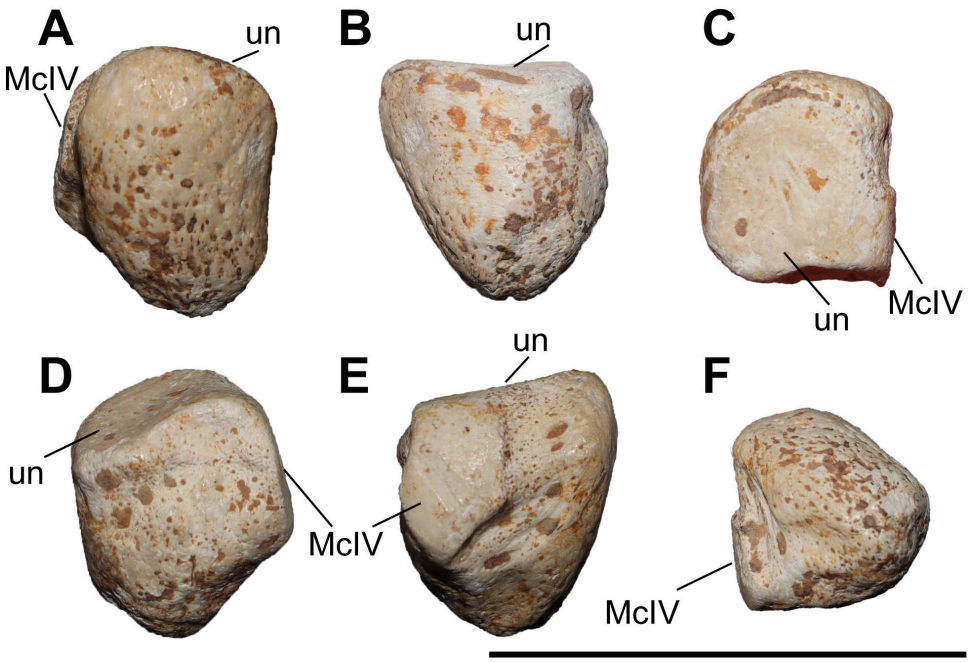


**Fig 11. The fifth metacarpal of *Chilotherium habereri* (Schlosser, 1903) [24] (GPIT/MA/04756, left) from Kutschwan.** A–F, McV in lateral (A), posterior (B), proximal (C), medial (D), anterior (E), and distal (F) views. Abbreviations: McV, articular facet for the McV; and un, articular facet for the unciform. Scale bar equals 5 cm.

https://doi.org/10.1371/journal.pone.0336590.g011

at all rudimentary, McV [81], comparable to the McV of *Aceratherium incisivum* from Höwenegg [74]. This is in stark contrast to *C. habereri* and *C. anderssoni*, which have a McV that is similarly highly reduced to extant rhinoceroses. Hence, the 'primitive' *Chilotherium* from Loc. 12 of the Sinap Formation is likely to not represent at all a chilothere, but some other aceratheriine. Representatives of *Chilotherium* overall do not have a functional McV, confirming the notion of Ringström (1924) [7] that *Chilotherium* has tridactyl limbs.

### Femur

Six femora of *C. persiae* from Maragheh, one of *C. habereri* from Kutschwan, and two of *C. schlosseri* from Samos were studied (Fig 12). Of these, only three, one of *C. persiae* and two of *C. schlosseri*, were complete enough to measure (almost) all dimensions of the bone. In most specimens the proximal part is either missing or damaged. The femoral head is protruding from the shaft and positioned higher than the greater trochanter, which is restricted to a slightly protruding, prominent tuberosity on the lateral side of the bone. On the posterior side of the femoral head, the fovea capitis is very high and narrow. On the lateral side, the convexity of the greater trochanter extends from the greater trochanter distally, creating the trochanteric fossa that is less prominent in specimen GPIT/MA/04835 of *C. habereri* (Fig 12G) than in the femora of *C. persiae* and *C. schlosseri* (Fig 12B, L). The lesser trochanter is represented by a small crest on the medial side of the bones, below the femoral head. The shaft narrows transversally towards the middle of the bone, with the third trochanter being moderately developed laterally and subtriangular when preserved, but is broken in almost all specimens. Distally, the trochlea for the patella is highly asymmetrical, with the medial lip extending much more proximally than the lateral one, in all specimens. On the anterior side, above the trochlea for the patella a deep fossa is visible (Fig 12A, K). On the posterior side, the two condyles for articulation to the tibia are slightly asymmetrical, with the medial one being wider and more rounded than the lateral one. They are separated by a deep intercondyloid fossa. The femur seems to be

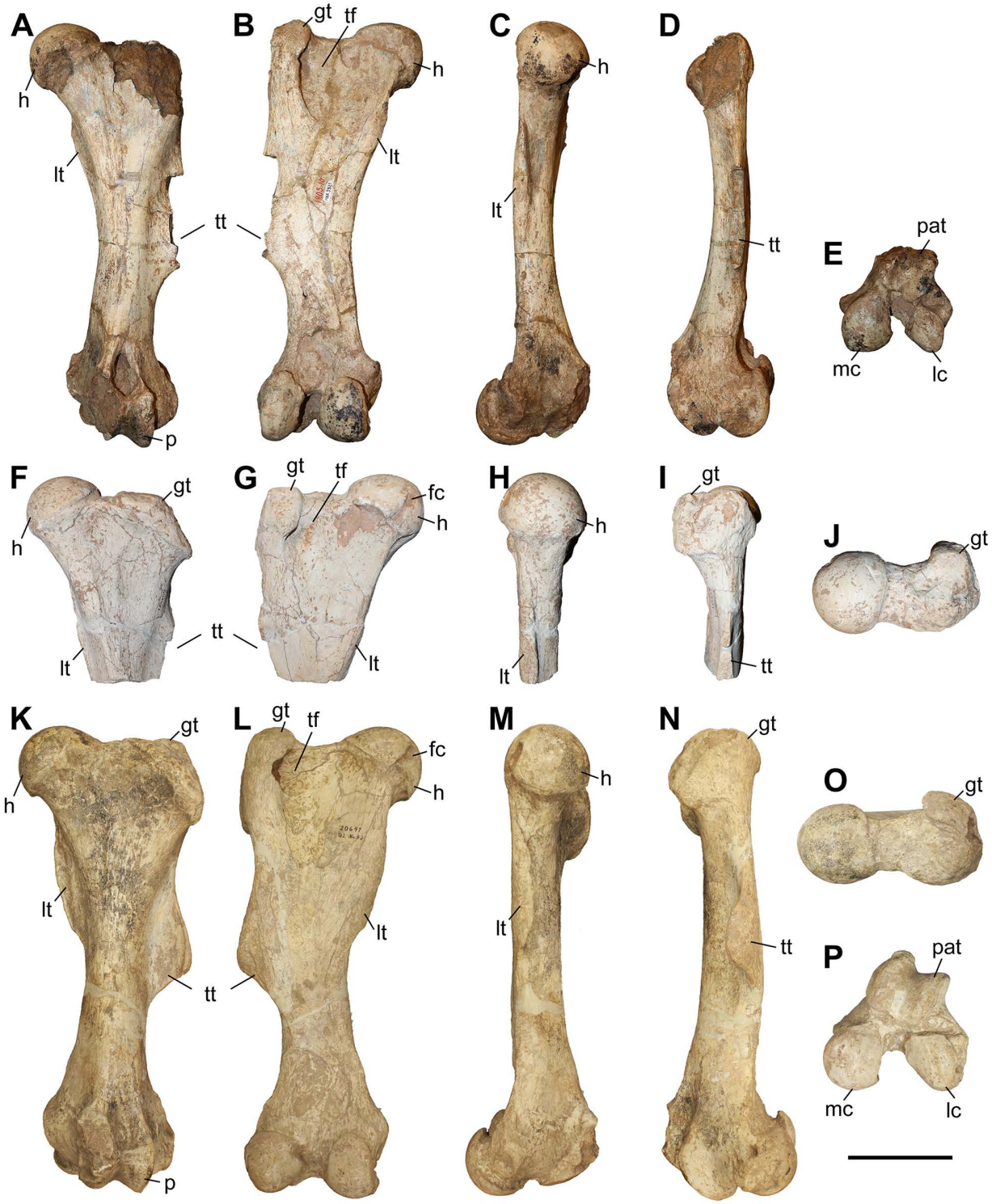


**Fig 12. The femur of chilotheres.** A–E, *Chilotherium persiae* (Pohlig, 1885) [19] (MNHN.F.MAR3921, left) from Maragheh (Iran), F–J, *Chilotherium habereri* (Schlosser, 1903) [24] (GPIT/MA/04835, left) from Kutschwan (China), and K–P, *Chilotherium schlosseri* (Weber, 1905) [14] (AMNH-20647, left) from Samos (Greece) in anterior (A, F, and K), posterior (B, G, and L), medial (C, H, and M), lateral (D, and N), proximal (J, and O), and distal (E, and P) views. Abbreviations: fc, fovea capitis, gt, greater trochanter; h, femoral head; mc, medial condyle; lc, lateral condyle; lt, lesser trochanter; pat, articular trochlea for the patella; tf, trochanteric fossa; and tt, third trochanter. Scale bar equals 10 cm.

https://doi.org/10.1371/journal.pone.0336590.g012

morphologically rather conservative within chilotheres, with most species looking almost identical [11,12,15,16]. Metrically, the femora of '*C.*' *wimani* from the Linxia Basin [16] exhibits the smallest dimensions, with its length not surpassing 400 mm. On the other hand, the femora of *C. orlovi* from Pavlodar seem to exhibit the largest dimensions, with a length ranging from 438 mm to 485 mm [12]. The dimensions of *C. schlosseri* (S1 Table 12) and *C. kowalevskii* from Grebeniki seem to be somewhat intermediate but closer to *C. orlovi*, whereas the dimensions of *C. sarmaticum* from Berislav somewhat closer to those of '*C.*' *wimani* [11,17].

### Patella

In total, 11 patellae of *C. persiae* from Maraghehand one of *C. habereri* from Kutschwan were studied (Fig 13, Table 6). The articular surface is asymmetrical, with the medial facet being higher than the lateral one, more so in *C. persiae* than in *C. habereri*. In *C. persiae*, the lateral side is narrow than in *C. habereri*. The base of the patella is rather high, projecting further proximally in *C. persiae* than in *C. habereri*. The apex is pointed in both species, but narrower in *C. persiae* and more rounded in *C. habereri* (compare Fig 13A, E). The medial process is rather prominent in both species but seems to be projecting slightly further in *C. persiae*. Metrically, the two species are very close (Table 6, S1 Table 13). The only other

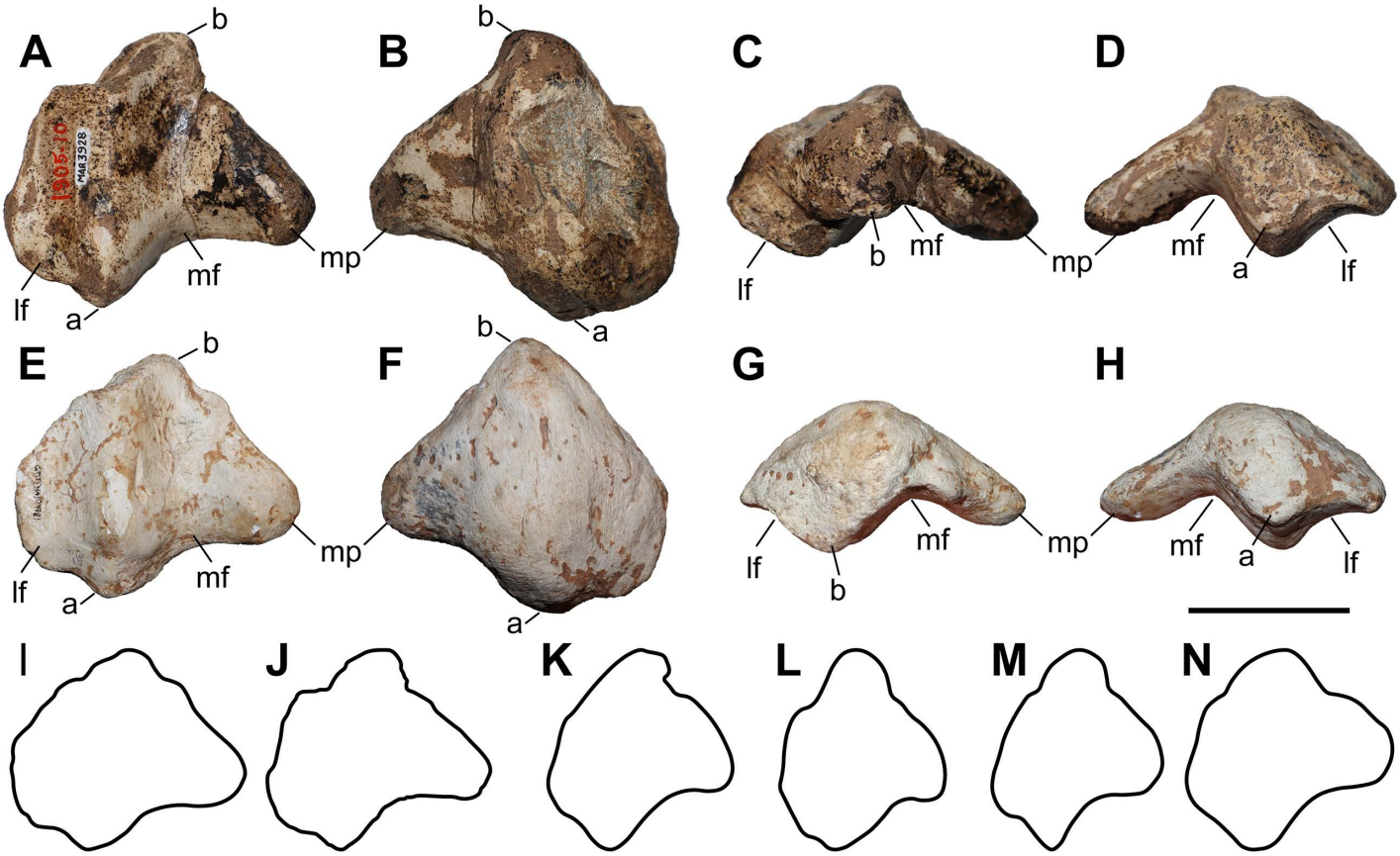


**Fig 13. The patella of chilotheres.** A–D, *Chilotherium persiae* (Pohlig, 1885) [19] (MNHN.F.MAR3928, left) from Maragheh (Iran), and E–H, *Chilotherium habereri* (Schlosser, 1903) [24] (GPIT/MA/04781, left) from Kutschwan (China), in anterior (A, E), posterior (B, F), proximal (C, G), and distal (D, H) views. I–N, outline of the patellae of *C. habereri* (I, drawn from ), *C. persiae* (J, drawn from Fig 13A), *C. kowalevskii* (K, drawn from [15]), *C. sarmaticum* (L, drawn from [11]), '*C.*' *wimani* (M, drawn from [16]), and *Aceratherium incisivum* (N, drawn from [74]) in anterior view. Abbreviations: a, apex; b, base; lf, lateral facet; mf, medial facet; and mp, medial process. Scale bar equals 5 cm for A–H. I–N are not in scale.

https://doi.org/10.1371/journal.pone.0336590.g013

**Table 6. Measurements (in mm) of patellae of the studied chilotheres.**

| | | L | TDprox max | TDprox art | APDprox |
|---|---|---|---|---|---|
| *C. persiae* | min | 76.2 | 82 | | 38 |
| | max | 89.8 | 95 | | 54.4 |
| | mean | 84.65 | 89.5 | 80 | 48.6 |
| | n | 8 | 5 | 1 | 9 |
| *C. habereri* | GPIT/MA/04781 | 83.4 | 90.7 | 76.2 | 45.6 |

https://doi.org/10.1371/journal.pone.0336590.t006

chilothere that has a patella with similar proportions is *C. orlovi* from Pavlodar [12]. The patella of '*C.*' *wimani* from the Linxia Basin differs from the patellae of *C. persiae* and *C. habereri*, in being higher proximodistally [16]. More specifically, in '*C.*' *wimani* the patella is higher than wide, which is not the case in *C. persiae* and *C. habereri*, which coincided with the proportions in *C. anderssoni* from Lok. 30 and *C. sarmaticum* from Berislav [7,11]. The measurements for a patella of *C. schlosseri* from Samos [14] are also close to these species and the proportions are a bit different from the patellae of *C. habereri* and *C. persiae* (S1 Table 13). The specimen itself was not figured [14] and was probably destroyed during WWII, along with the rest of the chilothere material from Samos that was housed in Munich [10,27,82]. For the patella of *C. kowalevskii* from Grebeniki no measurements are provided; based on the illustration provided by Pavlow (1913) [15], it seems to be very similar to that of '*C.*' *wimani* and *C. sarmaticum* [16,45]. However, in *C. sarmaticum* the apex of the patella is much more rounded than in *C. kowalevskii* and '*C.*' *wimani*. In the latter the tip of the apex is especially acute. The proportions of the patellae of *C. anderssoni*, '*C.*' *wimani*, *C. kowalevskii*, and *C. sarmaticum* are closer to those seen in *Acerorhinus zernowi* from Tung-Gur and *Aceratherium incisivum* from Höwenegg [74,75]. The morphology of the two illustrated patellae of *Aceratherium incisivum* differ significantly from each other [74: Abb. 49C, 50]. However, it is mentioned that only one is complete and the outline of this specimen (Fig 13N) is intermediate between the very wide patellae of *C. habereri* and *C. persiae* and the much narrower ones of '*C.*' *wimani*, *C. kowalevskii*, and *C. sarmaticum* (Fig 13I–M). Recently, Mallet and Houssaye (2024) [83] found that the shape of the patella in rhinoceroses and extant perissodactyls in general is strongly linked to their phylogenetic affinities and is less affected by functional constraints like body mass. Chilotheres seem to present an unexpected differentiation in the morphology of their patella and may be an exception to the otherwise rather conservative patella morphology among closely related taxa within Rhinocerotidae and other Perissodactyla.

### Tibia

Several tibiae of *C. persiae* from Maragheh, *C. habereri* from Kutschwan, and *C. schlosseri* from Samos have been studied (Fig 14, Table 7). However, only a few are adequately preserved to be able to measure the complete length of the bone and study their morphology in detail. They are rather similar with only a slight variability. The bone itself is relatively short, with the proximal epiphysis being quite wide. The lateral aspect of the tibia, on which the fibula is placed, is concave, whereas the medial side is straighter. In proximal view, the medial articular facet for the femur is larger than the lateral one. Both are concave and bend proximally towards the middle of the bone, creating a prominent ridge. Anterior to the articular facets for the femur a strong tibial tuberosityis placed, which functions as an attachment area for the patellar ligaments and merge distally into the tibial crest. The tibial tuberosity bears a wide and rounded tuberosity groove. The shape of the tibial tuberosity differs between *C. persiae* and *C. schlosseri* (compare Fig 13A, E). In proximal view, in *C. persiae* it is more transversally oriented, whereas in *C. schlosseri* it is anteroposteriorly oriented, being higher than wide. It is separated from the facet by a shallow groove. The central part of the diaphysis is relatively thin compared to the epiphyses, and relatively straight. On the lateral side of the distal epiphysis the rugose surface for the attachment of the fibula has a triangular outline. The articular surface for the astragalus has a subtrapezoidal outline in distal view, wider anteriorly than posteriorly, with the lateral malleolus of tibia and the posterolateral edge protruding.


**Fig 14. The tibia of chilotheres.** A–D, *Chilotherium persiae* (Pohlig, 1885) [19] (A–B, D: MNHN.F.MAR3931 and C: MNHN.F.MAR3933, both right) from Maragheh (Iran), and E–H, *Chilotherium schlosseri* (Weber, 1905) [14] (GMM 594, left) from Samos (Greece) in anterior (A, E), posterior (B, F), proximal (C, G), and distal (D, H) views. Abbreviations: a, articular facet for the astragalus; df, distal articular facet for the fibula; lf, lateral articular facet for the femur; mf, medial articular facet for the femur; mm, medial malleolus; tc, tibial crest; tg, tuberosity groove; and tt, tibial tuberosity. Scale bar equals 5 cm.

https://doi.org/10.1371/journal.pone.0336590.g014

**Table 7. Measurements (in mm) of tibiae of the studied chilotheres.**

| | | L | TDprox max | TDprox art | APDprox | TDdia | APDdia | TDdist max | TDdist artic | APDdist | APDdist art |
|---|---|---|---|---|---|---|---|---|---|---|---|
| *C. persiae* | min | 270.7 | 98 | 95.8 | 87.1 | 35.3 | 38 | 63 | 58.8 | 55 | 40.2 |
| | max | 302.1 | 118.6 | 99.3 | 110.4 | 53.2 | 52.4 | 90.4 | 69.9 | 64.2 | 47.5 |
| | mean | 287.2 | 105.6 | 97.1 | 102.4 | 41.8 | 46.9 | 81.9 | 63.5 | 59.3 | 44.3 |
| | n | 7 | 5 | 3 | 6 | 7 | 6 | 8 | 7 | 8 | 6 |
| *C. schlosseri* | min | 282.9 | 115 | 102 | 76.8 | 32.6 | 44 | 78.4 | 57 | 62.3 | 41.3 |
| | max | 317 | 128.9 | 113.8 | 116.9 | 49.9 | 74.9 | 94.5 | 73.7 | 73.2 | 50.6 |
| | mean | 300.1 | 121.9 | 110.7 | 107.9 | 42.4 | 62.5 | 88.7 | 67.3 | 66.2 | 47.6 |
| | n | 2 | 6 | 6 | 6 | 9 | 8 | 5 | 5 | 5 | 5 |
| *C. habereri* | | | | | | | 50.9 | 87.3 | 71.5 | 61.6 | 53 |

https://doi.org/10.1371/journal.pone.0336590.t007

The dimensions of the tibia are rather similar among chilotheres (Table 7, S1 Table 14), with the main differences being found in the total length and the dimensions of the proximal epiphysis [7,11,12,16]. *Chilotherium orlovi* from Pavlodar exhibits the greatest values for the length of the tibia, with rather large range of 280–340 mm (n = 11), which overlaps completely with the range for the length of the tibia of *C. kowalevskii* from Grebeniki (279–322 mm, n = 12). These value ranges, also cover the lengths measured in the tibiae of *C. schlosseri* from Samos (282.9–317 mm, n = 2), including also the tibia mentioned by Weber (1905) [14] from Samos with a length of 300 or 310 mm. The tibia mentioned by Kiernik (1913) [36] from Odessa has a lower length of 270/275 mm. The skull from the same locality can be assigned to *C. schlosseri*. The fact that the Odessa tibia is slightly smaller than the value range of *C. schlosseri*, is probably due to the small sample size (n = 2); especially when compared to the broad value range seen in *C. orlovi* and *C. kowalevskii*. The length of *C. persiae* tibiae from Maragheh is also very close to these values (270.7–302.1 mm, n = 7) and is almost identical to the value range given for *C. sarmaticum* from Berislav (271–301 mm, n = 11). The tibiae of '*C.*' *wimani* from the Linxia Basin seem to be placed at the lowest end of this range or even below it (269–282 mm, n = 7). The only measured tibia of *C. anderssoni* from Lok. 30 (280 mm) and the only tibia of *Chilotherium* indet. from Kavakdere on which the length could be measured (276 mm) seem to exhibit a somewhat intermediate length, compared to the other chilotheres.

### Astragalus

Concerning the astragalus, 14 specimens of *C. persiae* from Maragheh, two of *C. habereri* from Kutschwan, and five of *C. schlosseri* from Samos were studied (Figs 15–17, Table 8). Most of the specimens are fairly well preserved, allowing detailed descriptions. In anterior view, the articular facet for the tibia is fairly asymmetrical, in all studied specimens. The lateral lip of the trochlea is slightly wider and higher than the medial one. In *C. habereri*, this asymmetry is much more pronounced than in *C. schlosseri*, where the lips of the trochlea are much more similar in size (Fig 16A, F, K). In medial view (Fig 16C, H, M), the articular stripe for the medial malleolus of the tibia has a concave distal border and it narrows proximally. In lateral view, the articular stripe for the lateral malleolus of the fibula is very wide in *C. persiae* and *C. schlosseri* (Fig 16D, N) and less so in *C. habereri* (Fig 16I), but in all three species it retains a constant width and establishes a wide connection to the ectal calcaneal facet. The contact between that lateral articular facet for the malleolus of the fibula and the trochlea forms a sharp, almost right angle in *C. schlosseri*, whereas in *C. persiae* and *C. habereri* this angle is more rounded and wider. In distal view, the articular facets for the navicular and the cuboid share a wide contact and form a slight ridge between them (Fig 16E, J, O). The former is very large, subtrapezoidal, anteroposteriorly convex, and transversally concave. The latter is a much thinner stripe, which contacts the distal calcaneal facet. In posterior view, the morphology of the calcaneal facets varies significantly between the different *Chilotherium* species (Figs 16, 17) and some variability is observed within the same species from a given locality [7,11,12,16]. The sustentacular facet is relatively large

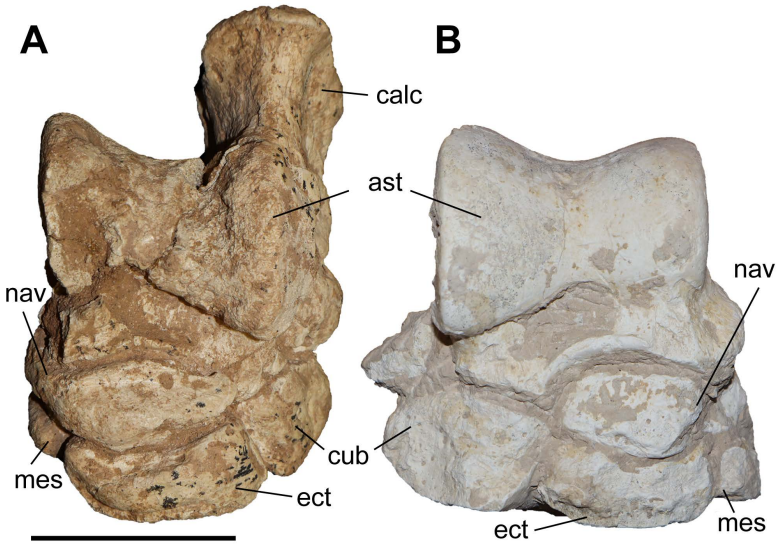


**Fig 15. The tarsus of chilotheres.** A, *Chilotherium persiae* (Pohlig, 1885) [19] (NHMW-GEO-2020/0014/0145, left) from Maragheh (Iran), and B, *Chilotherium schlosseri* (Weber, 1905) [14] (AMPG-SAM516, right) from Samos (Greece) in anterior view. Abbreviations: ast, astragalus; calc, calcaneum; cub, cuboid; ect, ectocuneiform; mes, mesocuneiform; and nav, navicular. Scale bars equal 5 cm.

https://doi.org/10.1371/journal.pone.0336590.g015

and its shape can vary from almost circular to high oval, and in some cases can have an irregular outline. In *C. habereri* and most studied specimens of *C. persiae* it remains separated from the articular facet of the navicular, cuboid and the distal calcaneal facet. However, in a few specimens a small contact with these facets can be established. In *C. schlosseri*, two astragali feature a completely isolated sustentacular facet, in two other specimens this portion cannot be studied, and in the last two astragali (GMM 571 and NHMW-GEO-1911/0005/0424) a unique condition is observed, where the sustentacular facet establishes a wide contact with the ectal calcaneal facet. This kind of connection is not observed in any other chilothere astragalus. The astragalus of '*C.*' *wimani* from the Linxia Basin (Fig 17H) variably shows a connection between the sustentacular facet, the cuboid facet and the distal calcaneal facet [16]. In *C. sarmaticum* from Berislav (Fig 17G) the astragalus exhibits a similar connection between the articular facets, but it is much wider and may also involve the navicular facet; this pattern is observed in 10 of the 12 astragali of *C. sarmaticum* [11]. Additionally, the sustentacular facet is more rounded in '*C.*' *wimani*, whereas in *C. sarmaticum* it is sub-trapezoidal (Fig 17H, G). The species *C. anderssoni*, *C. kowalevskii*, and *C. orlovi* exhibit the plesiomorphic arrangement of articular facets in rhinoceros' astragali, in which the sustentacular facet is isolated [7,11,12], similar to *C. habereri* and most *C. persiae* astragali and as seen in the astragalus of *Aceratherium incisivum* from Höwenegg (Fig 17A) and *Acerorhinus zernowi* from Tung-Gur [75]. Concerning the ectal calcaneal facet, it has a similar subtriangular outline in most species (Fig 17). In lateral view it is only little concave, compared to other rhinocerotids like *Aceratherium incisivum* from Höwenegg [74], in which it has a more prominently sigmoidal profile in lateral view. In all chilotheres, the ectal facet has a distally projecting tongue, which is usually relatively small and subtriangular to suboval in shape. In *C. schlosseri*, however, this distal tongue has a much bigger surface than in the other species; in this case, *C. schlosseri* exhibits a more derived morphology.

A last difference that can be observed in the astragalus of *C. schlosseri* in comparison to the other chilotheres is that in anterior view the medial lip is distally connected to the articular facet for the navicular, through a rugose bone growth which is observed in the six specimens where the area is observable (in the seventh this part is covered by sediment) In *C. persiae* and *C. habereri* the trochlea is separated by the distal articular facets for the navicular and the cuboid by a prominent groove, as is the case in most rhinoceroses.

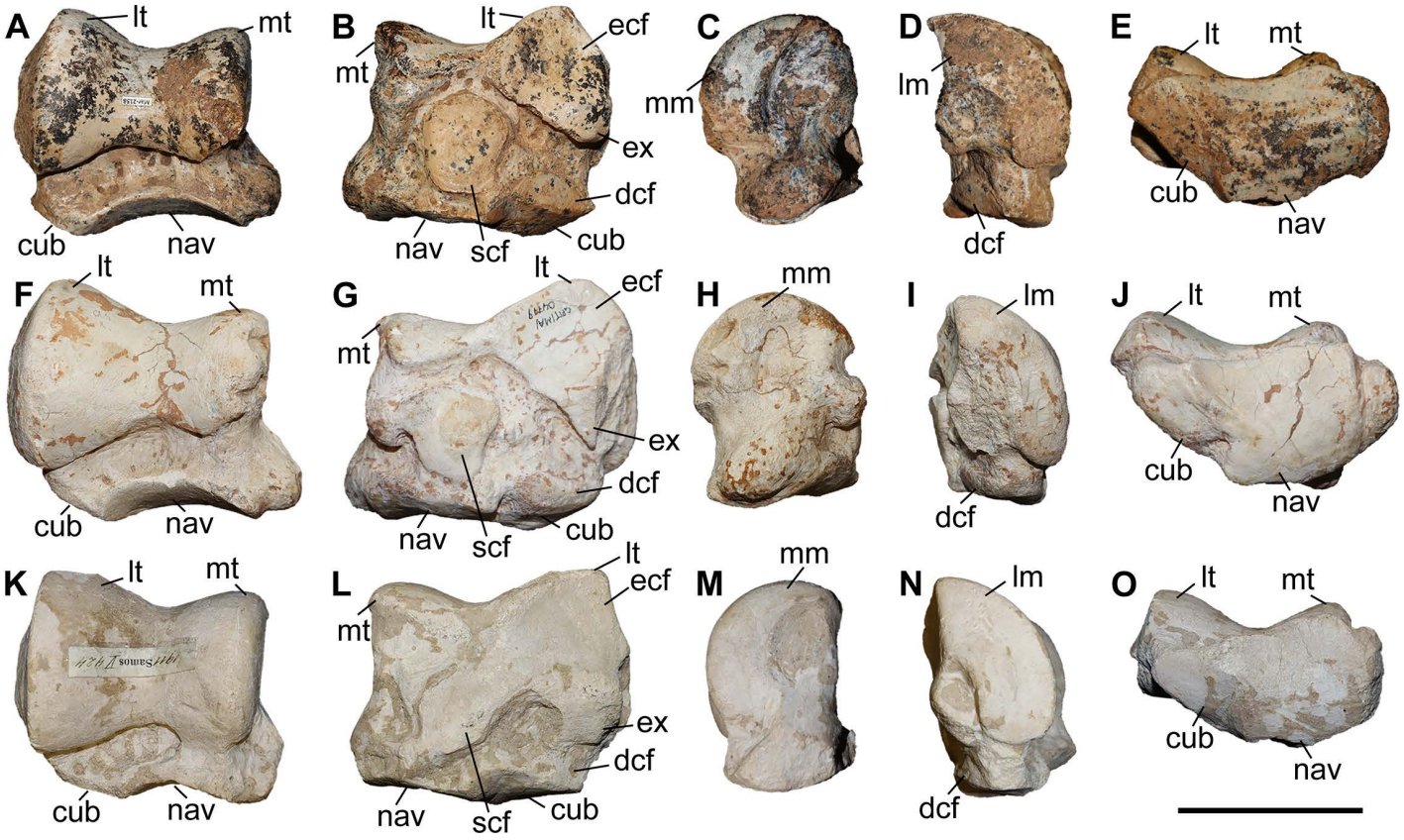


**Fig 16. The astragalus of chilotheres.** A–E, *Chilotherium persiae* (Pohlig, 1885) [19] (NHMW-GEO-2020/0014/01437, right) from Maragheh (Iran), F–J, *Chilotherium habereri* (Schlosser, 1903) [24] (GPIT/MA/04779, right) from Kutschwan (China), and K–O, *Chilotherium schlosseri* (Weber, 1905) [14] (NHMW-GEO-1911/0005/0424, right) from Samos (Greece) in anterior (A, F, and K), posterior (B, G, and L), medial (C, H, and M), lateral (D, I, and N), and distal (E, J, and O) views. Abbreviations: cub, articular facet for the cuboid; dcf, distal calcaneal facet; dpt; distally projecting tongue; ecf, ectal calcaneal facet; ex, distal expansion of the ectal calcaneal facet; lm, articular facet for thelateral malleolus of the fibula, lt, lateral lip of the trochlea, mm, articular facet for the medial malleolus of the tibia; mt; medial lip of the trochlea; nav, articular facet for the navicular; and scf, sustentacular calcaneal facet; Scale bar equals 5 cm.

https://doi.org/10.1371/journal.pone.0336590.g016

Overall, it seems very difficult to differentiate between most of the *Chilotherium* species, solely based on the astragalus morphology. However, *C. schlosseri* seems to be the exception, because half of the available specimens exhibit a connection between the sustentacular and ectal calcaneal facets, which is not observed in the other chilotheres. Additionally, the same species also exhibits a larger distally projecting tongue on the ectal calcaneal facet and the medial lip of the trochlea is connected to the navicular facet, which is not the case in the other chilotheres. Thereby, *C. schlosseri*, could be separated from the other *Chilotherium* species, based on some features. The variability of these features is, however, not clear and therefore the identification of isolated specimens remains ambiguous. Interestingly, the species '*C.*' *wimani* and *C. sarmaticum* feature a wide connection between the sustentacular and ectal calcaneal facets [11,16]. This is also observed in some specimens of *C. persiae*, but it is not clear whether this could be used as a diagnostic feature for some species or if it is a variable feature, which could potentially be observed in any given species, given a large enough sample.

### Calcaneum

In total, 19 calcanei of *C. persiae* from Maragheh, three of *C. habereri* from Kutschwan, and three of *C. schlosseri* from Samos were studied (Figs 15, 18, Table 9). Most are well-preserved and allow a detailed comparison for this bone. The

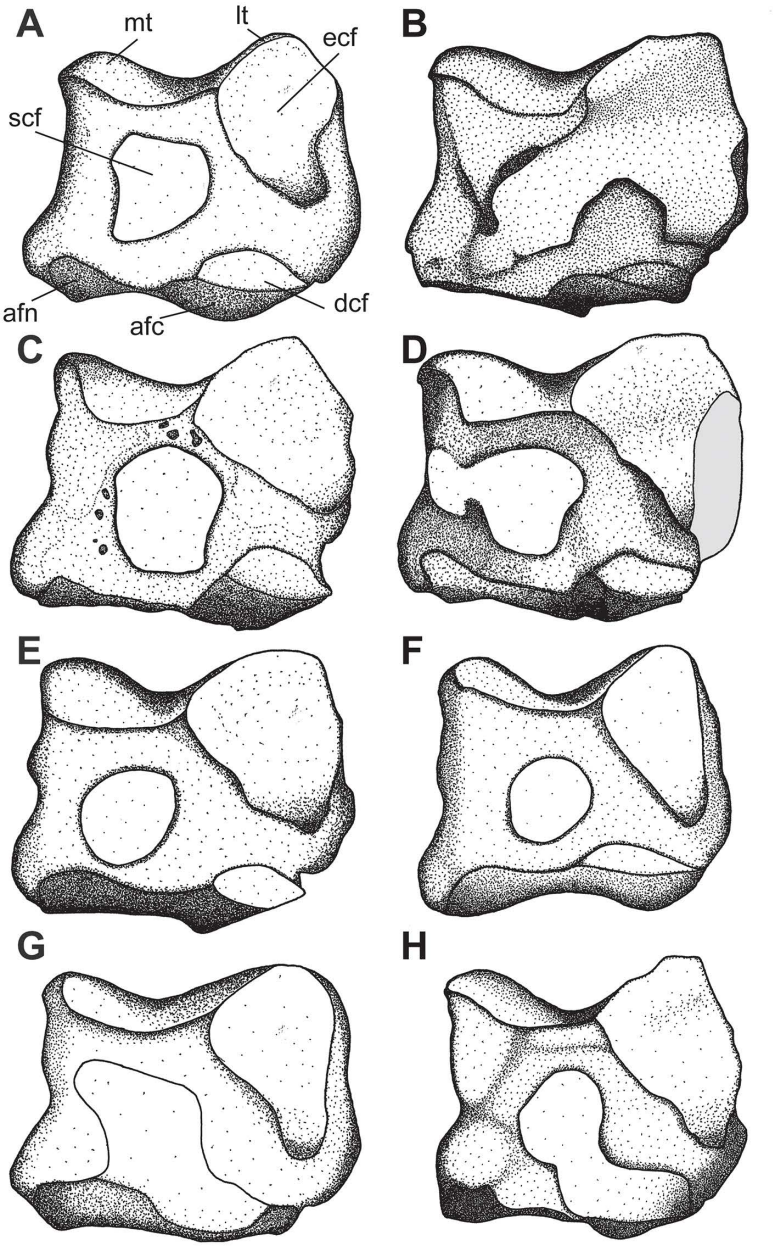


**Fig 17. Schematic comparison of chilothere astragali in posterior view.** A, *Aceratherium incisivum* Kaup, 1832 [80], B, *Chilotherium schlosseri* (Weber, 1905) [14], C, *Chilotherium persiae* (Pohlig, 1885) [19], D, *Chilotherium habereri* (Schlosser, 1903) [24], E, *Chilotherium orlovi* Bayshashov, 1982 [30], F, *Chilotherium kowalevskii* (Pavlow, 1913) [15], G, *Chilotherium sarmaticum* Korotkevitch, 1958 [45], and H, '*Chilotherium*' *wimani* Ringström, 1924 [7]. Abbreviations: afc, articular facet for the cuboid; afn, articular facet for the navicular; dcf, distal calcaneal facet; ecf, ectal calcaneal facet; lt, lateral lip of the trochlea; mt, medial lip of the trochlea; and scf, sustentacular calcaneal facet. Not to scale.

https://doi.org/10.1371/journal.pone.0336590.g017

tuber calcis is well-formed in all species and has a rugose surface. On the posterior side of the bone, the surface from the tuber calcis to the distal articular facet for the cuboid exhibits a very rugose secondary bone growth in most bones. The sustentacular facet for the astragalus is rounded in most specimens, varying in shape from almost circular to subtriangular. It is isolated from the other articular facets in all studied specimen. The ectal facet has a generally subtrapezoidal

**Table 8. Measurements (in mm) of astragali of the studied chilotheres.**

| | | H | DL | TD | TD maxi dist | APD art dist | TD art dist | APD inf |
|---|---|---|---|---|---|---|---|---|
| *C. persiae* | min | 61.2 | 47 | 67.4 | 62.6 | 31.5 | 54 | 40.7 |
| | max | 67.3 | 54.3 | 85.2 | 80.1 | 39.4 | 70.8 | 47.2 |
| | mean | 64.5 | 49.9 | 78.8 | 72.7 | 35.8 | 64.6 | 44.0 |
| | n | 13 | 14 | 14 | 14 | 14 | 14 | 13 |
| *C. habereri* | min | 73.3 | 54 | 84.2 | | 36.5 | | 48 |
| | max | 76.3 | 60.4 | 94 | | 43.7 | | 54.4 |
| | mean | 74.8 | 57.4 | 89.1 | 79.1 | 40.1 | 65.4 | 50.9 |
| | n | 2 | 3 | 2 | 1 | 2 | 1 | 3 |
| *C. schlosseri* | min | 63.7 | 53.9 | 76.6 | 68 | 34.8 | 58 | 37.7 |
| | max | 70 | 58.3 | 91.4 | 73.2 | 41.4 | 70.6 | 50.1 |
| | mean | 66.0 | 55.0 | 81.3 | 70.5 | 39.1 | 64.7 | 46.0 |
| | n | 6 | 5 | 6 | 6 | 5 | 5 | 6 |

https://doi.org/10.1371/journal.pone.0336590.t008

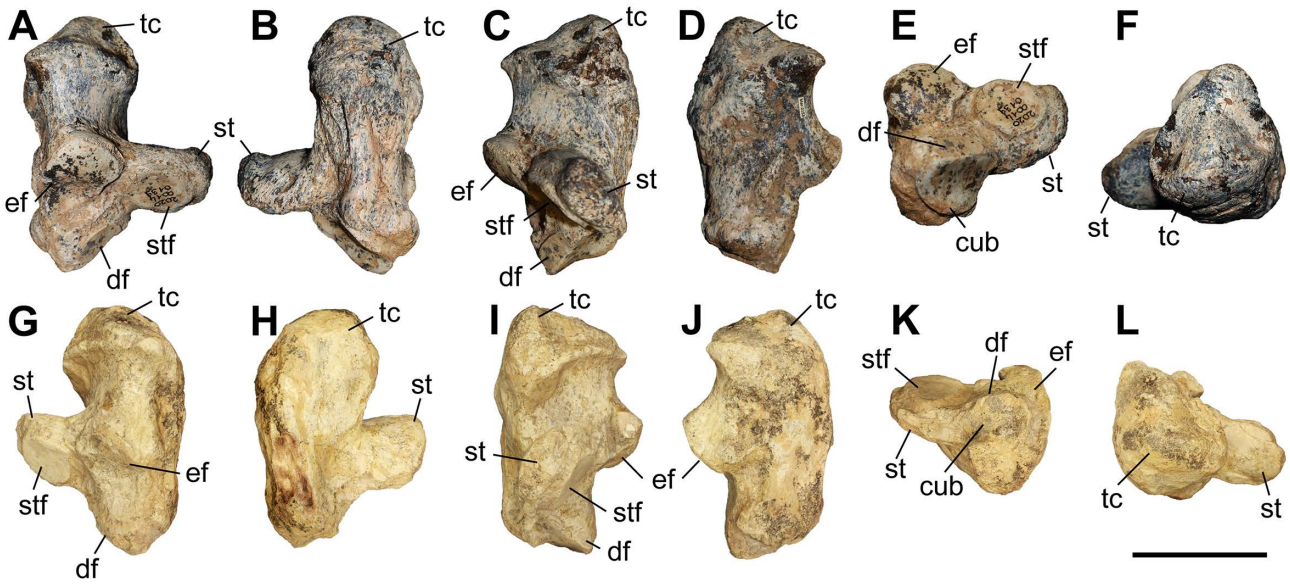


**Fig 18. The calcaneum of chilotheres.** A–F, *Chilotherium persiae* (Pohlig, 1885) [19] (NHMW-GEO-2020/0014/0139, right) from Maragheh (Iran), and G–L, *Chilotherium schlosseri* (Weber, 1905) [14] (AMNH-20794, left) from Samos (Greece) in anterior (A, G), posterior (B, H), lateral (C, I), medial (D, J), proximal (E, K), and distal (F, L) views. Abbreviations: cub, articular facet for the cuboid; df, distal articular facet, ef, ectal articular facet; st, sustentacular tali; stf, sustentacular articular facte; tc, tuber calcis. Scale bars equal 5 cm.

https://doi.org/10.1371/journal.pone.0336590.g018

outline and a sigmoidal profile in lateral view. It shares a wide contact with the semi-oval articular facet for the tibia in all three species. However, the tibia facet seems to be larger in *C. persiae* than in the other two species. The distal facet for the astragalus is elongated and subelliptical in most specimens. Distally it shares a wide contact with the articular facet for the cuboid, which is large and saddle-shaped.

The morphology of the studied specimen does not allow a separation between the three species, due to the extreme similarity of the species and the intraspecific variability observed in the Maragheh sample. For instance, the shape of the tuber calcis may vary, in some specimens of *C. persiae* it is more posteriorly developed than in others. Based on the measurements found in the literature, it seems that *C. orlovi* from Pavlodar is larger [12], and more specifically has a greater

**Table 9. Measurements (in mm) of calcanei of the studied chilotheres.**

| | | H | Hpost | APD sommet | TD sommet | TDmini post | APDbec | TDsust |
|---|---|---|---|---|---|---|---|---|
| *C. persiae* | min | 89.8 | 58.8 | 46.8 | 35 | 30.5 | 55.4 | 64 |
| | max | 106.1 | 72.9 | 61.1 | 51.9 | 41.9 | 64.3 | 78.3 |
| | mean | 99.3 | 69.6 | 55.9 | 45.0 | 35.6 | 58.5 | 71.5 |
| | n | 13 | 19 | 18 | 17 | 18 | 14 | 8 |
| *C. habereri* | GPIT/MA/04792 | 109.1 | 78 | 61 | 46 | 38 | 62.8 | 78.5 |
| *C. schlosseri* | min | 86.7 | | 60 | 36.6 | 31.5 | 57.4 | 62.8 |
| | max | 107 | | 63.2 | 55 | 48.5 | 64.1 | 80 |
| | mean | 96.9 | | 61.8 | 45.7 | 38.8 | 60.1 | 71.5 |
| | n | 4 | | 4 | 4 | 3 | 3 | 4 |

https://doi.org/10.1371/journal.pone.0336590.t009

height, than the other chilotheres. Whereas the calcanei of '*C.*' *wimani* from the Linxia Basin [16] and *C. sarmaticum* from Berislav [11] are clearly smaller. On the other hand, the studied calcanei of *C. schlosseri*, *C. persiae*, and *C. habereri* (Table 9) overlap with the dimensions of *C. anderssoni* from Lok. 30 and *C. kowalevskii* from Grebeniki [11] and seem to have an intermediate size (S1 Table 17). Therefore, a specific identification based on the calcaneum is rather difficult.

### Navicular

Six naviculars of *C. persiae* from Maragheh, one of *C. habereri* from Kutschwan, and one of *C. schlosseri* from Samos were studied (Fig 15, 19A–B). One navicular of *C. persiae* (NHMW 2020/0014/0145) and the single specimen of *C. schlosseri* are found in an articulated tarsus and their morphology cannot be assessed (Fig 15B). In proximal view, the articular facet for the astragalus is subrhomboidal and anteroposteriorly concave. In distal view, the three articular facets for the cuneiforms are separated by weak ridges exist. The medial facet for the entocuneiform is the smallest, obliquely placed, and its shape varies from subcircular to almost triangular. The central facet for the mesocuneiform has a subtrapezoidal outline. The lateral facet for the ectocuneiform is the largest and its shape varies from subtrapezoidal to an upturned "L". In lateral view, two articular facets for the cuboid exist. The proximal one is a narrow, anteroposteriorly oriented stripe, which is separated from the posterodistal facet by a shallow groove. The latter is obliquely placed and has an almost circular outline. The comparison of the studied material to chilotheres naviculars described in the literature shows that they are very similar. More specifically, Deng (2002) [16] described a very similar morphology for '*C.*' *wimani* from the Linxia Basin and even mentioned the fact that it bears two separated articular facets for the cuboid. Comparing the dimensions given in the literature for '*C.*' *wimani* [16] and *C. sarmaticum* from Berislav [11], it seems that *C. schlosseri* and *C. sarmaticum* have a similar height, which is lower than in *C. persiae* and '*C.*' *wimani*. However, the overall dimensions of '*C.*' *wimani* and *C. sarmaticum* are smaller [11,16] than in *C. schlosseri*, *C. persiae* and *C. habereri* (S1 Table 18). In the case of *C. orlovi* from Pavlodar [12] the measurements provided for the anteroposterior diameter of the navicular is greater than the transversal length, which is contrasting all other chilotheres and most rhinoceroses in general, therefore we assume that these values are in fact inversed. This would make the dimensions of *C. orlovi* fall into the size range of *C. schlosseri*, *C. persiae* and *C. habereri*, which is a much more plausible result.

### Cuboid

Three cuboids of *C. persiae* from Maragheh and only one of *C. schlosseri* from Samos were available for study (Fig 19C–G). Of these, only two (MNHN.F.MAR1427b and MNHN.F.MAR1414) of *C. persiae* were able to be studied in detail, because the third specimen of *C. persiae* and the only one of *C. schlosseri* are articulated with other tarsal bones (Fig 15). In proximal view, two articular facets are separated by a slight ridge (Fig 19C). The medial facet for the astragalus has a subtriangular outline. The lateral facet for the calcaneum is subtrapezoidal. Together they form a subtrapezoidal surface

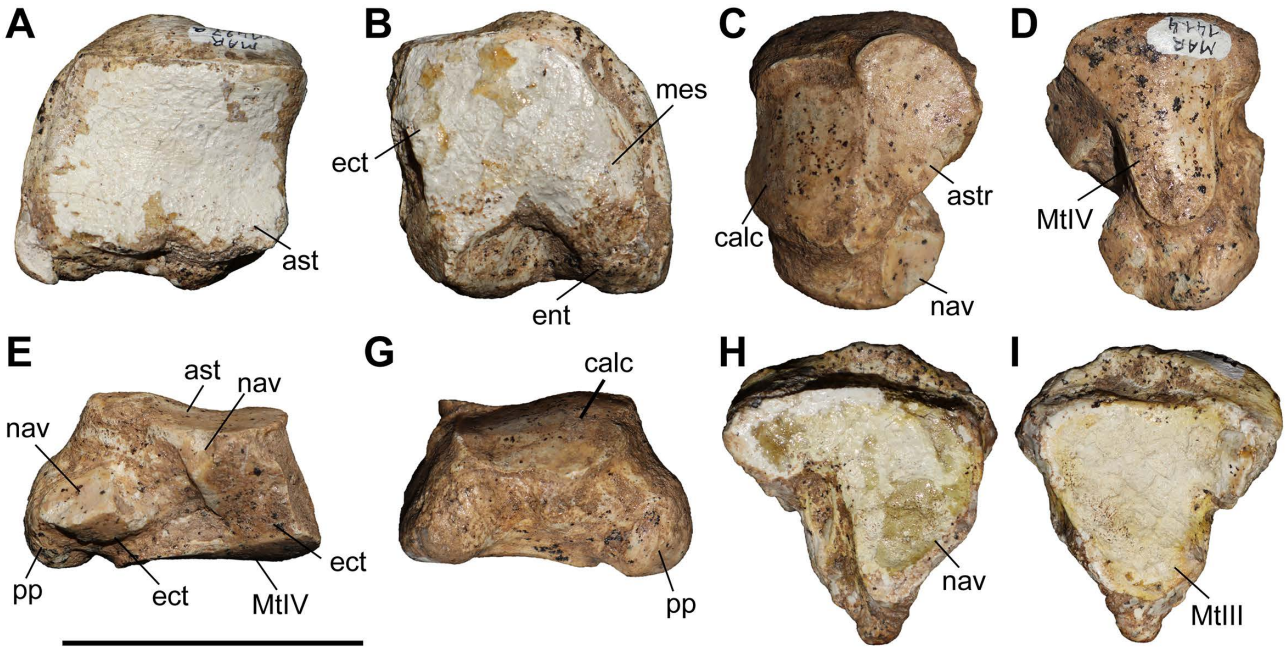


**Fig 19. Tarsals of *Chilotherium persiae* (Pohlig, 1885) [19] from Maragheh (Iran).** A–B, navicular (MNHN.F.MAR1427a, right) in proximal and distal views. C–G, cuboid (MNHN.F.MAR1414, left) in proximal, distal, medial, and lateral views. H–I, ectocuneiform (MNHN.F.MAR1424c, left) in proximal and distal views. Abbreviations: ast, articular facet for the astragalus; ect, articular facet for the ectocuneiform; ent, articular facet for the entocuneiform; mes, articular facet for the mesocuneiform; MtIII, articular facet for the MtIII; MtIV, articular facet for the MtIV; nav, articular facet for the navicular; and pp, posterior process. Scale bar equals 5 cm.

https://doi.org/10.1371/journal.pone.0336590.g019

with an irregular outline. In medial view, four articular facets are present that are connected in pairs, which are separated by a rugose groove (Fig 19E). In both pairs the proximal facet articulates to the navicular and the distal one to the ectocuneiform. The anterior facet for the navicular is a small triangle that contacts the proximal articular facet for the astragalus. The posterior one for the navicular is almost quadrangular and does not contact the facet for the astragalus. The anterior facet for the ectocuneiform is large, subrectangular, concave, and forms an obtuse angle with the anterior facet for the navicular, while also contacting the distal facet for the MtIV. The posterior facet is much smaller and almost quadrangular, forming an almost right angle with the posterior articular facet for the navicular and being separated from the MtIV facet. In distal view, the facet for the fourth metatarsal is large and almost triangular (Fig 19D). In the posterior part of the bone a large, rugose, and distally bent process is placed. The descriptions and illustrations provided for '*C.*' *wimani* from the Linxia Basin [16] and for *C. orlovi* from Pavlodar [12] are generally similar to the morphology observed in the Maragheh specimens, but many details cannot be compared. In both species the articular facet for the astragalus is separated from the anterior facet for the navicular facet, as in *C. persiae*. In distal view, the anterior articular facet for the ectocuneiform is visible in *C. orlovi* [12], but is seems small and not concave, thereby possibly differing from *C. persiae*. The comparison of the metrical data for cuboids of *C. kowalevskii* from Grebeniki [17], '*C.*' *wimani* [16], *C. sarmaticum* from Berislav [11], and *C. orlovi* [12] to the measured specimens of *C. schlosseri* and *C. persiae* (S1 Table 19) may offer some insight into the association of these specimen. More specifically, *C. persiae* has a relatively small cuboid with low length values (49.9 and 51.6 mm, n = 2) similar to *C. sarmaticum* (50.5 and 54.5 mm, n = 2) and '*C.*' *wimani* (53–59 mm, n = 3). Whereas *C. schlosseri* (62 mm, n = 1) seems to be closer to the larger *C. kowalevskii* (60.8–66.2 mm, n = 6). The species *C. orlovi* exhibits a length range that overlaps with the other species (55–61 mm, n = 5). Overall, no clear separation of the species can be observed, and the specific identification would currently be impossible based solely on the morphometry of the cuboid.

### Ectocuneiform

Three ectocuneiforms of *C. persiae* from Maragheh and a single one of *C. schlosseri* from Samos were able to be studied. Only a single specimen of *C. persiae* is completely preserved (Fig 19H–I) and the single specimen of *C. schlosseri* is articulated with the other tarsal bones (Fig 15B). In proximal view, the articular facet for the navicular has an upturned "L" shape and is weakly concave. In medial view, in the proximal part an articular stripe for the mesocuneiform exists, while in the distal part two articular facets for the second metatarsal exist, which are separated by a prominent notch. On the lateral side the ectocuneiform articulates to the cuboid. The morphology of the articular facet(s) for the cuboid cannot be assessed due to the damage in this part of the bone. In distal view, the articular facet for the MtIII is generally triangular and resembles a mirrored, upturned "L". The studied specimens fit the description for the ectocuneiform of '*C.*' *wimani* (therein referred to an entocuneiform) from the Linxia Basin [16]. The ectocuneiform has a rather simple and uniform morphology and does not exhibit any diagnostic features. The metrical comparison of *C. kowalevskii* from Grebeniki [17], '*C.*' *wimani* from the Linxia Basin [16], *C. sarmaticum* from Berislav [11], and *C. orlovi* from Pavlodar [12] to the measured specimens of *C. schlosseri* from Samos and *C. persiae* from Maragheh (S1 Table 20) shows that the dimensions of the ectocuneiform of most species overlaps even within the very small sample sizes. Therefore, any identification based on this bone seems impossible.

### Second metatarsal

Three MtII of *C. persiae* from Maragheh and one of *C. schlosseri* from Samos were studied (Fig 20, Table 10). Most of them are more or less complete and allow a detailed description and metrical comparison. In proximal view, the articular facet for the mesocuneiform has a semioval outline and laterally contacts the articular facet(s) for the ectocuneiform, forming a slightly obtuse angle. Anterior to the mesocuneiform facet a rugose protrusion is present in the proximal part of the shaft, which extends towards the medial side and continuesdistally. There it connects to a slight tuberosity that is placed in the proximal part of the shaft. In lateral view, the MtII bears two separated articular facets in the only specimen of *C. schlosseri* (GMM 572) and two specimens of *C. persiae* (MNHN.F.MAR1378 and MNHN.F.MAR1381). In the third specimen of *C. persiae* (MNHN.F.MAR1385), a single continuous facet for the ectocuneiform exists. The facets for the ectocuneiform are connected to two separate, small articular facets for the MtIII. In *C. schlosseri*, the articular facets for the MtIII seem to be somewhat larger compared to those of *C. persiae*. In both species, the shaft has a subtriangular cross-section in the proximal part and is more oval and transversally elongated in the distal part; however, in *C. persiae* the cross-section is somewhat more rounded than in *C. schlosseri*. In medial view, on the proximal half of the shaft of *C. persiae* a well-developed, bulbous rugosity for the attachment of the interosseous ligament is placed (Fig 20A); in *C. schlosseri*, this rugosity covers a similar surface but is much more weakly developed (Fig 20G). On the anterior side of the bone, above the distal trochlea two bilateral protuberances are placed for the attachment of the ligaments of the fetlock joint. These are much more pronounced anteriorly in *C. schlosseri* than in *C. persiae*. The distal articular head is relatively rounded, asymmetrical with a convex proximal border on the anterior side. The sagittal keel of the articular head is rather weak and located mainly in the posterior part of the bone. On the posterior side, above the articular head two bilateral rugose protrusions are located.

The morphological differences observed in the MTII of the two species are rather slight. Metrically, however, there seems to be a distinction between larger and smaller species (Table 10, S1 Table 21). This is evident in species, where a larger sample size has been reported, like *C. kowalevskii* from Grebeniki, *C. sarmaticum* from Berislav, and *C. orlovi* from Pavlodar [11,12,17]. All three of these species, exhibit similar values for the transversal and the anteroposterior diameter of the diaphysis (TDdia and APDdia) of the MtII, but differ in some other dimensions of the bone and most prominently in the length. More specifically, *C. kowalevskii* and *C. orlovi* exhibit a higher value range for the length of the MtII (94.6–114.2 mm, n = 13 and 98–106 mm, n = 7 respectively) than *C. sarmaticum* (86.2–93 mm n = 6). Based on these well-sampled species, it is possible to associate *C. schlosseri* (102–102.4 mm, n = 2), *C. persiae* (93.4–97.3 mm, n = 3), *C. anderssoni* (97–99, n = 3), and a potential primitive *Chilotherium* (100.7 mm) with the larger species *C. kowalevskii* and *C. orlovi* [7,14,81]. Additionally, *C. schlosseri* from Odessa (95–110 mm) also falls into this size range. On the contrary, '*C.*'

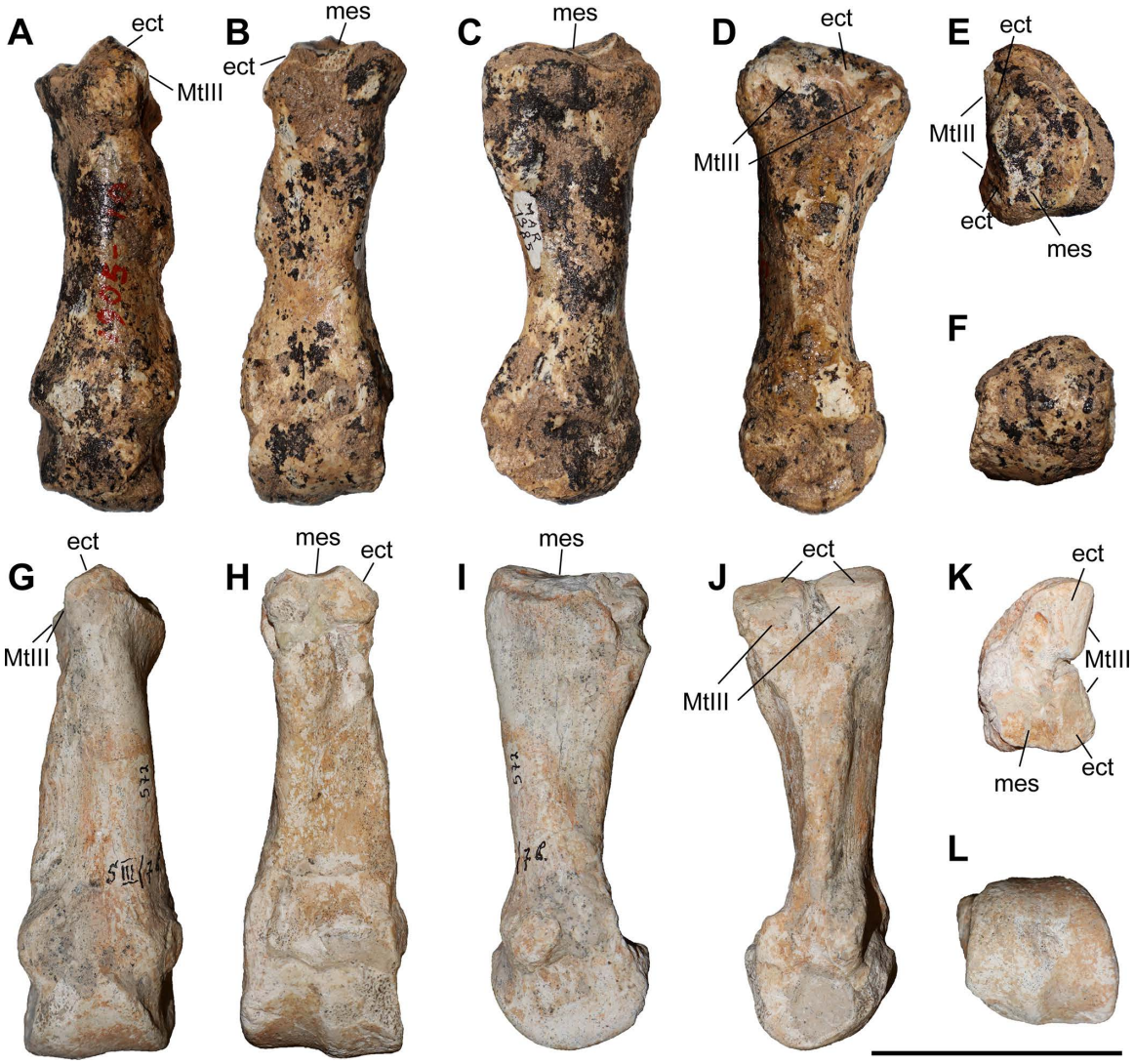


**Fig 20. Second metatarsal of chilotheres.** A–F, *Chilotherium persiae* (Pohlig, 1885) [19] (MNHN.F.MAR1385, left) from Maragheh (Iran), and G–L, *Chilotherium schlosseri* (Weber, 1905) [14] (GMM 572, right) from Samos (Greece) in anterior (A, G), posterior (B, H), medial (C, I), lateral (D, J), proximal (E, K), and distal (F, L) views. Abbreviations: ect, articular facet for the ectocuneiform; mes, articular facet for the mesocuneiform; MtIII, articular facet for the MtIII Scale bars equal 5 cm.

https://doi.org/10.1371/journal.pone.0336590.g020

**Table 10. Measurements (in mm) of second metatarsals of the studied chilotheres.**

| | | L | TDprox max | TDprox art | APDprox | TDdia | APDdia | TDdist max | TDdist artic | APDdist |
|---|---|---|---|---|---|---|---|---|---|---|
| *C. persiae* | min | 93.4 | 28.6 | 18.5 | 35.8 | 20.8 | 17.4 | 27.5 | 26.7 | 29.8 |
| | max | 99 | 32.1 | 20.8 | 38.6 | 27.8 | 19.7 | 33.6 | 27.7 | 31 |
| | mean | 96.6 | 30.4 | 19.7 | 37.2 | 24.6 | 18.7 | 30.7 | 27.2 | 30.4 |
| | n | 3 | 2 | 2 | 3 | 3 | 3 | 3 | 2 | 2 |
| *C. schlosseri* | min | 102 | | | | | | | | |
| | max | 102.4 | | | | | | | | |
| | mean | 102.2 | 23.5 | 20.3 | 36.3 | 25.2 | 21.7 | 35.1 | 32.8 | 33.7 |
| | n | 2 | 1 | 1 | 1 | 1 | 1 | 1 | 1 | 1 |

https://doi.org/10.1371/journal.pone.0336590.t010

*wimani* (89–94 mm, n = 3) and *Chilotherium* indet. from Kavakdere (85.2 mm) may be closer to the smaller *C. sarmaticum* [16,81]. It is rather surprising, that the MtII of the potential primitive *Chilotherium* from Loc. 72 of the Sinap Formation [81] has a length that is close to the length of species that are considered derived, such as *C. schlosseri*, *C. anderssoni*, and *C. orlovi* (S1 Table 21).

### Third metatarsal

Three MtIII of *C. persiae* from Maragheh and four specimens of *C. schlosseri* from Samos were studied (Fig 21, Table 11). Most of them are more or less complete and allow a detailed description and metrical comparison. Three specimens of *C. schlosseri* and one of the MtIII of *C. persiae* are completely preserved, except for some slight damage. The other

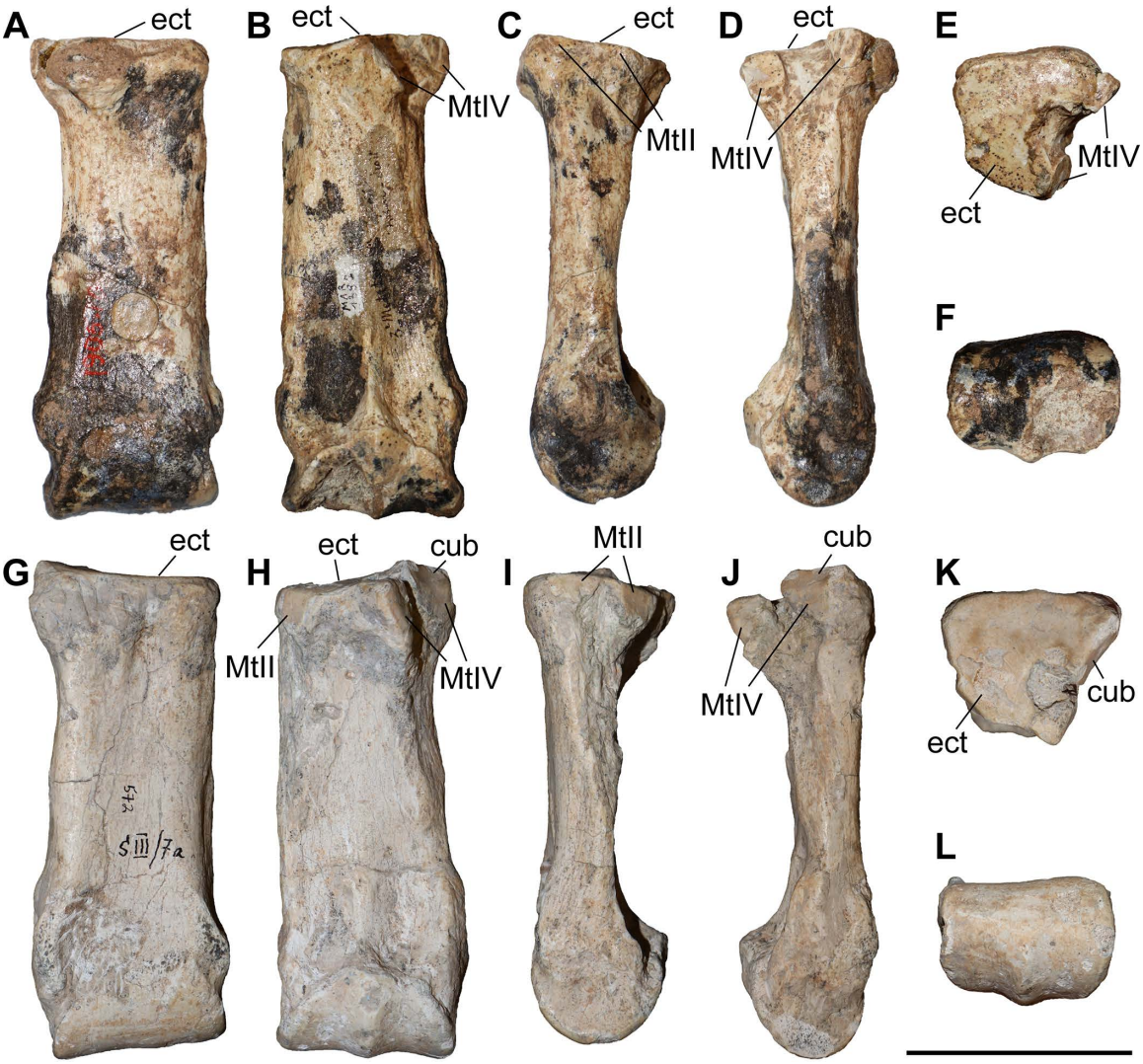


**Fig 21. Third metatarsal of chilotheres.** A–F, *Chilotherium persiae* (Pohlig, 1885) [19] (MNHN.F.MAR1385, right) from Maragheh (Iran), and G–L, *Chilotherium schlosseri* (Weber, 1905) [14] (GMM 572, right) from Samos (Greece) in anterior (A, G), posterior (B, H), medial (C, I), lateral (D, J), proximal (E, K), and distal (F, L) views. Abbreviations: cub, articular facet for the cuboid; ect, articular facet for the ectocuneiform; MtII, articular facet for the MtII; and MtIV, articular facet for the MtIV. Scale bars equal 5 cm.

https://doi.org/10.1371/journal.pone.0336590.g021

**Table 11. Measurements (in mm) of third metatarsals of the studied chilotheres.**

| | | L | TDprox max | APDprox | TDdia | APDdia | TDdist max | TDdist artic | APDdist |
|---|---|---|---|---|---|---|---|---|---|
| *C. persiae* | min | | 39 | 34.1 | 32 | 18.2 | | | |
| | max | | 40.4 | 37.7 | 35 | 20.1 | | | |
| | mean | 110.0 | 39.8 | 36.4 | 33.3 | 19.2 | 43.5 | 40.0 | 32.6 |
| | n | 1 | 3 | 3 | 3 | 2 | 1 | 1 | 1 |
| *C. schlosseri* | min | 111.2 | 41.3 | 33.8 | 36.7 | 18.2 | 46.2 | 42.4 | 30.3 |
| | max | 117 | 46.3 | 37 | 40 | 19.3 | 50 | 44.2 | 34.7 |
| | mean | 114.8 | 43.6 | 35.6 | 38.7 | 18.7 | 48.3 | 43.1 | 32.8 |
| | n | 4 | 4 | 3 | 4 | 3 | 3 | 3 | 3 |

https://doi.org/10.1371/journal.pone.0336590.t011

specimens are lacking the distal half. In proximal view, the articular facet for the ectocuneiform covers the complete proximal surface of the bone and is almost triangular. The anterior border of the articular facet for the ectocuneiform is almost straight in *C. schlosseri* and has a very slight indentation in MNHN.F.MAR1382 of *C. persiae*. In medial view, two distinct facets for the MtII are visible in all specimens of both species; both facets are small and have a semi-oval outline. On the lateral side, three out of the four specimens of *C. schlosseri* feature an articular facet for the cuboid. In the fourth specimen (AMNH-22818) the relevant portion is somewhat damaged, and the potential presence of a cuboid facet is not clear. In the three specimens of *C. schlosseri* where it can be observed, the cuboid facet is small and trapezoidal, placed between the articular facet for the ectocuneiform and the anterior one for the MtIV (Fig 21G, J). In contrast to that, all three studied *C. persiae* specimens lack a cuboid facet (Fig 21B, D). In lateral view, two articular facets for the MtIV are placed below the ectocuneiform facet. These two facets are separated by a deep groove, which is much wider in MNHN.F.MAR1382 of *C. persiae*. In anterior view, the shaft widens distally towards the bilateral protuberances for the attachment of the ligaments of the fetlock joint. In posterior view, the sagittal keel of the articular head for the proximal phalanx is well developed. It placed in the posterior part of the articular head and in distal view, reaches the level of its medial rim in distal view.

The presence of a cuboid facet in MtIII may present a diagnostic feature separating *C. schlosseri* from at least some of the other species like *C. persiae* (Fig 21D, J). The type species *C. anderssoni* from Lok. 30 also lacks the cuboid facet [7]. Deng (2002) [16] mentioned that in both *C. anderssoni* and '*C.*' *wimani* from the Linxia Basin (China) the MtIII does not bear an articular facet for the cuboid. Similarly, no cuboid facet has been described for *C. orlovi* from Pavlodar and in the illustrated MtIII, no such facet seems to be present between the articular facet for the ectocuneiform and that for the MtIV [12]. A MtIII from the Upper Miocene locality Küçükçekmece was assigned to *C. schlosseri* but was described as not having a cuboid facet. It is likely that this specimen, as well as the other *Chilotherium* specimens from Küçükçekmece actually belong to a different species and not *C. schlosseri*, which bears a cuboid facet. Unfortunately, for most chilotheres this condition has not been described or illustrated.

Metrically, however, there seems to be a slight distinction between larger and smaller species. More specifically, in *C. kowalevskii* from Grebeniki, *C. sarmaticum* from Berislav, and *C. orlovi* from Pavlodar the length of the MtIII seems to reach up to 120 mm, in the largest specimens [11,12,17]. The measured specimens of *C. schlosseri* (111.2–120 mm, n = 6) and *C. persiae* (110 mm) seem to have similar values to these species, with *C. schlosseri* having a mean value of about 116 mm, which is close to, but even higher than, the mean value of 113 mm seen in *C. kowalevskii* [11,17]. Respectively, *C. anderssoni* from China has a similar range for the length of the MtIII (110–118 mm, n = 3) as in these larger species [7]. The other Chinese species, '*C.*' *wimani*, on the other hand exhibits a rather low value range for the length of the MtIII (100–109 mm, n = 3), not surpassing 110 mm. Although the sample size is rather small for most species – in many instances three specimen or less – it seems that '*C.*' *wimani* differs somewhat from the other species, in having smaller dimensions. Similarly, the measured MtIII of a potential primitive *Chilotherium* from Loc. 72 of the Sinap Formation

(106 mm) and of *Chilotherium* indet. from Kavakdere (101.5 mm) are below the value ranges of *C. kowalevskii* and *C. orlovi* or barely reaching the lowest values. It seems that the material from Turkey [81] has more similar values to '*C.*' *wimani* and are also within the value range of *C. sarmaticum*.

### Fourth metatarsal

Four MtIV of *C. persiae* from Maragheh and two specimens of *C. schlosseri* from Samos have been studied (Fig 22, Table 12). Of these, only one specimen of each species (NHMW-GEO-2020/0014/0144 and GMM 572, respectively) is adequately preserved. The others are missing their distal parts in most cases. In proximal view, the articular facet for the cuboid is subtrapezoidal in GMM 572 of *C. schlosseri* and almost kidney shaped in NHMW-GEO-2020/0014/0144 of *C. persiae*. Below the articular facet for the cuboid, on the anterior side a small tubercle is present medially and a large one laterally, that covers the complete lateral side of the bone and weakens towards the posterior side. In medial view, the two

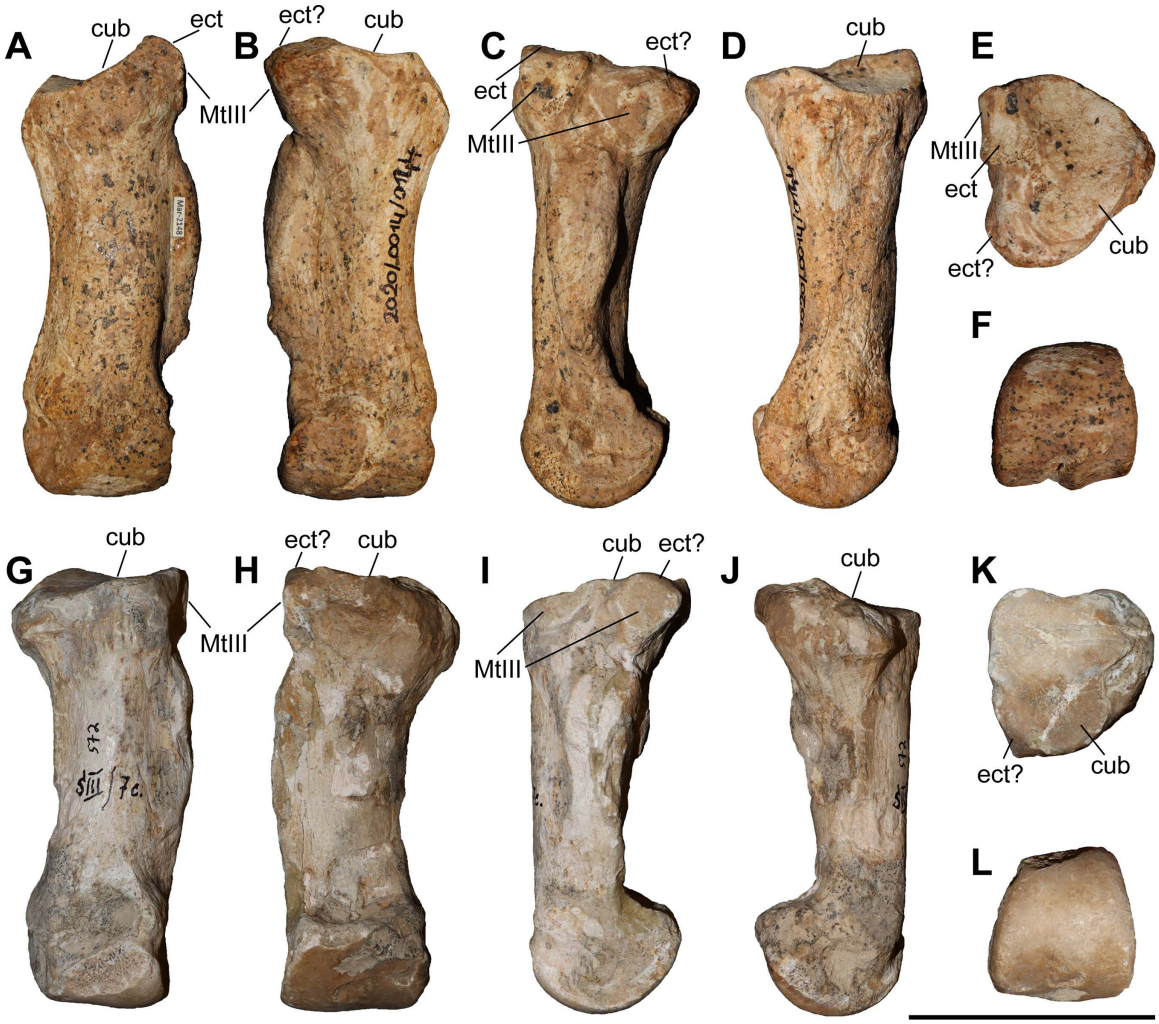


**Fig 22. Fourth metatarsal of chilotheres.** A–F, *Chilotherium persiae* (Pohlig, 1885) [19] (NHMW-GEO-2020/0014/0144, right) from Maragheh (Iran), and G–L, *Chilotherium schlosseri* (Weber, 1905) [14] (GMM 572, right) from Samos (Greece) in anterior (A, G), posterior (B, H), medial (C, I), lateral (D, J), proximal (E, K), and distal (F, L) views. Abbreviations: cub, articular facet for the cuboid; ect, articular facet for the ectocuneiform; and MtIII, articular facet for the MtIII. Scale bars equal 5 cm.

https://doi.org/10.1371/journal.pone.0336590.g022

**Table 12. Measurements (in mm) of fourth metatarsals of the studied chilotheres.**

| | | L | TDprox max | TDprox art | APDprox | TDdia | APDdia | TDdist max | TDdist artic | APDdist |
|---|---|---|---|---|---|---|---|---|---|---|
| *C. persiae* | min | | 35.5 | 30.3 | 32.3 | 29.2 | 18.2 | | | |
| | max | | 43.3 | 31 | 41.3 | 37.8 | 27.2 | | | |
| | mean | 94.3 | 38.9 | 30.7 | 37.15 | 33.5 | 21.6 | | 29.7 | 31 |
| | n | 1 | 4 | 3 | 4 | 2 | 3 | | 1 | 1 |
| *C. schlosseri* | min | 91.7 | 33.4 | 39.4 | 35.1 | | | | | |
| | max | 96 | 35.5 | 39.4 | 40.9 | | | | | |
| | mean | 93.9 | 34.5 | 39.4 | 38 | 28 | 26.1 | 19.5 | 32.1 | 30.1 |
| | n | 2 | 2 | 1 | 2 | 1 | 1 | 1 | 1 | 1 |

https://doi.org/10.1371/journal.pone.0336590.t012

articular facets that articulate to the MtIII vary in morphology between the two species. In *C. schlosseri* the anterior one is more elongated and thinner, while the posterior one is larger and rounded. In *C. persiae* the posterior one is similar to *C. schlosseri*, while the anterior one differs in being semi-oval and not elongated. Additionally, in *C. persiae* on the medial side, between the cuboid facet and the anterior MtIII facet, a small rectangular facet for the ectocuneiform is placed (Fig 22A, C, E). This differs from the morphology observed in *C. schlosseri*, where this facet is not found (Fig 22I). However, in both species the posterior MtIII facet seems to curve proximally, creating a very minute oblique surface, which could represent a ectocuneiform facet (Fig 22B, C, E, H, I, K), but cannot be confirmed, since there is no articulated set of tarsals and metatarsals. However, in both species the proximal portion of the posterior articular facet for the MtIII curves up, possibly creating a small articular surface for the ectocuneiform. Below the articular facets for the MtIII a prominent rugosity for the attachment of the interosseous ligament extends slightly beyond the middle of the shaft. This rugosity is more pronounced in *C. persiae* than in *C. schlosseri* (Fig 22A–C, G–I). The shaft of the bone is more or less straight. On the articular head for the proximal phalanx, there is only a very weak sagittal keel on the posterior side. In anterior view, the articular head is slightly asymmetrical.

The morphology of the articular facets for the tarsals and the MtIII may provide some insight into the separation of the species, as *C. persiae* and *C. schlosseri* exhibit significant differences. Most importantly, the existence of an ectocuneiform facet in the anterior part of the MtIV in *C. persiae* (Fig 22A, C, E) or the lack of it in *C. schlosseri* (Fig 22G, I, K) may present a diagnostic feature. Unfortunately, the presence of this facet cannot be assessed in the other chilotheres, as the descriptions and illustrations in the literature are not sufficient. However, this articulation is present in the non-chilothere aceratheriine *Aceratherium incisivum* from Höwenegg [74: Abb. 63]. No illustrations of the medial side of the MtIV is provided for *C. kowalevskii* from Grebeniki, but in anterior view it looks like such a articular facet for the ectocuneiform might be present [15,17]. The metrical comparison on the other hand seems to be more comparable (S1 Table 23). The species *C. kowalevskii* from Grebeniki and *C. orlovi* from Pavlodar have larger dimensions (length: 91.8–100.5 mm, n = 9 and 90–105 mm, n = 4, respectively) than *C. sarmaticum* from Berislav (length: 83.5–87 mm, n = 4), which do not overlap [11,12,17]. The length of the MtIV of *C. schlosseri* (91.7–96 mm, n = 4) and *C. persiae* (94.3 mm) fit much better the value ranges of the larger *C. kowalevskii* and *C. orlovi*. Whereas the dimensions of '*C.*' *wimani* from the Linxia Basin (83–90 mm, n = 4), the potential primitive *Chilotherium* from the Sinap Formation (106 mm), and *Chilotherium* indet. from Kavakdere (83.4 mm), fit better those of the smaller *C. sarmaticum* [16]. Therefore, despite the small sample size in most species, a separation into two size classes can be observed, similar to observation by other authors [84].

## Discussion

Detailed comparisons of the cranial and dental material of different chilothere taxa [e.g., 8,10,49] suggest that their separation is a rather delicate topic. Nonetheless, based on certain features in the skull most species can be distinguished. For instance, it was recently shown that *Eochilotherium samium* differs significantly from most members of the genus

*Chilotherium* and should be placed in its own genus within the Chilotheriina [10]. It was further established that two other species, '*C.*' *wimani* and '*C.*' *primigenium*, deviate from the typical *Chilotherium* morphology as exemplified by the type species *C. anderssoni* and probably also represent distinct genera [10,39]. Nonetheless, the tooth morphology of these species is remarkably consistent with *Chilotherium* and differs only in few features.

Within *Chilotherium* sensu stricto, the differentiation of species is less clear, as the skulls are very similar. The species *C. schlosseri* proves to be among the most recognisable species of the genus based on features such as the very prominent dorsally depressed skull and the very widely separated parietal crests (>70 mm, n = 12 [39]). Even the position of the nasal bones is affected by the frontal depression, and they are placed comparatively lower than in the other species, with the nasal bones being placed below the level of the dorsal border of the orbit in lateral view, in contrast to the other chilotheres [10,39]. However, there are characters that are able to also separate some of the other species. For instance, in the species *C. schlosseri* and *C. anderssoni* the skull is flattened, and the dorsal surface has a straight profile [10]. Whereas in species like *C. persiae*, *C. kowalevskii* and *C. sarmaticum* the skull is less flattened with the nuchal region being raised. Another morphological feature that could be used to separate some species is found in the frontal depression. More specifically, in some species like *C. persiae* and *C. kowalevskii* a faint longitudinal ridge is placed along the middle of the skull and is visible within the frontal depression [39]. This feature is not present in *C. schlosseri* and *C. anderssoni* [39]. Based on these features also a skull from the Upper Miocene locality of Reghiu (Romania), is morphologically closer to *C. kowalevskii* than to *C. schlosseri*. The two species were considered synonyms in the most recent re-evaluation of this skull, which led to the identification of the specimen as *C. schlosseri*, despite its closer affinities to *C. kowalevskii* [47]. This skull includes both a somewhat raised nuchal crest and a longitudinal ridge in the middle of the frontal depression like *C. kowalevskii*, also the parietal crests are 64.2 mm apart, thereby closer together than in *C. schlosseri* (>70 mm, n = 12), falling into the range of *C. kowalevskii* (40.1–66, n = 10) [10,17,39,47].

Unfortunately, in most cases within chilotheres the tooth morphology cannot solve the species determination. The lower teeth have an especially conservative morphology and are characterised by a notable uniformity within the group [8]. Despite that uniformity, the lower teeth can be used for the separation of chilotheres from other rhinoceroses, because in chilotheres the premolars are relatively shortened, resulting in a lower ratio of premolar to molar length [e.g., 42]. The morphology of the upper teeth is much more characteristic and can be used to separate chilotheres from all other rhinoceroses, but also includes some diagnostic features for the identification of some species within chilotheres. For instance, in the species *E. samium*, '*C.*' *wimani* and '*C.*' *primigenium* the premolars have either weakly constricted or unconstricted protocones. In the case of the P2, both the protocone and the hypocone are unconstricted and the median valley remains open even at a very late wear stage in these three species [10]. Also, the upper tooth morphology of *Shansirhinus* deviates from other chilotheres, exhibiting a prominent paracone fold and often a large number of enamel plications [73,76]. The sporadic occurrence of enamel plications is also observed in other chilotheres like *C. schlosseri*, where they are rather frequent, but not as abundant as in *Shansirhinus* [10].

Therefore, the taxonomy of the chilotheres has historically been very complicated and inconsistent but has started to be illuminated. In the present work we compare the postcranial material of chilothere species across Europe and Asia, in order to further elucidate the taxonomy of this group. Despite the relative abundance of cranial material from members of this group, the postcranial material is much more limited and rarely described in detail. This is probably due to a sampling bias towards skulls, which was especially common in the past. For instance, the *Chilotherium* material from the Upper Miocene of Kutschwan includes 11 cranial elements, but only 23 postcranial ones. Similarly, in the case of *C. schlosseri*, there are eight complete or almost complete skulls in different collections [39], but only very few collections house postcranial material of the species, namely the AMNH, AMPG, GMM, and NHMW.

Nonetheless, when Ringström (1924) [7] coined the genus *Chilotherium*, he distinctly mentioned the rather peculiar anatomy of the appendicular skeleton that characterises this rhinocerotid group. He specifically noted that the extremities are strongly shortened, both the manus and pes are tridactyl with short metapodials, and that the abaxial metapodials are

obliquely posteriorly oriented in comparison to the central one [7]. However, both in the work of Ringström (1924) [7] and the rest of the literature that was used in this context included rather short descriptions and comparisons of the postcranial elements of *Chilotherium* and their usefulness for taxonomic purposes was rather limited, as mainly the cranial and dental material was used to identify the species [e.g., 7,14,15]. However, the herein conducted comparison of the postcranial material of chilotheres confirms that there are several distinct features that characterise this genus, as already proposed by Ringström (1924) [7]. Most of these features are related to the shortening of the limbs. For instance, among the carpal bones the scaphoid is proximodistally notably shortened when compared to non-chilothere rhinocerotids for instance (Fig 23), with the only exception being teleoceratines like *Brachypotherium brachypus*. More specifically, most chilothere scaphoids have a height to length ratio between 50% and 69%, whereas in other Miocene rhinoceroses like *Dihoplus pikermiensis* and *Acerorhinus zernowi* this ratio can be higher, usually being above 70% and reaching up to 85% (Fig 23A). It has to be noted that this ratio is highly affected by the strongly proximodistally developed posterior tuberosity. In direct comparison it is clearly visible that the scaphoid of chilotheres is much shorter than that of extant horned rhinoceroses for instance (Fig 23B–E). More specifically, the anterior height is much lower than the posterior height in *Chilotherium*. This is a phylogenetically informative character also used in current morphological character matrices for rhinocerotids [34]. If only the anterior height was measured and used for the calculation, the ratio would be much lower. For *C. habereri* specifically instead of 66% it would be 53%, whereas in rhinocerotines the difference between the anterior and the posterior height in much less pronounced (Fig 23D–E). In most cases in the literature, only the maximal height is provided, without stating where it was measured, which complicates direct comparisons (Fig 23). In *Aceratherium incisivum* from Höwenegg (Germany) this ratio (70–73.4%, n = 4) is close to that of '*C.*' *wimani*, which shows the least degree of shortening of the limbs among any chilothere (Fig 23). In the European teleoceratine *Brachypotherium brachypus* the ratio (58.7–60.5%, n = 4, based on [85] and own data) is close to that of the chilotheres. This is also expressed in its morphology, which is much closer to that of *C. schlosseri* (compare Fig 23B, C). Though, the posterior tuberosity is not as strongly developed in

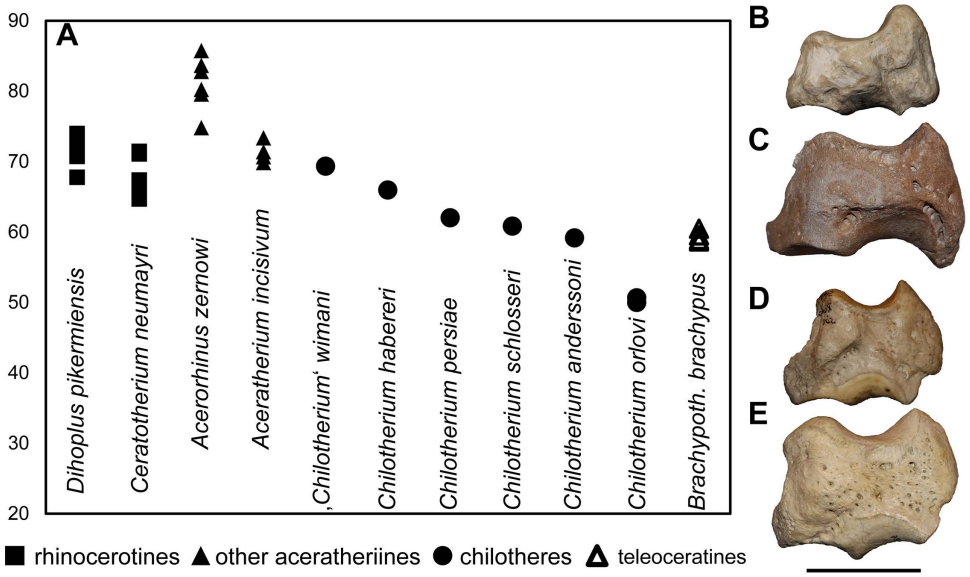


**Fig 23. Comparison of chilothere scaphoids.** A, univariate diagram of the height (H) to maximal length (L) ratio of the scaphoid of chilotheres compared to other rhinocerotids. B, left scaphoid of *Chilotherium schlosseri* (Weber, 1905) [14] (NHMW-GEO-2009z0089/0001) from the Upper Miocene of Samos (Greece); C, right scaphoid of *Brachypotherium brachypus* (GPIT/MA/03454, mirrored) from the Middle Miocene of Steinheim in Germany; D, left scaphoid of extant *Dicerorhinus sumatrensis* (NHMW-1500); and E, left scaphoid of extant *Ceratotherium simum* (NHMW-3086) in anterior view. Scale bar equals 5 cm. Measurements can be found in S1 Tables 4.

https://doi.org/10.1371/journal.pone.0336590.g023

*Brachypotherium brachypus* from Steinheim (Fig 23C). In the American short-limbed hornless rhinocerotid *Teleoceras*, the scaphoid seems to be similarly compressed (50–55%, n = 3) as in *Chilotherium orlovi* [86], which exhibits the lowest value of all chilotheres (Fig 23).

The most characteristic portion of the shortened limbs of chilotheres are the metapodials [7]. These are rather stout, especially when compared to other rhinocerotids (Fig 24) like the contemporaneous tandem-horned rhinocerotines *Dihoplus pikermiensis* and '*Ceratotherium' neumayri* or the Middle Miocene aceratheriine *Acerorhinus zernowi* from Tung Gur (China) [75]. *Aceratherium incisivum* from Höwenegg [74] seems to be somewhat closer to *Chilotherium* than to *Acerorhinus zernowi*, especially concerning the dimensions of the MtIII (Fig 24). In the MtIII diagram specifically, it is visible that there is a broad range in the values of '*C.*' *wimani*, which is however lower than that of *C. kowalevskii* for instance (Fig 24). The Middle Miocene European teleoceratine *Brachypotherium* exhibits similar ratios to the chilotheres (McIII: 39–46.1%, n=9, and MtIII: 38–47%, n=12 [85]), which overlap to an important degree with the ratios of *C. kowalevskii* (Fig 24). The American teleoceratine *Teleoceras* also exhibits similarly short or even shorter metapodials than *Chilotherium* [87], as indicated by the single data points for each species (Fig 24). A McIV (MNHN.F.TRQ329) from Küçükçekmece (Turkey) that was attributed to *C. schlosseri* [46], exhibits proportions that do not fit any chilothere. This McIV from Küçükçekmece is more slender (TDdia/L=22.3%) than the McIV of the chilothere compared herein (27.5–34.8%, n=14). Instead, its' proportions fit much better those of *Acerorhinus zernowi* from Tung Gur (19.8–23.9%, n = 3) [75]. In the same locality, the presence of another hornless rhinocerotid, *Persiatherium* sp., has been reported, which is not a chilothere and most likely had a more elongated appendicular skeleton. Therefore, this McIV (MNHN.F.TRQ329) could possibly belong to *Persiatherium* instead of *Chilotherium*. The MtIII from the same locality (MNHN.F.TRQ335) that was also assigned to *C. schlosseri* was described as not bearing a cuboid facet. However, in all *C. schlosseri* specimens from Samos that preserve the relevant portion a cuboid facet is indeed present. Therefore, it is most plausible that the MtIII MNHN.F.TRQ335, does not belong to this species. On the other hand a McIV from Loc. 26 in the Sinap region referred to as '*Acerorhinus* sp. nov.', has an index of 30.3% that falls well into the value range of the chilotheres (27.5–34.8%, n = 14) and the overall morphology of this bone also matches the morphology seen in *Chilotherium*. Therefore, it is most likely that this bone actually does belong to *Chilotherium* or another chilothere and not *Acerorhinus*.

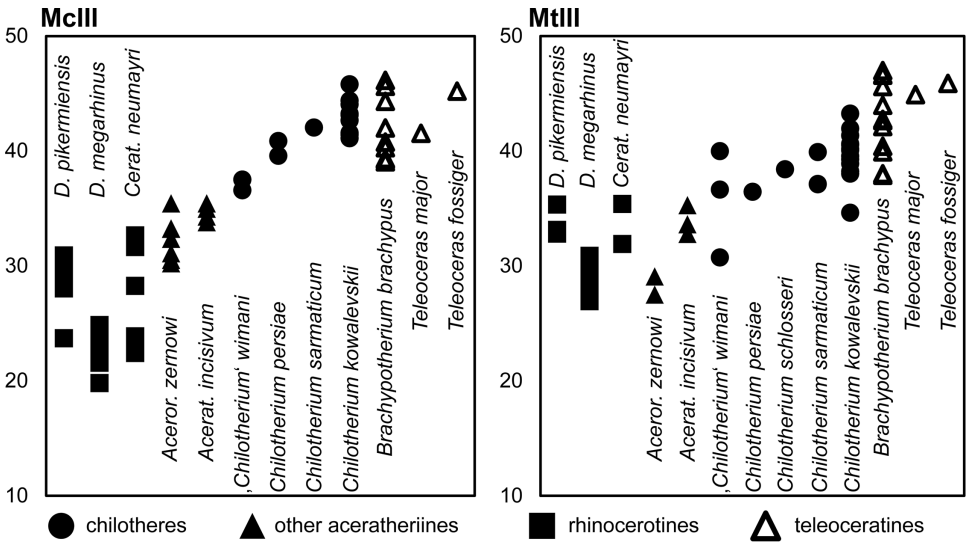


**Fig 24. Metrical comparison of chilothere metapodials.** Univariate diagrams of the proximal transversal diameter (DTprox max) to length (L) ratio of the McIII and MtIII of chilotheres compared to other rhinocerotids. Measurements can be found in S1 Tables 10 and 22.

https://doi.org/10.1371/journal.pone.0336590.g024

The trend of shortening the limbs is also demonstrated in other bones of the appendicular skeleton. For instance, the humeri and femora in chilotheres are also relatively stouter than in other aceratheriines, like *Aceratherium incisivum* and *Acerorhinus zernowi* (Fig 25). Within rhinocerotids only teleoceratines have reached a similar degree of limb shortening, as exemplified by *Teleoceras major* and *Teleoceras fossiger* in Fig 25. Although, in the Middle Miocene European teleoceratine *Brachypotherium brachypus* the femur is not quite as shortened (15.8%, n = 1 [85]), still being comparable to the lowest values of *Chilotherium* (Fig 25).

Within chilotheres there seems to be a gradual increase in size and further shortening of the limbs. More specifically, *E. samium* and '*C.*' *wimani*, which were considered as more "primitive" chilotheres, are somewhat smaller based on the dental and cranial material [e.g., 10]. This is also reflected in the appendicular skeleton, as confirmed by the comparison of the published postcranial data of '*C.*' *wimani* from the Linxia Basin (China) to that of other chilotheres (Figs 23–25, S1 Table). The only other well-sampled chilothere that seems to be comparable in size is the chronologically oldest European representative, *C. sarmaticum* from the Vallesian of Berislav (Ukraine) [11,45]. Whereas the younger, middle to late Turolian chilotheres *C. schlosseri* from Samos (Greece) and *C. orlovi* from Pavlodar (Kazakhstan) seem to be the largest chilotheres [84], while at the same time *C. orlovi* also seems to be among the species with the most pronounced shortening of appendicular skeleton. The only chilothere of younger geological age is *Shansirhinus*, which is, however, exclusively known from craniodental material. For the longest time, only teeth were known from this species [24,73,88] and only recently complete skulls were described from Upper Miocene and Lower Pliocene deposits from China [76,89,90], making it the youngest reported representative of the chilotheres until now and the only chilothere surviving into the Pliocene. Nonetheless, no postcranial material has been described for any *Shansirhinus* species to be used in our current comparisons.

The possible attribution of the aceratheriine material (a partial forelimb) from Loc. 12 of the Upper Miocene Sinap Formation in Turkey [81: fig. 12.15] to the genus *Chilotherium* is herein rejected, due to the existence of a well-developed, functional, and not at all reduced McV. It is known that in *Chilotherium* the McV is represented by a small and sesamoid-like rudimentary bone similar to what is observed in extant rhinoceroses and also seen in the herein studied *C. habereri*

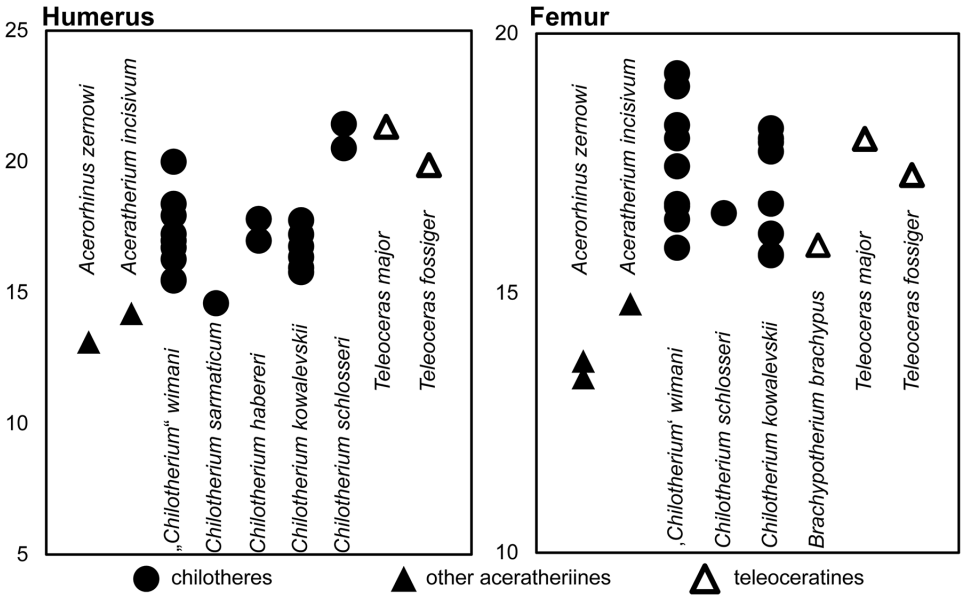


**Fig 25. Metrical comparison of chilothere humeri and femora.** Univariate diagrams of the transversal diameter of the diaphysis (TDdia) to length (L) ratio of the humerus and femur of chilotheres compared to other aceratheriines. Measurements can be found in S1 Tables 1 and 12.

https://doi.org/10.1371/journal.pone.0336590.g025

material from Kutschwan. That is why *Chilotherium* has been widely considered as tridactyl [3,7,16]. The condition of the Sinap specimen is more similar to *Aceratherium incisivum* from Höwenegg, which also includes a well-developed McV [74]. The shape and size of the McV from Sinap and those from Höwenegg are extremely similar. Also, the other associated metacarpals from Loc. 12 of Sinap, are overall similar in proportions and form to the metacarpals of *Aceratherium incisivum* from Höwenegg. The gracility index of these bones (McII: 28.5%, McIII: 27.9%, and McIV: 25.8%) is very close to the values in *Aceratherium incisivum* from Höwenegg (McII: 27.2–27.6%, McIII: 29.2–29.6%, and McIV: 24.3–27.4%, n = 4). Nonetheless, the Sinap material, with a length of 122 mm in the McIII from Loc. 12 [81], is smaller than *Aceratherium incisivum* from Höwenegg (140–144 mm, n = 4) [74]. It is more likely that the associated forelimb from Loc. 12 represents a non-chilothere aceratheriine, possibly closely related to *Aceratherium incisivum*; however, solely based on such material it is currently impossible to attempt any taxonomic attribution.

Bringing together the information from the literature based on the craniodental material that can be used for the identification of the chilotheres species and combining it with the results of the current study of the postcranial material refines their differentiations. The current study showed that one of the most promising elements for taxonomic distinction may be the astragalus. More specifically, the arrangement of the articular facet for the calcaneum seem to differ in some species. In *C. anderssoni*, *C. habereri*, *C. persiae*, *C. kowalevskii*, and *C. orlovi* all articular facets are well separated from each other [7,11,12], similar to *Aceratherium incisivum* from Höwenegg (Fig 17). The species '*C.*' *wimani* and *C. sarmaticum*, exhibit a connection between the sustentacular facet, the cuboid facet and the distal calcaneal facet (Fig 17) [11,16]. In *C. schlosseri*, the condition of these articular facets varies intraspecifically, with two astragali (GMM 571 and NHMW-GEO-1911/0005/0424) exhibiting a wide connection between the sustentacular facet and the ectal calcaneal facet, which is not observed in any other chilothere species (Fig 17B). The astragalus morphology of *C. schlosseri* further differs from the other chilotheres by having a connection between the medial lip for the articulation of the tibia and the articular facet for the navicular (Fig 16K). This character is observed in all available astragali of *C. schlosseri*; in other chilotheres there is a well-developed groove separating the medial lip and the navicular facet. Thereby it can be assumed that these features are apomorphic for *C. schlosseri* and can be added to the diagnostic characters for the species.

The studied axes of *C. persiae* and *C. schlosseri* also differ slightly from each other (Fig 2). The ventral crest of the axis is wider and looks more massive in *C. schlosseri*, whereas in *C. persiae* it seems compressed in its' middle. The posterior articular facet for third cervical vertebra has a high-oval shape with a slight, dorsal indentation in *C. schlosseri*, whereas in *C. persiae* it is more rounded, and the dorsal surface is flat. Additionally, in ventral view there is an indentation on the posterior side in *C. persiae*, whereas *C. schlosseri* does not feature such an indentation. Lastly, the area where the lateral walls of the neural canal of the axis connect to the vertebral body seems to extend more posteriorly in *C. schlosseri* than in *C. persiae*. Due to the small number of specimens, it is not possible to assess the intraspecific variability of these characters or whether they are also present in other species. In the scapula, the shape of the medial tuberosity, is more rounded in *C. persiae* and *C. schlosseri* and rather flattened in *C. habereri* but seems to be more protruding in *C. schlosseri* (Fig 3). In the humerus, the dimensions of the species seem to be most informative, since '*C.*' *wimani* and *E. samium* have the smallest humeri [14,16], *C. orlovi* has the largest humeri [12] and most other species, *C. persiae*, *C. habereri*, *C. schlosseri*, and *C. kowalevskii*, have humeri with intermediate dimensions. Additionally, *C. schlosseri* exhibits the most proximodistally compressed humerus among the compared species, being comparable to *Teleoceras* (Fig 25).

The patella also could be helpful for the taxonomic separation of chilotheres (Fig 13). The current comparison showed that there are two different morphotypes in the patella of chilotheres. The probably plesiomorphic '*C.*' *wimani* has a more proximodistally elongated patella than *C. habereri* and *C. persiae*. In the latter two species, the patella is much wider. In the case of *C. persiae*, the wider form of the patella corresponds to the mediolaterally oriented tuberosity in the proximal epiphysis of the tibia. If this is true, it would mean that *C. schlosseri*, that has a more anteroposteriorly oriented tuberosity in the tibia, would have a patella that is more similar to that of '*C.*' *wimani*. Besides the significance for taxonomy and

phylogeny, patellar morphology is known to be associated with ecological adaptations [91]. In primates for instance, it has been shown that a proximodistally elongated patella is associated with running, climbing, and leaping behaviour, whereas the wider patella found in great apes probably reflects a more mobile knee joint [e.g., 92,93]. Recently, it was suggested that in extant Perissodactyla patellar morphology is rather conservative, being correlated to their phylogenetic affinities [83]. Chilotheres seem to be an exception to this rule, and the patellar morphology may well be informative also for their ecology, with species like '*C.*' *wimani* that have a more proximodistally elongated patella being potentially somewhat more cursorial. However, additional material and analyses are needed to confirm such correlations.

Another postcranial element that seems to offer some taxonomic insight is the tibia. The dimensions of the bone already seem to help in the identification of the taxon, as some species like '*C.*' *wimani* are fairly small. More interestingly, the morphology of the lateral tuberosity of the proximal articulation, for the attachment of the patellar ligaments, is differently shaped in *C. schlosseri* and *C. persiae* (Fig 14C, G). In proximal view, in the former one it is anteroposteriorly oriented, being higher than wide, and in the latter one it is more mediolaterally oriented being wider than high. Unfortunately, the proximal view of the tibia is not provided for any other chilothere, therefore it is not possible to assess the state of this character in any other species.

Lastly, metapodial bones can be useful for the separation of some species. Their dimensions overall, and most prominently the length, are diagnostic. Korotkevitch (1970) [11], showed that *C. sarmaticum* from Berislav has shorter metapodials than *C. kowalevskii* from Grebeniki, based on the comparison of his own measurements to those provided by Krokos (1917) [11,17]. However, this study did not take into account data available from other localities such as Samos [14], Odessa [36], and the Red Clay localities from China [7]. Additionally, since then, there have been some new studies that have described postcranial material of chilotheres [12,16,46,81], which need to be considered. The combined comparison of the data from the literature and the newly studied material of *C. persiae* from Maragheh, *C. habereri* from Kutschwan, and *C. schlosseri* from Samos does not directly confirm the assumption of Korotkevitch (1970) [11], but shows that the chilothere species exhibit varying degrees of shortening of the limbs. Instead of *C. sarmaticum* having significantly shorter metapodials, it seems that the degree of shortening is similar, possibly even lower than that seen in *C. kowalevskii* (Fig 24). However, it seems that there is a general separation of chilotheres into two size classes. The large size group is represented by *C. kowalevskii*, *C. schlosseri*, *C. anderssoni*, *C. persiae*, and *C. orlovi*, whereas *C. sarmaticum*, '*C.*' *wimani*, *Chilotherium* indet. from Kavakdere, and possibly *E. samium* have smaller dimensions. A similar observation was also noted by Bayshashov et al. (2024) [84], who mentioned three size groups, with *C. sarmaticum* representing the small one, *C. schlosseri* (considered as the senior synonym of *C. kowalevskii* by these authors) and *C. anderssoni* representing the intermediate one, and only *C. orlovi* representing a distinctly larger size group. While *C. orlovi* seems to be the largest chilothere known to date, in our current study we divide the chilotheres in only two size groups, with *C. orlovi* being part of the large size group, for the purpose of this comparison. Additionally, there seems to be a temporal trend towards further shortening of the limb and becoming larger through time within the chilotheres. This is exemplified by the fact that the stratigraphically oldest chilotheres, like *C. sarmaticum* and '*C.*' *wimani* from the Vallesian, are in fact the smallest and have relatively longer limbs compared to younger chilotheres like *C. schlosseri* and *C. orlovi* from the middle to late Turolian.

Overall, these new findings that are based on the postcranium confirm previous assumptions about chilotheres being characterised by shortened limbs compared to other rhinocerotids [e.g., 3,7,16]. The only comparable group that independently acquired a similar bodyplan is the Teleoceratini [e.g., 86,87]. When comparing chilotheres with other Eurasian rhinoceroses that lived during the Late Miocene, like '*Ceratotherium*' *neumayri*, *Dihoplus pikermiensis*, and *Aceratherium incisivum* [27,74,94–96], it becomes clear that chilotheres differ significantly from the other members of the Rhinocerotidae and that despite often living in the same environment they were adapted to a different lifestyle. The results of our current study seem to also generally agree with what has been inferred from skull comparisons, concerning the relationship between different chilotheres. More specifically, it was already suggested that '*C.*' *wimani* represents a more

plesiomorphic chilothere, based on the very little separated parietal crests, the convex frontal region, the concave dorsal profile of the skull, the highly raised caudal portion of the skull, and the relatively simple tooth morphology [9,10,37]. This idea is corroborated by the comparatively small postcranial elements that are not quite as shortened as in other chilotheres (Fig 24). On the other hand, *C. schlosseri* was suggested to be a highly derived chilothere based on the strongly depressed frontal and nasal region of the skull, the generally flat and wide skull shape, and the complicated secondary enamel folds in the upper dentition [8,10]. This is further supported by the relatively large size and short appendicular elements, along with the derived morphology of the astragalus that differs from all other chilotheres.

Unfortunately, for many non-*Chilotherium* chilotheres, such as *E. samium*, *Shansirhinus* spp., and '*C.*' *primigenium*, no postcranial material is available [10,14,37,76,89,90]. This makes it impossible to assess how widespread the shortening of the limbs was within the chilotheres. Nonetheless, the fact that '*C.*' *wimani* – a species that is generally considered to be a "primitive" chilothere – exhibits shortened limbs in comparison to non-chilothere rhinocerotids, suggests that it is a plesiomorphic character within the chilothere group. It was recently suggested that '*C.*' *wimani* should actually represent a different genus within the chilotheres, because it lacks one of the key autapomorphies of the genus, which is the depression in the frontal region of the skull, similar to *E. samium* and '*C.*' *primigenium*, and unlike *C. anderssoni* and *C. schlosseri* [10]. The results of our study also support the notion that '*C.*' *wimani* differs from the typical species of *Chilotherium*. In the case where '*C.*' *wimani* is removed from the genus *Chilotherium* sensu stricto, the shortened limbs may actually prove to be a shared feature within chilotheres in general.

## Conclusion

The postcranial material of the hornless rhinocerotid group Chilotheriina has received little attention throughout their research history. Most studies have focussed on the skull and more specifically on the dental morphology. Herein, we describe the postcranium of three chilothere species: *Chilotherium persiae* from the Upper Miocene of Maragheh (Iran), *Chilotherium habereri* from the Upper Miocene of Kutschwan (China), and *Chilotherium schlosseri* from the Upper Miocene of Samos Island (Greece). We compared the newly described material with respective material of other chilotheres that is available in the literature and found some characters that seem to be taxonomically informative, including features in the scaphoid, tibia, patella, astragalus, and metatarsals. Additionally, we pointed out features that vary between the species, but due to the limited material their significance can presently not be evaluated. The new findings confirm that the shortening of the limbs is a key feature shared within chilotheres and support assumptions about the relationships between some species that were based only on cranial material until now.

## Supporting information

**S1 Table. Measurements of the studied material and species compared from the literature.**
(XLSX)

## Acknowledgments

We would like to thank J. Meng (AMNH), S. Roussiakis, G. Theodorou (AMPG), S. Trümper (GMM), U. Kotthoff (GPIH), I. Werneburg (GPIT), R. Rozzi, M. Albrecht (MLU), C. Argot (MNHN), U. Göhlich, F. Zachos, A. Bibl (NHMW), L. Costeur, F. Dammeyer (NMB), D. Nagel, M. Maslo (IPUW), R. Brocke, L. Kraus (SMF), and G. Rössner (SNSB-BSPG) for allowing us to study material under their care. We thank A. Athanassiou (Ephorate of Palaeoanthropology-Speleology at the Hellenic Ministry for Culture, Greece) and B. U. Bayshashov (Institut of Zoology in Akademgorodok, Kazakhstan) for providing information and literature about chilotheres. We kindly thank N. Kargopoulos (University of Zaragoza) for providing measurements and photos. We would like to thank J. Tissier and an anonymous reviewer for their useful comments that significantly improved our work and the Editor L. Pandolfi for the thorough and reliable handling of the manuscript.

## Author contributions

**Conceptualization:** Panagiotis Kampouridis, Nikolai Spassov, Madelaine Böhme.

**Investigation:** Panagiotis Kampouridis, Georgia Svorligkou.

**Visualization:** Panagiotis Kampouridis.

**Writing – original draft:** Panagiotis Kampouridis.

**Writing – review & editing:** Panagiotis Kampouridis, Georgia Svorligkou, Nikolai Spassov, Madelaine Böhme.

## References


1. Heissig K. Family Rhinocerotidae. The Miocene land mammals. Munich: Pfeil. 1999. p. 175–88.
2. Prothero DR. The evolution of North American rhinoceroses. Cambridge, UK: Cambridge University Press. 2005.
3. Heissig K. The Rhinocerotidae. The evolution of perissodactyls. New York, NY: Oxford University Press. 1989. p. 399–417.
4. Prothero DR, Guerin C, Manning E. The history of Rhinocerotoidea. The evolution of Perissodactyls. New York, NY: Oxford University Press. 1989. p. 321–40.
5. Antoine P-O, Downing KF, Crochet J-Y, Duranthon F, Flynn LJ, Marivaux L, et al. A revision of *Aceratherium blanfordi* Lydekker, 1884 (Mammalia: Rhinocerotidae) from the Early Miocene of Pakistan: postcranials as a key. Zoological Journal of the Linnean Society. 2010;160(1):139–94. https://doi.org/10.1111/j.1096-3642.2009.00597.x
6. Antoine P-O, Becker D, Pandolfi L, Geraads D. Evolution and Fossil Record of Old World Rhinocerotidae. Fascinating Life Sciences. Springer Nature Switzerland. 2025. p. 31–48. https://doi.org/10.1007/978-3-031-67169-2_2
7. Ringström T. Nashörner der Hipparion-Fauna Nord-Chinas. Palaeontologia Sinica. 1924;1:1–156.
8. Kampouridis P, Svorligkou G, Kargopoulos N, Augustin FJ. Reassessment of '*Chilotherium wegneri*' (Mammalia, Rhinocerotidae) from the late Miocene of Samos (Greece) and the European record of *Chilotherium*. Historical Biology. 2021;34(3):412–20. https://doi.org/10.1080/08912963.2021.1920939
9. Deng T. New material of *Chilotherium wimani* (Perissodactyla, Rhinocerotidae) from the Late Miocene of Fugu, Shaanxi. Journal of Vertebrate Paleontology. 2001;39:129–38.
10. Kampouridis P, Svorligkou G, Kargopoulos N, Spassov N, Böhme M. Revision of the Late Miocene hornless rhinocerotids from Samos Island (Greece) with the designation of neotypes and implications for the European chilotheres. Journal of Vertebrate Paleontology. 2023;43(1). https://doi.org/10.1080/02724634.2023.2254360
11. Korotkevich OL. The mammals of the Berislav late Sarmatian *Hipparion*-fauna. 5th ed. Naukova Dumka. 1970.
12. Bayshashov BU. Neogene rhinoceroses of Kazakhstan. Almaty: Academy of Sciences of Kazakhstan. 1993.
13. Mecquenem de R. Contribution à l'étude des fossiles de Maragha. Annales de Paléontologie. 1924;13:135–60, 1–36.
14. Weber M. Über tertiäre rhinocerotiden von der Insel Samos. Bulletin de la Société Imperériale des Naturalistes de Moscou. 1905;18:344–63.
15. Pavlow M. Mammifères tertiaires de la Nouvelle Russie, 1. Partie: Artiodactyla, Perissodactyla (*Aceratherium kowalevskii* n.s.). Nouveaux Mémoires de la Société Impériale des Naturalistes de Moscou. 1913;17:1–68.
16. Deng T. Limb bones of *Chilotherium wimani* (Perissodactyla, Rhinocerotidae) from the Late Miocene of the Linxia Basin in Gansu, China. 2002;40:305–16.
17. Krokos WI. *Aceratherium schlosseri* Web. du village de Grebeniki du gouvernement de Kherson. Memoires of the Agricultural Society of Southern Russia. 1917;82:1–96.
18. Wessel P, Luis JF, Uieda L, Scharroo R, Wobbe F, Smith WHF, et al. The Generic Mapping Tools Version 6. Geochem Geophys Geosyst. 2019;20(11):5556–64. https://doi.org/10.1029/2019gc008515
19. Pohlig H. Ueber eine Hipparionen-Fauna von Maragha in Nordpersien, über fossile Elephantenreste Kaukasiens und Persiens und über die Resultate einer Monographie der fossilen Elephanten Deutschlands und Italiens. Zeitschrift der Deutschen Geologischen Gesellschaft. 1885;37:1022–7.
20. Pandolfi L. *Persiatherium rodleri*, gen. et sp. nov. (Mammalia, Rhinocerotidae) from the upper Miocene of Maragheh (northwestern iran). Journal of Vertebrate Paleontology. 2015;36(1):e1040118. https://doi.org/10.1080/02724634.2015.1040118
21. Ataabadi MM, Bernor RL, Kostopoulos DS, Wolf D, Orak Z, Zare G, et al. Recent Advances in Paleobiological Research of the Late Miocene Maragheh Fauna, Northwest Iran. Fossil Mammals of Asia. Columbia University Press. 2013. p. 546–65. https://doi.org/10.7312/columbia/9780231150125.003.0025
22. Ataabadi MM, Kaakinen A, Kunimatsu Y, Nakaya H, Orak Z, Paknia M, et al. The late Miocene hominoid-bearing site in the Maragheh Formation, Northwest Iran. Palaeobio Palaeoenv. 2016;96(3):349–71. https://doi.org/10.1007/s12549-016-0241-4
23. Mecquenem R de. Contribution à l'étude du gisement des vertébrés de Maragha et de ses environs. Annales d'histoire naturelle. 1908;1:27–98.

24. Schlosser M. Die fossilen Säugethiere Chinas nebst einer Odontographie der recenten Antilopen. Abhandlungen der Königlichen Bayerischen Akademie der Wissenschaften. 1903;22:1–221.
25. Killgus H. Unterpliozäne Säuger aus China. PalZ. 1923;5:251–57. https://doi.org/10.1007/BF03160368
26. Killgus H. Die unterpliocaenen chinesischen säugetierreste der tafelschen sammlung zu tübingen. Eberhard-Karls University of Tübingen. 1922.
27. Giaourtsakis IX. The Fossil Record of Rhinocerotids (Mammalia: Perissodactyla: Rhinocerotidae) in Greece. Fossil Vertebrates of Greece Vol. 2. Springer International Publishing. 2021. p. 409–500. https://doi.org/10.1007/978-3-030-68442-6_14
28. Koufos GD, Kostopoulos DS, Vlachou TD, Konidaris GE. A synopsis of the late Miocene Mammal Fauna of Samos Island, Aegean Sea, Greece. Geobios. 2011;44(2–3):237–51. https://doi.org/10.1016/j.geobios.2010.08.004
29. Kostopoulos DS, Sen S, Koufos GD. Magnetostratigraphy and revised chronology of the late Miocene mammal localities of Samos, Greece. International Journal of Earth Sciences. 2003;92(5):779–94. https://doi.org/10.1007/s00531-003-0353-8
30. Bayshashov BU. A new rhinoceros species of the genus *Chilotherium* from Pavlodar. Mesozoic and Cenozoic vertebrate fauna and flora of North-Eastern and southern Kazakhstan. Almaty: Academy of Sciences of Kazakhstan. 1982. p. 72–83.
31. Guérin C. Les rhinocéros (Mammalia, Perissodactyla) du Miocène terminal au Pleistocène supérieur en Europe occidentale: comparaison avec les espèces actuelles. Documents des Laboratoires de Géologie de la Faculté des Sciences de Lyon. 1980. 1–1185.
32. Barone R. Anatomie comparée des mammifères domestiques. Paris: Vigot Frères. 2010.
33. Heissig K. Les Rhinocerotidae (Perissodactyla) de Sansan. Mammifères de Sansan. Paris: Muséum national d'Histoire naturelle. 2012. p. 317–485.
34. Antoine PO. Phylogénie et évolution des Elasmotheriina (Mammalia, Rhinocerotidae). 2002.
35. Mallet C, Cornette R, Billet G, Houssaye A. Interspecific variation in the limb long bones among modern rhinoceroses-extent and drivers. PeerJ. 2019;7:e7647. https://doi.org/10.7717/peerj.7647 PMID: 31579585
36. Kiernik E. Über einen Aceratheriumschädel aus der Umgebung von Odessa. Bulletin international de l'Académie des sciences de Cracovie. 1913;1913:808–64.
37. Deng T. A primitive species of *Chilotherium* (Perissodactyla, Rhinocerotidae) from the Late Miocene of Linxia Basin (Gansu, China). Cainozoic Research. 2006;5:93–102.
38. Heissig K. Rhinocerotidae aus dem Jungtertiär Anatoliens. Geologisches Jahrbuch (B). 1975;15:145–51.
39. Svorligkou G, Kampouridis P, Kargopoulos N, Pandolfi L. Craniodental anatomy of the hornless rhinocerotid *Chilotherium schlosseri* (Mammalia, Perissodactyla) from the Late Miocene of Samos Island, Greece. J Mammal Evol. 2025;32(4). https://doi.org/10.1007/s10914-025-09777-0
40. Andree J. Rhinocerotiden aus dem Unterpliocän von Samos. Paläontologische Zeitschrift. 1921;3:189–212.
41. Geraads D, Koufos G. Upper Miocene Rhinocerotidae (Mammalia) from Pentalophos-1, Macedonia, Greece. Palaeontographica Abteilung A. 1990;210:151–68.
42. Athanassiou A, Roussiakis SJ, Giaourtsakis IX, Theodorou GE, Iliopoulos G. A new hornless rhinoceros of the genus *Acerorhinus* (Perissodactyla: Rhinocerotidae) from the Upper Miocene of Kerassiá (Euboea, Greece), with a revision of related forms. pala. 2014;303(1–3):23–59. https://doi.org/10.1127/pala/303/2014/23
43. Lubicz-Niezabitowski E. *Teleoceras ponticus* n. sp. Vorläufige Notiz. Nowy Targ. 1912. 2.
44. Lubicz-Niezabitowski E. Über das Schädelfragment eines Rhinocerotiden (*Teleoceras ponticus* Niez.) von Odessa. Bulletin International de l'Académie des Sciences de Cracovie, Series B. 1913;:223–35.
45. Korotkevich OL. A new *Chilotherium* species from the Sarmatian deposits of the Ukraine. Dopovidi Akad Nauk Ukrainskoi RSR. 1958;12:1372–6.
46. Antoine P-O, Sen S. Rhinocerotidae and Chalicotheriidae (Perissodactyla, Tapiromorpha). Geodiversitas. 2016;38(2):245–59. https://doi.org/10.5252/g2016n2a6
47. Țibuleac P, Tissier J, Petculescu A, Becker D. *Chilotherium schlosseri* (Weber, 1905) (Rhinocerotidae, Mammalia) from the late Miocene of the foreland of the Eastern Carpathians in Romania. Comptes Rendus Palevol. 2023;(36). https://doi.org/10.5852/cr-palevol2023v22a36
48. Geraads D, Spassov N. Rhinocerotidae (Mammalia) from the Late Miocene of Bulgaria. pala. 2009;287(4–6):99–122. https://doi.org/10.1127/pala/287/2009/99
49. Sun DH, Li Y, Deng T. A new species of *Chilotherium* (Perissodactyla, Rhinocerotidae) from the Late Miocene of Qingyang, Gansu, China. Vertebrata PalAsiatica. 2018;56:216–28. https://doi.org/10.19615/j.cnki.1000-3118.180109
50. Mecquenem de R. Le lac d'Ourmiah. geo. 1908;17(92):128–44. https://doi.org/10.3406/geo.1908.18216
51. Pohlig H. On the Pliocene of Maragha, Persia, and its resemblance to that of Pikermi in Greece. Quarterly Journal of the Geological Society of London. 1886;42:177–9.
52. Bernor RL. Mammalian biostratigraphy, geochronology, and zoogeographic relationships of the Late Miocene Maragheh fauna, Iran. Journal of Vertebrate Paleontology. 1986;6(1):76–95. https://doi.org/10.1080/02724634.1986.10011600
53. Campbell BG, Amini MH, Bernor RL, Dickinson W, Drake R, Morris R, et al. Maragheh: a classical late Miocene vertebrate locality in norhtwestern Iran. Nature. 1980;287(5785):837–41. https://doi.org/10.1038/287837a0

54. Osborn HF. Phylogeny of the rhinoceroses of Europe. Bulletin of the American Museum of Natural History. 1900;12:229–67.
55. Kampouridis P, Mirzaie Ataabadi M, Hartung J, Augustin FJ. The easternmost occurrence of the Late Miocene schizotheriine chalicothere *Ancylotherium pentelicum* at the classical locality of Maragheh (Iran). J Mammal Evol. 2024;31(3). https://doi.org/10.1007/s10914-024-09730-7
56. Salminen J, Paknia M, Kaakinen A, Ataabadi MM, Zare G, Orak Z, et al. Preliminary magnetostratigraphic results from the late Miocene Maragheh Formation, NW Iran. Palaeobio Palaeoenv. 2016;96(3):433–43. https://doi.org/10.1007/s12549-016-0239-y
57. Lu X-K, Deng T, Pandolfi L. Reconstructing the phylogeny of the hornless rhinoceros Aceratheriinae. Front Ecol Evol. 2023;11. https://doi.org/10.3389/fevo.2023.1005126
58. Kargopoulos N, Kampouridis P, Hartung J, Böhme M. Hyaenid remains from the Late Miocene of Kutschwan (Shanxi Province, China). PalZ. 2023;97(3):653–66. https://doi.org/10.1007/s12542-023-00658-6
59. Kampouridis P, Hartung J, Ferreira GS, Böhme M. Reappraisal of the late Miocene elasmotheriine *Parelasmotherium schansiense* from Kutschwan (Shanxi Province, China) and its phylogenetic relationships. Journal of Vertebrate Paleontology. 2021;41(6). https://doi.org/10.1080/02724634.2021.2080556
60. Koufos GD. The late Miocene mammal faunas of the Mytilinii basin, Samos Island, Greece: new collection: 1. history of the samos fossil mammals. Beiträge zur Paläontologie. 2009;31:1–12.
61. Kostopoulos DS, Koufos GD, Sylvestrou IA, Syrides GE, Tsombachidou E. The late Miocene mammal faunas of the Mytilinii basin, Samos Island, Greece: New collection: 2. Lithostratigraphy and fossiliferous sites. Beiträge zur Paläontologie. 2009;31:13–26.
62. Koufos GD, Kostopoulos DS, Vlachou TD. The late Miocene mammal faunas of the Mytilinii basin, Samos Island, Greece: New collection 16. Beiträge Paläontol. 2009;31:397–408.
63. Toula F. Das gebiss und reste der nsenbeine von *Rhinoceros* (*Ceratorhinus* Osborn) *hundsheimensis*. Abhandlungen der k.k Geologischen Reichsanstalt. 1906;20:1–38.
64. Weber M. Ueber tertiäre Rhinocerotiden von der Insel Samos. Bulletin de la Société Impériale des Naturalistes de Moscou. 1904;17:477–501.
65. Drevermann F. Aus der Zeit des dreizehigen Pferdes. Natur und Museum. 1930;60:2–13.
66. Leonardi P. Resti fossili inediti di rhinoceronti conservati nelle collezioni dell'instituto geologico dell'università di Padova. Memorie dell'Instituto Geologico. 1948;15:2–30.
67. Gürich G. Fossile Säugetierreste aus Samos. Verhandlungen des Naturwissenschaftlichen Vereins in Hamburg. 1911;3:79.
68. Linnaeus C. Systema naturae. Stockholm: Laurentii Salvii. 1758.
69. Owen. Description of Teeth and portions of Jaws of two extinct Anthracotheroid Quadrupeds (*Hyopotamus vectianus* and *Hyopbovinus*) discovered by the Marchioness of Hastings in the Eocene Deposits on the N. W. coast of the Isle of Wight: with an attempt to develope Cuvier's idea of the Classification of Pachyderms by the Number of their Toes. QJGS. 1848;4(1–2):103–41. https://doi.org/10.1144/gsl.jgs.1848.004.01-02.21
70. Gray JE. On the natural arrangemenet of vertebrose animals. London Medical Repository. 1821;15:297–310.
71. Dollo L. Rhinocéros vivants et fossiles. Revue de Questions Scientifiques. 1885;17:293–9.
72. Qiu ZX, Xie JY, Yan DF. A new chilothere skull from Hezheng, Gansu, China, with special reference to the Chinese "*Diceratherium*". Scientia Sinica B. 1987;:545–52.
73. Kretzoi M. Bemerkungen zum System der Nachmiozänen Nashorn-Gattungen. Földtani Közlöny. 1942;72:4–12.
74. Hünermann KA. Die nashornreste (*Aceratherium incisivum*) aus dem jungtertiär vom höwenegg im hegau. Andrias. 1989;6:5–116.
75. Cerdeno E. Rhinocerotidae from the Middle Miocene of the Tung-gur Formation, Inner Mongolia (China). American Museum Novitates. 1996;44.
76. Deng T. New cranial material of *Shansirhinus* (Rhinocerotidae, Perissodactyla) from the Lower Pliocene of the Linxia Basin in Gansu, China. Geobios. 2005;38(3):301–13. https://doi.org/10.1016/j.geobios.2003.12.003
77. Rodler A. Verhandlungen der kaiserlich-königlichen geologischen Reichsanstalt. 1885;14:333–7.
78. Gaudry A. V.—Palæontology in Germany and Austria. Geol Mag. 1885;2(12):556–9. https://doi.org/10.1017/s0016756800152756
79. Bernor RL, Semprebon GM, Damuth J. Maragheh Ungulate Mesowear: Interpreting Paleodiet and Paleoecology from a Diverse Fauna with Restricted Sample Sizes. Annales Zoologici Fennici. 2014;51(1–2):201–8. https://doi.org/10.5735/086.051.0220
80. Kaup J. Über *Rhinoceros incisivus* Cuv., und eine neue Art, *Rhinoceros schleiermacheri*. Isis von Oken. 1832;:898–904.
81. Fortelius M, Heissig K, Saraç G, Sen S. Rhinocerotidae (Perissodactyla). In: Fortelius M, Kappelman J, Sen S, Bernor RL, editors. Geology and paleontology of the Miocene Sinap Formation, Turkey. New York, NY: Columbia University Press. 2003. p. 282–307.
82. Nothdurft W, Smith JB. The lost dinosaurs of Egypt. New York: Random House. 2002.
83. Mallet C, Houssaye A. Deciphering the influence of evolutionary legacy and functional constraints on the patella: an example in modern rhinoceroses amongst perissodactyls. PeerJ. 2024;12:e18067. https://doi.org/10.7717/peerj.18067 PMID: 39469593
84. Baishashov BU, Nigmatova SA, Seidali AL, Madiyarova IT, G. Lucas S. Paleogeographical reconstruction of the late neogene in the north-eastern part of Central Kazakhstan (The «Goose Passage» Site). EJSU. 2024;146(5):32–44. https://doi.org/10.51301/ejsu.2024.i5.05
85. Cerdeño E. Étude sur *Diaceratherium aurelianense* et *Brachypotherium brachypus* (Rhinocerotidae, Mammalia) du Miocène moyen de France. Bulletin du Muséum national d'histoire naturelle, Paris. 1993;15:25–77.

86. Prothero DR, Manning EM. Miocene rhinoceroses from the Texas Gulf Coastal Plain. J Paleontol. 1987;61(2):388–423. https://doi.org/10.1017/s0022336000028559

87. Short RA, Wallace SC, Emmert LG. A new species of *Teleoceras* (Mammalia, Rhinocerotidae) from the late Hemphillian of Tennessee. FLMNH. 2019;56(5):183–260. https://doi.org/10.58782/flmnh.kpcf8483

88. Ringström T. Über quartäre und jungtertiäre rhinocerotiden aus China und der Mongolei. Palaeontologia Sinica. 1927;4:1–21.

89. Lu X, Chen S, He W. New skulls of Shansirhinus ringstroemi from the upper Neogene of the Linxia Basin, and their paleoenvironmental context. Quaternary Research. 2015;35:539–49. https://doi.org/10.11928/j.issn.1001-7410.2015.03.06

90. Deng T, Lu X, Sun D, Li S. Rhinocerotoid fossils of the Linxia Basin in northwestern China as late Cenozoic biostratigraphic markers. Palaeogeography, Palaeoclimatology, Palaeoecology. 2023;614:111427. https://doi.org/10.1016/j.palaeo.2023.111427

91. Samuels ME, Regnault S, Hutchinson JR. Evolution of the patellar sesamoid bone in mammals. PeerJ. 2017;5:e3103. https://doi.org/10.7717/peerj.3103 PMID: 28344905

92. Pina M, Almécija S, Alba DM, O'Neill MC, Moyà-Solà S. The Middle Miocene ape *Pierolapithecus catalaunicus* exhibits extant great ape-like morphometric affinities on its patella: inferences on knee function and evolution. PLoS One. 2014;9(3):e91944. https://doi.org/10.1371/journal.pone.0091944 PMID: 24637777

93. Ward CV, Ruff CB, Walker A, Teaford MF, Rose MD, Nengo IO. Functional morphology of *Proconsul* patellas from Rusinga Island, Kenya, with implications for other Miocene-Pliocene catarrhines. Journal of Human Evolution. 1995;29(1):1–19. https://doi.org/10.1006/jhev.1995.1045

94. Antoine PO, Saraç G. Rhinocerotidae (Mammalia, Perissodactyla) from the late Miocene of Akkaşdaği, Turkey. Geodiversitas. 2005;27:601–32.

95. Svorligkou G. Study and taxonomical identification of carpal and metacarpal bones of rhinocerotids *Dihoplus pikermiensis* and "*Diceros*" *neumayri* (Mammalia, Perissodactyla) from the Turolian of Pikermi. National and Kapodistrian University of Athens. 2018.

96. Heissig K. The fossil rhinoceroses of Rudabánya. Palaeontographia Italica. 2004;90:217–58.

# Appendix 6

*Publication 6*

Deciduous dentition and ontogenetic development of the skull and teeth of *Chilotherium* (Mammalia, Perissodactyla, Rhinocerotidae) from the Late Miocene of Eurasia

**Panagiotis Kampouridis**[a,b]*, Luca Pandolfi[c], Christina Kyriakouli[a,b], Nikolai Spassov[d], Madelaine Böhme[a,b]

[a]Department of Geoscience, Eberhard Karls University of Tübingen, Tübingen, Germany;

[b]Senckenberg Centre for Human Evolution and Palaeoenvironment, Tübingen, Germany;

[c]Dipartimento di Scienze della Terra, Università di Pisa, Pisa, Italy;

[d]National Museum of Natural History at the Bulgarian Academy of Sciences, Sofia, Bulgaria

Published in

Fossil Record 29(1), 373–410

DOI: 10.3897/fr.29.192018

Date of online publication: 04.06.2026

Fossil Record 29 (1) 2026, 373–410 | DOI 10.3897/fr.29.192018

PENSOFT

MUSEUM FÜR NATURKUNDE BERLIN

# Deciduous dentition and ontogenetic development of the skull and teeth of *Chilotherium* (Mammalia, Perissodactyla, Rhinocerotidae) from the Late Miocene of Eurasia

Panagiotis Kampouridis[1,2], Luca Pandolfi[3], Christina Kyriakouli[1,2], Nikolai Spassov[4], Madelaine Böhme[1,2]

1 *Department of Geoscience, Eberhard Karls University of Tübingen, Hölderlinstraße. 12, 72074, Tübingen, Germany*
2 *Senckenberg Centre for Human Evolution and Palaeoenvironment (HEP Tübingen), Hölderlinstraße. 12, 72074, Tübingen, Germany*
3 *Università di Pisa, Dipartimento di Scienze della Terra, via S. Maria 53-56126, Pisa, Italy*
4 *National Museum of Natural History at the Bulgarian Academy of Sciences, Sofia, Bulgaria*

*https://zoobank.org/33C26AAA-328C-4047-A52C-340260017491*

Corresponding author: Panagiotis Kampouridis (pkampouridis94@gmail.com)

Academic editor: Florian Witzmann ♦ **Received** 18 March 2026 ♦ **Accepted** 19 May 2026 ♦ **Published** 4 June 2026

## Abstract

The hornless rhinoceros genus *Chilotherium* is characterised by high taxonomic complexity, with more than 30 species having been included in the genus at some point. This frequently prevents the identification of incomplete material, which has historically limited understanding of the genus's diversity and evolution. Although recent work has enhanced the comprehension of the systematics of hornless rhinoceroses, the ontogeny of the cranium and deciduous dentition of chilotheres is still poorly known. Herein, juvenile skulls and mandibles at different ontogenetic stages are investigated, along with the deciduous teeth of four Late Miocene chilothere species: *Chilotherium persiae* from Maragheh (Iran), *Chilotherium habereri* from Kutschwan (China), *Chilotherium schlosseri* from Samos (Greece), and *Chilotherium anderssoni* from Daijiagou (China). The results show that several dental characters in the deciduous premolars are informative for species discrimination. The eruption sequence of the deciduous teeth is broadly uniform within the genus. Only the relative eruption of D1 and D4 varies, with *C. schlosseri* showing delayed D1 eruption. Lastly, enamel hypoplasia is also documented in the deciduous teeth. Although d/D2 and d/D3 exhibit hypoplasias only sporadically, d/D4 consistently bears prominent hypoplasias associated with the individual's birth. The position of the latter hypoplasia is consistent across chilotheres, occurring in the middle of the tooth crown, except in *C. schlosseri*, where it is located at the base of the crown.

## Key Words

Milk teeth, morphology, Neogene, pathology, rhinoceros, taxonomy

## Introduction

Mammals are generally characterised by highly specialised dentition that reflects ecological adaptations (Ungar 2010). A major modification in the evolutionary history of mammals was diphyodonty: the existence of only two generations in dental replacement, initially the deciduous or milk teeth and then the permanent teeth (e.g. Jäger et al. 2019; Cabreira et al. 2022). Despite their potential systematic value (e.g. Fernández et al. 2021; Gomes Rodrigues et al. 2021; Kampouridis et al. 2023a), deciduous teeth are rarely studied in detail or used in phylogenetic and taxonomic analyses.

The significance of the deciduous dentition for the reconstruction of phylogenetic relationships was recently highlighted for Hippopotamoidea (Gomes Rodrigues et al. 2021). Although many studies have addressed the phylogenetic relationships of rhinoceroses, in the past, most did not include any characters related to the deciduous teeth (e.g. Heissig 1981; Fortelius and Heissig 1989; Cerdeño 1995).

Antoine (2002) incorporated nearly 20 characters specifically related to deciduous dentition into his newly compiled comprehensive character matrix, which set the framework for subsequent rhinocerotid phylogenetic analyses. However, chilotheres are underrepresented in most phylogenetic analyses, with only a few including any chilothere taxa (e.g. Deng 2006a; Pandolfi 2016; Lu et al. 2023). The morphology of the deciduous dentition in chilotheres is also almost unknown for most taxa, as it is usually not explicitly described. A first step to resolving this is describing the morphology of the milk teeth of chilotheres and their variability.

The hornless rhinoceros genus *Chilotherium* Ringström, 1924, was autochthonous to Eurasia and lived only during the Late Miocene (e.g. Deng and Downs 2002; Deng 2006b; Kampouridis et al. 2022b). Its biogeographical distribution ranged from eastern China to the Balkan Peninsula in the west (e.g. Deng 2006b; Geraads and Spassov 2009; Spassov et al. 2018). The genus was initially described by Ringström (1924), who revised several hornless rhinoceroses, most of which had been attributed to the genus *Aceratherium* Kaup, 1832, until then. The most characteristic features that connected these species were the depression in their frontals, widely separated parietal crests, a wide mandibular symphysis with large tusk-like lower second incisors, and short limb bones (Ringström 1924). While the permanent dentition of chilotheres is well known and presents many diagnostic features differentiating the group from other rhinoceroses (e.g. Geraads and Spassov 2009; Kampouridis et al. 2023b; Țibuleac et al. 2023), little is known about the deciduous dentition of these animals.

The aim of the present study is to describe juvenile crania, mandibles, and teeth of the hornless rhinoceros *Chilotherium*. This allowed a better understanding of their tooth morphology, including potential variability, dental eruption, and skull development, to shed light on aspects of their systematics and ecology.

## Abbreviations

**AMNH**, American Museum of Natural History, New York (USA); **AMPG**, Palaeontological and Geological Museum of the University of Athens (Greece); **BSPG**, Bayerische Staatssammlung für Paläontologie und Geologie (Germany); **GMM**, Geomuseum of the University of Münster (Germany); **GPIH**, Geologisch-Paläontologisches Institut der Universität Hamburg (Germany); **GPIT**, Geologisch-Paläontologisches Institut der Universität Tübingen (Germany); **MLU**, Martin-Luther Universität Halle-Wittenberg (Germany); **MNHN**, Muséum national d'Histoire naturelle, Paris (France); **NHMUK**, Natural History Museum, London (UK); **NHMW**, Naturhistorisches Museum in Wien (Austria); **PMU**, Museum of Evolution (Palaeontological Museum), Uppsala (Sweden); **SMF**, Senckenberg Museum in Frankfurt (Germany); **SMNS**, Staatliches Museum für Naturkunde Stuttgart (Germany); and **SNSB**, Staatliche Naturwissenschaftliche Sammlungen Bayerns (Germany).

## Fossil sites

### Samos

The island of Samos (Fig. 1) has been known to yield Late Miocene vertebrate fossils since the 19th century, with the first excavations taking place in the 1880s, led by C. I. Forsyth Major (Koufos 2009). Since then, numerous palaeontologists and fossil hunters have visited the island to collect fossils (Koufos 2009). This led to several impressive collections of Samos material in major natural history museums throughout the world, including the AMNH, the NHMW, and the SMNS. Most recently, the Aristotle University of Thessaloniki, led by Professor George Koufos, excavated on Samos Island, bringing to light a rich collection of mammalian remains (e.g. Kostopoulos et al. 2009; Koufos 2009). The material was studied in detail, providing crucial information about the biostratigraphical context and the fauna itself (e.g. Kostopoulos et al. 2003, 2009; Koufos et al. 2009, 2011). The rhinoceros material from Samos has been assigned to several different taxa over the years (for an overview, see Giaourtsakis 2022). Today, it is generally accepted that two large tandem-horned rhinoceroses are present, *Ceratotherium neumayri* (Osborn, 1900) and *Dihoplus pikermiensis* (Toula, 1906), along with two smaller, hornless rhinocerotids belonging to the chilotheres. The taxonomy of chilotheres has experienced many difficulties in the past, with the variously suggested presence of five species – *Chilotherium schlosseri* (Weber, 1905), *Eochilotherium samium* (Weber, 1905), *Chilotherium wegneri* (Andree, 1921), *Chilotherium angustifrons* (Andree, 1921), and *Chilotherium kowalevskii* (Pavlow, 1913) – depending on the authors (Weber 1905; Krokos 1917; Andree 1921; Giaourtsakis 2003, 2009, 2022; Athanassiou et al. 2014). Recently, it was suggested that *C. wegneri* and *C. angustifrons* represent junior synonyms of *C. schlosseri* (e.g. Giaourtsakis 2022; Kampouridis et al. 2023b). The identification of *C. kowalevskii* in Samos stems from the erroneous synonymisation of this species with *C. angustifrons* (see Kampouridis et al. 2022b). Therefore, *C. schlosseri* and *E. samium* are the two valid chilothere species present in Samos (Kampouridis et al. 2022b, 2023b, 2025; Giaourtsakis 2022; Svorligkou et al. 2025).

### Maragheh

The locality of Maragheh is situated in northwestern Iran (Fig. 1). The Late Miocene fauna has been well known since the late 19th century (Rodler 1885; Pohlig 1886; Mecquenem 1908b; Mirzaie Ataabadi et al. 2013, 2016). Several fossil sites have been excavated over more than 100 years; recent studies have suggested the existence of three distinct fossiliferous levels and were able to associate the historical fossil sites with them (Campbell et al. 1980; Bernor 1986). Material from this locality is scattered throughout many collections, such

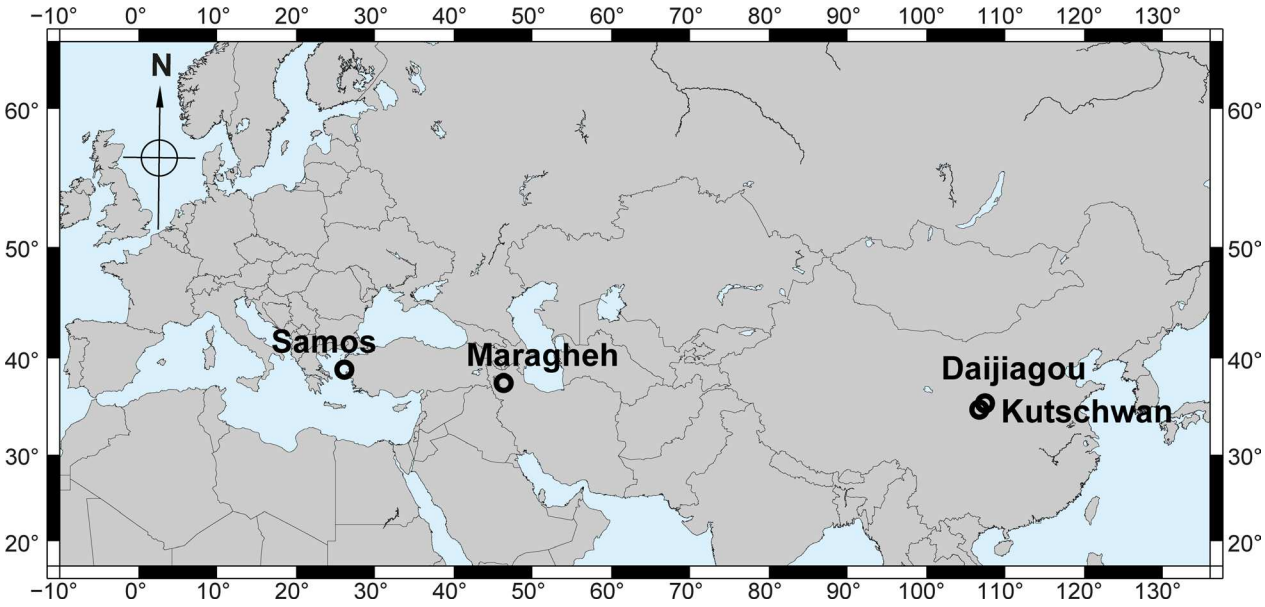


**Figure 1.** Geographical map. Fossil localities from which the material studied herein comes (Samos in Greece, Maragheh in Iran, Daijiagou, and Kutschwan in China) are shown. The map was generated using Generic Mapping Tools 6 (GMT6) (Wessel et al. 2019).

as the NHMW, MLU, MNHN, NHMUK, and SNSB-BSPG. The rhinoceros assemblage in Maragheh is quite rich and includes the large single-horned *Iranotherium morgani* (Mecquenem, 1908a), the large tandem-horned *Ceratotherium neumayri*, and two small hornless rhinoceroses, *Chilotherium persiae* (Pohlig, 1885) and *Persiatherium rodleri* Pandolfi, 2016 (e.g. Pohlig 1885; Mecquenem 1924; Pandolfi 2016; Kampouridis et al. 2025). Notably, Maragheh represents the type locality for all these rhinocerotid species. *Chilotherium persiae* is the most common and most characteristic representative of the family in the Maragheh fauna, and several juvenile dental elements have been found and studied in the context of the present study. These fossils were excavated at different fossil sites in the area around Maragheh that correspond to different stratigraphical sections, although exact information about the site is often not provided on the collection labels (e.g. Pohlig 1886; Mecquenem 1908b; Kampouridis et al. 2024).

Daijiagou

The fossil site of Daijiagou (also spelled Taijiagou and Taichiakou or called Lok. 30) is found close to the Yellow River (Huang He), situated in the county of Baode in Shanxi Province, China (Fig. 1). This fossil site was discovered and excavated in the context of the Sino-Swedish expedition led by J. G. Andersson in the late 1910s and early 1920s, which created the Lagrelius Collection at the University of Uppsala. The excavation of this locality, which is referred to as "Lok. 30" in several publications, and many other localities in China between 1921 and 1923 was undertaken by O. Zdansky and later by other palaeontologists such as B. Bohlin, who also studied part of the excavated material (e.g. Zdansky 1924, 1925a, 1925b, 1927a, 1927b; Bohlin 1926, 1935). The Late Miocene faunal assemblages were mainly composed of horses, bovids, and rhinoceroses (Ringström 1923, 1924, 1927; Sefve 1927; Bohlin 1935). Based on this material, Ringström (1924) erected the genus *Chilotherium* and its type species, *Chilotherium anderssoni* Ringström, 1924. However, several other rhinoceroses, including further chilotheres, were erected by T. Ringström based on material from these excavations (Ringström 1923, 1924). The locality of Daijiagou represented only a small portion of the overall excavated material during the Sino-Swedish expedition; nonetheless, in addition to a large sample of *C. anderssoni* specimens, the elasmotheriine *Sinotherium lagrelii* Ringström, 1923, was also erected based on a left M3, and additional material was described later (Ringström 1923, 1924). The stratigraphy of these classical Upper Miocene localities in the Baode area was recently re-evaluated and the age of many localities was refined, dating Daijiagou to approximately 5.7 Ma (Kaakinen et al. 2013).

Kutschwan

The locality of Kutschwan is of Late Miocene age and was discovered by the German geographer Albert Tafel in Shanxi during his trip to China in 1905 (Killgus 1923). No information about the exact location of the fossil site is known, but the material was collected from horizontal red clay deposits close to the Yellow River (Huang He) in Shanxi Province, China (Fig. 1; Killgus 1923). The material excavated by Tafel included a large collection of mammalian remains, with many cranial and postcranial elements. The whole collection was initially prepared at the SMNS (Germany), then given to the GPIT (Germany), and is still housed there today. Hugo Killgus studied the whole collection for his Ph.D. dissertation (Killgus 1922) and recognised a quite rich mammalian fauna, based

on this limited material, including two rhinoceroses, *Chilotherium habereri* and *Parelasmotherium schansiense* Killgus, 1923, a hipparionine, *Schansitherium tafeli* Killgus, 1923, four bovids, and a hyaenid (Killgus 1923). More recently, Kampouridis et al. (2022a) re-examined the holotype of *Parelasmotherium schansiense* using micro-computed tomography to reveal unknown features important for the taxonomy and phylogeny of this taxon, and Kampouridis et al. (2025) studied the postcranial material of *C. habereri* from Kutschwan in an overview of the postcranial anatomy of the genus.

# Material and methods

## Material

The material investigated herein includes four species of *Chilotherium* from different Upper Miocene localities across Eurasia (Fig. 1). The first species is *C. persiae* from the Upper Miocene of Maragheh (Iran). Most of the material is housed at the MNHN and NHMW, and additional cranial, mandibular, and dental material is housed at the MLU and NHMUK. The second species is *C. habereri* from the Upper Miocene of Kutschwan (China). The material includes several partial skulls, mandibles, and isolated deciduous teeth housed in the GPIT. The third species is *C. schlosseri* from the Upper Miocene of Samos (Greece), with material of this species spread throughout different institutions, such as the AMPG, GMM, NHMW, SMF, and SMNS. The last species is *C. anderssoni* from the Upper Miocene site of Daijiagou (also referred to as "Lok. 30") in Shanxi, China. The material includes four partial skulls from the historical fossiliferous site that are housed in the collections of the AMNH and SMF. These specimens, along with other chilothere material described by Ringström (1924), were collected during the Sino-Swedish expedition led by J. G. Andersson (Mateer and Lucas 1985) and were later donated by the PMU to the SMF between 1927 and 1929 (according to the catalogues of the SMF) and to the AMNH.

## Anatomical nomenclature

The anatomical nomenclature of the skull and dentition (Fig. 2) follows Guérin (1980), Peter (2002), and Antoine (2002). The ontogenetic age of the specimens was determined for more detailed comparisons between the species and the assessment of potential intraspecific ontogenetic changes in skull morphology. The ages were determined based on the wear stages of the teeth as described by Hillman-Smith et al. (1986) for the extant *Ceratotherium simum* and further elaborated for fossil rhinocerotid species by Hullot and Antoine (2020). The data concerning the wear stages of the teeth and the suggested age classes can be found in Suppl. material 1: table S1.

## Enamel hypoplasia

Enamel hypoplasia is a defect in tooth development, leading to the underdevelopment of enamel in part of a tooth, and represents a unique marker of high levels of stress in an individual (e.g. Goodman and Rose 1990; Guatelli-Steinberg 2001; Hullot et al. 2021; Hullot and Antoine 2022). Herein, enamel hypoplasia was studied in the deciduous teeth of four *Chilotherium* species. For this purpose, hypoplasia in the deciduous premolars, upper and lower second (d/D2), third (d/D3), and fourth (d/D4) premolars was investigated. In total, 152 teeth were studied. If hypoplasia appeared on the same tooth position on both sides, it was counted as a single occurrence. Teeth with damaged enamel or those that had not fully erupted were excluded from this study. Additionally, in cases where teeth from Kutschwan and Samos had not fully erupted, the respective specimens were CT-scanned, as proposed by Hullot and Antoine (2022), to investigate the occurrence of potential hypoplasia.

## µCT-scanning

To study the cranial and dental morphology in detail, micro-computed tomography (µCT) scans were acquired for some specimens with a Nikon XT H 320 µCT scanner operated by the 3D Imaging Lab Senckenberg Centre for Human Evolution and Palaeoenvironment and the Eberhard Karls University Tübingen, Germany. An X-ray tube containing a multi-metal reflection target with a maximum acceleration voltage of 225 kV was used. Specimen GPIT/MA/04842 (partial skull of *C. habereri*) was scanned at 215 kV and 210 µA with a voxel size of 0.05999687 mm, using a copper filter of 1.0 mm thickness. Specimen GPIT/MA/04818 (mandible of *C. habereri*) was scanned at 165 kV and 200 µA with a voxel size of 0.03678904 mm, using a copper filter of 0.25 mm thickness. Specimen GPIT/MA/04820 (mandible of *C. habereri*) was scanned at 190 kV and 130 µA with a voxel size of 0.04216668 mm, using a copper filter of 0.25 mm thickness. Specimen GPIT/MA/04849 (mandible of *C. habereri*) was scanned at 200 kV and 160 µA with a voxel size of 0.03750121 mm, using a copper filter of 0.5 mm thickness. Specimen GPIT/MA/04817 (isolated D4 of *C. habereri*) was scanned at 175 kV and 180 µA with a voxel size of 0.03139582 mm, using a copper filter of 0.1 mm thickness. Specimen SMNS 47913 (partial skull of *C. schlosseri*) was scanned at 200 kV and 205 µA with a voxel size of 0.06508365 mm, using a copper filter of 0.1 mm thickness. Specimen SMNS 47914 (partial skull of *C. schlosseri*) was scanned at 225 kV and 215 µA with a voxel size of 0.05487692 mm, using a copper filter of 2.5 mm thickness. Images were processed using VG Studio Max. The results are virtual orthoslices of the actual teeth, used for the detailed comparison of the hypoplasia observed in the deciduous teeth. The scans are available on MorphoSource (https://www.morphosource.org/) under the Project ID 000840545.

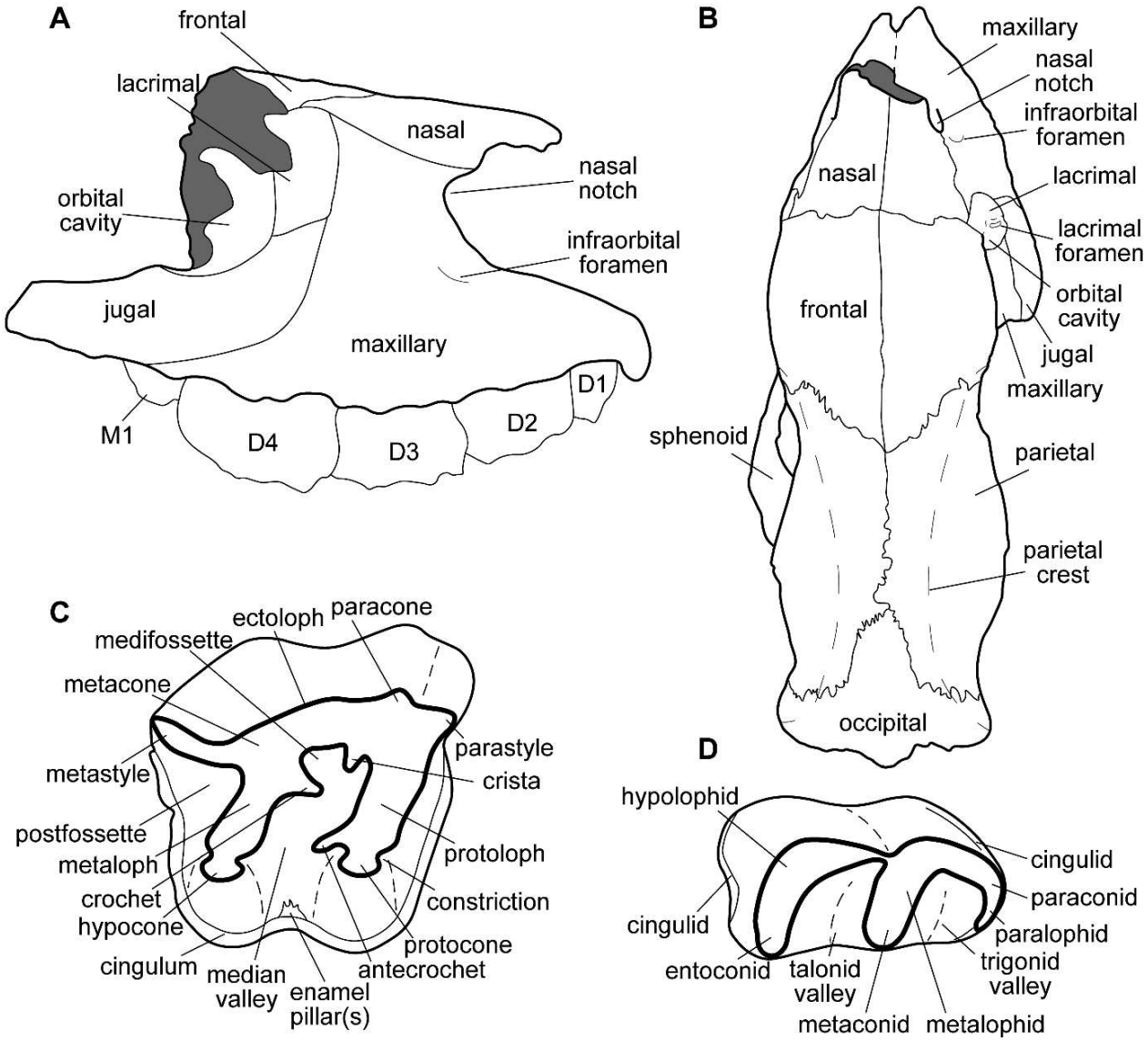


**Figure 2.** Anatomical nomenclature used in this study. **A.** Juvenile skull (MNHN.F.MAR3053) of *Chilotherium persiae* (Pohlig, 1885) from the Upper Miocene of Maragheh in Iran in lateral view; **B.** Juvenile skull (SMF M 3592) of *Chilotherium anderssoni* Ringström, 1924, from the Upper Miocene of Daijiagou in China in dorsal view; **C.** Upper molar; and **D.** Lower molar in occlusal view showing the anatomical nomenclature used in this study. Not to scale.

## Systematic palaeontology

**Class Mammalia Linnaeus, 1758**
**Order Perissodactyla Owen, 1848**
**Family Rhinocerotidae Gray, 1821**
**Subfamily Aceratheriinae Dollo, 1885**
**Subtribe Chilotheriina Qiu et al., 1987 (*sensu* Kampouridis et al. 2023b)**

**Genus *Chilotherium* Ringström, 1924**

**Type species.** *Chilotherium anderssoni* Ringström, 1924 from Daijiagou in Shanxi (China).

**Included species.** *Chilotherium persiae* (Pohlig, 1885), *Chilotherium habereri* (Schlosser, 1903), *Chilotherium schlosseri* (Weber, 1905), *Chilotherium kowalevskii* (Pavlow, 1913), '*Chilotherium*' *wimani* Ringström, 1924, *Chilotherium sarmaticum* Korotkevich, 1958, *Chilotherium xijangensis* (Ji et al., 1980), *Chilotherium orlovi* Bayshashov, 1982, '*Chilotherium*' *primigenium* Deng, 2006a, *Chilotherium licenti* Sun et al., 2018.

**Occurrence.** Upper Miocene deposits of Eurasia.

***Chilotherium persiae* (Pohlig, 1885)**
Figs 3–5

**Type material.** Pohlig (1885) originally erected this species based on a collection of four adult and one juvenile skull from Maragheh, but he did not mention where exactly these specimens are housed (Pohlig 1884a, 1884b, 1885, 1886); therefore, the type material was never properly defined. He mentioned that the material he collected himself in Maragheh (Iran) was sent to Halle (Germany)

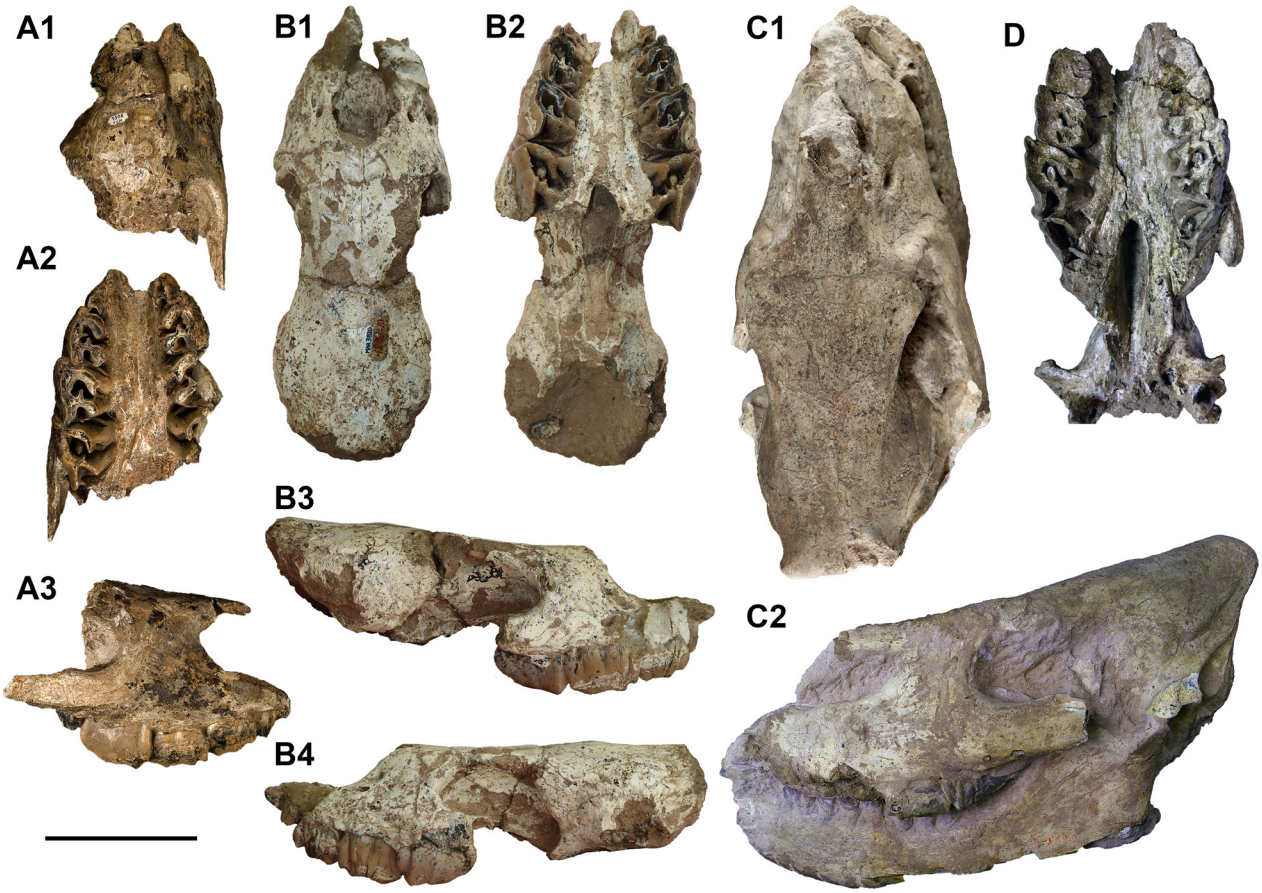


**Figure 3.** Juvenile skulls of *Chilotherium persiae* (Pohlig, 1885) from the Upper Miocene of Maragheh (Iran). MNHN.F.MAR3053 (**A**), MNHN.F.MAR3820 (**B**), MLU.GeoS.8030 (**C**), and NHMW-GEO-2020/0014/0093 (**D**) are juvenile skulls in dorsal (**A1**, **B1**, and **C1**), ventral (**A2**, **B2**, and **D**), and lateral (**A3**, **B3–4**, and **C2**) views. Scale bar: 10 cm.

(Pohlig 1886) and is now housed in the palaeontological collection of the MLU. However, Pohlig (1885, 1886) did not specify whether he collected the specimens he referred to as "*Rhinoceros persiae*" himself or saw them in another collection, such as the NHMW. Therefore, until further information becomes available, the type material cannot be determined with certainty, as already discussed by Kampouridis et al. (2025).

**Type locality.** Upper Miocene deposits of Maragheh (Iran); exact locality unknown

**Material.** An almost complete juvenile skull preserving D1–D4 with its associated mandible, preserving d2–d4 (MLU.GeoS.8030); a partial juvenile skull preserving part of the nasals and the frontals, and the maxillae, with D1–D4 (MNHN.F.MAR3053); a partial juvenile skull preserving the left D1–D4 and right D3–D4 (MNHN.F.MAR3078–3079); a partial juvenile skull preserving D2–D4 and M1, and its associated mandible, preserving the right d2–d4 and the left d3 (NHMW-GEO-2020/0014/0093); a partial juvenile skull preserving D2–D4 (MLU.GeoS.8028); a right maxilla preserving D1–D4 (MLU.GeoS.8029); a left juvenile maxilla preserving D2–D4 and M1 (NHMW-GEO-2020/0014/0034); a right maxilla preserving D1–D4 (NHMW-GEO-2020/0014/0030); a partial left maxilla preserving D1–D4 (MLU.GeoS.8025); a partial subadult skull preserving, on both sides, P2, P3, D4, M1, and M2, in addition to the left D1 (NHMW-GEO-2020/0014/0099); a partial juvenile skull preserving D1–D4 on both sides (NHMW-GEO-2020/0014/0006); a left partial maxilla preserving D2–D3 (NHMUK M 2006); eight isolated D4s (MLU.GeoS.8027, MLU.GeoS.8031, NHMW-GEO-2020/0014/0032, NHMW-GEO-2020/0014/0070, NHMW-GEO-2020/0014/0081, NHMW-GEO-2020/0014/0056, and NHMW-GEO-2020/0014/0067); a partial juvenile mandible preserving the left d2–d4 and the right d1–d4, with erupting m1 (MNHN.F.MAR3859); a partial juvenile mandible preserving d2–d4 and erupting m1 on both sides (NHMUK M 3916); a partial mandible preserving d2–d4 on both sides (NHMW-GEO-2020/0014/0033); a partial mandible preserving d2–d3 on both sides (MLU.GeoS.8034); a partial mandible preserving d3–d4 and m1 on both sides, in addition to the left d2 (NHMW-GEO-2020/0014/0100); a partial juvenile mandible preserving the right d2–d3 and m1, and the right d1 (MNHN.F.MAR3889); a left hemimandible preserving d4 and erupting m1 (MLU.GeoS.8031); a left hemimandible preserving d2–d4 (NHMUK M 3917); and a partial mandible preserving i2 and d1–d4 on both sides, in addition to the right i1 (NHMW-GEO-2020/0014/0037).

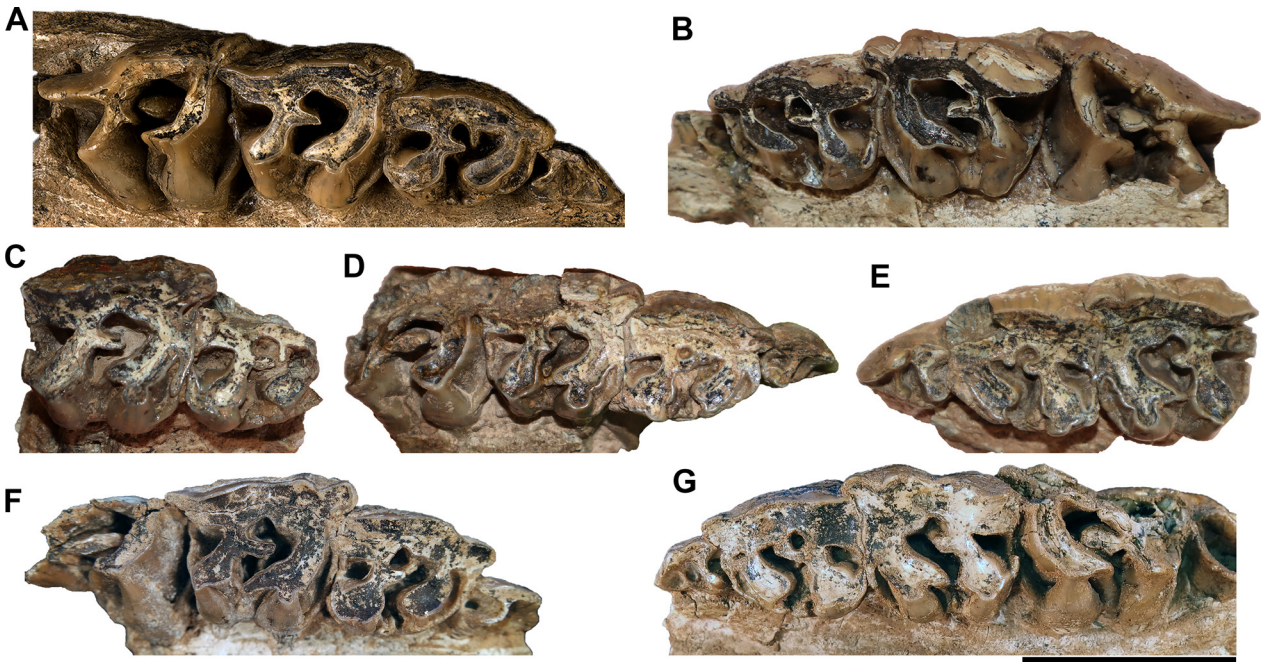


**Figure 4.** Upper deciduous dentition of *Chilotherium persiae* (Pohlig, 1885) from the Upper Miocene of Maragheh (Iran). **A.** MNHN.F.MAR3053 (right D1-D4); **B.** MNHN.F.MAR3820 (left D1-D4); **C.** MNHN.F.MAR3840 (right D2-D3); **D.** MNHN.F.MAR3841 (right D1-D4); **E.** MNHN.F.MAR3841 (left D1-D3); **F.** NHMW-GEO-2020/0014/0030 (right D1-D4); and **G.** NHMW-GEO-2020/0014/0006 (left D1-D4) in occlusal view. Scale bar: 5 cm.

**Description.** One almost complete and several partial juvenile skulls of *C. persiae* from the Upper Miocene of Maragheh (Iran) were studied (Fig. 3). The premaxillary bones are absent in all specimens. The nasals are thin, lack any pneumatisation, and share a long, central, prominent suture. In dorsal view, the suture between the nasals and the frontals is an almost straight mediolateral line. In lateral view, the suture between the nasals and the maxillary is relatively straight, starting from the nasal notch and ending at the lacrimal. The nasal notch is situated above the anterior portion of D3. In lateral view, the nasal and lacrimal also share a short suture, separating the maxillary from the frontal. The maxillary exhibits several infraorbital foramina on each side; their exact number cannot be assessed due to the state of preservation of the specimens. The maxillary is partially broken in most specimens, but the few preserved ones feature long, posteriorly projecting pockets for the unerupted molars (as seen in MLU.GeoS.8030, MNHN.F.MAR3078–3079, and NHMW-GEO-2020/0014/0099). The lacrimal is relatively small; it connects ventrally to the frontal and the nasal, anteriorly to the maxillary, and ventrally to the jugal. The jugal shares a wide suture with the maxillary. Immediately behind the orbit, it exhibits a well-developed postorbital process. In ventral view, the maxillary constitutes the largest portion of the palatine. Posteriorly, the maxillary is sutured to the palatinal; the latter reaches anteriorly to the level of the posterior edge of D3. The palatine forms the largest part of the choana. Two symmetrical foramina are present at the level of the posterior portion of D4, near the maxillary-palatinal suture.

Concerning the upper dentition (Fig. 4), several specimens preserve at least some teeth, and some skulls or maxillae preserve the complete deciduous series at least on one side (MLU.GeoS.8029, MLU.GeoS.8030, MNHN.F.MAR3053, MNHN.F.MAR3079, MNHN.F.MAR3820, MNHN.F.MAR3841, NHMW-GEO-2020/0014/0006, and NHMW-GEO-2020/0014/0030). D2 to D4 are hypsodont and highly molarised. D1 has an almost continuous lingual cingulum. The most prominent enamel fold is the metaloph, which separates a comparably large postfossette. No other enamel folds are visible within the tooth. The parastyle and metastyle are relatively well developed in comparison to the generally reduced D1. In specimen MNHN.F.MAR3820, D1 is barely starting to erupt, while D4 has already erupted, though it is not yet worn.

The morphology of D2 can be observed at different wear stages between the different specimens. D2 features a protocone that is somewhat smaller than the hypocone and bears a posterior constriction, forming an antecrochet; the latter does not bend lingually in most specimens. A discontinuous lingual cingulum is present. At the entrance of the median valley, a small enamel pillar is present, but its size varies slightly among the different specimens. In MNHN.F.MAR3079, the antecrochet features a very weak connection to the enamel pillar at the entrance of the median valley. The median valley remains open until the tooth is almost completely worn (as seen in MLU.GeoS.8029). Relatively strong crochet and crista are present; when heavily worn, they can connect to close off the medifossette in some specimens. Very strong anterior and posterior cingula are present, forming a small, closed-off prefossette and a

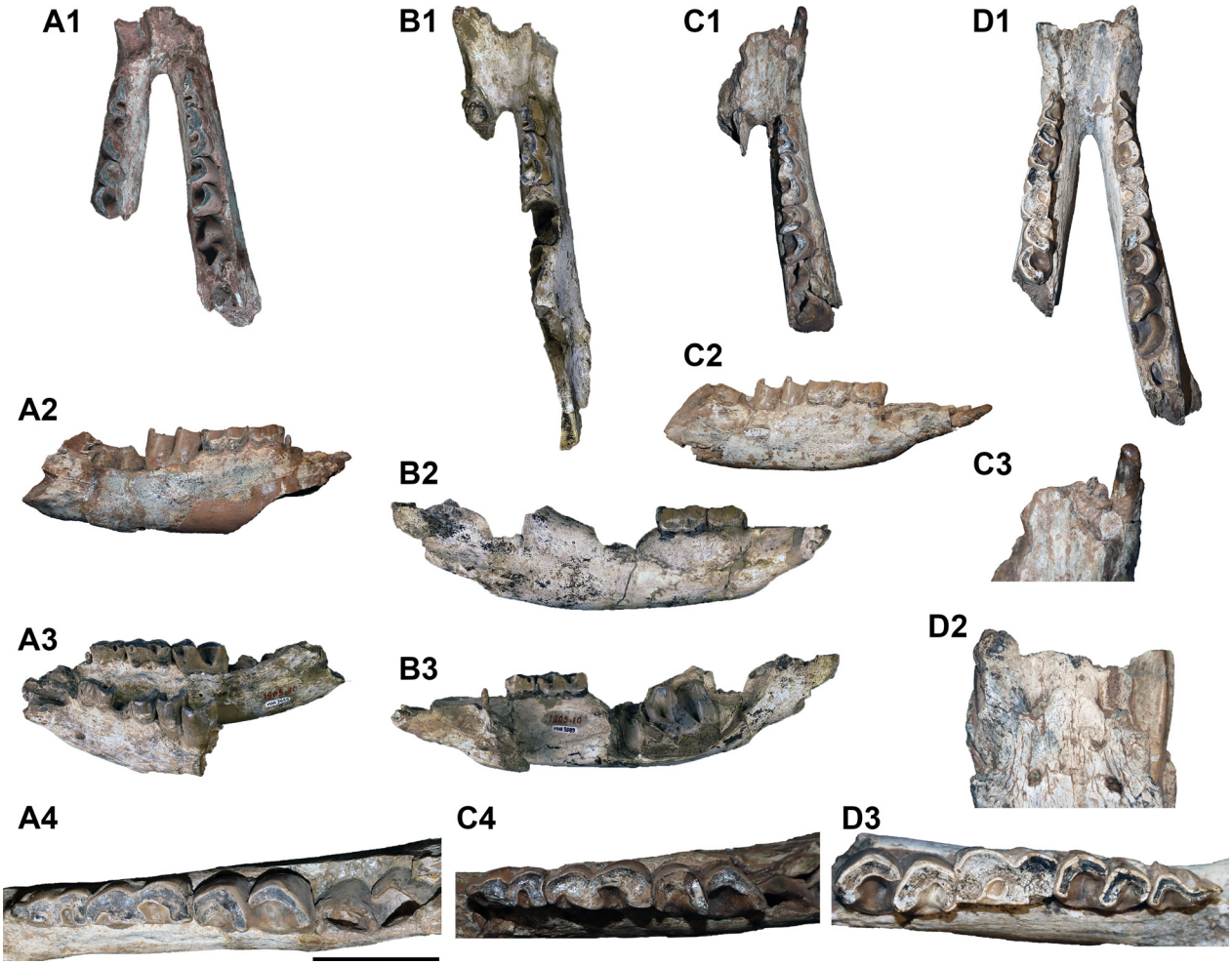


**Figure 5.** Juvenile mandibles of *Chilotherium persiae* (Pohlig, 1885) from the Upper Miocene of Maragheh (Iran). MNHN.F.MAR3859 (**A**), MNHN.F.MAR3889 (**B**), MNHN.F.MAR3069 (**C**), and MNHN.F.MAR (**D**) are juvenile mandibles in dorsal (**A1**, **B1**, **C1**, and **D1**), lateral (**A2–3**, **B2–3**, and **C2**), and occlusal (**A4**, **C4**, and **D4**) views. Detailed views of the anterior part of the mandibular symphysis in dorsal (**C3**) and ventral (**D2**) views are also given. Scale bar: 10 cm (**A1–3**, **B1–3**, **C1–2**, and **D1**); 5 cm (**A4**, **C3–4**, and **D2–3**).

wide postfossette. The parastyle and metastyle are wide, while the paracone and metacone folds are extremely weak and rounded.

In D3 and D4, the protocone is somewhat larger than the hypocone and bears strong anterior and posterior constrictions, forming an antecrochet that bends lingually in some specimens; the hypocone bears only an anterior constriction. The lingual cingulum is absent on both D3 and D4. At the entrance of the median valley, a small enamel pillar is present in some D3 specimens, such as MNHN.F.MAR3053, while it is absent in D4. A crochet is always present on D3 and D4. A small crista can be present on D3, as seen in NHMW-GEO-2020/0014/0093, where it fuses with the crochet and closes off the medifossette, but is absent in D4. Strong anterior and posterior cingula are present on both deciduous teeth, as well as a large postfossette. The parastyle and metastyle are well developed on both D3 and D4; the paracone fold is rather strong, while the mesostyle and metacone fold are weak. D4 is more hypsodont than D3. All D4s exhibit thin horizontal grooves on the lingual side at the base of the enamel and "ω"-shaped grooves on the buccal side in the middle of the enamel, which can be interpreted as hypoplasias (Mead 1999; Böhmer and Rössner 2018; Hullot and Antoine 2020).

Several juvenile mandibles of *C. persiae* from the Upper Miocene of Maragheh (Iran) are documented in the studied collections (Fig. 5). One specimen preserves the deciduous incisors on the right side of the symphysis (Fig. 5C3). The di1 is tiny, barely projecting from the bone, whereas di2 is much larger but still quite small, with a diameter of approximately 1 cm. Both di1 and di2 are elongated, with a round cross-section. In di1, no enamel is preserved, and in di2, the tooth crown is rounded and slightly asymmetrical. Some specimens preserve a very small, rudimentary d1, at least on one side (Fig. 5A2, A3, B3). When present, it is single-rooted and very short, and its crown has a single tip, without any distinct morphological features. The d2 is well formed; its paralophid is anteriorly oriented and bears a buccal constriction at the level of the anterior valley. The metalophid projects lingually, as does the hypolophid, and is relatively wide, with a lingual constriction. The anterior valley remains open until completely worn. The

posterior valley may form an extremely small fossettid before being completely worn down. A shallow ectolophid groove exists buccally. A relatively weak posterior cingulum is also visible. On the buccal and lingual sides, weak discontinuous cingula are present. In d3, the paralophid projects lingually, with its tip slightly curving posteriorly. A slight constriction in the metalophid can be observed. The ectolophid groove is relatively shallow but deeper than in d2. An anterior and a posterior cingulum are visible, with the anterior one extending towards the buccal side to some degree. In d4, the paralophid projects lingually and is smaller than the metalophid and hypolophid, which are similarly well developed. The trigonid and talonid are not yet connected due to wear. The ectolophid groove is deep and bears a small enamel pillar at its base. Anterior and posterior cingulids are present, and only the anterior one extends slightly to the buccal side. All d4s exhibit thin horizontal grooves in the enamel, clearly visible on the buccal side, which can be interpreted as hypoplasias (Mead 1999; Böhmer and Rössner 2018; Hullot and Antoine 2020).

### *Chilotherium habereri* (Schlosser, 1903)

Figs 6–8

**Lectotype.** A set of associated P3 and P4 (SNSB-BSPG 1900 XII 622), described and illustrated by Schlosser (1903, pl. 5, fig. 18) and designated as the lectotype of the species by Kampouridis et al. (2025).

**Type locality.** Upper Miocene red clay deposits in Shanxi Province (China); exact locality unknown

**Material.** A partial juvenile skull preserving, on both sides, parts of D3, D4, and erupting M1 (GPIT/MA/04830); an almost complete juvenile skull preserving, on the right side, D2–D4 and, on the left side, D1–D4 (GPIT/MA/04843); a partial juvenile skull preserving D1–D4 on both sides (GPIT/MA/04842); a partial subadult skull preserving the heavily worn D4s on both sides (GPIT/MA/04840); a subadult maxilla preserving the heavily worn D4 (GPIT/MA/04844); an almost unworn, complete D4 (GPIT/MA/04821); a D2 (GPIT/MA/04821); a D3 (GPIT/MA/04821); an almost complete subadult mandible preserving the left d4 (GPIT/MA/04826); a partial juvenile mandible preserving, on the right side, d1–d3 and erupting d4 and, on the left side, d2–d3 and erupting d4 (GPIT/MA/04849); a partial juvenile mandible preserving d2–d3 on both sides (GPIT/MA/04820); a partial right juvenile hemimandible preserving d2–d4 (GPIT/MA/04818); and a partial left juvenile hemimandible preserving part of d2 and the unworn d3 (GPIT/MA/04821).

**Remarks.** The Kutschwan material housed in the GPIT was studied more than a century ago by Hugo Killgus for his PhD (Killgus 1922). He attributed the chilothere material to *Aceratherium habereri* (Killgus 1922, 1923). Soon after, Ringström (1924) erected the genus *Chilotherium* and included this species in it after he revised it. Ringström (1924) also agreed with Killgus (1922, 1923) in referring the Kutschwan chilothere to the species *Chilotherium habereri*. This identification was also supported by Kampouridis et al. (2025).

**Description.** Three partial juvenile skulls preserving most of the deciduous teeth (Fig. 6), along with one subadult skull and a partial subadult maxilla preserving the D4s with the permanent dentition of *C. habereri*, are present in the material from the Upper Miocene of Kutschwan (China) housed in the GPIT. The premaxillary bones are absent in all specimens. In specimen GPIT/MA/04842, the suture between the premaxillary and maxillary bones seems to start approximately above D1. In one specimen (GPIT/MA/04830), the nasals are completely broken off, while, in the other two specimens, part of the nasals is still preserved, showing that they are thin, lack any pneumatisation, and share a long, prominent suture. In dorsal view, the suture between the nasals and the frontals is an almost straight mediolateral line (Fig. 6B1, C1). The frontals are flat and seem quite porous in the younger two specimens (GPIT/MA/04843 and GPIT/MA/04842), whereas, in the somewhat older skull (GPIT/MA/04830), they are massive and bear a slight depression, resembling those of adult individuals (Fig. 6A1, B1, C1). In specimen GPIT/MA/04830, the parietal crests are very weak but widely separated, with the minimum preserved distance being 55 mm.

In lateral view, the suture between the nasals and the maxillary is relatively straight, starting from the nasal notch and ending at the lacrimal (Fig. 6A3, B4, C4). The nasal notch is situated above the middle portion of D3 in the younger specimens (GPIT/MA/04843 and GPIT/MA/04842) and above the anterior portion of D4 in the slightly more mature individual (GPIT/MA/04830). In lateral view, the nasal and lacrimal also share a short suture, separating the maxillary from the frontal. Immediately behind the orbit, at the widest part of the dorsal side of the cranium, a well-developed postorbital process is present in the frontal. From there, the frontal-parietal crests reach the nuchal crest. The maxillary exhibits several infraorbital foramina, which can vary significantly, even in the same individual, from three to up to six foramina of variable size. The intraspecific variability of this feature has also been mentioned in previous works (e.g. Ringström 1924, p. 29). Posteriorly, the maxillary features long pockets, which include the unerupted molars. The size and length of these pockets seem to depend strongly on the ontogenetic stage of the individual, as they vary in the three specimens: from more than 50 mm in the youngest individual (GPIT/MA/04842: unworn D4) to 85 mm in the slightly more mature individual (GPIT/MA/04843: slightly worn D4) to 99 mm in the oldest individual (GPIT/MA/04830: moderately worn D4). The lacrimal is relatively small, and it connects ventrally to the frontal and the nasal, anteriorly to the maxillary, and ventrally to the jugal. The jugal shares a wide suture with the maxillary. Immediately behind the orbit, the jugal exhibits a less prominent postorbital

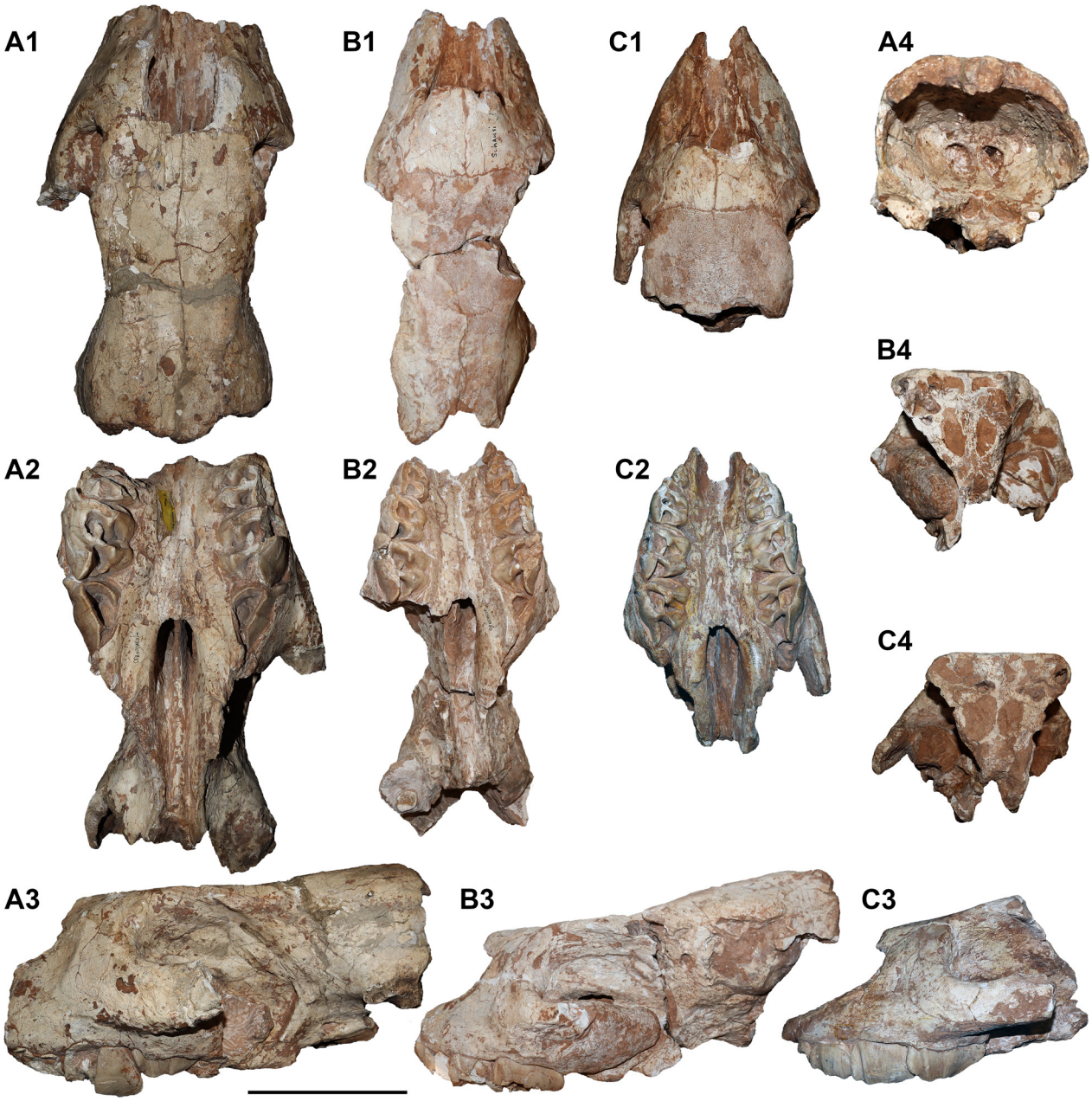


**Figure 6.** Juvenile skulls of *Chilotherium habereri* (Schlosser, 1903) from the Upper Miocene of Kutschwan (China). GPIT/MA/04830 (**A**), GPIT/MA/04843 (**B**), and GPIT/MA/04842 (**C**) are juvenile skulls in dorsal (**A1**, **B1**, and **C1**), ventral (**A2**, **B2**, and **C2**), lateral (**A3**, **B3**, and **C3**), and caudal (**A4**, **B4**, and **C4**) views. Scale bar: 10 cm.

process compared to the slightly more posteriorly positioned postorbital process on the frontals. The squamosal shares a suture with the jugal, starting at the postorbital process. In specimen GPIT/MA/04830, the posterior portion of the squamosal is sutured to the parietal. The zygomatic arch, along with the post-tympanic and paroccipital processes, is broken off.

In lateral view, one of the most prominent parts is the orbital cavity, which is placed very high dorsally, creating a thin dorsal orbital rim (Fig. 6A3, B4, C4). The anterior portion of the orbital cavity is formed by the frontal, lacrimal, and jugal bones. The lacrimal bone bears two small lacrimal foramina, although in specimen GPIT/MA/04843, only one lacrimal foramen is present on each side. A distinct lacrimal process is not present. The maxillary foramen is visible at the anteroventral portion of the lacrimal-maxillary suture. The sphenopalatine foramen is present at the ventral limit within the orbital cavity. The optic foramen is located posteriorly to the postorbital process, above the posterior edge of the maxillary pocket. In the more complete skull specimen GPIT/MA/04830, the sphenorbital and rotundum foramina are fused and located posteroventrally to the optic foramen, immediately behind the posterior end of the maxillary pocket. In the same specimen, a well-formed caudal alar foramen is visible on the lateral side of the sphenoid bone, immediately behind the large fused sphenorbital and rotundum foramen. Inside the orbital cavity, the sutures for the palatine and sphenoid are not distinguishable, even at this early ontogenetic stage.

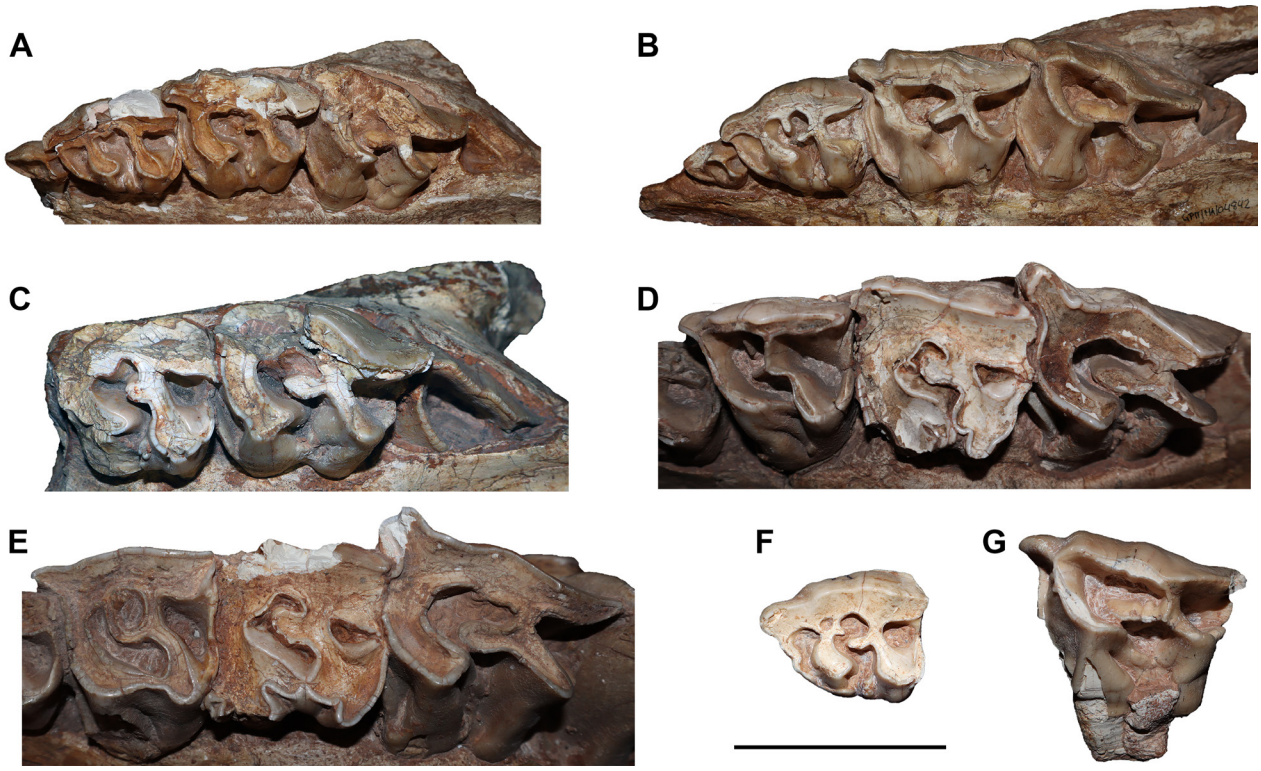


**Figure 7.** Upper deciduous dentition of *Chilotherium habereri* (Schlosser, 1903) from the Upper Miocene of Kutschwan (China). **A.** GPIT/MA/04843 (left D1–D4); **B.** GPIT/MA/04842 (left D1–D4); **C.** GPIT/MA/04830 (left D3–D4, erupting M1); **D.** GPIT/MA/04840 (left P3, D4, and M1); **E.** GPIT/MA/04844 (P3, D4, and M1); **F.** GPIT/MA/04821 (left D2); and **G.** GPIT/MA/04817 (left D4) in occlusal view. Scale bar: 5 cm.

In ventral view, the maxillary constitutes the largest portion of the palate. The anterior edge of the maxillary-palatine suture reaches the level of the posterior end of D3 (Fig. 6A2, B2, C2). The palatine forms the largest part of the choana. Two symmetrical foramina are present at the maxillary-palatine suture, at the level of the posterior portion of D4. In posterior view, all specimens are damaged and expose features of the endocranium. Specimens GPIT/MA/04843 and GPIT/MA/04842 are broken in the middle of the frontal bones, thus revealing several small cavities inside the skull, which are at least partially separated by thin bone layers. They represent the frontal sinuses, which have also been described for *Chilotherium* by Edinger (1937). In these specimens, there seem to be several rather small extensions of the frontal sinus. It is possible that, when complete, they were all connected, as also described by Edinger (1937) for *C. anderssoni*.

The upper dental material of *C. habereri* comprises the dentition of three partial juvenile skulls, two subadult skulls, and three isolated teeth (Fig. 7). In two partial skulls (GPIT/MA/04843 and GPIT/MA/04842), D1 is preserved and almost unworn. In specimen GPIT/MA/04842, D1 starts being worn before the eruption of D4. D2 to D4 are hypsodont and highly molarised. The morphology and dimensions of D1 are identical in both specimens. It has a single, large root and an almost continuous lingual cingulum. The most prominent enamel fold is the metaloph, which separates a comparably large postfossette. A relatively weak enamel fold in the middle of the tooth probably corresponds to the protocone. The parastyle and metastyle are relatively well developed compared to the generally reduced D1. The maximum height of the tooth crown is 18 mm.

D2 is preserved in the two younger skulls (GPIT/MA/04843 and GPIT/MA/04842). Additionally, one isolated left D2 (GPIT/MA/04821) is present in the studied collection. In all teeth, the protocone is smaller than the hypocone and bears a posterior constriction forming a short antecrochet. A small anterior constriction is present in the hypocone in GPIT/MA/04843. A slightly variable, discontinuous lingual cingulum is present in all teeth, in addition to an enamel pillar at the entrance of the median valley. The protoloph and metaloph are relatively thin. In GPIT/MA/04842 and GPIT/MA/04821, D2 bears a relatively strong crochet and crista, whereas, in GPIT/MA/04843, only a slight enamel bump is present instead of a crista. In GPIT/MA/04821, the crista connects to the protoloph, closing off a small fossette, and a secondary fold splits off from the crista. Strong anterior and posterior cingula are present, forming large pre- and postfossettes. Both cingula continue slightly onto the ectoloph. The parastyle and metastyle are very large. Weak paracone and metacone folds are present only in GPIT/MA/04821.

D3 is preserved in all three partial skulls, and an isolated lingual portion of a D3 (GPIT/MA/04821) is also present in the Kutschwan collection. In all specimens, the protocone is somewhat larger than the hypocone and

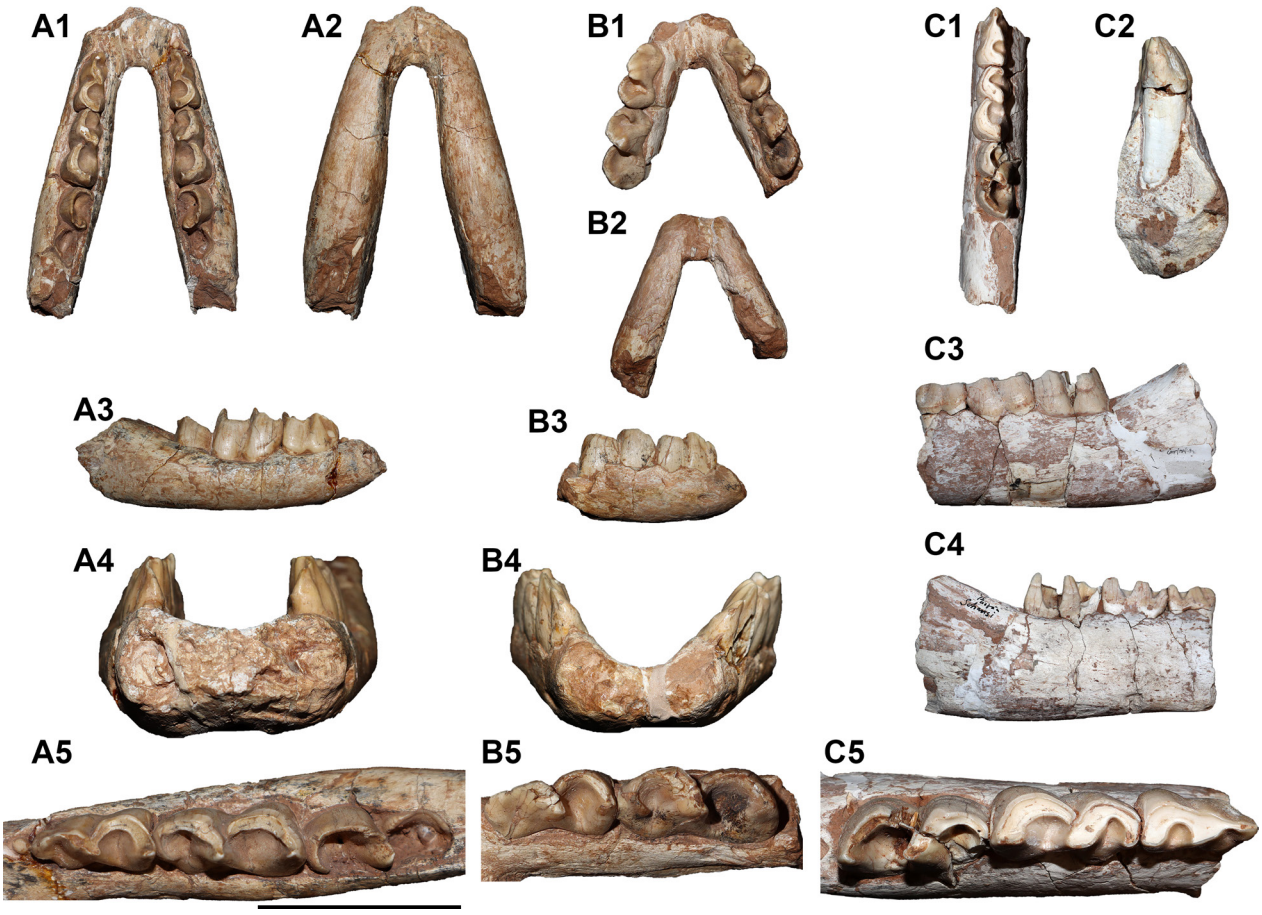


**Figure 8.** Juvenile mandibles of *Chilotherium habereri* (Schlosser, 1903) from the Upper Miocene of Kutschwan (China). GPIT/MA/04849 (**A**), GPIT/MA/4820 (**B**), and GPIT/MA/4818 (**C**) are juvenile mandibles in dorsal, ventral, lateral, anterior, and occlusal views. Scale bar: 10 cm (**A1–3**, **B1–3**, **C1**, and **C3–4**); 5 cm (**A4–5**, **B4–5**, **C2**, and **C5**).

bears a slight anterior and a strong posterior constriction, forming an antecrochet. The lingual cingulum is absent. At the entrance of the median valley, a small to prominent enamel pillar is present in all specimens. A crochet is always present, though its size may vary. A small crista is present in two specimens (GPIT/MA/04821 and GPIT/MA/04830). In GPIT/MA/04843, the crista is represented by a small enamel bump, whereas, in GPIT/MA/04842, it is completely missing. Strong anterior and posterior cingula are present, forming a short prefossette and a large postfossette. The parastyle and metastyle are well developed. The paracone fold is strong in the specimens where it is not broken off (GPIT/MA/04843 and GPIT/MA/04842), whereas the metacone fold is weak.

D4 is preserved in all partial skulls, and an isolated D4 (GPIT/MA/04821) is also present in the Kutschwan collection. The morphology of D4 resembles that of D3, but it is more hypsodont, and the antecrochet is more prominent and bends lingually. A large crochet is always present, but no crista is visible in any of the specimens. A strong anterior cingulum is present, and a strong posterior cingulum forms a wide postfossette. The parastyle is well developed, and the metastyle is large. The paracone fold is present in all specimens, along with a weak metacone fold. All D4s exhibit thin horizontal grooves in the lower part of the enamel on the lingual side of the tooth and "ω"-shaped grooves in the middle of the ectoloph, which are interpreted as hypoplasias (Mead 1999; Böhmer and Rössner 2018; Hullot and Antoine 2020). Below these enamel defects, the enamel becomes rougher and more irregular. The D4 of GPIT/MA/04842 also exhibits small pits in the enamel, slightly above the groove, which can also be interpreted as hypoplasias, whereas the D4 of GPIT/MA/04843 bears such small pits directly on the horizontal groove. Interestingly, in both specimens, the pits are present only on the protocone. Additionally, the D4 of GPIT/MA/04843 also features a second hypoplasia in the middle of the enamel, approximately 8 mm above the first one.

Four partially preserved mandibles (GPIT/MA/04849, GPIT/MA/04818, GPIT/MA/04820, and GPIT/MA/04821) are available in the Kutschwan collection of the GPIT (Fig. 8). Specimen GPIT/MA/04849 preserves an extremely small and short rudimentary d1 on its right hemimandible. It is single-rooted, and its crown is rounded, approximately 4 mm in diameter and only a few millimetres tall, without any morphological features. The d2 is well developed in all specimens. Its paralophid is anteriorly oriented and bears a buccal constriction, opposite to the anterior valley. The metalophid projects

lingually, as does the hypolophid, and is relatively wide, with a lingual constriction. Both the anterior and posterior valleys remain open until completely worn. A shallow ectolophid groove exists buccally. A relatively weak posterior cingulum is visible. No anterior, lingual, or buccal cingula exist in any d2 studied. In d3, the paralophid projects lingually, and its tip is slightly posteriorly curved. The paralophid is less developed than the metalophid and hypolophid. A slight constriction in the metalophid can be observed in all specimens except GPIT/MA/04818 due to its more advanced wear stage. The hypolophid also bears a slight anterior constriction. Both the anterior and posterior valleys remain open until completely worn. In only two specimens (GPIT/MA/04818 and GPIT/MA/04820), it is possible to observe an extremely small fossettid that might form immediately before being completely worn down. The ectolophid groove is relatively shallow but deeper than in d2. Anterior and posterior cingulids are visible, whereas lingual or buccal cingulids are absent. The d4 is preserved only in three specimens (GPIT/MA/04818, GPIT-PV115054, and GPIT/MA/04826); in GPIT/MA/04826, d4 is the only remaining deciduous tooth, next to permanent teeth. The paralophid is larger than in d3 but still smaller than the metalophid and hypolophid, which are similarly well developed. Both the metalophid and hypolophid exhibit a weak anterior constriction. At the base of the posterior valley, a small enamel pillar is present. The ectolophid groove is deep. Anterior and posterior cingulids are present, but they do not continue on the buccal or lingual sides. All d4s exhibit thin horizontal grooves in the enamel, best visible on the buccal side, which can be interpreted as hypoplasias (Mead 1999; Böhmer and Rössner 2018; Hullot and Antoine 2020).

### *Chilotherium schlosseri* (Weber, 1905)

Figs 9–11

**Neotype.** A well-preserved skull (GPIH 3015) with an associated mandible (GPIH 3015a), designated by Kampouridis et al. (2023b).

**Type locality.** Upper Miocene deposits of Samos Island (Greece); exact locality unknown.

**Material.** An almost complete juvenile skull preserving D1–D4 and M1 on both sides (NHMW-GEO-2009z0088/0001); a partial juvenile skull preserving the maxillary with D1–D4 on both sides (SMNS 47913); a partial juvenile skull preserving only the maxillary, which bears D2–D4 on both sides (SMNS 47914); an isolated D1 (MGL 106691); two isolated D2s (GMM 570 and MGL 107103); a partial mandible preserving the right i2, p2, p3, d4, m1, and m2 and the left i2, p3, d4, m1, and m2 (NHMW-GEO-1911/0005/0033); a partial mandible preserving the right d1–d4, erupting m1, the left d2–d4, and erupting m1 (SMF M 6814); a partial mandible preserving the right p2, d3–d4, erupting m1, the left p2, d3–d4, and erupting m1 (SMF M 6815); and a partial juvenile mandible preserving d2–m1 on both sides, while the i2s are erupting (GMM 593).

**Description.** One almost complete (NHMW-GEO-2009z0088/0001) and one partial juvenile skull (SMNS 47913), along with some partial maxillae of *C. schlosseri*, exist in the studied material from the Upper Miocene of Samos in Greece (Fig. 9). The premaxillary bones are broken off in all specimens. In dorsal view, the suture between the nasals and the frontals is a relatively straight mediolateral line at the level of the anterior edge of the orbit. The suture between the two frontals is a straight line, when present, and the bones seem quite porous in comparison to the more massive nasals. In the youngest partial skull (SMNS 47913), no frontal-parietal crests are visible. In the ontogenetically older NHMW-GEO-2009z0088/0001, the frontal-parietal crests are well formed and already widely separated (minimum distance = 64 mm). The frontal-parietal suture forms a 50° angle to the frontal suture. Posteriorly, the frontal suture merges with the suture between the parietals.

In lateral view, the suture between the nasals and the maxillary is relatively straight, starting from the nasal notch and ending at the lacrimal. The position of the nasal notch slightly varies in the three available *C. schlosseri* specimens. In the youngest specimen (SMNS 47914), the nasal notch reaches the level of the contact between D2 and D3, whereas, in the slightly more mature SMNS 47913, it reaches the level of mid-D3. In the ontogenetically oldest specimen (NHMW-GEO-2009z0088/0001), the nasal notch reaches the level of the contact with D3 and D4. In lateral view, the nasal and lacrimal share a short suture, thus separating the maxillary from the frontal. Immediately behind the orbit, the beginning of the postorbital process on the frontal is visible in SMNS 47914. The maxillary and lacrimal are positioned below the nasals and frontals. The maxillary exhibits several infraorbital foramina, which can vary significantly, even in the same individual, from three to up to four foramina of variable size. Posteriorly, the maxillae extend into pockets, which house the unerupted molars. The lacrimal is relatively small, and it connects dorsally to the frontal and nasal, anteriorly to the maxillary, and ventrally to the jugal. The jugal shares a wide suture with the maxillary. The zygomatic arches are not preserved on any of the specimens. In lateral view, one of the most prominent parts is the orbital cavity, which is placed very high dorsally and has a thin dorsal margin. In ventral view, the maxillary constitutes the largest portion of the palatine. Posteriorly, the maxilla is sutured to the palatine. The palatine forms the anterior part of the choana, and two symmetrical foramina are placed near the maxillary-palatinal suture, at the posterior portion of D4.

The upper dental material of *C. schlosseri* can be studied based on a number of complete or partial deciduous tooth rows and some isolated teeth (Fig. 10). The D1s in SMNS 47913 are not fully erupted, as they are placed well below the occlusal level of the other teeth (Fig. 9B3, B4, 9C). Thus, D1 seems to finalise

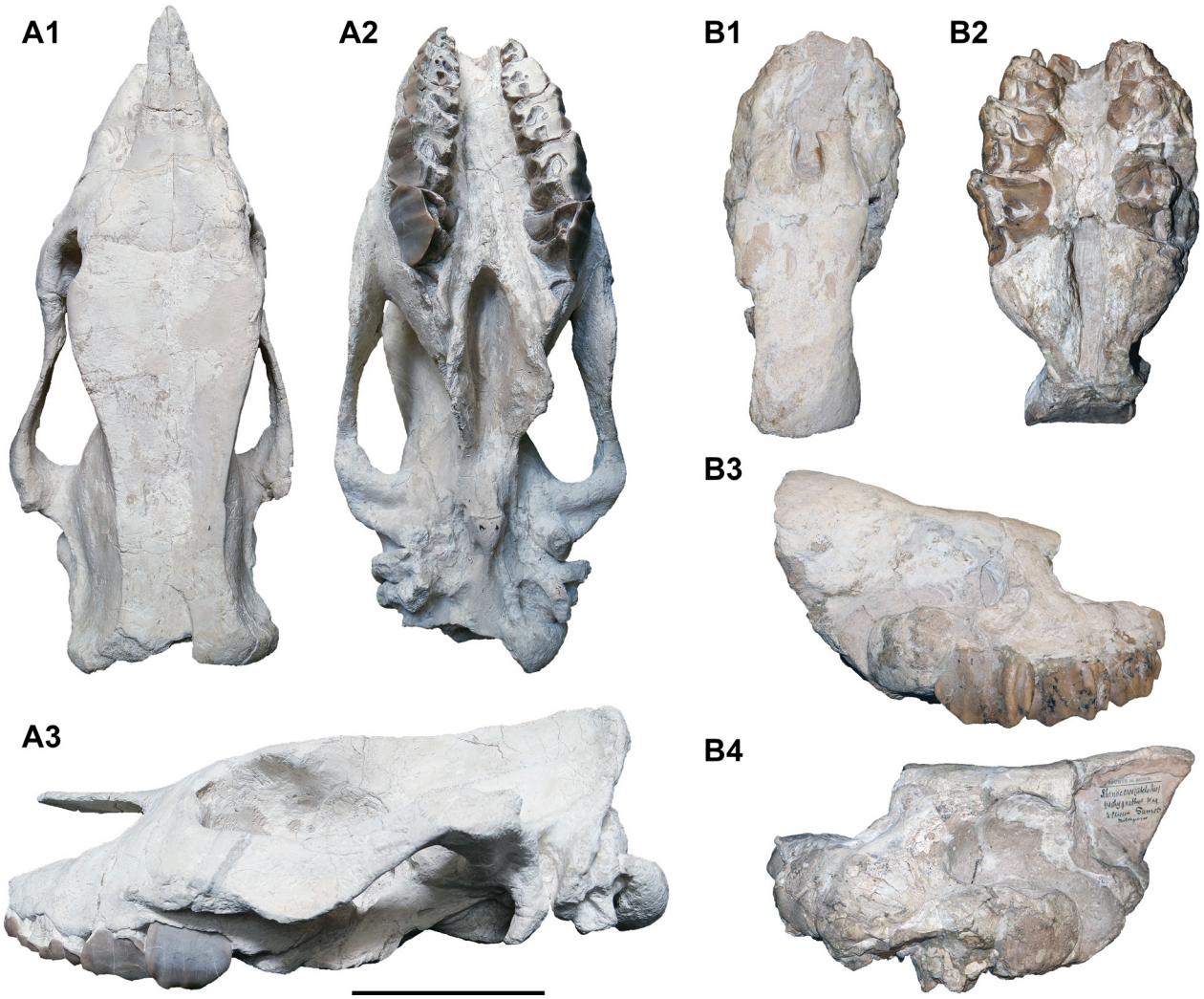


**Figure 9.** Juvenile skulls of *Chilotherium schlosseri* (Weber, 1905) from the Upper Miocene of Samos Island (Greece). NHMW-GEO-2009z0088/0001 (**A**) and SMNS 47913 (**B**) in dorsal (**A1** and **B1**), ventral (**A2** and **B2**), and lateral (**A3** and **B3–4**) views. Scale bar: 10 cm.

its eruption and start being worn after D4. The root of the tooth in this specimen is not yet formed, also demonstrating the early developmental stage of D1 in SMNS 47913. A continuous lingual cingulum is present, which continues on the posterior side of the tooth, becoming stronger and extremely high. The most prominent enamel fold is probably the metaloph, separating a large postfossette. Another weaker enamel fold in the middle of the tooth probably corresponds to the protoloph. The protocone and metacone seem to be connected to some degree lingually. The parastyle and metastyle are relatively well developed in comparison to the generally reduced D1.

Concerning the other deciduous premolars, D2 to D4 are hypsodont and highly molarised. In D2, the protocone is slightly smaller than the hypocone and bears a posterior and very weak anterior constriction, forming a short antecrochet. A small anterior constriction is present in the hypocone. An enamel pillar is present at the entrance of the median valley in all specimens. A very strong, continuous lingual cingulum is also present in all specimens except SMF M 6805 and NHMW-GEO-2009z0088/0001. The protoloph and metaloph are relatively thin, and a closed medifossette is always present. In all specimens that are adequately worn, a secondary fold splits off the crista and connects to the protoloph, creating a prominent fossette anterior to the medifossette. Very strong anterior and posterior cingula are present, forming large pre- and postfossettes. Both cingula continue slightly onto the ectoloph, even forming an extremely weak buccal cingulum in SMNS 47913. The parastyle and metastyle are very large. Weak paracone and metacone folds are present. All three specimens bear some enamel plications in the median valley. They are most prominent in the medifossette of the left D2 of SMNS 47913, where five small plications are visible.

In D3, the protocone and hypocone are of comparable size. The protocone bears strong anterior and posterior constrictions, forming an antecrochet. The hypocone is weakly constricted anteriorly. An almost continuous lingual cingulum is present in many specimens, although it is very weak in NHMW-GEO-2009z0088/0001 and

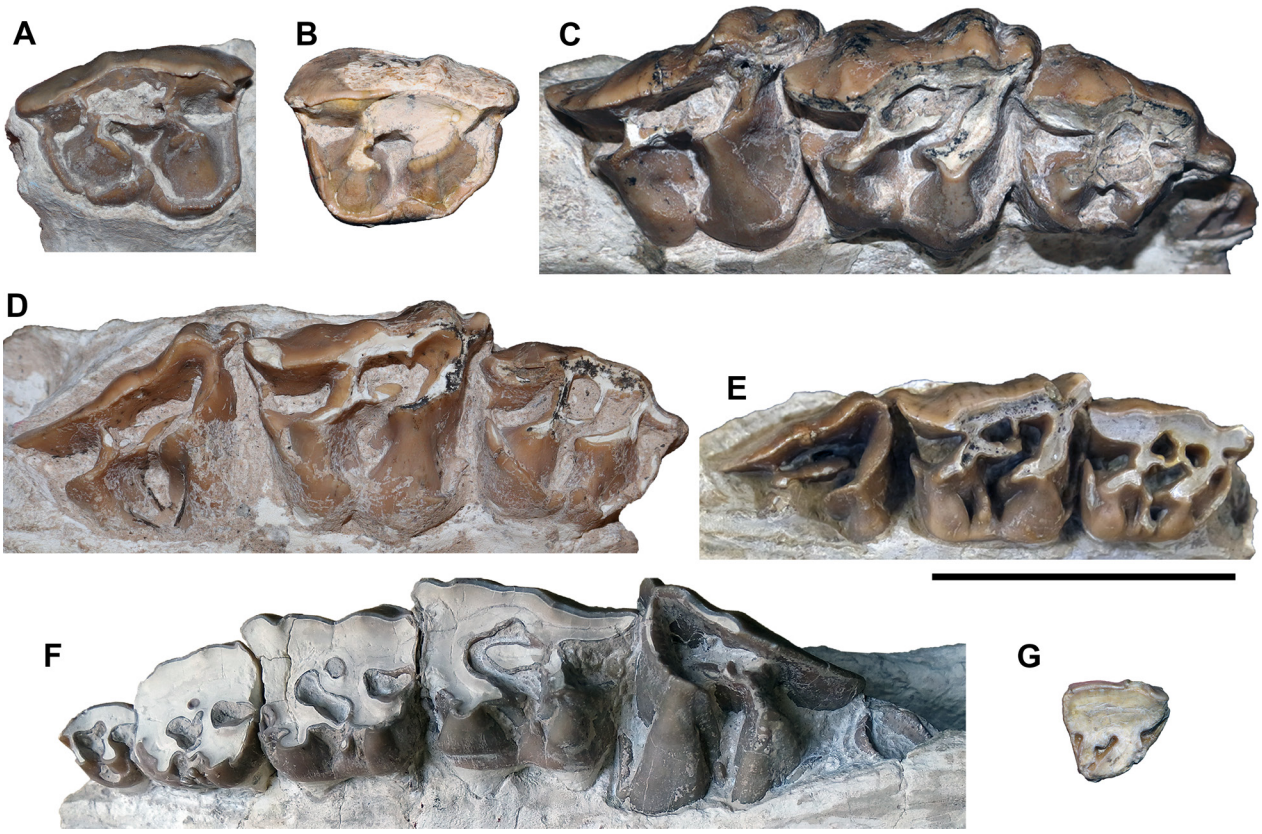


**Figure 10.** Upper deciduous dentition of *Chilotherium schlosseri* (Weber, 1905) from the Upper Miocene of Samos Island (Greece). **A.** GMM 570 (left D2); **B.** MGL 107103 (right D2); **C.** SMNS 47913 (right D1–D4); **D.** SMNS 47913 (right D1–D4); **E.** SMF M 6805 (right D2–D4); **F.** NHMW-GEO-2009z0088/0001 (left D1–D4, M1); and **G.** MGL 106691 (right D1) in occlusal view. Scale bar: 5 cm.

absent in SMF M 6805. At the entrance of the median valley, a small enamel pillar is present in all specimens. A well-developed crochet is always present. A small crista is present in all specimens, varying in size and shape. Strong anterior and posterior cingula are present, forming a large postfossette. The parastyle and metastyle are well developed. The paracone fold is strong, the mesostyle is extremely weak, and the metacone fold is faintly visible.

D4 has a similar morphology to D3, although the protocone is somewhat larger than the hypocone. The protocone bears strong anterior and posterior constrictions, forming a prominent antecrochet. The hypocone bears only an anterior constriction. A slight, discontinuous lingual cingulum is present in some D4 specimens. A large crochet is always present, but the crista is lacking in all specimens, although a very weak enamel bump might be present instead. A strong anterior cingulum is present, and a strong posterior cingulum forms a wide postfossette. The parastyle is well developed and the metastyle large. The paracone fold is well developed, a slight mesostyle is present, and a weak metacone fold is faintly visible. All D4s exhibit thin horizontal grooves at the base of the crown on the lingual and buccal sides of the enamel, which can be interpreted as hypoplasias (Mead 1999; Böhmer and Rössner 2018; Hullot and Antoine 2020).

Branching furrows are visible on the teeth of three specimens (MGL 107103, SMNS 47913, and SMNS 47914). The traces occur as a branched network of shallow, bleached furrows, covering large parts of the teeth of SMNS 47913 and SMNS 47914 (Fig. 10C, D) and almost the whole ectoloph of MGL 107103 (Fig. 10B). The concentration of these furrows varies significantly. Some areas are only sporadically covered with a few furrows, while in other areas, the furrows cover the surface of the enamel so densely that a continuous, bleached area is produced. These branching furrows represent root etching, which is commonly observed in extant and fossil bones and usually takes the form of irregular furrows, indicating that the bones were altered by plant growth (Behrensmeyer 1978; Andrews and Cook 1985; Fisher 1995; Montalvo 2002; Bader et al. 2009). Humic acids – produced by the plant roots to extract nutrients from the substrate – cause shallow depressions and bleaching of the bone (Behrensmeyer 1978; Morlan 1980), which can result in the pattern seen on the enamel of the studied teeth.

Four juvenile *C. schlosseri* mandibles from Samos in Greece (Fig. 11) were studied. One of them, GMM 593, was published by Andree (1921, pl. 2, figs 4, 5) and originally referred to as *Aceratherium wegneri*?, a junior synonym of *C. schlosseri* (Kampouridis et

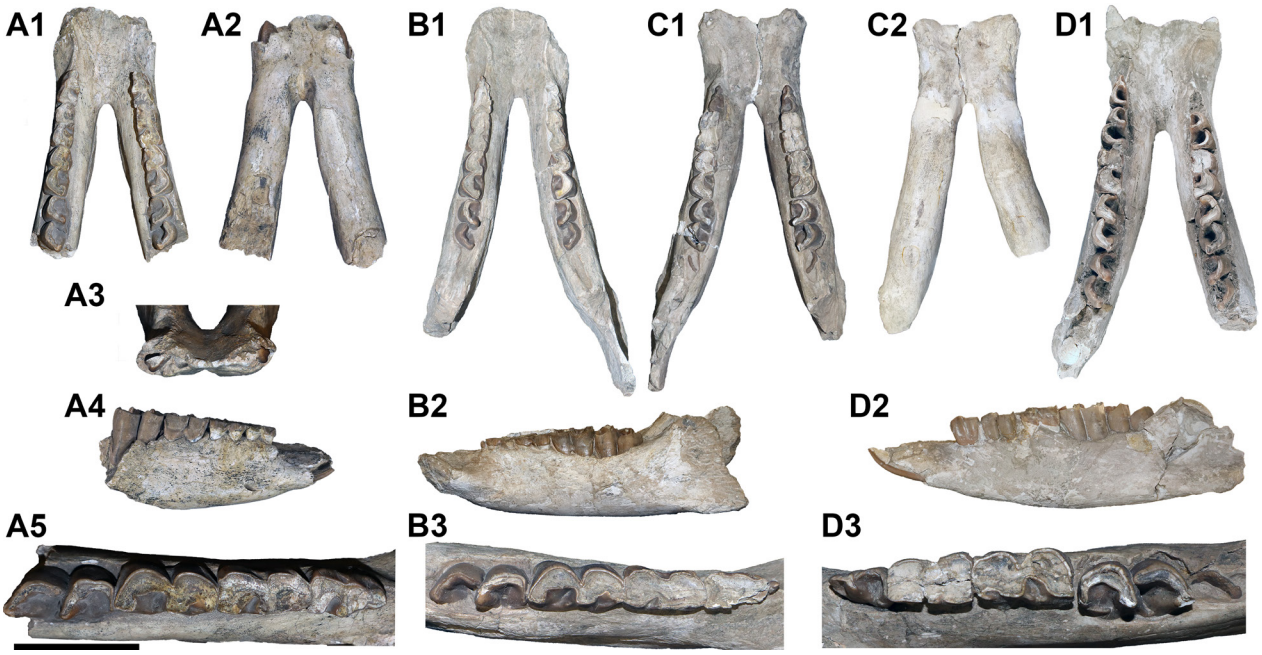


**Figure 11.** Juvenile mandibles of *Chilotherium schlosseri* (Weber, 1905) from the Upper Miocene of Samos Island (Greece). GMM 593 (**A**), SMF M 6814 (**B**), SMF M 6815 (**C**), and NHMW-GEO-1911/0005/0033 (**D**) in dorsal (**A1**, **B1**, **C1**, and **D1**), ventral (**A2** and **C2**), anterior (**A3**), lateral (**A4**, **B2**, and **D2**), and occlusal (**A5**, **B3**, and **D3**) views. Scale bar: 10 cm (**A1–4**, **B1–2**, **C1–2**, and **D1–2**); 5 cm (**A5**, **B3**, and **D3**).

al. 2022b; Svorligkou et al. 2025). Three additional mandibles are preserved in the studied collections (NHMW-GEO-1911/0005/0033, SMF M 6814, and SMF M 6815). Only one of these specimens, SMF M 6814, preserves the left d1. This tooth is extremely small and has a single, rounded tip that is approximately 6 mm in diameter and 10 mm in height. The d2 is preserved in only two specimens (GMM 593 and SMF M 6814) but is heavily worn in both, with the trigonid and talonid widely connected. The paralophid is constricted and anteriorly oriented. The metalophid projects lingually and slightly distally. The hypolophid projects lingually and is slightly wider than the metalophid. Both anterior and posterior valleys remain open until completely worn. A shallow ectolophid groove exists buccally. A slightly discontinuous buccal cingulum is visible, and it is probably connected to the anterior and posterior cingula, which are not preserved due to wear. The preserved d3s are quite worn down in all specimens, and a wide connection between the trigonid and talonid has been established. The paralophid is less developed than the metalophid and hypolophid. A weak constriction in the metalophid is visible in GMM 593, though only faintly, due to heavy wear. Both the anterior and posterior valleys remain open until completely worn in GMM 593; while in SMF M 6814, the anterior valley is already completely worn off, a small remnant of the posterior valley is still present. In SMF M 6815, both the anterior and posterior valleys are already worn off. The ectolophid groove is relatively shallow but deeper than in d2. A discontinuous cingulid is visible in buccal view, and a very small discontinuous cingulid is also visible lingually at the entrance of the anterior valley. The d4 is moderately to heavily worn in the studied specimens. A narrow connection between the trigonid and talonid is established in the ontogenetically youngest specimens, GMM 593 and SMF M 6814. In NHMW-GEO-1911/0005/0033 and SMF M 6815, the connection between the trigonid and talonid is somewhat wider. The paralophid is relatively short, whereas the metalophid and hypolophid are similarly well developed. In GMM 593, the paralophid of the right d4 exhibits a small distal projection, which is not visible on any other d4. The hypolophid exhibits an anterior constriction in GMM 593 and SMF M 6814. The anterior valley is quite small, whereas the posterior one was probably larger. The anterior valley probably would close shortly before being completely worn due to a small cingulid being present at its entrance in most d4s. The ectolophid groove is deep, and a small enamel pillar is located at its base in all four specimens. High anterior and posterior cingulids are present; they continue faintly on the buccal side and less so on the lingual side.

### *Chilotherium anderssoni* Ringström, 1924

Fig. 12

**Type material.** The species was erected based on a number of cranial and postcranial elements, without the designation of a holotype (Ringström 1924). Therefore, all material referred by Ringström (1924) to *Chilotherium anderssoni* represents the syntype, including the specimens described herein.

**Type locality.** Upper Miocene deposits of Daijiagou in Shanxi Province (China), also referred to as “Lok. 30” (Ringström 1924) of the Lagrelius Collection.

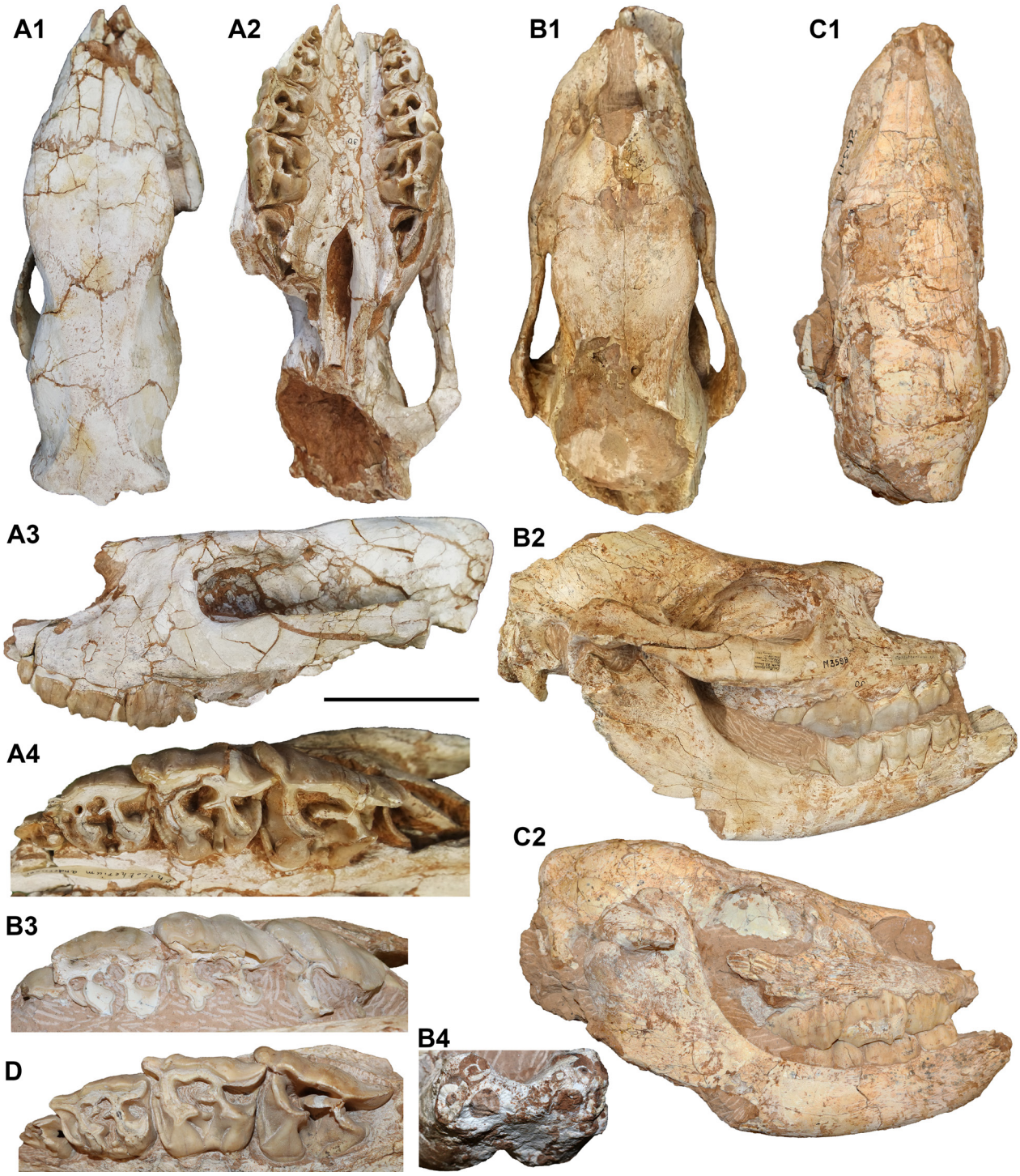


**Figure 12.** Juvenile skulls and upper dentition of *Chilotherium anderssoni* Ringström, 1924 from the Upper Miocene of Daijiagou (China). SMF M 3592 (**A**), SMF M 3598 (**B**), AMNH FM 26341 (**C**), and AMNH FM 26340 (**D**) in dorsal (**A1**, **B1**, and **C1**), ventral (**A2**), lateral (**A3**, **B2**, and **C2**), occlusal (**A4**, **B3**, and **D**), and anterior mandibular (**B4**) views. Scale bar: 10 cm (**A1–3**, **B1–2,** and **C1-2**); 5 cm (**A4**, **B3-4,** and **C**).

**Material.** Two almost complete juvenile skulls with their associated mandibles, both preserving all deciduous premolars (AMNH FM 26341 and SMF M 3598); an almost complete skull preserving D1–D4 on both sides (SMF M 3592); and a partial skull preserving D1–D4 on both sides (AMNH FM 26340).

**Description.** Four juvenile skulls of *C. anderssoni* from the Upper Miocene of Daijiagou or "Lok. 30" (China) are housed in the collections of the AMNH and SMF (Fig. 12) and were donated to these collections by the PMU, where they were originally housed. Specimens AMNH FM 26341 and SMF M 3598 are almost complete skulls with articulated mandibles. In both specimens, the skulls are slightly damaged, with parts of the nasals and zygomatic arches missing, and in SMF M 3598, the parietal and nuchal regions are heavily damaged.

The premaxillary bones are present only in AMNH FM 26340 and are broken off in all other specimens. In dorsal view, the suture between the nasals and the frontals is an almost straight transverse line. The frontals are flat, already slightly showing the frontal depression known in chilotheres. The parietal crests are already visible in all specimens except AMNH FM 26340 and are clearly separated in AMNH FM 26341 and SMF M 3592.

In lateral view, the suture between the nasals and the maxillary is relatively straight, starting from the nasal notch and ending at the lacrimal. The nasal notch is situated above D3 in all specimens, at slightly different levels. The nasal and lacrimal share a very short suture, separating the maxillary from the frontal. Immediately behind the orbit, a well-developed postorbital process is present in the frontal, at the widest part of the dorsal side of the cranium, which is especially well visible in SMF M 3592. From this point, the frontal-parietal crests extend towards the nuchal crest. The maxillary exhibits several infraorbital foramina; three on each side are visible in SMF M 3592. Posteriorly, the maxillary features long pockets, which include the unerupted molars. The lacrimal is relatively small; it connects dorsally to the frontal and nasal, anteriorly to the maxillary, and ventrally to the jugal. The jugal shares a wide suture with the maxillary. Immediately behind the orbit, it exhibits a less prominent postorbital process compared to the slightly more posteriorly positioned postorbital process on the frontals. The squamosal shares a suture with the jugal, starting at the postorbital process. The squamosal is posteriorly sutured to the parietal.

In lateral view, one of the most prominent parts is the orbital cavity, which is placed very high dorsally, creating a thin dorsal orbital rim. The anterior portion of the orbital cavity is formed by the frontal, lacrimal, and jugal. Two small lacrimal foramina are visible in SMF M 3598; they are placed next to each other within a cavity, while in the other specimens, only one foramen is visible. However, it is possible that this is due to remaining sediment covering the distinct foramina. No distinct lacrimal process is visible in either specimen, though it is not certain whether this is the normal morphology or a preservational bias. Within the orbital cavity, no more detailed observations can be made because of the presence of sediment and, in part, due to preservation.

Only AMNH FM 26340 and SMF M 3592 can be studied directly in ventral view, due to the still-attached mandible in the other two specimens. Additionally, Ringström (1924, pl. 3, fig. 1) provided illustrations of another juvenile skull, which is housed in the collections of the PMU, in ventral view. The maxillary constitutes the largest portion of the palate. Posteriorly, the maxillary is sutured to the palatine, which anteriorly reaches the level between D3 and D4. The palatine forms the largest part of the choana. In the palatine, close to the maxillary-palatinal suture, an asymmetrical number of foramina is present at the level of the unerupted M1; on the right side, three foramina are present, whereas on the left side, probably two are present, placed very close to each other.

In posterior view, three of the specimens are damaged. In AMNH FM 26340, the posterior portion is completely missing. In SMF M 3592, only the dorsal portion is preserved, including the nuchal crest, but the posterior side is almost completely covered by a layer of sediment. In SMF M 3598, only the ventral portion, including the foramen magnum, is preserved, while dorsally the brain cavity is exposed; the latter is filled with sediment. In AMNH FM 26341, most of the occipital region is preserved, with only slight damage and some parts partially covered by sediment. The outline of the skull is bell-shaped, and the central tubercle of the nuchal crest is rather weak. The occipital fossa seems fairly shallow, and the occipital crests are weak and fairly wide. The foramen magnum is large and shows a dorsal incision with a rounded end.

The upper deciduous dentition of *C. anderssoni* can be observed in all studied specimens, as well as in the specimen housed in the PMU illustrated by Ringström (1924, table 3, fig. 6). The occlusal surface of the upper dentition of SMF M 3598 is visible only for the left tooth row; however, even there, the lingual portion is still covered in sediment, and it is not possible to assess certain features, such as the lingual cingula and development of the proto- and hypocone constrictions, along with the antecrochet. D2 to D4 are hypsodont and highly molarised. D1 is present in all three specimens and has already been worn. In SMF M 3598, D4 has also just started being worn, based on the continuous wear facet from the parastyle to the protoloph. In AMNH FM 26340 and the specimen illustrated by Ringström (1924, table 3, fig. 6), D4 has barely started being worn, based on a tiny wear facet on the protoloph, while D1 exhibits a more extensive wear facet. Therefore, D1 erupts slightly before D4 in this species. A continuous lingual cingulum is present; it extends on the posterior side in both SMF M 3592 and the Ringström specimen. The hypocone is well formed in all specimens; in SMF M 3592, it is not directly connected to the metaloph, whereas, in the Ringström specimen, this connection is very weak. The metaloph separates a large postfossette. The protocone is smaller than the hypocone, and the protoloph is similar in size to the metaloph. The parastyle is well developed and anteriorly projecting. The metastyle is slightly shorter than the parastyle, but still relatively long.

On D2, the protocone is smaller than the hypocone and bears a posterior and weak anterior constriction, forming a short antecrochet. A weak anterior constriction is present in the hypocone. A moderate, discontinuous lingual cingulum is present, along with an enamel pillar at the entrance of the median valley. In SMF M 3592, there seems to be an enamel pillar next to the base of the antecrochet in the right D2. The protoloph is thinner than the metaloph. A strong crochet is present, along

with a crista; these folds are fused in the Ringström specimen and may also fuse in the other two specimens with further wear, forming a closed medifossette. In AMNH FM 26340 and SMF M 3592, a secondary fold splits off the crista and connects to the protoloph, closing off a prominent fossette anterior to the still-open medifossette. In SMF M 3598, a small secondary enamel fold branches off from the protoloph and nearly connects to the crista; with slightly more wear, it would likely fuse, creating the same fossette. In the Ringström specimen, the medifossette is already closed, and with further wear, it is possible that a similar fossette may form anterior to it. Very strong anterior and posterior cingula are present, forming large pre- and postfossettes. The posterior cingulum extends slightly onto the ectoloph. The parastyle and metastyle are very strong, whereas the paracone and metacone folds are weak.

In D3, the protocone and hypocone are of comparable size. The protocone bears strong anterior and posterior constrictions, forming an antecrochet, whereas the hypocone is only weakly constricted anteriorly. No lingual cingulum is present, but a small enamel pillar occurs in all specimens at the entrance of the median valley. A well-developed crochet is always present. A long crista is present in the Ringström specimen, while only a small enamel bump is visible in the other specimens. Strong anterior and posterior cingula are present, with the latter forming a large postfossette. The parastyle and metastyle are well developed. The paracone fold is strong, and an extremely weak mesostyle is present.

In D4, the protocone is somewhat larger than the hypocone. The protocone bears strong anterior and posterior constrictions that form a prominent antecrochet, and the hypocone bears an anterior constriction. An enamel pillar is present at the entrance of the median valley in SMF M 3592 but is absent in AMNH FM 26340. A large crochet is always present, and an enamel bump in place of a crista appears to be present. A strong anterior cingulum is present, and a strong posterior cingulum forms a wide postfossette. The parastyle is well developed, and the metastyle is wide. The paracone fold is well developed, the mesostyle is weak, and the metacone fold is faintly visible. D4 shows thin horizontal grooves at the base of the crown on the lingual side, as well as "ω"-shaped grooves in the middle of the ectoloph, which can be interpreted as enamel hypoplasias (Mead 1999; Böhmer and Rössner 2018; Hullot and Antoine 2020). In AMNH FM 26340, the hypoplasia is visible only on the lingual side because the D4s are not fully erupted. In AMNH FM 26341, the presence of hypoplasia cannot be assessed because the D4s are largely unerupted and the skull is still attached to the mandible, preventing evaluation of the lingual side.

Only one juvenile mandible of *C. anderssoni* from the Upper Miocene of Daijiagou (China) housed at the SMF and a specimen figured by Ringström (1924, table 3, figs 2, 5) can be studied. Specimen SMF M 3898 is articulated to the previously described skull (Fig. 12B2, B3), and the occlusal surfaces of the teeth are observable only on the right tooth row. Specimen AMNH FM 26341 also includes a skull and mandible that are attached, but the dentition cannot be observed in this specimen. In all three specimens, the anterior portion can be studied to some extent. In Ringström's specimen, two deciduous incisors, di1 and di2, are preserved, including the crowns of the teeth, which are very short, small, and rounded; di1 is less than half the size of di2. In SMF M 3898, only the roots of these teeth are visible, but both deciduous incisors are present (Fig. 12B4). The roots have a rounded cross-section and are small, with di1 being smaller than di2, though the size difference is less pronounced than in Ringström's specimen. In AMNH FM 26341, the anterior part is broken and covered by sediment, preventing observation of the incisor roots. SMF M 3898 preserves d1 on both tooth rows, whereas in Ringström's specimen, it is visible only on the right side. In AMNH FM 26341, d1 is not present on either side. Ringström (1924) noted that the presence of this tooth varies among specimens and may even differ between the right and left sides within the same individual, as in the specimen he illustrated (Ringström 1924, table 3, fig. 2). This tooth is extremely small and bears a single, rounded cusp. The d2 is moderately worn in both specimens, and the trigonid and talonid are connected. The paralophid is anteriorly oriented and constricted. The metalophid projects lingually and distally, and the hypolophid is slightly wider and also projects lingually. Both the anterior and posterior valleys seem to remain open until completely worn. An ectolophid groove exists buccally and appears deeper in Ringström's specimen than in SMF M 3898. No cingulids are visible. The d3 is likewise moderately worn in both specimens, with the trigonid and talonid already connected. The paralophid is less developed than the metalophid and hypolophid. A slight constriction of the metalophid is visible in Ringström's specimen. Both the anterior and posterior valleys probably remain open until completely worn, although, in Ringström's specimen, a weak lingual cingulid may be present in the anterior portion of the tooth. The ectolophid groove is relatively deep. No discontinuous cingulid is visible in buccal view in SMF M 3598. The morphology of d4 cannot be properly assessed, neither in SMF M 3598, because the tooth is embedded in sediment, nor in Ringström's specimen, because it is not fully erupted and properly worn. In Ringström's specimen, the paralophid is relatively short, whereas the metalophid and hypolophid are similarly well developed. A weak and most likely discontinuous cingulid seems to be present at the entrance of the anterior valley in d4 of Ringström's specimen. The ectolophid groove is deep, and a weak enamel bump is located at its base in SMF M 3598. In the latter specimen, an "ω"-shaped groove is visible approximately at the middle of the d4 crown in buccal view, which represents enamel hypoplasia (Mead 1999; Böhmer and Rössner 2018; Hullot and Antoine 2020).

# Comparison

## Late Miocene horned rhinoceroses

During the Late Miocene, several different Rhinocerotidae species occurred in Eurasia. Along with the hornless rhinocerotids or aceratheriines, horned rhinocerotines (e.g. Geraads and Koufos 1990; Antoine and Saraç 2005; Deng 2006b; Geraads and Spassov 2009; Antoine and Sen 2016; Hullot et al. 2023) and elasmotheriines were widespread on the continent (e.g. Chow 1958; Deng 2005b, 2006b, 2008; Kampouridis et al. 2022a; Antoine et al. 2025).

The differentiation of the studied material from elasmotheriines is very easy, as elasmotheriines are much larger in size, their teeth are highly hypsodont, and their enamel pattern is very complex, usually involving very long crochets, cristae, antecrochets, and, in the more derived elasmotheriines, enamel plications as a prominent feature (see Antoine 2002, 2003; Antoine et al. 2002; Deng 2007, 2008; Geraads and Zouhri 2021; Kampouridis et al. 2022a). For instance, the height of an almost unworn D4 of *C. habereri* (GPIT/MA/04830) from the Upper Miocene locality of Kutschwan (China) is 48 mm, whereas the height of a heavily worn D4, which is close to being shed, of *Parelasmotherium schansiense* (GPIT-PV-86051) from the same locality is 41 mm. Additionally, the teeth of elasmotheriines, including the deciduous ones, display more strongly developed cristae, crochets, antecrochets, and sometimes also strong enamel plications compared to chilotheres (e.g. Antoine 2002; Lu et al. 2023). In the case of *P. schansiense* (GPIT-PV-86051), D4 has a branched crochet and antecrochet (Kampouridis et al. 2022a, fig. 1A), along with multiple enamel plications, which are more pronounced when heavily worn (Kampouridis et al. 2022a, fig. 2A1).

The distinction of the studied material from rhinocerotines is more difficult and needs a more detailed comparison of the upper tooth morphology (Fig. 13; Table 1). For many species, the morphology of the deciduous teeth is not known at all or only poorly known, except for some well-sampled species. There are significant morphological differences in the deciduous dentition of horned rhinoceroses, such as *Dihoplus pikermiensis* and *Ceratotherium neumayri* (Fig. 13I, J) from the Upper Miocene of the Balkan-Iranian zoogeographical province (e.g. Geraads 1988; Giaourtsakis et al. 2006; Geraads and Spassov 2009; Giaourtsakis 2009); *Pliorhinus megarhinus* (de Christol, 1835) from the Upper Miocene to Early Pliocene of Europe (e.g. Dawkins 1865; Fukuchi et al. 2009; Pandolfi et al. 2021); *Pliorhinus ringstromi* (Arambourg, 1959) (Ringström 1924; Li et al. 2024) from the Upper Miocene of China; as well as *Lartetotherium sansaniense* (Lartet in Laurillard, 1848) from the Middle Miocene of Europe and *Lartetotherium cixianensis* (Chen & Wu, 1976) from the Middle Miocene of China (Cerdeño 1996; Heissig 2012; Li and Deng 2023), compared to the studied chilotheres (Fig. 13, Table 1).

For instance, D1 is generally smaller in chilotheres than in these horned species, and the morphology is not as well developed; it bears weaker and shorter proto- and metalophs, and the cusps are generally much smaller or even absent in chilotheres. In a sample of 35 studied *Chilotherium* D1s, the width is between 12.8 and 20.3 mm, whereas in *Ceratotherium neumayri*, it is at least 20.6 mm (Giaourtsakis et al. 2006, table 2; Geraads and Spassov 2009, table 5, $n = 8$; Alifieri 2019, table 2); in *D. pikermiensis*, it is at least 21.8 mm (Giaourtsakis et al. 2006, table 2; Geraads and Spassov 2009, table 5, $n = 15$; Alifieri 2019, table 2); in *Dihoplus schleiermacheri* (Kaup, 1832), D1 width is at least 24 mm ($n = 2$; Guérin 1980); and in *P. megarhinus*, it is at least 22 mm ($n = 2$; Guérin 1980). The only rhinocerotine species that bears a narrower D1 is *Lartetotherium*, where the width is between 16 mm and 23 mm (Guérin 1980; Cerdeño 1996; Heissig 2012; Li and Deng 2023), thereby somewhat overlapping with the value range of chilotheres. In D2, a prefossette is always present and relatively large, whereas in rhinocerotines, the prefossette is usually absent. The postfossette is larger and the paracone rib much weaker in chilotheres than in the mentioned horned rhinoceros species (Fig. 13). Additionally, the protocone constriction is more prominent in chilotheres than in any of the compared horned rhinoceroses; notably, the protocone is not at all constricted in *Ceratotherium neumayri* (Fig. 13) or *Lartetotherium* spp. Additionally, chilotheres have a much longer parastyle in D2 compared to the horned species (Fig. 13). In D3 and D4, the protocone bears strong mesial and distal constrictions, creating a strong antecrochet, whereas in *Ceratotherium neumayri*, the protocone is not constricted, and in *Lartetotherium sansaniense*, *D. pikermiensis*, *P. ringstromi*, and *P. megarhinus*, it is only slightly constricted, creating either no antecrochet or only a faint one (Fig. 13). Additionally, the hypocone is always constricted, moderately in D3 and strongly in D4 of chilotheres, whereas in *Ceratotherium neumayri*, it is not constricted at all, and in *Lartetotherium sansaniense*, *D. pikermiensis*, *P. ringstromi*, and *P. megarhinus*, it is only slightly constricted. Based on these features, a maxilla from Samos that was assigned to *Rhinoceros schleiermacheri* by Weber (1904, pl. 16, fig. 1) belongs to a chilothere, as previously suggested (Giaourtsakis et al. 2006). Based on the specific features that can be observed in this specimen, such as the protocone constriction, along with the strong and continuous lingual cingulum in D2 and a discontinuous lingual cingulum in D3, an assignment to *C. schlosseri* seems plausible. This specimen was housed in the collections of the SNSB-BSPG and was destroyed during the Second World War, along with a large part of the palaeontological collection (Nothdurft and Smith 2002; Kampouridis et al. 2023b). Concerning cranial morphology, when fairly complete skulls are available, it is very easy to distinguish chilotheres from any horned rhinoceros, including elasmotheriines, as the former are characterised by shorter and dorsally flattened crania that lack any nasal horn boss, which is documented in juvenile rhinocerotines (Figs 3A1,

**Table 1.** Morphological differences in the upper deciduous dentition of Late Miocene chilotheres and rhinocerotines. The latter are exemplified by *Ceratotherium neumayri* and *Dihoplus pikermiensis* (modified after Giaourtsakis et al. 2006, table 3).

| | Feature | *Ceratotherium neumayri* | *Dihoplus pikermiensis* | Chilotheres |
|---|---|---|---|---|
| **D1** | Relative size | Slightly reduced | Normal | Very reduced |
| | Protoloph | Very long, bends posterolingually, blocking the entrance of medisinus | Normal, vertical, does not bend | Reduced, very short and narrow, if present |
| | Metaloph | Reduced, very short | Normal, long | Reduced, very short |
| **D2** | Lingual cingular pillar | Present in front of the entrance of medisinus | Absent | Usually present in front of the entrance of medisinus |
| | Protocone constriction | Unconstricted | Slightly constricted | Constricted |
| | Prefossette | Absent | Absent | Present, large |
| | Size of postfossete | Very small and narrow, if present | Large, wide | Very large, wide |
| | Hypostyle | Not developed or distinct from posterior cingulum | Present, distinct from posterior cingulum | Not developed or distinct from posterior cingulum |
| | Paracone rib | Very strong, usually double | Strong, always single | Weak |
| | Metacone rib | Absent or faint, only at the top of the crown | Present, clearly marked and continuous down to the base of the crown | Absent or faint only at the top of the crown |
| | Parastyle | Moderate | Moderate | Long |
| **D3 and D4** | Lingual cingular pillar | Present in front of the entrance of medisinus | Absent | Present in front of the entrance of medisinus (not always in D4) |
| | Protocone constriction | Unconstricted | Slightly constricted | Strongly constricted |
| | Hypocone constriction | Unconstricted | Slightly constricted | Moderately in D3, strongly in D4 |
| | Antecrochet | Absent | Weak | Strong |
| | Crista | Always present | Always absent | Sometimes present but weak |
| | Medifossete | Usually present | Always absent | Sometimes present |
| | Metacone rib | Absent or faint, only at the top of the crown | Present, clearly marked and continuous down to the base of the crown | Weak, only at the top of the crown |

2C1, 8A1, 11B). This morphology is well exemplified by the beautifully preserved juvenile *C. schlosseri* skull housed in the NHMW (NHMW-GEO-2009z0088/0001) and well-preserved skulls of *C. persiae* (MNHN.F.MAR3053 and MLU.GeoS.8030) and *C. anderssoni* (AMNH FM 26341 and SMF M 3598), in contrast to the morphology observed in *Ceratotherium neumayri* (Giaourtsakis et al. 2006, fig. 2a; Giaourtsakis 2009, pl. 2, fig. 2), *Lartetotherium* spp. (Cerdeño 1996, pl. 1, figs 1–2; Li and Deng 2023, fig. 1A–B), *P. ringstromi* (Li et al. 2024, fig. 5a), and *D. pikermiensis* (NHMW-GEO-1863/0001/0018).

In the mandible, there are also several features that can distinguish the studied chilothere material from horned rhinoceroses. For instance, chilotheres have a very wide mandibular symphysis, even in very young individuals, that fuses at a very early ontogenetic stage. In GPIT/MA/4820 of *C. habereri*, which is the ontogenetically youngest chilothere individual studied here, d2 and d3 are barely worn, and yet the symphysis is already fully fused. In GPIT/MA/04849, the anterior portion of the mandibular symphysis is broken off, but the root of the right di2 is visible, and its cross-section is round and approximately 10 mm in diameter. In MNHN.F.MAR3069 of *C. persiae*, all deciduous premolars have erupted and are moderately worn, and the symphysis is already rather wide and features a very long diastema between d2 and di2, with a crest running along it; this mandible also preserves a tiny di1. Two mandibles of *C. anderssoni* – SMF M 3598 and the specimen figured by Ringström (1924, pl. 3, figs 2, 5) – preserve both deciduous incisors, as also specifically mentioned by Ringström (1924). The condition concerning the incisors in horned rhinoceroses such as *Ceratotherium neumayri*, *Lartetotherium* spp., *D. pikermiensis*, *P. ringstromi*, and *P. megarhinus* differs from that observed in chilotheres. In the juvenile mandibles HLMD-Sam.77 and GPIH 3017 of *Ceratotherium neumayri*, there are no deciduous incisors, but it is possible that very small, diminutive incisors were present and are lacking in the specimens studied due to their state of preservation. In *D. pikermiensis*, *D. ringstromi*, and *D. megarhinus*, both deciduous incisors may be present (Ringström 1924, pl. 1, fig. 4; Giaourtsakis et al. 2006; Alifieri 2019, fig. 12; Pandolfi et al. 2021). However, the size and form of the symphysis differ significantly, as the symphysis in *Dihoplus* and *Pliorhinus* species is narrow compared to that in chilotheres and does not feature a prominent crest on the diastema (see Ringström 1924, pl. 1, fig. 4; Giaourtsakis et al. 2006). Another striking difference between chilotheres and rhinocerotines is the development of d1, which in chilotheres is either absent or, when present, extremely reduced and small, having a small, rounded tip with a diameter of 5 mm. In *Lartetotherium sansaniense*, *Ceratotherium neumayri*, *D. pikermiensis*, *D. ringstromi*, and *D. megarhinus*, d1 is always present and is not reduced; its length is usually more than 15 mm, and it has distinct morphological features (Dawkins 1865, figs 6, 7; Ringström 1924, pl. 1, fig. 4; Giaourtsakis 2009, pl. 7, figs 7–9; Heissig 2012),


**Figure 13.** Comparative figure with upper dentition (left D1-D4) of the studied Late Miocene chilothere species and rhinocerotines. **A, B.** *Chilotherium persiae* from Maragheh in Iran (**A.** MNHN.F.MAR3820 and **B.** MNHN.F.MAR3053, mirrored); **C, D.** *Chilotherium habereri* from Kutschwan in China (**C.** GPIT/MA/04842 and **D.** GPIT/MA/04843); **E, F.** *Chilotherium schlosseri* from Samos in Greece (**E.** SMNS 47914, mirrored, and **F.** NHMW-GEO-2009z0088/0001); **G, H.** *Chilotherium anderssoni* from Daijiagou in China (**G.** AMNH FM 26341 and **H.** SMF M 3598); **I.** *Ceratotherium neumayri* (HLMD-Sam.231); and **J.** *Dihoplus pikermiensis* (NHMW-GEO-1911/0005/0030) from Samos (Greece). Scale bar: 5 cm.

unlike in chilotheres. Additionally, the morphology of the other deciduous lower premolars differs between chilotheres and rhinocerotines. In d2 of the rhinocerotines *Lartetotherium sansaniense*, *Ceratotherium neumayri*, *D. pikermiensis*, *P. ringstromi*, and *P. megarhinus*, after moderate wear, a closed-off fossettid forms in the talonid (Dawkins 1865; Ringström 1924, pl. 1, fig. 4; Lehmann 1984, pl. 1, fig. 4; Giaourtsakis 2009, pl. 4, figs 8, 9; Heissig 2012, figs 59, 60; Alifieri 2019, fig. 12). Lastly, in d2, and in some cases in d3 as well, the paralophid splits into two lobes in these species, which may connect to form a small fossettid, as observed in some d3s of *Ceratotherium neumayri*, such as in GPIH 3017 and Giaourtsakis (2009, pl. 4, fig. 8).

## Late Miocene aceratheriines

The distinction of the chilothere material studied herein from other hornless rhinocerotids that lived during the Late Miocene in Eurasia is even more difficult than their separation from horned rhinoceroses. One of the issues that makes their distinction so difficult is that, for many species, no deciduous dentition has been described so far. Juvenile specimens are available for some species: a juvenile skull of *Acerorhinus yuanmouensis* Zong, 1998 was recently described from the Yuanmou Basin (China) (Lu 2013); the species *Persiatherium rodleri* is based on a subadult skull from Maragheh (Iran) that still bears D4 (Pandolfi 2016); a juvenile skull with its

associated mandible of *Acerorhinus neleus* Athanassiou et al., 2014 was recently reported from the Upper Miocene locality of Pikermi (Greece) (Giaourtsakis et al. 2018); and *Alicornops complanatum* (Heissig, 1972), *sensu* Antoine et al. (2003), was reported from Upper Miocene beds of the Siwaliks (Heissig 1972, table 7, fig. 13). Additionally, a few characters on the deciduous dentition of *Aceratherium incisivum* Kaup, 1832 can be partially extrapolated from Guérin (1980). The comparison with these specimens shows that *A. neleus* has a much narrower mandibular symphysis, even in juvenile specimens. This is especially evident when the mandible of *A. neleus* and the mandible GMM 593 of *C. schlosseri* from Samos are compared, which are of similar ontogenetic age – the d4s are moderately worn, representing wear stage 6 or 7 (Hillman-Smith et al. 1986; Hullot and Antoine 2020). In GMM 593 of *C. schlosseri*, the symphysis is already very wide and massive, showing a long diastema between d2 and the (d)i2 alveolus, with a crest running along the diastema, whereas the symphysis of *A. neleus* is much narrower. Also, in all four of these non-chilothere aceratheriines, as well as in *Aceratherium incisivum*, the protocone in D3 and D4 is not as strongly constricted as in chilotheres, which also display a prominent and lingually projecting antecrochet. In *Alicornops complanatum*, the paracone fold is much stronger than in chilotheres; this difference is especially evident in D2, which in chilotheres bears a very weak paracone fold, whereas in *Alicornops*, it is very strong (Heissig 1972, table 7, fig. 13). In contrast to the other aceratheriines, some of the studied chilothere specimens preserve a thin layer of cement coating on the ectoloph – although this feature can vary significantly, and the cement layer can often be removed during the preparation of the specimens.

## Chilotheriina

The material of the different studied *Chilotherium* species is rather similar, and any specific identification is very difficult (Fig. 13). There are several characters that show some degree of variation; however, it is often very difficult to assess whether this represents intraspecific variation or interspecific variation of taxonomic significance. For instance, the distance between the orbit and the nasal notch (nasal-orbital bar) and the relative position of the nasal notch seem to vary between the considered species. The length of the nasal-orbital bar depends significantly on the ontogenetic age of the individual but exhibits an approximately linear increase with age (Fig. 14). The comparison of the studied chilothere species shows that the values of *C. persiae*, *C. habereri*, and *C. anderssoni* are close and overlap to some degree. Especially *C. persiae* and *C. habereri* present incredibly similar values with almost perfectly overlapping trendlines (Fig. 14). In contrast to these three species, the values of *C. schlosseri* are consistently lower (Fig. 14). It must be noted here that, in adult skulls, the nasal-orbital bar seems to be of similar size at least in *C. persiae* (79 mm, $n = 1$), *C. habereri* (79–85 mm, $n = 2$), and *C. schlosseri* (72–80 mm, $n = 2$). This would suggest different ontogenetic development in *C. schlosseri*, corresponding either to a somewhat longer period of development or accelerated development towards the later juvenile/subadult life of the individual.

The size of D1 varies amongst chilotheres, with *C. habereri* exhibiting the lowest values within the group, separating this species from all other chilotheres (Fig. 15), whereas *C. persiae* exhibits the greatest length values and *Shansirhinus ringstromi* Kretzoi, 1942 from the Upper Miocene of China the greatest width values in D1 (Fig. 15). In the same diagram (Fig. 15), *C. schlosseri* overlaps with *C. persiae*, *Shansirhinus ringstromi*, and *C. anderssoni*, while *Shansirhinus ringstromi* and *C. persiae* only marginally overlap. More specifically, in *C. habereri*, both the length and width of D1 are lower than those of *C. persiae* and *C. schlosseri*. The few values of *C. anderssoni* overlap with *Shansirhinus ringstromi* and *C. schlosseri*; Ringström (1924) provided value ranges for D1 of the *C. anderssoni* specimens that he studied ($L = 18–21$ and $W = 15–17$), which do not fully agree with the measured values. Nonetheless, they show that *C. anderssoni* overlapped little with the other species and mainly filled the gap between the small D1 of *C. habereri* and the larger D1s of *C. persiae* and *C. schlosseri*. This suggests that the size of D1 can be used to some extent for taxonomic purposes within the genus *Chilotherium* and Chilotheriina in general, with *C. habereri* exhibiting the lowest values in general and *Shansirhinus ringstromi* the greatest width. When other chilotheres are also compared, the picture becomes even more complicated and diverse, with D1 of *E. samium* having almost the same dimensions ($L = 20$ mm and $W = 18.2$ mm, based on the adult neotype SMF M 3601) as *C. anderssoni*, the type species of the genus (Ringström 1924). The dimensions for D1 of '*Chilotherium*' *wimani* from the Upper Miocene of Beihougou in China, based on measurements of the type material provided by Ringström (1924, pp. 50–51), are also rather close to those values, with one specimen having exactly the same dimensions as two *C. anderssoni* D1s, while another specimen has slightly smaller dimensions ($L = 18$ mm and $W = 18$ mm). Deng (2001, table 3) provided measurements of a D1 of '*C.*' *wimani* ($L = 15$ mm and $W = 18$ mm) with a significantly lower length value; it is possible that the intraspecific variation in the size of D1 is relatively broad in this species, possibly similar to the value range provided by Ringström (1924) for *C. anderssoni*. Deng (2005a) and Lu et al. (2015) described cranial and dental material of *Shansirhinus ringstromi*, providing measurements for six D1s, in addition to a D1 of the same species that was measured on a skull housed at the SNSB-BSPG (SNSB-BSPG-2002-I-1). The value range is very broad and seems to vary more significantly than in the studied *Chilotherium* species ($L = 17.7–22.4$ mm and $W = 14.9–21.9$), but D1 is generally larger than in most chilotheres that were measured, with the greatest overlap with *C. schlosseri* (Fig. 15), which is one of the largest *Chilotherium* species (Kampouridis et al. 2025).

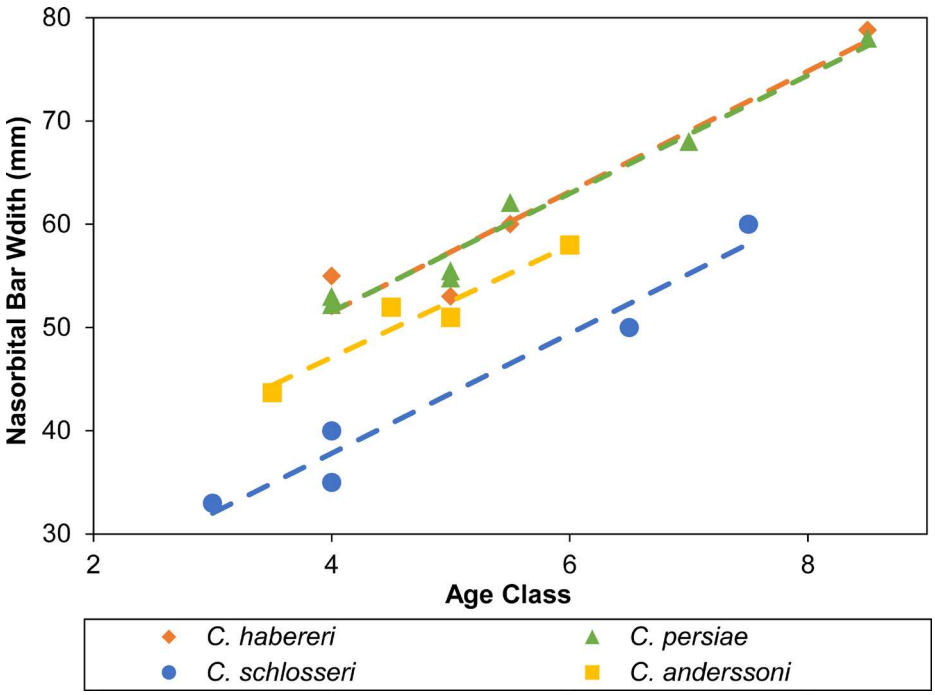


**Figure 14.** Ontogenetic development of the nasal-orbital bar. Scatter diagram of the distance between the orbit and nasal notch (nasal-orbital bar) and the age class of the respective specimen, along with the trendline showing the ontogenetic development of the length of the nasal-orbital bar in each of the studied Late Miocene chilotheres: *Chilotherium persiae* from Maragheh (Iran), *Chilotherium habereri* from Kutschwan (China), *Chilotherium schlosseri* from Samos (Greece), and *Chilotherium anderssoni* from Daijiagou (China). For detailed data, see Suppl. material 1: table S1.

The morphology of D1 is extremely uniform throughout aceratheriines and shows some degree of intraspecific variability, as also reported by Ringström (1924, p. 31) for *C. anderssoni*. Within chilotheres, it seems that a few characters differ between the considered species (Fig. 13). For instance, while all species exhibit a lingual cingulum, it is discontinuous in *C. persiae* and *C. habereri*, whereas it is continuous in *C. schlosseri* and *C. anderssoni*. In *C. schlosseri*, this cingulum continues into a strong and very high distal cingulum that closes off a postfossette at an early wear stage. In *C. persiae* and *C. habereri*, the postfossette is similarly large but closes off at a later wear stage, whereas in *C. anderssoni*, the metaloph is either absent or very thin, with a weak distal cingulum – possibly leaving an open postfossette. The protoloph and protocone are represented by a small enamel fold in most specimens. In *C. persiae* and *C. anderssoni*, this fold is more pronounced and reaches higher up; in *C. habereri*, this fold is very small and is found almost at the base of the crown, whereas in *C. schlosseri*, this fold is quite strong and closes off the median valley after moderate wear.

In D2, *C. schlosseri* seems to have a consistently closed medifossette, and at least in some specimens, some enamel plications are present in the median valley and medifossette (Fig. 13E, F). The D2 described by Weber (1905, pl. 8, fig. 4) as *C. schlosseri* and D2 of the maxilla described by Weber (1904, pl. 16, fig. 1) as *Rhinoceros schleiermacheri* (assigned herein to *C. schlosseri*) also feature a closed medifossette, though no enamel plications are visible in the published drawings. In other *Chilotherium* species, the closure of the medifossette seems variable. Ringström (1924) figured a D2 of *C. anderssoni* (Ringström 1924, pl. 3, fig. 6) and a D2 of '*C.*' *wimani* (Ringström 1924, pl. 7, fig. 4), both with a closed medifossette, but mentioned the variability of this feature (Ringström 1924, p. 32). In *C. habereri* from Kutschwan, none of the D2s feature a closed medifossette (Fig. 13C, D). Similarly, in D2 of *C. persiae* (MNHN.F.MAR3053), the medifossette remains open, though the crista is well developed and almost reaches the crochet (Fig. 13A, B). The D2 of *C.* '*habereri* var. *laticeps*' Ringström, 1924 (synonymised with *C. anderssoni* by Heissig 1975, table 6), illustrated by Ringström (1924, table 5, fig. 2), also exhibits an open medifossette, despite its advanced wear stage. Also, none of these three species features any enamel plications. In *C. kowalevskii*, the medifossette seems to, at least occasionally, close, and enamel plications also seem to be present at least in some cases (Pavlow 1913, pl. 17, figs 2, 3). The D2 of *E. samium* (Weber 1905, pl. 9, fig. 4) also features a completely closed medifossette and a small enamel plication below the lingual wall of the medifossette. Additionally, the lingual cingulum differs among the studied chilotheres. In *C. schlosseri*, it is usually more pronounced than in *C. anderssoni*, *C. habereri*, *C. wimani*, *C. persiae*, and *C. kowalevskii* (Fig. 13). A very strong lingual cingulum is also clearly visible in D2 of *C. schlosseri,* described by Weber (1905, pl. 8, fig. 4), whereas that of *E. samium* (Weber 1905, pl. 9, fig. 4) features a discontinuous

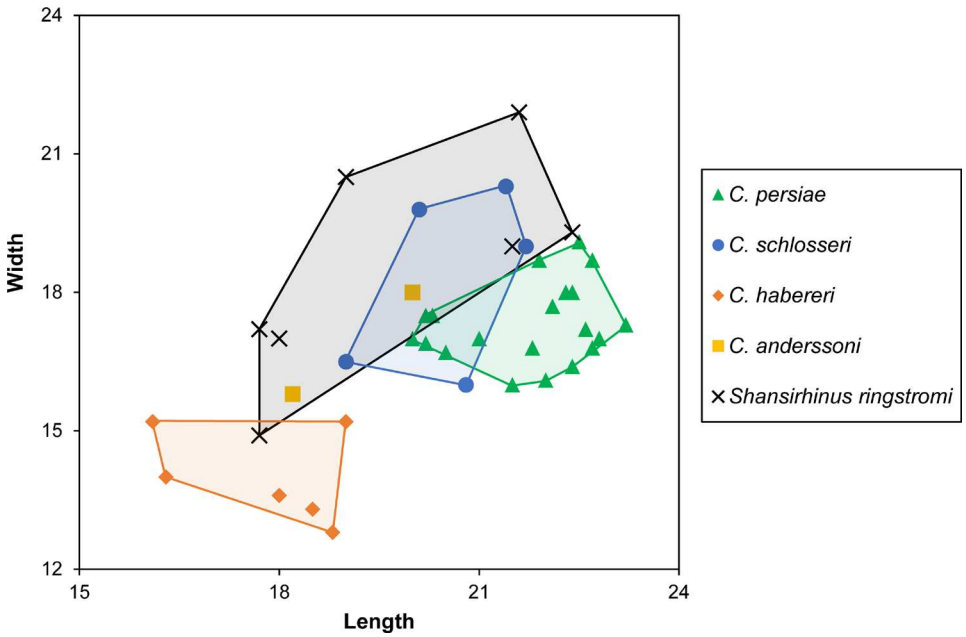


**Figure 15.** Size differences in D1 of chilotheres. Scatter diagram of the length and width of D1 in the Late Miocene chilotheres *Chilotherium persiae* from Maragheh (Iran), *Chilotherium habereri* from Kutschwan (China), *Chilotherium schlosseri* from Samos (Greece), *Chilotherium anderssoni* from Daijiagou (China), and *Shansirhinus ringstromi* from China. For detailed data, see Suppl. material 1: table S1.

cingulum. While in most studied chilothere specimens D2 features both closed-off pre- and postfossettes, in *C. persiae*, the prefossette is not always closed. In D2 of '*C.*' *wimani* (Ringström 1924, pl. 7, fig. 4), the parastyle is shorter compared to the other chilotheres.

D3 seems to have a very conservative morphology throughout chilotheres. Ringström (1924) described D3 of *C. anderssoni* as usually lacking an enamel pillar at the entrance of the median valley and a lingual cingulum and having an 'insignificant' crista, but he illustrated a D3 (Ringström 1924, table 3, fig. 6) with both an enamel pillar and a long crista that closes the medifossette when slightly more worn. In one *C. anderssoni* specimen (SMF M 3592), an enamel pillar is present at the entrance of the median valley, whereas the other studied specimens do not exhibit an enamel pillar. Instead of a crista, the three *C. anderssoni* specimens only exhibit a weak enamel bump in D3 (Fig. 13G, H). In *C.* '*habereri* var. *laticeps*' (Ringström 1924, table 5, fig. 2) and '*C.*' *wimani* (Ringström 1924, table 7, fig. 4), neither a crista nor a continuous lingual cingulum is visible, though an enamel pillar exists at the entrance of the median valley. Similarly, in *C. habereri* from Kutschwan, the size of the crochet and crista vary within the three studied specimens (Fig. 13C, D). In GPIT/MA/04843, D3 has a very small crochet and a small enamel bump in place of the crista, whereas the other two specimens have longer crochets, and in GPIT/MA/04830, a small but distinct crista is also present. In *C. persiae* from Maragheh, all studied specimens feature a well-developed crochet, whereas a crista is present only in some specimens, closing off the medifossette (i.e. NHMW-GEO-2020/0014/0093). In *C. kowalevskii*, the crista seems to be small or absent and the crochet large (Pavlow 1913, table 17, figs 1–3). In *C. schlosseri*, a crista is present in all D3s studied herein and may close off the medifossette after moderate wear. In the illustration of a D3 of *C. schlosseri* by Weber (1905, table 8, fig. 4), a crista is not visible. Another feature in *C. schlosseri* that seems to differ from other chilotheres is the existence of a continuous or slightly discontinuous lingual cingulum on D3, which is present in all three specimens studied herein and in the *C. schlosseri* D3 depicted by Weber (1905, table 8, fig. 4). Moreover, the *C. schlosseri* specimens also feature some small enamel plications, as seen in SMNS 47913 and SMNS 47914. Overall, the presence and development of the crista and enamel plications also seem to vary within *C. schlosseri* but might be most commonly present.

D4 is morphologically very similar to D3 but is the most molarised tooth among the deciduous premolars, often being confused with M1 or M2. A long crochet, a strongly constricted protocone, and a well-developed antecrochet are present in all the considered species (Fig. 13). Also, no crista is present in any of the studied specimens, although a small enamel bump might at least be present. The only features that seem to be somewhat common in *C. schlosseri* but lacking or less developed in the other species are the presence of enamel plications and a discontinuous lingual cingulum. Neither *C. persiae*, *C. habereri*, nor *C. anderssoni* exhibits any lingual cingulum in D4. Interestingly, in both deciduous dentitions for *C. schlosseri* and *E. samium* illustrated by Weber (1905), a lingual cingulum seems to be present in D4. The D4 that was assigned to *E. samium* (Weber 1905, table 9, fig. 4) even features several enamel plications on the crochet. The deciduous tooth row assigned

to *E. samium* by Weber (1905, table 9, fig. 4) exhibits several features that are otherwise characteristic of *C. schlosseri*, such as the closed medifossette in D2 and D3 and the multiple enamel plications in D4, suggesting that this specimen belongs to *C. schlosseri*.

# Discussion

## Taxonomy

The taxonomy of chilotheres is a complicated and often debated topic. There are many controversies about the validity of species and their potential synonymy (e.g. Kiernik 1913; Krokos 1917; Heissig 1975; Deng 2006a; Țibuleac 2014; Kampouridis et al. 2022b, 2023b). Originally, Ringström (1924) suggested that the cranial morphology of most species is too similar to be used for their distinction, and he used dental morphology, including that of deciduous teeth, to separate the different species. However, it is now known that dental morphology is often interspecifically very uniform and can vary greatly depending on the wear stage (see Țibuleac 2014; Antoine and Sen 2016). Cranial morphology, instead, is more diagnostic than initially expected (Kampouridis et al. 2023b), and many species can be distinguished based on the morphology of their skulls. For instance, *C. sarmaticum* differs from *C. kowalevskii* in having shorter nasal bones and more widely separated parietal crests. *Chilotherium schlosseri* has more widely separated parietal crests than any other chilothere (Svorligkou et al. 2025). These three species, along with *C. persiae*, *C. habereri*, *C. anderssoni*, *C. orlovi*, *C. xijangensis*, and *C. licenti*, represent *Chilotherium sensu stricto* and bear a prominent depression in the frontal region, which is lacking in *Shansirhinus* spp., *E. samium*, '*C.*' *wimani*, and '*C.*' *primigenium*. For this reason, the latter three species have been proposed to be removed from the genus *Chilotherium* (Kampouridis et al. 2023b). Few studies have also attempted to use postcranial morphology for the taxonomic identification of chilotheres (Korotkevich 1970; Deng 2002; Kampouridis et al. 2025), which showed that at least some features in the postcranium present diagnostic characters. For instance, a recent study suggested that the morphology of the articular facets of the astragalus for the calcaneum can be used to separate some species, and the patella and tibia are helpful for species identification, though more material is needed to confirm these hypotheses and refine these diagnostic characters (Kampouridis et al. 2025).

The deciduous dentition of chilotheres is often overlooked, and little is known about its potential taxonomic value. It is known that, in some rhinoceros groups, deciduous teeth can be used to identify the genus or even the species (e.g. Guérin 1980; Heissig 1984; Giaourtsakis et al. 2006; Becker et al. 2009; Böhme et al. 2021a; Kampouridis et al. 2022a). Nonetheless, Ringström (1924, p. 41) suggested that the deciduous dentition of *C. habereri* and *C. anderssoni* varies intraspecifically to a degree that does not allow their specific separation. The results of the comparisons suggest that, although the morphology of the deciduous dentition is rather uniform, some characters can be used to help with the identification of the abovementioned species (Fig. 13). The size and morphology of D1 vary between the species, with *C. habereri* from Kutschwan (China) exhibiting the smallest dimensions for D1 (Fig. 15) and also featuring a shorter protoloph and weaker protocone than the other species. *Chilotherium schlosseri* from Samos (Greece) often includes some enamel plications in the deciduous premolars, which are much rarer in the other studied chilothere species, *C. persiae*, *C. habereri*, and *C. anderssoni*. This has also been observed in the permanent dentition of the species (Kampouridis et al. 2023b). Additionally, *C. schlosseri* exhibits more pronounced enamel folds in the deciduous teeth than other chilotheres, such as a mesial and distal protocone constriction in D2, a crista in D3, a closed-off medifossette in both D2 and D3, and commonly strong lingual cingula. Lastly, the prefossette in D2 is always present in *C. habereri* and *C. schlosseri*, whereas it is absent in some specimens of *C. persiae* (Fig. 13).

## Tooth eruption in *Chilotherium*

Tooth eruption in rhinoceroses is usually conservative, without much variation between different species (Koenigswald et al. 2007). For this reason, it has been studied in only a few taxa (e.g. Goddard 1970; Hillman-Smith et al. 1986; Koenigswald et al. 2007; Böhmer et al. 2016), and consequently, it has never been described for chilotheres. Herein, the eruption sequence of the deciduous and permanent dentition of the four studied species of chilotheres is evaluated, also taking into account the literature for other chilothere species (Pavlow 1913; Ringström 1924; Deng 2005a). In all chilothere species, d/D2 and d/D3 are the first teeth to erupt, which must start immediately after birth, since there is no single specimen where these teeth are still unerupted. The ontogenetically youngest specimen is the mandible GPIT/MA/04820 of *C. habereri* from Kutschwan, in which d2 and d3 have erupted but exhibit only very weak wear, with very small wear facets in the posterior part of the talonid of d2 and the trigonid of d3 (Fig. 8B). In this specimen, there are no signs of a distal wear facet on d3 for d4; therefore, d4 had not erupted yet. The d1 is not always present, and it is not possible to assess its eruption compared to the other lower teeth. D1 and d/D4 erupt later, and some disparity is observed. In most studied specimens of chilotheres, such as *C. habereri*, *C. persiae*, and *C. kowalevskii* (Pavlow 1913, pl. 17, figs 1, 2; Ringström 1924, pl. 3, figs 1, 6), D1 erupts before or simultaneously with D4. In *C. schlosseri*, only one specimen preserves both teeth, allowing assessment of the relative eruption time (SMNS 47913): D4 is already fully erupted, though unworn, whereas D1 is

only beginning to erupt, with its tip barely reaching the level of the tooth crown base of the D2 crown, thereby deviating from the pattern observed in other chilotheres. In a specimen of *C. persiae* (MNHN.F.MAR3820), a similar condition can be observed: D4 is at the same eruption stage as in SMNS 47913 of *C. schlosseri*, and D1 is not fully erupted yet, though the tip of D1 reaches the middle of D2, thereby being at a more advanced eruption stage than in SMNS 47913. It is difficult to determine the exact eruption sequence of these two teeth with certainty because they erupt at approximately the same time, and their relative eruption timing appears to vary at least in *C. persiae*. D1 is the only deciduous tooth that is not replaced and is retained into adulthood, being retained even in ontogenetically very old specimens such as NHMW-GEO-1911/0005/0128 (see Svorligkou et al. 2025, fig. 6a).

## Enamel hypoplasia in *Chilotherium*

Enamel hypoplasia is a deficiency in enamel thickness resulting from stress when a certain threshold is met (Goodman and Rose 1990, fig. 14) during the secretory phase of amelogenesis (Goodman and Rose 1990). Linear enamel hypoplasia (LEH) is the most common form of these defects (Goodman and Rose 1990). Though well studied in some mammalian groups such as humans, enamel hypoplasia is a topic that, until recently, had received little attention in rhinoceroses (e.g. Bratlund 1999; Mead 1999; Roohi et al. 2015; Böhmer and Rössner 2018). However, in recent years, several studies have dealt with the topic, trying to standardise the study of hypoplasias in rhinoceroses based on work in other groups (e.g. Hullot et al. 2021, 2023, 2024a, 2024b, 2024c; Hullot and Antoine 2022).

The aetiology of enamel hypoplasias in general is a very complex and controversial topic, but it has been extensively discussed in primates (Skinner 1986; Eckhardt and Protsch von Zieten 1993; Hillson and Bond 1997; Guatelli-Steinberg and Lukacs 1998; Guatelli-Steinberg and Skinner 2000; Guatelli-Steinberg 2001; Hannibal and Guatelli-Steinberg 2005; Chollet and Teaford 2009; Skinner et al. 2014). Their taxonomic distribution in primates seems to be somewhat dichotomous because they are very rare in monkeys (Guatelli-Steinberg and Lukacs 1998; Guatelli-Steinberg 2000, 2001; Chollet and Teaford 2009) but very common in great apes, often having multiple defects in one tooth (Skinner 1986; Eckhardt and Protsch von Zieten 1993; Hannibal and Guatelli-Steinberg 2005). The reason for this taxonomic discrepancy in the distribution of linear enamel hypoplasias has been discussed by many authors and includes the length of tooth maturation (Guatelli-Steinberg 2000; Newell et al. 2006; Chollet and Teaford 2009), crown morphology (Guatelli-Steinberg 2000), differences in the spacing of perikymata (Hannibal and Guatelli-Steinberg 2005), and differences in enamel thickness (Lukacs 1999), though it seems to overlap in some taxa (Shellis et al. 1998) and probably does not relate to the occurrence of hypoplasias (Hannibal and Guatelli-Steinberg 2005; Chollet and Teaford 2009). However, Hannibal and Guatelli-Steinberg (2005) demonstrated that, within the great apes, gorillas exhibit a low frequency of enamel hypoplasias compared to chimpanzees and orangutans, which they correlate with their somewhat different diet and the perikymata spacing. They also observed that, within the same taxon group, chimpanzees and gorillas, the hypoplasia frequency varies by location but were unable to correlate it with any kind of food availability or pathogens that differ between the two regions (Hannibal and Guatelli-Steinberg 2005). Chollet and Teaford (2009) investigated the presence of enamel hypoplasias in *Cebus* canines from Brazil in relation to some environmental factors. They found that hypoplasias were more prevalent in semi-deciduous forests and lower average temperatures than in coastal regions or tropical rainforests and high temperatures and were unable to trace any correlation with precipitation (Chollet and Teaford 2009).

Concerning the presently studied material, numerous deciduous teeth were found featuring hypoplasia (Fig. 16). More specifically, hypoplasias in d/D2 and d/D3 are rather rare, whereas hypoplasia in d/D4 was observed in all available specimens in all four studied species (Figs 16–18, Table 2). In the studied sample of *C. persiae* from Maragheh (Iran), only two teeth of the 33 d/D3s show hypoplasia, whereas none of the 29 d/D2s exhibit hypoplasia. In contrast, in the 34 d/D4 specimens, every single one exhibits hypoplasia, always in the same position. In the studied sample of *C. habereri* from Kutschwan (China), of the six d/D2s and eight d/D3s, only one specimen (GPIT/MA/04849) shows hypoplasias. In this specimen, both d2 and d3 present multiple weakly developed hypoplasias in the lower part of the respective teeth on both sides. The hypoplasias in d2–3 are almost at the same level in the tooth crowns in both teeth and were most probably caused by the same event(s), which further indicates that these teeth developed at the same time. Another specimen (GPIT/MA/04820) exhibits more subtle hypoplasias in d2 and d3 that are represented by small pits (Fig. 17A, B), as described by Hullot et al. (2021), in the lower half of the tooth crown. Concerning the d/D4s of *C. habereri*, all seven specimens feature hypoplasia, all located in the middle of the tooth crown. In the mandible GPIT/MA/04849, the d4s have not erupted yet, with only the tip of the tooth crown visible. The CT scan of the specimen revealed the d4 hypoplasia, which was well pronounced (Fig. 17C, D). In the studied sample of *C. schlosseri* from Samos (Greece), not a single hypoplasia was found among the 17 d/D2s and d/D3s, whereas among the nine examined d/D4s (Table 2), all exhibit hypoplasia (see Fig. 17I–O). This hypoplasia differs from the hypoplasias found in d/D4 in the other three studied species.

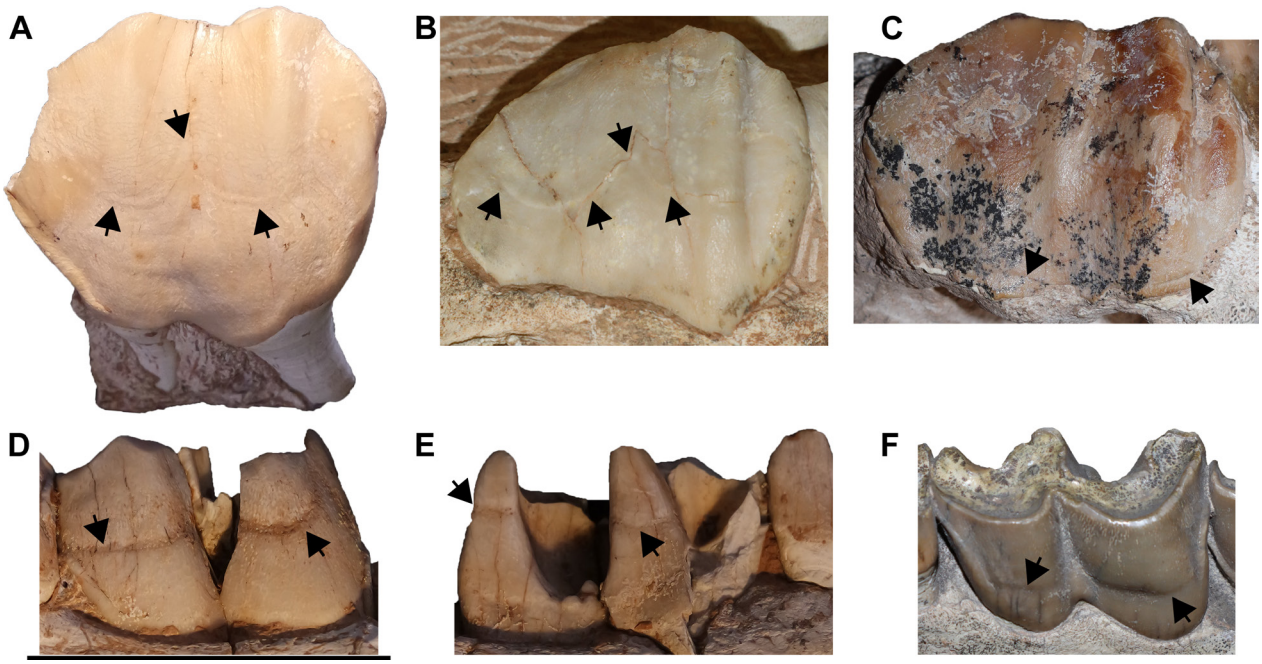


**Figure 16.** Hypoplasias in d4 and D4 of the studied Late Miocene chilotheres. *Chilotherium habereri* from Kutschwan in China (**A.** GPIT/MA/04817, D4; and **D–E.** GPIT/MA/04818, d4 in buccal and lingual views), *Chilotherium anderssoni* from Daijiagou in China (**B.** SMF M 3598, D4), and *Chilotherium schlosseri* from Samos in Greece (**C.** SMNS 47914, D4 and **E.** GMM 593, d4). Black arrows indicate enamel hypoplasias. Scale bar: 5 cm.

In the upper D4 of *C. persiae*, *C. habereri*, and *C. anderssoni*, the hypoplasia is represented by a horizontal groove close to the base of the crown on the lingual side of the tooth and an "ω"-shaped groove in the middle of the ectoloph (Figs 16A, B, 17G, H). In D4 of *C. schlosseri*, it has a different form and is found at a different position (Figs 16C, 17I–O) in all specimens. The hypoplasia is found at the base of the crown on both the lingual and buccal sides, and on the ectoloph (Fig. 17J, N), it takes the shape of an almost straight horizontal line (Fig. 16C) instead of an "ω", which is seen in the other chilotheres. The position and "ω"-shaped form of the enamel defect on the buccal side of d/D4 are consistent with what has been observed in other rhinoceroses. It is comparable to the hypoplasia reported in *Prosantorhinus germanicus* (Wang, 1928) from the Miocene of Sandelzhausen (Germany) (Böhmer and Rössner 2018) and *Teleoceras* from the Miocene of North America (Mead 1999; Gajewski 2026). Bratlund (1999) studied a large collection of *Stephanorhinus kirchbergensis* (Jäger, 1839) specimens (368 teeth), of which only nine featured some kind of enamel hypoplasia. Hullot et al. (2021) investigated the ecology of different Miocene rhinoceros species from France with a multiproxy approach consisting of micro- and mesowear and an investigation of enamel hypoplasias. Hullot et al. (2023) studied the ecology of the rhinoceros assemblage that inhabited the Balkan-Iranian zoogeographical province during the Late Miocene, also investigating hypoplasias in these animals, including some chilothere species such as *C. persiae* from Maragheh (Iran), *C. schlosseri* from Samos, and *E. samium* from Pentalophos (Greece).

**Table 2.** Prevalence of hypoplasia in the deciduous teeth of the studied chilotheres by species and tooth.

| Species | Hypoplasia | d/D2 | d/D3 | d/D4 |
|---|---|---|---|---|
| ***C. persiae*** - Maragheh (Iran) | present | 0 | 2 | 33 |
| | absent | 28 | 30 | 0 |
| | Prevalence (%) | 0 | 6 | 100 |
| ***C. habereri*** - Kutschwan (China) | present | 2 | 2 | 7 |
| | absent | 4 | 6 | 0 |
| | Prevalence (%) | 33 | 25 | 100 |
| ***C. schlosseri*** - Samos (Greece) | present | 0 | 0 | 9 |
| | absent | 8 | 9 | 0 |
| | Prevalence (%) | 0 | 0 | 100 |
| ***C. anderssoni*** - Daijiagou (China) | present | 0 | 0 | 4 |
| | absent | 4 | 4 | 0 |
| | Prevalence (%) | 0 | 0 | 100 |
| ***Chilotherium* spp.** | present | 2 | 4 | 53 |
| | absent | 44 | 49 | 0 |
| | Prevalence (%) | 4 | 8 | 100 |

Although in the d/D4s of chilotheres, hypoplasia is always present, when the other deciduous teeth are concerned, hypoplasias are rather rare, with only 4% and 8% of d/D2s and d/D3s, respectively, exhibiting hypoplasia (Fig. 18, Table 2). The presence of hypoplasias on deciduous teeth can vary from species to species and from locality to locality but is usually not very frequent (Hullot et al. 2023, 2024a, 2024c). In a comparative sample of *D. pikermiensis* specimens from Pikermi and Samos (Greece), one of eight studied d/D2s (12.5%) and two of eight d/D3s (25%) have hypoplasia. Hullot et al. (2023) studied hypoplasias in the same species, mainly based on material from Bulgarian Late Miocene localities, and

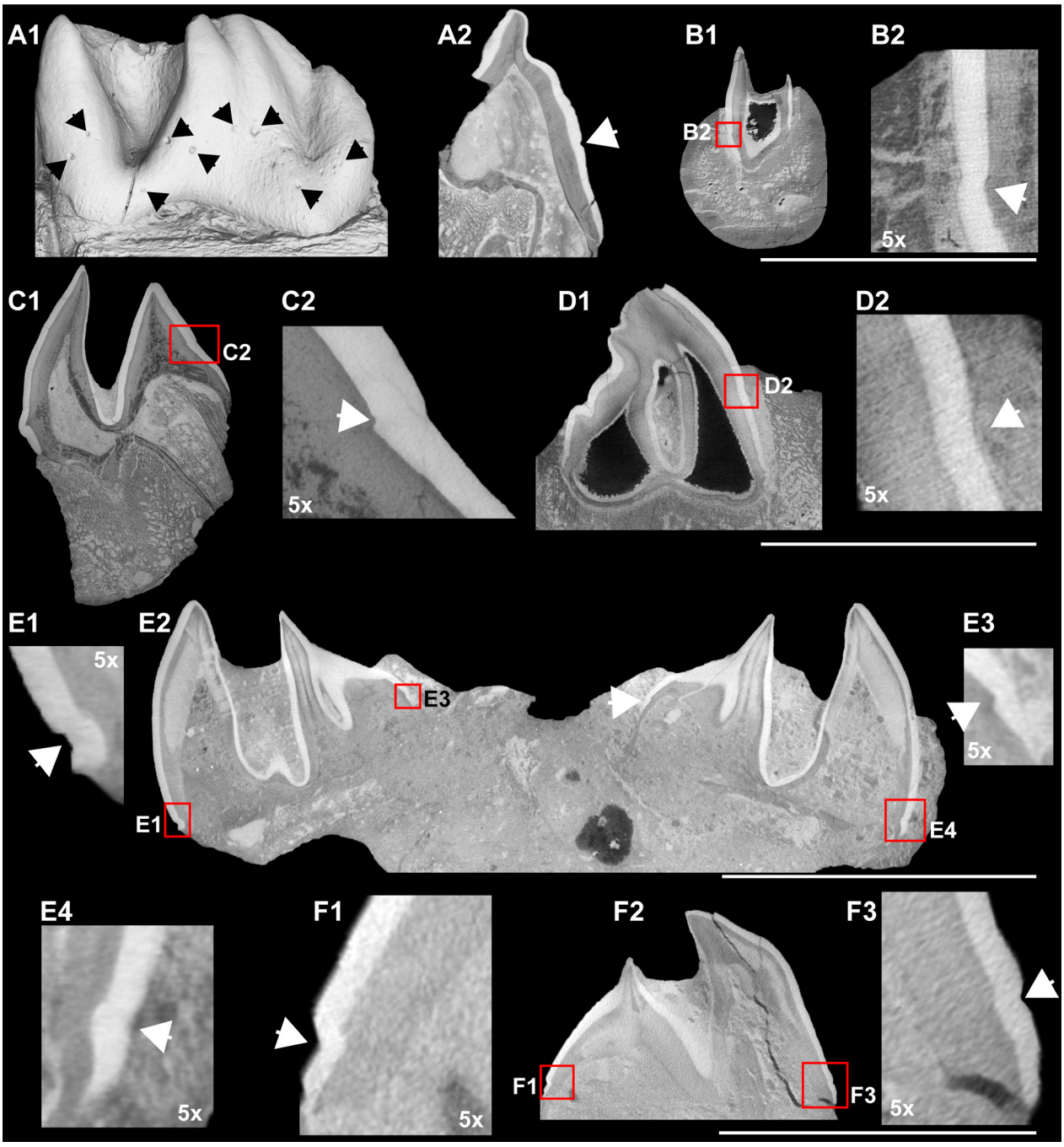


**Figure 17.** Hypoplasias in the deciduous dentition of the studied Late Miocene chilotheres through µCT scans. Virtual cross-sections of µCT scans of: **A–D.** *Chilotherium habereri* from Kutschwan in China (**A.** GPIT/MA/04820, d2; **B.** GPIT/MA/04849, d4; **C.** GPIT/MA/044817, D4; and **D.** GPIT/MA/04820, D4); and **E–F.** *Chilotherium schlosseri* from Samos in Greece (**E.** SMNS 47914, D4s; and **F.** SMNS 47913, D4). Black arrows indicate pit-shaped hypoplasias in d2, and white arrows indicate linear enamel hypoplasias in d/D4. Scale bar: 5 cm for **A1**, **B1**, **C1**, **D1**, **E2**, and **F2**, and 1 cm for the magnified images **A2**, **B2**, **C2**, **D2**, **E1**, **E3–4**, **F1**, and **F3**, indicated with "5x".

found a similar prevalence in these tooth positions. This defect in chilotheres shows a lower frequency in these deciduous premolars, though it also varies between localities and species, as seen in the relatively high prevalence in the rather limited sample of *C. habereri* from Kutschwan (33% for d/D2 and 25% for d/D3, Table 2).

As already mentioned, hypoplasia in d/D4 is constantly present in all chilothere specimens studied here, contrary to the contemporaneous horned rhinoceros *D. pikermiensis* from Pikermi and Samos (Greece), for which only two (22.2%) of the nine studied d/D4s exhibited hypoplasia. In a sample of 14 d/D4s of another horned rhinoceros, *Ceratotherium neumayri*, seven (50%) specimens exhibit hypoplasia, demonstrating a much higher prevalence. In a relatively small sample of five juvenile crania of the extant black rhinoceros from the Kunene

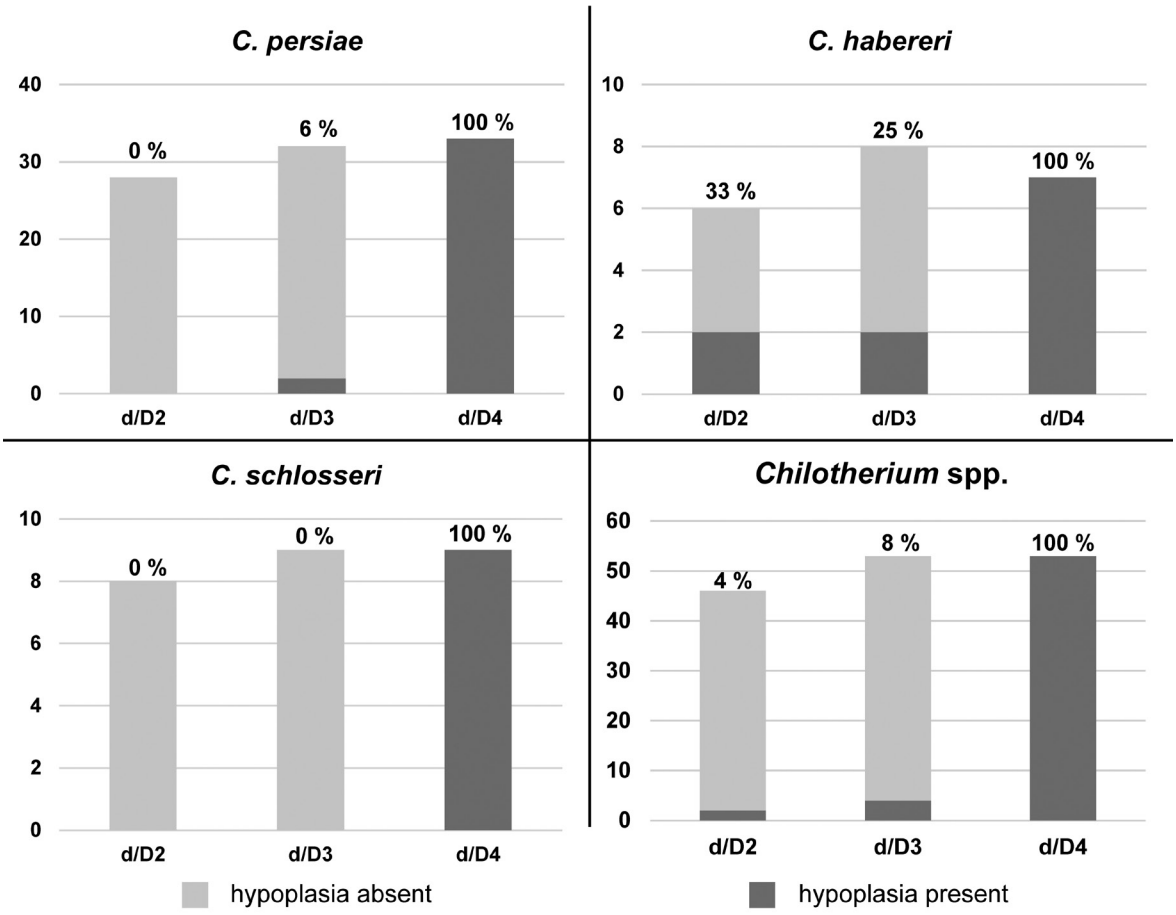


**Figure 18.** Prevalence of hypoplasias in the deciduous teeth of the studied Late Miocene chilotheres. Detailed diagrams for *Chilotherium persiae* from Maragheh (Iran), *Chilotherium habereri* from Kutschwan (China), *Chilotherium schlosseri* from Samos (Greece), and data from all three species, along with *Chilotherium anderssoni* from Daijiagou (China), merged. For detailed data, see Table 2.

Region (Namibia) studied at the facilities of the Save the Rhino Trust, all specimens exhibit hypoplasia in d/D4. It is not known how the presence of this defect may vary in these species or to what degree its presence is affected by environmental conditions or other external pressures.

The main causes of enamel hypoplasias include: 1. localised trauma, 2. genetic defects, and 3. physiological and systemic stress (nutritional). Enamel hypoplasia as a result of localised trauma appears only in a few teeth on the side of injury (Goodman and Rose 1990). This contrasts with the hypoplasias present in the studied material of *Chilotherium*, where the defects are present on both sides of the same maxilla or mandible and, in the case of d/D2 and d/D3, can affect multiple teeth if they were formed at the same time. Enamel hypoplasia as a result of a genetic defect typically occurs in all teeth and often occurs with other congenital anomalies (Goodman and Rose 1990). On the contrary, in the *Chilotherium* material, no other anomalies can be observed in the studied material, and hypoplasia is usually present only in one single tooth position, as in the case of d/D4. Lastly, enamel hypoplasia resulting from systemic stress, whether nutritional or disease-related, appears in all teeth that were developing at the time of the stress (Goodman and Rose 1990), thereby presenting the only fitting explanation.

The fact that enamel hypoplasias in the studied sample are primarily found in d/D4 in both the mandible and maxilla requires further clarification. In the extant white rhinoceros, d4 can start erupting as early as the second month (Hillman-Smith et al. 1986). Based on a radiographical image provided by Goddard (1970, pl. 2a), in the extant black rhinoceros, d4, which starts erupting a few months after birth, is already fully formed in a 5.5-month-old calf. Thus, Mead (1999) correlated the hypoplasias in d/D4 of *Teleoceras* with the timing of birth of the individuals. Enamel hypoplasias in different mammalian groups have been linked to high-stress situations, such as birth (e.g. Goodman and Rose 1990; Upex and Dobney 2012), and a study concerning hypoplasias in extant white-tailed deer correlated linear enamel hypoplasias in d4 with the timing of birth or the first week following birth (Davis and Mead 2013).

The hypoplasias reported herein in d/D4 of *Chilotherium* are consistent throughout several individuals of three distinct species, being situated in the same portion of the tooth crown, and while, in *C. schlosseri*, the position of the d/D4 hypoplasia differs, it is intraspecifically extremely consistent being always at the base of the crown, without any variation. Other enamel defects were extremely rare or absent. Consequently, a random

event that caused hypoplasia at the same exact position in all d/D4s can be excluded. An event that could cause such a defect in amelogenesis and is normal and undeviating in the life of all individuals and at a common ontogenetic stage, during the formation of d/D4, must be looked for as a cause. The only such event that could cause a stressful situation during the formation of d/D4 is the birth of the animal. Therefore, Mead (1999) and Hullot et al. (2021) are followed in supporting that this enamel hypoplasia is the result of birth-related stress.

In the present case, the prevalence of hypoplasias in d/D2 and d/D3 is rather similar and remarkably low in *C. schlosseri*, *C. anderssoni*, and *C. persiae*, with only d/D3 of *C. persiae* exhibiting any hypoplasias (6%, *n* = 32, Fig. 18, Table 2). Hullot et al. (2023) provided the first results on hypoplasias in chilothere teeth, with none found in 12 d/D2s and d/D3s of *E. samium* (referred to as *C. kiliasi* in their study) from Pentalophos-1 in Greece. This is the only other chilothere present during the Late Miocene in Greece, and even though Pentalophos-1 is of Vallesian age (late MN9) and Samos is Turolian (MN11–13, depending on the horizon), it does not present any hypoplasia in these teeth, as in *C. schlosseri* from Samos. On the contrary, *C. habereri* from Kutschwan (China) exhibits a comparably very high prevalence of hypoplasias in d/D2 (33%, *n* = 6) and d/D3 (25%, *n* = 8) in a rather limited specimen sample (Fig. 18, Table 2).

Regarding d/D4, the results of the present study show that there is no taxonomic disparity in the prevalence of hypoplasias because hypoplasia is found in all specimens. However, there is an important discrepancy between the present results and those of Hullot et al. (2023) in the prevalence of hypoplasias in the studied chilotheres. Most importantly, Hullot et al. (2023) studied the *C. persiae* material housed in the NHMW, which is also the subject of the current study, and listed several d/D4s that do not exhibit hypoplasia. They mentioned that, in 22 d/D4s, only 15 (68.2%) feature hypoplasia. However, the deviating results seem to stem from the exclusion in our study of worn-down and damaged specimens, in which the portion of the tooth where the hypoplasia would be visible is not preserved, along with teeth that are at least partially covered by cement, which complicates the observation of potential hypoplasia.

While hypoplasia was found to always be present in d/D4 of chilotheres, a significant disparity was observed in the position of the hypoplasia in *C. schlosseri* from Samos. As mentioned above, in this species, the hypoplasia is an almost straight line and is placed at the base of the tooth crown, whereas, in *C. persiae*, *C. habereri*, and *C. anderssoni*, the hypoplasia is placed in the middle of the tooth and has an "ω" shape on the buccal side of D4. In both cases, the creation of hypoplasia can be correlated with the birth of the individual, as the only constant event that could cause that much stress in so many individuals, as also discussed above. The observed deviation of the position of the hypoplasia might be related to some external environmental factor or interspecific differences, or a combination of both may affect the timing of birth to some degree.

The four studied chilothere species come from different localities across Eurasia, with *C. schlosseri* representing the westernmost species, found in Samos in Greece, *C. anderssoni* and *C. habereri* representing the easternmost species, both coming from Shanxi Province, China, and *C. persiae* having an intermediate position in Maragheh in Iran (Fig. 1). While all four localities are placed in the Upper Miocene, they differ in age, with Maragheh preserving the oldest record, spanning from 9 to 7.4 Ma (Mirzaie Ataabadi et al. 2013, 2016), and Daijiagou, the type locality of *C. anderssoni*, being the youngest locality, having been dated to 5.7 Ma (Kaakinen et al. 2013). The fossiliferous horizons on Samos Island stratigraphically overlap to a large degree with the Maragheh levels, having been dated to 8–6.7 Ma (Kostopoulos et al. 2003; Koufos et al. 2011), whereas Kutschwan is the only fossil site for which no information about the exact location and age is available (Kampouridis et al. 2022a; Kargopoulos et al. 2023). Overall, the Late Miocene was a time of changing environments, with the expansion of more open habitats and grasslands (Böhme et al. 2017, 2021b; Denk et al. 2018; Kaya et al. 2018; Fortelius et al. 2019; Li et al. 2020). In northeastern China, the palaeoenvironment was a C3 steppe with mild seasonality that was most probably affected by summer monsoons during the Late Miocene (Ciner et al. 2015; Li et al. 2020) but was subject to significant environmental changes, with the expansion of C4 plants and climatic changes resulting from the uplift of the Tibetan Plateau (Li et al. 2014; Liu et al. 2016). In western Asia, the climate was mainly characterised by winter rainfall and differed significantly from the climatic conditions in Europe (Böhme et al. 2021b). This could have led to different environmental conditions to which each chilothere was adapted, depending on the area in which it lived, thus resulting in subtle or more pronounced changes in their ecology, especially between the European (*C. schlosseri*) and eastern Asian (*C. anderssoni* and *C. habereri*) species. Nonetheless, even with these potential environmental differences, it is unlikely that, by themselves, they would have led to a significant change in the position of d/D4 hypoplasia. Nevertheless, in combination with additional factors, they may have contributed to the observed displacement of the hypoplasia.

Interspecific differences may have affected this divergence of the hypoplasia placement in d/D4 of *C. schlosseri* from Samos. They could reflect some change in the physiology of this species, such as a deviating tooth height, earlier development of d/D4 or all deciduous teeth, a longer pregnancy length, or a different breeding season. Comparing the complete heights of D4 is very difficult because only few isolated, complete, and unworn specimens were investigated. In the few specimens that were studied, *C. schlosseri* did, in fact, exhibit the shortest tooth crown (39–41 mm, *n* = 2), though only marginally shorter than *C. anderssoni* (42 mm, *n* = 1). Most importantly, while *C. persiae* (45–47 mm, *n* = 2) and *C. habereri* (49 mm, *n* = 1) did exhibit higher tooth

crowns, the hypoplasias were found closer to the crown tip, which is the starting point during tooth development. In *C. schlosseri*, the hypoplasia exhibits the greatest distance from the crown tip (~36 mm, $n = 2$), compared to the other three studied chilothere species (22–26 mm). Therefore, tooth height by itself does not explain the observed differences in the position of the hypoplasia. Earlier development of d/D4 would probably also result in earlier eruption of this tooth, which would mean that the already erupted deciduous teeth, d/D2 and d/D3, would be comparably less worn in *C. schlosseri*. However, the comparison of the wear stages of D2 and D3 in SMNS 47913 of *C. schlosseri* (Fig. 10C) and GPIT/MA/04842 of *C. habereri* (Fig. 7B) suggests that D4 erupts almost at the exact same time in these two species, based on the extremely similar wear stages, with the teeth of *C. habereri* being even slightly less worn than those of *C. schlosseri*. Therefore, a hypothesis about earlier development of d/D4 in *C. schlosseri* cannot be supported. Differences in breeding season or gestation period cannot be tested for the studied extinct taxa, but it is known that extant rhinoceroses present some variability. For instance, it is generally accepted that rhinoceroses today are non-seasonal breeders, but African rhinoceroses have preferred breeding seasons, in contrast to Asian rhinoceroses, which do not (Kretzschmar et al. 2004; Schwarzenberger and Hermes 2023). Further, a slight intraspecific variation in gestation length has also been observed that is associated with the season of breeding and climatic conditions (Schwarzenberger and Hermes 2023).

Therefore, a combination of different climatic conditions that may affect breeding and gestation time and some interspecific differences, such as slight differences in crown height, would be a plausible explanation for the lower placement of hypoplasia in d/D4 of *C. schlosseri*. Nonetheless, proving the existence of such differences in fossil taxa is very difficult. A potential difference in the gestation of the animal could only be investigated using Ca isotopes that may expose differences in the isotope composition before and after birth (e.g. Hassler et al. 2021). Based solely on external morphology, it is impossible to confirm such differences. However, the morphology and position of the D4 hypoplasia differ significantly from those of the other chilotheres, and it is possible that this could even represent a distinguishing feature for the species.

## Concluding remarks

Deciduous dentition is commonly overlooked in many groups, including rhinoceroses. This is particularly true for chilotheres, which have long been affected by taxonomic uncertainty. A careful examination of the deciduous dentition of four chilothere species – *Chilotherium persiae* from Maragheh (Iran), *Chilotherium habereri* from Kutschwan (China), *Chilotherium schlosseri* from Samos (Greece), and *Chilotherium anderssoni* from Daijiagou (China) – shows that deciduous teeth can be a unique source of taxonomic information. Chilotheres have generally rather molarised deciduous premolars. In particular, the presence and development of the lingual cingulum and enamel plications can be used for the identification of *C. schlosseri*, whereas the dimensions and morphology of D1 seem to differ in *C. habereri*. Additionally, the ontogenetic development of the nasal-orbital bar varies among the studied species, with *C. persiae* and *C. habereri* showing broadly similar trends, slightly differing from *C. anderssoni*, and *C. schlosseri* exhibiting the greatest deviation. It was possible to determine the eruption sequence of the deciduous dentition and the order in which the teeth are shed and replaced. The d/D2 and d/D3 erupt first, very early in ontogeny, followed by D1 and d/D4. The relative eruption timing of D1 and D4 seems to vary. Replacement of the deciduous teeth by the permanent dentition begins with d/D2, followed by d/D3 and lastly d/D4, whereas D1 is retained into adulthood. Finally, it was detected that d/D2 and d/D3 rarely exhibit enamel hypoplasia (4% and 8%, respectively), whereas d/D4 consistently shows hypoplasia at nearly the same position on the crown in *C. persiae*, *C. habereri*, and *C. anderssoni*. In these three species, the defect shows an "ω" shape near the middle of the tooth crown, whereas in *C. schlosseri*, it is a straight line near the base of the crown. The constant presence of hypoplasia in d/D4 suggests that its aetiology is linked to birth. Overall, these results show that chilothere deciduous dentition potentially preserves consistent, taxonomically and phylogenetically informative characters and should be incorporated into future systematic and developmental studies.

## Acknowledgements

The authors thank M. Hullot (Jurassica Museum, Porrentruy, Switzerland), who generously provided comparative information and photos of rhinoceros teeth with hypoplasias that she studied. The authors thank A. Gishlick, J. Meng (AMNH), S. Roussiakis, G. Svorligkou, G. Theodorou (AMPG), S. Trümper (GMM), U. Kotthoff (GPIH), I. Werneburg (GPIT), M. Blume, O. Sandrock (HLMD), A. Pictet (MGL), R. Rozzi, M. Albrecht (MLU), C. Argot (MNHN), S. Pappa (NHMUK), U. Göhlich (NHMW), R. Brocke, L. Kraus (SMF), E. Amson (SMNS), G. Rössner (SNSB-BSPG), and the Save the Rhino Trust for access to and photographs of material under their care. The authors thank G. Ferreira (University of São Paulo) and the 3D Imaging Lab of the SHEP at the Eberhard Karls University of Tübingen, Germany, for the acquisition of µCT scans of part of the material. PK acknowledges support from the Joachim Herz Stiftung (Add-on Fellowship for Interdisciplinary Life Science 2024) and the AMNH's Richard Gilder Graduate School (Collection Study Grant) for visiting collections. The authors thank the Editor-in-Chief F. Witzmann, J. Tissier, and an anonymous reviewer for their helpful comments on the manuscript.

# References


Alifieri E (2019) Morphological study of cranial material from the rhinocerotids (Mammalia, Perissodactyla) from the old excavations of Pikermi, Attica. Undergraduate Thesis. National and Kapodistrian University of Athens.

Andree J (1921) Rhinocerotiden aus dem Unterpliocän von Samos. Paläontologische Zeitschrift 3: 189–212. https://doi.org/10.1007/bf03190415

Andrews P, Cook J (1985) Natural Modifications to Bones in a Temperate Setting. Man 20: 675–691. https://doi.org/10.2307/2802756

Antoine P-O (2002) Phylogénie et évolution des Elasmotheriina (Mammalia, Rhinocerotidae). Mémoires du Muséum National d'Histoire Naturelle 188: 1–359.

Antoine P-O (2003) Middle Miocene elasmotheriine Rhinocerotidae from China and Mongolia: taxonomic revision and phylogenetic relationships. Zoologica Scripta 32: 95–118. https://doi.org/10.1046/j.1463-6409.2003.00106.x

Antoine P-O, Saraç G (2005) Rhinocerotidae (Mammalia, Perissodactyla) from the late Miocene of Akkaşdağı, Turkey. Geodiversitas 27: 601–632.

Antoine P-O, Sen S (2016) Rhinocerotidae and Chalicotheriidae (Perissodactyla, Tapiromorpha). Geodiversitas 38: 245–259. https://doi.org/10.5252/g2016n2a6

Antoine P-O, Alférez F, Iñigo C (2002) A new elasmotheriine (Mammalia, Rhinocerotidae) from the Early Miocene of Spain. Comptes Rendus Palevol 1: 19–26. https://doi.org/10.1016/S1631-0683(02)00005-2

Antoine P-O, Duranthon F, Welcomme J-L (2003) *Alicornops* (Mammalia, Rhinocerotidae) dans le Miocène supérieur des Collines Bugti (Balouchistan, Pakistan) : implications phylogénétiques. Geodiversitas 25: 575–603.

Antoine P-O, Becker D, Pandolfi L, Geraads D (2025) Evolution and Fossil Record of Old World Rhinocerotidae. In: Melletti M, Talukdar B, Balfour D (Eds), Rhinos of the World. Fascinating Life Sciences. Springer Nature Switzerland, Cham, 31–48. https://doi.org/10.1007/978-3-031-67169-2_2

Arambourg C (1959) Vertébrés continentaux da Miocène supérieur de l'Afrique du Nord. Publications du Service de la Carte Géologique de l'Algérie (Nouvelle Série) Paléontologie, Mémoires 4: 1–159.

Athanassiou A, Roussiakis SJ, Giaourtsakis IX, Theodorou GE, Iliopoulos G (2014) A new hornless rhinoceros of the genus *Acerorhinus* (Perissodactyla: Rhinocerotidae) from the Upper Miocene of Kerassiá (Euboea, Greece), with a revision of related forms. Palaeontographica Abteilung A 303: 23–59. https://doi.org/10.1127/pala/303/2014/23

Bader KS, Hasiotis ST, Martin LD (2009) Application of forensic science techniques to trace fossils on dinosaur bones from a quarry in the Upper Jurassic Morrison Formation, northeastern Wyoming. Palaios 24: 140–158. https://doi.org/10.2110/palo.2008.p08-058r

Bayshashov BU (1982) A new rhinoceros species of the genus *Chilotherium* from Pavlodar. In: Mesozoic and Cenozoic vertebrate fauna and flora of North-Eastern and southern Kazakhstan. Academy of Sciences of Kazakhstan, Almaty, 72–83.

Becker D, Bürgin T, Oberli U, Scherler L (2009) *Diaceratherium lemanense* (Rhinocerotidae) from Eschenbach (eastern Switzerland): systematics, palaeoecology, palaeobiogeography. Neues Jahrbuch für Geologie und Paläontologie - Abhandlungen 254: 5–39. https://doi.org/10.1127/0077-7749/2009/0002

Behrensmeyer AK (1978) Taphonomic and ecologic information from bone weathering. Paleobiology 4: 150–162. https://doi.org/10.1017/S0094837300005820

Bernor RL (1986) Mammalian biostratigraphy, geochronology, and zoogeographic relationships of the Late Miocene Maragheh fauna, Iran. Journal of Vertebrate Paleontology 6: 76–95. https://doi.org/10.1080/02724634.1986.10011600

Bohlin B (1926) Die Famillie Giraffidae. Palaeontologia Sinica, Series C 4: 1–178.

Bohlin B (1935) Cavicornier der *Hipparion*-Fauna Nord-Chinas. Palaeontologia Sinica, Series C 9: 1–166.

Böhme M, Kampouridis P, Markov GN, Hristova L, Spassov N (2021a) Large mammals (Proboscidea, Perissodactyla) from the late Miocene Burel Basin in West Bulgaria. Neues Jahrbuch für Geologie und Paläontologie - Abhandlungen 302: 117–129. https://doi.org/10.1127/njgpa/2021/1022

Böhme M, Spassov N, Majidifard MR, Gärtner A, Kirscher U, Marks M, Dietzel C, Uhlig G, El Atfy H, Begun DR, Winklhofer M (2021b) Neogene hyperaridity in Arabia drove the directions of mammalian dispersal between Africa and Eurasia. Communications Earth & Environment 2: 85. https://doi.org/10.1038/s43247-021-00158-y

Böhme M, Spassov N, Ebner M, Geraads D, Hristova L, Kirscher U, Kötter S, Linnemann U, Prieto J, Roussiakis S, Theodorou G, Uhlig G, Winklhofer M (2017) Messinian age and savannah environment of the possible hominin Graecopithecus from Europe. Macchiarelli R (Ed.). PLoS ONE 12: e0177347. https://doi.org/10.1371/journal.pone.0177347

Böhmer C, Rössner GE (2018) Dental paleopathology in fossil rhinoceroses: etiology and implications. Journal of Zoology 304: 3–12. https://doi.org/10.1111/jzo.12518

Böhmer C, Heissig K, Rössner GE (2016) Dental Eruption Series and Replacement Pattern in Miocene *Prosantorhinus* (Rhinocerotidae) as Revealed by Macroscopy and X-ray: Implications for Ontogeny and Mortality Profile. Journal of Mammalian Evolution 23: 265–279. https://doi.org/10.1007/s10914-015-9313-x

Bratlund B (1999) Taubach revisited. Jahrbuch des Römisch-Germanischen Zentralmuseums Mainz 46: 61–174.

Cabreira SF, Schultz CL, da Silva LR, Lora LHP, Pakulski C, do Rêgo RCB, Soares MB, Smith MM, Richter M (2022) Diphyodont tooth replacement of *Brasilodon*—A Late Triassic eucynodont that challenges the time of origin of mammals. Journal of Anatomy 241: 1424–1440. https://doi.org/10.1111/joa.13756

Campbell BG, Aminit MH, Bernor RL, Dickinsont W, Drake R (1980) Maragheh: a classical late Miocene vertebrate locality in northwestern Iran. Nature 287: 837–841. https://doi.org/10.1038/287837a0

Cerdeño E (1995) Cladistic Analysis of the Family Rhinocerotidae (Perissodactyla). American Museum Novitates 3143: 1–25.

Cerdeño E (1996) *Lartetotherium* (Rhinocerotidae) en la fauna con *Hispanotherium* de! Mioceno Medio de La Retama, Cuenca, Espana. Revista Española de Paleontología 11: 193–197.

Chen GF, Wu WY (1976) Mammalian fossils from the Miocene Jiulongkou locality, Cixian County, Heibei Province. Vertebrata PalAsiatica 14: 6–15.

Chollet MB, Teaford MF (2009) Ecological stress and linear enamel hypoplasia in *Cebus*. American Journal of Physical Anthropology: NA-NA. https://doi.org/10.1002/ajpa.21182

Chow M (1958) New elasmotherine rhinoceros from Shansi. Vertebrata PalAsiatica 2: 131–142.

de Christol M (1835) Recherches sur les caractères des grandes espèces de Rhinocèros fossiles. Annales des Sciences Naturelles 2: 44–112. https://doi.org/10.5962/bhl.title.16189

Ciner B, Wang Y, Deng T, Flynn L, Hou S, Wu W (2015) Stable carbon and oxygen isotopic evidence for Late Cenozoic environmental change in Northern China. Palaeogeography, Palaeoclimatology, Palaeoecology 440: 750–762. https://doi.org/10.1016/j.palaeo.2015.10.009

Davis H, Mead AJ (2013) Enamel Hypoplasia as an Indicator of Nutritional Stress in Juvenile White-Tailed Deer. Georgia Journal of Science 71: 95–101. https://doi.org/10.1515/9780820367521-032

Dawkins WB (1865) On the dentition of *Rhinoceros megarhinus*. The Natural History Review 5: 399–414. https://doi.org/10.1144/gsl.jgs.1867.023.01-02.36

Deng T (2001) New material of *Chilotherium wimani* (Perissodactyla, RHinoceritdae) from the Late Miocene of Fugu, Shaanxi 39: 129–138.

Deng T (2002) Limb bones of *Chilotherium wimani* (Perissodactyla, Rhinocerotidae) from the Late Miocene of the Linxia Basin in Gansu, China. Vertebrata PalAsiatica 40: 305–316.

Deng T (2005a) New cranial material of *Shansirhinus* (Rhinocerotidae, Perissodactyla) from the Lower Pliocene of the Linxia Basin in Gansu, China. Geobios 38: 301–313. https://doi.org/10.1016/j.geobios.2003.12.003

Deng T (2005b) New discovery of *Iranotherium morgani* (Perissodactyla, Rhinocerotidae) from the late Miocene of the Linxia Basin in Gansu, China, and its sexual dimorphism. Journal of Vertebrate Paleontology 25: 442–450. https://doi.org/10.1671/0272-4634(2005)025[0442:ndoimp]2.0.co;2]2.0.CO;2

Deng T (2006a) A primitive species of *Chilotherium* (Perissodactyla, Rhinocerotidae) from the Late Miocene of Linxia Basin (Gansu, China). Cainozoic Research 5: 93–102. https://doi.org/10.1016/j.geobios.2008.01.006

Deng T (2006b) Neogene Rhinoceroses of the Linxia Basin (Gansu, China). Courier des Forschungsinstituts Senckenberg 256: 43–56.

Deng T (2007) Skull of *Parelasmotherium* (Perissodactyla, Rhinocerotidae) from the Upper Miocene in the Linxia Basin (Gansu, China). Journal of Vertebrate Paleontology 27: 467–475. https://doi.org/10.1671/0272-4634(2007)27[467:sopprf]2.0.co;2]2.0.CO;2

Deng T (2008) A new elasmothere (Perissodactyla, Rhinocerotidae) from the late Miocene of the Linxia Basin in Gansu, China. Geobios 41: 719–728. https://doi.org/10.1016/j.geobios.2008.01.006

Deng T, Downs WR (2002) Evolution of Chinese Neogene Rhinocerotidae and Its Response to Climatic Variations. Acta Geologica Sinica 76: 139–145. https://doi.org/10.1111/j.1755-6724.2002.tb00080.x

Denk T, Zohner CM, Grimm GW, Renner SS (2018) Plant fossils reveal major biomes occupied by the late Miocene Old-World Pikermian fauna. Nature Ecology & Evolution 2: 1864–1870. https://doi.org/10.1038/s41559-018-0695-z

Dollo L (1885) Rhinocéros vivants et fossiles. Revue de Questions Scientifiques 17: 293–299.

Eckhardt RB, Protsch von Zieten R (1993) Enamel hypoplasias as indicators of developmental stress in pongids and hominids. Human Evolution 8: 93–99. https://doi.org/10.1007/BF02436608

Edinger T (1937) Ein Steinkern der Gehirn-, Nasen- und Nebenhöhlen von *Chilotherium*. Bulletin of the Geological Institution of the University of Uppsala 27: 32–41.

Fernández M, Fernicola JC, Cerdeño E (2021) Deciduous dentition and dental eruption sequence in Interatheriinae (Notoungulata, Interatheriidae): implications in the systematics of the group. Journal of Paleontology 95: 861–885. https://doi.org/10.1017/jpa.2021.7

Fisher JW (1995) Bone Surface Modifications in Zooarchaeology. Journal of Archaeological Method and Theory 2: 7–68. https://doi.org/10.1007/bf02228434

Fortelius M, Heissig K (1989) The phylogenetic relationships of the Elasmotherini. Mitteilungen der Bayerischen Staatssammlung für Paläontologie und historische Geologie 29: 227–233.

Fortelius M, Bibi F, Tang H, Žliobaitė I, Eronen JT, Kaya F (2019) The nature of the Old World savannah palaeobiome. Nature Ecology & Evolution 3: 504–504. https://doi.org/10.1038/s41559-019-0857-7

Fukuchi A, Nakaya H, Takai M, Ogino S (2009) A preliminary report on the Pliocene rhinoceros from Udunga, Transbaikalia, Russia. Asian Paleoprimatology 5: 61–98.

Gajewski JA (2026) Ontogeny and the Effects of Perinatal Stress in the First Immature Skeleton of *Teleoceras aepysoma* (Perissodactyla, Rhinocerotidae). Master's Thesis. East Tennessee State University

Geraads D (1988) Révision des Rhinocerotinae (Mammalia) du Turolien de Pikermi. Comparaison avec les formes voisines. Annales de Paléontologie 74: 13–41.

Geraads D, Koufos G (1990) Upper Miocene Rhinocerotidae (Mammalia) from Pentalophos-1, Macedonia, Greece. Palaeontographica Abteilung A 210: 151–168.

Geraads D, Spassov N (2009) Rhinocerotidae (Mammalia) from the Late Miocene of Bulgaria. Palaeontographica Abteilung A 287: 99–122. https://doi.org/10.1127/pala/287/2009/99

Geraads D, Zouhri S (2021) A new late Miocene elasmotheriine rhinoceros from Morocco. Acta Palaeontologica Polonica 66. https://doi.org/10.4202/app.00904.2021

Giaourtsakis IX (2003) Late Neogene Rhinocerotidae of Greece: distribution, diversity and stratigraphical range. Deinsea 10: 235–253. https://doi.org/10.1525/9780520942509-018

Giaourtsakis IX (2009) The Late Miocene Mammal Faunas of the Mytilinii Basin, Samos Island, Greece: New Collection 9. Rhinocerotidae. Beiträge zur Paläontologie 31: 157–187. https://doi.org/10.1525/9780520942509-018

Giaourtsakis IX (2022) The Fossil Record of Rhinocerotids (Mammalia: Perissodactyla: Rhinocerotidae) in Greece. In: Vlachos E (Ed.), Fossil Vertebrates of Greece Vol. 2. Springer International Publishing, Cham, 409–500. https://doi.org/10.1007/978-3-030-68442-6_14

Giaourtsakis IX, Svorligkou G, Roussiakis S (2018) A juvenile skull of the hornless rhinocerotid *Acerorhinus neleus* (Rhinocerotidae, Mammalia) from the Late Miocene locality of Pikermi (Attica, Greece). In: Bristol, UK, 81. https://doi.org/10.13140/rg.2.2.14335.46244/1

Giaourtsakis IX, Theodorou G, Roussiakis S, Athanassiou A, Iliopoulos G (2006) Late Miocene horned rhinoceroses (Rhinocerotinae, Mammalia) from Kerassia (Euboea, Greece). Neues Jahrbuch für Geologie und Paläontologie - Abhandlungen 239: 367–398. https://doi.org/10.1127/njgpa/239/2006/367

Goddard J (1970) Age criteria and vital statistics of a black rhinoceros population. East African Wildlife Journal 8: 105–121. https://doi.org/10.1111/j.1365-2028.1970.tb00834.x

Gomes Rodrigues H, Lihoreau F, Orliac M, Boisserie J-R (2021) Characters from the deciduous dentition and its interest for phylogenetic reconstruction in Hippopotamoidea (Cetartiodactyla: Mammalia).

Zoological Journal of the Linnean Society 193: 413–431. https://doi.org/10.1093/zoolinnean/zlaa147

Goodman AH, Rose JC (1990) Assessment of systemic physiological perturbations from dental enamel hypoplasias and associated histological structures. American Journal of Physical Anthropology 33: 59–110. https://doi.org/10.1002/ajpa.1330330506

Gray JE (1821) On the natural arrangemenet of vertebrose animals. London Medical Repository 15: 297–310.

Guatelli-Steinberg D (2000) Linear enamel hypoplasia in gibbons (*Hylobates lar carpenteri*). American Journal of Physical Anthropology 112: 395–410. https://doi.org/10.1002/1096-8644(200007)112:3<395::aid-ajpa9>3.0.co;2-h

Guatelli-Steinberg D (2001) What can developmental defects of enamel reveal about physiological stress in nonhuman primates? Evolutionary Anthropology: Issues, News, and Reviews 10: 138–151. https://doi.org/10.1002/evan.1027

Guatelli-Steinberg D, Lukacs JR (1998) Preferential expression of linear enamel hypoplasia on the sectorial premolars of rhesus monkeys (*Macaca mulatta*). American Journal of Physical Anthropology 107: 179–186. https://doi.org/10.1002/(sici)1096-8644(199810)107:2<179::aid-ajpa4>3.3.co;2-q

Guatelli-Steinberg D, Skinner M (2000) Prevalence and Etiology of Linear Enamel Hypoplasia in Monkeys and Apes from Asia and Africa. Folia Primatologica 71: 115–132. https://doi.org/10.1159/000021740

Guérin C (1980) Les Rhinocéros (Mammalia, Perissodactyla) du Miocène terminal au Pleistocène supérieur en Europe occidentale: comparaison avec les espèces actuelles. Documents des Laboratoires de Géologie de la Faculté des Sciences de Lyon 79: 1–1185. https://doi.org/10.1016/s0016-6995(06)80220-2

Hannibal DL, Guatelli-Steinberg D (2005) Linear enamel hypoplasia in the great apes: Analysis by genus and locality. American Journal of Physical Anthropology 127: 13–25. https://doi.org/10.1002/ajpa.20141

Hassler A, Martin JE, Ferchaud S, Grivault D, Le Goff S, Albalat E, Hernandez J-A, Tacail T, Balter V (2021) Lactation and gestation controls on calcium isotopic compositions in a mammalian model. Metallomics 13: mfab019. https://doi.org/10.1093/mtomcs/mfab019

Heissig K (1972) Paläontologische und geologische Untersuchungen im Tertiär von Pakistan 5. Rhinocerotidae (Mamm.) aus den unteren und mittleren Siwalik-Schichten. Bayerische Akademie der Wissenschaften Mathematisch-Naturwissenschaftliche Klasse Abhandlungen - Neue Folge 152: 1–112.

Heissig K (1975) Rhinocerotidae aus dem Jungtertiär Anatoliens. Geologisches Jahrbuch (B) 15: 145–151.

Heissig K (1981) Probleme bei der cladistischen Analyse einer Gruppe mit wenigen eindeutigen Apomorphien: Rhinocerotidae. Paläontologische Zeitschrift 55: 117–123. https://doi.org/10.1007/BF02986041

Heissig K (1984) Nashornverwandte (Rhinocerotidae) aus der Oberen Süsswassermolasse und ihre Bedeutung für deren Lokalstratigraphie. Heimatliche Schriftenreihe des Landkreises Günzburg 2: 62–74.

Heissig K (2012) Les Rhinocerotidae (Perissodactyla) de Sansan. In: Mammifères de Sansan. Muséum national d'Histoire naturelle, Paris, 317–485.

Hillman-Smith AKK, Owen-Smith RN, Anderson JL, Hall-Martin AJ, Selaladi JP (1986) Age estimation of the White rhinoceros (*Ceratotherium simum*). Journal of Zoology 210: 355–379. https://doi.org/10.1111/j.1469-7998.1986.tb03639.x

Hillson S, Bond S (1997) Relationship of enamel hypoplasia to the pattern of tooth crown growth: A discussion. American Journal of Physical Anthropology 104: 89–103. https://doi.org/10.1002/(sici)1096-8644(199709)104:1<89::aid-ajpa6>3.0.co;2-8

Hullot M, Antoine P-O (2020) Mortality curves and population structures of late early Miocene Rhinocerotidae (Mammalia, Perissodactyla) remains from the Béon 1 locality of Montréal-du-Gers, France. Palaeogeography, Palaeoclimatology, Palaeoecology 558: 109938. https://doi.org/10.1016/j.palaeo.2020.109938

Hullot M, Antoine P-O (2022) Enamel hypoplasia on rhinocerotoid teeth: Does CT-scan imaging detect the defects better than the naked eye? Palaeovertebrata 45: e2. https://doi.org/10.18563/pv.45.1.e2

Hullot M, Laurent Y, Merceron G, Antoine P-O (2021) Paleoecology of the Rhinocerotidae (Mammalia, Perissodactyla) from Béon 1, Montréal-du-Gers (late early Miocene, SW France): Insights from dental microwear texture analysis, mesowear, and enamel hypoplasia. Palaeontologia Electronica 24: a27. https://doi.org/10.26879/1163

Hullot M, Martin C, Blondel C, Rössner GE (2024a) Life in a Central European warm-temperate to subtropical open forest: Paleoecology of the rhinocerotids from Ulm-Westtangente (Aquitanian, Early Miocene, Germany). The Science of Nature 111: 10. https://doi.org/10.1007/s00114-024-01893-w

Hullot M, Antoine P-O, Spassov N, Koufos GD, Merceron G (2023) Late Miocene rhinocerotids from the Balkan-Iranian province: ecological insights from dental microwear textures and enamel hypoplasia. Historical Biology 35: 1417–1434. https://doi.org/10.1080/08912963.2022.2095910

Hullot M, Martin C, Blondel C, Becker D, Rössner GE (2024b) Evolutionary palaeoecology of European rhinocerotids across the Oligocene–Miocene transition. Royal Society Open Science 11: 240987. https://doi.org/10.1098/rsos.240987

Hullot M, Martin C, Blondel C, Becker D, Rössner GE (2024c) Paleobiology and paleoecology of the woolly rhinoceros (*Coelodonta antiquitatis*) in Northern and Central Europe: New insights from multi-proxy data. Quaternary International 713: 109573. https://doi.org/10.1016/j.quaint.2024.10.005

Jäger GF (1839) Über die fossilen Säugetiere welche in Würtemberg in verschiedenen Formationen aufgefunden worden sind, nebst geognotischen Bemerkungen über diese Formationen. Carl Erhard Verlag, Stuttgart, 139 pp.

Jäger KRK, Gill PG, Corfe I, Martin T (2019) Occlusion and dental function of *Morganucodon* and *Megazostrodon*. Journal of Vertebrate Paleontology 39: e1635135. https://doi.org/10.1080/02724634.2019.1635135

Ji HX, Xu QQ, Huang WB (1980) The *Hipparion* fauna from Guizhong Basin, Xizang. In: Palaeontology of Xizang, Book 1. The Comprehensive Scientific Expedition to the Qinghai-Xizang Plateau of the Chinese Academy of Sciences. Science Press, Beijing, 18–32.

Kaakinen A, Passey BH, Zhang Z-Q, Liu L-P, Pesonen Z, Fortelius M (2013) Stratigraphy and Paleoecology of the Classical Dragon Bone Localities of Baode County, Shanxi Province. In: Fortelius M, Wang X, Flynn L (Eds) Fossil Mammals of Asia. Columbia University Press, 203–217. https://doi.org/10.7312/columbia/9780231150125.003.0007

Kampouridis P, Hartung J, Ferreira GS, Böhme M (2022a) Reappraisal of the late Miocene elasmotheriine *Parelasmotherium schansiense*

from Kutschwan (Shanxi Province, China) and its phylogenetic relationships. Journal of Vertebrate Paleontology 41: e2080556. https://doi.org/10.1080/02724634.2021.2080556

Kampouridis P, Svorligkou G, Kargopoulos N, Augustin FJ (2022b) Reassessment of '*Chilotherium wegneri*' (Mammalia, Rhinocerotidae) from the late Miocene of Samos (Greece) and the European record of *Chilotherium*. Historical Biology 34: 412–420. https://doi.org/10.1080/08912963.2021.1920939

Kampouridis P, Mirzaie Ataabadi M, Hartung J, Augustin FJ (2024) The easternmost occurrence of the Late Miocene schizotheriine chalicothere *Ancylotherium pentelicum* at the classical locality of Maragheh (Iran). Journal of Mammalian Evolution 31: 36. https://doi.org/10.1007/s10914-024-09730-7

Kampouridis P, Svorligkou G, Spassov N, Böhme M (2025) Postcranial anatomy of the Late Miocene Eurasian hornless rhinocerotid *Chilotherium*. PLoS ONE 20: e0336590. https://doi.org/10.1371/journal.pone.0336590

Kampouridis P, Hartung J, Augustin FJ, El Atfy H, Ferreira GS (2023a) Dental eruption and adult dentition of the enigmatic ptolemaiid *Qarunavus meyeri* from the Oligocene of the Fayum Depression (Egypt) revealed by micro-computed tomography clarifies its phylogenetic position. Zoological Journal of the Linnean Society: zlad065. https://doi.org/10.1093/zoolinnean/zlad065

Kampouridis P, Svorligkou G, Kargopoulos N, Spassov N, Böhme M (2023b) Revision of the Late Miocene hornless rhinocerotids from Samos Island (Greece) with the designation of neotypes and implications for the European chilotheres. Journal of Vertebrate Paleontology. https://doi.org/10.1080/02724634.2023.2254360

Kargopoulos N, Kampouridis P, Hartung J, Böhme M (2023) Hyaenid remains from the Late Miocene of Kutschwan (Shanxi Province, China). PalZ. https://doi.org/10.1007/s12542-023-00658-6

Kaup J (1832) Über *Rhinoceros incisivus* Cuv., und eine neue Art, *Rhinoceros schleiermacheri*. Isis von Oken: 898–904.

Kaya F, Bibi F, Žliobaitė I, Eronen JT, Hui T, Fortelius M (2018) The rise and fall of the Old World savannah fauna and the origins of the African savannah biome. Nature Ecology & Evolution 2: 241–246. https://doi.org/10.1038/s41559-017-0414-1

Kiernik E (1913) Über einen *Aceratherium* schädel aus der Umgebung von Odessa. Bulletin international de l'Académie des sciences de Cracovie 1913: 808–864.

Killgus H (1922) Die Unterpliocaenen Chinesischen Säugetierreste der Tafelschen Sammlung zu Tübingen. Ph.D. Dissertation. Eberhard-Karls University of Tübingen

Killgus H (1923) Unterpliozäne Säuger aus China. Paläontologische Zeitschrift 5: 251–257. https://doi.org/10.1007/bf03160375

Koenigswald W, Smith BH, Arbor A, Keller T (2007) Supernumerary teeth in a subadult rhino mandible (*Stephanorhinus hundsheimensis*) from the middle Pleistocene of Mosbach in Wiesbaden (Germany). Paläontologische Zeitschrift 81: 416–428. https://doi.org/10.1007/bf02990253

Korotkevich OL (1958) A new *Chilotherium* species from the Sarmatian deposits of the Ukraine. Dopovidi Akad. Nauk Ukrainskoi RSR 12: 1372–1376.

Korotkevich OL (1970) The mammals of the Berislav late Sarmatian *Hipparion*-fauna. In: The Natural Environment and the fauna of the past. Naukova Dumka, 121.

Kostopoulos DS, Sen S, Koufos GD (2003) Magnetostratigraphy and revised chronology of the late Miocene mammal localities of Samos, Greece. International Journal of Earth Sciences 92: 779–794. https://doi.org/10.1007/s00531-003-0353-8

Kostopoulos DS, Koufos GD, Sylvestrou IA, Syrides GE, Tsombachidou E (2009) The Late Miocene Mammal Faunas of the Mytilinii Basin, Samos Island, Greece: New Collection: 2. Lithostratigraphy and Fossiliferous Sites. Beiträge zur Paläontologie 31: 13–26. https://doi.org/10.1016/j.geobios.2010.08.004

Koufos GD (2009) The Late Miocene Mammal Faunas of the Mytilinii Basin, Samos Island, Greece: New Collection: 1. History of the Samos Fossil Mammals. Beiträge zur Paläontologie 31: 1–12. https://doi.org/10.1016/j.geobios.2010.08.004

Koufos GD, Kostopoulos DS, Vlachou TD (2009) The Late Miocene Mammal Faunas of the Mytilinii Basin, Samos Island, Greece: New Collection 16. Biochronology. Beiträge zur Paläontologie 31: 397–408. https://doi.org/10.1016/j.geobios.2010.08.004

Koufos GD, Kostopoulos DS, Vlachou TD, Konidaris GE (2011) A synopsis of the late Miocene Mammal Fauna of Samos Island, Aegean Sea, Greece. Geobios 44: 237–251. https://doi.org/10.1016/j.geobios.2010.08.004

Kretzschmar P, Ganslo\u00dfer U, Dehnhard M (2004) Relationship between androgens, environmental factors and reproductive behavior in male white rhinoceros (*Ceratotherium simum simum*). Hormones and Behavior 45: 1–9. https://doi.org/10.1016/j.yhbeh.2003.08.001

Krokos WI (1917) *Aceratherium schlosseri* Web. du village de Grebeniki du gouvernement de Kherson. Memoires of the Agricultural Society of Southern Russia 82: 1–96.

Laurillard F (1848) Rhinoceros fossiles. In: Dictionnaire universel d'Histoire naturelle, volume 11. Renard Martinet & Cie édit, Paris, 99–102.

Lehmann U (1984) Notiz für Säugerreste von der Insel Samos in der Sammlung des Geologisch-Paläontologischen Instituts und Museums Hamburg. Mitteilungen des Geologisch-Paläontologischen Instituts der Universität Hamburg 57: 147–156.

Li J, Fang X, Song C, Pan B, Ma Y, Yan M (2014) Late Miocene–Quaternary rapid stepwise uplift of the NE Tibetan Plateau and its effects on climatic and environmental changes. Quaternary Research 81: 400–423. https://doi.org/10.1016/j.yqres.2014.01.002

Li S, Sanisidro O, Wang S, Yang R, Deng T (2024) New materials of *Pliorhinus ringstromi* from the Linxia Basin (Late Miocene, eastern Asia) and their taxonomical and evolutionary implications. Journal of Mammalian Evolution 31: 6. https://doi.org/10.1007/s10914-023-09698-w

Li S-J, Deng T (2023) Restudy of Rhinocerotini fossils from the Miocene Jiulongkou Fauna of China. Vertebrata PalAsiatica 61: 198–211.

Li Y, Deng T, Hua H, Zhang Y, Wang J (2020) Isotopic record of palaeodiet of a 7.4 Ma Hipparionine fauna from the central Loess Plateau, northern China: Palaeo-ecological and palaeo-climatic implications. Chemical Geology 532: 119353. https://doi.org/10.1016/j.chemgeo.2019.119353

Linnaeus C (1758) Systema naturæ per regna tria naturæ, secundum classes, ordines, genera, species, cum characteribus, differentiis, synonymis, locis. Editio decima, reformata, Holmiae, Laurentii Salvii, 824 pp.

Liu J, Li JJ, Song CH, Yu H, Peng TJ, Hui ZC, Ye XY (2016) Palynological evidence for late Miocene stepwise aridification on the northeastern Tibetan Plateau. Climate of the Past 12: 1473–1484. https://doi.org/10.5194/cp-12-1473-2016

Lu X (2013) A juvenile skull of *Acerorhinus yuanmouensis* (Mammalia: Rhinocerotidae) from the Late Miocene hominoid fauna of the Yuanmou Basin (Yunnan, China). Geobios 46: 539–548. https://doi.org/10.1016/j.geobios.2013.10.001

Lu X, Chen S, He W (2015) New skulls of *Shansirhinus ringstromi* from the upper Neogene of the Linxia Basin, and their paleoenvironmental context. Quaternary Research 35: 539–549. https://doi.org/10.11928/j.issn.1001-7410.2015.03.06

Lu X-K, Deng T, Pandolfi L (2023) Reconstructing the phylogeny of the hornless rhinoceros Aceratheriinae. Frontiers in Ecology and Evolution 11: 1005126. https://doi.org/10.3389/fevo.2023.1005126

Lukacs JR (1999) Enamel hypoplasia in deciduous teeth of great apes: Do differences in defect prevalence imply differential levels of physiological stress? American Journal of Physical Anthropology 110: 351–363. https://doi.org/10.1002/(sici)1096-8644(199911)110:3<351::aid-ajpa7>3.0.co;2-2

Mateer NJ, Lucas SG (1985) Swedish vertebrate palaeontology in China: A history of the Lagrelius Collection. Bulletin of the Geological Institutions of the University of Uppsala, New Series 11: 1–24.

Mead AJ (1999) Enamel hypoplasia in Miocene rhinoceroses (*Teleoceras*) from Nebraska: evidence of severe physiological stress. Journal of Vertebrate Paleontology 19: 391–397. https://doi.org/10.1080/02724634.1999.10011150

Mecquenem R de (1908a) Contribution à l'étude du gisement des vertébrés de Maragha et de ses environs. Annales d'histoire naturelle 1: 27–98.

Mecquenem R de (1908b) Le lac D'ourmiah. Annales de Géographie 17: 128–144. https://doi.org/10.3406/geo.1908.18216

Mecquenem R de (1924) Contribution à l'étude des fossiles de Maragha. Annales de Paléontologie 13–14: 135–160, 1–36.

Mirzaie Ataabadi M, Bernor RL, Kostopoulos DS, Wolf D, Orak Z, Zare G, Nakaya H, Watabe M, Fortelius M (2013) Recent Advances in Paleobiological Research of the Late Miocene Maragheh Fauna, Northwest Iran. In: Fortelius M, Wang X, Flynn L (Eds) Fossil Mammals of Asia. Columbia University Press, 546–565. https://doi.org/10.7312/columbia/9780231150125.003.0025

Mirzaie Ataabadi M, Kaakinen A, Kunimatsu Y, Nakaya H, Orak Z, Paknia M, Sakai T, Salminen J, Sawada Y, Sen S, Suwa G, Watabe M, Zaree G, Zhaoqun Z, Fortelius M (2016) The late Miocene hominoid-bearing site in the Maragheh Formation, Northwest Iran. Palaeobiodiversity and Palaeoenvironments 96: 349–371. https://doi.org/10.1007/s12549-016-0241-4

Montalvo CI (2002) Root traces in fossil bones from the Huayquerian (Late Miocene) faunal assemblage of Telén, La Pampa, Argentina. Acta geologica hispanica 37: 37–42.

Morlan RE (1980) Taphonomy and Archaeology in the Upper Pleistocene of the Northern Yukon Territory: A Glimpse of the Peopling of the New World. University of Ottawa Press, Ottawa, 428 pp. https://doi.org/10.2307/j.ctv16tq6

Newell EA, Guatelli-Steinberg D, Field M, Cooke C, Feeney RNM (2006) Life history, enamel formation, and linear enamel hypoplasia in the Ceboidea. American Journal of Physical Anthropology 131: 252–260. https://doi.org/10.1002/ajpa.20436

Nothdurft W, Smith JB (2002) The lost dinosaurs of Egypt. Random House, New York, 256 pp.

Osborn HF (1900) Phylogeny of the rhinoceroses of Europe. Bulletin of the American Museum of Natural History 12: 229–267.

Owen R (1848) Description of teeth and portions of jaws of two extinct anthracotherioid quadrupeds (*Hyopotamus vectianus* and *Hyop. bovinus*) discovered by the Marchioness of Hastings in the Eocene deposits on the N.W. coast of the Isle of Wight; with an attempt to develop Cuvier's idea of the classification of pachyderms by the number of their toes. Quarterly Journal of the Geological Society of London 4: 103–141. https://doi.org/10.1144/gsl.jgs.1848.004.01-02.21

Pandolfi L (2016) *Persiatherium rodleri* , gen. et sp. nov. (Mammalia, Rhinocerotidae) from the upper Miocene of Maragheh (northwestern iran). Journal of Vertebrate Paleontology 36: e1040118. https://doi.org/10.1080/02724634.2015.1040118

Pandolfi L, Pierre-Olivier A, Bukhsianidze M, Lordkipanidze D, Rook L (2021) Northern Eurasian rhinocerotines (Mammalia, Perissodactyla) by the Pliocene–Pleistocene transition: phylogeny and historical biogeography. Journal of Systematic Palaeontology 19: 1031–1057. https://doi.org/10.1080/14772019.2021.1995907

Pavlow M (1913) Mammifères tertiaires de la Nouvelle Russie, 1. Partie: Artiodactyla, Perissodactyla (*Aceratherium kowalevskii* n.s.). Nouveaux Mémoires de la Société Impériale des Naturalistes de Moscou 17: 1–68.

Peter K (2002) Odontologie der Nashornverwandten (Rhinocerotidae) aus dem Miozän (MN5) von Sandelzhausen (Bayern). Zitteliana 22: 3–168.

Pohlig H (1884a) Geologische Untersuchungen in Persien. Verhandlungen der kaiserlich-königlichen geologischen Reichsanstalt 14: 281–284.

Pohlig H (1884b) Ueber weitere Reiseergebnisse des Herrn Dr. Pohlig in Persien. Sitzungsberichte der naturforschenden Gesellschaft in Bonn: 173–175.

Pohlig H (1885) Ueber eine Hipparionen-Fauna von Maragha in Nordpersien, über fossile Elephantenreste Kaukasiens und Persiens und über die Resultate einer Monographie der fossilen Elephanten Deutschalnds und Italiens. Zeitschrift der Deutschen Geologischen Gesellschaft 37: 1022–1027.

Pohlig H (1886) On the Pliocene of Maragha, Persia, and its resemblance to that of Pikermi in Greece. Quaterly Journal of the Geological Society of London 42: 177–179. https://doi.org/10.1144/gsl.jgs.1886.042.01-04.20

Qiu ZX, Xie JY, Yan DF (1987) A new chilothere skull from Hezheng, Gansu, China, with special reference to the Chinese "*Diceratherium*". Scientia Sinica B: 545–552.

Ringström T (1923) *Sinotherium lagrelii*. Ringström. A new fossil rhinocerotid from Shansi, China. Bulletin of the Geological Survey of China 5: 91–93.

Ringström T (1924) Nashörner der Hipparion-Fauna Nord-Chinas. Palaeontologia Sinica 1: 1–156.

Ringström T (1927) Über quartäre und jungtertiäre Rhinocerotiden aus China und der Mongolei. Palaeontologia Sinica, Series C 4: 1–21.

Rodler A (1885) Das Knochenlager und die Fauna von Maragha. Verhandlungen der kaiserlich-königlichen geologischen Reichsanstalt 14: 333–337.

Roohi G, Raza SM, Khan AM, Ahmad RM, Akhtar M (2015) Enamel Hypoplasia in Siwalik Rhinocerotids and its Correlation with Neogene Climate. Pakistan Journal of Zoology 47: 1433–1443.

Schlosser M (1903) Die fossilen Säugethiere Chinas nebst einer Odontographie der recenten Antilopen. Abhandlungen der Königlichen Bayerischen Akademie der Wissenschaften 22: 1–221.

Schwarzenberger F, Hermes R (2023) Comparative analysis of gestation in three rhinoceros species (*Diceros bicornis*; *Ceratotherium simum*; *Rhinoceros unicornis*). General and Comparative Endocrinology 334: 114214. https://doi.org/10.1016/j.ygcen.2023.114214

Sefve I (1927) Die Hipparionen Nord-Chinas. Palaeontologia SInica, Series C 4: 1–91.

Shellis RP, Beynon AD, Reid DJ, Hiiemae KM (1998) Variations in molar enamel thickness among primates. Journal of Human Evolution 35: 507–522. https://doi.org/10.1006/jhev.1998.0238

Skinner MF (1986) Enamel hypoplasia in sympatric chimpanzee and gorilla. Human Evolution 1: 289–312. https://doi.org/10.1007/BF02436704

Skinner MF, Rodrigues AT, Byra C (2014) Developing a pig model for crypt fenestration-induced localized hypoplastic enamel defects in humans: Localized Enamel Hypoplasia In Pigs. American Journal of Physical Anthropology 154: 239–250. https://doi.org/10.1002/ajpa.22497

Spassov N, Geraads D, Hristova L, Markov GN, Garevska B, Garevski R (2018) The late Miocene mammal faunas of the Republic of Macedonia (FYROM). Palaeontographica Abteilung A 311: 1–85. https://doi.org/10.1127/pala/2018/0073

Sun D-H, Li Y, Deng T (2018) A new species of *Chilotherium* (Perissodactyla, Rhinocerotidae) from the Late Miocene of Qingyang, Gansu, China. Vertebrata PalAsiatica 56: 216–228. https://doi.org/10.26879/838

Svorligkou G, Kampouridis P, Kargopoulos N, Pandolfi L (2025) Craniodental anatomy of the hornless rhinocerotid *Chilotherium schlosseri* (Mammalia, Perissodactyla) from the Late Miocene of Samos Island, Greece. Journal of Mammalian Evolution 32: 36. https://doi.org/10.1007/s10914-025-09777-0

Țibuleac P (2014) Presence of the genus *Choerolophodon* (Proboscidea: Mammalia) within the Moldavian Platform framework (Eastern Carpathians Foreland, Romania). Comptes Rendus Palevol.

Țibuleac P, Tissier J, Petculescu A, Becker D (2023) *Chilotherium schlosseri* (Weber, 1905) (Rhinocerotidae, M ammalia) from the late Miocene of the foreland of the Eastern Carpathians in Romania. Comptes Rendus Palevol 22: 729–752. https://doi.org/10.5852/cr-palevol2023v22a36

Toula F (1906) Das Gebiss und Reste der Nsenbeine von *Rhinoceros* (*Ceratorhinus* Osborn) *hundsheimensis*. Abhandlungen der k.k. Geologischen Reichsanstalt, Wien 20: 1–38.

Ungar PS (2010) Mammal Teeth: Origin, Evolution, and Diversity. JHU Press, 316 pp. https://doi.org/10.1353/book.485

Upex B, Dobney K (2012) Dental enamel hypoplasia as indicators of seasonal environmental and physiological impacts in modern sheep populations: a model for interpreting the zooarchaeological record. Kitchener A (Ed.). Journal of Zoology 287: 259–268. https://doi.org/10.1111/j.1469-7998.2012.00912.x

Wang K-M (1928) Die obermiozänen Rhinocerotiden von Bayern. Paläontologische Zeitschrift 10: 184–212. https://doi.org/10.1007/BF03041571

Weber M (1904) Ueber Tertiäre Rhinocerotiden von der Insel Samos. Bulletin de la Société Impériale des Naturalistes de Moscou 17: 477–501.

Weber M (1905) Über Tertiäre Rhinocerotiden von der Insel Samos. II. Bulletin de la Société Imperériale des Naturalistes de Moscou 18: 344–363.

Wessel P, Luis JF, Uieda L, Scharroo R, Wobbe F, Smith WHF, Tian D (2019) The Generic Mapping Tools Version 6. Geochemistry, Geophysics, Geosystems 20: 5556–5564. https://doi.org/10.1029/2019GC008515

Zdansky O (1924) Jungtertiäre Carnivoren Chinas. Palaeontologia Sinica, Series C 2: 1–149.

Zdansky O (1925a) Fossile Hirsche Chinas. Palaeontologia Sinica, Series C 2: 1–94.

Zdansky O (1925b) Quartäre Carnivoren aus Nord-Chiina. Palaeontologia Sinica, Series C 2: 1–25.

Zdansky O (1927a) Weitere Bermerkungen über fossile Carnivoren aus China. Palaeontologia Sinica, Series C 4: 1–30.

Zdansky O (1927b) Weitere Bermerkungen über fossile Cerviden aus China. Palaeontologia Sinica, Series C 5: 1–21.

Zong GF (1998) A new evidence of dividing in the Neogene stratigraphy of Yuanmou Basin. Memories of Beijing Natural History Museum 56: 159–178.

# Supplementary material 1

## Measurements of D1 and nasal-orbital bar

Authors: Panagiotis Kampouridis, Luca Pandolfi, Christina Kyriakouli, Nikolai Spassov, Madelaine Böhme

Data type: xlsx



Link: https://doi.org/10.3897/fr.29.192018.suppl1